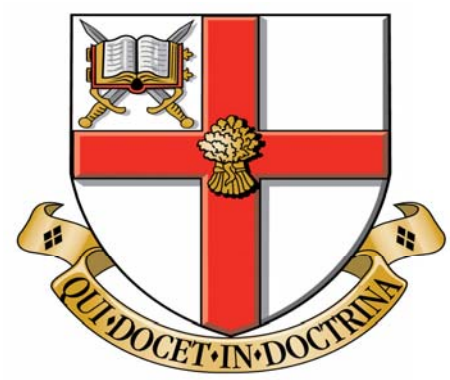

University of Chester

A Multidisciplinary Approach to Structuring in Reduced Triacylglycerol Based Systems

Thesis submitted in accordance with the requirements of the University of Chester for the degree of Doctor of Philosophy

by

Paul Wassell

May 2013

Declaration of Originality

I hereby declare that work contained here is original and is entirely my own work (unless indicated otherwise). It has not been previously submitted in support of a Degree, qualification or other course.

I wish to acknowledge the Swedish Institute for Food and Biotechnology (SIK). Göteborg, Sweden, who contributed to the research leading to Chapter 3, by supporting experiments through analysis and interpretation of data for the Ultrasonic Velocity Profiling with Pressure Difference studies (Wassell et al., 2010b; Young et al., 2008).

I wish to acknowledge the Laboratory of Food Biophysics, Hiroshima University, Higashi-Hiroshima, Japan, who contributed to the research leading to Chapter 6, by making the requested measurements and data analysis for the Synchrotron Radiation Macrobeam and Microbeam X-ray Diffraction studies of Interfacial Crystallisation of Fats in Water-in-Oil Emulsions (Wassell et al., 2012).

Signed

Date

Acknowledgements

I would like to thank the following friends and colleagues who have inspired, helped and supported me, before and during this study:

Allan Bech, Thue Christensen, Fernanda Davoli, Mark Farmer, Brad Forrest, Torben Isak, Henrik Kragh, Cecilie Kristensen, Neils Krog, Christian Kjølby, Jorgen Madsen, John Neddersen, Mogens Nielsen, Birgitte Pedersen, Lisbeth Dahl Pedersen, John Podmore, Kirsten Aaby Sorensen, Jorn Borch Søe, Ralph Timms, Stuart Warner, Niall Young and many others too numerous to mention.

I wish to acknowledge the contribution made by Danisco / DuPont and particularly mention the technical support and the excellent library team in Brabrand.

Thanks to my supervisors (Professors) at the University of Chester especially to Graham Bonwick and Niall Young for being available in the good and testing times.

I need to thank Dr. Johan Wiklund and all those involved in the joint collaboration between Danisco / DuPont and the Swedish Institute for Food and Biotechnology (SIK). Göteborg, Sweden.

Especially, I wish to thank very much Airi Okamura and Professors Kiyo Sato and Satoru Ueno involved in the joint collaboration between Danisco / DuPont and the Laboratory of Food Biophysics, Hiroshima University, Higashi-Hiroshima, Japan, for their time and patience.

Finally, of course, Julia, for all your incredible support. Thank you.

List of Publications, Patents and Presentations

Papers:

Paper 1 Wassell, P. & Young, N.W.G (2007). Food applications of *trans* fatty acid substitutes. International Journal of Food Science and Technology, 42, 503–517.

Paper 2 Wassell, P. Bonwick, G., Smith, C. J., Almiron-Roig, E. & Young, N.W.G. (2010) Towards a Multidisciplinary Approach to Structuring in Reduced Saturated Fat- Based Systems – A Review. International Journal of Food Science & Technology, 45, 642–655.

Paper 3 Young, N.W.G., Wassell, P, Wiklund, J. & Stading, M. (2008). Monitoring Structurants of Fat Blends with Ultrasound Based In-Line Rheometry (UVP-PD). International Journal of Food Science and Technology, 43, 2083–2089.

Paper 4 Wassell, P., Wiklund, J,. Stading, M., Bonwick, G., Smith, C. J., Almiron-Roig, E. & Young, N. W. G. (2010) Ultrasound Doppler Based In-Line Viscosity and Solid Fat Profile Measurement of Fat Blends. International Journal of Food Science and Technology, **45**, 877 - 883.

Paper 5 Wassell, P., Okamura, A., Young, N.W.G., Bonwick, G., Smith, C., Sato, K., and Ueno, S., (2012) Synchrotron Radiation Macrobeam and Microbeam X-ray Diffraction Studies of Interfacial Crystallization of Fats in Water-in-Oil Emulsions. Langmuir 28 (13), 5539-5547.

Book Chapters

Young, N.W.G. and Wassell, P. (2008). Margarines and Spreads. In: G.L. Hasenhuettl and R.W. Hartel (eds.), Food Emulsifiers and Their Applications, 2nd ed. Springer, New York.

Wassell, P. (2014). Bakery fats. In: Fats in Food Technology (edited by K.K. Rajah), 2nd edn. Oxford, UK: Wiley-Blackwell (for publication).

Patents:

Patent 1 Wassell, P., Farmer, M., Warner, S.A., Bech, A.T., Young, N.W.G., Bonwick, G., Smith, C., DuPont Nutrition Biosciences APS, (2012). *Food or Feed Including Moringa Oil*. World Intellectual Property Organisation No. WO2012168722.

Patent 2 Wassell, P., Farmer, M., Warner, S.A., Bech, A.T., Young, N.W.G., Bonwick, G., Smith, C., DuPont Nutrition Biosciences APS, (2012). *Triglyceride Fat Crystallisation*. World Intellectual Property Organisation No. WO2012168727.

Patent 3 Wassell, P., Farmer, M., Warner, S.A., Bech, A.T., Young, N.W.G., Bonwick, G., Smith, C., DuPont Nutrition Biosciences APS, (2012). Low Fat Spread. World Intellectual Property Organisation No. WO2012168726.

Patent 4 Wassell, P., Farmer, M., Warner, S.A., Bech, A.T., Young, N.W.G., Bonwick, G., Smith, C., Forrest, B.A., DuPont Nutrition Biosciences APS, (2012). *Dispersion of Triglycerides*. World Intellectual Property Organisation No. WO2012168723.

Patent 5 Wassell, P., Farmer, M., Warner, S.A., Bech, A.T., Young, N.W.G., Bonwick, G., Smith, C., DuPont Nutrition Biosciences APS, (2012). *Spread*. World Intellectual Property Organisation No. WO2012168724.

Patent 6 Bech, A.T., Farmer, M., Forrest, B.A., Wassell, P., Young, N.W.G., DuPont Nutrition Biosciences APS, (2013). *Composition*. World Intellectual Property Organisation No. WO2013050944.

Presentations (Oral)

Ultrasound Doppler Based In-Line Viscosity and Solid Fat Profile Measurement of Fat Blends. Wassell, P., Lecture presentation: Hiroshima International Forum on Functionality of Lipids 24 -27 March, (2010). Hiroshima University, Higashi-Hiroshima, Japan.

Ultrasonic Based Methods for Acoustic Characterization, In-Line Viscosity and Solid Fat Content (SFC) Measurements of Fat Blends. Levenstam Bragd, E., Wiklund, J., Wassell, P. and Young, N.W.G., 7th International Symposium on Ultrasound Doppler Techniques. Annual European Rheology Conference. April 7-9, (2010). Göteborg, Sweden.

Ultrasound Doppler Based In-Line Viscosity and Solid Fat Profile Measurement of Fat Blends. Bhattacharya, K., Wassell, P., Wiklund, J., Stading, M., Bonwick, G., Smith, C., Almiron-Roig, E., Young, N.W.G., Physical Chemistry Lecture., 9th Euro Fed Lipid Congress, Rotterdam, 18-21 September (2011).

Presentations (Poster)

Influence of Emulsifiers in W/O Low Fat Spreads for Fat Crystallization. Okamura, A., Wassell, P., Young, N.W.G., Bonwick, G., Smith, C., Almiron-Ruig, E., Sato, K., Ueno, S., Physical chemistry, poster session (PC-007). 9th Euro Fed Lipid Congress, Rotterdam, 18-21 September (2011).

Influences of Emulsifiers in W/O Low Fat Spreads on Fat Crystallization. Okamura, A., Wassell, P., Young, N.W.G., Bonwick, G., Smith, C., Almiron-Ruig, E., Sato, K., Ueno. Poster, AAOCS biennial conference. November 9-11th, (2011), Sebel Playford Adelaide, Australia.

Abstract

This study (Wassell & Young 2007; Wassell et al., 2010a) shows that behenic (C22:0) fatty acid rich Monoacylglycerol (MAG), or its significant inclusion, has a pronounced effect on crystallisation (Wassell et al., 2010b; 2012; Young et al., 2008) and interfacial kinetics (3.0; 4.0). New interfacial measurements demonstrate an unusual surface-interactive relationship of long chain MAG compositions, with and without Polyglycerol Polyricinoleate (PGPR). A novel MAG synthesised from *Moringa oleifera* Triacylglycerol (TAG) influenced textural behaviour of water-in-oil (W/O) emulsions and anhydrous TAG systems (4.0: 5.0; 6.0).

Emulsifier mixtures of PGPR and MAG rich in C18:1 / 18:2 and C16:0 / C18:0 do not decrease interfacial tension compared with PGPR alone. Only those containing MAG with significant proportion of C22:0 impacted interfacial behaviour. A mixture of C22:0 based MAG and PGPR results with decreasing tension from ~20°C and is initially dominated by PGPR, then through rearrangement, the surface is rapidly dominated by C22:0 fatty acids.

A *Moringa oleifera* based MAG showed unusual decreased interfacial behaviour not dissimilar to PGPR. All other tested MAG (excluding a C22:0 based MAG), irrespective of fatty acid composition resulted with high interfacial tension values across the measured temperature spectrum (50°C to 5°C). A relative decrease of interfacial tension, with decreased temperature, was greater, the longer the chain length (Krog & Larsson 1992). Moreover, results from bulk and interfacial rheology showed that the presence of C22:0 based MAG has a pronounced effect on both elastic modulus (G') and viscous modulus (G'').

Through a multidisciplinary approach, results were verified in relevant product applications. By means of ultrasonic velocity profiling with pressure difference (UVP-PD) technique, it was possible to examine the effect of a C22:0 based MAG in an anhydrous TAG system whilst in a dynamic non-isothermal condition (3.0). The non-invasive UVP-PD technique conclusively validated structural events.

The application of a *Moringa oleifera* based MAG in low TAG (35% - 41%), W/O emulsions, results in high emulsion stability without a co-surfactant (PGPR). The bi-functional behaviour of *Moringa oleifera* based MAG is probably attributed to miscibility (Ueno et al., 1994) of its fatty acids, ranging ~30% of saturated fatty acids (SAFA), with ~70% of C18:1 (5.0). It is concluded that the surface-interactive behaviour of *Moringa oleifera* based MAG, is attributed to approximately 10% of its SAFA commencing from C20:0.

When examined separately and compared, results showed that physical effect of a *Moringa oleifera* based MAG was not dissimilar to PGPR, influencing the crystallisation kinetics of the particular anhydrous TAG system. When either was combined with a C22:0 rich MAG, enhanced gelation onset and strong propensity to form dendrite structure occurred (5.0).

Macrobeam and synchrotron radiation microbeam small angle x-ray diffraction (SR-μ-SAXD) was utilized (6.0) to assess behavior of C22:0 rich MAG, with and without PGPR (Wassell et al., 2012). The C22:0 based MAG combined with PGPR promoted TAG crystallisation as observed by differential scanning calorimetry (DSC). Polarised optical microscopy (POM) observations indicated that C22:0 based MAG eliminates formation of large crystal aggregates, resulting in the likely formation of tiny Pickering TAG / MAG crystals (6.0).

It is concluded that the presence and interactive behaviour of Pickering surface-active MAG, is strongly linked to increased fatty acid chain length, which induce increased textural resilience owing to viscoelasticity (4.0; 5.0).

A multidisciplinary approach was able to verify structuring behaviour (4.0; 5.0), using multiple analyses (Wassell et al., 2010b; 2012; Young et al., 2008). Novel structuring solutions in reduced TAG based systems have been provided (4.0; 5.0). This study both enhances current understanding of structuring in low TAG W/O emulsions and has led to novel MAG compositions, which address emulsification, structuring and texture in TAG based food systems (Wassell et al., 2010a; 2012a; 2012b; 2012c; 2012d; 2012e; Bech et al., 2013).

Table of Contents

List of Figures

1.0 General Introduction

4.0 Rheology and Interfacial Surface-Interactive Behaviour of Mixed Surfactant Systems

List of Tables

1.0 General Introduction

Abbreviations

CLSM	confocal laser scanning microscopy
DAG	diglyceride or diacylglycerol
DSC	differential scanning calorimetry
DSD	droplet size distribution
G’	storage modulus /elastic
G’’	loss modulus /viscosity
G_i’	complex elastic modulus
G_i’’	complex viscous modulus
G*	complex modulus
HDL	high-density lipoproteins
HIPRE	high internal phase ratio emulsions
IRS	interfacial rheology system
IU	international unit
IV	iodine value
LDL	low-density lipoproteins
MAG	monoacylglycerol; mono & di-glyceride; monoglyceride (E471)
mN/m	millinewton per meter
ND	no date
O/W	oil-in-water
Pas	viscosity
PGPR	polyglycerol polyricinoleate (E476)
PLM	polarised light microscopy
POM	polarised optical microscopy
ppm	parts per million

Pst	palm stearin
pNMR	pulsed nuclear magnetic resonance
RBD	refined bleached deodorised
SAFA	saturated fatty acids
SAXD	small angle x-ray diffraction
SFC	solid fat content
SR-μ-SAXD	synchrotron radiation microbeam small angle x-ray diffraction
SSHE	scraped surface heat exchanger
St.dev	standard deviation
TAG	triacylglycerol; triacylglyceride; triglyceride
TFA	*trans* fatty acids
UVP-PD	ultrasonic velocity profiling with pressure difference
WAXD	wide angle x-ray diffraction
W/O	water-in-oil
w/g	watts per gram (heat flow)
wt%	weight percent
XRD	x-ray diffraction

Symbols

α	alpha
β	beta
β’	beta prime
θ	contact angle
T°C	temperature

$T\gamma$	critical interfacial temperature
η^*i	complex interfacial viscosity
μm	micrometer
χ	azimuthal angle
$\Delta\chi$	half width of χ value

1.0 General Introduction

As a result of overwhelming concerns about health issues (Swinburn et al., 2011; Wang, Y.C., McPherson, Marsh, Gortmaker & Brown,, 2011), the food industry has shown continued interest in the reduction of saturated fatty acids, including *trans* fatty acids in foods (Mozaffarian, Jacobson & Greenstein, 2010; NICE, 2010). Current literature confirms this (Bot et al., 2011; Morris, 2011; Wassell & Young, 2007; Wassell, Bonwick, Smith, Almiron-Roig, & Young, 2010a) and discussions continue about the positives and negatives of achieving reduction of saturated fatty acids (Micha & Mozaffarian, 2010; Siri-Tarino, Sun, Hu, & Krauss, 2010; Yamagishi et al., 2010; Swinburn et al., 2011; Wang Y.C. et al., 2011). Irrespective of this, there is a need to find alternative structuring materials, since many food products, especially fat based food dispersions and emulsions, are currently still highly dependent on the presence of saturates and traditional emulsifiers (Wassell et al., 2010a).

Herein lies the problem, removal of these 'building' blocks, i.e. saturates and their *trans* isomer from fat systems, make it difficult to achieve food products which are functionally acceptable to the consumer. The mechanics and successful removal of saturated and *trans* fatty acids in foods (Wassell & Young, 2007) is a complex problem, as is the successful structuring of low or reduced fat based foods, that require additional reduction of total saturates (Wassell et al., 2010a; Young & Wassell 2008). Accomplishing any net reduction of saturated fatty acid materials for dietary requirements (Winwood, 2011) without negative impact on structure and functional properties of a particular food (Wassell & Young, 2007; Wassell et al., 2010a) is more problematic for foods which are already regarded as low saturated. Therefore, the challenge is intensified for food manufacturers to find innovative solutions to structuring issues whilst meeting consumer expectations.

This study examines this current situation through a literature review. It then reports on a small pilot study which investigated the effect of several emulsifiers on crystallisation behaviour in dispersion and emulsion systems, and consequently led to a critical review. As a result of this preliminary research, extensive work explored the use of traditional and novel materials, methods of measurement and analysis. This is subsequently described.

To set the scene, the following sections present a brief overview and history of oils and fats and their use in water – oil emulsions.

1.1 Oils and Fats – Triacylglycerol Based Structurants

Both oils and fats are composed of triacylglycerols (TAG), generally known as triglycerides and are liquid and solid at ambient temperatures, respectively. A triglyceride consists of glycerol esterified with three fatty acids, which can either be three similar ones, called a simple triglyceride, or two or three different ones, in which case it is a mixed triglyceride. A schematic example is given in Figure 1.1.1 (Madsen, 2003).

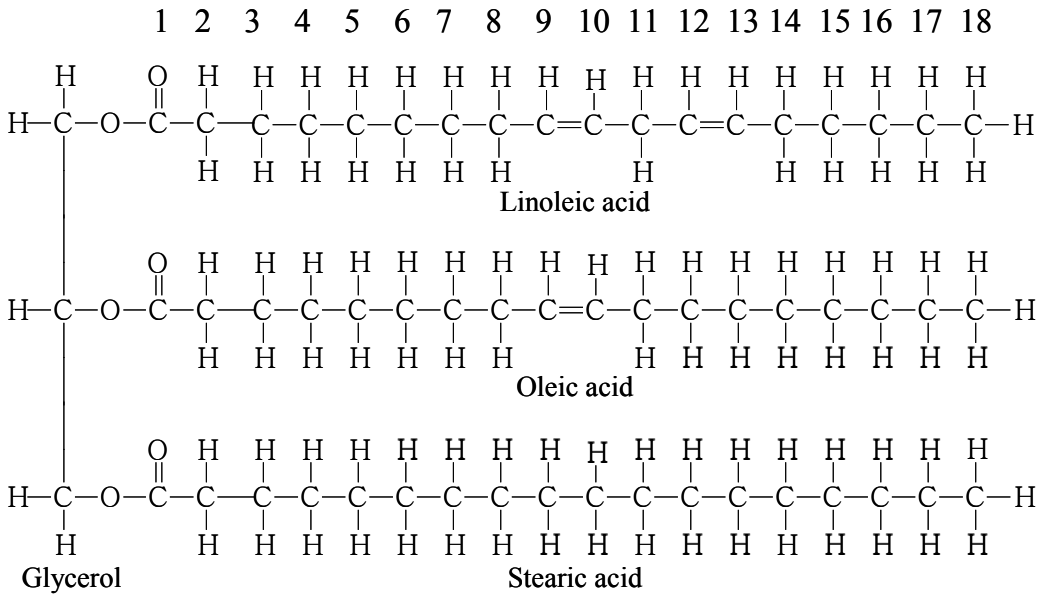

Figure 1.1.1 Schematic example of a mixed triglyceride (Madsen, 2003)

As can be seen in Figure 1.1.1, double bonds are present in some of these fatty acids. Modification of the fatty acids, usually by means of hydrogenation, is where the unsaturated fatty acids are transformed into saturated fatty acids. Here, an example could be C18:1 (oleic acid) going to C18:0 (stearic acid). Such modifications offer the oils and fats manufacturer a greater flexibility and the chance to dramatically alter the melting point of the fat. The fatty acid composition of some natural fats along with other important information is summarised in Table 1.1.1. Given current trends, the down side to hydrogenation is that during the addition of hydrogen, *trans* fatty acids are formed, which are schematically

shown in Figure 1.1.2. Selective hydrogenation involves the saturation of the most polyunsaturated fats first, such that the *trans* fatty acid concentration increases up to a point until they themselves are hydrogenated. If the reaction runs to completion, then the *trans* isomer is absent. The *trans* fatty acids can have substantially higher melting points than the corresponding *cis* fatty acid, where the difference can be in excess of 30°C.

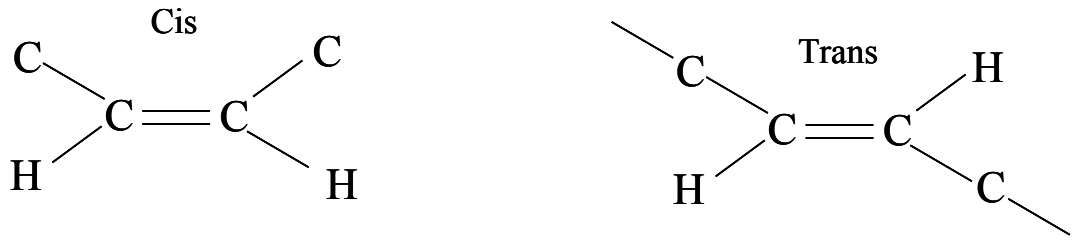

Figure 1.1.2 Schematic diagrams of cis and *trans* configurations (Young and Wassell 2008).

Table 1.1.1 gives the melting points of the individual oils that are used to make up the fat blends, but it is also important to know and recognise the melting points of the fatty acids themselves. These are outlined together with the number of double bonds they contain in Table 1.1.2.

Table 1.1.1 Composition of fatty acids in vegetable oils and fats (Madsen, 2003). T = trace. [a] refers to the typical value, and [b] refers to the range due to natural variability – valid throughout the entire table.

Oil / Fatty acid	Castor	Coconut	Palm kernel	Palm	Ground-nut	Cotton-seed	Soya bean	Sunflower	Linseed	Rapeseed
Caproic, C6:0		0.5[a] 0.2-0.8[b]	0.5 T-1.6							
Caprylic C8:0		8 6-9	4 3-10							
Capric C10:0		7 6-10	5 3-14							
Lauric C12:0		48 44-51	50 37-52							
Myristic C14:0		17 13-18	15 7-17	2 0.5-5		1 0.5-2	T	T		0.5 0-1.5
Palmitic C16:0	2 1-2	9 8-10	7 2-9	42 32-47	10 7-12	21 20-27	8 7-10	6 4-8	5 4-7	2 1-4
Stearic C18:0	1 1-2	2 1-3	2 1-3	5 2-8	3 2-6	2 1-3	4 3-6	4 2-5	4 2-5	1 0.5-2
Arachidic C20:0			T T-0.6		3 2-4	0.5 0.2-1	0.5 0-2	0.5 0-1	T	0.5 0-1
Behenic C22:0					2 T-3			0.5 0-1		1 0.5-1.5
Lignoceric C24:0				T	2 1-3				T	1 1-2
Palmitoleic C16:1		0.2 T-0.4	0.5 T-0.6		T	0.5 0-2	0.5 T-1	T		T
Oleic C18:1	7 T-8.5	7 5.5-7.5	15 11-23	41 40-52	50 35-70	29 22-35	28 20-35	28 20-40	22 12-34	15 11-24
Gadoleic C20:1										7 5-12
Eurcic C22:1										50 40-55
Ricinoleic C18:1	87 86-92									
Linoleic C18:2	3 3-6	1.3 T-2.5	1 1-3	10 5-11	30 20-25	45 42-54	53 40-57	61 45-68	17 14-20	15 11-29
Linolenic C18:3						1 T-2	6 5-14	T	52 35-65	7 6-13
Pure Glycerine	8.8-9.8	13.2-13.5	12.2-12.8	5.5-10.0	8.7-9.9	10.6	10.2	10-12	0.4-10.5	9-9.7
I_2 value (Wijs)	81-91	7.5-10.5	14-23	44-54	84-100	99-113	120-141	126-136	55-205	97-108
Saponification Value	177-187	250-264	245-255	195-205	188-195	189-198	189-195	186-194	188-196	170-180
Melting point °C	-10 b. -12	23-26	24-26	27-50	-2	-2b. +2	-20 b. -23	-10	-20	-9
Titer °C		20-24	20-24	40-47	26-32	30-37	20-21	16-20	19-21	11-15

Table 1.1.2 Common fatty acids showing their melting points and the number of double bonds they naturally contain (Source: Chemical Abstracts Service, www.cas.org)

Fatty Acid	No. of Double Bonds	Melting point °C
Lauric C12:0	-	44 – 46°C
Myristic C14:0	-	52 – 54°C
Myristoleic C14:1	1	Liquid at 5°C
Palmitic C16:0	-	61 – 62.5°C
Palmitoleic C16:1	1	Liquid at 5°C
Stearic C18:0	-	67 – 72°C
Oleic C18:1	1	13 – 14°C
Linoleic C18:2	2	Liquid at 5°C
Linolenic C18:3	3	Liquid at 5°C
Arachidic C20:0	-	74 – 76°C

1.1.1 Modification of Oils and Fats

Probably all oils and fats will undergo some form of modification before use in a food product. The most well used modifications are hydrogenation, interesterification and fractionation. Depending on the naturally occurring starting point of saturation or unsaturation of the said oil, the degree of modification might result in a more saturated or unsaturated fat having a higher or lower melting point than the starting material. The importance of this cannot be overemphasised, because it provides structure, texture and hardness to the food product, lubrication, and in terms of emulsion stability, can provide specific crystallisation behaviour, necessary for continuous fat phase dispersions / emulsions. The extent and degree of satisfying these criteria are dependent on the amount of solid fat, size, shape and interactions of the crystals (Wassell & Young, 2007). Figure 1.1.3, shows

schematically, the degree of modification liquid oil required to obtain the desired solid fat structure, which could be used, for example, in margarine or shortening production. Detailed reviews about the subject of structuring edible fat based systems are discussed by Wassell & Young (2007) and Wassell et al., (2010a).

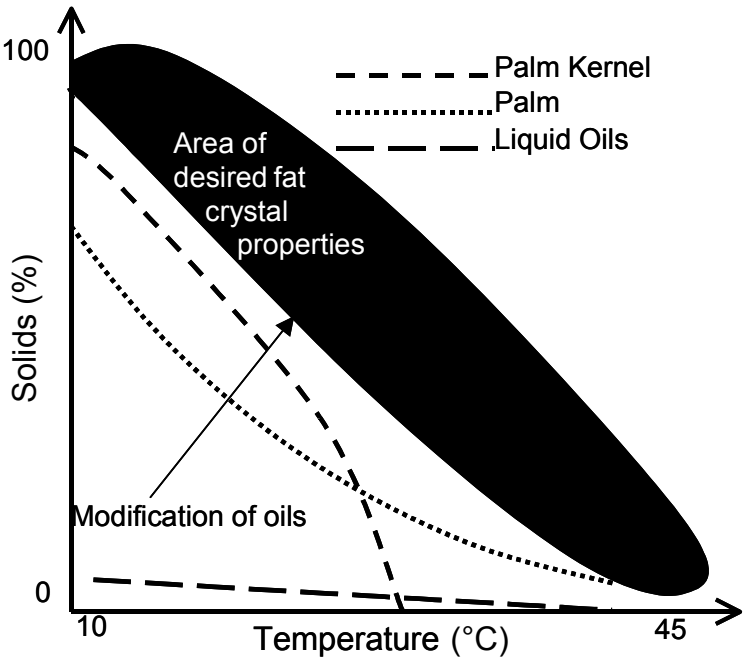

Figure 1.1.3 Desired solid phase lines for hardstocks (dark area) compared to naturally occurring oils and fats (adapted from van Duijn et al., 2006).

1.2 Edible Water-in-Oil Emulsions – Background

1.2.1 History

The term "margarine and spreads", refers to a group of products, which are likened to butter, but have different fat contents. Margarine was invented in response to a request from the French Government of Napoleon III for a less expensive, longer life replacement for butter, available in higher quantities and at a lower price. The big difference between butter and margarine is the source of the raw materials. Butter is made with the cream of cow's milk and margarine with vegetable oils or in the beginning with animal fat (Young & Wassell, 2008; Verstraete, 2011).

1.2.2 Structure of Margarine

According to the council regulation 2991/94 of the European Community concerning fats, margarine is a water-in-oil emulsion with a fat content ranging from 80 to 90%. Most commonly, margarines consist of 80% fats and oils, and 20% of an aqueous phase. The fat phase is a network of fat crystals and agglomerates of fat crystals with liquid oil in between. The fat phase contains fat-soluble ingredients like fat-soluble flavours, vitamins, colourants and emulsifiers. The aqueous phase contains maximum 16% of water. The other 4% are the water-soluble ingredients. These may be salt, water-soluble flavours, milk or milk solids and preservatives (Bockisch, 1998; Young & Wassell, 2008).

The definition of margarine has been established. Anything below 80% fat content, by definition, is not margarine, and must be referred to as a spread; reduced fat, low fat or otherwise. Legislation is complex and terms such as three-quarter fat, half-fat and fat content X% are routinely seen. Three-quarter fat refers to a fat percentage of 60-62%, half-fat to 39-41% specifically. Reduced fat falls

within the range 41-62%, and low fat or light products under 39%. Overall, there is a general consensus that a fat spread product, butter, margarine or other must have a fat content between 10 and 90%. These options are summarised in Table 1.2.1

Table 1.2.1 Product type versus their fat content in percent Source [a] Article 5 of the Council Regulation (EC) No. 2991 / 94, laying down standards for spreadable fats, [b] Other industry classifications

Product Type	**Fat content %**
Butter	80[a]
Margarine	80[a]
Three-quarter fat	60-62[a]
Half-fat	39-41[a]
Reduced fat	>41 to < 62[a]
Low fat / Light	< 39[a]
Very Low Fat	20 – 30[b]
Water Continuous	10 – 15[b]

Margarine is classified as water-in-oil (W/O) emulsion and is characterised as having a water phase, or the dispersed phase, distributed (homogenised) within the fat / oil phase, the continuous phase, as droplets. These products are a complex mix of proteins, emulsifiers, salts, flavours, colours and vitamins. Understanding the chemistry and mechanics of the fat phase is therefore important for producing a stable margarine / spread product. Table 1.2.2 gives the average composition of European margarines and table spreads.

Table 1.2.2 The average composition of margarine and table spreads in Europe

Component	Amount	Examples
Oils/fats	80 %	Soybean oil, rapeseed oil, sunflower oil, palm oil,
Emulsifiers	0.2-0.6%	Lecithin, mono & diglycerides, Citrems, PGPR (in low-fat <41%)
Milk components	<6 %	Whole & skimmed milk, butter milk, whey
Acids	0.1-0.3%	Citric acid solution, lactic acid solution
Sodium Chloride	0.1-0.4%	
Flavour	Traces %	Oil and water soluble
Preservative	<0.12 %	Sorbic acid, benzoic acid (in reduced-fat margarines)
Water	100 %	Tap water
Vitamins	1500 (IU)	Vitamin A
	100 (IU)	Vitamin D
	100-300 ppm	Vitamin E
Stabilisers		In reduced-fat and low-fat margarines
Colour		Carotene

1.2.3 Design and Control of the Fat Blend

The specification of a given fat blend is chosen as a result of many factors (Chrysan, 2005; Wassell & Young, 2007). An oil/ fat blend for margarines can be designed by simple blending, which may encompass a combination of fractions (which can either be fully hydrogenated or not), with liquid oil and/or interesterified oil (which may be hydrogenated hardstocks).

1.2.4 Hardness

The hardness or consistency is a measurement of the texture of the margarine. It may be linked to the type of fats and oils used and the process conditions. The correlation between the hardness and percentage of solid fat content (SFC%) is

debated. One study found the hardness of the margarine has no linear correlation with the SFC (Moziar, De Man, & De Man, 1989). However, hardness is also linked to the total lipid composition (including emulsifiers), polymorphism, crystallisation behaviour and the microstructure. (Vereecken, Meeussen, Lesaffer, & Dewettinck, 2010; Wassell et al., 2010a).

1.2.5 Solid Fat Content (SFC)

There are strong correlations between the SFC% and the plasticity of margarine. This also has implications for the overall melting characteristics of margarines and spreads at various temperatures. This is particularly important for low fat spreads. At low temperatures, i.e. 4–10°C the value of the SFC% will lead to an indication of spreadability when the product is removed straight from the fridge. The SFC values should not exceed 32% at 10°C (Lida & Ali, 1998). Higher ambient temperatures – of 20–22°C – determine the product stability and resistance to oil exudation in domestic conditions and therefore the SFC should be at least 10%. SFC's at approx. 35–37°C provides data on the thickness and mouth feel characteristics as well as flavour release, and should be around 1–3% (Wassell & Young, 2007).

The determination of a required SFC profile, must be factored according to the local climatic, distribution chain and performance demanded in the margarine's application (Yusoff, Kifli, Lida, & Rozie, 1998).

Ideally, the SFC, melting profile, and crystallisation process is such that texturally the fat blend gives the optimal structure and sensory properties characteristic of table margarine or spread (Chrysan, 2005).

1.2.6 Reduced - Low Fat Spreads

Typically, reduced and low fat spreads have fat contents of 60% and 40% respectively. They are primarily used for spreading on bread or cracker products (Chrysan, 2005; Madsen, 1990).

As discussed in 1.2.5, the SFC% must be determined so as to allow the emulsion to attain spreadibility. Selected fat blends tend to be softer where there is much less fat content and therefore, demands on the emulsifier are greater to maintain the stabilisation of the water phase. The preconditions for a stable low fat spread are small water droplets and a stable emulsion. Other components in the system, such as milk proteins, act to give a more open emulsion resulting in improved flavour release; but they also make controlling the water dispersion more difficult, with the consequence of shorter shelf life. The selection of emulsifier therefore depends not only on the fat content of the spread product, but also on the aqueous phase and its composition. This involves consideration of things such as local water hardness, proteins, and hydrocolloids.

1.2.7 Emulsifiers

Emulsifiers reduce interfacial tension in oil-in-water (O/W) and W/O emulsions to aid emulsification and stability. Polar lipids tend to fit this definition and contain a hydrophilic part and a hydrophobic (lipophilic) part. The hydrophobic part that repels water may consist of a fatty acid.

When an emulsifier is added to a mix of oil and water a spontaneous self-organisation takes place at the interface between the two phases.

On the interface, the hydrophilic groups are in contact with water and the hydrophobic groups are in contact with the oil. The interfacial tension is then reduced by the emulsifier, resulting in an easy mixing of oil and water.

Typically in margarine spread type W/O emulsions, the most common emulsifiers (surfactants) used are monoacylglycerols (know as Mono and diglycerides or monoglycerides or E471) or MAGs (Juriaanse & Heertje, 1988), which have amphiphilic properties (Krog, 1977). Table 1.2.3 shows distilled monoglycerides with varying degrees of saturation (a higher iodine value = more unsaturation), and its relationship to emulsion stability.

1.2.8 PGPR

In low-fat spreads with high water and milk protein content, polyglycerol polyricinoleate (PGPR), known for its exceptional water-binding properties secures the necessary emulsion stability and water dispersion. According to the EC Directive 95/2/EC, PGPR (E-476) is allowed in low-fat spread with 41% fat and less in a maximum dosage of 0.4% (Bastida-Rodríguez, 2013).

For very low fat spreads the use of a combination of monoglyceride and polyglycerol ester emulsifiers is claimed to result in wider processing latitude and enhanced finished product stability (Chrysan, 2005; Stewart & Hughes, 1972)

Table 1.2.3 Stability of a 40% W/O emulsion over time (Information received from Danisco / DuPont Oils & Fats, 2009)

	WATER SEPARATION	
DISTILLED MONOGLYCERIDE	10 min	20 min
Iodine value 1	60%	75 %
Iodine value 55	8 %	27 %
Iodine value 80	3 %	16 %
Iodine value 105	3 %	14 %
Iodine value 80 + PGPR	0 %	0 %

In the preparation of the margarine / spread and depending on the ratio of water to oil in the said emulsion, it is usually necessary to select the correct type of emulsifiers to aid product integrity. Table 1.2.4 shows typical emulsifier selection according to fat content and presence of protein.

Table 1.2.4 Typical emulsifier selection for W/O spreads with and without proteins (Information received from Danisco / DuPont Oils & Fats, 2009).

VLFS	Low Fat		Reduced Fat	High Fat
< 25%	< 41%	50%	60 - 70%	80% +
Soft eg. unsaturated sunflower	Mono-di texture RBD palm			Hard eg. fully sat palm
High IV 105	Iodine Value IV 60 - 80		IV 30 - 60	Low IV 2

without protein 0.5% Dimodan U/J 0.4% Grindsted PGPR 90	**without protein** 0.6% Dimodan U/J 0.2% Dimodan P	0.5% Dimodan P or 0.3 - 0.5% Dimodan HP	0.2 - 0.5% Dimodan HP
with protein 0.6% Dimodan U/J 0.4% Grindsted PGPR 90	**with protein** 0.6% Dimodan U/J 0.2% Dimodan P 0.2 - 0.4% Grindsted PGPR 90		
Spreadable low fat butter 0.2% - 0.5% Dimodan U/J 0.3% Grindsted Citrem SP 70 0.1% - 0.2% Grindsted PGPR 90			

Dimodan = Distilled monoglyceride	
Dimodan U/J	Sunflower (IV 105)
Dimodan P	Palm (IV 80)
Dimodan HP	Palm (IV 2)
Grindsted Citrem SP 70	Citric acid ester of Mono & diglycerides
Grindsted PGPR 90	polyglycerol polyricinoleate

1.2.9 Quality Criteria

There are several common tests for emulsion stability (Chrysan, 2005), these being electrical resistance (conductivity), droplet size distribution (DSD), cardboard test (simple backward and forwards spreading action), ambient and cooled storage to assess oiling out and texture analysis. The principles and methods of these and other analyses used within the scope of this thesis are discussed in the General Materials and Methods (2.0). The physical properties of the emulsion can have microbiological implications (Juriaanse & Heertje, 1988; Charteris, 2007); this does not form part of this study.

1.3 Crystallisation and Crystal Growth

1.3.1 Introduction

An overview of some key areas in the physical properties of fats and oils (triacylglycerols / TAG) are presented in brief, and where appropriate additional explanation is provided.

Within edible oils and fats, the subject of crystallisation is usually discussed in the context of two kinds of nucleation:

> Homogenous nucleation - No impurities are present in the liquid oil (Martini, Awad, & Marangoni, 2006).
>
> Heterogeneous nucleation - Nucleation is induced at a higher temperature than that expected for pure oil due to impurities, dust, vessel surface, air bubbles, interface of the emulsion droplets, monoglyceride reverse micelles (Himawan, Starov, & Stapley, 2006; Martini et al., 2006).

Once stable nuclei have formed, these grow into crystals by incorporating molecules in the interface from the melted oil. So that as crystallisation continues, the degree of super-saturation in the system decreases (Timms, 1985).

Once a fat has crystallised, the individual crystals may aggregate to form a three dimensional network which traps liquid oil through capillary forces. With time, crystals transform into more stable state, depending on the chemical composition of the fat and environmental conditions. The rate of crystal growth is proportional to the degree of supercooling and inversely proportional to the viscosity of the melt (Hartel, 2001; Timms, 2007).

During crystal growth, heat is released. Rapid cooling of the melted oil leads to the simultaneous formation of many nuclei which grow into small crystals. Slow cooling leads to a smaller amount of nuclei which have time to grow into larger crystals (Himawan et al., 2006).

1.3.2 Polymorphism and its Identification

X-ray diffraction is commonly used to ascertain the identity of polymorphs (where a solid material is able to exist in more than one form or crystal structure). For each polymorph to produce a different X-ray pattern there must be a fundamental difference in structure. In Triacylglycerol, crystallisation characteristic is due to the packing arrangement of the hydrocarbon chains. Polymorphism of most fats is dependent on the planes of the fatty acid chains within a crystal arrangement. There are three main basic forms: α, β' and β (Kristott, 1999; Timms, 1984).

Fat (triacylglycerol) crystal configuration can be viewed as being like a stacked chair in double or triple layers. X-ray crystallography can measure the spacing across this arrangement to determine its d-spacing (double or triple long spacing). The angle of molecular tilt determines if the polymorph is double or triple long spacing (LS). This is indicated by including -2 or -3 to the basic structure. These are schematically shown in Figure 1.3.1, where (a) shows β' fats normally used in the margarine industry, and (b) shows β for cocoa butter.

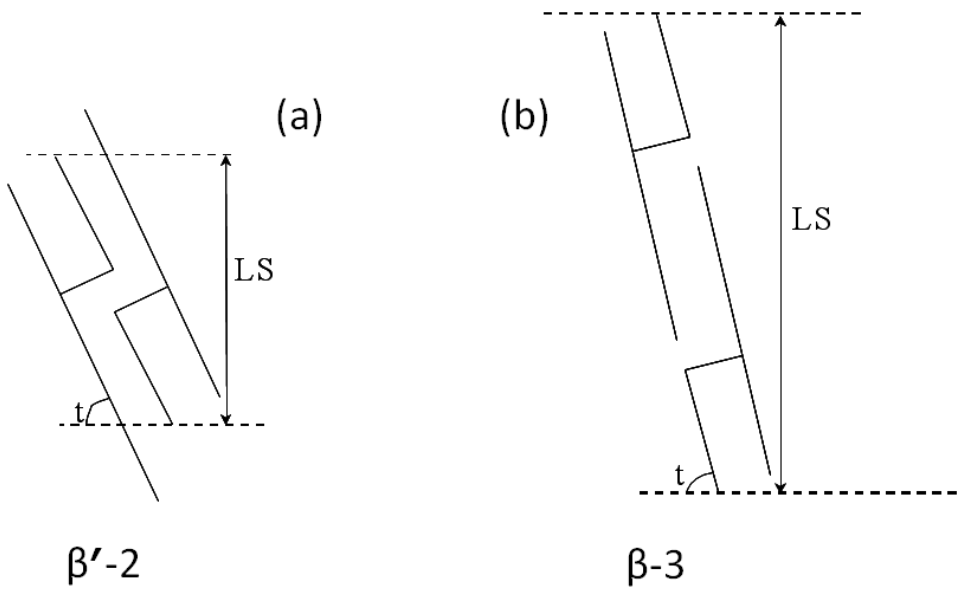

Figure 1.3.1 A schematic of triacylglycerol arrangement in the β'-2, and β-3 form. LS is the long spacing, t is the angle of tilt of the triglyceride configuration (adapted from Timms, 1984).

The angle of tilt, t, will depend on the LS value such that larger LS values result in smaller angles of tilt and vice versa.

The short spacings, shown schematically in Figure 1.3.2, represent distance between the fatty acid chains, and these can accurately be measured by X-ray crystallography. The typical values of the short spacings of the three crystal types are: α - 4.15Å, β' – 3.8Å and 4.2Å, and β - 4.6Å.

α, β' and β crystals (Hoerr, 1960) can be formed directly from the melt, or α to β' to β, but this is not reversible. Although any polymorph can be returned to the liquid phase by raising the temperature above its melting point, polymorphic transformations are irreversible, where β cannot transform back to β' and β' cannot revert back to α (Sato, 1989).

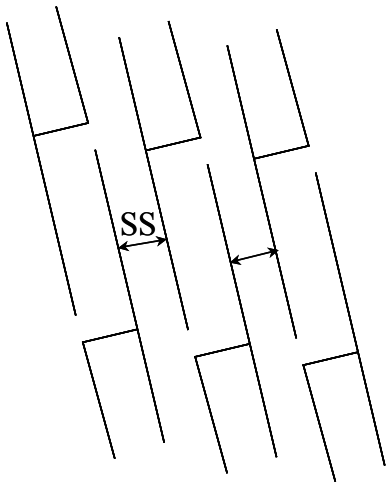

Figure 1.3.2 Fatty acid units showing the short spacing between the individual fat units (source: Young & Wassell, 2008)

Measurement of short spacing between the fatty acids enables quantification of the type and ratio of the fat crystal forms in a given blend. A number of analytical techniques have established that margarines and spreads are preferred when the crystal polymorph is in the β'crystal form, because this form imparts desirable textural qualities (Wassell & Young, 2007; Wassell et al., 2010a).

The influence of processing however can have dramatic impact on crystallisation kinetics. Palm oil is probably the most widely used of vegetable oils. It is naturally β' tending, largely because of its diverse fatty acid profile and particularly high content of palmitic acid (Berger & Idris, 2005). However, if processed incorrectly, these benefits are lost, and because palm oil also contains unusually high content of diglycerides ~ 6 to 7 %, the diglycerides have anti-crystallisation properties that can influence crystal kinetics (Siew, 2002).

The different crystal types, α, β' and β each have their own configurations, shown in Figure 1.3.3., (Hernqvist, 1988), and it is well known that fat crystals with similar chain lengths, e.g. hydrogenated sunflower oils, transform more quickly from the β' to β form (Yap, deMan, & deMan, 1989).

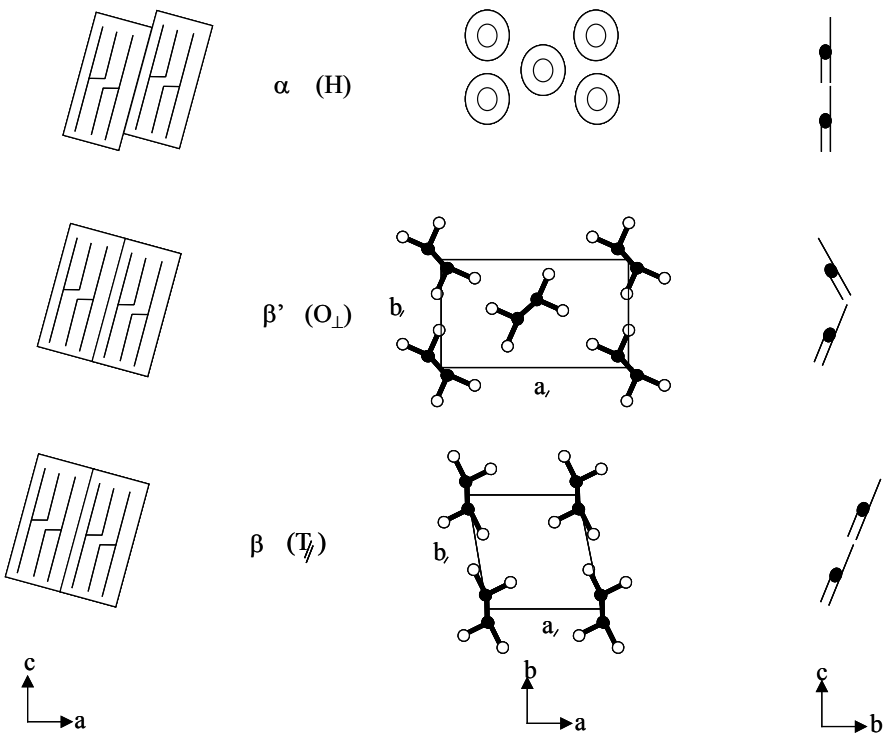

Figure 1.3.3 The three projections of α, β', and β crystal forms (Source: Hernqvist, 1988).

As the crystal form changes, the texture likewise changes. This typically takes place under storage, with the usual transition being from β' to β. During this transition crystal size increases dramatically, from ~3-5 microns to ~100 microns respectively, and likewise melting point. The result is that the margarine now infers a sandy / gritty mouth feel (Kristott, 1999).

The crystals in margarine, spreads and shortenings are bound together by a network of crystal-to-crystal contact bindings. The functionality of the semi-solid margarine, termed plastic fat, is influenced by the ratio of liquids to solids in the lipid phase, and the crystal packing arrangement developed during processing (Timms, 1991). Control of crystal form, size, and shape must be balanced with careful blend selection, and are critical for final application in bakery products. Often these inter-crystal associations are classified as primary (irreversible) and secondary (reversible) bindings, which can be reliably measured using creep – recovery techniques (Marangoni, 2005).

1.3.3 Supercooling

Crystallisation can take place once a liquid phase is cooled below its melting point. This is due to activation energy (ΔG*), which must be overcome before the transition from liquid to solid (Figure 1.3.4). Crystallisation of a single species of TAG molecules requires lowering the temperature of the melted fat below its melting point. The degree of sub-cooling, known as ΔT, is simply the difference between the melting point and the actual temperature. The lower the temperature, the higher the driving force for crystallisation.

The degree of supercooling depends on the chemical structure of the oil, contaminants and cooling rate.

Pure oils can be supercooled by more than 10°C, before any crystallisation is observed.

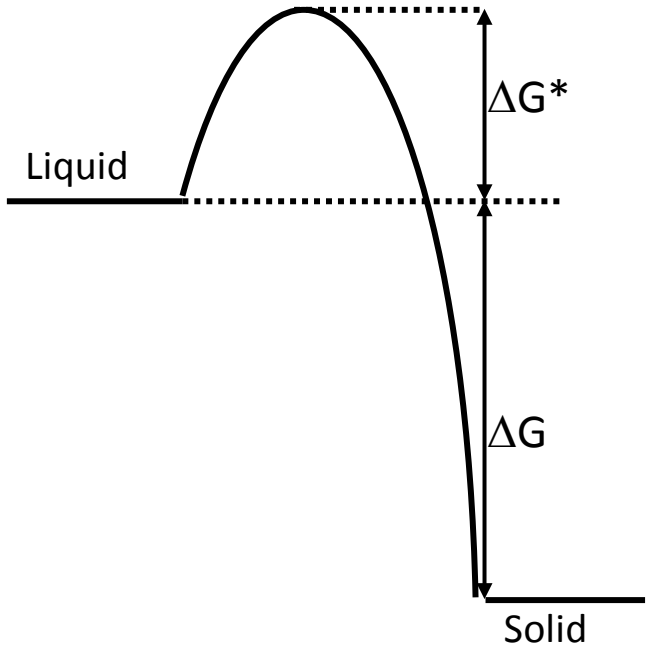

Figure 1.3.4 Diagram of the energy barrier to crystallisation (Source: McClements, 1999)

Table 1.3.1 The influence of supercooling on the solubility and radius of triglyceride crystals.

RADIUS OF CRYSTAL		SUPERCOOLING (°C)	INCREASE IN SOLUBILITY
(μ)	(Å)		
10	**100,000**	**0.004**	**1.001**
1	**10,000**	**0.036**	**1.007**
0.1	**1,000**	**0.36**	**1.1**
0.01	**100**	**3.6**	**2.1**
0.001	**10**	**7.2**	**1380**

Data for Table 1.3.1 is supplied from Dr. Ralph Timms (Danisco AS, lecture, 2003 & 2004).

Table 1.3.1 shows that small crystals have an enormously increased solubility and require a lot of supercooling to cause expanded crystallisation. It can be seen that at a radius <10Å the degree of supercooling required would be very large. Hence spontaneous or homogeneous nucleation rarely, if ever, occurs.

1.3.4 Post-Crystallisation

Fat hardness increases during post-crystallisation and Figure 1.3.5 shows a process described as "sintering", according to the following sequence:

A. Nucleation

B. Crystal growth

C. Solid bridge formation

D. Flocculation of small nuclei between fat crystals

(Johansson & Bergenstahl, 1995).

Some mechanisms of post-crystallisation are:

Ostwald ripening

- Large-size particles grow at the expense of small-size particles
- Driving force: excess interfacial energy for small-size particles

Polymorphic crystallisation and transformation

- More stable forms crystallise at later stage
- More stable forms grow at the expense of less stable forms

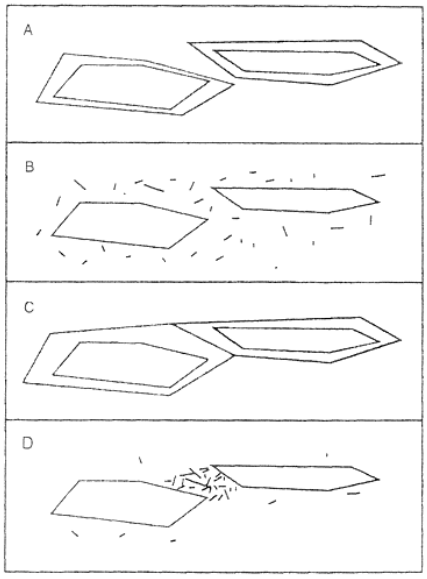

Figure 1.3.5 Schematic stages of sintering (Source: Johansson & Bergenstahl, 1995)

1.3.5 Technical Impact of Process Conditions on Post-Crystallisation

The control of post-crystallisation is important, especially for fat containing products such as W/O emulsions, which are directly influenced by the selected processing conditions. One noticeable impact of cooling and shear, seen during manufacture is the thermal response behaviour of the product. If sub-optimal crystallisation occurs, this often results in hardening (post-crystallisation), and it may have technical consequences for its ability to achieve any subsequent performance e.g. aeration capacity and plasticity, as in the case of margarines and shortenings (Wassell & Young, 2007).

The texture of reduced fat spread products can be critical, especially where reduction of fat in very low fat spread products leads to loss of texture due to "uncontrolled" post-crystal growth (Sato, 2001). Again, cooling and agitation (Bell, Gordon, Jirasubkunakorn, & Smith, 2007) in the production process may influence product quality as shown in Figure 1.3.6. This effect could be experienced by the end-user noticing textural issues such as graininess.

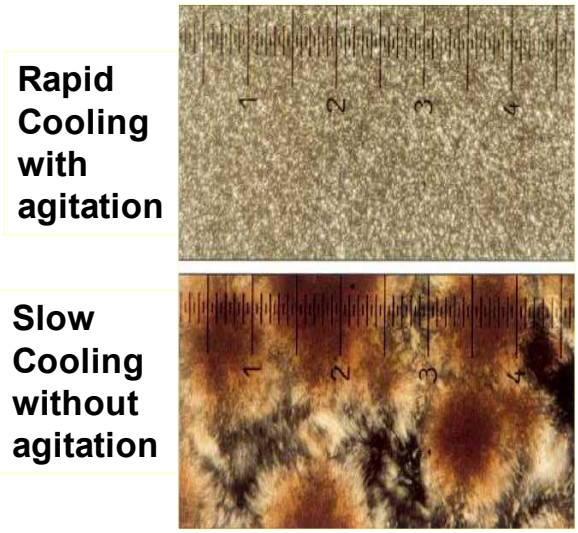

Figure 1.3.6 Effect of cooling and agitation on crystal growth. One scale unit = 100 microns. (Image supplied courtesy of Danisco / DuPont in their Technical Paper: Fat Crystallography – a Review. TP1504-2e)

1.3.6 Palm Oil

The effect of switching to *trans* free fat blends, has usually meant working with palm oil products. Palm oil is not the subject of this thesis, but it is considered necessary to acknowledge its use within the edible oils and fats industry and thereby provide some general back ground to it (Basiron, 2005). Palm oil is inherently β' tending and has a natural semisolid consistency, useful to margarine applications.

In tackling the issue of reducing *trans* saturates, palm oil offers a natural solution. It does not necessarily require a hydrogenation step, which can lead to formation of (dependant on degree of hydrogenation) *trans* isomers (Wassell & Young, 2007). The whole palm oil naturally contains significant amounts of saturates (Wassell et al., 2010a).

Palm is probably the most important oil in terms of fractionation because of its unique fat profile (Sahasranamam, 2005) which can be broken down into individual fractions and will naturally and obviously, become more or less saturated (Timms, 2007). The degree of unsaturation of the palm oil (fractions), can present crystallisation issues due to their inherent diacylglyceride (DAG) content (Siew, 2002; Wassell & Young, 2007; Wassell et al., 2010a). The presence of DAG slows the crystallisation process and changes the melting behaviour (Siew & Ng, 1990; Siew, 2002). Slowing of the crystallisation process leads to post-hardening during storage of palm-based margarines (Wassell & Young, 2007). By gaining control over the DAG content of palm oil, Kristensen and Wassell (2006) showed that not only control, but also improvement over the crystallisation rate was possible (Kristensen, Wassell, Mikkelsen, & Søe, 2005).

Control of the crystallisation rate can be altered by either varying the degree of cooling, type of additive and its concentration, or by manipulating the DAG content (Wassell & Young, 2007). The selection and concentration of emulsifier to enhance crystallisation kinetics has been reviewed extensively (Smith, Bhaggan, Talbot, & van Malssen, 2011; Wassell & Young, 2007).

1.4 Literature Review

1.4.1 Introduction and Background

The issue of *trans* fatty acid (TFA) replacement has been the subject of much discussion and debate within the food industry (Wassell & Young, 2007) as well as in the clinical field for health reasons (FSA, 2008). Now, there is even stronger focus on reducing total saturated fatty acid contents (Beaglehole et al., 2011; Bradley, 2012; Gortmaker et al., 2011; Micha & Mozaffarian, 2010; Mozaffarian et al., 2010; NICE, 2010; Siri-Tarino et al., 2010; Yamagishi et al., 2010; Swinburn et al., 2011; van Camp, Hooker, & Lin, 2012; Vesper, Kuiper, Mirel, Johnson, & Pirkle, 2012; Wang, Y.C. et al., 2011; WHO, 2011; Winwood, 2011). Currently, some governments are considering its taxation to control its presence in foods (Lucas & Rappeport, 2012). However, reformulating is often expensive and not simple, because consumers expect particular textural properties in a given food product.

1.4.1.1 Texture

The aroma, texture and mouth sensations experienced when consuming foods are strongly dependent on their fat content and can eventually shape dietary choices in the long term (Drewnowski, Shrager, Lipsky, Stellar, & Greenwood, 1989; Drewnowski & Almiron-Roig, 2009). Thus, the idea of reformulating familiar foods which historically contained significant amounts of fats and oils (and usually contain significant levels of saturated fat) into lower fat versions, is challenging not only technologically (Pothiraj, Zuñiga, Simonin, Chevallier, & Le-Bail, 2012), but also from a consumer acceptance point of view. Research into consumer perceptions of a new food product, is often compared to memorized experience from a similar consumed food. Consumers may tend to conclude their decisions on the basis of their memory of a food, and not on the basis of their actual perceptions (Mojet & Koster, 2005; Wassell et al., 2010a).

1.4.1.2 Health

It is reported that the consumption of TFA's may raise low-density lipoprotein (LDL) cholesterol levels, and lower high-density lipoprotein (HDL) cholesterol levels, thus contributing to atherosclerosis and an increased risk of apoplexy (Wassell et al., 2010a). However, there is still debate as to the relevance of the intake of TFA from naturally occurring ruminant sources (Willett & Mozaffarian, 2008) and of the importance of saturated fats. McNeill (2009) clearly showed that despite a large body of epidemiological data being generated over the last two decades in respect of their adverse effects, there are also apparently certain important positive effects. Thus the effects of saturated fats on cardiovascular disease are complex.

1.4.1.3 Legislation

Legislation, and literature (WHO, 2011; Wassell et al., 2010a) state that *trans* fatty acids should be removed from food, but current research (Stender, Astrup, & Dyerberg, 2009) suggests that this is insufficient in terms of creating healthy foods. Removal of, or at least drastic reduction of, not only *trans* containing fats, but all saturated fats is also required (Beaglehole et al., 2011; Bradley, 2012; Gortmaker et al., 2011; Micha & Mozaffarian, 2010; Mozaffarian et al., 2010; NICE 2010; Siri-Tarino et al., 2010; Yamagishi et al., 2010; Swinburn et al., 2011; van Camp et al., 2012; Vesper et al., 2012; WHO, 2011; Wassell & Young, 2007; Wassell et al., 2010a).

Realising the legislative requirements of governments, and consumer expectations for the food industry, is a tremendous challenge (Wassell et al., 2010a). Achieving the balance of adequate structure in fat based food systems whilst lowering the total saturated fatty acid content is a major objective of the food ingredient industry which remains elusive. For well over a decade the issue of *trans* fatty acid

removal from bulk fat based systems has been the main focus of research in this field (Wassell & Young, 2007), and in some countries remains so (Wassell et al., 2010a), e.g. Brazil and USA. However, the predominant global attention is on reducing total saturated fats, which of course includes *trans* fats (Wassell & Young, 2007; Wassell et al., 2010a). That said, while the problem is global; for some cases in emerging economies, the degree of importance placed on providing food products with lower *trans* and saturated fats has taken lower priority (Wassell et al., 2010a).

1.4.1.4 Interim Conclusion

Whilst there is general agreement that total fat levels should be reduced, there is disagreement as to the best route (Wassell et al., 2010a). Talbot, Favre, and Thörig (2007), advocate the use of saturated fats preferably from natural sources (Wassell et al., 2010a). Marangoni (2007) suggests that the use of saturated fat in the absence of *trans* fats is not a solution.

The dramatic switch to palm oil products and away from high *trans* containing oils created challenges for food producers to satisfy nutritional demands, and still deliver acceptable functional performance (Wassell & Young, 2007; Wassell et al., 2010a).

A review article entitled: *Food applications of trans fatty acid substitutes* (Wassell & Young, 2007), assessed the increasing pressure to remove trans fatty acids from food products. Further, it reviewed how practical applications of *trans*-free solutions could be successfully implemented and suggested this might be achieved via multiple routes (Wassell & Young, 2007).

When pulled together using a multidisciplinary approach several areas are thought to demand further study. As a consequence, following on from Wassell & Young (2007) a review to study the current state of the art was continued and identified important areas for consideration: Raw materials, reducing total saturates; crystallisation kinetics and interfacial behaviour (Wassell et al., 2010a). These are discussed next.

1.4.2 Raw Materials

As TAGs are responsible for the network structure in traditional systems, it is difficult to entirely remove saturated fats without compromising some sensory and physical characteristics. Modified hard stocks composed largely of saturated fatty acids, contain significant amounts of *trans* isomers (Kodali, 2005; Flöter & van Duijn, 2006; Podmore, 2008; Wassell & Young, 2007; Wassell et al., 2010a). As a natural, semi-solid product that requires little or no modification, palm oil currently continues to dominate. However, as explained earlier (1.4.1.2), nutritionists and health experts exert increasing demands to achieve a lower degree of total saturates (FSA 2008).

Modification techniques and uncomplicated selection of alternative oils, for example, rice bran oil, allanblackia (Wassell & Young, 2007; Wassell et al., 2010a), have demonstrated the possibility of minimising and controlling the *trans* / saturated content of oil blends and of successfully formulating alternative hardstocks (Wassell et al., 2010a). Consequently, edible oil processors continue to explore more exotic and novel sources. Others have explored providing structure without TAGs (Bot, Veldhuizen, del Adel, & Roijers, 2009; Hughes, Marangoni, Wright, Rogers, & Rush, 2009; Rogers, 2009; Halliday, 2011; Wassell et al., 2010a).

1.4.3 Reducing Total Saturates (Emulsions)

The initiatives to either phase out or to reduce *trans* fatty acids, have not entirely addressed the issue of total saturates; nor have they entirely addressed the debate over inclusion of fully hydrogenated oil and fats (van Duijn, Dumelin, & Trautwein, 2006), which are *trans*-free (Wassell & Young, 2007; Wassell et al., 2010a).

In terms of water-oil emulsions and dispersions, several methods to successfully produce margarines and anhydrous shortenings with acceptable structure and

texture were reviewed and all were TAG based solutions (Wassell & Young, 2007). Currently, the literature acknowledges the necessity to couple traditional TAG based solutions with novel materials, because it is unlikely that one novel structurant could satisfy all requirements. An example might be to use a novel lipid based mixture in a TAG-based dispersion or W/O emulsion, a more realistic approach (Johansson, Bergenståhl, & Lundgren, 1995; Rousseau & Hodge, 2005; Wassell et al., 2010a). Whichever route is adopted, this would have implications on either crystallisation behavior or emulsification, or both.

1.4.4 Crystal Kinetics and Interfacial Behaviour

The effect of switching to alternative raw materials for TAG based systems (with or without aqueous phase), and reducing total saturates, will likely influence kinetic behaviour and eventually textural properties. This could be more prevalent in those retail products to which consumers are accustomed. It is likely that synergies obtained through several disciplines, coupled with an understanding of the thermodynamic mechanical properties and critical design of real systems, play a vital influence (Wassell et al., 2010a).

Technology, using long-chain hydrophobic surfactants (Sucrose behenic esters and polyglycerol behenic esters) are known to influence crystallisation kinetics (Sakamoto et al., 2003; 2004). Using this technology, reviews of previous studies have shown several strategies for improving both crystallisation and emulsification, which might transpose to low saturated food formula (Wassell et al., 2010a; Arima, Ueji, Ueno, Ogawa, & Sato, 2007; Awad & Sato, 2001; 2002; Fujiwara, Nagahisa, Yano, Ueno, & Sato, 2000; Sakamoto et al., 2003). One practical approach e.g. inclusion of an aqueous phase, automatically reduces the total fat content, so that incorporation of a significantly larger water phase could utilise W/O low fat emulsion technology (Garti & Remon, 1984; Goubran & Garti, 1988; Rousseau 2000; Wassell & Young, 2007).

For low TAG W/O, it is usual to soften the TAG continuous phase, which automatically results in less saturation. However, this results in less solid TAG content, hence reduced steric stabilisation of the internal (aqueous) phase (Krog, 1990), from a three dimensional network of crystal aggregates. As a consequence, there is potential compromise of the particle attachment to the water-in-oil interface which is essential to Pickering stabilisation (Johansson et al., 1995; Ghosh, Tran, & Rousseau, 2011; Pickering 1907). To compensate, aid from a surface active material that could possibly fulfil both crystallisation and emulsification tasks is likely needed. This situation may be strongly linked to the rate of fat crystallisation in the TAG phase as well as on the amount and form of fat crystals formed. Variations in temperature and/or shear rate may also be important (Johansson et al., 1995).

1.4.5 Conclusion

A review of TAG based materials, crystal kinetics and interfacial behaviour shows that whilst low fat emulsion technology is not new, the use of one or several novel applications of long-chain behenic based emulsifiers to low or reduced TAG based W/O emulsions is not found in the literature (Wassell & Young, 2007). Stabilising W/O emulsion structures at lower TAG levels, using these alternate strategies, required more investigation.

To support this, pilot studies were conducted. First, the use of MAG / TAG mixtures for enhancing crystallisation rates in several anhydrous dispersions. Second, an investigation of the effect of diversified fatty acid mixtures of MAG in the presence of an aqueous interface (shown in 1.5).

1.5 A Pilot Study – Preliminary Investigations for Enhancing Crystallisation of Anhydrous TAG Dispersions and W/O Emulsions

1.5.1 Introduction and Background

Several aspects of crystallisation have been considered previously (1.3 and 1.4). There is no intention to repeat the theory of crystallisation and nucleation in lipid based systems as this has been presented and discussed by others (Garti & Sato, 2001; Himawan et al., 2006; Povey, 2001; Timms, 1984; 1985; Wassell & Young, 2007).

For practical reasons, it was thought necessary to provide supporting data from preliminary investigations to show the effects of MAG / TAG additives on the behaviour of anhydrous continuous model systems. These considerations provide additional comprehensive background to support this thesis, but which is not specifically detailed in publicly available literature.

A review of food applications of *trans* fatty acid substitutes, highlighted a trend to switch away from high *trans* containing fat blends to lower or "zero" (1% max) fat blends. A global move to TAGs containing non-*trans,* has brought other technical challenges. For example, palm oil products containing DAG are known to interfere with crystallisation kinetics (Wassell & Young, 2007).

The literature review (1.4) identified that long-chain emulsifiers are thought to be potentially important. A pilot study was conducted on the use of a MAG based on C22:0.

The following are pilot study results and data from investigations into crystallisation behaviour of anhydrous dispersions together with available MAG and TAG materials.

1.5.1.1 Materials and Methods

It is known that a saturated monoglyceride, preferably of low iodine value (IV) of approx IV<10 can assist crystallisation (Bech, Wassell, & Hornholt, 2008). A distilled monoglyceride, known as DIMODAN® HP (based on fully hydrogenated C16:0, palm), is one such monoglyceride (IV = 2). A second distilled monodiglyceride, rich in C22:0 was compared in order to observe its pro-crystalliser properties. DIMODAN® MB-90 (based on fully hydrogenated C22:0 rape), was compared with DIMODAN® HP in standard refined bleached and deodorised (RBD) palm oil at several concentrations.

DIMODAN® HP and DIMODAN® MB-90 (currently known as GRINDSTED® CRYSTALLIZER 110), were supplied by Danisco / DuPont, Grindsted, Denmark.

Arbitrary concentrations were used simply to observe effect and achieve proof of concept. It was not to focus on prohibitive commercial or legal issues on the use of a behenic based emulsifier. Samples were assembled and tested as follows:

Std RBD Palm oil

Palm Oil + 1% DIMODAN® HP

Palm Oil + 2% DIMODAN® HP

Palm Oil + 3% DIMODAN® HP

Palm Oil + 1% DIMODAN® MB-90

Palm Oil + 2% DIMODAN® MB-90

Palm Oil + 3% DIMODAN® MB-90

A series of crystallisation curves were made and quantified using Bruker pNMR as a measure of SFC% over time. Samples were melted in a water bath at 90°C for 1 hour and then measured after each consecutive 1 minute interval from a water bath at 20°C (ambient) for 20 minutes. Differential scanning calorimetry (DSC) was used to examine thermal behaviour on cooling.

1.5.1.2 Results - Crystallisation of RBD Palm Oil and Commercial Hard and Soft Anhydrous Fat Blends

Based on Figure 1.5.1 it is possible to see that adding DIMODAN® HP (HP) and DIMODAN® MB-90 (MB-90) impacts on solid fat content of palm oil. The solid fat content was increased. Examination of Figure 1.5.2 shows this more clearly. A plateau occurs at 3-5 minutes, as emulsifier concentration was increased, this resulted in a direct relative influence on SFC%.

1% MB-90 showed increased performance compared to 1% HP. Nucleation onset was most significant from time zero.

As crystallisation continued, a concentration above 1% of either HP or MB-90 showed similar performance compared to 1% MB-90. This suggested from this test, no clear advantage with addition of MB-90 beyond 1% in RBD palm oil.

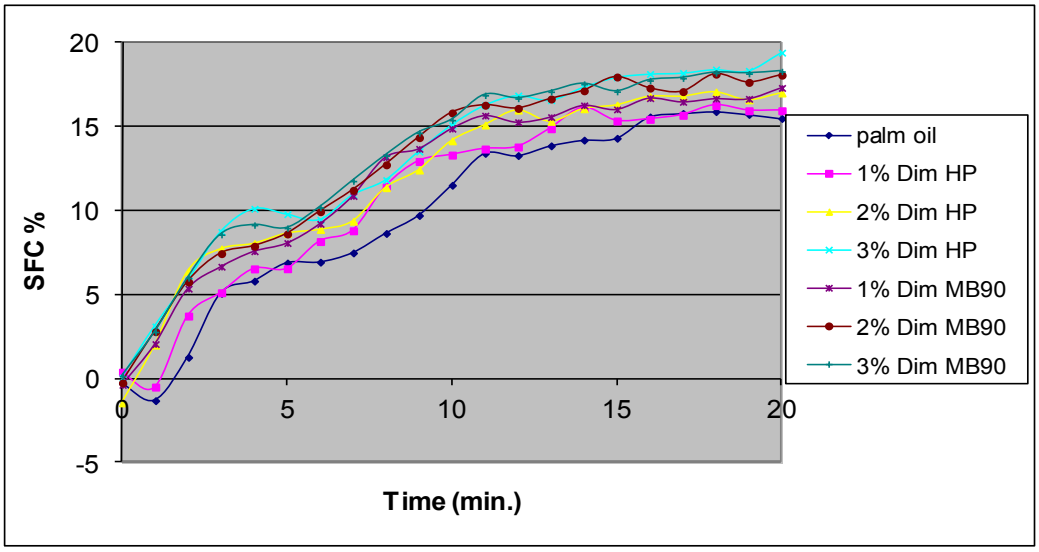

Figure 1.5.1 SFC curves to **20min**

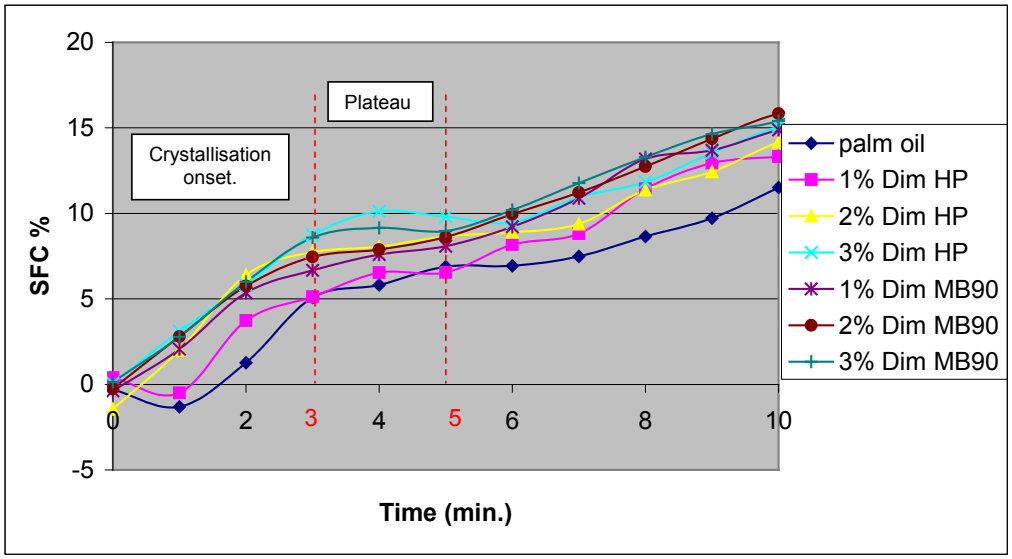

Figure 1.5.2 SFC curves to **10min**

Further trials using two commercial fat blends, a hard (H) and soft (S) fat blend were conducted. Their fatty acid compositions are shown in Table 1.5.1. The rate of crystallisation results are shown in Figures 1.5.3 and 1.5.4. DSC results are shown in Table 1.5.2, where data is based on the crystallisation onset starting point.

Table 1.5.1 Fatty acid profiles of two palm based fat blends.

Fatty Acid (%) Profile Methyl-ester:	**Hard blend (H)**	**Soft blend (S)**
C8:0	0.2	<0.1
C10:0	0.2	<0.1
C12:0	2.6	0.3
C14:0	1.7	0.7
C15:0	0.1	0.1
C16:0	40.9	28.7
C16:1	0.1	0.3
C17:0	0.2	0.2
C18:0	4.6	3.5
C18:1	33.4	44.3
C18:2	10.4	13.8
C18:3	3.4	5.2
C20:0	0.4	0.5
C20:1	0.5	0.8
C20: unclassified	0.2	0.3
C22:0	0.2	0.3
C24:0	0.1	0.1
Total	99.32	99.12

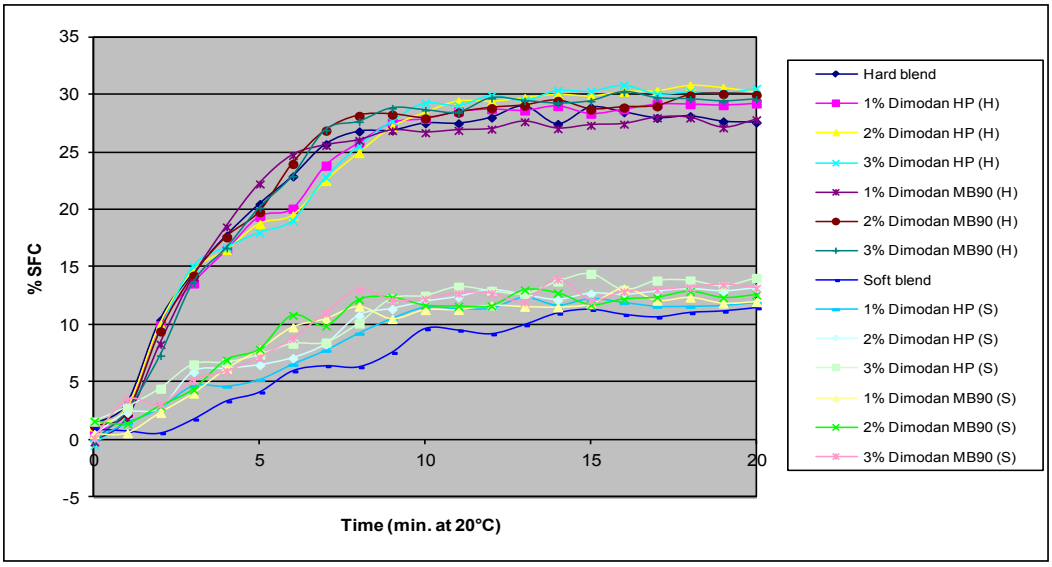

Figure 1.5.3 SFC curves at **20min**

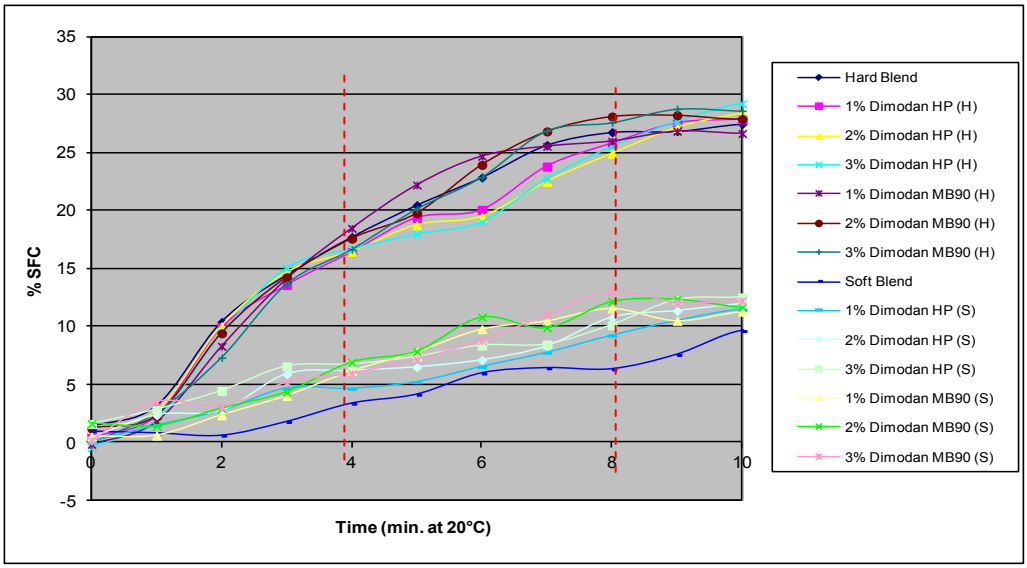

Figure 1.5.4 SFC curves at **10min**

Rate of Crystallisation:

Hard Blend (H): From Figure 1.5.3 it is difficult to say which and/or if the emulsifiers promoted any effect. However, in Figure 1.5.4, it can be seen that between 4 and 8 minute, MB-90 curves are above the pure H, whereas HP curves are below. So, it seems that MB-90 presented a greater and more pronounced effect than HP.

Soft Blend (S): It is much easier to see the emulsifier effect on S than H. Both emulsifiers (all concentrations) presented higher SFC% than S. Figure 1.5.4 shows that at 4 to 8 minutes, all emulsifier curves are above S and MB-90 is above HP.

DSC:

Table 1.5.2 DSC data to show the start of crystallisation onset.

Crystallisation onset starting point (~°C) [#]				
	Hard (H)		Soft (S)	
Pure Fat	24.6		18.7	
Emulsifier	DIMODAN® HP	DIMODAN® MB-90	DIMODAN® HP	DIMODAN® MB-90
1%	25.4	35.0	22.9	38.2
2%	29.2	45.0	32.7	47.6
3%	34.5	50.7	51.1	54.6

[#]Data extracted from DSC corresponds to average of first peak "Right Limit".

Hard Blend (H): The tabulated DSC data shown in Table 1.5.2, shows that H starts crystallisation onset at ~24.6°C. With the addition of 1% HP, there was little emulsifier effect noted. This suggests that DSC of pure H and H+1% HP are similar. Increasing to 2% HP, it was possible to see some effect, where the crystallisation onset started at a higher temperature (~29.2°C). Whereas, increasing to 3% HP significantly enhanced the crystallisation onset, which then started at ~34.5°C.

In comparison, Table 1.5.2 shows that adding 1% MB-90 to blend H, had a similar effect to that of adding 3% HP. The addition of 2% MB-90 significantly increased the crystallisation onset to ~45.0°C. Increasing the MB-90 to 3%, raised onset to ~50.7°C.

Soft Blend (S): The DSC data (Table 1.5.2) revealed that S started crystallisation onset at ~18.7°C. The inclusion of 1% HP had a small effect, increasing the crystallisation onset to 22.9°C. The addition of 2% HP and 3% HP increased the effect further, so that crystallisation onset began at ~32.7°C and ~51.1°C respectively.

In comparison, the addition of 1% MB-90 to S, increased onset to ~38.2°C. This is significantly more functional, than the addition of 2% HP. At 2% MB-90, crystallisation onset started at ~47.6°C, almost 10°C higher than with 1% MB-90. Increasing to 3% MB-90, led to crystallisation onset at ~54.6°C, which is only slightly greater than the effect of 3% HP.

These results showed both HP and MB-90 had the most impact on the crystallisation onset temperature in the soft (S) fat blend.

In the soft fat blend (S), the comparative effect of MB-90 to HP was greater at lower concentrations (1-2%), but when the concentration was increased to 3%, MB-90 showed only a small advantage.

Comparing the two emulsifiers, it was shown that MB-90 had a greater effect than HP in both fat blends.

To show the relative increase of the hard (H) and soft (S) blends (Table 1.5.1) compared to RBD Palm oil, the rate of crystallisation of the three pure fats are plotted together in Figure 1.5.5 which shows their relative SFC% increase over time.

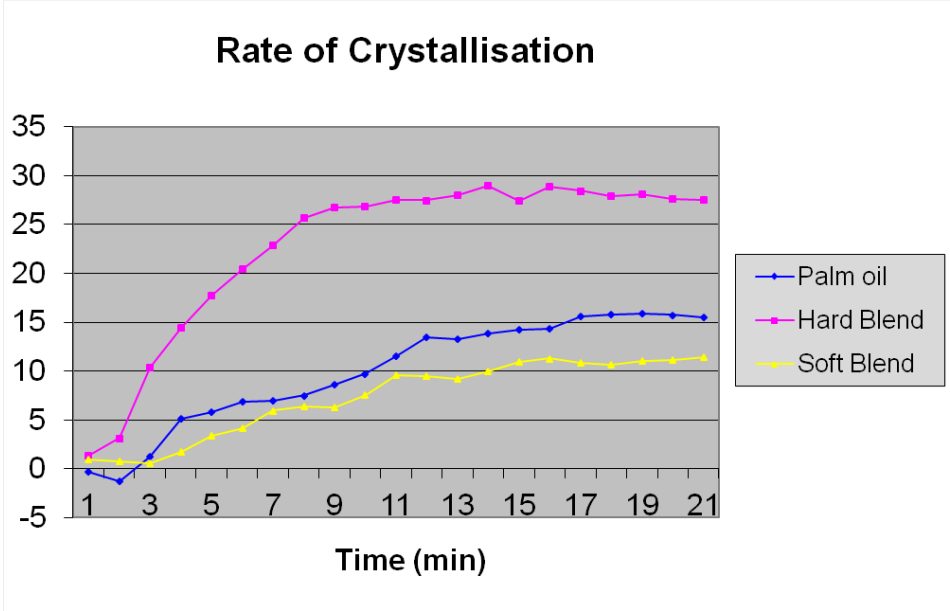

Figure 1.5.5 Relative increase in SFC% of RBD Palm Oil, Hard and Soft blends

1.5.1.3 Interim Conclusions of Pilot Study on Crystallisation

The results showed that MB-90 tends to increase both SFC and crystallisation onset compared to HP. The influence of both these distilled monoglycerides seemed dependent on both the concentration and the chain length of the fatty acids.

Based on this conclusion and independent findings (Appendix A), an extensive second pilot study was conducted (Appendix B, C, D). Twelve emulsifier combinations ((using Monoglyceride (MAG) and/or Triglycerides (TAG)), were tested and applied into commercially available fat blends. Due to the difficulty of unlimited combinations of possible oil blend formulations, this supplementary study was limited to typical commercial fat blends, which were arbitrarily selected to observe the effect of the MAG/TAG mixtures on the crystallisation onset of industrial "hard" fat blends (relatively harder to RBD Palm oil) and a soft fat blend (typical for retail spreads) relatively softer than RBD Palm oil.

Overall, there was a positive effect on the selected fat blends, when a MAG rich in C22:0 was included. This promoted a higher rate of crystallisation and earlier onset than other tested MAG / TAG mixtures. In this work it was generally concluded that the harder the fat blend, the greater the influence of the monoglyceride performance when compared to triglyceride. Whereas, for the softer TAG based blend, when C22:0 rich MAG (MB-90) and HLEAR (fully hardened low erucic acid rapeseed oil) were combined 1:1, this resulted in equal affect compared to a single C22:0 based MAG.

The measurement of the nucleation and crystal growth rates of MAG in TAGs is not precise (Himawan et al., 2006). However, this is partially solved by the determination of overall crystallisation kinetics and the use of models such as the Avrami equation, which is not considered central to this investigation, because in a number of industrial applications fat crystallisation occurs in dispersions (emulsions). MAGs have been found to accelerate not only the onset of crystallisation of various fats under agitation, but also in the presence of water (Chrysan, 2005; Himawan et al., 2006). Since retail fat blends tend to be a softer

(less saturation) continuous phase together with a secure internal aqueous phase, this has implications not only for crystallisation but also emulsification, especially where C22:0 rich MAGs are present. This was explored next.

1.5.2 Interface and Diversity: Effect of Fatty Acids on W/O Emulsions

1.5.2.1 Introduction and Background

Real food systems are normally emulsions and inherently have interfaces which are most often stabilised by the assistance of emulsifiers (Krog, 1975; 2001). As already described (1.2.7), emulsifiers concentrate at the surface, either creating interfacial film or strongly influencing other material at or close to the interface. They thereby act as a mechanical barrier between two immiscible liquids, preventing flocculation or coalescence (Krog, 1977).

The stability and rheological properties of emulsions are largely determined by the size of the dispersed droplets and how they interact with each other. The degree of particle-particle interactions is mainly dependent on the structure and composition of the interfacial film which may consist of adsorbed layer of proteins and/or emulsifiers as in the case of a W/O interface (Johansson et al., 1995; Krog, 1990; Krog & Larson, 1992; Krog & Sparsø, 2003).

Usually distilled monoglycerides (E471) are used for margarine and spread production. A distilled monglyceride composition is related to the fat source from which it is made (1.4). Depending on the fatty acid residue of the distilled monoglyceride, the interfacial film can have different rigidity or visco-elastic behaviour (Krog & Sparsø, 2003; Rousseau, 2000). The type of film affects not only stability of the emulsion during formation but also stability of the final product during shelf life and consumption (spreading, eating properties).

A surface monolayer of unsaturated monoglycerides forms a loose packed film because the fatty acid double bonds hinder close packing. Saturated monoglycerides form more close packed monolayers resulting in rigidity due to

strong van der Waals attraction forces between the hydrocarbon chains (Krog, 1997). Emulsifiers in adsorbed monolayers can act as templates for the surface crystallisation of triglycerides. Further, emulsifiers which contain saturated hydrocarbon chains are known to be effective initiators of fat crystallisation, whereas those with unsaturated chains are less effective (Euston, 2008; Wassell & Young, 2007).

It should be noted that the standard hydrophilic - lipophilic balance (HLB) was not used in this pilot study because the mixing complex properties of several emulsifiers is removed from individual emulsifiers and is therefore an unreliable guide for emulsion stability (Boyd, Parkinson, & Sherman, 1972). Further, Bergenståhl (2008), says the HLB values do not include the important crystallisation properties of monoglycerides; fatty acid composition is more important (Keogh, 2006).

1.5.2.2 Reduced TAG W/O Emulsion

In the context of reduced or low TAG W/O emulsions, the degree of saturation / unsaturation of the fatty acids have a direct bearing on the technical influence of the emulsifier (Chrysan, 2005). Compared to lower TAG contents, it is known (Garti & Remon, 1984) that a distilled highly saturated fatty acid based MAG e.g. (IV 2), is more suitable for full-fat margarine. Whereas for low TAG spreads, a distilled TAG with more unsaturation (>IV 40) has a theoretically more flexible film (interface) because of the loosely packed monolayers, stabilising the emulsion and final product when spread. However, this is not always correct and can only be used as a rough guideline.

The surface viscosity of interfacial films is an important factor for emulsion stability. This is likely to be more critical with lower TAG contents, because high interfacial film viscosity may have implications to corresponding resistance to film rupture during shear and increase emulsion stability towards droplet coalescence (Rousseau, Ghosh, & Park, 2009).

The effect of emulsifiers on interfacial tension between oil and water is highly influenced by temperature (Krog, 1990). It is also known that the actual composition of the emulsion droplet surface is the key denominator of most surface interactions (Bergenståhl, 2008). There appears to be no information or practical examples reported in the literature about a wide distribution of MAG fatty acid chain compositions to aid stability. The effect at the interface of temperature and fatty acid diversity is shown in Figure 1.5.6, where four preparations are made and held at three temperature regimes. It is easy to observe how, depending on the selected temperature and degree of saturation, there is a tendency for mono-crystal formations to occur towards the bulk oil or towards the aqueous phases. Subsequently, as part of this pilot study, this was explored next.

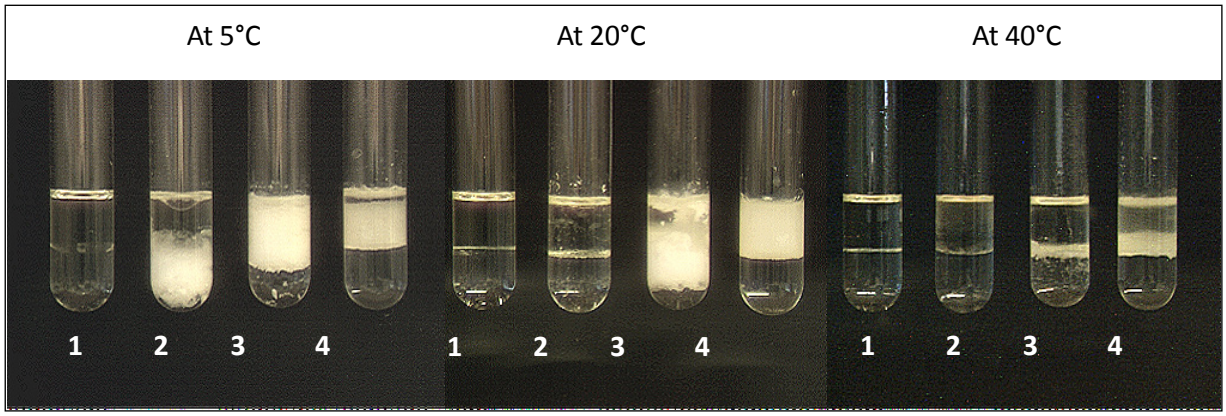

1 = no emulsifier, 2 = cis-unsaturated MAG., 3 = trans-unsaturated MAG., 4 = saturated MAG

Figure 1.5.6 The effect of temperature and fatty acid diversity at the interface: a preparation of water-soybean oil (1:1) with or without 4% emulsifier (E471) in the oil phase is observed at three temperatures 5°C, 20°C & 40°C (Image supplied courtesy of Danisco A/S., 2003)

1.5.2.3 Materials and Methods

Several commercially available distilled monoglycerides were tested in W/O reduced 50% TAG emulsions. The emulsifiers tested (from DuPont, formally Danisco A/S, Denmark) are shown in Table 1.5.3 and show distilled monoglycerides based on partially hardened rapeseed oil, partially hardened

soybean oil, palm oil, sunflower oil and fully hardened palm oil. The last column shows a fatty acid composition of two emulsifiers: Fully hardened Palm (DIMODAN® HP) and Sunflower (DIMODAN® U/J) in a ratio of 1:1 This mixture or ratio, results in a more diverse fatty acid composition, which hypothetically may lead to additional emulsifying properties (Bergenståhl 2008).

Table 1.5.3 Commercial distilled monoglycerides and their prevalent fatty acids (*approx. 50% *trans* fatty acids)

DIMODAN®	R-T*	S-T*	U/J	P	UP	HP	HP+U/J (1:1)
Source oil / Fatty acids (%) residue	Partially hardened Rapeseed	Partially hardened Soybean	Sunflower oil	Palm oil	Sunflower /palm oils	Fully hardened palm oil	Fully Hardened Palm / Sunflower
C14:0	0.1	0.1	0.1		0.5	1	0.5
C16:0	6	**11**	7	**44**	**22**	**55**	**31**
C18:0	**14**	8	5	5	4	**43**	**24**
C18:1 (cis+*trans*)	**75**	**76**	**28**	**39**	**30**	0.1	**14**
C18:2	2	3	**58**	**10**	**43**	0.2	**29**
C18:3	0.3	0.3	0.1	0.3	0.1		0.1
C20:0 and longer	3	1	1	0.2	0.9	0.7	0.6
C18 total	*91.3*	*87.3*	*91.1*	*54.3*	*81.1*	*43.3*	*67.1*
Saturated total	*23*	*20*	*12*	*49*	*26*	*100*	*56*
IV (approx.)	*60*	*60*	*105*	*45*	*80*	*2*	*54*

Application trials were performed on reduced fat 50% spreads with milk proteins, using an abnormal (hard) fat blend under typical scraped surface pilot plant processing conditions (refer to General Materials and Methods 2.0). The formulation used, is described in Table 1.5.4 to test the following: a) Milk proteins against monoglycerides, destabilising emulsion during production; b) high water

content giving risk of emulsion inversion during production; c) hard fat blend, crystals of which can cause water separation (coalescence) when spread (worked).

Samples were assessed using a simple cardboard test; an abuse test, by spreading back and forth across the cardboard surface and then subjectively gauging the degree of separation of the emulsion.

Droplet Size Distribution (DSD) using pNMR, is a more qualitative examination of emulsion behaviour, in terms of its average droplet size (refer to General Materials and Methods 2.0).

Table 1.5.4 Formula of 50% reduced fat W/O emulsions and details of the major fatty acids (SMP = skimmed milk powder).

Trial no.	1	2	3	4	5
WATER PHASE:					
Water	48	48	48	48	48
Salt	0.5	0.5	0.5	0.5	0.5
SMP	1	1	1	1	1
pH	5.5	5.5	5.5	5.5	5.5
FAT PHASE:					
Coconut oil (fully hardened)	15	15	15	15	15
RBD liquid Rapeseed oil	15	15	15	15	15
Soya 41°C	50	50	50	50	50
RBD Palm oil	20	20	20	20	20
FAT total	49.8	50	50	50	50
DIMODAN® HP (C16:0+C18:0)	**0.4**				***0.2***
DIMODAN® S-T (C18:1+C16:0)		**0.4**			
DIMODAN® UP (C18:2+C18:1+C16:0)			**0.4**		
DIMODAN® U/J (C18:2+C18:1)				**0.4**	***0.2***
Lecithin	**0.2**				
PPM ß-carotene	6	6	6	6	6
Butter Flavouring	0.01	0.01	0.01	0.01	0.01

1.5.2.4 Results and Evaluation test

A simple evaluation test was carried out by “abuse” test on cardboard with stainless steel knife moving the prepared emulsion back and forth over the surface of the cardboard as shown in Figure 1.5.7

Figure 1.5.7 Image of cardboard evaluation test by spreading (Image supplied courtesy of Danisco A/S., 2009)

A separation test does not give a complete, objective picture of sample stability; it is a subjective evaluation, but nevertheless, it is very informative. Regarding the five samples prepared in Table 1.5.4, the following was observed:

1. Free water. Discarded.
2. Stable, but free water released when spread.
3. Same as 2.
4. As 1.
5. As 2, but separated less water on spreading (worked)

A more quantitative measurement is analysis of water droplet distribution by means of Droplet Size Distribution (DSD). The results showed the sample comprising the more mixed fatty acid profile, had the smallest water droplets (Table 1.5.5). In this case it demonstrated, that a simple MAG mixture of highly unsaturated and highly saturated fatty acids based on C16:0, C18:0, C18:1, C18:2 enhanced the emulsification properties of a reduced TAG emulsion.

Table 1.5.5 Results of preparations from Table 1.5.4; the average water droplet size distribution

Droplet size distribution (DSD)[#]	2.5%	50%	97.5%
Sample 2 DIMODAN® S-T 0.4%	<0.62µm	<11.47µm	<225.56µm
Sample 3 DIMODAN® UP 0.4%	<0.73µm	<16.14µm	<364.92µm
Sample 5 Mixed system (1:1) DIMODAN® HP 0.2% DIMODAN® U/J 0.2%	<0.47µm	<3.95µm	<33.65µm

[#]Samples 1 & 4 not measurable using DSD

1.5.2.5 Conclusion

These results showed that capability to secure a narrow droplet size distribution was likely the result of diversified fatty acid residue in the lypophilic part of the monoglyceride mixtures, thereby aiding interfacial and functional properties. In this case it was an improvement on using individual monoglycerides that may not have had sufficient fatty acid diversity.

As total TAG levels decrease below 50% of the total emulsion, and therefore by default naturally follow a decrease in total saturates, the emulsifier interactions may become more critical especially where proteins are still present. (Chrysan, 2005; Madsen, 1987).

There are still unanswered questions as to the effects on W/O emulsion, when utilising a range of diversified fatty acid mixtures, incorporating the use of hydro-carbons beyond C18:0 chain length. As reported earlier, there appear to be some benefits to using much longer saturated chain lengths (1.4).

1.5.3 Very Low W/O TAG (12%) Based Emulsion - With and Without MAG/TAG Additive

1.5.3.1 Introduction and Background

In the case of those products already classified as low fat (<41%), reducing total saturates by re-engineering to lower fat contents, or improving the general melting / firmness of W/O spreads, presents a problem for the product developer. This is because TAG's are the building blocks of the continuous phase for W/O emulsions. Therefore, if reducing the structuring material, a "scaffold" of sorts is still necessary.

A second obstacle is the increasing use of palm oil products, which may potentially (depending on degree of DAG content) effect crystallisation. Thirdly, PGPR is often utilised in this product category to secure emulsion stability (Garti & Remon, 1984; Goubran & Garti, 1988; Rousseau, 2000). It is well documented that blending emulsifiers will always produce a more stable emulsion (ICI Americas Inc. 1980) as opposed to using a single emulsifier, by the fact that combining a water soluble hydrophilic one with an oil soluble lipophilic type will produce a denser interfacial film due to the hydrophilic and lipophilic portions of the molecules sitting on different sides of the interface (Garti & Remon, 1984).

1.5.3.2 Materials and Methods

Based on the preliminary findings in 1.5.2 for the 50% reduced fat W/O emulsion (Table 1.5.4), a series of application trials were made to produce a very low W/O TAG (12%) emulsion (Table 1.5.6); a significant proportion of the aqueous phase contained a polydextrose (Litesse® Ultra – DuPont, Denmark).

Table 1.5.6 12% very low fat spread formula, assembled on Gerstenberg scraped surface pilot plant. (interesterified blend = PK4 INES, a palm stearin / lauric. Cargill GmbH)

Ingredient Name	1	2	3	4
Water phase				
Water (Tap)	74,975	64,975	74,975	64,975
Salt (sodium chloride)	0,900	0,900	0,900	0,900
GRINDSTED® LFS 560 Stabiliser System	2,000	2,000	2,000	2,000
Litesse® Ultra™ polydextrose	**10,000**	**20,000**	**10,000**	**20,000**
Potassium Sorbate	0,100	0,100	0,100	0,100
CALCIUM DI SODIUM EDTA	0,015	0,015	0,015	0,015
Butter Flavouring T02807	0,010	0,010	0,010	0,010
Water phase total	**88,000**	**88,000**	**88,000**	**88,000**
pH	5,5	5,5	5,5	5,5
Fat phase				
Interesterified blend	15,000	15,000	15,000	15,000
Rapeseed oil	85,000	85,000	85,000	85,000
Fat blend total	**100,000**	**100,000**	**100,000**	**100,000**
Other fat ingredients				
DIMODAN® U/J Distilled Monoglyceride	0,600	0,600	0,600	0,600
GRINDSTED® PGPR 90	0,300	0,300	0,300	0,300
GRINDSTED® CRYSTALLIZER 100, Emulsifier blend			**0,200**	**0,200**
2% sol. beta-carotene	0,010	0,010	0,010	0,010
Butter flavouring T03085	0,020	0,020	0,020	0,020
Other fat ingredients total	**0,930**	**0,930**	**1,130**	**1,130**
Fat phase total	**12,000**	**12,000**	**12,000**	**12,000**
RECIPE total (calc. batchsize)	**100,000**	**100,000**	**100,000**	**100,000**

The emulsifier system was based on highly unsaturated (DIMODAN® U/J – based on sunflower C18:1, C18:2) and highly saturated (Grindsted® Crystallizer 100 – containing significant levels of C22:0, abbreviated CRY100) distilled monoglycerides (a combination of DIMODAN® MB-90 + HLEAR (fully hardened low erucic acid rapeseed oil)). It is highly unusual to consider the use of a MAG based on C22:0 for aqueous binding properties in a W/O emulsion where the total fat content is either low and or very soft (Garti & Remon, 1984). One specific reason for introducing C22:0 as previously shown, is that behenic fatty acid seems to have a generally positive influence on crystallisation and additional influence on emulsification (1.4; 1.5.1.3; Wassell & Young, 2007).

With regards to the stabilisation of the W/O low TAG emulsions and the choice of saturated MAG, why were MAG's based on C16:0 or C18:0 not considered? The answer is because of partial hydrogenation (presence of *trans* isomer) and/ or the MAG being palm based, with additional commercial implications (1.4). Irrespective of these factors, palm triglycerides were used for the fat continuous systems in this study. To aid and or secure emulsion stability, a co-surfactant, PGPR was still part of the emulsifier system (Garti & Remon, 1984; Goubran & Garti, 1988; Rousseau, 2000).

Samples were prepared using a G&A pilot plant, and then assessed by DSD and Texture Analysis (refer to General Materials & Methods 2.0)

1.5.3.3 Results

Results from water droplet size distribution were not available. However, results from texture test using Stable Micro Systems TX2 Texture Analyser revealed interesting data; both samples 3 and 4 exhibited additional resilience (Figure 1.5.8). Both contained the MAG rich in C22:0.

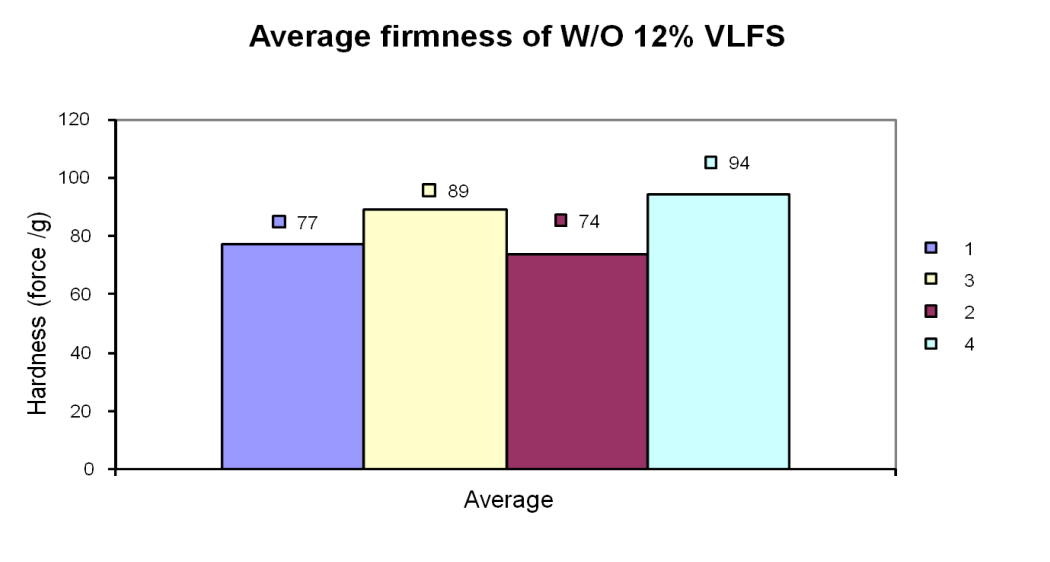

Figure 1.5.8 Textural firmness at 5°C of W/O 12% very low fat spread emulsion

To determine if the resilience was because of the addition of the emulsifiers increasing the total solid fat content (SFC), the SFC% using Bruker p-NMR, was measured on three samples (Table 1.5.7), two of which were the same emulsifier combination as used in the 12% very low fat spread formula (Table 1.5.6). A third sample was also added to include Grindsted Crystallizer 110, abbreviated CRY110 (refer to Materials & Methods, 2.0).

Table 1.5.7 Anhydrous bulk TAG blend with emulsifier mixtures: three samples assembled for SFC% determinations

% of TAG blend + emulsifier	0.6% Dim UJ + 0.3% PGPR90	0.6% Dim UJ+ 0.3% PGPR90 + 0.2% CRY100	0.6% Dim UJ + 0.3% PGPR90 + 0.2% CRY110
15% PK4 INES / 85% RP	99.1	98.9	98.9
Dimodan UJ	0.6	0.6	0.6
PGPR 90	0.3	0.3	0.3
Crystallizer 100		0.2	
Crystallizer 110			0.2
Total	100	100	100

Samples were triple determined and results presented in Table 1.5.8, then graphically in Figure 1.5.9. The SFC% for all samples appears to be very similar. Arguably, those samples with either CRY100 or CRY110 should, at 5°C, be differentiated because of additional saturation. However, an emulsifier contribution of 0.2% in either case on the total TAG / emulsifier load is thought to be negligible (Smith et al., 2011) because a significant increase in the total SFC% is not observed.

Theoretically, it would seem that the emulsifier mixtures containing unusually diverse fatty acid composition for these W/O low TAG emulsions are resulting in additional emulsifying properties (Bergenståhl, 2008).

Table 1.5.8 Triple SFC% determinations for emulsifier mixtures in Table 1.5.7

SFC% **Triple determination**

Fat blends		Sample 1			Sample 2			Sample 3		
		0.6% Dim UJ + 0.3% PGPR90			0.6% UJ + 0.3% PGPR90 + 0.2% CRY100			0.6% UJ + 0.3% PGPR90 + 0.2% CRY110		
		SFC %	average	stdv	SFC %	average	stdv	SFC %	average	stdv
5°C	a	9.37	8.61	0.73	7.55	7.82	1.09	8.84	8.51	0.30
	b	8.54			9.02			8.24		
	c	7.91			6.88			8.46		
10°C	a	6.58	6.43	0.18	6.24	6.72	0.42	6.36	6.20	0.14
	b	6.22			6.96			6.09		
	c	6.49			6.97			6.15		
20°C	a	1.54	2.17	0.72	1.35	2.35	0.87	2.77	2.78	0.29
	b	2.02			2.77			2.49		
	c	2.96			2.93			3.08		
30°C	a	1.24	1.07	0.14	0.51	0.64	0.14	1.27	0.91	0.32
	b	0.97			0.61			0.75		
	c	1.00			0.79			0.69		
35°C	a	0.62	0.22	0.35	0.00	0.15	0.23	0.30	0.30	0.30
	b	0.04			0.41			0.00		
	c	0.00			0.04			0.60		
40°C	a	0.18	0.06	0.10	0.00	0.00	0.00	0.11	0.04	0.06
	b	0.00			0.00			0.00		
	c	0.00			0.00			0.00		

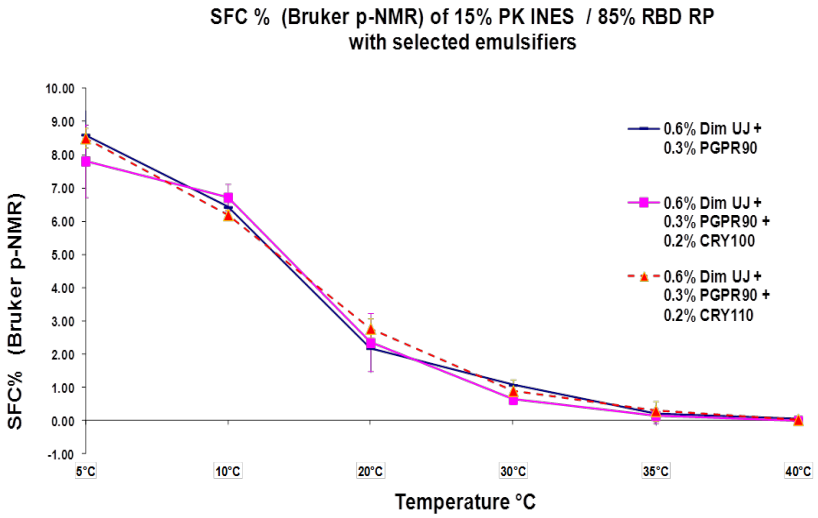

Figure 1.5.9 Graph to show SFC% of MAG/TAG and PGPR mixtures in 15% PKINES / 85% RBD RP (re: Table 1.5.7 / 1.5.8)

1.5.3.4 Conclusion

These interim results seem to suggest that the presence of a fully hydrogenated TAG/MAG containing significant presence of behenic (C22:0) monoglyceride, seems to have a technical influence on interfacial properties, causing apparent thickening of the final emulsion. The results from SFC% showed no appreciable differences to suggest firmness is attributed to increase in overall total SFC% in the samples containing CRY100 or CRY110. This leads to the question - what is the cause of the apparent increase in emulsion resilience? If the textural response is not attributed to increased SFC%, then it can only be attributed to the emulsifier relationship of PGPR, CRY110 with or without UJ. This needs to be investigated further.

1.5.4 General Conclusion of Pilot Studies

Exploratory pilot studies were conducted and indicated that MAG / TAG mixtures give an enhancing effect on the crystallisation rates in several anhydrous dispersions (1.5.1; Appendix A,B,C,D). Second, the effect of diversified fatty acid mixtures of MAG in the presence of an aqueous interface (shown in 1.5.2) was shown to have a positive influence, increasing the W/O emulsion stability. Third, pilot studies showed it was possible to stabilise exceptionally low TAG W/O emulsion structures (1.5.3) using an application of long-chain behenic based emulsifier. This approach is not known to be reported in the literature.

Based on these pilot studies, a critical review of current issues behind finding alternative structuring mechanisms for water-oil emulsions and for aiding structure in TAG based systems, needed to be undertaken.

1.6 A Critical Review of Current Issues: Alternative Mechanisms for Aiding Structure in TAG Based Systems

1.6.1 Introduction and Background

Exploratory pilot studies have shown that saturated MAG / TAG mixtures give an enhancing effect on the crystallisation rates in TAG based anhydrous dispersions (1.5.1; Appendix A,B,C, D). Secondly, diversified fatty acid mixtures of MAGs in the presence of an aqueous interface (1.5.2) have a positive influence for W/O emulsion stability. Thirdly, interim pilot studies suggested it is possible to stabilise exceptionally low TAG W/O emulsion structures (1.5.3) using the application of a long-chain behenic based emulsifier. This approach is not known to be reported in the literature.

Since conducting a literature review (1.4) and series of pilot studies (1.5), a more critical review is now necessary. This is because to progress this learning into finding new and novel approaches to structuring, a consideration for current issues is required. Realistically, this must therefore also encompass issues surrounding the sourcing of alternative, natural lipid materials, their sustainability and a consideration of the techniques used to observe and quantify structural and interfacial events.

1.6.2 New Applications and Novel Materials

An edible oil and its commoditised fractions which has grown widely in use (Wassell & Young, 2007) and status since the 1990's, is palm oil. While palm oil is not necessarily regarded as a low saturated fat, it does have many fractions, some of which are more unsaturated, eg. olein fractions. However, despite being

inherently natural, there is controversy surrounding agricultural ethics and sustainability of palm oil (Carmichael, 2011; Young, 2011).

In sourcing alternative natural lipid materials, China (the largest vegetable oil-consuming country in the world) is, as part of its continued growth strategy, developing several uncommon oil resources (Table 1.6.1). This is to minimise its land dependence and achieve maximum yield. It is also regulatory friendly to "Novel foods" or food components which are not traditionally used in China (Wang, Xu, & Jiang, 2012).

Table 1.6.1 Approved novel foods related to fats and oils (source: Wang et al., 2012)

Novel foods	**Year approved**
Plant stanol ester	2008
Conjugated linoleic acid	2009
Conjugated linoleic acid glycerides	2009
Eucommia ulmoides Oliv. seed oil	2009
Tea camellia seed oil	2009
Fish oil (extract)	2009
Diacylglycerol oil	2009
Docosahexaenoic acid algal oil	2010
Plant sterol ester	2010
Plant sterol	2010
Arachidonic acid oil	2010
Poppy seed oil	2010
Elaeagnus mollis Diels oil	2011
Acer truncatum Bunge seed oil	2011
Peony seed oil	2011

Other researchers have explored different strategies including, lipid crystal engineering (Schaink, van Malssen, Morgado-Alves, Kalnin, & van der Linden, 2007); phytosterol systems (Bot et al., 2009); organogel-based emulsion systems (Duffy, Blonk, Beindorff, Cazade, Bot, & Duchateau, 2009) and wax technology to form 'lipo-colloid' structures (Shigemi, 2006). A comprehensive discussion of possibilities is put forward by Pernetti, van Malssen, Flöter, & Bot, (2007), who state succinctly that finding alternatives to traditional triacylglyceride (TAG) structuring whilst maintaining healthy properties, versatility and performance, is a tremendous challenge. More recent and current reviews confirm the same (Rogers 2009) and have considered the influence of minor components (Smith et al., 2011) e.g. emulsifiers, functional ingredients and their characterisation at micro and nano-scale (Marangoni et al., 2012; Sato & Ueno, 2011; Silva, Cerqueira, and Vicente, 2011).

Additionally, it is clear that population increase and the issues of sustainability are indirect catalysts to finding alternate lipid materials for the function of structuring / stabilising food products (Carmichael, 2011; Wang et al., 2012; Wassell & Young, 2007; Young, 2011). Whatever forms of approach are adopted, removal of, or at least drastic reduction of all saturated fats is also required (Beaglehole et al., 2011; Bradley, 2012; Gortmaker et al., 2011; Micha & Mozaffarian, 2010; Mozaffarian et al., 2010; NICE, 2010; Siri-Tarino et al., 2010; Yamagishi et al., 2010; Swinburn et al., 2011; van Camp et al., 2012; Vesper et al., 2012; WHO, 2011; Merchant et al., 2008; Wassell & Young, 2007; Wassell et al., 2010a).

1.6.3 Techniques for Analysis

To characterise crystallisation properties, new analytical approaches to observe interactions both in model and real time dynamic measurements are increasingly necessary (Povey, Awad, Huo, & Ding, 2007; Ishizuka, Ahmed, Arima, & Aramaki, 2009; Ojijo, Neeman, Eger, & Shimoni, 2004; Pernetti et al., 2007;

Schaink et al., 2007; Arima, Ueno, Ogawa, & Sato, 2009; Rogers, 2009; Tanaka, Tanaka, Yamato, Ueno, & Sato, 2009; Young et al., 2008).

Interactions of and between surfactants and their interactions as template structures, for example in heterogeneous nucleation events (Fujiwara et al., 2000), are not easily explained with typical crystallisation measurements at zero shear, e.g. DSC measurements (De Graef, Dewettinck, Verbeken, & Foubert, 2006; Pernetti et al., 2007; Povey et al., 2007). Most studies have been performed under isothermal conditions where observation of crystal behaviour is potentially quite different from that observed within a dynamic environment (Garbolino, Bartoccini & Flöter, 2005; Janssen & MacGibbon, 2007; Maleky, Campos & Marangoni, 2007; Pérez-Martínez, Reyes-Hernández, Dibildox-Alvarado & Toro-Vazquez, 2012; Povey et al., 2007; Wang, Liu, Jin, Huang, Meng & Wang, 2011).

New techniques are necessary to observe and quantify structural properties and events in both static and under dynamic conditions. (Arima et al., 2009; Boodhoo, Humphrey, & Narine, 2009; Tang & Marangoni, 2006). This should help provide stronger information that could be transposed to, for example, "real" emulsion systems. One example is ultrasonic velocity profiling with pressure difference (UVP-PD) instrumentation, allowing non-invasive in-line rheological measurement. Another is synchrotron radiation microbeam small-angle XRD (SR-μ-SAXD) technique which more precisely observes microstructures of fat crystals (Awad, Moharram, Shaltout, Asker, & Youssef, 2012; De Graef et al., 2006; Maleky et al., 2007; Mazzanti, Guthrie, Sirota, Marangoni, & Idziak, 2003; 2005; McClements & Rao, 2011; Okamura, Wassell, Young, Bonwick, Smith, Almiron-Ruig, Sato, Ueno, 2011; Pernetti et al., 2007; Prakash & Ramana, 2003; Silva et al., 2011; Tanaka et al., 2009; Young et al., 2008).

1.6.4 Structure – Effects of Minor Components

Recent publications have discussed the use of "crystal structure modifiers" (Garbolino et al., 2005; Pernetti et al., 2007; Rousseau, Hodge, Nickerson, & Paulson, 2005; Young et al., 2008), addition of a co-surfactant (Foster et al., 2007; Rogers, 2009), inclusion of an additive, accelerant (Fujiwara et al., 2000; Katsuragi, 1999), or impurity (Awad & Sato, 2001 & 2002).

Pernetti et al., (2007) suggest crystal structure modifiers are potentially interesting not only within traditional systems, but also within novel structures and mixtures, where a combination of these materials might provide several functions. The effects of hydrophobic adsorption properties of additives, template behaviour and acceleration of nucleation have been studied (Awad & Sato, 2001 & 2002; Cerdeira, Martini, Hartel, & Herrera, 2003; Cerdeira, Pastore, Vera, Martini, Candal, & Herrera, 2005; Cerdeira, Martini, Candal, & Herrera 2006; Sakamoto et al., 2003; Sakamoto et al., 2004). More recently, the advanced analysis of the behaviour of unsaturated and saturated surfactants, their polymorphism and time temperature effects (Arima et al., 2009; Tanaka et al., 2009), has provided information on the interactions of minor components (Vereecken, Foubert, Smith, & Dewettinck, 2009a) and crystallisation with and without a water phase (Vereecken, Foubert, Meeussen, Lesaffer, & Dewettinck, 2009b; Vereecken, Meeussen, Foubert, Lesaffer, Wouters, & Dewettinck, 2009c; Vereecken et al., 2010). However, it is important to gain a clearer understanding on the effects of mixed surfactant systems, and how these interactions influence TAG mixtures in W/O emulsions (Pernetti et al 2007; Rogers, 2009).

One investigation of the kinetic stabilisation of emulsions within low TAG concentrations (Rousseau et al., 2005) found TAG polymorphic behaviour could be manipulated through a multidisciplinary approach, involving the presence of polyglycerol polyricinoleate (PGPR), together with variable crystallisation

conditions e.g. static vs. dynamic crystallisation (Young et al., 2008). Rousseau et al. (2005) suggest liquid emulsifiers such as PGPR compared to emulsifiers such as saturated MAG are not as likely to influence crystallisation unless PGPR is combined with agitation conditions, where polymorphic transformation was retarded. They found that static crystallisation in the presence of PGPR showed no "apparent" differences. This relationship ought to be more clearly understood, especially within the area of high internal-phase-ratio emulsions (HIPREs), where interfacial film strength and mechanical flexibility will probably impact on final textural properties (Charteris, 2007; Povey et al., 2007; Pothiraj et al., 2012), and primarily where both MAGs and PGPR are combined (Garti & Remon, 1984; Garti, Binyamin, & Aserin, 1998; Goubran & Garti, 1988).

Structures based on traditional TAGs, and/or novel combinations of these approaches, are thought to lead to some potentially interesting physical properties (also refer to pilot studies 1.5).

A review of several studies by Rogers (2009) looked at the effects of a number of minor ingredients, including MAGs, and found the addition of MAGs was important for reduced droplet size and improved spreadability. However, in a separate study Hughes et al. (2009) found that even when fairly large water droplets were formed, they remained stable. This has implications for the formation of HIPREs emulsions where its internal phase is a relatively large aqueous volume. In the context of low (<41%) and reduced TAG W/O emulsions (spreads), irrespective of droplet size (ignoring microbiological implications), the visco-elastic interfacial behaviour of the continuous phase is critical to stability (Johansson et al., 1995; Garti et al., 1998; Bergenståhl, 2008) as found in non-edible applications (Peng et al., 2009).

Therefore, attempts to find novel strategies for making healthier (reduced fat) spreadable butters or to improve total saturated fatty acid contributions in low fat spreads (W/O), may be limited by the diversity of accepted (FAO/WHO, 2011) raw materials. As a result, to bring forth any subsequent or new improvements, there is requirement to better understand current application of traditional ingredients (e.g. emulsifiers), and/or to explore new possibilities with novel ingredients to perform similar and or improved function.

1.6.5 Conclusion

The literature shows first, the necessity to move away from the addition of hard fatty material and substitute with alternative structure forming strategies (Dassanayake, Kodali, & Ueno, 2011; Wassell & Young, 2007). Second (related to first theme) is the need to cause beneficial interactions through inclusion of a small amount of additive such as an emulsifier (Smith et al., 2011).

Given the aforementioned approaches, there are two areas for consideration; not just structure and assembly within the bulk oil, but the mechanism of structure at interfaces e.g. W/O emulsions, and how the interface might be modified through emulsifier initiated processes (Krog, 1975; 2001) to provide adequate structure, strength, and flexibility via a range of mechanisms (Povey et al., 2007). One mechanism is to employ the use of "traditional" TAG based structurants (Lupi, Gabriele, de Cindio, Sánchez, Gallegos, 2011b; Smith at al., 2011), coupled with novel structuring material (Duffy et al., 2009; Pernetti et al., 2007). The addition of a co-surfactant could aid nucleation through standard thermodynamic events (Pernetti et al., 2007; Rogers, 2009). Co-surfactants such as MAGs derived from TAGs, which are commonly used for W/O emulsions (Garti & Remon 1984), could fit this description, as they can enhance textural properties which consumers are familiar with (Foster et al., 2007; Pothiraj et al., 2012).

Among the TAG components discussed by Rogers (2009), fatty acids, particularly long chain fatty acids, are ignored due to the negative health implications associated with traditional TAG based networks. However, there are still unanswered questions regarding the use of emulsifiers synthesised from them (Vereecken et al., 2009c & 2010). Pernetti et al. (2007) suggested that longer chain fatty acids tended to have more structuring potential per gram of material than shorter chains. Further investigation of how these subtle variations in the amounts and chain length of structurants influence the structural properties of TAG based systems is of interest (Krog & Larsson 1992). This is especially the case when combining surfactants of differing molecular structure, e.g. monodiglyceride and polyglycerol polyricinoleate (PGPR) – a classic combination, for low fat W/O emulsions (Garti & Remon 1984; Garti et al., 1998; Annon, 2005).

Sakamoto et al. (2003) reported that polyglycerol behenic esters promoted nucleation, but inhibited crystal growth of palm oil and promoted the β' polymorph. Arima et al. (2007) reported stabilisation and retardation effects when combining two surfactants; they observed heterogeneous crystallisation in O/W emulsions and prohibition of morphological change, due to adsorption at the interfacial membrane. This situation might provide interesting mechanisms for structuring in low TAG based W/O emulsion systems.

Learning how a surfactant might work as part of a combination, rather than focusing purely on single components, ought to provide more practical and meaningful information. This might be found through an investigation into real systems e.g. water-in-oil emulsions, where aqueous phases are employed (Fujiwara et al., 2000; Pernetti at al., 2007; Sakamoto et al., 2003 & 2004; Tanaka et al., 2009).

In the case of a given interfacial emulsifier concentration, temperature, and shear rate (Lupi, Gabriele, de Cindio, 2011a), the surface of water droplets will be optimally or sub-optimally covered, especially in the context of HIPREs. However, explaining these mechanisms could be problematic, in that laboratory scale techniques using standard models / methods could be limited because of their inability to provide data whilst under true dynamic conditions (Young et al., 2008).

During isothermal / non-isothermal conditions, the mechanical orientation of TAG and non–TAG stabilisation could be critical, especially where e.g. TAG structures in themselves do not exhibit polar behaviour. However, at a certain surfactant concentration, the TAG crystals become more polar in behaviour because the surfactant is adsorbed to the TAG surface (Johansson et al., 1995). This theoretically produces a more uniform structure (Arima et al., 2009; Shinohara, Takamizawa, Ueno, Sato, Kobayashi, Nakajima, & Amemiya, 2008; Tanaka et al., 2009), so that at a given concentration and ratio of specific surfactants, the surface of water droplets (W/O emulsions) are more optimally covered. Possibly, this is indirectly aided by induction of heterogeneous nucleation to form molecular aggregates, which then act as a template for nucleation. Shinohara et al., (2008) suggests the curvature of the interface interferes with the crystallisation at the interface. Therefore, in attempting to reduce the degree of saturates in food systems, it will be necessary to observe and to analyse any relationship when co-surfactant structures are used and how this may influence interfacial film behaviour.

A multiple approach, involving the use of SR-μ-SAXD (a microscopic analysis of the lamellar plane directions and structural domains), coupled with measurement of structurant interactions, both in model and dynamic real-time e.g. rheometery and UVP-PD, might provide a deeper insight into the crystallisation and

rheological mechanics of W/O emulsions (Arima et al., 2009; Awad et al., 2012; Ishizuka et al., 2009; Ojijo et al., 2004; Pernetti et al., 2007; Povey et al., 2007; Rogers, 2009; Schaink et al., 2007; Young et al., 2008). Pothiraj et al., (2012) explain that low TAG W/O emulsions cannot easily be formulated to mimic butter or similar, because of the challenges to developing melting behaviour, which is largely governed by emulsion characteristics such as volume of the aqueous phase and size of water droplets.

The literature demonstrates the need to achieve a clearer understanding of how to reformulate and structure low or reduced fat spread products (Wassell & Young, 2007). Hence, exploring how novel structures behave, particularly within W/O emulsions, is warranted within the context of increasing new product launches of reduced fat emulsion products (Ford, 2012). Consequently, it will likely become important to understand how novel emulsifiers will behave at or near the interface and in the bulk continuous (Wassell et al., 2010a).

1.7 Aims and Objectives

1.7.1 Background

There is a need to find alternative structuring materials, since many food products, especially fat based food dispersions and emulsions are currently still highly dependent on the presence of saturated fats and traditional emulsifiers. However, the problem, of removing these 'building' blocks, i.e. saturates and their *trans* isomer from fat systems, make it difficult to produce food products which are functionally acceptable to the consumer. The mechanics and successful removal of saturated and *trans* fatty acids in foods (Wassell & Young, 2007) is a complex problem, as is the successful structuring of low or reduced fat based foods, that require additional reduction of total saturates (Wassell et al., 2010a; Young and Wassell 2008). Achieving further reduction of saturated fatty acid materials for dietary requirements (Winwood, 2011) without negative impact on structure and functional properties, presents challenges for those food systems already regarded as low saturated. The challenge is for food manufacturers to find innovative solutions to structuring whilst meeting consumer expectations (Wassell & Young, 2007; Wassell et al., 2010a).

Improving emulsification kinetics is considered to offer additional benefit, because it has been demonstrated (1.5) that the addition of small quantities of long chain fatty acids to food systems containing less saturated fats, could potentially enhance structuring and texturing whilst retaining functionality in low and reduced fat food systems (1.4; 1.6).

New innovative solutions were researched to address the challenges of structuring, texturing and associated issues in the production of fat based food systems within the areas of dispersions (Wassell et al., WIPO No. WO2012168722, 2012a; WO2012168723, 2012d), crystallisation (Wassell et al., WO2012168727 2012b; Bech et al., WO2013050944, 2013), water-in-oil low fat spreads (Wassell et al., WO2012168726, 2012c), reduced fat water-in-oil spreads (Wassell et al., WO2012168724, 2012e). This was carried out using new techniques such as real-

time process rheology (Young, Wassell, Wiklund, & Stading, 2008; Wassell, Wiklund, Stading, Bonwick, Smith, Almiron-Roig, & Young, 2010b) and analytical X-ray measurement (Wassell, Okamura, Young, Bonwick, Smith, Sato, & Ueno, 2012).

1.7.2 Outstanding problems

In terms of MAG (E471), no literature could be found on the effectiveness of a C22:0 based MAG in W/O emulsions. Several have looked at the effect of chain length and saturation in W/O emulsions using MAG (Vereecken et al., 2009a, 2009b; 2010). However, it is still not known to be reported in real W/O emulsion systems beyond C18:0. The work by Vereecken et al (2010) only tested in full fat margarine type products, but not reduced or low fat W/O emulsions. Studies on interfacial behaviour by Krog, (1990) and Krog and Larsson (1992), researched the effects of temperature and concentration on long, medium and short chain fatty acids, but these were only examined as single MAG.

A pilot study (1.5) looked at the effect of MAG on crystallisation time and diversifying their fatty acids. This included mixing C22:0 with other MAG chain lengths and TAG mixtures. Some positive influence was found when tested in anhydrous dispersions (Basso et al., 2010). The degree of benefit was influenced also by the degree of saturation of the solvent (TAG mixtures). An effect was also found on the visco-elastic properties of a very low TAG W/O emulsion by minor addition of a C22:0 based MAG (1.5.1; 1.5.2; 1.5.3; 1.5.4).

Currently, many low cost emulsifiers tend to be based on palm TAG products, characterised by its major fatty acids C16:0 / C18:1 and its intrinsically natural, unmodified arrangement. Alternative TAG materials which are natural, unmodified and provide a whole range of fatty acids may currently be difficult to source in sufficient quantities. Hence, other naturally occurring novel resources must be considered (Dierig & Thompson, 1993; Dierig, Thompson, & Nakayama, 1993). Moringa TAG, has a significant range of saturated fatty acids to unsaturated fatty acids, including naturally occurring saturated fatty acids >C16:0 – C24:0 (Abdulkarim, Long, Lai, Muhammad, Ghazali, 2005; Lalas & Tsaknis, 2002).

In low or reduced fat systems it is known that as the oil phase is decreased, and water phase increased, the emulsifiers usually become softer, more liquid in form (Table 1.2.4). Furthermore, as the fat content is reduced, there is also tendency to soften the SFC, so that both the continuous TAG phase and the emulsifier are similar in rigidity (Garti & Remon 1984). So that, whilst utilisation of a MAG based on e.g. liquid sunflower or similar (IV = ~105) is able to facilitate assembly of a W/O emulsion, in W/O of approximately <41% this may not be entirely secure. Hence, where TAG content is <41% it is common to use both PGPR and a second emulsifier (a co-emulsifier) e.g E476 (EU max permitted use – 0.4%).

For commercial and product quality reasons, several manufacturers have requested replacement of PGPR because of its negative effect on the sensory melting behaviour (too stable) and to achieve clean label by removing E-numbers. Another reason is because of handling re-melt (a given volume of product will re-circulate through the production process), where the WO emulsion must be re-melted and sometimes separated. PGPR is very robust at binding water.

Single component emulsifiers are generally cheaper to supply than multi-component blends. Finding a one-stop solution without PGPR is challenging and in very low fat <20%, it is near impossible unless relying on MAG to dominate the continuous phase at high concentration (5% MAG – 95% aqueous).

1.7.3 Empirical Quantification

In the context of real, low TAG based W/O emulsion systems, there is still a need to report the affects of the interfacial behaviour of MAG mixtures with other common emulsifiers e.g. PGPR (Garti & Remon 1984; Garti et al., 1998). While texture analysis (1.5.3.3) revealed “apparent” increased firmness in the finished product, it is more difficult to quantify affects in a dynamic state. This leads to another necessity; to find a method to measure rheological change in real-time so that rheological interactions can be reported both off-line and in-line.

Empirical quantification to determine how much impact a minor ingredient e.g. a MAG based on significant quantities of saturated longer chain >C18:0, may have on a "real", low or reduced TAG based W/O emulsion system has not been reported in the literature. Only the behaviour of behenic (C22:0) based emulsifiers in O/W systems is reported (Arima et al., 2007; Awad & Sato, 2001; 2002; Fujiwara et al., 2000; Sakamoto et al., 2003; Wassell & Young, 2007) and not in W/O. Therefore, as part of a multidisciplinary investigation, the rheological and interfacial properties after the addition of a >C18:0 based MAG within the bulk and W/O emulsion needs to be characterised. Then to quantify its impact in a dynamic state, requires both direct and indirect methods of analysis.

Solutions to these outstanding technical challenges were investigated through a multidisciplinary approach (Wassell & Young, 2007; Wassell et al., 2010a) by:

1) Combining traditional techniques with novel structurant technology;

2) Developing and validating a dynamic measurement technique;

3) Investigating real emulsion systems, as opposed to exclusively single phase model systems.

1.7.4 Experimental Approach

The intention was to investigate how structuring and texturing low saturated fat based systems can be achieved through a multidisciplinary route (Wassell & Young, 2007). The innovative nature of this approach intended to provide answers to these outstanding questions:

1) What can be achieved when combining traditional techniques with novel structuring technology?

2) What can be learned from developing and validating in-line dynamic measurement techniques?

3) What is revealed through investigating real emulsion systems, as opposed exclusively to single phase model systems?

Specifically, the thesis reviews current approaches to structuring fat based foods / emulsions and points to potential new mechanisms to modify fat crystallisation and emulsion behaviour (Wassell & Young, 2007; Wassell et al., 2010a) and considers new ways with which to measure these phenomena (Young et al., 2008; Wassell et al., 2010b; 2012).

In utilising alternative measurement techniques, the crystallisation kinetics can be more robustly observed under real dynamic process conditions, thereby instilling confidence in the food engineer when testing formulations developed in real-time, and/ or with less saturated oil/fat. (Young et al., 2008; Wassell et al., 2010b; 2012)

This thesis aims to show the potential of reducing total saturated fats by using existing and novel emulsifiers, demonstrating their impact on functionality (Wassell et al., 2012a; 2012b; 2012c; 2012d; 2012e; Bech et al., 2013).

A decrease in total fats tends to lead to increase in the water phase (in respect to water – oil emulsions) of the emulsion system. This being the case, the thesis takes into consideration fat mimetic properties (Wassell & Young, 2007; Wassell et al., 2010a). The objective therefore is to investigate behaviour and influence of emulsifiers both at the interface and in the bulk to demonstrate how their role is critical to the ultimate mechanics of structuring fat based dispersions and emulsions (Wassell et al., 2012a; 2012b; 2012c; 2012d; 2012e; Bech et al., 2013).

One line of investigation is to examine induced structural changes, using "crystalliser" to see if addition of a relatively longer chain saturated fatty acid can influence and initiate fat crystal formation (Young et al., 2008; Wassell et al., 2010b).

The uses of novel structuring agents are investigated within this thesis to observe their influence on final fat texture and functionality. Within the scope of this work,

extensive focus is given to a novel emulsifier developed from an innovative source of edible oil (Wassell et al., 2012a; 2012b; 2012c; 2012d; 2012e; Bech et al., 2013). The study looks at emulsifiers that do not necessarily conform to the broad international legislative demands, but which nonetheless, provide deeper insight into structuring and texturing of low saturated fat based systems.

It is intended to show that innovation and novelty can be provided not only through combining the use of emulsifiers (nucleation inducers) in real systems, but also analysis through static and dynamic conditions. Techniques to analyse the functionality of the given systems under static and dynamic conditions, include controlled stress rheology, interfacial rheology, tensiometry, X-ray diffraction, CLSM, DSC, DSD, UVP-PD.

A dynamic real-time rheological measurement to assess both viscosity and solid fat content in-line, is approached using the UVP-PD apparatus. Novel data and effective conclusions are made from observing fat crystallisation within real systems (Wassell et al., 2010; Young et al., 2008).

A relatively new technique is utilised to look at the orientation of fat crystals surrounding a single water droplet via means of wide angle and small angle X-ray diffraction (WAXD / SAXD), (Ueno & Sato 2008; Wassell et al., 2012).

The key aim of this multidisciplinary approach was to develop a more thorough and complex understanding of the mechanics and development of structure within commercially relevant, novel, low saturated fat based systems. Successful achievement of the key aim would therefore enable development of new routes to structuring fat based systems, either by enhancing traditional options, or switching to new alternatives and away from traditional methods which are currently under legislative scrutiny and lobbying pressure to be abandoned (Wassell et al., 2010a; Smith et al., 2011; Wang et al., 2012).

1.7.5 Analytical Approach

1.7.5.1 UVP-PD

A study of physical crystallisation of TAG based systems using UVP-PD, to be able to profile the effects of a behenic (C22:0) based MAG in TAG, using a non-invasive in-line rheological measuring technique would help to quantify structural events (viscosity) under dynamic conditions. This method has several advantages, where it is able to monitor opaque, highly concentrated, non-Newtonian suspensions and allow measurements not possible with common rheometers. The capability to determine dynamic rheological, non-isothermal, real-time influence of a structuring MAG based material on viscosity, would have strong commercial value, particularly when assessing "real" emulsion systems.

1.7.5.2 Tensiometry

An interfacial examination of single and mixed MAG behaviour is necessary to determine the effect of saturation and chain length on interfacial behaviour. Specifically, the intention of this study is to observe the effect of MAG based on C22:0, on interfacial tension through temperature changes, and by varying fatty acid chain length, degree of saturation (introducing other MAG) and hydrophilic properties of the emulsifiers with / without PGPR and novel MAG material. Thermal treatment (cooling) of the preparations would provide new information about any improvement to surface inter-active behaviour of emulsifier compositions not yet reported in the literature. New interfacial information could have important implications for potential viscoelastic behaviour.

1.7.5.3 Rheology

Following interfacial tensiometry, an examination of single and mixed MAG behaviour using interfacial rheology system (IRS) is required in order to determine

any previously observed effects (interfacial behaviour) of saturation and chain length in anhydrous bulk and water-oil systems. The intention of this study is to observe the rheological behaviour of selected emulsifiers through temperature, varying fatty acid chain length, degree of saturation with / without PGPR and novel MAG material. Any undiscovered improvement to viscoelastic behaviour would have important commercial value for water – oil emulsions and other food systems. This knowledge is currently unreported in the literature.

1.7.5.4 A Study Series of Application Tests: Observations on the Behaviour of Novel MAG, Behenic rich MAG and PGPR in Real Systems

Following investigations studying the rheological and interfacial behaviour of MAG, including a *Moringa Oleifera* based MAG (1.7.2), assessment of the effect of saturation, chain length and how these may transpose to and influence real bulk food dispersions or W/O emulsions is considered necessary. Any new improvements would need product validation (proof of concept) in typical commercial bulk and real emulsion preparations. Techniques, including Droplet Size Distribution (DSD), Confocal Laser Scanning Microscopy (CLSM), Textural Analysis, and Polarised Microscopy, are used to evaluate crystallisation, emulsion and final sensory properties.

1.7.5.5 Synchrotron Radiation X-ray Diffraction (SR-XRD) Macrobeam and Microbeam small angle X-ray Diffraction (SR-µ-SAXD) Analysis

Finally, a synchrotron radiation macrobeam and microbeam X-ray diffraction technique is used to determine interfacial crystallisation and clarify the effects of emulsifier additives on commercial low-fat W/O emulsions. This technique can more precisely observe microstructures of the lamellar plane directions and may provide explanation about mechanical and physical structure at the interfacial region as a result of surface active MAG and a co-emulsifier (PGPR).

2.0 General Materials and Methods

2.1 Emulsifiers

Emulsifiers used in this research were distilled monoacylglycerols (MAG); fully saturated, partially saturated and unsaturated. Emulsifiers were DIMODAN® HP, P, RT, U/J, GRINDSTED® Crystallizer 110 (CRY110), PR40, and samples of distilled monoglycerides based on triacylglyceride (TAG) of refined bleached deodorised (RBD) Ricebran oil, *Lesquerella fendleri* oil and *Moringa oleifera* oil (Appendix F, G). A polyglycerol ester emulsifier, known as GRINDSTED® PGPR 90 (Polyglycerol polyricinoleate) was also used. All emulsifiers were obtained from Danisco A/S, (known as DuPont – Bioscience ApS, Denmark) and tested, either individually, or combined, without further modifications.

Moringa oleifera oil (Code: 126089, Batch No: DE05040243, Ref: 804903823/1) was obtained from Earth Oil Plantations Ltd. Lichfield, Staffordshire, United Kingdom. RBD ricebran oil was obtained from Thai Edible Oil Co., Ltd. (Bangkok, Thailand). RBD *Lesquerella fendleri* oil was obtained through Danisco A/S (known as DuPont – Bioscience ApS, Denmark).

2.2 Fatty Acid and Monoacylglycerol Compositions (%)

Emulsifiers and their source are shown (Tables 2.1, 2.2, 2.3, 2.4, 2.5, 2.6, 2.7, 2.9, 2.10, 2.11) and characterised (Table 2.8) by one or two specific fatty acids: DIMODAN® HP is characterised by palmitic acid (C16:0); DIMODAN® P by palmitic acid (C16:0) and oleic acid (C18:1c); Crystallizer 110 by behenic acid (C 22:0); DIMODAN® UJ by linoleic acid (C18:2c), and RT by oleic acid (C18:1c) and linoleic acid (C18:2c). Table 2.1 also shows degree of saturation by iodine value (IV).

Table 2.1 Emulsifier fatty acid carbon chain lengths

Fatty acid carbon chain length (%)	RT	U/J	PR40	P	HP	CRY110
C14:0	0.1	0.1	< 1	< 1	1	< 1
C16:0	6	7	25	44	55	1
C18:0	14	5	3	5	43	2
C18:1	75	28	28	39	0.1	< 1
C18:2	2	58	12	10	0.2	< 1
C18:3	0.3	0.1	6	0.3	< 1	< 1
C20:0	< 1	1	< 1	0.2	0.7	5
C22:0	< 2	< 1	< 1	< 1	< 1	89
C24:0	< 1	< 1	< 1	< 1	< 1	< 2
Saturated total	*24*	*12*	*28*	*49*	*100*	*100*
IV (app.)	*60*	*105*	*65*	*45*	*2*	*2*

Table 2.2 Distilled Ricebran monoglyceride from RBD ricebran oil (Table 2.10)

Fatty acid and GC (%)	Ricebran as distilled monoglyceride
Glycerol	0.2
Diglycerol	0.2
FFA	0.3
Mono	98.2
Di	1.1
Tri	< 0.1
C14:0	0.4
C15:0	< 0.1
C16:0	20.5
C16:1	0.3
C17:0	< 0.1
C.18:0	2.1
C18:1	41.3
C18:2	32.5
C18:3	1.3
C20:0	0.7
C20:1	0.6
C22:0	0.2
C24:0	0.1
Unknown	0.6

Table 2.3 Fatty acid composition of *Moringa oleifera* TAG and Moringa monoglyceride

Analysis (%)	**Moringa TAG / mono**	**Analysis (%)**	**Moringa TAG / mono**
C14	0.1	C19	0.1
C15	<0.1	C20	3.4
C16	5.8	C20:1	2.2
C16:1	1.8	C22	**5.8**
C17	0.2	C22:1	0.1
C18	5.4	C24	1.0
C18:1	**73.0**	C26	-
C18:2	0.7	Unknown	0.2
C18:3	0.2		

Table 2.4 Analyses of *Moringa oleifera* TAG

Analysis	***Moringa oleifera* TAG**
Iodine value (calculated)	68
Acid value	3.2
Unsaponifiable matter	0.4%
FFA	1.5%
Diglyceride	3.3%

Table 2.5 Analyses of Moringa monoglyceride

Analysis (Mono, di, tri) %	**Moringa Monoglyceride**
Glycerol	0.76
Diglycerol	0.07
FFA	0.3
Monoglyceride	**91.15**
Diglyceride	**7.75**
Triglyceride	0

Table 2.6 Analyses of Lesquerella monoglyceride

Analysis (Mono, di, tri) %	**Distilled Lesquerella MAG**
Glycerol	0.2
Monoglyceride (MAG)	**94.1**
Diglyceride	6.1
Triglyceride	< 0.1
Total	100 ±0.5

Table 2.7 Table of Fatty acid profile and saturation (IV) of *Lesquerella fendleri* TAG

Analysis (Fatty acids %)	**Lesquerella TAG**
C14	<0.1
C16	1.5
C16:1	0.6
C18	1.9
C18:1	14.9
C18:2	9.5
C18:3	11.1
C20	0.2
C20:1	0.9
Densipolic acid	0.4
Ricinoleic acid	0.6
Lesquerolic acid	**55.2**
Auricolic acid	3.2
Iodine Value (IV)	**107.8**

Table 2.8 Emulsifiers are characterised by source from which they were produced

Name	Abbreviation	Description
DIMODAN® HP	Dim HP	Distilled saturated monoacylglycerol based on fully hydrogenated palm
DIMODAN® P	Dim P	Distilled partially saturated monoacylglycerol based on refined palm oil
GRINDSTED® Crystallizer 110	CRY 110	Distilled saturated monoacylglycerol based on fully hydrogenated high-erucic rapeseed oil
DIMODAN® UJ	Dim UJ	Distilled unsaturated monoacylglycerol based on sunflower oil
GRINDSTED® Mono-di PR40	PR40	Monoacylglycerol made from edible, refined rapeseed and / or palm oil.
DIMODAN® RT	Dim RT	Distilled monoacylglycerol based on rapeseed oil
GRINDSTED® PGPR 90	PGPR90[a]	Polyglycerol ester of polycondensed fatty acids from castor oil
Ricebran	RB[b]	Distilled unsaturated monoacylglycerol based on refined ricebran oil.
Moringa	Moringa[c, d]	Partially and fully distilled Moringa, based on *Moringa oleifera*
Lesquerella	Lesquerella[e]	Distilled unsaturated monoacylglycerol based on *Lesquerella fendleri* oil

a. PGPR, for description see Table 2.9

b. RBD Ricebran, for description as triglyceride see Table 2.10

c. Moringa, for description as *Moringa oleifera* triglyceride see Table 2.11. Partial and fully distilled methyl-ester description is shown in Table 2.12 and 2.16

d. Details of additional distilled and mono-diglyceride distillations are found in Wassell et al., 2012a; 2012b; 2012c; 2012d; 2012e

e. Lesquerella, for description as *Lesquerella fendleri* triglyceride see Table 2.7

Table 2.9 PGPR specification (Danisco A/S, Denmark)

PGPR 90[#] Analysis %	C16	C17	C18	C18:1	C18:2	C20	C18:1 Ricinoleic acid	C18:1 oleic acid	unknowns
	1.3	0.0	1.3	3.6	5.1	0.0	86.1	0.0	2.4

[#] PGPR Palsgaard 4150 also known as PGPR 90 Plus

Table 2.10 RBD Ricebran oil (Thai Edible Oil Co., LTD (Bangkok, Thailand)

DESCRIPTION	SPECIFICATION	METHOD
1. APPEARANCE	CLEAR, SLIGHTLY YELLOW	BY EYE
2. COLOUR (LOVIBOND) 5 1/4"CELL (Ex-FACTORY)	MAX. 4.0 R, 35.0 Y	AOCS Ce 13 j - 97
3. ACID VALUE	MAX. 0.30	AOCS Cd 3d - 63
(MILLIGRAM KOH PER 1 GRAM OIL)		
4. PEROXIDE VALUE (Ex-FACTORY)	MAX. 1.50	AOCS Cd 8 - 53
(MILLIGRAM EQUIVALENT/Kg. OIL)		
5. WATER AND VOLATILE MATTER	MAX. 0.10 %	AOCS Ca 2c - 25
(% BY WEIGHT)		
6. IODINE VALUE (WIJS)	92 - 115	AOCS Cd 1d - 92
7. SAPONIFICATION VALUE	180 - 195	AOCS Cd 3 - 25
8. ORYZANOL (ppm.)	MIN. 2,000 ppm.	spectrophotometer

Table 2.11 *Moringa oleifera* (Earth Oil Plantations Ltd. Lichfield, Staffs., UK)

Tests[a]	Specification
Physical State	MOBILE LIQUID -MAY SOLIDIFY
Colour	PALE YELLOW -YELLOW/ORANGE
Peroxide Value (Meq)	Maximum 6
Free Fatty Acid content (%)	Maximum 3
Fatty Acid profile	PASS
Palmitic Acid (16:0)	2.0 -10.0
Palmitoleic Acid (16:1)	1.0 -5.0
Stearic Acid (18:0)	2.0 -7.5
Oleic Acid (18:1)	65.0 -85.0
Linoleic Acid (18:2)	Maximum 1
Arachidic Acid (20:0)	2.0 -5.0
Gadoleic Acid (20:1)	Maximum 4

a = Test parameters not specified within material specification

2.3 Additional Distillations of Natural *Moringa oleifera*

Moringa monoglycerides with differing mono-di contents were made. The following glyceride contents are shown in Table 2.12 (see also Table 2.3, 2.4, 2.5). In Tables 2.12, 2.14 and 2.16, the abbreviations stand for; GL – Glycerol, Digl – Diglycerol, FFA – Free Fatty Acids, Mono – Monoglycerides, Di – Diglycerides, and Tri – Triglycerides.

Table 2.12 Other partial and full distillations of natural Moringa monoglyceride with mono, di- and triglyceride specifications

Analysis (%)	**2559/102**	**2559/104**	**2472/191**
GL	0.11	1.27	0.76
Digl	0.05	0.08	0.07
FFA	0.2	0.4	0.3
Mono	53.16	82.55	91.14
Di	42.05	15.67	7.75
Tri	4.39	0.02	< 0.1
Approx mono content %	53	82	91

2.4 Synthetic Monoglycerides

Monoglycerides described in Table 2.1 and Table 2.8 are mixed to provide a similar fatty acid profile to natural distilled Moringa monoglycerides (Table 2.3), and similar GC (Table 2.5) are shown in Table 2.13. Resultant compositions are shown in Table 2.14.

Table 2.13 Blends of mono and diglycerides

Synthetic Moringa monoglyceride	**SM 90 [a]**	**SM 60 [b]**	**SM 80 [c]**
GRINDSTED® CRYSTALLIZER 110	10	10	10
DIMODAN® RT [d]	90		50
GRINDSTED® MONO-Di PR40 [e]		90	40
Total %	100	100	100
Final mono content % (approximate)	96	64	82

a., b., c., are named SM 90, SM 60, SM 80, merely as means of identification and approximate mono content.

d. DIMODAN® RT is a distilled monodiglyceride made from partially hydrogenated rapeseed oil

e. GRINDSTED® MONO·DI PR40 is a monodiglyceride made from edible, refined rapeseed and/or palm oil. Total monoglyceride = 55%. Iodine value = 65

Table 2.14 Analysis of synthetic Moringa monoglycerides

Analysis (%)	**SM 90**	**SM 60**	**SM 80**
GL	0.16	0.24	0.20
Digl	0.14	0.1	0.18
FFA	0.30	0.40	0.40
Mono	96.50	64.56	82.87
Di	2.64	29.02	15.28
Tri	0.22	2.59	1.10

In summary the natural samples, align approximately with synthetic samples and are as follows:-

Natural		**Synthetic**
2472/**191**	=	SM 90
2559/**102**	=	SM 60
2559/**104**	=	SM 80

The fatty acid compositions of synthetic Moringa monoglycerides are shown in Table 2.15.

Table 2.15 Fatty acid composition of synthetic Moringa monoglycerides

Fatty acids (%)	**SM 90**	**SM 60**	**SM 80**
C10:0	<0.1	0.0	0.0
C12:0	0.1	0.1	0.1
C14:0	0.1	0.5	0.3
C15:0	<0.1	<0.1	<0.1
C16:0	5.3	21.5	12.7
C16:1	0.1	0.1	0.2
C17:0	0.1	0.1	0.1
C18:0	10.9	4.1	7.8
C18:1	64.6	23.9	47.6
C18:2	5.2	10.8	7.7
C18:3	0.0	3.8	2.0
C20:0	1.3	1.0	1.0
C20:1	1.4	2.6	1.8
C20:unsaturated	0.1	0.9	0.7
C22:0	**10.7**	**8.8**	**7.2**
C22:1	0.0	20.7	10.0
C22:unsaturated	0.0	0.8	0.4
C24:0	0.3	0.3	0.3
C24:1	0.0	0.4	0.2

2.5 High and Low Temperature Distillation of *Moringa oleifera* TAG

High temperature distillation of the *Moringa oleifera* TAG (Table 2.11) enables preservation of the whole fatty acid distribution being carried over into the resultant monoglyceride. The effects of producing fully distilled Moringa MAG at a low (185°C) and high (210°C) temperature are shown in Table 2.16.

Table 2.16 Effect of high / low temperature distillation on *Moringa oleifera* TAG

	Monoglyceride	**Monoglyceride**	***Moringa oleifera* TAG**
	2559/132	2559/134	starting material
Distillation °C	**210°C**	**185°C**	-
Analysis (%)			
GL	0.88	0.52	-
DIGL	0.15	0.22	-
FFA	0.2	0.2	-
MONO	86.92	97.95	-
DI	11.80	1.06	-
TRI	0.03	0.02	-
C12:0	<0.1	<0.1	0.2
C14:0	0.1	0.1	0.1
C16:0	6.3	6.4	5.9
C16:1	1.9	1.9	1.8
C17:0	0.1	0.1	0.1
C18:0	5.5	5.7	5.5
C18:1	72.6	75.3	71.8
C18:2	1.5	1.5	1.6
C18:3	0.2	0.2	0.0
C20:0	**3.2**	**2.9**	**3.3**
C20:1	1.8	1.7	1.9
C20:u	0.2	0.2	0.1
C21:0	<0.1	0.0	-
C22:0	**5.8**	**3.6**	**6.3**
C22:1	0.1	0.0	0.1
C23:0	<0.1	<0.1	1.0
C24:0	0.8	0.3	0.1

2.6 Triacylglycerol (TAG) for Water-in-Oil (W/O) Emulsions and Anhydrous Dispersions

The multidisciplinary approach used throughout this study, led to the use of several base TAGs. These are listed and described in Table 2.17

Table 2.17 Major TAGs for W/O emulsions and anhydrous dispersions

	TAG						
°C [l]	ChocoFill BR60[a]	PK4 INES[b]	Palmotex B[c]	Palmotex 98[d]	Palmovit 200[e]	Kokowar 31[f]	COLZAO[g,k]
10		72 - 80		82	10		
20	45 - 48	49 - 55		64	1	60	
25	31					29	
30	10 - 14	23-28		42		9	
35	1 - 2			27		4	
40		3 – 4					
Slip melt[h] °C	33	37 - 42	36	53 - 57		31	
Iodine Value[i]	22 - 32			35	min 63		110 - 121
SAT %[j]	74	74			39		7
MONO %[j]	22	31			47		62
POLY %[j]	4	5			14		30
trans %[j]	<1	max 2		<1	max 1	<4	max 1

a = Interesterified palm stearin / lauric (previous names include: Akomic or Akocrem M), Aarhus Karlshamn (AAK), Denmark.

b = Interesterified palm stearin / lauric. Cargill GmbH., Hamburg, Germany.

c = RBD Palm oil. AarhusKarlshamn (AAK), Denmark.

d = Palm Stearin. AarhusKarlshamn (AAK), Denmark.

e = RBD Palm Olein. ADM Hamburg AG, Hamburg.

f = hydrogenated and lauric oil based on coconut oil. Aarhus Karlshamn (AAK), Denmark.

g = RBD Rapeseed oil. AarhusKarlshamn (AAK), Denmark.

h = AOCS Cc 3-25

i = IUPAC 2.205

j = IUPAC 2.304

k = Cloudpoint (°C) -16, ASTM D97 SS-EN (23015)m

l = Solid Fat Content (%), IUPAC 2.150a

RBD Peanut oil (Lot no: J0112KA) supplied by Columbus Foods Company, inc. Des Plaines, IL., USA), with following specifications:-

Colour (Lovibond): 0.5 (Cc13b-45); Flavour: Bland; Free Fatty Acid (%): 0.025 (Ca5a-40); Peroxide Value meq/kg: 0.25 (Cd8b); Iodine Value: 90.3 (Cd1-25); Cold Test: 5.5 Clear & Brilliant (Cc11-53); Additives: none.

2.7 Other and Minor Ingredients for W/O Emulsions

2.7.1 Hydrocolloid

GRINDSTED® LFS 560 Stabiliser System, E440 (Amidated pectin standardised) and E401 (Sodium alginate). Danisco A/S, Gums & Systems, Denmark.

2.7.2 Flavours

Butter flavour (water phase) 050001 T03007, and Butter flavour (oil phase) 050001 T04184, (Firmenich. Denmark).

2.7.3 Antioxidant

GRINDOX TOCO 50 (Danisco A/S. Denmark).

2.7.4 Skimmed Milk Powder

MILEX 240 – ARLA Foods (Viby, Denmark).

2.7.5 Salt:

SUPRASEL· FINE SALT, (Akzo Nobel Salt A/S, Denmark).

2.7.6 Antimicrobial

Potassium sorbate 105119, (Merck KGaA, Germany).

2.7.7 β-carotene and Preparation

BC-3000-OSS (Chr. Hansen GmbH. Lubeck. Germany). Carotenoid of BC-3000-OSS: nature-identical β-carotene. Formulation is a liquid suspension of microcrystalline β-carotene in vegetable-oil:

	30% β-carotene	6.7 %
+	Rapeseed Oil	93.3 %
β -carotene sol. (2%)		100%

1. Heat the oil to approx. 100°C
2. Add β -carotene and mix well.

2.7.8 EDTA:

EDTA (Kirsch Pharma GmbH), dosage is normally used at 0.015%, for chelating.

2.7.9 Tap Water Specification (Data on Water Hardness, Aarhus, Denmark)

The hardness of the water in Aarhus is between 12°dH - 20°dH* as shown in Table 2.18

Table 2.18 Tap Water hardness characterisation

Hardness in ^{o}dH	Characterisation
12 – 18	Quite hard
18 – 30	Hard

*** German degrees (Deutsche Härte)**

2.8 Preparation of W/O Emulsions and Bulk Anhydrous – TAG Systems

Besides the chemical properties of the fat blend, the process conditions have a major impact on the finished product. Emulsions are subjected to applied cooling temperatures and shear, whilst passing through a series of scraped surface units, often referred as A-units, and pin-workers, often referred as B-units. Depending on the pump speed and back-pressure, the residence time of the product can be controlled. These process parameters will strongly determine the properties of the margarine / spread and are very important to obtain margarine with a good quality and storage stability.

2.8.1 Equipment and Processing

35%, 40% and 60% water-in-oil (W/O) emulsions and continuous bulk oil compositions were processed (Table 2.19) on a cooled scraped surface heat exchanger pilot plant (Figure 2.1), known as a Gerstenberg & Schröder (previously named Gerstenberg & Agger) : 3-tube pilot perfector 3x57 (Serial No: 11803). Design pressure 80 bar – 120bar. Refrigerant: Ammonia (NH3), from SPX Flow Technology Copenhagen A/S, Vibeholmsvej 22, Brøndby, Denmark. Specifications are as follows: Scraped surface heat exchanger (SSHE): Diameter/length 57mm/430mm. Annular space 6.5 mm. Volume 0.42ltr. Cooling surface area /tube: 0.0567m^2. RPM each tube: 200-1000. Cooling (max) $^{-}$25°C. High pressure 3-piston pump (Model: P-3-15/35-Labo). Capacity: 20-210 l/h. Max pressure: 160 bar. Centrifugal Pump type: CS 25 (serial no: 48258) with a 115mm inbuilt propeller, 0.55KW Bi Polar motor 0.75 hp motor (2900rpm). AISI316 stainless steel heated pump housing (Model T82)

The Processed 35%, 40% and 60% W/O emulsions and or bulk oils were assembled as per the following general procedure:

2.8.1.1 Water Phase

Water was heated to 80°C

All dry ingredients were weighed and mixed and slowly added to the water phase, while stirring intensively for 4 minutes. The water phase was then allowed to cool to 40°C or adjusted accordingly (see Table 2.19). The pH of the water phase was adjusted with standard citric acid (Citric Acid Anhydrous, (Food Grade) CAS No. 77-92-9)).

2.8.1.2 Fat Phase

The emulsifiers, beta carotene (2% solution) and the selected oils and fats were weighed into the same container and then heated to 80°C. Periodically, the fat phase was stirred to ensure homogeneous melting.

The fat phase was then cooled to 40°C or adjusted accordingly (see Table 2.19), until required for processing. In the case of emulsions, the water phase was carefully added to the fat phase while stirring intensively.

2.8.1.3 Lab Pilot Scale Process Conditions

Unless otherwise indicated, emulsions were processed using the following conditions shown in Table 2.19 for 35%, 40% and 60% W/O emulsions.

Table 2.19 Processing parameter using Gerstenberg & Schröder 3-tube lab scale scraped surface heat exchanger units

Processing parameter using Gerstenberg & Schröder 3-tube lab scale scraped surface heat exchanger units	**Default 35% w/o**	**Default 40% w/o**	**Default 60% w/o**
Oil phase temperature (°C)	40	40	50
Water phase temperature (°C)	40	40	20
Emulsion temperature (°C)	40	40	50
Centrifugal pump %	20 - 30	Auto	Auto
Capacity high pressure pump (kg/h)	25	40	40
Cooling (NH3) tube 1: (°C)	-15	-10	-10
Cooling (NH3) tube 2: (°C)	-15	-10	-10
Cooling (NH3) tube 3: (°C)	N/A	-10	-10
SSHE (Rpm) tube 1:	1000	1000	1000
SSHE (Rpm) tube 2:	1000	1000	1000
SSHE (Rpm) tube 3:	N/A	1000	1000

Measurements of process conditions are recorded using Gerstenberg and Schröder datalogger (D.S. Engineering, Nyborg, Denmark).

The pilot scale scraped surface heat exchanger units are shown in Figure 2.1

Figure 2.1 A Gerstenberg & Schröder pilot scale: 3-tube Pilot Perfector 3x57

(Source: SPX Flow Technology Copenhagen A/S, Brøndby, Denmark).

2.9 Confocal Laser Scanning Microscopy (CLSM)

In the confocal microscope, all structures not in focus are suppressed at image formation. This is obtained by a pair of pinholes which limit the specimen's focal plane to a confined volume. Relatively thick specimens can be imaged in successive volumes by acquiring a series of sections along the optical axis of the microscope. This results in image stacks that can be reconstructed into images showing the 3D structure of the sample. Structural information can thus be obtained with minimum risk of integrity to the sample under examination.

The sample to be imaged by CLSM must be labelled with a fluorescent probe, if not autofluorescent themselves. Fluorescent probes are available for a wide range of biological materials, such as proteins, lipids. CLSM can be used either to obtain static images or to provide dynamic imaging.

The CLSM system in this study enabled simultaneous detection of signals from four photo multipliers, including one for transmitted light which allowed use of ordinary light microscopy. There were 3 detection channels for simultaneous staining with fluorescent probes and 6 laser lines available for inducing maximum available fluorescence. The protein was dyed using FITC, which turns green. The fat was dyed using Nile Red, which turns red. Both of these are fluorescent colours, which are dissolvable in acetone.

2.9.1 Method

A Leica TCS SL module 2 CLSM system with a Leica DM IRE2 inverted microscope (Leica Microsystems, Germany), serial no. 192216. The system was equipped with 3 lasers: Ar/Green He/HeNe and four detector channels (incl. transmitted light detector).

The water-in-oil emulsions were placed and pushed lightly upon a 1.5 x 1 x 0.5 cm dyed cover glass (using 15µL FITC, Flourescein-5-Isothiocyanate, dissolved in acetone, and 15µL Nile Red, dissolved in acetone), then placed in refrigerator at

5°C for dying for a minimum of 30 minutes. Final analysis occurred at ambient approximately 21°C.

2.9.1.1 Reagents

Acetone CAS.no: 67-64-1 R 11

Nile Red CAS.no: 230-966-0

FITC (Flourescein-5-Isothiocyanate)

Acridin Orange.

Use solutions of 50-200 µg/ml

2.9.1.2 Equipment Beam Path Settings

Laser power: 488: 50 % 543: 50 %

Splitter filter: DD 488/543

PMT 1: 483-500 Blue reflection

PMT 2: 503-533 Green protein

PMT 3: 605-675 Red fat

2.9.1.3 Calculations

Four images at two magnifications were taken using a 40X and 100X object lenses respectively. CLSM images were then run through a MATLAB program R2009b (MathWorks, Matrix House, Cambridge Business Park, Cambridge, UK) to remove the blue reflection channel, and to 'colour combine' the images. The images are then reproduced (scaled) to 375 x 375 µm and 188 x 188µm.

2.10 Differential Scanning Calorimetry (DSC)

Differential Scanning Calorimetry (DSC) is a thermo analytical technique principally for monitoring changes in the physical or chemical properties of materials (Narine, & Marangoni, 1999). The changes are measured as a function of temperature by detecting the heat changes associated with the sample compared to the control – usually a sealed empty pan. These are positioned on a sensor plate to detect thermal resistance.

Fats exist in a number of different crystal forms, depending on fat type and the thermal treatment it receives: this is called polymorphism. The most important of these crystal forms are α, β' and β. DSC helps to identify the polymorphic behaviour of an emulsifier subjected to specific thermal treatments.

A Mettler Toledo TA 8000 System consisting of a DSC820 measuring module and cryostat cooler; equipped with STAR^e Software (Mettler-Toledo Ltd., 64 Boston Road, Beaumont Leys Leicester, UK) was used to examine the polymorphic behaviour of water-in-oil emulsion samples forming one part of a composite analysis with microbeam X-ray analysis described later within the general methods (2.20).

2.11 Gas Chromatography (GC)

2.11.1 GC Analysis

GC is a common type of chromatography used in analytical chemistry for separating and analysing compounds that can be vaporised without decomposition.

The GC principle operation follows a flow-through narrow tube known as the column, through which different chemical constituents of a sample pass in a gas stream (carrier gas, mobile phase) at different rates depending on their various chemical and physical properties and their interaction with a specific column filling, called the stationary phase. As the chemicals exit the end of the column,

they are detected and identified electronically. How the final data is displayed is based on the computer and software.

2.11.2 Monoglyceride Analysis Method: Fatty Acid Methyl Ester (FAME) and Glycerols (Tri, Di, Mono)

The equipment used for the chromatographic data is listed below:

A Perkin Elmer model Autosystem XL gas chromatograph was used fitted with a Perkin Elmer AS-8300 automatic injector, programmable temperature vaporiser (PTV), flame ionisation detector and TotalChrom software for data analysis (PerkinElmer Instruments, Massachusetts, USA). The chromatographic column used was a WCOT fused silica 12.5m x 0.25mm ID x 0.1µ film thickness, with coating: 5% phenyl methyl silicone (figures are length of column x diameter x thickness of the coating).

This following method was used for determination of fatty acid composition in all monoglycerides and fat containing samples.

Carrier gas: Helium, 10-12 psi inlet pressure. Automatic injector programming: injection time 1 second, rinse cycle 10-20 seconds. 0.1-0.2 µl of sample injected if on-column injection is used, and 1-2 µl of sample injected if split injection is used. Injector: 0.01 minutes after injection, the temperature of the PTV is increased to 400°C. The Oven was programmed from 60-80°C to 200°C at 15-20°C/min., then to 360°C at 10-TC/min and held at 360°C for 7-12 minutes. The Detector temperature was 385°C. Detector gases: H_2 35 ml/min., and air 430 ml/min.
Data processing: peak data was collected and computed using a Perkin Elmer mini-computer based integrating system.

2.11.3 Preparation of Methyl Esters for GC Determination

The following describes the preparation of methyl esters for GC determination. The GC analysis determined the fatty acid compositions as weight% of fatty acid methyl ester: Reagents used were:

Methyl-tert-butyl-ether (MTBE), Heptane, Methanol, anhydrous.

Ethanol 95-99% (190-200 proof).

Hydrochloric acid (HCl), half normal (0.5 N) in methanol.
For preparation, approximately 95 ml of methanol anhydrous was cooled in a 100 ml Erlenmeyer flask to approximately –15°C by means of dry ice and ethanol. Then 5 ml of acetyl chloride was added drop wise by means of a pipette while stirring. This was diluted to 100 ml with methanol anhydrous.
Next, 20 mg of the sample was weighed into a 5 ml reactivial (Figure 2.4). Then 1 ml 0.5 N HCl in methanol and 200 µl heptanes were added. The reactivial was then placed into a Reacti-Therm for 30 min. ±2 minutes at 100°C, and shaken several times during the 30 minutes, then left to cool. After cooling, 2 ml of MTBE and 1 ml of deionised water was added and the sample shaken. This was then transferred to the upper phase in a 10 ml glass container with screw cap containing 200-300 mg sodium sulphate, anhydrous. The sample was then ready for GC.

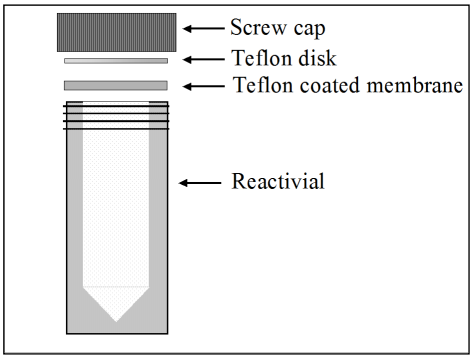

Figure 2.2 Schematic of reactivial for preparation of methyl esters for GC determination

2.12 Polarised Light Microscopy (PLM)

Polarised light microscopy images are useful to observe effects of environmental conditions on lipid crystallisation behaviour as a consequence of thermal manipulation. The treatment of several emulsions and bulk continuous systems to Isothermal and non-isothermal conditions can provide strong correlations to actual crystallisation behaviour within TAG continuous commercial food systems.

2.12.1 Method

Several analyses of W/O emulsions and continuous bulk oil phase systems were observed using an Olympus BX60 optical microscope (Serial no: 6M02546), fitted with polarised filter (Olympus Optical Co. GmbH. Hamburg, Germany). The desired amount of sample (~40 mg) is placed on a carrier glass slide which has been pre-cooled or preheated to ~5°C. A cover slip was then placed parallel to the plane of the carrier slide and centred on the drop of sample to ensure uniformity and desirability of sample thickness. The micrograph of the crystal was taken at 40x and 200x magnification unless otherwise indicated. A number of images were acquired each representing a typical field. Scale bars were added as appropriate.

2.12.2 Induction Heat / Cool / PLM Micrographs

Micrograph images were collected in polarised light using an Evolution Colour-camera (MP 5.0 RTV 32-0041C-309) supplied from Media Cybernetics (Media Cybernetics, Inc.USA.), attached to the Olympus BX60 optical microscope with following parameters: Heat step 50°C/minute to 85°C, tempering for 2 minutes. Then cooling rate: 1°C/minute - 10°C/minute - 50°C/minute and 100°C/minute to final stop temperature 20°C.

Cooling rate: 1°C/min. 108 PLM images at every 30 seconds.

Cooling rate: 10°C/min. 27 PLM images at every 10 seconds.

Cooling rate: 50°C/min. 12 PLM images at every 3 seconds.

Cooling rate: 100°C/min. 8 PLM images at every 3 seconds.

2.13 Rheology

2.13.1 Interfacial Rheological System (IRS) Measurements

The IRS allows measurements of interfaces covered with surface active molecules. The raw data is produced by well known rheological standard tests and the interfacial properties can then be calculated by analysing the raw data.

Interfacial Rheology and Bulk Rheology, was measured using Physica MCR 301 (Figure 2.3a) and data driven from RHEOPLUS/32 V3.21 software (Anton Paar GmbH, Germany). Oscillatory interfacial method was used to measure interfacial properties of interfaces covered with surface active molecules. The IRS bicone system is shown in Figure 2.3b & c. Geometries used for measurements were as follows: Interfacial Rheology: Bicone - BIC68-5 (Figure 2.4a), and Bulk rheology: Bob/cup - CC27 (Figure 2.4b).

Oil phase: Emulsifiers were weighed for rheology measurements at 0.2% w/w (unless otherwise indicated) and the RBD sunflower oil balanced to 100%. The preparation is heated to 10°C above melting point of emulsifier, and held for 1 hour, then cooled to ambient temperature and deaerated (~12hrs).

Water phase: Demineralised water is deaerated using a Desiccator (Sigma-Aldrich, Denmark A/S. Copenhagen, Denmark). Oscillation measurements were conducted at the following parameter settings: Temperature sweep: 50°C - 5°C, 0.3°C/min. 151 data points. Strain 0.1%. Frequency 1%. Held 15 min at 5°C. Then strain Sweep**:** Strain: 0.001-100%, Ramp log+ (points/decade), Slope: 6 pt/Dec. Frequency 1% at temperature 5°C.

A very low strain was chosen to make sure that at every stage in the crystallisation process, measurements were performed within the linear viscoelastic region so as to avoid disturbing the crystallisation process. The low frequency was preferred in order to minimise influence of crystallisation as little as possible. Rheograms were obtained by plotting dynamic change in the elastic modulus (G') and viscous

modulus (G'') of the crystallising sample as a function of the crystallisation temperature (non-isothermal).

The analysis method for calculation of complex interfacial viscosity η^*_i by frequency sweep measurements, with a bicone measuring system, are produced by known rheological and mathematical formula (4.2.2). Interfacial properties can then be calculated by analysing the raw data. The precalculated data were then computed using RHEOPLUS/32 V3.21 software and recalculated. Ideally, the calculation of complex interfacial viscosity η^*_i, is determined for each of the 151 data points.

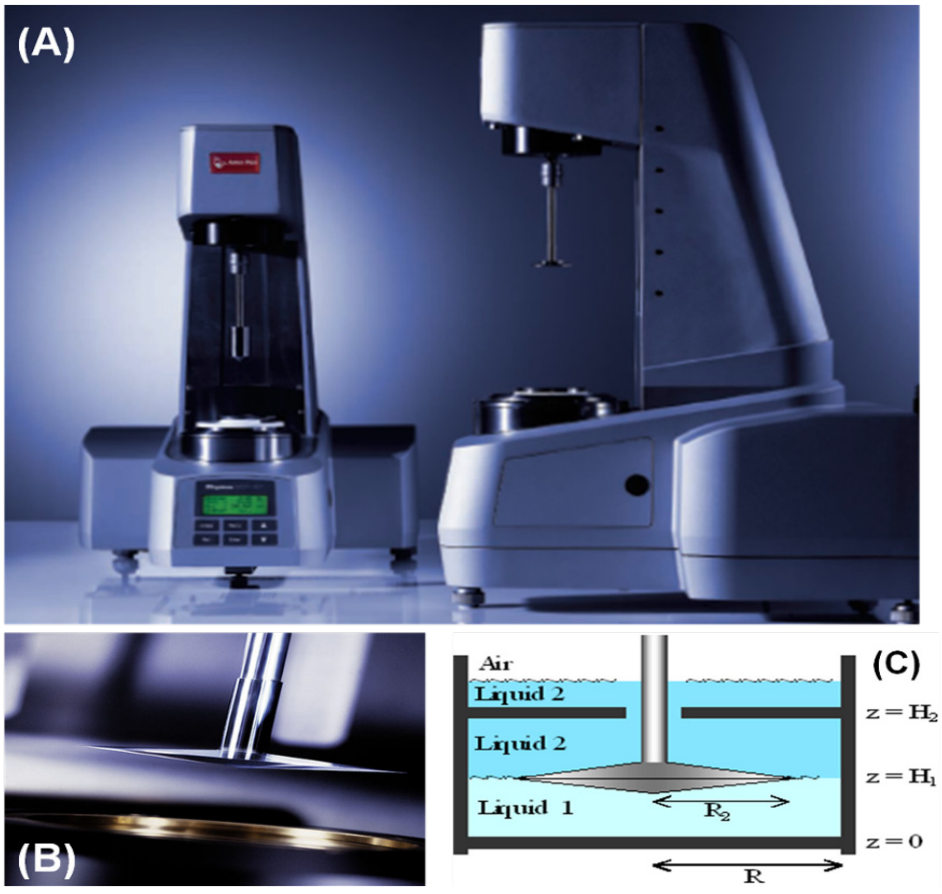

Figure 2.3 (a) Anton Paar Physica MCR Interfacial Rheology System (IRS) and (b / c) Bicone measuring system

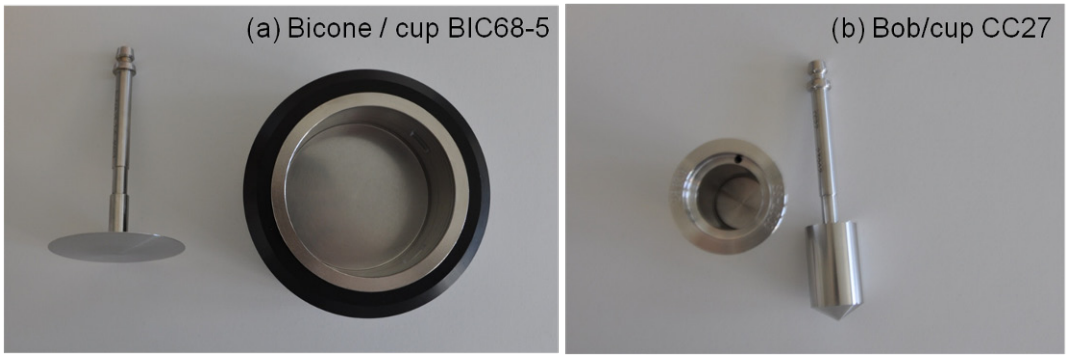

Figure 2.4 Geometries used for measurements: (a) Interfacial Rheology: Bicone - BIC68-5 and (b) Bulk rheology: Bob/cup - CC27

Bulk rheology measurements were used to provide real constants for upper fluid density and viscosity values for interfacial analyses (Appendix I).

2.13.2 Haake Controlled Stress Rotational Rheometer

A controlled stress rheometer (Haake RS 150, from Fisher Scientific Ltd, Bishop Meadow Road, Loughborough, Leicestershire, UK), was set up to run from 0.001 - 60Pa of stress range, and it was programmed to measure over a period 300s, in a logarithmic distribution. Geometries were used as follows: Bob Diameter = 20.000mm. Measuring gap = 0.850mm. Cup Diameter = 21.700mm. Sample volume = 8.20cm^3. The Haake internally calculates the stress range and time range. Software: RheoWin version 3.610004 (Thermo Fischer group, UK) was used for computation of readings at the stress corresponding to an even log distribution over stress and time range requested.

2.13.3 Rheometrics Controlled Stress Rotational Rheometer

Investigation of bulk oil blends subjected to the effects of controlled cooling rate while under shear were analysed using a shear stress controlled rotational rheometer, Rheometrics SR 5 (proRheo, Germany), operating in simulated rate control mode. Target shear rate of 10 s^{-1}. Crystal history was removed by melting and holding at 90°C for 15 minutes before loading onto the rheometer. A parallel plate geometry (40mm diameter top plate. Gap = 1mm) with thermoelectric cooling plate using Peltier cooling was used. The temperature ramp was 70°C to 25°C at either 1°C/min, 10°C/min, 30°C/min, was used. A 2 minute delay without shear at 70°C prior to thermo-cooling was also used.

The fat blend tested in all cases comprised of a base of 70% palm stearine (35 IV) and 30% palm olein (56 IV), to which the emulsifiers GRINDSTED® Crystallizer 110, GRINDSTED® PGPR 90, and Monoglycerides of Moringa were added at 1%, 0.5% and 1% respectively (2.1, 2.2, 2.3, 2.6)

2.14 SFC Determination

Following the AOCS Official Method Cd 16b-93 (Firestone, 2004), the SFC of the samples was determined on a PC120 pulsed nuclear magnetic resonance (pNMR) spectrometer (Bruker AXS GmbH. Karlsruhe, Germany). The sample was placed in the NMR tube and successively melted at 80°C for 30 min, tempered at 0°C for 90 min, and then kept at the desired temperature (10°C, 20°C, 25°C, 30°C, 35°C 40°C) for 30 min before measurement was recorded. Triplicate measurements were obtained.

2.15 Isothermal Rate of Crystallisation (RoC) Test

The SFC of the separated fat was measured at isothermal crystallisation conditions using the following procedures: samples were successively filled into the glass NMR tube (each~3 g), heated to 80°C and then maintained for 60 minutes, and placed into a refrigerated bath circulator set at ambient 20°C. SFC readings were obtained at 1 minute intervals for 20 minutes for each RoC test. The crystallisation curves (SFC vs. time) were produced under isothermal conditions. Triplicate measurements were obtained (Appendix B & C).

2.16 Surface Tension - Interfacial Tensiometry

Interfacial tension is an important property of liquid/liquid systems. It serves as an index of the relative forces of intermolecular attraction and as a measure of the free energy per unit area of the interface, and also provides information about emulsification. The reduction in interfacial tension is due to the increased adsorption of emulsifier molecules at the interface, because their solubility in the oil phase decreases as the temperature decreases. Figure 2.5 shows preparation of interfacial tension measurement between two the two liquids, oil (O) and water (W)

and is also known as the Wilhelmy plate method. This method is ideal for measuring solutions containing surfactants and observing change of surface tension over time without disturbing the liquid surface.

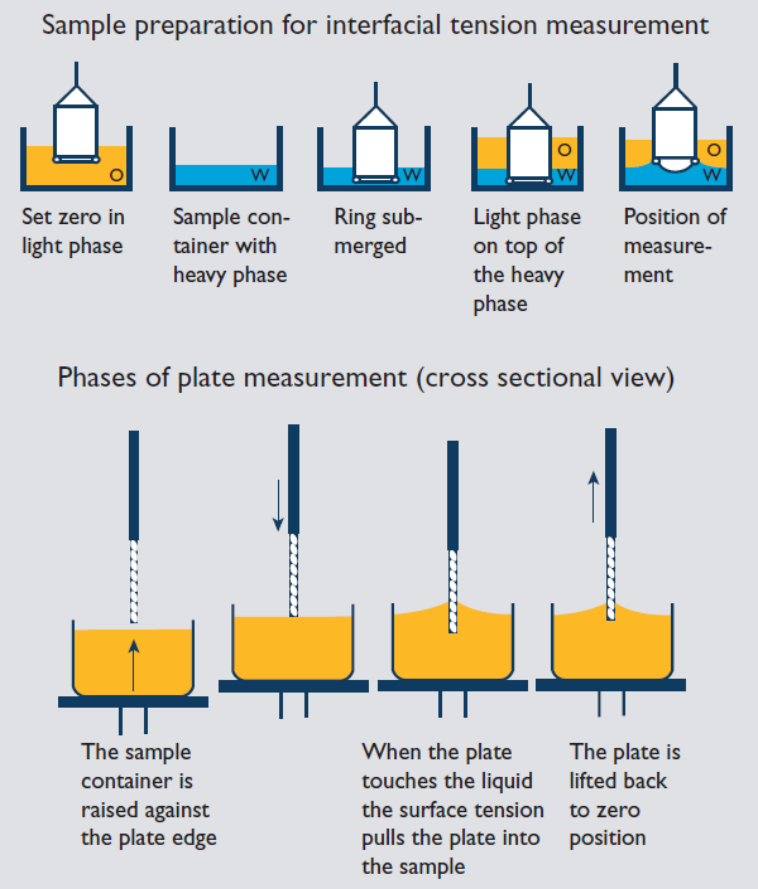

Figure 2.5 Principle action of the Wilhelmy plate method (Source: Danisco Physical Food Science, Brabrand, Denmark).

The Wilhelmy plate consists of a thin plate usually on the order of a few square millimetres in area. The plate is often made from glass or platinum which may be roughened to ensure complete wetting. The plate is cleaned thoroughly and attached to a scale or balance via a thin metal wire. The force on the plate due to wetting is measured via a tensiometer or microbalance and used to calculate the surface tension (γ) using the **Wilhelmy equation**:

$$\gamma = \frac{F}{l \cdot \cos\theta} \qquad \text{Eq. (2.1)}$$

where l is the wetted perimeter ($2w + 2d$) of the Wilhelmy plate and θ is the contact angle between the liquid phase and the plate. In practice the contact angle is rarely measured, instead either literature values are used, or complete wetting ($\theta=0$) is assumed (Holmberg 2002).

2.16.1 Tensiometry Materials and methods

2.16.1.1 Solvent

Refined, bleached and deodorised (RBD) sunflower oil, iodine value 127, was obtained from AAK (Aarhus, Denmark). Purification was then carried out using the following procedure: Mix 30g of Fluorisil PR60/100 mesh (Sigma-Aldrich Denmark A/S) with 500g Sunflower Oil in a vessel. The mixture was stirred for 60 min at 80°C, and protected from UV light. After cooling over 12hrs, the sunflower oil was passed slowly at room temperature through a glass column, containing filter paper (glass fibre GA55, 47 mm) into 800ml UV light protected beaker. This procedure results in the sunflower oil having an interfacial tension at 20°C of 28-30mN/m (oil – water)

2.16.1.2 Preparation of Samples

Oil phase: Emulsifiers were weighed for tensiometer measurements at 0.02% w/w (unless otherwise indicated) and the RBD sunflower oil balanced to 100%. The preparation was heated to 10°C above the melting point of emulsifier, and held for 1 hour, then cooled to ambient temperature and deaerated (~12hrs).

Water phase: Demineralised water was deaerated using a Desiccator (Sigma-Aldrich, Denmark A/S. Copenhagen, Denmark). Both phases were ready to use after heating to 50°C.

2.16.1.3 Interfacial Tension Method

The interfacial tension of oil/water systems was measured on a Digital-Tensiometer, Figure 2.6 (model K10ST, Krüss Germany), using the Wilhelmy plate method (Holmberg 2002), and recorded continuously by connecting a high resolution data recorder (PicoLog ADC-20, using PicoLog for windows 5.13.4 from Pico Technology Ltd, Cambridgeshire. United Kingdom) to the tensiometer. A second channel on the recorder was used to monitor the temperature of the oil/water system in the tensiometer. The oil/water phase was controlled by a programmable water bath (model: Thermo Haake® DC10-K10, with a refrigerated recirculation unit (Sigma-Aldrich, Denmark A/S. Copenhagen, Denmark), which allowed the temperature to be changed from 50°C to 5 °C. Prior to initializing measurement the tensiometer K10ST was calibrated for the oil phase to show more than 27mN/m at 20°C and held constant for 15 min, enabling both oil and instrument to reach equilibrium.

Measurements were started at 50°C after preheating the oil phase and the water phase to 50°C separately. Prior to commencing with a temperature sweep, the interfacial tension was maintained at 50°C for 5 minutes to achieve equilibrium between the oil and water phases. Then the temperature was decreased to 5°C at 0.3°C/min and kept at 5°C for 5 minutes.

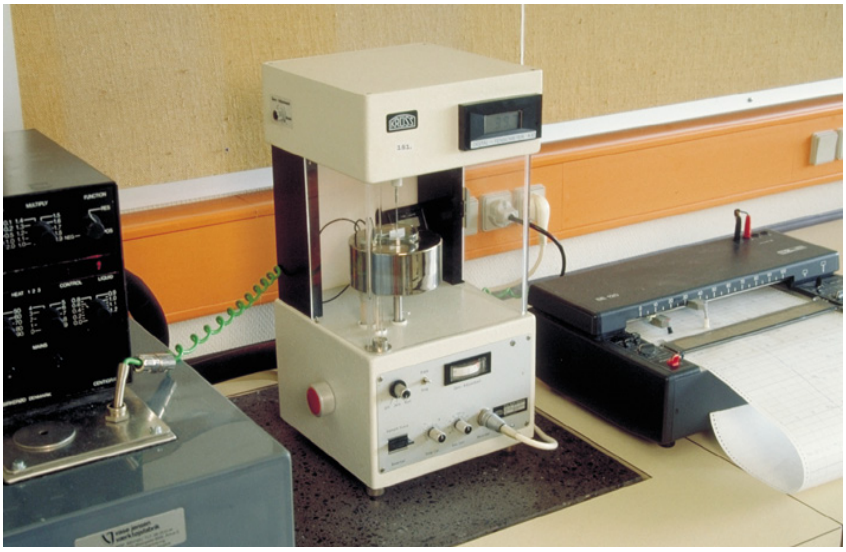

Figure 2.6 Digital-Tensiometer K10ST from Krüss, Germany

2.17 Texture Analysis (TA-XT2i)

Texture analysis was measured using a Stable Micro Systems Texture analyser: TA-XT2i and Software Texture expert Exceed version 2.64, from Stable Micro Systems Ltd., Godalming, Surrey, United Kingdom. In all measurements the probe was: SMS P/0.5 (½ diameter cylinder: Ebonite) and samples were prepared directly from the scrapped surface cooling plant (Gerstenberg & Schroder pilot plant), described in the methods (2.8). All samples were measured at 5°C and force was according to standard compression test at 1mm/s to depth of 15mm. The maximum penetration force was recorded. Hardness is reported as the maximum penetration force (g) based on triplicate measurements. Test settings are shown in Appendix J.

2.18 Droplet Size Distribution (DSD) in Low-Fat Spread

One of the important features of an emulsion is its Droplet Size Distribution (DSD). The droplet size influences many characteristics, for instance the rheology (Asano & Sotoyama 1999), and the stability of an emulsion (Basheva, Gurkov, Ivanov, Bantchev, 1999) and emulsion liquid membrane performance (Chakraborty, Bhattacharya, & Datta, 2003). Droplet size distribution in low-fat spread is important with respect to appearance, flavour release and microbiological stability. In protein-containing low-fat spreads, stabilisers are added to secure emulsion stability. These also have a profound effect on water droplet size.

The water droplet size distribution of margarine influences the microbiological stability, the hardness, mouth feel and flavour release of the margarine. A product with a coarse water droplet distribution and with low preservatives and salt will be susceptible to fast microbial contamination. Microbiological spoilage is also influenced by protein content and pH.

The smaller the water droplet size, the less attractive the environment for the micro-organisms since less nutrients are available to them. A small water droplet size (average droplet range from 5 to 50 microns) increases the shelf life of the product, and this is aided by the side function of emulsifiers which are able to influence texture and stability.

When the droplet size is less than 10 microns, this environment will be more restrictive to microbiological growth (Charteris, 2007; Delamarre & Batt, 1999). In reality, good manufacturing practice (GMP) will come into play, because the

margarine and spreads (water-in-oil) industry is generally regarded as low risk, sometimes larger size droplets are found because of the acceptable trade-off to attain a required flavour release (Young & Wassell, 2008).

2.18.1 Method

Pulsed NMR analysis using a pulsed gradient unit Bruker Minispec mq 20, 20MHz low field pulsed pNMR Analyzer, Magnet unit ND2172, equipped with a Pulsed Gradient Unit 1059. High / low temperature probe head assembly mq-PA231 (-120°C - +200°C). Software: SSL, system status logging. Pulsed gradient system for 10mm tubes (10 x 180 x 0.6mm = diameter x length x thickness). Mq-SOFT EDMs Oil droplets / Water droplets and Diffusio. Bruker gas tempering unit for high and low temperature analysis: mq-BVT3000c (for minispec probe PA231). Measurements are performed at 20°C and field gradients of 2.0 T/m (Telsa per meter) or higher.

2.18.2 Analytical Principle

A Hahn spin echo experiment with field gradient pulses involves calculating the reduction in spin echo amplitude compared with the Hahn spin echo amplitude without field gradient pulses (R).

Determining diffusion coefficient of water molecules: If protons can move unhindered in the liquid, then free diffusion is taking place, and the diffusion coefficient D can be determined directly from R.

Determining droplet size distribution in w/o emulsions: If proton movement is restricted by the boundaries of a droplet, an R value plateau is obtained reflecting the droplet size. When measuring at several pulse lengths, the corresponding R plateau values give a fingerprint of the droplet size distribution. Measurements are

performed at 5°C and with 8 R values. Log-normal particle size distribution is typically seen in w/o emulsions and is used in the mathematical calculation of droplet size distribution. Results are given as volume and number size distribution (Table 2.20) and derived from a log-scale using values of standardised normal distribution (Table 2.21).

Table 2.20 Droplet size distribution results presented as volume and number size distribution

2.5 % of droplet volume is smaller than "x" µm
50% of droplet volume is smaller than "x" µm
97.5 % of droplet volume is smaller than "x" µm

Table 2.21 Droplet size distribution calculated from log-scale values of standardised normal distribution

2.5% <µ	**50% <µ**	**97.5% <µ**
(d_{lower})	***($d_{50,3}$)***	***(d_{upper})***

2.19 Ultrasonic Velocity Profiling with Pressure Difference (UVP-PD) Materials and Methods

The fats described earlier (Table 2.17) were blended forming the following:

25% Akomic (non *trans* fat filling based on non-hydrogenated partly lauric vegetable oils and fats; Aarhus Karlshamn, Karlshamn, Sweden) and 75% rapeseed oil – the control.

25% Akomic, 74% rapeseed oil and 1% GRINDSTED® Crystallizer 110 (distilled monoglyceride based on behenic acid; Danisco / DuPont, Grindsted, Denmark).

Fats used for off-line (Haake) rheological measurements (2.13) shown in Figure 3.3 (3.0), were Kokowar and Akocrem (see footnote in Table 2.17)

Fat blends used for the SFC measurements (2.19.4; 2.19.5) consisted of 30% of palm stearin, added to 70% rapeseed oil before being processed (2.19.1).

At time of writing the Akomic (Table 2.17) has been renamed to Chocofill BR 60 (Aarhus Karlshamn, Karlshamn, Sweden).

The GRINDSTED® PS 209 (material no. 126324), was a composition of mono-, di and triglycerides based on fully hydrogenated (IV 2) rapeseed and palm oil and contained a maximum monoglyceride content 12% (supplied by Danisco / DuPont, Denmark).

2.19.1 Pilot Plant (Gerstenberg-Schröder A/S)

All experimental water-in-oil emulsion samples were prepared and measurements made on a Gerstenberg-Schröder oils and fats pilot plant (refer to 2.8.1) consisting of a flow loop (closed stainless steel tubular circulation system) into which the UVP-PD equipment was incorporated (Figure 2.7). The tubular diameter of the pilot plant was 12 mm, and the sample enters this system from a holding tank and passes through a centrifugal pump. The UVP-PD equipment was connected to the

pilot plant via quick valve expansion couplings such that a smooth transition to the UVP-PD tube diameter of 22.5 mm was achieved. The sample then flowed through the UVP-PD equipment and exited directly into 150ml plastic cups or collected and re-melted before sending the fat blend on a repeat process. The measurement apparatus was attached directly at and immediately after the pin worker, the area where the greatest heat of crystallisation occurs.

The fat blends were independently introduced to the pilot plant at 80°C, and thermodynamic drive constants: ammonia -30°C, Flow rate at high-pressure pump = 70 kg/h. Pressure on transducers <4 bars. Shaft rotation speed perfector 1 = 1000 r.p.m. Pin rotor =302 r.p.m. These conditions achieved an approximate exit temperature in the order of 18°C after ~2 min flow time.

2.19.2 UVP-PD System

The UVP-PD system and method for in-line rheometry used here are well described in the literature (Wiklund, 2007; Wiklund, Shahram, & Stading, 2007; Wiklund & Stading, 2008). However, the upgraded system including new hardware and new transducers used in this work has not been described in detail before (Young et al., 2008; Wassell et al., 2010b).

The UVP-PD testing section was designed and manufactured by SIK – The Swedish Institute for Food and Biotechnology, Goteborg, Sweden SIK, Sweden and AB WI-KA Mekaniska Verkstad, Sweden and connected to the Gertenberg & Schröder pilot plant (refer to 2.8.1) using a series of quick valve expansion couplings, facilitating rapid movement of UVP-PD test sections between different measuring points. Figure 2.12 shows the pilot plant and testing section including the by-pass loop and the flow adapter cell for housing the ultrasound transducers, located towards the exit point, prior to sampling.

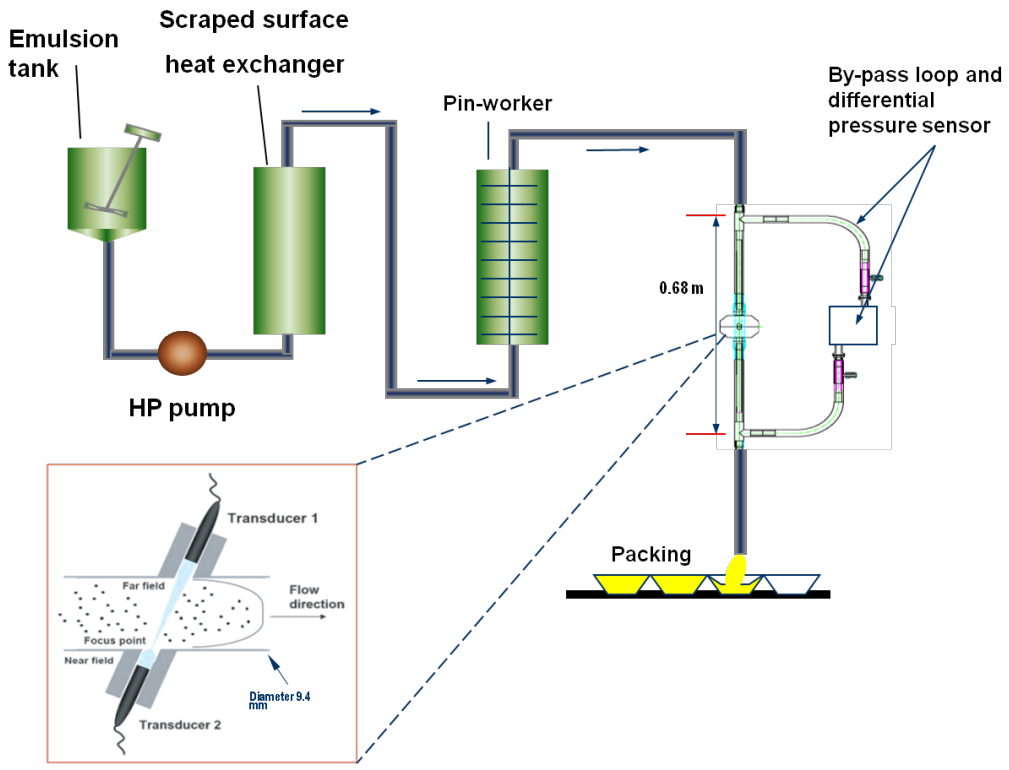

Figure 2.7 Schematic image of pilot scale scraped surface heat exchanger unit and pin rotor units with flow-cell and by-pass loop measuring apparatus with differential pressure gauge and ultrasound transducers.

The testing section comprised a flow adapter cell for housing a pair of custom made 4 MHz high-temperature ultrasound transducers (TR0405LH-X., Signal-Processing SA., Savigny, Switzerland). The high temperature transducers, at the time of writing are a new development and part of confidential contract work, allowing measurements directly from the transducer front and thus to record more or less zero velocity at the wall. As a result, higher precision in determining the wall positions were achieved compared to previous work (Young et al 2008).

The transducers were mounted opposite each other at a fixed angle of inclination (20°), which allowed simultaneous non-invasive measurement of the flow velocity profiles and monitoring of the acoustic properties. The active diameter of the piezo

was 5 mm and the transducers were in contact with the liquid but were pulled back 6.9 mm to avoid measurements within the near field region where the acoustic pressure field is irregular (Young et al 2008). The testing section also contained a differential pressure sensor, (ABB 265DS; ETP80, ABB Automation Technology Products AB, Sollentuna, Sweden), and the pressure drop was measured over a distance of 0.68m (shown in Figure 2.7).

The UVP-PD system used consisted of a customised pulser/receiver, UVP-DUO-MX model with a Multiplexer, (Met-Flow SA, Lausanne, Switzerland). The UVP-DUO-MX instrument features modified firmware that gives direct access to demodulated echo amplitude (DMEA) data, i.e. raw data, which is not available using standard instrumentation. Wiklund et al (2007) and Birkhofer et al (2008), have recently shown that direct access to DMEA data from the pulser/receiver instrument makes it possible to say something about the quality of the acquired data and to correct it in real-time thus leading to improved measurement accuracy.

A high-speed digitiser card (Agilent Acquiris; Agilent Technologies, Kista, Sweden) was used as an integral part of the data acquisition scheme, enabling simultaneous measurement of the flow velocity profiles and acoustic properties.

The pulser/receiver and the differential pressure sensor were connected to a master PC via Ethernet and a high-speed DAQ card (National Instruments Sweden AB). UVP data acquisition was implemented with an ActiveX library (Met-Flow SA, Switzerland). All data acquisition, data processing and analysis were made using novel software, RheoFlow™, developed at SIK, Sweden for in-line UVP-PD-based rheological measurements.

2.19.3 UVP-PD Method and experimental parameters

The UVP-PD in-line rheometer system used in this work only required initial calibration of the transducer angle. No other calibration was needed since only physical parameters i.e. velocity, pressure and velocity of sound are measured

directly. The emitting frequency of the ultrasound was set to 4 MHz, 150V with 2-4 cycles per pulse and 512 repetitions resulting therefore in a sampling rate of 300ms per demodulated echo amplitude (DMEA) data set. Short bursts of ultrasonic pulses were emitted and then echoed back towards the transducer by reflective surfaces such as particles moving with the flowing suspension. The local velocities are obtained by detecting the Doppler shift frequency of the reflected ultrasound and the local position of the particles by simultaneous measurements of the time delay between emission and echo reception. The power density spectra of one set of profiles, typically 25-40 were determined using Fast Fourier Transform (FFT) algorithm and averaged. The Doppler shift frequency (flow velocity) was then determined from the geometrical mean of the spectra above an offset. The total measurement time per recorded and processed velocity profile was 450ms. Thus, radial velocity profiles can be continuously obtained in real-time both in the direction of the flow and counter to the direction of the flow, and the volumetric flow rate were obtained by integration of the velocity profiles.

The shear rate distribution could be determined directly from the velocity gradient of the acquired velocity profiles. Shear viscosities and rheological model parameters presented here were determined from a non-linear fit to the integrated form of the power-law model.

Power-law model: $\tau = K\dot{\gamma}^n$ Eq. (2.2)

Integrated form: $v(r) = \left(\frac{R\Delta P}{2LK}\right)^{1/n} \cdot \frac{R}{\left(1+1/n\right)} \cdot \left[1 - \left(\frac{r}{R}\right)^{\left(1+1/n\right)}\right]$ Eq. (2.3)

Where τ and $\dot{\gamma}$ are the shear stress and shear rate, K is the consistency index and n is the flow exponent. In the integrated form of the model r and R are the inner and outer radius, ΔP is the pressure drop and L is the length of pipe section used for ΔP. Details on the UVP-PD system and method for in-line rheometry used in this work have been published in the literature (Young et al., 2008; Wassell et al., 2010b).

2.19.4 Solid Fat Content (SFC) Measurement – p-NMR

The solid fat content was determined off line using the established p-NMR technique as described by IUPAC (1987) and the calculation principle outlined by van Putte and van den Enden (1974). Also refer to 2.14

2.19.5 Solid Fat Content (SFC) Measurement – Ultrasound

A method for determining the solid fat content in-line using an ultrasonic velocity technique has been improved. The method is based on the pulse transmission technique described e.g. by McClements and Povey (1987; 1988) where an equation derived by Urick (1947) is used to convert the ultrasonic velocity in a sample into SFCs for many oil/fat mixtures. The velocity of sound in a two-component suspension of particles or emulsion of droplets depends on the mean density and mean compressibility and is given by the Urick (1947) equation:

$$v = \frac{1}{\sqrt{\kappa\rho}} \quad \text{Eq. (2.4)}$$

where, $\rho = (1-\phi)\rho_1 + \phi\rho_2$ Eq. (2.5)

and $\kappa = (1-\phi)\kappa_1 + \phi\kappa_2$ Eq. (2.6) according to Wood (1964).

Here ϕ is the volume fraction of the dispersed phase, ρ is the density, κ is the adiabatic compressibility, v is the velocity of sound and the subscripts 1 and 2 represent the continuous and dispersed phases respectively. Equation (2.5) can be rewritten as a cubic equation in terms of ϕ. For oil- and fat based systems an analytical solution exists:

$$\phi = \left(-B - \left(B^2 - 4AC\right)^{1/2}\right)/2A \quad \text{Eq.(2.7)}$$

Where,

$$A = v_1^2\left(1-\rho_1/\rho_2\right)+v_2^2\left(1-\rho_2/\rho_1\right),$$

$$B = v_2^2\left(\rho_2/\rho_1-2\right)+v_1^2\rho_1/\rho_2,$$

$$C = v_2^2\left(1-v_1^2/v_{total}^2\right)$$

The SFC is then calculated by converting the volume fraction ϕ, into a mass percentage

$$SFC = 100\phi\rho_2/\rho_{total} \quad \text{Eq.(2.8)}$$

The velocities in, and densities in the solid and liquid phases are required to determine SFC from Eq. (2.8). The densities were measured using a Densito-30PX instrument (Mettler-Toledo AB, Stockholm, Sweden). The sound velocity in palm stearin at 10°C was determined to 1548 ±5 m/s and its density 899 ±1 kg/m^3. The density in rapeseed oil was determined to 916 ±1 kg/m^3. The sound velocity in rapeseed oil was determined as function of temperature using a pulsed method to c = 1536.4-3.487xT m/s with a correlation coefficient of 0.997. This procedure was needed to allow for temperature compensation of the measured sound velocities. A significant limitation of the ultrasonic technique is that vacuole formation may occur in the sample during cooling, which practically restricts SFCs to less than about 40% according to McClements and Povey (1988).

2.20 Synchrotron Radiation X-ray Diffraction (SR-XRD) using Microbeam small angle X-ray Diffraction, (SR-μ-SAXD)

To determine the detailed mechanisms of interfacial heterogeneous crystallisation, a technique which relies on X-ray focusing optics and a synchrotron radiation X-ray source is used (Wassell et al., 2012). This enables use of X-rays and the generation of an intense X-ray microbeam with a divergence small enough to perform X-ray diffraction studies. By scanning the X-ray microbeam (μ-SAXD) on a thin section of the sample in two dimensions with steps on the order of the beam size and by collecting each two-dimensional (2D) X-ray diffraction pattern with a 2D X-ray-sensitive area detector, it is possible to construct 2D micrometer-dimension images. In principle, simultaneous observation of small-angle and wide-angle diffraction patterns can be achieved to obtain the lamellar distance and sub-cell structure.

This study encompassed multiple analyses using DSC, PLM, macrobeam and microbeam synchrotron radiation X-ray diffraction (SR-XRD), experiments on fat crystals in the continuous phase of W/O emulsions (35 wt. % fat).

2.20.1 Method

Preparations of 35% W/O emulsions were assembled using ingredients described in Tables 2.22 and 2.23. Emulsifier additives were provided by Danisco/DuPont (Grindsted, Denmark). Emulsion preparation and processing conditions (Table 2.19) using a Gerstenberg & Schröder pilot scale SSHE plant were described previously in 2.8.

Table 2.22 Sample recipes for 35% W/O emulsions

Sample:	**PGPR**	**PGPR + MB**
Water (tap)	64.0%	64.0%
Salt (Nacl)	1.0%	1.0%
Water phase total	65.0%	65.0%
Fat blend: solid fat (interesterified: palm stearin / lauric kernel) / liquid oil (RBD Rapeseed oil) = 1/3	34.6%	34.45%
Other fat ingredients		
GRINDSTED® PGPR 90-K[a]	0.4%	0.4%
GRINDSTED® Crystallizer 110-K[b]		0.15%
Fat phase total	35.0%	35.0%

[a] GRINDSTED® PGPR 90-K; polyglycerol polyricinoleate, a polyglycerol ester of polycondensed fatty acids from castor oil.

[b] GRINDSTED® Crystallizer 110-K; distilled saturated monobehenoyl (MB) based on fully hydrogenated high-erucic rapeseed oil (HEAR)

Table 2.23 Properties of fats used for W/O emulsions

SFC%[a]	Interesterified palm stearin/lauric[b]	RBD Rapeseed oil[c, d]
10°C	72 - 80	
20°C	49 – 55	
25°C		
30°C	23-28	
35°C		
40°C	3 - 4	
Slip melt[e] °C	37 - 42	
Iodine Value[f]		110 - 121
SAT %[g]	74	7
MONO %[g]	21	62
POLY %[g]	5	30
trans %[g]	max 2	max 1

a = Solid Fat Content (%), IUPAC 2.150a

b = Cargill GmbH., Hamburg, Germany

c = AarhusKarlshamn (AAK)., Denmark.

d = Cloudpoint (°C) -16, ASTM D97 SS-EN (23015)m

e = AOCS Cc 3-25

f = IUPAC 2.205

g = IUPAC 2.304

2.20.2 Macrobeam X-ray Diffraction (XRD) Measurements

In order to observe the macroscopic crystallisation behaviour of fats in the emulsion, synchrotron radiation (SR)-XRD experiments with a normal macrobeam (beam width 0.5x0.5mm^2) were carried out at two different beamlines (BL-15A) of the SR source Photon Factory (PF) in the National Laboratory for High-Energy Physics (Tsukuba, Japan). For both beamlines, a double-focusing camera was operated at a wavelength of 0.15nm. Two different detectors were used: a CCD camera for small-angle data and a PSPC for wide-angle data. SAXD and WAXD measurements were performed simultaneously. The SAXD pattern was used to determine the chain length structure of the TAG, and the WAXD pattern enabled identification of the polymorphic forms. The temperature program applied to the sample was controlled by a Mettler DSC-FP84 (Mettler Instrument Corp., Greifensee, Switzerland) with FP99 software. A 2mm-thick sample was placed in a stainless-steel sample cell with Kapton film windows.

2.20.3 Microbeam Small-angle X-ray Diffraction Measurements

The basic principle of SR-μ-SAXD has been reported elsewhere (Ueno, Nishida, Sato, 2008; Shinohara et al 2008; Arima et al 2009; Tanaka et al 2009; Wassell et al., 2012). By scanning the X-ray microbeam on a thin section of the sample two dimensions with steps on the order of the beam size, and by collecting each two-dimensional (2D) XRD pattern with a 2D X-ray sensitive area detector, the polymorphic structure can be assessed by measuring the long spacing value, which is calculated by the diffraction angle (2θ) extension (Fig. 2.10a). In addition, the lamellar plane direction (Fig. 2.10b) of the fat crystal can be assessed by measuring the azimuthal angle (χ) extension pattern at a fixed 2θ position (Fig. 2.10c).

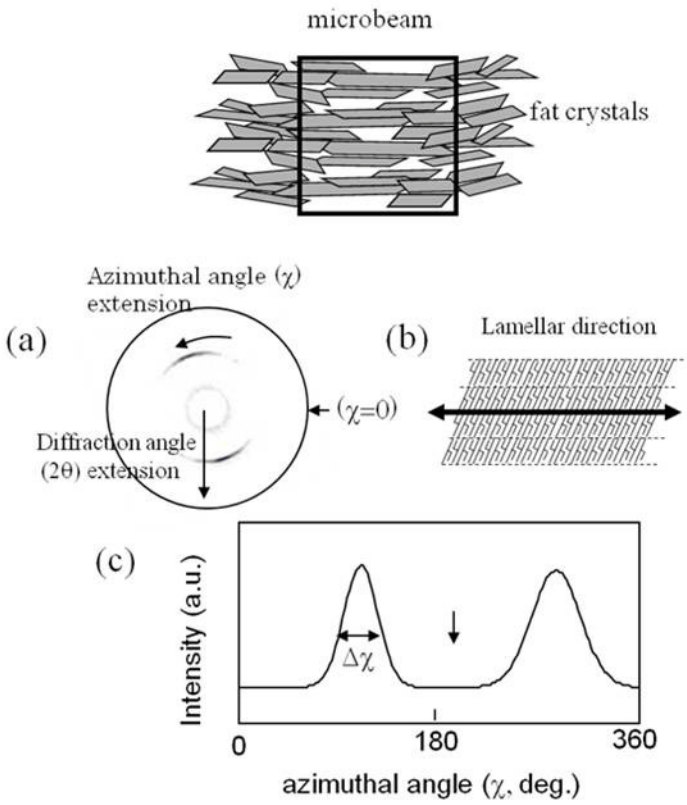

Figure 2.8 Data analyses of SR-μ-SAXD patterns. (**a**) 2D SR-μ-SAXD pattern. (**b**) Lamellar direction in a fat crystal. (**c**) χ extension pattern

When all the fat crystals are highly oriented, two sharp 2D diffraction peaks (arc peaks) should appear because of the preferred orientation of crystals. The average direction of the lamellar planes of the fat crystals is directed normal to the direction connecting the two arc peaks. For example, in Figure 2.8(c), sharp arc peaks appear at $\chi = 110°$ and $\chi = 290°$, which are superimposed by a 180° rotation. This set of two peaks (twin peaks), correspond to the symmetric diffraction peaks from the crystals whose lamellar planes are aligned along the same direction at $\chi = 200°$ (arrow in Figure 2.8(c)).

The degree of orientation of the lamellar planes of TAG crystals can be evaluated by calculating the half width of χ value ($\Delta\chi$). A smaller $\Delta\chi$ yields a higher degree of orientation of the lamellar planes (Arima et al., 2009).

The μ-SAXD measurement was performed at BL-4A of the Photon Factory, the synchrotron radiation facility of the High-Energy Accelerator Research Organization (KEK) in Tsukuba, Japan. Details of the μ-SAXD method have been reported previously (Riekel, Burghammer, & Muller, 2000).

The X-ray microbeam wavelength was 0.11nm, and the beam area was 5 x 5μm^2. The emulsion sample was sealed in a 50μm-thick cell made of mica covered with polyethylene terephthalate (PET) film, and set on a temperature controlled stage (Figure 2.9). The sample was thermally treated using a Linkam (Linkam, UK) as follows. First, the sample was kept at 60°C for 5min. The temperature was then reduced to 5°C at a rate of 2°C/min and kept at 5°C during the μ-SAXD measurement. An image of the Linkam temperature control stage unit is shown in Figure 2.10.

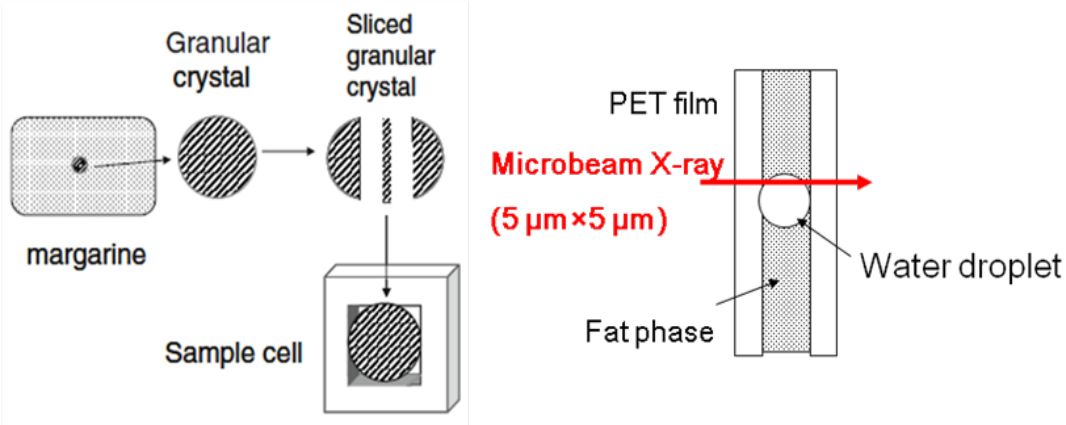

Figure 2.9 Schematic showing cold stage temperature control for the W/O emulsion preparation (Ueno et al. 2008)

It was necessary to decrease the distance between the sample and the 2D detector to 30cm so that both the small- and wide-angle diffraction patterns could be imaged on a 2D detector with a 6in x 6in (15.24 x 15.24cm) area. Keeping the microbeam position fixed, the measured sample was moved by an x-y-z stepping motor for observation by an optical microscope (magnification ×200). The sample was moved automatically within a 2D plane in 5μm steps.

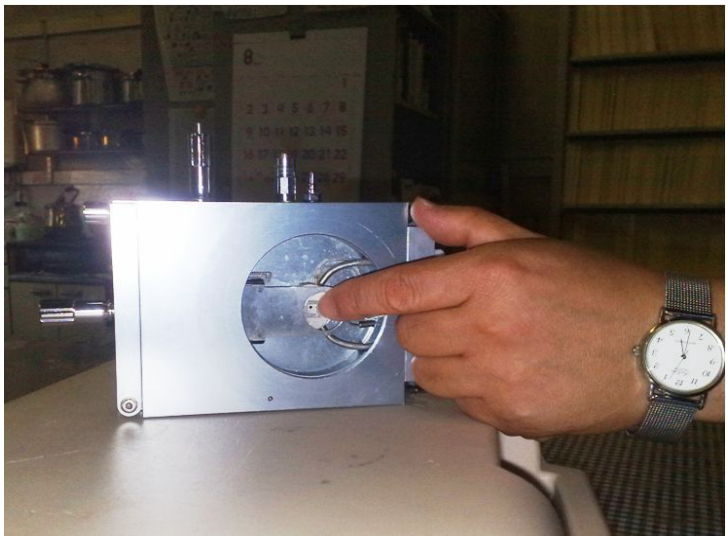

Figure 2.10 Image of Linkam temperature control stage unit

2.20.4 DSC Measurements

DSC analyses were performed using a differential scanning calorimeter model XRD-DSCII (Rigaku, Tokyo, Japan). First, 10mg of the sample was weighed in an aluminium pan. Before analysis, the sample was heated to 60 °C at a rate of 10 °C/min and held under isothermal conditions for 5min to erase its previous thermal history. The sample was then cooled to 0°C at a rate of 2°C/min and heated again to 60°C to obtain the cooling and heating thermograms. All experiments were performed under a nitrogen flow of 50 mL/min, and an empty aluminium pan was used as a reference for all. Duplicated experiments were conducted for each emulsion, and the same results were obtained.

2.20.5 Polarised Optical Microscopic (POM) Observation

Water droplet distribution and fat crystal morphology were observed using a CX31-P POM (Olympus Co., Tokyo, Japan) with a DP 12 digital camera (Olympus). The POM was set under the crossed Nicols condition. Samples were set in a Linkam (TU-600PM, Cambridge, UK) furnace set to a temperature of 5°C and placed on the sample stage of the POM.

3.0 A Study on the Crystallisation of TAG Based Systems using UVP-PD

3.1 Introduction and Background

The physical properties of Triacylglycerol (TAG) based systems have mainly been studied and performed under isothermal conditions where observations of crystal behaviour can be quite different from those observed whilst in or from a dynamic, non-isothermal environment (Wassell et al., 2010a). Ultrasonic velocity profiling with pressure difference (UVP-PD), offers the chance to probe the mechanics of TAG blend physics under real, dynamic conditions.

There are many potential factors influencing crystal nucleation and many have been reviewed (Povey et al., 2007). There is a need for methods to analyse and understand the crystallisation processes occurring under dynamic conditions. A range of different analytical techniques have been reported to study TAG crystallisation processes, including rheology, DSC, pNMR, ultrasonic spectroscopy (De Graef et al., 2006; Janssen & MacGibbon, 2007; Maleky et al., 2007; Martini et al., 2006; Wassell et al., 2010a), but so far all these techniques have been constrained to static, and semi-static conditions. None of these analyses measure while the material is potentially in a dynamic – supercooled condition, where crystallisation occurs very quickly and in bulk (Garbolino et al., 2005). Ultrasound is regarded as the most sensitive (Povey & Challis 2006).

3.2 Effect of Cooling

In real process conditions, nucleation is induced at a higher temperature than that expected for pure TAG due to impurities, dust, vessel surface, air bubbles, interface of the emulsion droplets, and for example, emulsifier e.g. monoacylglycerol (MAG) or monoglyceride reverse micelles. Once stable nuclei have formed, these grow into crystals by incorporating molecules in the interface from the melted TAG. As crystallisation continues, the degree of super-saturation in the system decreases. Importantly, the rate of crystal growth is proportional to the degree of supercooling, whereby rapid cooling of the melted TAG leads to the simultaneous formation of many nuclei which grow into small crystals. Slow cooling leads to smaller numeration of nuclei, eventually with time, these grow to larger crystals.

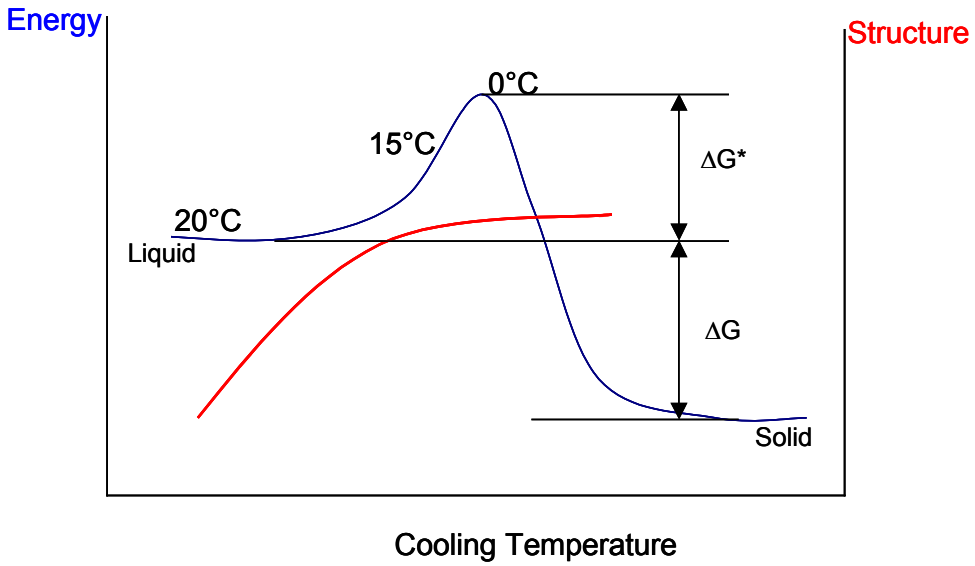

Figure 3.1 Schematic diagrams of the energy barrier to crystallisation and the relative amount of structure formed as a function of cooling temperature.

The effect cooling on the structure forming ability of a system is shown in Figure 3.1, where a schematic energy diagram depicts the amount of activation energy (McClements, 1999) required to 'kick start' nucleation; energy on the y-axis and cooling temperature on the x-axis, and structure on the second y-axis. Reducing the cooling rate to 15°C causes a small change. Reducing to 0°C and cooler,

suggests an optimum has been reached. The energy barrier to crystallisation is surpassed. The benefit of moving to lower cooling rates, together with mechanical contact (shear), encourages the process of crystallisation (refer 1.3).

3.3 Ultrasonic Velocity Profiling with Pressure Difference (UVP-PD)

A method for in-line rheometry combining the Doppler-based ultrasound velocity profiling (UVP) technique with pressure difference (PD) measurements, commonly known as UVP-PD, has recently been investigated by several authors (Birkhofer, Jeelani, Windhab et al., 2008; Wiklund, 2007; Wiklund & Stading, 2008; Wassell & Young 2007; Wassell et al., 2010a). The UVP-PD method has several advantages over commercial process rheometers in being applicable to monitor, opaque, highly concentrated, non-Newtonian suspensions and allows measurements not possible with common rheometers. Other researchers are indirectly interested in ultrasound techniques for other reasons, such as crystallisation kinetics (Sato & Ueno 2011), specifically in the area of ultrasound analysis, processing and quality control of food systems (Awad et al., 2012).

Until now, a relatively new technique (Young et al., 2008; Wassell et al., 2010b) using UVP-PD, draws attention to a new method of observing rheological behaviour of a crystallising TAG blend under real fluid / dynamic process conditions, neatly demonstrating fundamental differences. Importantly, this non-invasive technique is also able to observe, the effect on additions of minor additives, e.g. addition of a relatively small inclusion of a longer chain MAG such as monobehenate (see 1.5; 1.6). These additives are known to influence crystallisation mechanics (seeding / promoting crystal networks). This aspect is well documented (Sakamoto et al., 2003 & 2004). The effect has been less easily observed in real dynamic processing conditions, until now.

Measurements used to quantify crystallisation events are typically DSC or pNMR, both being off-line static measurements, and both limited to the degree of thermal treatments typically found in real food processes.

A review of findings (Wassell et al., 2010a) clearly shows the necessity for a multiple approach to structuring. Part of this multiple discipline highlights investigation into the use of crystal modifiers; specifically, this being the use of MAG. The influence of the longer chain behenic MAG has been discussed in review (Wassell & Young 2007), and offers some influence on nucleation (For comprehensive supporting detail, refer 1.6). Indirectly, the UVP-PD technique was used to quantify the effect of crystallisation on a typical TAG blend; the TAG blend being anhydrous. This investigation was to characterise a true in-line measurement, under real processing conditions.

Figure 3.2 shows schematics of the test section (Appendix E shows previous and current photo images of UVP test sections). The study characterised the influence of an additive, based on behenic based MAG (GRINDSTED® Crystallizer 110) on the selected TAG blend (Young et al., 2008).

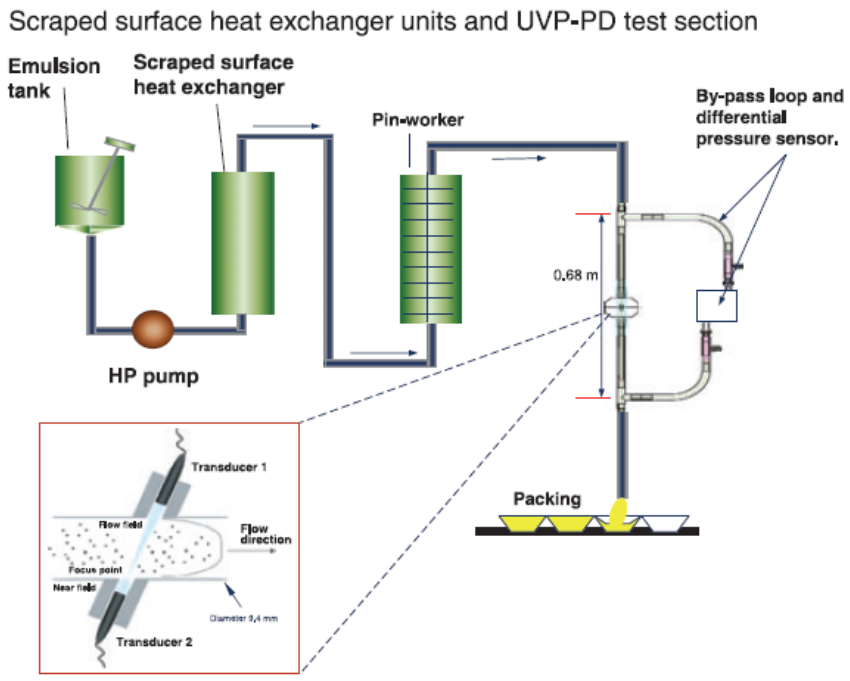

Figure 3.2 Schematic image of pilot scale scraped surface heat exchanger unit and pin rotor units with flow-cell and by-pass loop measuring apparatus with differential pressure gauge and ultrasound transducers.

3.3.1 Off-line Haake Measurements

For comparison, several MAG / TAG mixtures were first measured off-line on a controlled stress rheometer from Haake (Thermo Electron Corp., Karlsruhe, Germany) (Haake RS 150), using a cup-bob geometry where the bob is of 20 mm diameter (refer to 2.13.2). The temperature was cooled from 70°C to 40°C at 1°C min^{-}1 and the shear rate was held constant at 10 s^{-1}. Results for viscosity as a function of temperature are given in Figure 3.3.

The samples represent filling fats and were chosen for their resemblance to the model systems to be tested with the UVP equipment. The filling fats (refer to materials and methods Table 2.17) are: Kokowar, (hydrogenated, deodorised lauric oil based on coconut) from Aarhus Karlshamn, Akocrem (the same as Akomic), GRINDSTED® PS 209 (a blend of MAG and TAG, fully hydrogenated rapeseed and palm-based oil) from Danisco A/S, GRINDSTED® Crystallizer 110 (frequently abbreviated throughout the subsequent text as CRY110 and described previously in 2.0) and Dimodan® HP (fully distilled MAG, from fully hydrogenated palm TAG, described previously in 2.0).

The data in Figure 3.3 depicts that, at a given temperature, in this case c.48°C, there is the onset of a dramatic rise in viscosity, not seen in the samples where the additive (CRY110) is absent. This increase in viscosity continues for the duration of the experiment, whereby the actual viscosity increase is approaching a factor of 2 for the sample with the lowest viscosity and still significantly higher than the previous highest result.

The results show a distinct trend for the viscosity increase as a result of CRY110 addition under the semi-static conditions of the rheometer, where shear rates and cooling rates are predominantly lower than those experienced in real process conditions. Hence, the need to be able to characterise the same rheological parameters in-line and under real process conditions, which gives not only real commercial value, but adds to the understanding of TAG crystallisation discipline generally.

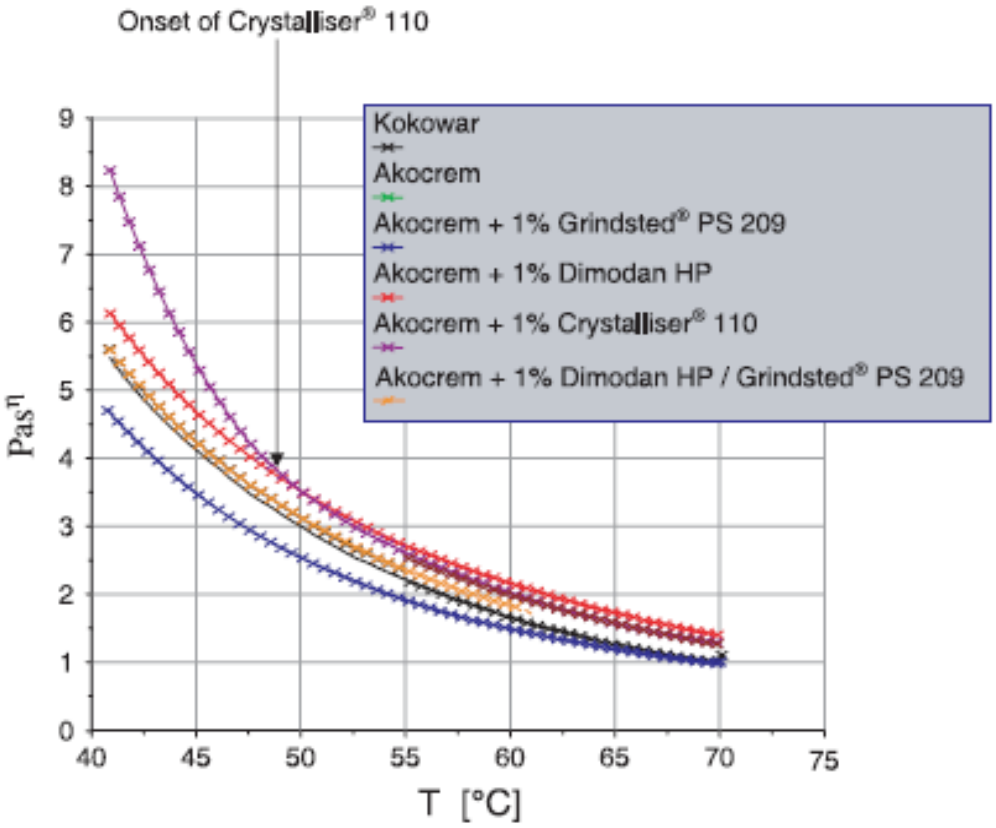

Figure 3.3 Viscosity as a function of temperature for TAG blends measured off-line

Table 3.1, presents measurements of live process conditions recorded using Gerstenberg and Agger datalogger (D.S. Engineering, Nyborg, Denmark), two of which show typical product responses to process modification, e.g. addition of CRY110. The thermodynamic drive constants: ammonia (31.7°C), high-pressure pump capacity (71 kg h) and shaft rotation speeds of perfector 1 (1000 r.p.m.), Pin rotor (302 r.p.m.), clearly shows a typical isothermal (exothermic) gain from 2 to 12.8°C observed in sample no. 11. However, a greater isothermal transition is seen with the addition of 1% CRY110 (sample 15) with a heat gain from 3.9 to 22°C. The additional heat energy gained in sample 15 can be attributed to increased

heterogeneous nucleation induced by the CRY110, thereby promoting a more solid TAG-crystal network structure. Isothermal change is partially explained by increased energy consumption (ampere) drawn when supercooling the samples (Amps first tube). Additional energy consumption (c. 1.8%) is drawn on the sample with CRY110, while still maintaining steady-state thermodynamic-processing conditions. Ideally, control of in situ isothermal heat of crystallisation can help minimise post-structural changes, post-process. Most importantly, these tests provided sufficient continual structural changes to be 'captured' downstream at the point of UVP measurement.

Table 3.1 Influence of cooling to the degree of exothermic crystallisation, recorded at pin-worker (PRM) unit with data log – prior to UVP-PD

Sample no.	11	15
Time (h)	13:36	15:30
Log	–	–
Pump capacity (kg)	71.00	71.00
Centrifugal pump (bar)	0.50	0.50
Pump pressure (bar)	2.60	1.90
Emulsion temperature (°C)	55.40	57.70
NH3 (first tube) (°C)	–31.70	–31.70
Temp (first tube) (°C)	2.00	3.90
Temp PRM (°C)	12.80	22.00
Amp (first tube)	269.00	274.00
Speed Perf 1 (r.p.m.)	1000	1000
Speed PRM (r.p.m.)	302	302
Akomic + rapeseed	x	
Akomic + rapeseed + 110		x

Temp, temperature; PRM, pin rotor machine; AMP, ampere; Perf, perfector.

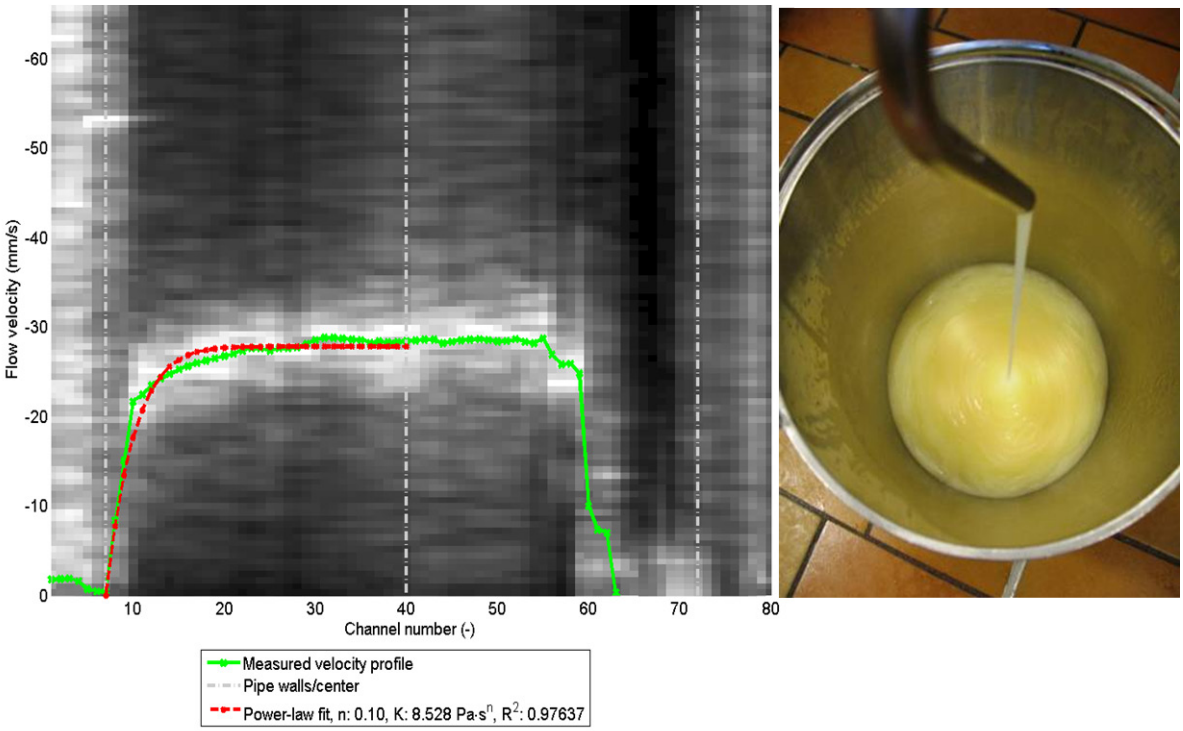

Figure 3.4 Spectral plot together with an arithmetic average of some 30 measured profiles (green) together with the resulting power-law fit (red) for the control system, i.e. 25% Akomic / 75% rapeseed TAG at a flow rate of 70 kg/h

As seen for the sample without additive (CRY110) in Figure 3.4, there is a strong shear-thinning behaviour, the power-law index is 0.1, and consistency index K is 8.53 Pas. The fit coefficient is satisfactory at $R^2 = 0.98$. However, the consistency index K between the two TAG blends is almost double for the fats blend with the CRY110 additive (Figure 3.5) at 14.4 Pas. The fit coefficient is satisfactory at $R^2 = 0.98$.

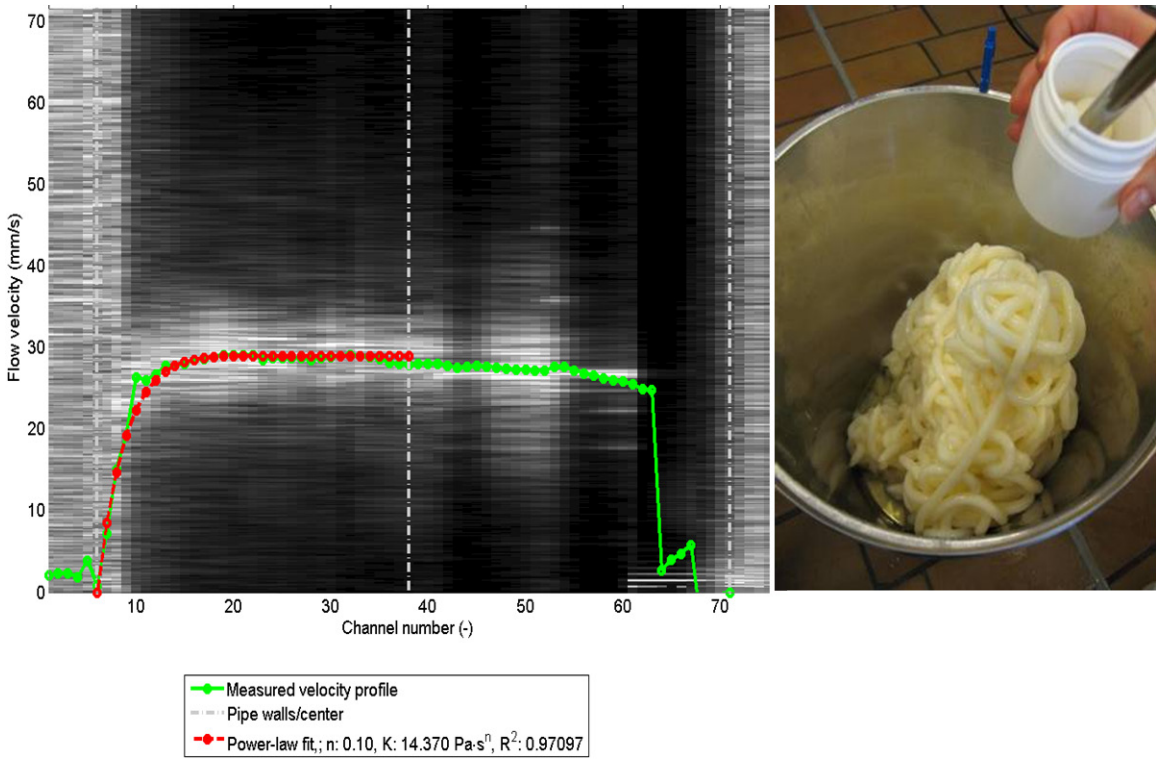

Figure 3.5 Corresponding spectral plot and ultrasound profile as an arithmetic average of 30 measured profiles (green) and resulting power-law fit (red) for the 25% Akomic / 74% rapeseed TAG and 1% CRY110 (Distilled monoglyceride) at 70 kg/h.

To appreciate the significance of these in-line results (Figure 3.4 & 3.5), the flow curves constructed from the velocity profiles for the samples with and without added CRY110 are given in Figure 3.6.

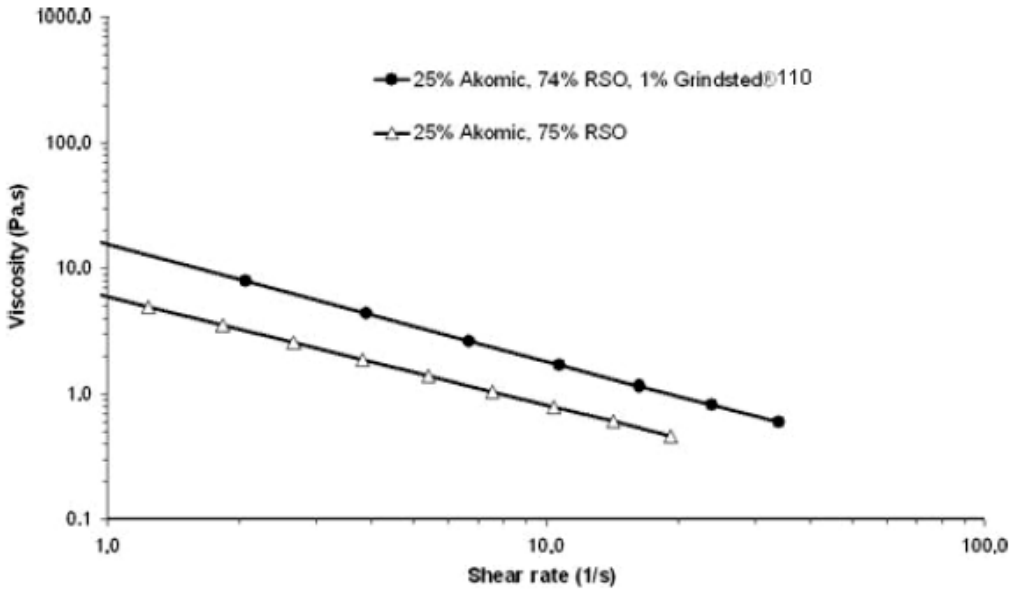

Figure 3.6 Comparison of the Akomic / Rapeseed (RSO) TAG blends; without additive (tetrahedrons) and with 1% CRY110 (circles)

The results in Figure 3.6 indicate that the sample containing the CRY110 had increased the viscosity of the control, and these in-line results were in agreement with previous off-line results, using a Haake Rheometer (3.3.1). It is clearly shown that the UVP-PD method could rheologically differentiate the TAG blend, with CRY110 (GRINDSTED® Crystallizer 110) and without additive. The viscosity of the TAG blend increased by almost a factor of 2 after the addition of CRY110 and thereby showed good agreement with the Haake off-line measurements.

The UVP-PD method directly allows measurements that were previously not possible with common rheometers; namely the inline determination of rheological properties and velocity profiles in real time. This therefore offers advantages over commercially available process rheometers and off-line measurements.

The systems tested were limited to model systems because of current transducer limitations and flow cell diameters, but nevertheless, a significant difference, essentially a doubling of the viscosity, was measured and quantified (Young et al., 2008).

3.4 Comparison and Validation

A further exploration was the next step, using upgraded UVP-PD apparatus with new upgraded transducers, measuring to wider temperature and pressure range, combined with rapid super-cooling in real-time. At this point the SFC values were determined under dynamic conditions and these values were compared from the UVP-PD measurement from those obtained from p-NMR data. This allowed comparison and validation between the two techniques.

The data presented in Wassell et al. (2010b), clearly shows the upgraded UVP-PD apparatus is comparable to the data reported previously (Young et al., 2008). Specifically, when considering the velocity profiles found within Figures 3.7 and 3.8, there is obvious effect in the power law consistency index values e.g. 6.6 – 6.7Pas, compared to 14.2 – 14.3Pas, the latter, being with the CRY110. These results (Wassell et al., 2010b) compare favourably with previous results (Young et al., 2008).

Clearly, the sample with added CRY110 has a shear viscosity of twice that found in the TAG blend without this additive. This compares well with previous off-line data (3.3.1) measurements (Young et al., 2008).

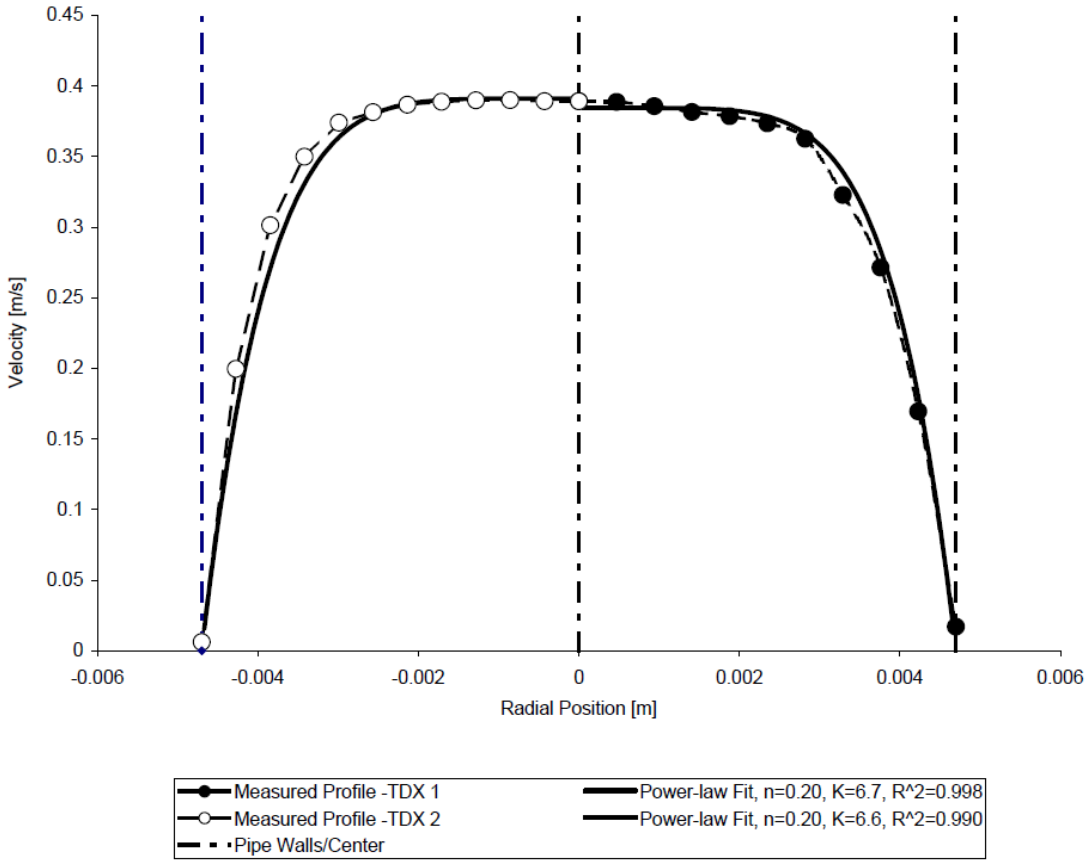

Figure 3.7 Measured arithmetic average over 28 velocity profiles and the resulting power-law fit for 25% Akomic / 75% rapeseed TAG without additive at a flow rate of 70 kg h^{-1} (The profiles were measured both opposite to- (Transducer 1, TDX1) and in the direction of the flow (Transducer 2, TDX2))

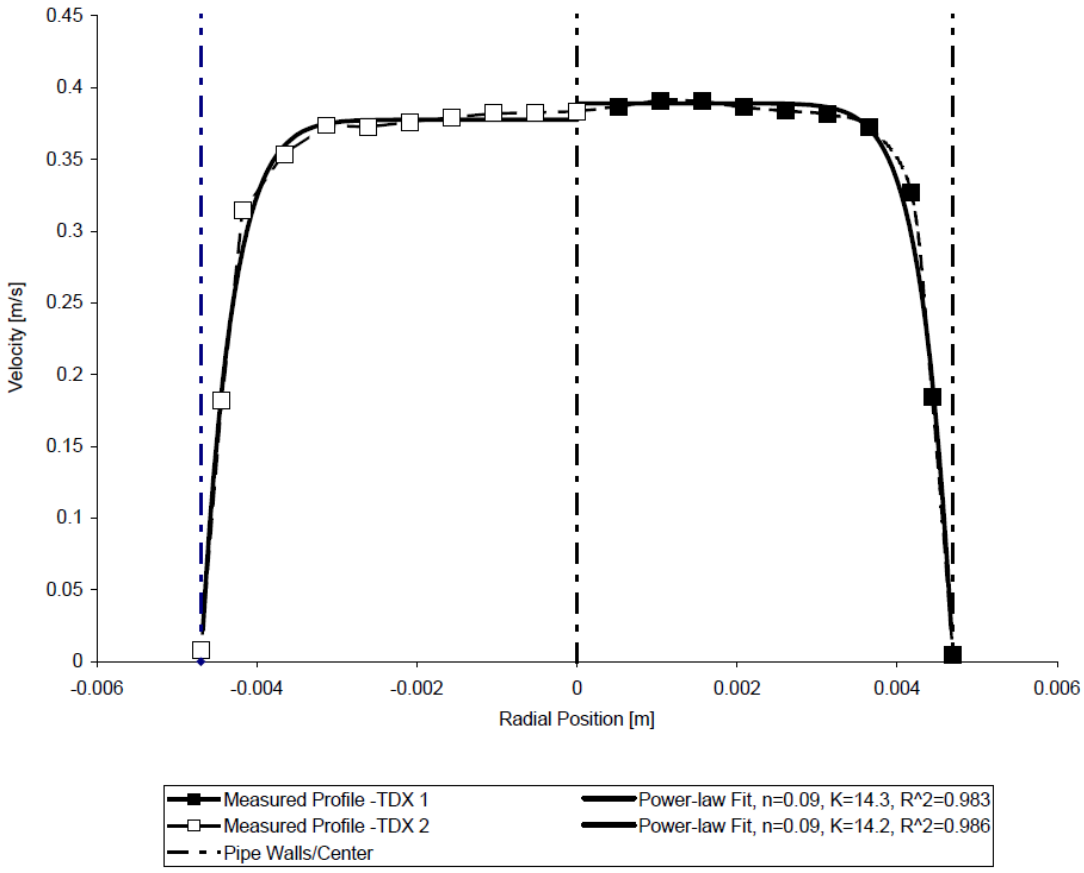

Figure 3.8 Measured arithmetic average over 39 velocity profiles and the resulting power-law fit for 25% Akomic / 74% rapeseed TAG with 1% CRY110 at a flow rate of 70 kg h^{-1} (The profiles were measured both opposite to- (Transducer 1, TDX1) and in the direction of the flow (Transducer 2, TDX2))

The evidence is convincing; the addition of 1% CRY110, leads to significant increase in viscosity of the TAG blend. This occurs in spite of the SFC of the TAG blends being similar (Wassell & Young 2007). No consequential influence on the SFC of either TAG blend is observed. These results imply that the mechanical strength of the TAG crystal network is not only determined by the SFC, but also points to a degree of structural changes developed within the TAG blend, where physical changes also influence the final structure.

Table 3.2 (Wassell et al., 2010b), shows response behaviour when subjected to process modification, where exothermic behaviour is observed at the pin-worker prior to UVP measurement.

Table 3.2 Exothermic crystallisation behaviour recorded after pin-worker, prior to UVP-PD measurement

Sample No.	A	B
Pump capacity (kg)	71.00	71.00
Centrifugal Pump (bar)	0.90	0.90
Pump pressure (bar)	3.00	2.50
Emulsion temp. C	54.60	55.50
NH3 (1st tube) °C	–28.30	–26.70
Temp (1st tube) °C	2.30	5.30
Temp PRM °C	12.70	17.90
Amp (1st tube)	270.00	278.00
Speed Pert 1 [rpm]	1000	1000
Speed PRM [rpm]	302	302
Akomic + Rapeseed	X	
Akomic + Rapeseed + Cryst. 110		X

This in-situ effect is potentially helpful to minimising any negative effects on the TAG blend during post-process storage. Therefore, the net effect is possibly more pronounced in the TAG blend containing CRY110, because this may minimise observable structural changes within the transducer flow-cell, in respect to the location (down-stream) of the UVP-PD analysis (Figure 3.2).

3.5 In-line Solid Fat Content

In line solid fat content (SFC) measurement was also explored and compared to a well established method using Bruker p-NMR (2.14). Other reviewed authors (Wassell et al., 2010a; Young et al., 2008), have examined the prospects of following TAG crystallisation by means of ultrasonic, in-line analysis. They have shown in-line detection of SFC is possible. However, SFC results gained under true dynamic processing conditions had not yet been reported until now (Wassell et al., 2010b). Results are presented in Figure 3.9, showing the SFC values as a function of temperature for a 30% palm stearin / 70% rapeseed TAG blend (Table 2.17), comparing the two methods, p-NMR and UVP-PD. While there is good correlation, the largest deviation is observed at the high temperature (40°C) and low temperature (10°C).

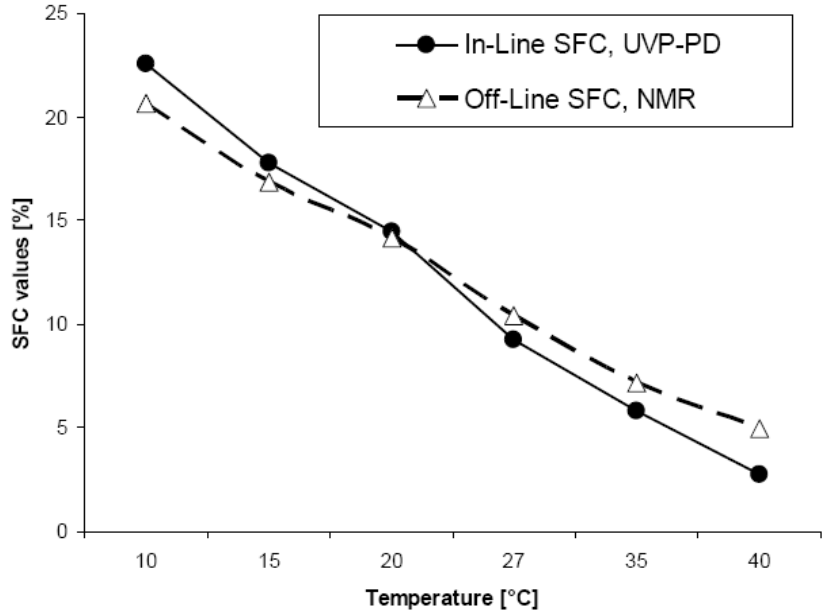

Figure 3.9 Solid fat content (SFC) expressed as percentage values versus temperature for 30% palm stearin / 70% rapeseed TAG measured by standard p-NMR technique (triangles) and in-line dynamic conditions from UVP-PD (circles)

A correlation of the data and minimal variation, confirms from the initial hypothesis (Young et al., 2008), that the UVP-PD can monitor the in-line rheology of anhydrous TAG blends, with a dynamic process condition. Specifically, the SFC measured differences are shown to result in a variation of not more than +/- 2% over the entire range, and within accepted experimental variation.

3.6 Conclusions and Recommendations

Many studies (Flöter & van Duijn 2006; Frederick et al., 2008; Garbolino et al., 2005; Mazzanti et al., 2005) have been performed using isothermal conditions where observations of crystal behaviour can be quite different from those observed whilst in a dynamic, non-isothermal environment (Wassell et al., 2010a).

The UVP-PD methodology clearly shows that true in-line rheological measurements of TAG blends are possible. The UVP-PD (Wassell et al., 2010b; Young et al., 2008) methodology (2.0) provided relative evaluation with accuracy in a dynamic state, when comparing in-line SFC values against off-line p-NMR (Povey & Challis 2006). Using this new technique as part of a composite / multidisciplinary perspective, it has been possible to examine the effect of a behenic fatty acid based MAG in a anhydrous TAG system whilst in a dynamic environment (3.0; Povey and Challis 2006).

Investigation of the TAG continuous phase, where there is predominate interest centred on reducing either *trans* fatty acids and or total saturates does not address the problem entirely. The addition of a water phase, creating an emulsion, automatically reduces the TAG content into the final application and can therefore redress the balance of total saturates. However, to effectively follow this route requires balanced emulsifier technology, because over and above a selected TAG blend, the combination of emulsifiers are also important as their interaction and influence on the TAG components can change the crystallisation behaviour and hence adjust texture (Wassell & Young 2007; Wassell et al., 2010a; Wassell et al., 2012a; 2012b; 2012c; 2012d; 2012e; Bech et al., 2013). It is recognised that

ultrasound can be used in an entirely different way, to stimulate nucleation by applying high-intensity ultrasound (Sato & Ueno 2011). This approach was not within the scope of the UVP-PD investigation, where the intention was to characterise bulk crystallisation, not stimulate it.

Future work is still necessary to observe behaviour and robustness of water – oil emulsion systems. The next apparent step is to introduce a water phase to observe effects of emulsifiers on physical behaviour. Testing a water-in-oil (W/O) emulsion proved problematic, due to the effects of pressure across the test apparatus (to be maintained below 4 bar max), specifically on the flow cells, due to potential stress and weakening to the prototype transducer housings. Despite this current limitation, it will be necessary to run these experiments with updated transducer housings (at time of writing, the transducer casing was upgraded. Refer to Figure E4: Appendix E) in order for instrumentation to cope with additional back-pressures. If several formulas are measured with a range of process parameters, information ought to become available about the optimal addition of a structurant e.g. single, mixed emulsifiers or other additive in reduced TAG dynamic environments (Wassell et al., 2010a; 2010b; Young et al., 2008). While this is important, because normally water droplet size is a usual parameter and indicator for emulsion integrity, it is not the only parameter. Attention was therefore turned towards interfacial tensiometry (4.0).

Additionally, palm oil crystallisation containing varied diglyceride (DAG) concentration ought to be investigated. DAG slows the crystallisation process and changes the melting behaviour (Siew & Ng, 1990; Siew, 2002). Control of the DAG content of palm oil may result with improvement of its crystallisation properties (Kristensen et al., 2005; Kristensen & Wassell 2006; Wassell & Young 2007). To compare the effect of several DAG concentration on rheological properties of TAG (RBD Palm) based systems (with and without aqueous phase), a static off-line rheological profile, together, using the UVP-PD method, could provide new rheological information.

4.0 Rheology and Interfacial Surface-Interactive Behaviour of Mixed Surfactant Systems

4.1 Summary

As part of a multidisciplinary approach in attempting to reach a clearer explanation of the functionality of low saturated fat systems, it is necessary to examine response changes in fat crystallisation as a function of interfacial and rheological behaviour. Furthermore, what effect would introduction of a novel food structuring material have on the interfacial behaviour of well known and regulatory approved materials?

This work follows a natural progression from the pilot study examinations of crystallisation speed and fatty acid diversity (1.5; 3.0).

As part of a diverse experimental approach, a series of measurements using tensiometry and rheology are used to examine MAG of differing degrees of saturation and chain length. In the context of emulsions, the behaviour of selected MAG is also examined with and without the use of PGPR.

The interfacial tensiometry measurements of a Moringa MAG have shown unusual decreased interfacial tension (γ) behaviour not dissimilar to PGPR. All other tested MAG (excluding a behenic based MAG), irrespective of their fatty acid compositions resulted in higher γ tension values across a wide temperature spectrum (50°C to 5°C). Both IRS and bulk rheology measurements showed visco-elastic / structural changes. A Moringa based MAG and its interactive behaviour with a behenic based MAG (CRY110) may be significant.

New learning from these measurements helps to provide important data, which supports several new patent applications (Wassell et al., 2012a; 2012b; 2012c; 2012d; 2012e; Bech et al., 2013).

4.2 Interfacial Tension - An Interfacial Examination of Single and Mixed MAG Behaviour: Effect of Saturation and Chain Length

4.2.1 Introduction

Although many food products are essentially emulsions, interest in the structuring of water-continuous emulsions is not necessarily straightforward, especially where more novel structuring materials are used either wholly or partially to replace traditional structurants (Wassell et al., 2010a).

In attempting to reduce the degree of saturates in food systems, it is necessary to observe effects on mixed structurants and analyse the relationship when co-surfactant structures are used and how this may influence interfacial film thickness, viscosity, strength and flexibility. These parameters will likely have varying degrees of influence towards interfacial stability of the formed emulsion and hence potentially aid maximum stability against coalescence (Krog 1977).

In the production of low fat spreads it is common to employ at least two emulsifiers (Garti & Remon 1984). In this regard, Garti and Remon (1984), studied the degree of unsaturation and the relationship between nature of vegetable oil, emulsifier and the stability of WO emulsions. Their study (Garti & Remon, 1984), focused on reduced fat 60% emulsions prepared with 5 wt % of a treated polyglycerol ester (specification not provided). These results showed that as the nature of the solvent edible oil became more unsaturated, there is a tendency towards more stability when selecting emulsifiers of similar unsaturation. Goubran and Garti (1988) reported the benefit of using high molecular weight polyglycerols (PGPR) and recognised that while much had been reported on their behaviour in OW emulsions, there appeared to be lack of understanding regarding their behaviour in WO emulsions.

Theory, suggests some emulsifiers are able to act as templating agents with other surfactants, thereby resulting in increased strength of the interfacial membrane between the oil and water phases. At a given interfacial emulsifier concentration, temperature, and time, the surface of the water droplets will be partially or totally

covered (Johansson et al., 1995; Garti et al., 1998) with fatty acid chains likened to a fat crystal surface (Krog & Larsson 1992).

In the case where PGPR and a MAG are used, the MAG is used to form template or monolayer for heterogeneous crystallisation, while the PGPR may be used for emulsion stability. However, at a certain critical micelle concentration (CMC) and or change in temperature, the interaction to maintain, or form further template formations may be either disturbed or strengthened. The formation for a template for further crystallisation (Arima et al., 2009) is described in Figure 4.1.

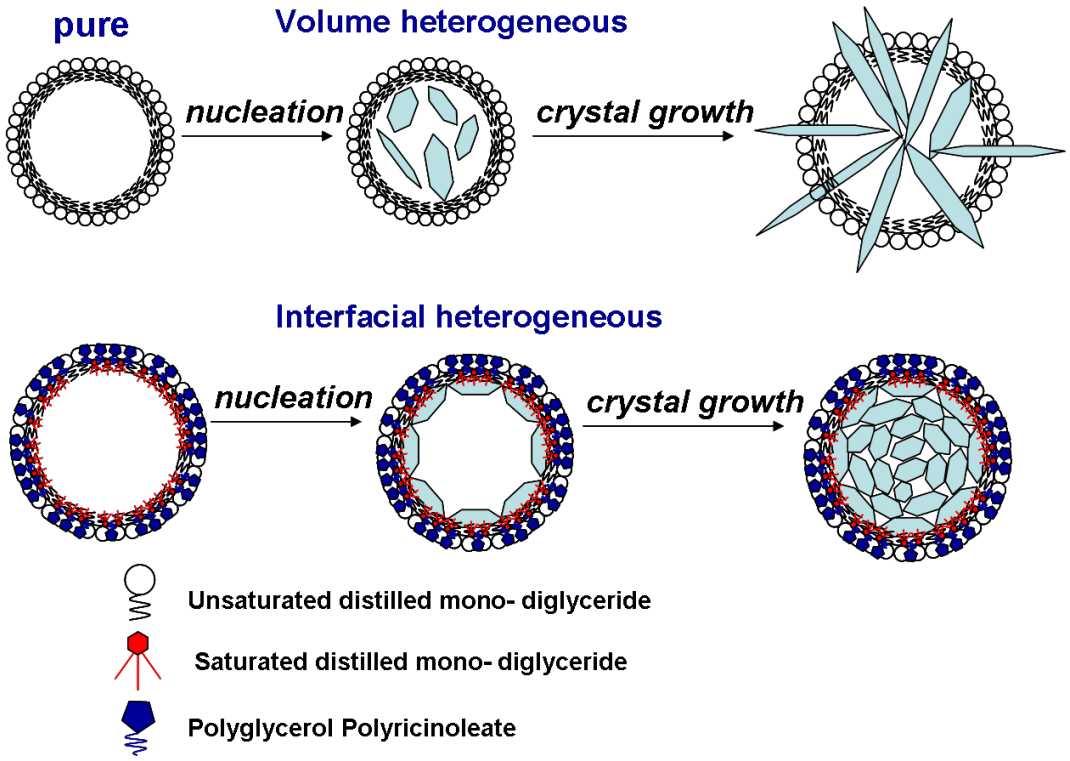

Figure 4.1 Schematic of template mechanism for heterogeneous crystallisation of O/W emulsion with additive (Saturated distilled mono-diglyceride). Adapted from Arima et al., 2007 (Wassell et al., 2010a)

Although Figure 4.1 describes an O/W emulsion and the type of emulsifier could be different from case to case, it nevertheless shows the basic principle of interaction and can be applied to Figure 4.2 which describes the same process with a W/O emulsion.

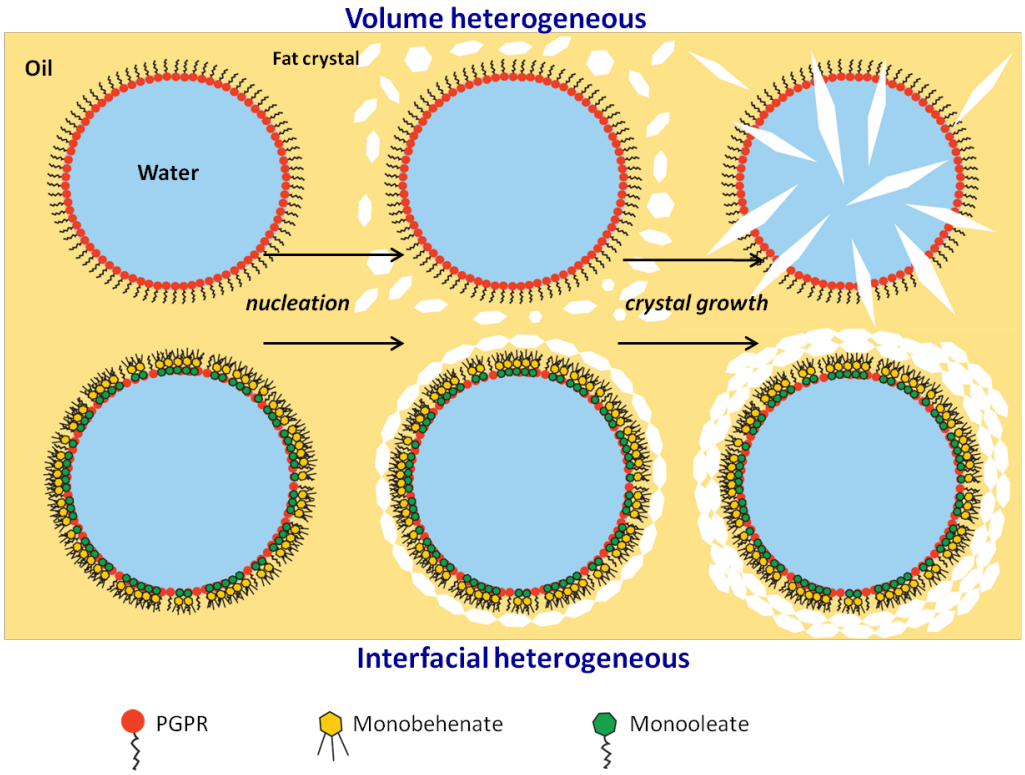

Figure 4.2 Schematic of proposed template mechanism for heterogeneous crystallisation of W/O emulsion with additives (PGPR, Monooleate, Monobehenate) (Wassell et al., 2010a)

The saturated distilled MAG acting as a "crystalliser" forms a template for heterogeneous crystallisation at a particular concentration. In the case of W/O emulsion, which is applicable to low fat W/O spreads, the scenario is possibly as proposed in Figure 4.3, where the additive (crystalliser) is behaving as a template. This situation might explain the increased textural behaviour of the very low fat (12%) W/O emulsions observed in 1.5.3

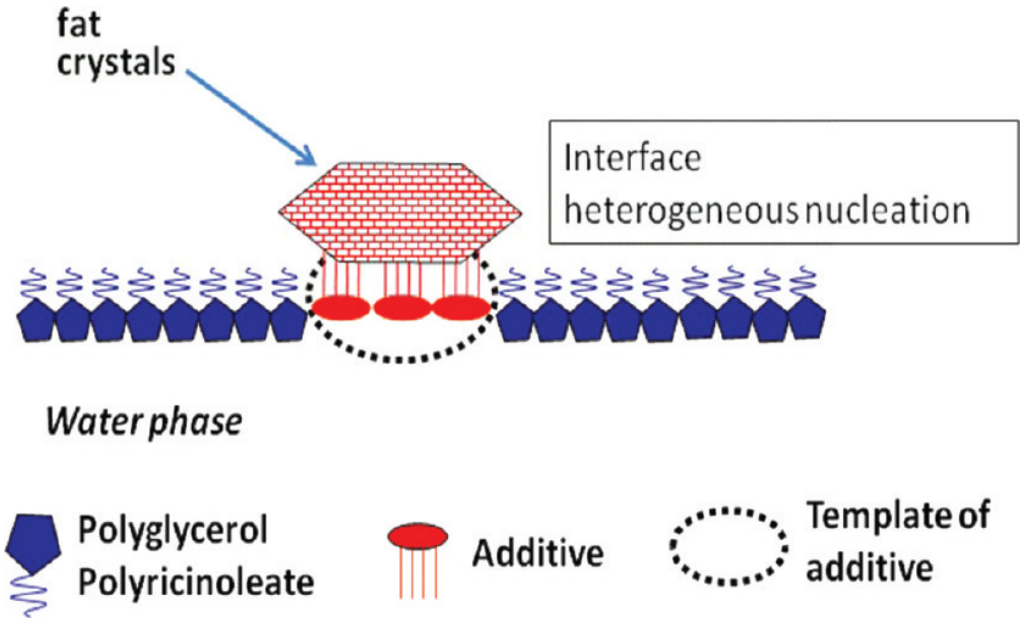

Figure 4.3 Proposed schematic showing interfacial crystallization at the water-in-oil interface (Source: Wassell et al., 2012)

Surprisingly little is found in the literature about the surface-interactive behaviour of mixed surfactant systems (1.6; 1.7; Wassell et al., 2010a). A preliminary examination, by way of a pilot study (1.5) clearly shows there is apparent influence of behenic based (C22:0) MAG (GRINDSTED® Crystallizer 110, abbreviated CRY110) on the physical properties of fat blends (1.5.1; 3.0) and emulsions (1.5.3). Therefore, as part of this multidisciplinary approach to discover physical differences that affect the surface interface, strength and elasticity for making reduced saturated emulsions, a study of interfacial tension of oil / water systems containing emulsifiers was made.

The intention of this study is to show the effect of temperature induced changes through a series of complementary non-isothermal measurements as a function of temperature rather than time (De Graef et al., 2006); then to investigate the surface tension and rheology of several MAG of differing fatty acid profiles (different saturation and chain length), which are examined as single MAG and mixed MAG. These are also combined with novel Moringa MAG and PGPR.

4.2.2 Materials and Methods

Previous studies found in the literature, chose a lower starting temperature, decreasing from within a range of 40°C to 5°C (Krog 1990; Krog & Larsson 1992). This investigation measures from a higher temperature (50°C) to account for melting behaviour of a variety of MAG (2.0). The individual emulsifier concentrations in these tests were 0.02% (unless otherwise indicated) with no additional proteins. Krog (1990) measured at higher concentrations (0.2% - 0.3%), possibly to account for the water phase containing a default concentration of milk protein (0.01%). The emulsifier inclusion rate was initially selected at 0.002% but response behaviour was below the limit of meaningful detection. No comparisons could be made. Emulsifier concentration was increased to 0.02%. The interfacial tension of oil/water systems was measured on a Digital-Tensiometer, model K10ST (Krüss Germany), using the Wilhelmy plate method (Refer to general Materials & Methods, 2.0).

4.2.3 Results and Discussion

Figure 4.4 shows considerable difference in tension behaviour between sunflower based distilled MAG - DIMODAN® UJ (UJ) at 0.02 / 0.06% and PGPR 90 at 0.02%. Increasing UJ to 0.06% resulted in slight decrease compared to 0.02% inclusion. When both UJ & PGPR combined, results showed a small increase in tension compared to PGPR only.

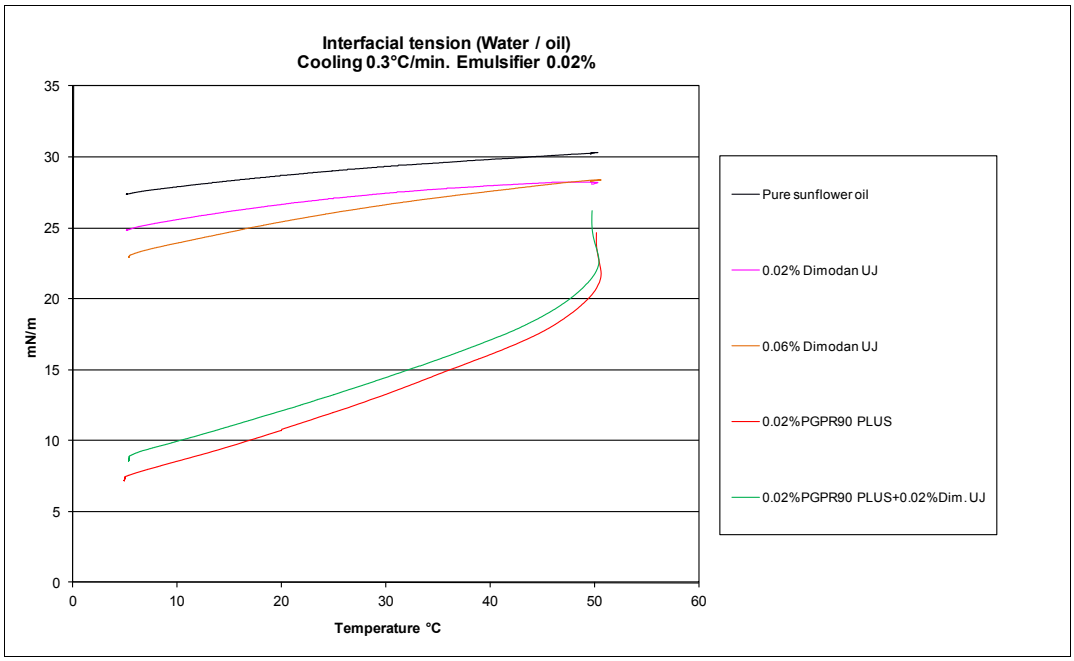

Figure 4.4 Tensiometry values for PGPR 90 compared with unsaturated MAG based on sunflower oil (DIMODAN® UJ)

Assuming that PGPR inhibits the effect of CRY110, then the following question must be addressed: What is the effect of CRY110 and does it have any interaction with PGPR or Dim UJ?

Figure 4.5 shows that a fully saturated MAG, rich in C22:0 (CRY110) both individually and together with UJ (C18:1 / C18:2). Upon reaching towards 20°C, a critical temperature is attained and a considerable rate of reduction in surface tension occurs.

Where PGPR is present there is initial rapid decrease of ~5mN/m, from the starting temperature at 50°C. All PGPR containing variants continued to gradually decrease in tension from ~22mN/m to ~12mN/m, following a linear slope. When reaching a critical interfacial tension temperature (Tγ) 15°C the PGPR blends fall dramatically to 10°C. However, the PGPR alone continues on a linear slope to approximately 5°C where measurement continues for 5 minutes. No further reduction in tension occurs.

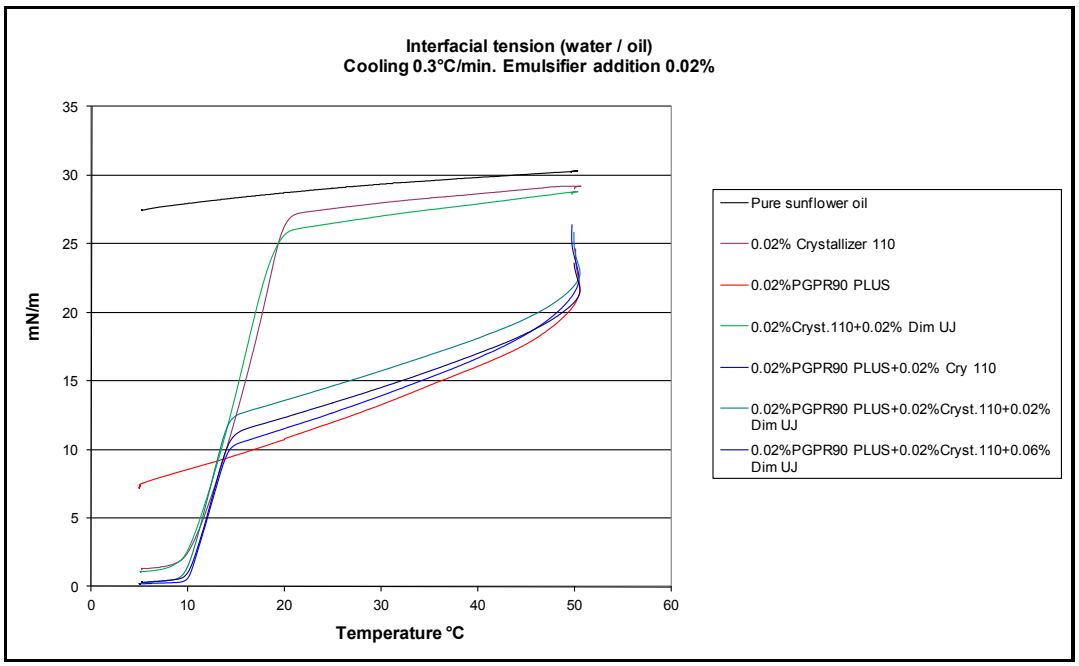

Figure 4.5 Interfacial tension behaviour of emulsifiers used in preliminary application tests for 12% WO emulsion (1.5)

Where PGPR is present, the situation in Figure 4.5 occurs in all cases irrespective of emulsifier concentration, ratio, relative to PGPR (Dim UJ at 0.06%).

Given that PGPR and CRY110 are entirely different emulsifiers, it would seem reasonable to assume, that through exchange, competitive adsorption occurs (Krog 1990). Both CRY110 and PGPR are lipophilic. PGPR is highly polar towards water, having a larger hydrophilic head group (polyglycerol) compared with CRY110 (MAG) and also has a large hydrophobic polyricinoleic acid chain.

The situation in Figure 4.5, strongly suggests PGPR is highly surface active (Wassell et al., 2010a), at lower concentrations, dominating the interface (Dedinaite & Campbell, 2000; Rousseau, 2000). The likely reason for this is due to required physical properties of MAG, which are governed by temperature (Krog & Larsson, 1992). The development of surface-active formations from the CRY110 does not occur until the C22:0 rich MAG reaches Tγ.

Table 4.1 Emulsifier specifications supplied courtesy of Danisco A/S, Denmark

DIMODAN®	U/J	RO	P	HP	CRY110
TAG source / Fatty acids (%)	Sunflower	Ricebran	Palm	Fully Hardened Palm	FHHEAR [#]calculated
C14:0	0.1	0.4	-	1	-
C16:0	7	**20.5**	**44**	**55**	-
C18:0	5	2.1	5	**43**	**5**
C18:1	**28**	**41.3**	**39**	0.1	-
C18:2	**58**	**32.5**	**10**	0.2	-
C18:3	0.1	1.3	0.3	-	-
C18:0 total	*91.1*	*75.9*	*54.3*	*43.3*	*5*
C20:0 >	1	2.2	0.2	0.7	**95**
C22:0 total	-	*0.2*	-	-	*85*
Saturated total	*12*	*24*	*49*	*100*	*100*
IV (app.)	*105*	*103*	*45*	*2*	*2*

PGPR combined with a second or third emulsifier is perhaps more surface active until ~15°C, whereby Tγ is observed. Standalone or mixtures of CRY110 with PGPR follow a near linear shift from 20°C to 10°C, and converge with the same inflection where PGPR is present as a single emulsifier at ~15°C. This suggests a rearrangement / displacement (Marze, 2009) of the PGPR at the interface; and is effectively "forced" or exchanged into a new geometry in the presence of CRY110. PGPR continues to dominate (Gülseren & Corredig 2012) the surface arrangement until broken at 15°C (Shimada & Ohashi, 2003). Therefore, the effect of PGPR suppression is now dominated by CRY110 at a Tγ ~15°C onwards. The behenic rich (C22:0) MAG crystals are more surface active and an exchange through competitive adsorption occurs (Krog 1990).

Speculation exists as to whether a similar effect might be observed when interchanging the C22:0 based MAG for one predominately rich in C16:0 or C18:0, where not only the degree of saturation but also the chain length might have an interaction (Table 4.1). The next step asked whether this happens specifically because the MAG is C22 chain length.

Figure 4.6 shows DIMODAN® P, a partially saturated MAG based on refined palm oil and DIMODAN® HP, a fully saturated MAG based on fully hydrogenated palm. The latter, DIMODAN® HP - rich in C16:0 / C18:0, appears to decrease tension very slightly in relation to the former, DIMODAN® P (C16:0).

It would seem that MAG as single emulsifiers are affected by temperature on interfacial tension. This seems to be more pronounced with long-chain MAG than with short-chain MAG. Furthermore, the relative decrease in interfacial tension, when the temperature is lowered, is higher the longer the chain length. This confirms the same findings as Krog and Larsson (1992), who did measure C18:0 rich MAG and showed these gave lower tension values compared to C16:0, but did not lower tension values near or lower to MAG rich in C22:0.

A mixture of PGPR and MAG rich in C18:1 / 18:2 (DIMODAN® UJ) & C16:0 / C18:0 (DIMODAN® HP) did not improve on PGPR alone. Only a mixture of PGPR and MAG rich in C18:1 / 18:2 (DIMODAN® UJ) & C22:0 (CRY110) resulted on tension impact at $T\gamma$ ~15°C. This effect must be entirely influenced by C22:0 rich MAG (CRY110).

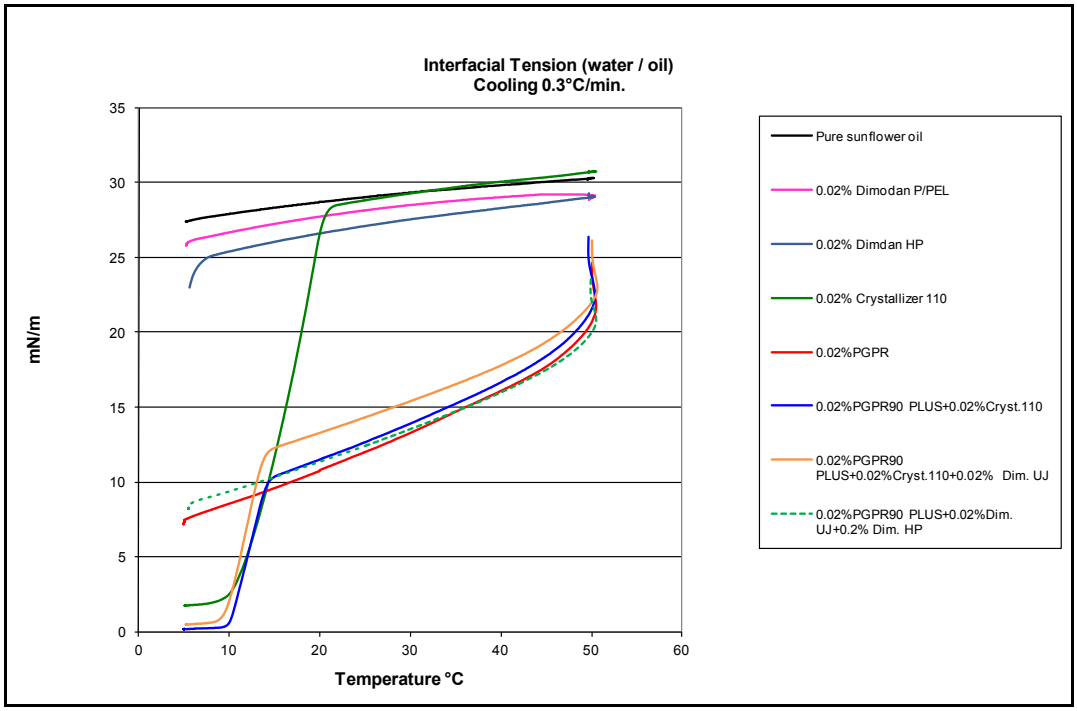

Figure 4.6 Single MAG: DIMODAN® P, a partially saturated MAG (rich in C16:0) and DIMODAN® HP, a fully saturated MAG (rich in C16:0 / C18:0), compared with CRY110 (rich in C22:0); and mixture of DIMODAN® HP (dotted line), compared to mixtures of CRY110

After an initial steady fall in tension from the upper temperature towards lower temperature, results from Krog (1990) showed dramatic fall of interfacial tension once a critical temperature ($T\gamma$) had been reached. This behaviour could possibly have occurred more accentuated if the emulsifier concentration had been increased to individual concentrations of between 0.03% - 0.3%. However, a risk of total emulsifier overload could possibly mask small differentiations.

In this examination only liquid sunflower oil was used as the solvent. Where there were obvious signs of crystallisation, the test samples containing C22:0 changed the translucence of the oil, turning milky white. In the context and study of interfacial behaviour, crystallisation at the surface or interface is suggested to be faster than nucleation and crystal growth in the bulk oil, particularly when the

emulsification process also involves cooling. As the emulsifier crystals orientate, they position methyl end group towards the oil and the polar heads towards water. These are referred to as *surface-active* crystals (Krog & Larsson 1992).

4.2.4 Conclusion

This study not only confirms findings from the pilot study preliminary investigations (1.5), where it was shown that behenic fatty acid based MAG or dilutions have a pronounced effect on crystallisation; These new interfacial measurements clearly demonstrate an unusual surface-interactive relationship. They may also partially explain textural behaviour previously observed in application trials of 12% WO emulsions (1.5).

MAG as single emulsifiers are affected by temperature on interfacial tension. This seems to be more pronounced with long-chain MAG than with short-chain MAG. The relative decrease in interfacial tension, when the temperature is lowered, is higher the longer the chain length. This confirms the same findings as Krog and Larsson (1992), who did measure C18:0 rich MAG's and showed these gave lower tension values compared to C16:0, but did not lower tension values near or lower to MAG rich in C22:0.

A mixture of PGPR and MAG rich in C18:1 / 18:2 (DIMODAN® UJ) & C16:0 / C18:0 (DIMODAN® HP) did not improve on PGPR alone. Only a mixture of PGPR and MAG rich in C18:1 / 18:2 (DIMODAN® UJ) & CRY110 resulted on tension impact at $T\gamma$ ~15°C. This effect must be entirely dominated by C22:0 rich MAG (CRY110).

Whether similar behaviour could be observed in other solvents e.g liquid / solid TAG mixtures remains to be discovered. Irrespective of this, it may be beneficial to re-run these samples in controlled rheological measurements to observe if there is any functional effect on viscoelastic behaviour, the outcome of which may have implications for real bulk TAG and W/O (TAG) emulsions.

4.3 A Rheological and Interfacial Examination of Single, Mixed and Novel MAG Behaviour: Effect of Saturation and Chain Length in Anhydrous Bulk and Water-Oil Systems.

4.3.1 Introduction

Based on the conclusion in 4.2.4, attention was turned to interfacial and bulk behaviour where single, mixed and novel MAG behaviour was examined to observe the effects of saturation and chain length in anhydrous bulk and water-oil systems. This is important, because in real emulsion systems, interest lies in the properties of the interfacial film and its viscoelastic behaviour, where surface elasticity is thought to be the determining factor in minimising film rupture (Boyd et al., 1972) and hence coalescence. The strength of the interfacial film formed by the emulsifier may be more important than its effect on interfacial tension (Scherze, Knotha, Muschiolika, 2006).

Rheograms were obtained by plotting dynamic change in the elastic modulus (G') and viscous modulus (G'') of the crystallising sample as a function of the crystallisation temperature (non-isothermal).

4.3.2 Interfacial Rheological System (IRS) Measurements

Interfacial rheology and bulk rheology, were investigated using Physica MCR 301, and data driven from RHEOPLUS/32 V3.21 software (Anton Paar, Germany GmbH). Oscillatory interfacial method was used to measure interfacial properties of interfaces covered with surface active molecules. Emulsifiers were weighed for rheology measurements at 0.2% w/w (unless otherwise indicated) and the solvent (RBD sunflower oil) balanced to 100% (Refer to general Materials & Methods 2.0).

Bulk rheology measurements were used to provide real constants for upper fluid density and viscosity values for interfacial analyses. Complex viscosity is based on constants of upper fluid density and viscosity parameter for Sunflower oil at 50°C and the lower fluid density and viscosity parameter for water was 50°C. These constants were used as a function of all 151 data points. The analysis method for calculation of complex interfacial viscosity (η*i) by frequency sweep measurements, with a bi-cone measuring system, are computed by known rheological and mathematical regression formula (Oh & Slattery, 1978; Ray, Lee, Jiang, & Jiang, 1987; Lee, Jiang, Jiang, & Avramdis, 1991; Nagarajan, Chung, & Wasan, 1998). The interfacial properties are then calculated by analysing the raw data using RHEOPLUS/32 V3.21 software. Ideally, the calculation of complex interfacial viscosity eta-i, is completed for each of the 151 data points.

4.3.3 "True" Dynamic Complex

Further explanation is required here regarding complex interfacial viscosity η*i, this is difficult and remains a limitation of the mathematics controlling the software. For each temperature change, density as well as the viscosity of the bulk and upper phase change, simultaneous regression analysis becomes too complex to solve, because there are too many changing parameters at the same time. Further, RHEOPLUS/32 V3.21 software is unable to accommodate changing densities. When calculations are based on absolute values, this presents problems in the regression analysis, where a small negative G' is introduced, causing "overcompensation". This artefact is difficult to eliminate (Appendix H).

4.3.4 Results and Discussion

It is important to note that where measured and studied, the viscous (G'') and elastic (G') moduli of several types of commercial MAG, using interfacial rheology system (IRS), shown in Figure 4.7 were observed only with CRY110 and mixtures of other MAG that resulted in development of both G'' / G' in samples. Pure CRY110 is highly surface active at <20°C as shown from previous tensiometer measurements (4.2).

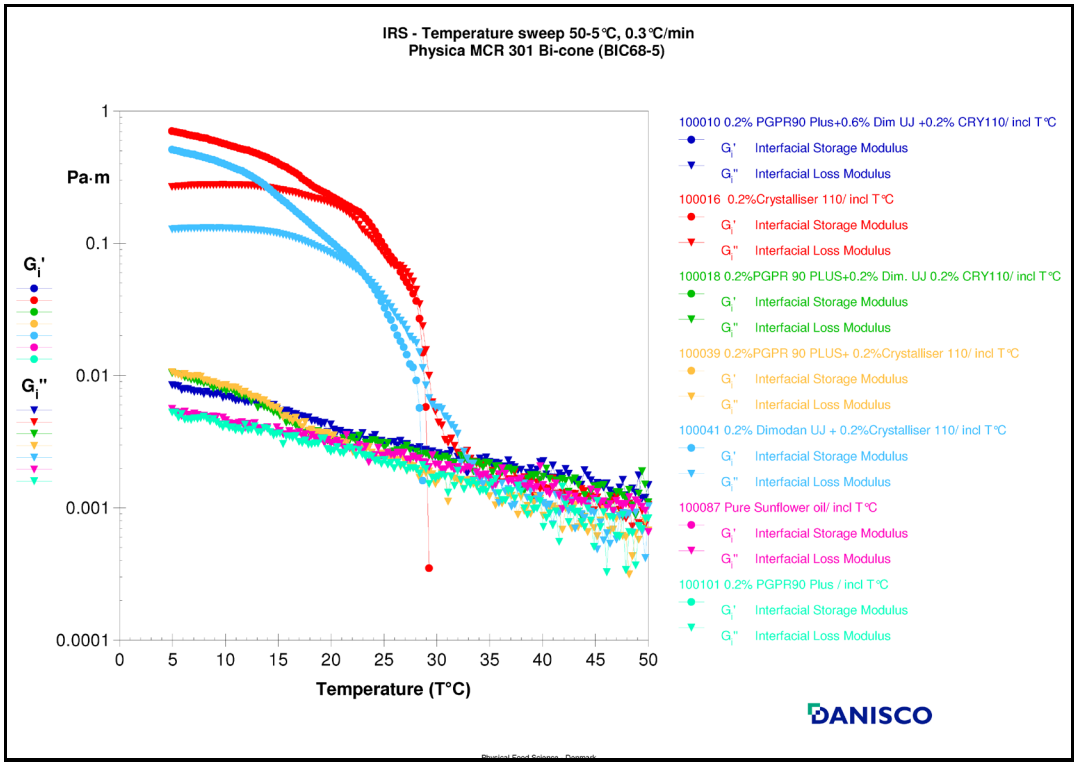

Figure 4.7 Interfacial Rheology System (IRS) temperature sweep and resulting complex modulus G_i' and G_i'' of CRY110 (rich in C22:0) alone compared to PGPR and other emulsifier mixtures.

The temperature sweep shows that CRY110 is quite different from PGPR. The presence of highly unsaturated MAG – Dim U/J with CRY110, impacts on both G_i' and G_i''. The bulk oil phase reveals a similar picture (Figure 4.8), in that CRY110 shows an elastic modulus (G'). The presence of an aqueous interface

(Figure 4.7) affects the onset of both G_i' and G_i'' at 30°C compared with the anhydrous (Figure 4.8) bulk phase.

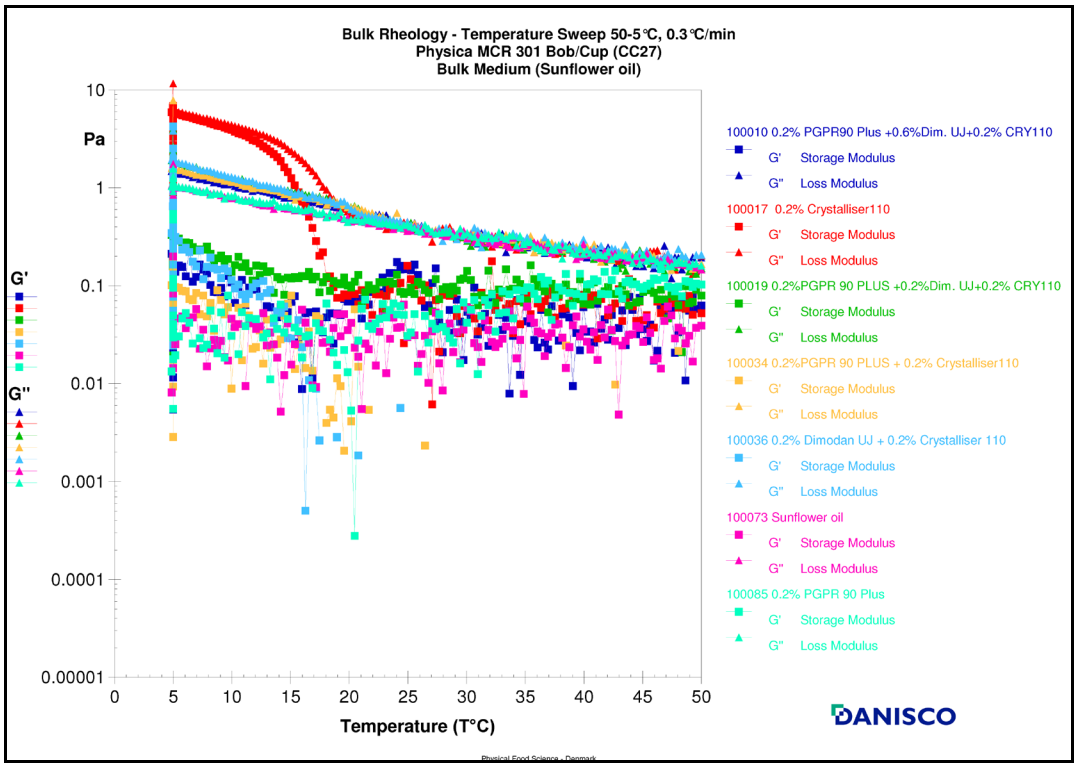

Figure 4.8 Bulk temperature sweep and resulting G' and G'' of CRY110 (rich in C22:0) alone compared to PGPR and other emulsifier mixtures.

The results shown in Figure 4.7 and 4.8 seem to correspond to the tensiometer measurement in Fig. 4.5 (see 4.1). It is suggested that the behaviour is due to a development of stronger monolayer formation and corresponding affinity to the oil phase is observed because of its C22 fatty acid configuration. This argument is now supported by results from interfacial rheology (Figure 4.7), whereby with continued onset of cooling to ~29°C, both G' and G'' begin to develop. Upon reaching 18 – 20°C, the CRY110, with and without Dim U/J attains a G'' plateau. At a similar gradient, a continued trend is observed in development of the elastic modulus G'.

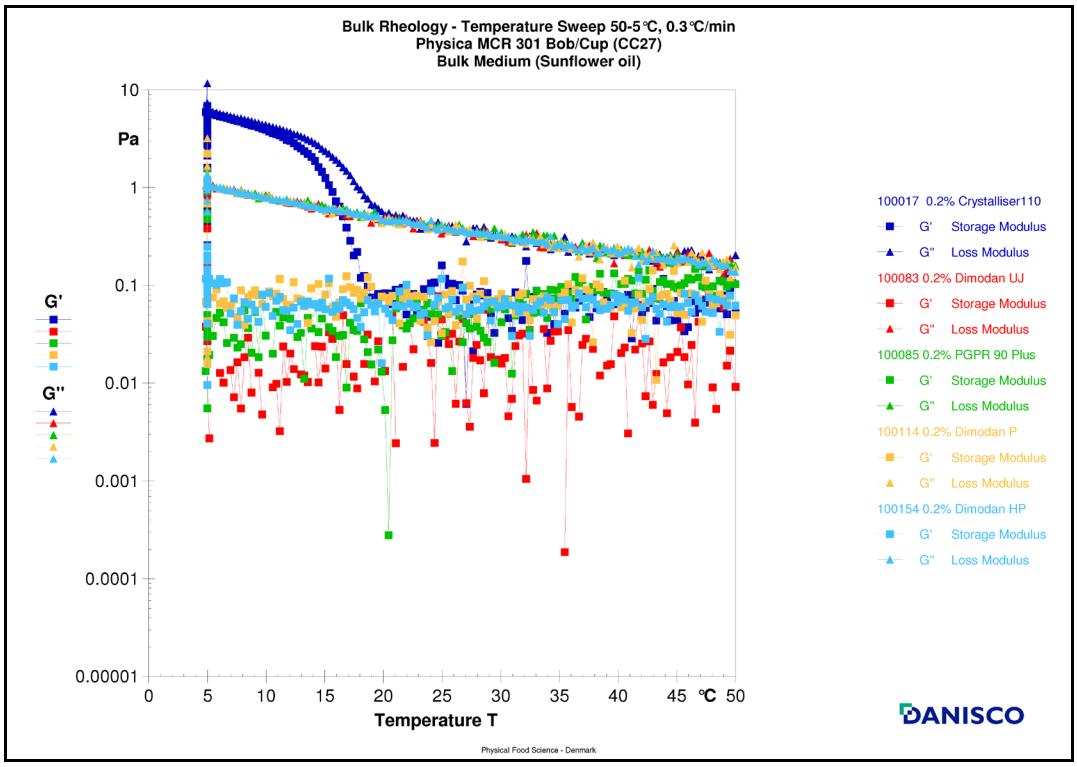

Figure 4.9 Bulk measurement of the single emulsifiers compared to CRY110

In Figure 4.9 and 4.10, the bulk and interfacial temperature sweeps show the same single emulsifiers measured using tensiometry (Figure 4.4 / Figure 4.5). Only the DIMODAN® HP (C16:0 / C18:0) exhibited a small increase in G'' compared to CRY110.

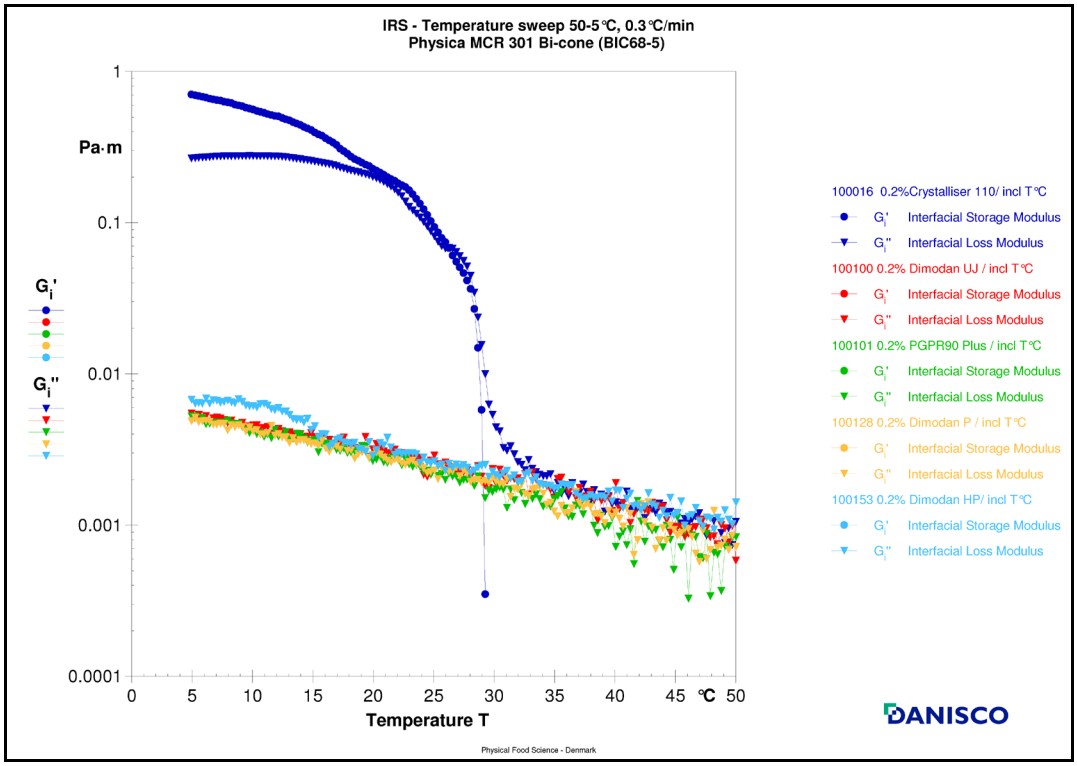

Figure 4.10 Comparison of interfacial behaviour of single emulsifiers compared to CRY110 (C22:0). Dim HP shows small change in G''

When combined with PGPR and UJ, the CRY110 has slightly greater G'' values compared with DIMODAN® HP. The tensiometry readings in Figure 4.6 clearly showed the effect of combining PGPR with UJ, and CRY110 or HP. A MAG rich in C22:0 (CRY110) has stronger interaction with PGPR / UJ compared to HP. A similar evidence is seen in Figure 4.11 and Figure 4.12 which show a small deviation observed from ~15°C – 18°C where there is a small build-up of G'' in bulk and interfacial behaviour. A slight build-up of G' is also found in the bulk.

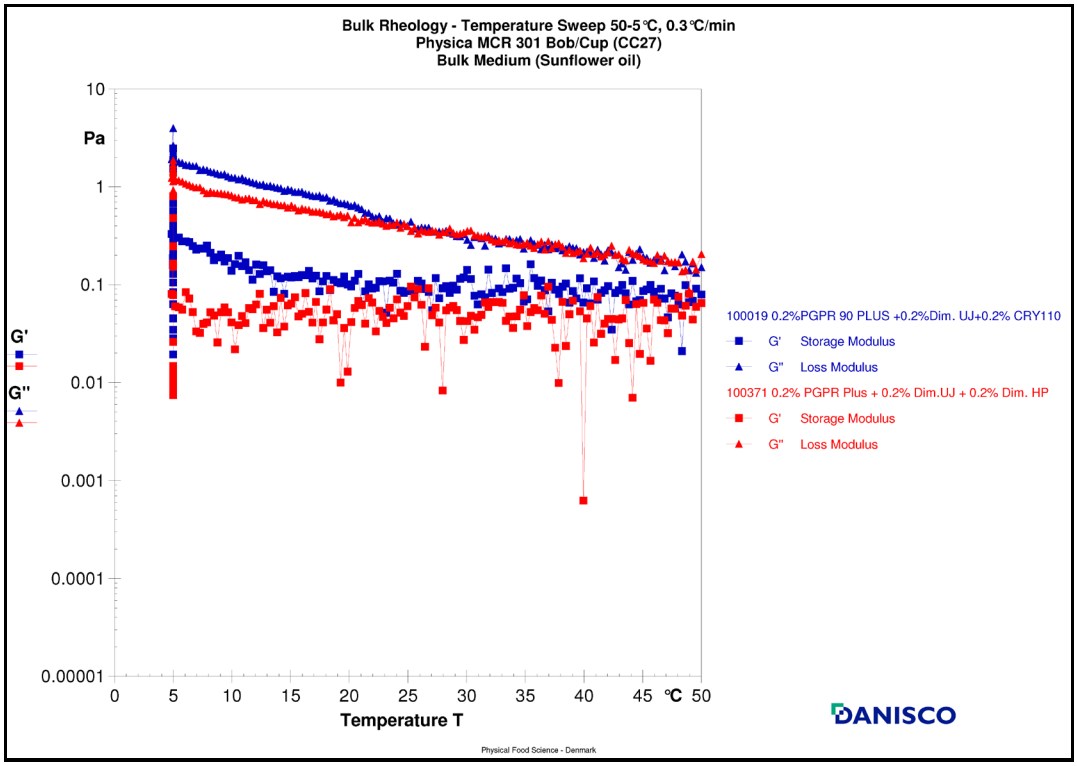

Figure 4.11 The influence of a MAG rich in C22:0, where CRY110 affects both G'' and G'

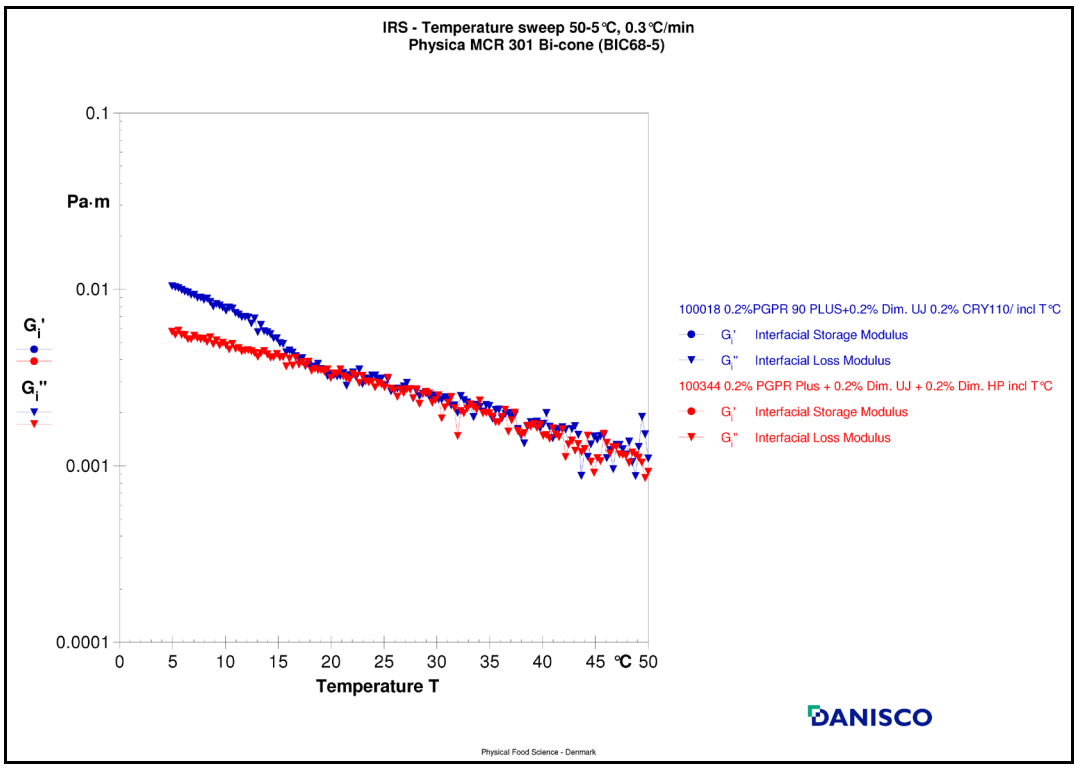

Figure 4.12 The effect of CRY110 compared with HP in combination with PGPR and UJ

The results from IRS and bulk rheology seem to concur with tensiometry data; when PGPR is not present, higher tension values are observed. The interfacial rheology data show higher viscosity without PGPR. At 18 – 20°C in both interfacial rheology and tensiometry, there is clear increase in G' and sharp decrease in interfacial tension respectively (Figure 4.5 & 4.7). This particular effect is likely observed because of the factors previously mentioned (temperature / time dependant changes occur). A similar outcome occurs whether in the bulk phase, or with additional presence of an interface (water), so that while PGPR does seem to suppress CRY110, this does not occur across the whole measured temperature range.

A form of synergy seems to occur, where one emulsifier (PGPR) lowers interfacial tension – early in process and the second emulsifier (CRY110) dominates the surface tension faster as the material approaches a dramatic fall of interfacial tension once a critical temperature (Tγ) had been reached (Krog 1990). A comparison of IRS and bulk rheology suggests this behaviour is onset earlier in the presence of a water phase. This will be examined in more detail through application measurements (5.0).

4.3.5 Emulsifier Similarity

In the Bulk oil phase (Figure 4.8) PGPR or Dim U/J are causing suppression to G' development, whereas interfacial rheology (Figure 4.7) demonstrates that Dim U/J is not disrupting assemblies or causing displacement because there is definite build up of G' in the presence of CRY110. Similar is observed in Figure 4.5, where Dim U/J does not have strong interaction with CRY110 to cause earlier tension drop and follows the same pattern as standalone CRY110. Possibly this occurs due to similar affinity at the interface and or similar dielectric compatibility to each other so that despite these structures having radically different fatty acid configurations, these binary MAG mixtures are apparently still miscible (Ueno, Suetake, Yano, Suzuki, & Sato, 1994). However, a broader examination of binary ratio's of MAG, coupled with a new temperature constant for each change in density as well as the viscosity of the bulk and upper phase change, if this was possible (refer to 4.3.3), may reveal undiscovered transition temperatures (Ueno et al., 1994).

4.3.6 Tension Reduction

The interactive behaviour of a MAG combined with PGPR observed within the scope of these measurements has significance for real W/O emulsions, specifically e.g. low fat spreads. It is found to be the case that tension is very low at typical product packing temperatures, between 10°C – 20°C. The interfacial tension of C22:0 fatty acids (in CRY110) and interactive behaviour of surface active 'crystals' may partially explain the presence of G'. Further, when CRY110 is combined with PGPR, it is considered potentially important as a partial explanation to the cause of why apparent thickening is observed (1.5).

If it was possible to find a novel emulsifier from an edible oil source, being non-hydrogentated (unmodified), this would have potential commercial advantages (Wassell & Young 2007; Wassell et al., 2010a; Wassell et al., 2012a; 2012b; 2012c; 2012d; 2012e; Bech et al., 2013).

4.3.7 Novel MAG

It is reasonably established from the tensiometry and IRS temperature sweeps that CRY110 functions because of it having a relatively rich source of C22:0, having a longer fatty acid moiety than other common MAG with shorter fatty acid chains. However, the problem to date is finding and developing surfactants which contain a significant source of C22:0 and or other long chain moieties, and yet have not undergone hydrogenation or other modification steps.

The following measurements of two potentially novel MAG show non-hydrogenated Ricebran (Table 4.1, section 4.2.3) and Moringa (Wassell et al., 2012a; 2012b; 2012c; 2012d; 2012e; Bech et al., 2013; Appendix F) MAG were tested with Interfacial tensiometry.

Figure 4.13 shows several MAG which, irrespective of their fatty acid compositions, all give high tension measurements across a wide temperature spectrum (50°C to 5°C). The ricebran MAG (predominant in C18:1/C18:2 and ~20% C16:0) gave a tension value similar to those grouped with MAG previously show in Figure 4.4 and 4.6. This result is not surprising given that it has a similar IV value (103) to sunflower based DIMODAN® UJ (105).

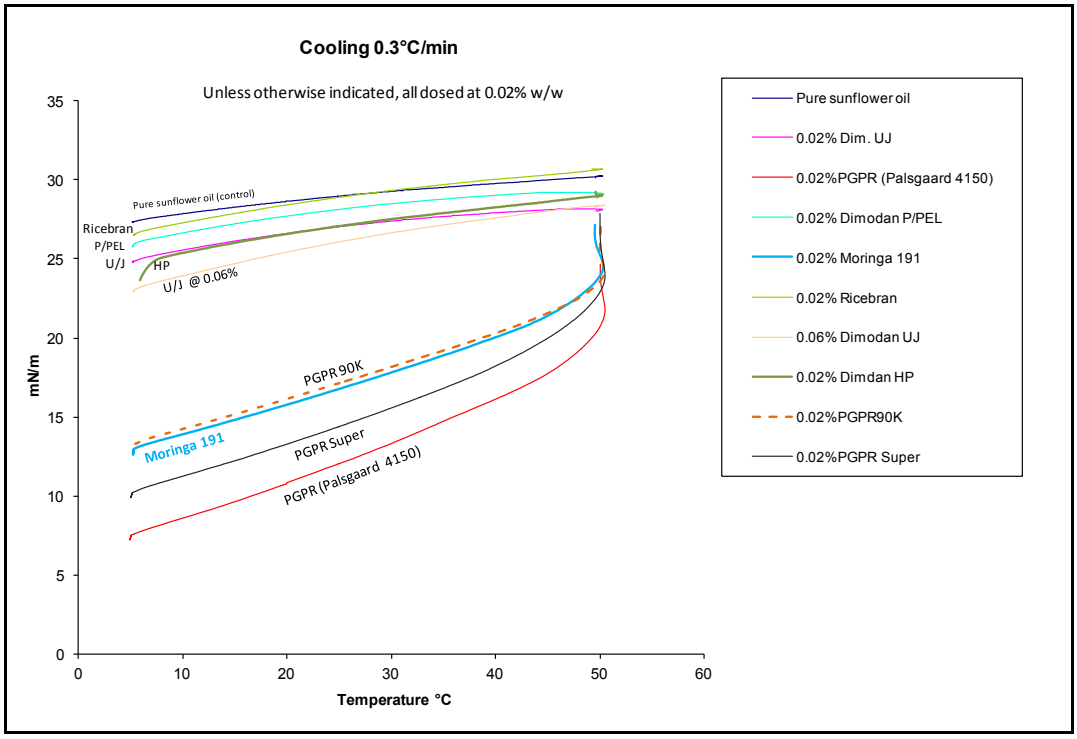

Figure 4.13 Interfacial tension measurements for several MAG, including novel ricebran and Moringa, compared to several PGPR's (PGPR Palsgaard 4150, known as PGPR 90 Plus)

Most interesting is the Moringa MAG (natural non-hydrogenated and source of behenic acid, approximately 6 – 8%, containing approximate >C20:0 of >10% and IV ~68) which gave a tension measurement, similar to PGPR. Moringa also seems to have subtle effect on CRY110, causing earlier onset of Tγ.

Moringa, as a standalone emulsifier, gives a similar γ to PGPR Plus, and is actually similar to PGPR 90 (Figure 4.13). Possibly the Moringa behaviour is dominating at the surface, causing the early onset of Tγ, when combining CRY110 and Moringa (Figure 4.14). From a commercial prospective, this gives certain labelling advantages because both emulsifiers are declared E471.

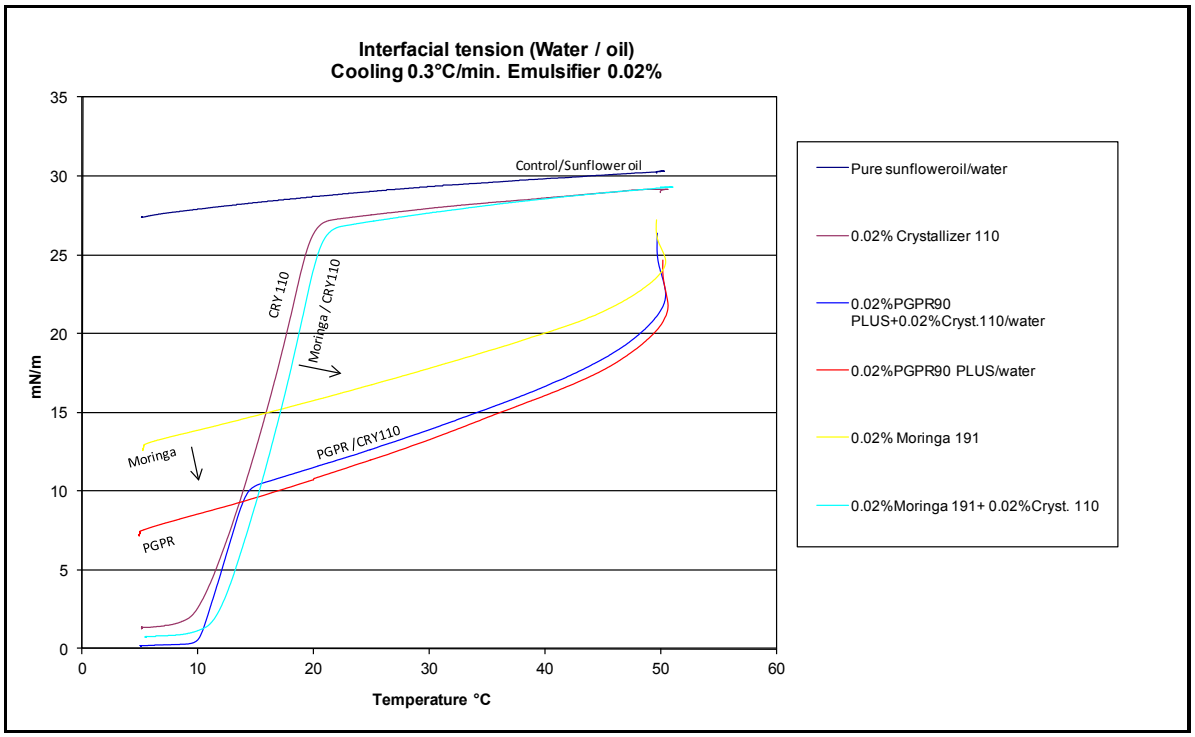

Figure 4.14 Interfacial tension of CRY110 compared with a novel MAG (Moringa) and in comparison to PGPR Plus.

IRS and bulk rheology measurements also provide evidence of visco-elastic structural changes. Results in Figure 4.15, show that in the bulk, Moringa alone, does not have significant differences in response behaviour compared with PGPR (seen clearer in Figure 4.16). There is a small effect from approximately 10°C, when combined with CRY110 (Figure 4.17). A sharp increase in G' from 0.1Pa to ~0.4Pa is observed.

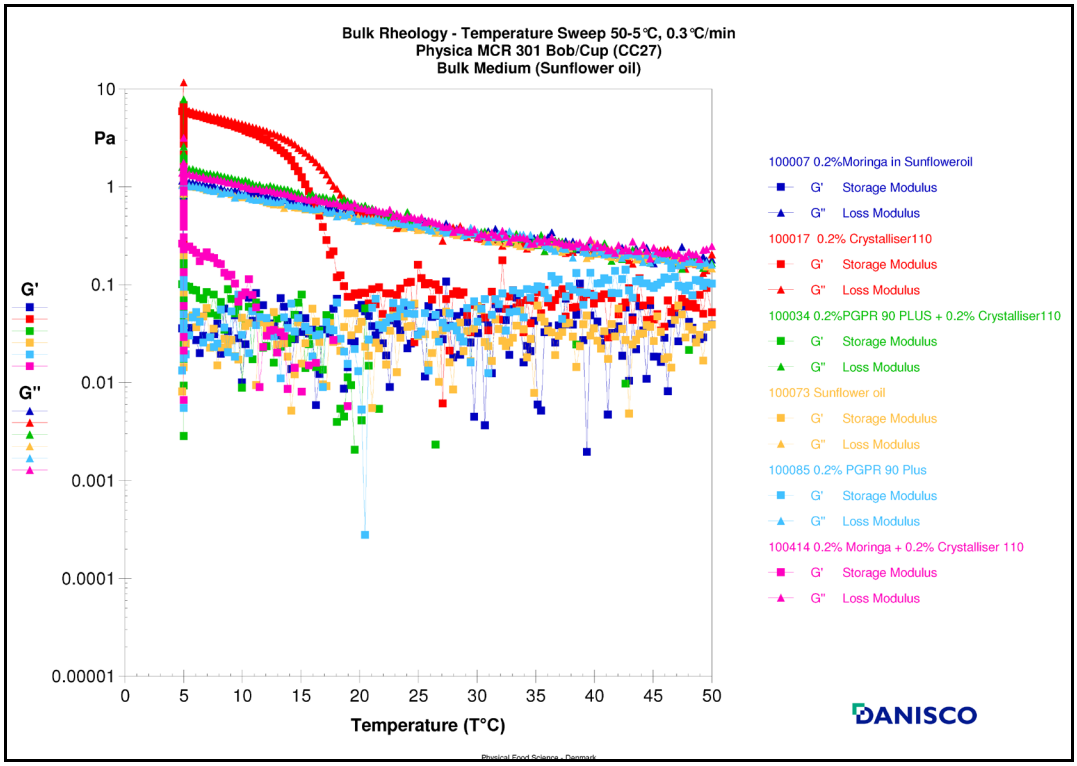

Figure 4.15 Bulk behaviour of Moringa MAG v CRY110 with PGPR

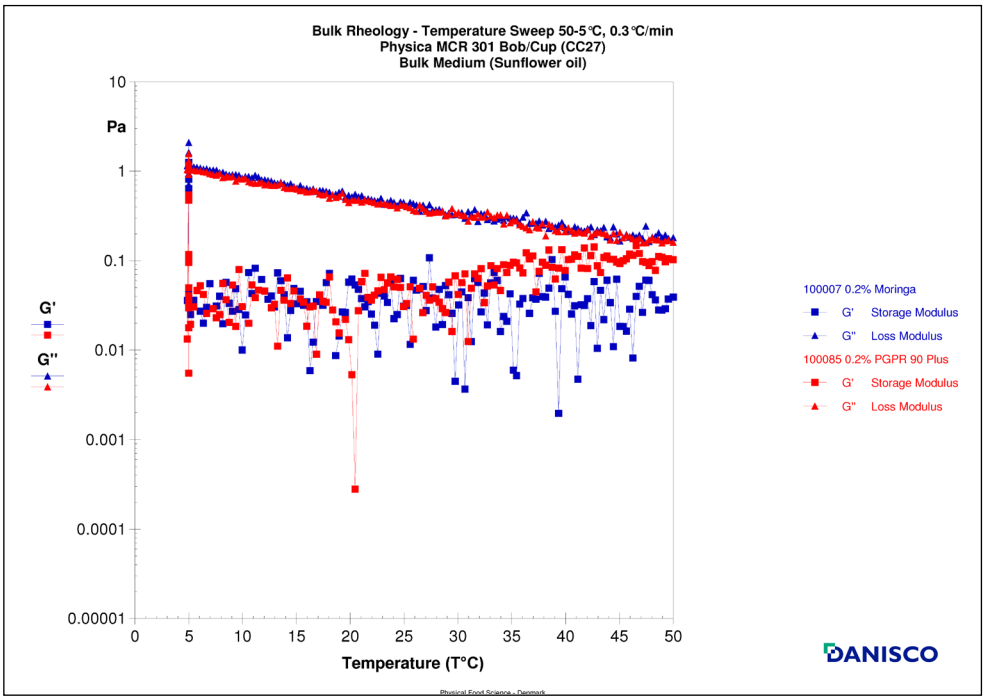

Figure 4.16 Bulk behaviour of Moringa MAG v PGPR

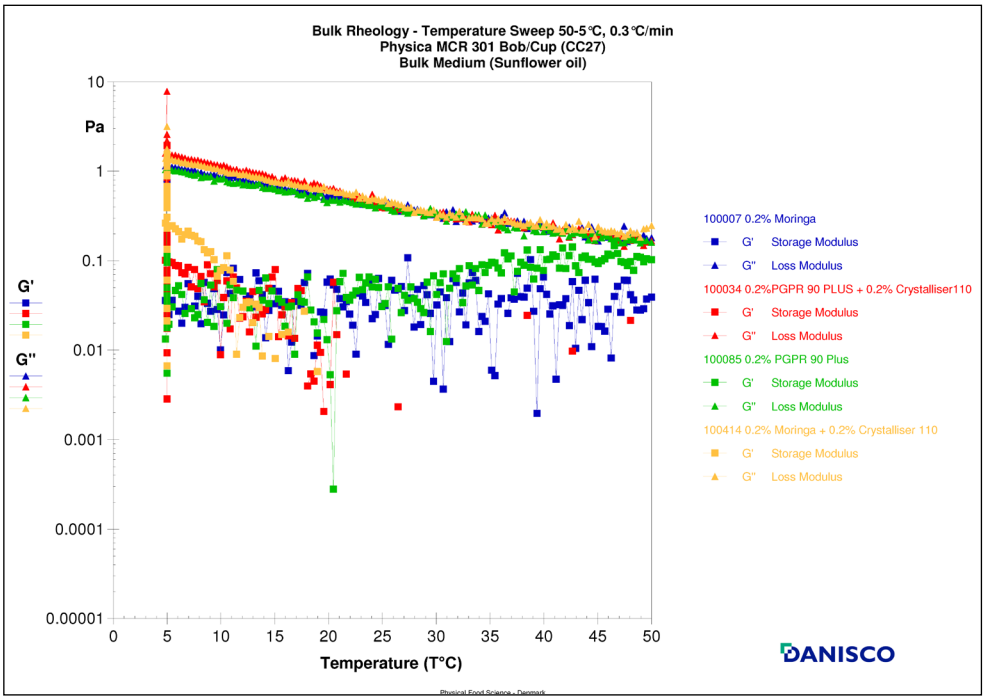

Figure 4.17 Bulk behaviour of Moringa and CRY110 compared to PGPR and CRY110

Turning attention to the interfacial behaviour, it is apparent from Figure 4.18 that Moringa / CRY110 combination is active in the G' / G''. The response curve is similar to CRY110 / UJ shown in Figure 4.7.

When comparing Figure 4.5 and Figure 4.14, the tension value is slightly lower overall with the CRY110 / Moringa. It is more surface active. But crucially, it seems Moringa MAG is able to enhance and or build structure similar to CRY110 and yet compared with PGPR 90 (Figure 4.13), have remarkably similar γ behaviour.

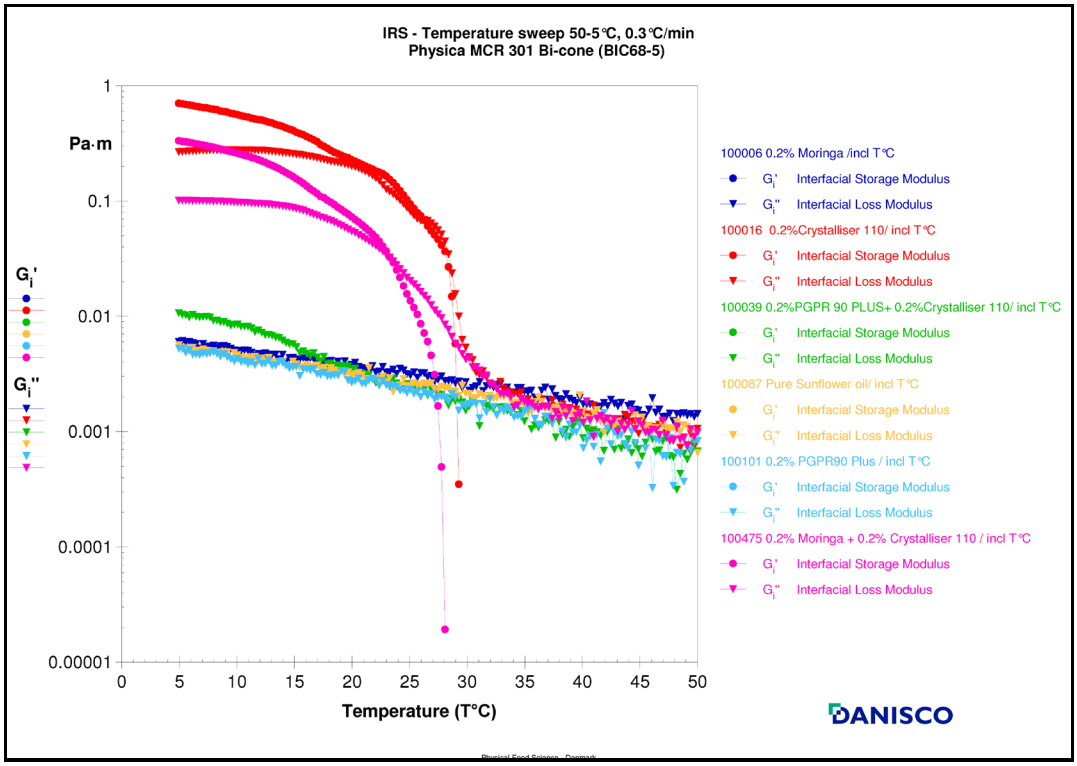

Figure 4.18 The complex IRS for Moringa MAG / CRY110 or PGPR

Another possible reason for the large differences in response behaviour shown in Figure 4.19 and Figure 4.20 is because the PGPR 90 Plus is more surface active compared to PGPR 90 and Moringa. This is seen in Figure 4.13 and helps to explain the reason for Moringa having more G'' compared with PGPR 90 Plus as shown in Figure 4.20

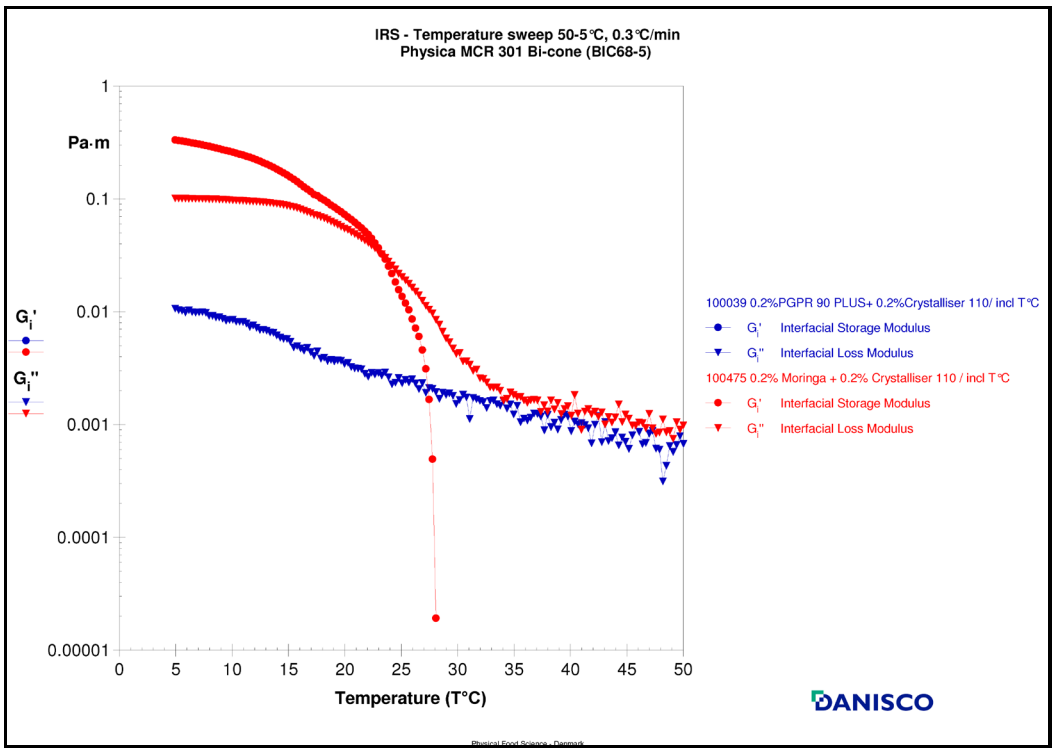

Figure 4.19 Complex IRS: CRY110 & Moringa v CRY110 & PGPR

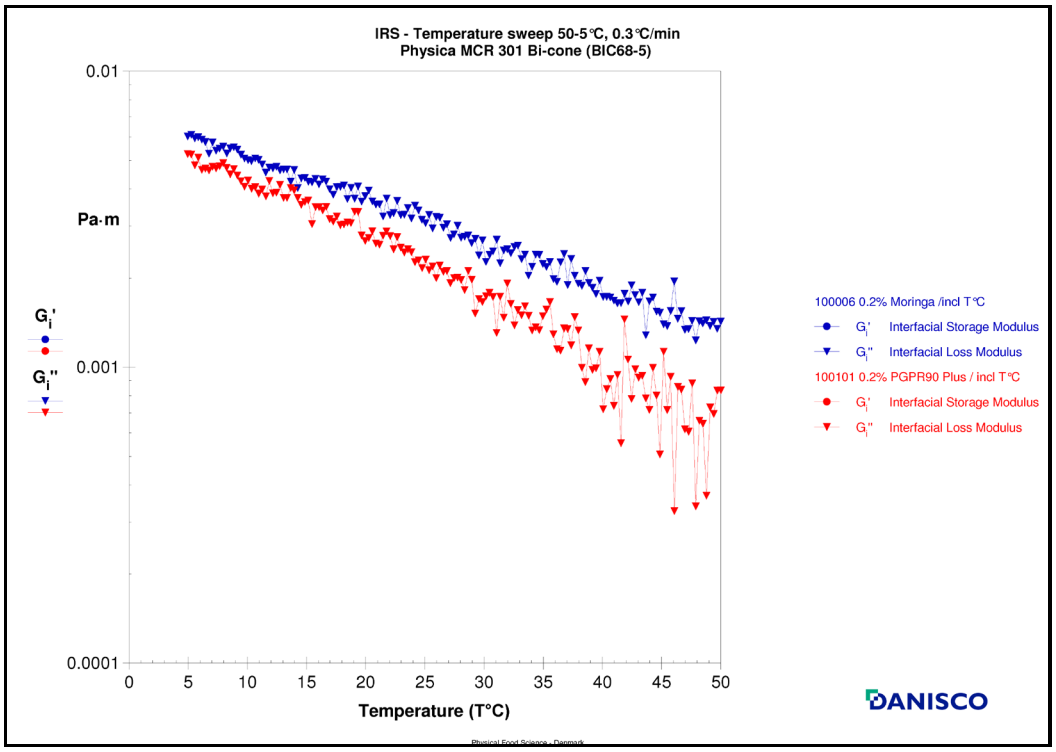

Figure 4.20 The effect on G'' after interfacial temperature sweep for Moringa MAG v PGPR

4.3.8 Conclusions and Recommendations

The interfacial tensiometry measurements of a Moringa MAG have shown unusual decreased γ tension behaviour not dissimilar to PGPR. All other tested MAG (excluding CRY110), irrespective of their fatty acid compositions resulted in higher γ tension values across a wide temperature spectrum (50°C to 5°C).

IRS and bulk rheology measurements provided evidence of visco-elastic / structural changes. The total saturated fatty acid > C20:0 spectrum of a Moringa based MAG and its interactive behaviour with a behenic based MAG (CRY110) may be significant.

If it was possible for the Anton Paar RheoPlus software to handle complex regression analysis for absolute values and each density / viscosity for each of the 151 data plots, the IRS and bulk rheology information would surely be more informative and accurate (4.3.3). However, this was not possible because only one T°C constant could be used. If a low T°C constant was used, then high T°C plots would be inaccurate or lost. Conversely, in this procedure 50°C was the T°C constant, which likely resulted in the low T°C plots being less reliable. However, this does not minimise the information about viscoelastic crystallisation behaviour, which could not be provided from more classic techniques e.g. pNMR, DSC (De Graef et al., 2006, Wassell et al., 2010a)

As part of a multidisciplinary investigation there is still a need to discover how these results transpose to and influence behaviour in bulk food dispersions or the interfacial behaviour in W/O emulsions. For a typical TAG blend (solvent) used for e.g. low fat W/O emulsion there is usually a proportion which is higher melting. This higher melt will eventually crystallise out of solution and in doing so establish additional surfaces (other than water droplets) for the emulsifier to adsorb to. Alternatively, in the case of higher melting emulsifier (CRY110) when crystallising out of solution, it may establish a template structure of micro or nano crystalline material (Taylor, 2011) for new born crystal growth within the TAG.

The TAG solvent used for both tensiometry and IRS rheology was pure liquid sunflower oil. In this situation, it not known if interstitial (Shiota, Iwasawa, Kotera, Konno, Isogai, & Tanaka, 2011) liquid crystalline TAG structures may have formed during thermal treatment in the presence of PGPR and or MAG containing C22:0. As with interfacial tensiometry (4.2.4) there were obvious crystallisation events where MAG containing C22:0 changed the translucence of the oil at and near the interface, turning milky white. These must be *surface-active* crystals (Krog & Larsson 1992), which may account for the resulting interfacial behaviour, which in turn may have important implications for droplet stabilisation in W/O low TAG emulsions specifically (Rousseau, Zilnik, Khan, & Hodge, 2003). Surface active PGPR was clearly dominant at the upper temperature region, but as thermal treatment continued towards lower temperatures, insoluble surface active crystalline MAG then competes at the interface. Rousseau et al (2003), suggest a highly viscous and rigid interfacial film would result from sufficient monolayer coverage, in effect – Pickering stabilisation (Pickering, 1907). In the case of PGPR / CRY110 mixture, competitive adsorption (Bergenståhl, 2008), together with previous factors discussed in this conclusion may explain these rheological and interfacial results and therefore help to explain the textural "thickening" observed in very low TAG (12%) W/O emulsions, from earlier preliminary studies (1.5.3).

Other methods such as rotational rheology and or synchrotron microbeam X-ray analysis might possibly lead to a clearer understanding and conclusions (Wassell et al., 2012; Wassell et al., 2012a; 2012b). Subsequent studies would likely benefit from using a thermal controlled rheo-microsope (Anton Paar) as used by other researches (Ghosh & Rousseau 2010). This would monitor TAG crystallisation combined with mixing and cooling, whilst measuring and recording visco-elastic information about the emulsion microstructure.

A dynamic interfacial tension measurement (Krüss DSA 100) would enable the observation of thermal conditions where surface-active ingredients are still mobile and molecular organisation is incomplete. Drop shape analysis video can measure

on time scales ranging from 5 minutes to 30 seconds. Comparing this information with a fixed isothermal condition using a Krüss K10ST analysis (2.0) e.g. at ex-packing (~10°C – 15°C) and domestic refrigeration conditions (~5°C), might show new data, which if found, could provide additional insight into affects of chain length transitions (Larsson et al., 1969). New information could potentially be extended to other food and non-food applications (Carmichael 2011; Marangoni & Garti 2011; Menaa et al., 2013; Piller 2011; Wang et al., 2012)..

Results obtained from tensiometry and interfacial rheology now require testing (Wassell & Young 2007; Wassell et al., 2010a; Wassell et al., 2012) within conditions that replicate those of the actual food products in which MAG combinations, with and without PGPR, will be used (McClements, 2007), e.g. W/O emulsions. These application trials and additional measurements will reveal their emulsification capabilities and crystallisation behaviour under real dynamic conditions.

5.0 A Study Series on the Behaviour of a Moringa MAG, Behenic Based MAG and PGPR

5.1 Introduction

The application of structurant materials in the replacement of saturated TAGs (Wassell & Young 2007; Wassell et al., 2010a) is broad. Specifically for water-in-oil product applications (low TAG spreads), it is important to know how emulsifier mixtures or novel emulsifiers contribute to the visco-elastic properties of W⁄O emulsions (Wassell et al., 2010a).

The presence of interfaces, as in emulsions, clearly is an important element which contributes a significant influence on the complete macro-structure and hence sensory properties (Wassell et al., 2010a). These structures are highly influenced by the way they are assembled and processed by mechanical mixing, shearing and thermal treatment (5.0), which subsequently influences functional properties often still obtained by protracted trial and error scaled procedures (Mazzanti et al., 2005).

The interfacial tensiometry measurements of a Moringa MAG have shown unusual decreased γ tension behaviour not dissimilar to PGPR. IRS and bulk rheology measurements (4.0) have provided evidence of visco-elastic / structural changes occurring with a Moringa MAG and its interactive behaviour with CRY110. Both contain significant proportion of the behenic (C22:0) fatty acid which is considered to be significant (3.0; 4.0).

As part of a multidisciplinary investigation (Wassell & Young 2007; Wassell et al., 2010a; Young et al., 2008; Wassell et al., 2010b) there is still a need to discover how the rheological and interfacial behaviour of a Moringa monoglyceride (MAG) and the effect of saturation and chain length transpose to and influence bulk food dispersions or W/O emulsions.

In attempting to discover the practical capabilities and application of the emulsifying properties of novel Moringa MAG and other long chain fatty acid mixtures, a series of application measurements are made. While reviews (Wassell & Young 2007; Wassell et al., 2010a), techniques (Young et al., 2008; Wassell et al., 2010b; 2012) and methodologies (2.0) for characterisation of emulsions or dispersions have been made to test emulsifier efficiency (McClements 2007), a consideration to the characteristics of the food in which the emulsifier is present is key. Consequently, it is preferable to examine the effectiveness of an emulsifier within conditions relevant to those used in the actual food product in which it will be used (McClements 2007).

The intention from these application tests (proof of concept) is to provide important practical data, which support new patent applications (Refer to 5.12) for the following:

Fat based food systems, including dispersions (Wassell et al., WIPO No. WO2012168722, 2012a; WO2012168723, 2012d), crystallisation (Wassell et al., WO2012168727 2012b; Bech et al., WO2013050944, 2013), water-in-oil low fat spreads (Wassell et al., WO2012168726, 2012c), reduced fat water-in-oil spreads (Wassell et al., WO2012168724, 2012e).

5.2 A Rheological Evaluation on a Moringa Monoglyceride (MAG) and PGPR in Triacylglyceride (TAG)

5.2.1 Introduction

The work described herein investigated the functionality of Moringa MAG, based on *Moringa oleifera* TAG and PGPR (GRINDSTED® PGPR 90) specifically in peanut TAG – for peanut butter dispersions, and more generally in rapeseed TAG.

The rationale of the study was to investigate the effect of adding either Moringa MAG or PGPR over a range of concentrations to peanut TAG or rapeseed TAG respectively by measuring the rheological properties during cooling. This work supports inventive claims for a texturant for bulk food, TAG blend and emulsion (Wassell et al., 2012a; 2012b; 2012c; 2012d; 2012e; Bech et al., 2013).

5.2.2 Materials & Methods

RBD Peanut TAG and RBD rapeseed TAG (specification in 2.0) were used as the base TAGs, to which a Moringa monoglyceride (MAG) and a PGPR (GRINDSTED® PGPR 90) were added such that the concentrations were 0.1, 0.2, 0.4, 1, and 3%. Fatty acid content and various analyses of *Moringa oleifera* TAG and monoglyceride are given in Table 5.2.1, 5.2.2 and 5.2.3. Refer to General Materials & Methods (2.0) for additional detail.

Table 5.2.1 Fatty acid composition of *Moringa oleifera* TAG and MAG

Analysis (%)	Moringa TAG / MAG	Analysis (%)	Moringa TAG / MAG
C14	0.1	C19	0.1
C15	<0.1	C20	3.4
C16	5.8	C20:1	2.2
C16:1	1.8	C22	**5.8**
C17	0.2	C22:1	0.1
C18	5.4	C24	1.0
C18:1	**73.0**	C26	-
C18:2	0.7	Unknown	0.2
C18:3	0.2		

Table 5.2.2 Analyses of *Moringa oleifera* TAG

Analysis	***Moringa oleifera* TAG**
Iodine value (calculated)	68
Acid value	3.2
Unsaponifiable matter	0.4%
FFA	1.5%
Diglyceride	3.3%

Table 5.2.3 Analyses of Moringa MAG.

Analysis (%)	**Moringa MAG**
Glycerol	0.76
Diglycerol	0.07
FFA	0.3
Monoglyceride	**91.15**
Diglyceride	**7.75**
Triglyceride	< 0.1

Each sample was then pre-heated in a microwave oven for 2 minutes at maximum power before testing. This was to ensure the temperature exceeded 90°C, thereby removing crystal history before the sample was then loaded and cooled on the rheometer. In each case the measurements were carried out using a controlled stress Haake RS 150 rheometer (2.13.2) fitted with a serrated parallel plate of 35mm in diameter, both top and bottom. Cooling took place from 85°C to 25°C at the rate of 1°C per minute. The strain used was 0.004, 120 data points were collected, the frequency was fixed at 0.5Hz, and the gap was reduced to 0.5mm. Polarised Light Microscopy (PLM) was carried out at x20 magnification using a polarised microscope (Olympus SC300).

5.2.3 Results and Discussion

Figures 5.2.1 and 5.2.2 show the results for the effect of PGPR and Moringa MAG on rapeseed and peanut TAG respectively.

In Figure 5.2.1, the full concentration range of 0.1%, 0.2%, 0.4%, 1% and 3% PGPR is tested, along with only Moringa MAG at 1% and 3% in rapeseed TAG. The assumption was that with 1% Moringa displaying the same behaviour as the raw rapeseed TAG sample, the results for the lower Moringa concentrations would have followed a similar trend. For concentrations 0.1%, 0.2%, 0.4% and 1% together with the pure rapeseed TAG the dynamic viscosity measured was essentially constant between 0.03 and 0.04 Pas, whereas for 3% PGPR and 3% Moringa MAG, differences were seen. For PGPR there is an observed shift in the curve to a higher constant viscosity centred at 0.06 Pas, but for Moringa MAG, dramatic changes in the profile of the curve occurred.

The Initial viscosity for Moringa MAG at the lower concentrations was 0.03 – 0.04Pas, but at a temperature corresponding to 32°C the onset of a dramatic increase in viscosity is seen. Viscosity value increased to ~20 Pas, approaching 3 orders of magnitude greater than its start point, and occurred over a temperature range of 6 – 7°C (25°C – 32°C).

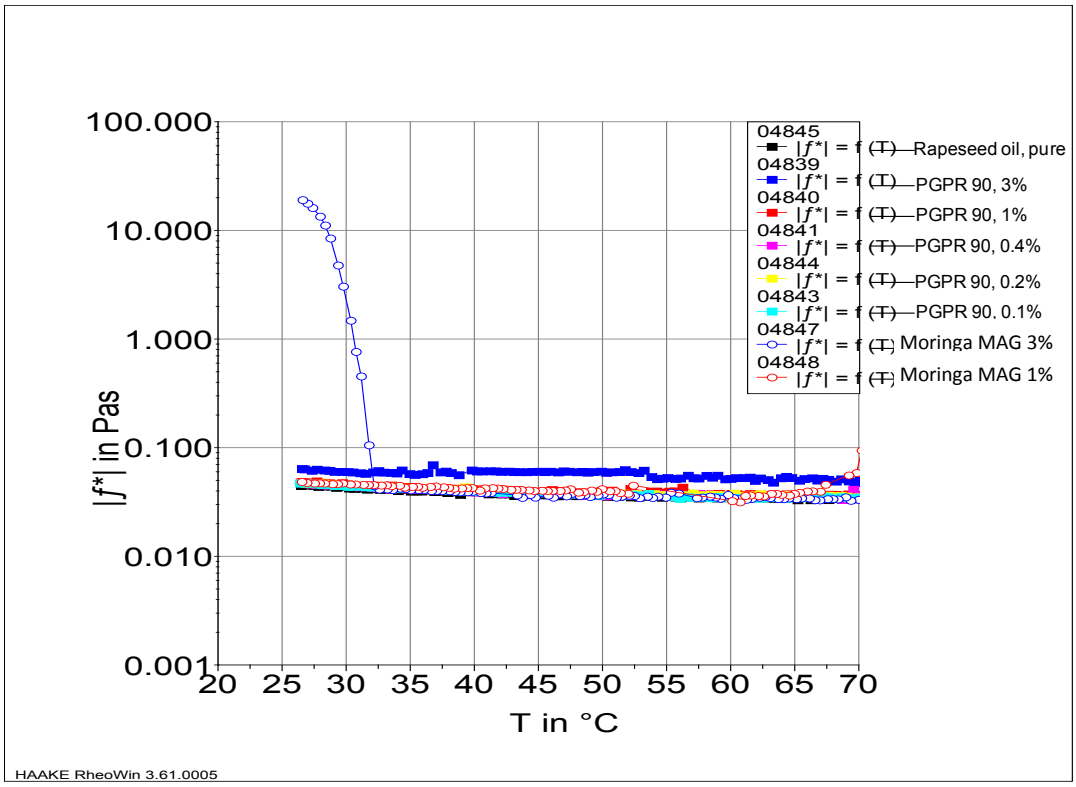

Figure 5.2.1 Effect of Moringa MAG and PGPR in Rapeseed TAG

In Figure 5.2.2, where the results for Peanut TAG are presented, essentially the same picture is seen. For concentrations of PGPR below 3% and for Moringa MAG at 1% the measured viscosity starts at around 0.03 Pas, and rises upon cooling in a steady state to a value of 0.05 – 0.06 Pas, i.e. there is a greater rise in viscosity of peanut TAG compared to rapeseed TAG. This however, can be explained by the fact that the peanut TAG itself follows this curve, and could likely be attributed to either its intrinsic wax content, or natural content of C22:0 of ~1.5 – 4.5%, and the generally more saturated nature, IV 86 – 107, of the peanut TAG (FAO/WHO 2011). PGPR at 3% does show greater viscosity than the samples so far mentioned, but not to the same extent as it did in Figure 5.1. Here the viscosity begins at 70°C around 0.04 Pas and ends around 0.06 Pas at 26°C. Moringa MAG at 3% mirrors the tendency displayed from Figure 5.2.1, i.e. in this case it follows the same gently increasing viscosity of the other samples until a

temperature of 30°C, a similarly dramatic increase in viscosity is recorded. The increase is less than in Figure 5.2.1, with a final measured value plateau round 7 Pas, but still enough to record a 2 order of magnitude increase.

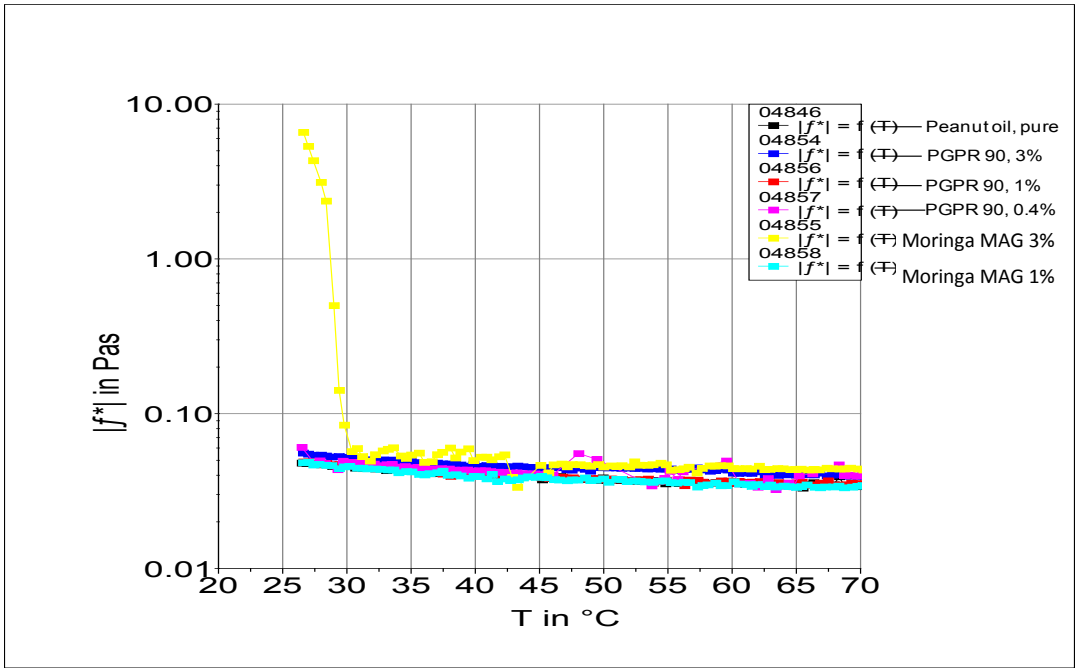

Figure 5.2.2 Effect of Moringa MAG and PGPR in Peanut TAG

Below a concentration of 3% it appears as though the function of Moringa MAG is behaving similarly to PGPR. This assumption however needs to be confirmed with additional model or application tests – preferably both because PGPR is extremely hydrophilic, and hence, very surface active in the presence of an aqueous phase. On a molecular scale, PGPR and MAGs are quite different (Garti & Remon 1984; Garti et al., 1998; Goubran & Garti 1988; Annon 2005).

The results from Figures 5.2.1 and 5.2.2 show that both the tested TAGs (rapeseed and peanut) are affected at around 30°C to 32°C, which does not occur in samples below the Moringa MAG concentration of 3%. The reason why Moringa MAG shows this dramatic increase in viscosity, can likely be attributed to its own fatty acid composition, which is retained when synthesised from the original TAG (refer to 5.11). *Moringa oleifera* TAG fatty acid composition is C16:0 – 6.0%, C16:1 – 1.4%, C18:0 – 4.0%, C18:1 – 75.0%, C20:0 – 2.5%, C20:1 – 2.5%, C22:0 – 5.8%,

and >C24:0 - 1.0% (Abdulkarim et al., 2005; Lalas & Tsaknis, 2002) which is in good agreement with the analysis in table 5.2.1. There is a significant proportion of Moringa MAG with C22:0 fatty acids (behenic acid), similar to CRY110 (refer to 1.5; 2.0; 3.0; 4.0). Therefore, it is reasonable to suggest that the increase in viscosity is likely due to the presence of long chain saturated fatty acids, which also include C20:0 and >C24:0.

Supporting evidence as to why the viscosity rise occurs is shown via microscopy. The micrographs for the 3% samples of both PGPR and Moringa MAG in the rapeseed and peanut TAGs are shown in Figure 5.2.3.

Figures 5.2.3a and 5.2.3c show 3% Moringa MAG in rapeseed and peanut TAG respectively show a higher level of crystalline structure than Figures 5.2.3b or 5.2.3d with 3% PGPR in the same respective TAGs. Figures 5.2.3a and 5.2.3c, shows the presence of crystalline entities, which may be attributed to the presence of the Moringa MAG. In contrast Figures 5.2.3b and 5.2.3d detailing 3% PGPR in the same rapeseed or peanut TAG show much less in the way of crystal formation, and thereby explain why the viscosity profile remains at the low levels see in Figures 5.2.1 and 5.2.2.

The micrograph images provide evidence of tangible difference between Moringa MAG at 3% compared to PGPR at the end temperature of 25-26°C. These differences are likely attributable to > C20:0 fatty acids present in the Moringa MAG.

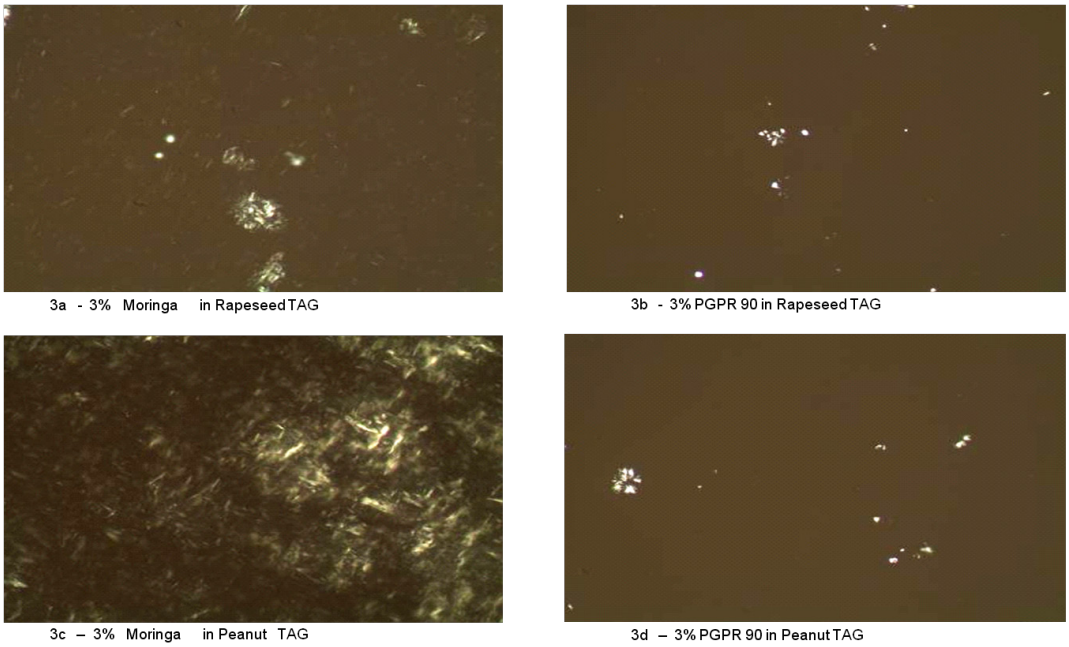

Figure 5.2.3 Micrographs of 3% Moringa MAG in rapeseed and peanut TAG (3a, 3c), and 3% PGPR in rapeseed and peanut TAG (3b, 3d) at approximately 25°C – 26°C

5.2.4 Conclusion

The rheological behaviour of Moringa MAG and PGPR 90 in two different liquid TAGs are essentially the same once below a concentration of 3%. At 3% there is a significant increase in dynamic viscosity from a temperature of 32°C for rapeseed TAG and 30°C for peanut TAG. The increase continues reaching levels up to 3 orders of magnitude greater than the start point. This increase is attributed to the greater fat crystal density seen in the Moringa samples, as shown by the micrographs; in the peanut TAG specifically, there may also likely be another factor where the TAG solvent i.e. degree of its total saturation, may also have a contributing factor. However, a Moringa based MAG with a fatty acid specification similar to those described in tables 5.2.1, 5.2.2 and 5.2.3 is thought to be the reason for the proliferation of crystal growth (Wassell & Young 2007; Wassell et al., 2012a; 2012b; 2012c; 2012d; 2012e; Bech et al., 2013). This aspect requires further investigation.

5.3 Crystallisation Effects of Natural Moringa MAG, a Synthetic Behenic Based MAG Composition and PGPR by Cold Stage Polarised Light Microscopy

5.3.1 Introduction

A study is performed to examine the formation of TAG crystals resulting in the cooling of samples containing Moringa MAG – both natural and synthetic, - PGPR and CRY110, with the purpose of providing evidence to support claims for invention disclosures which deal with texturing / stabilising of TAG based bulk dispersions, emulsions and crystallisation properties (Wassell et al., 2012a; 2012b; 2012c; 2012d; 2012e; Bech et al., 2013).

A Moringa (*Moringa oleifera* TAG) based MAG possibly has some unusual similarities to PGPR in certain applications (refer to 5.2). This investigation attempts to provide clear visual evidence to confirm these similarities. Through an examination of samples cooled by controlled thermal induction, and then using a polarised light microscope, it is possible to gain optical evidence, resulting in a snapshot of the crystal structure at a given temperature. Therefore, an induction heat /cool regime can provide evidence that is being sought.

5.3.2 Materials and Methods

The samples were used from the melt after pre-heating to remove crystal history, starting at 85°C and then cooling to 20°C at a temperature cooling rate of 1°C per minute. Photographic images were taken approximately once every 2°C and recorded. Using an Olympus BX 60 microscope, all images were taken under polarised light at a magnification of x200.

The TAG blend used in all cases was 70% Palm Stearin, with an iodine value (IV35) and 30% Palm Olein (IV 56). 1% of either Moringa MAG or GRINDSTED® Crystallizer 110 (CRY110) or 0.5% GRINDSTED® PGPR 90 (PGPR) was added (2.0)

Moringa MAG samples, were either classified as natural (sourced from: *Moringa oleifera* TAG) or synthetic, i.e. the natural samples are true Moringa sourced materials (2.0), whereas the synthetic samples have been assembled by attempting to blend a similar fatty acid and glyceride content similar to that of the natural samples as given in Table 5.3.1.

To try and match the natural Moringa MAG in Table 5.3.1, a series of synthetic samples were blended (Table 5.3.2) and dosed at the same 1% inclusion rate.

Table 5.3.1 Natural Moringa MAG with the breakdown of mono, di- and tri-glycerides

Analysis (%)	**2559/102**	**2559/104**	**2472/191**
GL	0.11	1.27	0.76
Digl	0.05	0.08	0.07
FFA	0.2	0.4	0.3
Mono	53.16	82.55	91.14
Di	42.05	15.67	7.75
Tri	4.39	0.02	0
Approx mono content %	53	82	91

In Tables 5.3.1 and 5.3.3, the abbreviations stand for; GL – Glycerol, Digl – Diglycerol, FFA – Free Fatty Acids, Mono – Monoglycerides, Di – Diglycerides, and Tri – Triglycerides.

Synthetic MAG: Blends of commercial MAG (Table 5.3.2) were assembled in such a way as to provide a similar fatty acid profile to natural distilled Moringa monoglycerides (Table 5.3.4). Resultant compositions are shown in Table 5.3.3 and 5.3.5. The predominant fatty acid base for all three compositions is based on Table 5.3.6.

Table 5.3.2 Blends of MAG with resulting mono contents

Synthetic Moringa monoglyceride	**SM 90 [a]**	**SM 60 [b]**	**SM 80 [c]**
GRINDSTED® CRYSTALLISER 110	10	10	10
DIMODAN® RT [d]	90		50
GRINDSTED® MONO-Di PR40 [e]		90	40
Total %	100	100	100
Final mono content % (approximate)	96	64	82

a., b., c., are named SM 90, SM 60, SM 80, merely as means of identification and approximate mono content.

d. DIMODAN® RT is a distilled monodiglyceride made from partially hydrogenated rapeseed oil

e. GRINDSTED® MONO·DI PR 40 is a monodiglyceride made from edible, refined rapeseed and/or palm oil. Total monoglyceride = 55%. Iodine value = 65

Table 5.3.3 Glyceride distribution of synthetic Moringa MAG (mono, di-, tri-glycerides)

Analysis (%)	**SM 90**	**SM 60**	**SM 80**
GL	0.16	0.24	0.20
Digl	0.14	0.1	0.18
FFA	0.30	0.40	0.40
Mono	96.50	64.56	82.87
Di	2.64	29.02	15.28
Tri	0.22	2.59	1.10

The natural MAG samples, align approximately with synthetic MAG samples as follows:-

Natural		**Synthetic**
2472/**191**	=	**SM 90**
2559/**102**	=	**SM 60**
2559/**104**	=	**SM 80**

The iodine values (IV) of these samples was calculated according to the principles reported by Kyriakidis, and Katiloulis (2000) as:

SM 90 IV total: 66 (Sat 28.8 Mono unsat 66.1 Poly unsat 5.3)

SM 60 IV total: 70 (Sat 36.4 Mono unsat 47.3 Poly unsat 16.3)

SM 80 IV total: 71 (Sat 29.5 Mono unsat 66.1 Poly unsat 5.3)

The fatty acid compositions of the natural Moringa MAG and synthetic MAG are shown in Tables 5.3.4 and 5.3.5.

Table 5.3.4 Fatty acid composition of the natural Moringa MAG

Fatty acid chain length (%)	% present
C12:0	<0.1
C14:0	0.1
C15:0	<0.1
C16:0	6.5
C16:1	1.8
C17:0	0.2
C18:0	5.8
C18:1	71.2
C18:2	1.5
C18:3	0.3
C20:0	3.4
C20:1	1.9
C20 unsaturated	0.3
C22	6.0
C22 unsaturated	0.2
C24	0.8

Table 5.3.5 Fatty acid composition of synthetic Moringa MAG: sample 1 (SM 90), sample 2 (SM 60) and sample 3 (SM 80)

Analysis (%)	(Sample 1) SM 90	(Sample 2) SM 60	(Sample 3) SM 80
C10:0	<0.1	0.0	0.0
C12:0	0.1	0.1	0.1
C14:0	0.1	0.5	0.3
C15:0	<0.1	<0.1	<0.1
C16:0	5.3	21.5	12.7
C16:1	0.1	0.1	0.2
C17:0	0.1	0.1	0.1
C18:0	10.9	4.1	7.8
C18:1	64.6	23.9	47.6
C18:2	5.2	10.8	7.7
C18:3	0.0	3.8	2.0
C20:0	1.3	1.0	1.0
C20:1	1.4	2.6	1.8
C20:unsaturated	0.1	0.9	0.7
C22:0	10.7	8.8	7.2
C22:1	0.0	20.7	10.0
C22:unsaturated	0.0	0.8	0.4
C24:0	0.3	0.3	0.3
C24:1	0.0	0.4	0.2

Table 5.3.6 Predominant fatty acids of GRINDSTED® Crystallizer 110

Predominant fatty acids (%)	% present
C18:0	2.0
C20:0	5.0
C22:0	89.0
C22:1	0.2
C24:0	3.0

Refer to General Materials & Methods (2.0) for additional detail.

5.3.3 Results and Discussion

The micrographs shown in Figure 5.3.1a to 5.3.1f depict the crystal structure as seen via microscope at 20°C after the samples were cooled from 85 – 20°C at a cooling rate of 1°C per minute. The samples represented from Figure 5.3.1a to 5.3.1f respectively are:

1a the blank control

1b 1% GRINDSTED® Crystallizer 110

1c 1% GRINDSTED® Crystallizer 110 + 0.5% GRINDSTED® PGPR 90

1d 0.5% GRINDSTED® PGPR 90,

1e 1% Moringa (191) and 1% GRINDSTED® Crystallizer 110

1f 1% Moringa (191)

Moringa (191) refers to the Moringa MAG being fully distilled (see Table 5.3.1 – sample 2472/191)

The blank sample, Figure 5.3.1a, shows clear evidence of TAG crystallisation, with pentagonal and hexagonal snowflake like patterned crystal structures. Figure 5.3.1b, shows 1% of CRY110, with many small discrete TAG crystals. A similar micrograph image has recently been reported (Basso et al., 2010) when adding a behenic based monoglyceride. The dramatic difference between Figures 5.3.1a and 5.3.1b is possibly attributed to the crystallisation onset, which may occur at higher temperatures where the CRY110 is present. The solubility and degree of total saturation of the TAG solvent will also have a bearing (Refer to 5.2, A rheological evaluation on a Moringa Monoglyceride (MAG) and PGPR in TAG and 1.5, A Pilot Study – preliminary investigations for enhancing crystallisation of anhydrous TAG dispersions and W/O Emulsions) .

The next four micrographs from Figure 5.3.1 are examined in pairs, starting next with the single samples of PGPR and Moringa MAG (191). In Figures 5.3.1d and 5.3.1f respectively, there are clear dendrite structures (Mullin, 1993) with the presence of PGPR. Though not as comparatively large, Figure 5.3.1f (Moringa MAG 191) is densely populated with irregular crystal structures of which also dendrite structures are present. There is also evidence of several large cluster formations, which were seen in Figure 5.3.1a, but without doubt it is the dendrite like structure which dominates. This is completely different from the crystal structure of Figure 5.3.1b, and given that all observed images are in reality an intertwined 3-D network of interpenetrating crystal flocculation's, then the physical dimensions of the dendrite structures by their surface area, suggests these could have high function in real food systems.

The similarities between Figure 5.3.1d and 5.3.1f leads to the suggestion that the behaviour of Moringa MAG could be similar to PGPR, but given that the dendrite structures in 5.3.1f are not so well "developed", then performance will need to be determined in application trials.

The potentially similar functionality of Moringa MAG and PGPR can be seen when comparing the last two micrographs of Figure 5.3.1, i.e. Figure 5.3.1c and Figure 5.3.1e. These refer to a combination of two samples, where Figure 5.3.1c is a combination of 1% CRY110 and 0.5% PGPR and Figure 5.3.1e is 1% Moringa MAG (191) and 1% CRY110. In both cases the micrograph show an entirely different picture compared to these components in isolation i.e. Figure 5.3.1b, 1d, 1f. This suggests that whatever the effect, the interaction of adding PGPR or Moringa MAG (191) to the CRY110 has a similar outcome.

Three important observations come from Figure 5.3.1, first; Moringa MAG (191) which naturally contains ~6% behenic acid (C22:0) behaves differently to CRY110, which contains a high source of C22:0. Second, Moringa MAG (191) appears to have some similar crystal structures to PGPR, suggesting the possibility of similar behaviour.

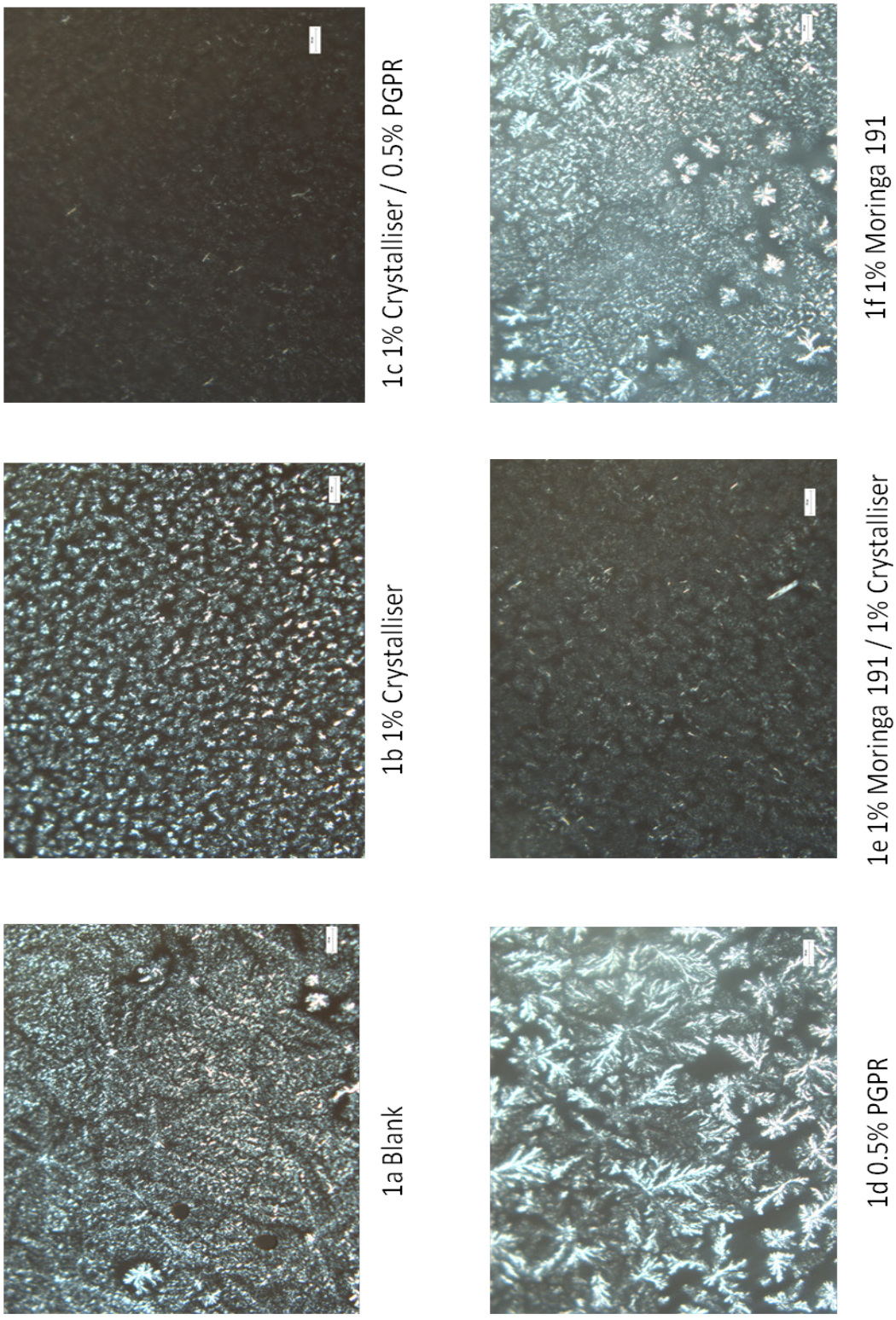

Figure 5.3.1 Micrographs showing the crystal structures of samples 1a – 1f at 20°C in 70% Palm Stearin (IV35) and 30% Palm Olein (IV 56) (scale bars = 20µm)

Third, Moringa MAG (191) and PGPR appear to demonstrate similar interaction with CRY110. These conclusions strongly point to the potential of Moringa MAG (191) possessing similar properties to PGPR.

Moringa TAG (*Moringa oleifera*), being a natural source of saturated fatty acids (Abdulkarim et al., 2005; Anwar and Rashid 2007; Fahey 2005; Lalas and Tsaknis, 2002; Mohammed et al., 2003) gives this material potentially attractive nutrition labelling. Currently, while TAG from *Moringa oleifera* is a known source of food energy and has multipurpose use (Marikkara & Ghazali 2011; Pandey et al., 2011), it is not currently recognised as a commodity TAG at present. However, once synthesised to a MAG it could (subject to Codex & Novel foods regulation) be identified as E471. This is advantageous for low TAG W/O emulsions < 41%, where it is not unusual to combine both a MAG (E471) and PGPR (E476); it may be possible to use only E471. The use of mono- and di-glycerides prepared from *Moringa oleifera* TAG has not previously been taught for such applications (Wassell et al., 2012a; 2012b; 2012c; 2012d; 2012e; Bech et al., 2013).

5.3.3.1 Synthetic Moringa MAG

Given the results observed in the application of a natural Moringa MAG (sample 2472/191 in Table 5.3.1), could a "synthetic" mix of fatty acids and Mono, Di, Tri composition offer similar properties as the natural Moringa MAG. Three synthetic versions of specific fatty acid composition were assembled (Table 5.3.2) and tested.

In to order investigate comparatively, a further two natural monoglycerides of Moringa (from *Moringa oleifera* TAG) were synthesised and finalised according to Table 5.3.1, these were sample numbers 2559/102 and 2559/104 and these shared the same fatty acid composition as 2472/191 (Table 5.3.4), but had differing total mono% contents.

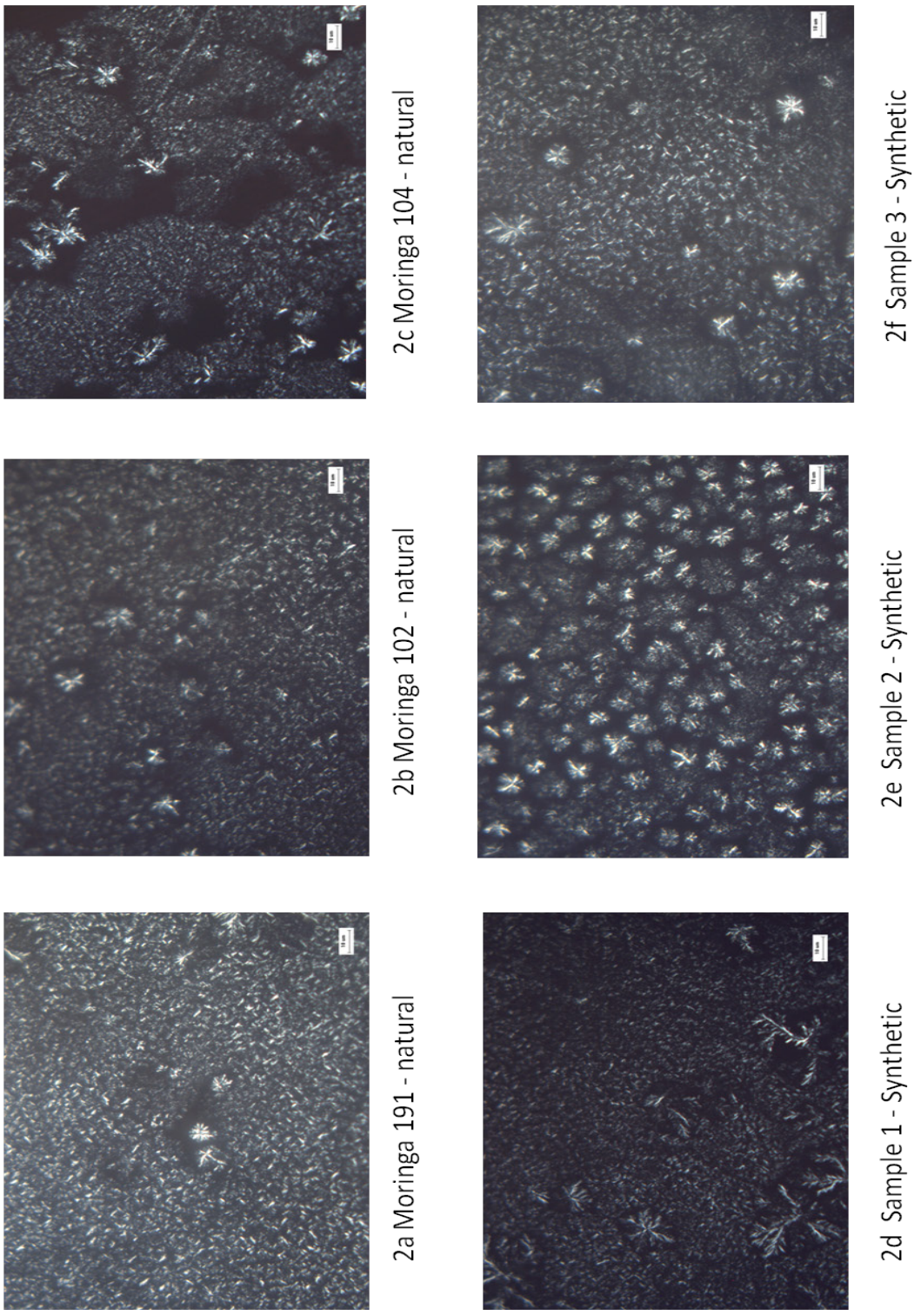

Figure 5.3.2 Micrographs 2a – 2f show crystal structures of natural and synthetic Moringa MAG (dose 1%) at 20°C in 70% Palm Stearin (IV35) and 30% Palm Olein (IV 56) (scale bars = 10µm)

The results in Figure 5.3.2 show Figures 5.3.2a to 5.3.2f, where 2a, 2b, and 2c represent the natural Moringa MAG, and 2d, 2e, and 2f represent the synthetic blends made to match the natural Moringa MAG components (fatty acid profile).

In general the micrographs in Figure 5.3.2 seem to show that synthetic Moringa MAG samples have similar fractural patterns, compared to the natural Moringa MAG. More specifically, Figures 5.3.2a, and 5.3.2d which represent the natural and synthetic versions at 91.14%, 96.5% mono content respectively, both show the scattered TAG crystallisation in the bulk, but also the evidence of single larger branched clusters together with the dendrite structures similar to those seen in Figure 5.3.1d and 5.3.1f. Both are clearly distinct from CRY110 (Figure 5.3.1b).

Figures 5.3.2b and 5.3.2e, natural and synthetic versions of 53.16% and 64.56% mono content respectively; Figure 5.3.2e shows larger clusters as opposed to the discrete nuclei of the CRY110 in Figure 5.3.1b. Less evident in both cases is the dendrite structures associated with PGPR (Figure 5.3.1d) and Moringa 191 (Figure 5.3.1f) at higher monoglyceride contents. However, Figure 5.3.2e has structures found in both Figure 5.3.2a and 5.3.2b, i.e. structures that equate to as yet underdeveloped fern-like structures, which may be signs of a delayed crystal development due to the higher di-glyceride (DAG) content within the TAG olein.

Figures 5.3.2c and 5.3.2f, natural and synthetic versions at 82.55%, 82.87% mono content respectively, show similar smaller crystals coupled with several large clusters. This is not dissimilar to 5.3.2b.

Summarising Figure 5.3.2 it is concluded that firstly the ability to make synthetic samples of Moringa by blending MAG to achieve a fatty acid composition is possible. Secondly, it seems as though either the mono or di-glyceride content is important, but this matter requires further investigation before explanations can be attributed.

5.3.4 Conclusion

This study has shown that based on micrograph evidence, the influence on TAG crystallisation of Moringa MAG (191) is different from CRY110, despite Moringa MAG (191) containing some 5.8% - 6% of C22:0 (behenic acid) and yet exhibiting behaviour not dissimilar to PGPR 90.

Figure 5.3.1f shows the TAG blend with added Moringa MAG to be essentially like viewing a composite image of Figures 5.3.1a and 5.3.1d together, where bulk TAG crystallisation and obvious evidence of fern-like dendrite structures are present. Given that both aspects are now present in a single system, this may possibly provide evidence as to why the interfacial tension measurements (Figure 4.14 in 4.2) showed PGPR and a Moringa MAG behaving with not dissimilar tensiometry values.

Combining Moringa MAG (191) with CRY110, and PGPR with CRY110 resulted in similar micrograph observations.

Results have also demonstrated that it is possible to make a composition to mimic natural Moringa MAG by blending suitable MAG, characterised by specific fatty acid arrangements. It is also possible that the content of MAG / DAG ratio may be important.

It would be interesting to discover how these findings would transpose to real emulsions and how these could be used to support new inventions (Wassell et al., 2012a; 2012b; 2012c; 2012d; 2012e; Bech et al., 2013).

5.4 High and Low TAG W/O Emulsion Application Trials: A Functional Evaluation of MAG based on Moringa, Lesquerella, Rapeseed, Sunflower TAG and a PGPR

5.4.1 Introduction

It has been shown (4.0) that a MAG based on *Moringa oleifera* TAG, can have similar interfacial and crystallisation (5.2 & 5.3) characteristics to PGPR (GRINDSTED® PGPR 90). Previous examinations have centred on model systems. In real emulsion systems, interest lies in the properties of the interfacial film and its viscoelastic behaviour, where surface elasticity is thought to be the determining factor in minimising film rupture (Boyd et al., 1972) and hence coalescence. The strength of the interfacial film formed by the emulsifier may be more important than its effect on interfacial tension (Scherze, Knotha, Muschiolika, 2006). An emulsifier which is very effective in stabilising an emulsion may be much less effective in aiding the construction of an initial small water droplet and narrow DSD, i.e. it may help form visco-elastic films at the TAG / water interface, but may result in emulsions of relatively large DSD. This may be irrespective of its hydrophobic influence on reducing interfacial tension to low values (Boyd et al., 1972). To obtain confirmation about the functionality of Moringa MAG, proof of concept by way of application trials were required. A series of W/O emulsion spreads are prepared at 60% and 40% TAG concentration respectively. Results from water Droplet Size Distribution (DSD) analysis, Confocal Laser Scanning Microscopy (CLSM) imaging, texture analysis and sensory tasting are used as a basis for evaluation.

5.4.2 Materials and Methods

High and low TAG WO emulsion application trials were prepared for evaluation of monoglycerides based on *Moringa oleifera* TAG and *Lesquerella fendleri* TAG (Appendix F, G); commercial rapeseed based (DIMODAN® RT); sunflower based (DIMODAN® UJ) and a PGPR (GRINDSTED® PGPR 90).

The W/O emulsion samples were made according to formula and process conditions given below for 60% W/O TAG spreads in Tables 5.4.1 and 5.4.2, and for 40% W/O TAG spreads in Tables 5.4.3 and 5.4.4.

The chosen emulsifier concentration is arbitrarily based on typical minimum / maximum levels (refer to 1.2). For 60% TAG, a partially saturated / hydrogenated (IV 60) monoglyceride (Rapeseed based) – DIMODAN® RT is for control and comparison. For 40% TAG an unsaturated (IV105) monoglyceride (Sunflower based) – DIMODAN® UJ is for control and comparison. PGPR was used at a dose of 0.2% between maximum permitted use (0.4%) and total absence (refer to 1.2).

For more details of emulsifier and general process conditions and analysis, refer to Materials and Methods (2.0)

Table 5.4.1 Recipe for 60% TAG spreads trials 1-6

Ingredients in %						
Ingredient Name	**1**	**2**	**3**	**4**	**5**	**6**
Water phase						
Water (Tap)	38.400	38.400	38.400	38.400	38.400	38.400
Salt	1.000	1.000	1.000	1.000	1.000	1.000
Skimmed milk powder (MILEX 240)	0.500	0.500	0.500	0.500	0.500	0.500
Potassium Sorbate	0.100	0.100	0.100	0.100	0.100	0.100
Water phase total	**40.000**	**40.000**	**40.000**	**40.000**	**40.000**	**40.000**
pH	5.5	5.5	5.5	5.5	5.5	5.5
Fat phase						
PK4 - INES	25.000	25.000	25.000	25.000	25.000	25.000
Rapeseed oil	75.000	75.000	75.000	75.000	75.000	75.000
Fat blend total	**100.000**	**100.000**	**100.000**	**100.000**	**100.000**	**100.000**
Other fat ingredients						
Distilled Lesquerella Monoglyceride					0.300	0.600
DIMODAN R-T PEL/B - K	0.300	0.600				
Moringa MAG (191)			0.300	0.600		
TOCO 50	0.010	0.010	0.010	0.010	0.010	0.010
2% sol. beta-carotene	0.020	0.020	0.020	0.020	0.020	0.020
Other fat ingredients total	**0.330**	**0.630**	**0.330**	**0.630**	**0.330**	**0.630**
Fat phase total	**60.000**	**60.000**	**60.000**	**60.000**	**60.000**	**60.000**
RECIPE total (calc. batchsize)	**100.000**	**100.000**	**100.000**	**100.000**	**100.000**	**100.000**

The emulsifiers tested in 60% W/O TAG spreads samples according to Table 5.4.1 are as follows:

1. DIMODAN® RT 0.3%
2. DIMODAN® RT 0.6%
3. Moringa MAG (191) 0.3%
4. Moringa MAG (191) 0.6%
5. Lesquerella 0.3% (Fatty acid details in 2.0)
6. Lesquerella 0.6%

Table 5.4.2 Pilot plant processing conditions for the 60% TAG spread samples

Pilot Plant						
Processing (3-tube lab perfector):	**1**	**2**	**3**	**4**	**5**	**6**
Oil phase temperature	50	50	50	50	50	50
Water phase temperature	20	20	20	20	20	20
Emulsion temperature	50	50	50	50	50	50
Centrifugal pump	Auto	Auto	Auto	Auto	Auto	Auto
Capacity high pressure pump	40	40	40	40	40	40
Cooling (NH3) tube 1:	-10	-10	-10	-10	-10	-10
Cooling (NH3) tube 2:	-10	-10	-10	-10	-10	-10
Cooling (NH3) tube 3:	-10	-10	-10	-10	-10	-10
Rpm tube 1:	1000	1000	1000	1000	1000	1000
Rpm tube 2:	1000	1000	1000	1000	1000	1000
Rpm tube 3:	1000	1000	1000	1000	1000	1000

Table 5.4.3 Recipe for 40% TAG spreads trials 11-19

Ingredients in %									
Ingredient Name	**11**	**12**	**13**	**14**	**15**	**16**	**17**	**18**	**19**
Water phase									
Water (Tap)	57.300	57.300	57.300	57.300	57.300	57.300	57.300	57.300	57.300
Salt	1.000	1.000	1.000	1.000	1.000	1.000	1.000	1.000	1.000
Skimmed milk powder (MILEX 240)	0.100	0.100	0.100	0.100	0.100	0.100	0.100	0.100	0.100
GRINDSTED® LFS 560	1.500	1.500	1.500	1.500	1.500	1.500	1.500	1.500	1.500
Potassium Sorbate	0.100	0.100	0.100	0.100	0.100	0.100	0.100	0.100	0.100
Water phase total	**60.000**	**60.000**	**60.000**	**60.000**	**60.000**	**60.000**	**60.000**	**60.000**	**60.000**
pH	5.5	5.5	5.5	5.5	5.5	5.5	5.5	5.5	5.5
Fat phase									
Fat blend									
PK4 – INES	25.000	25.000	25.000	25.000	25.000	25.000	25.000	25.000	25.000
Rapeseed oil	75.000	75.000	75.000	75.000	75.000	75.000	75.000	75.000	75.000
Fat blend total	**100.000**	**100.000**	**100.000**	**100.000**	**100.000**	**100.000**	**100.000**	**100.000**	**100.000**
Other fat ingredients									
Distilled Lesquerella Monoglyceride			0.300			0.600			0.300
DIMODAN U/J – K	0.300			0.600			0.300		
Moringa MAG (191)		0.300			0.600			0.300	
PGPR 90 – K							0.200	0.200	0.200
TOCO 50	0.010	0.010	0.010	0.010	0.010	0.010	0.010	0.010	0.010
2% sol. beta-carotene	0.020	0.020	0.020	0.020	0.020	0.020	0.020	0.020	0.020
Other fat ingredients total	**0.330**	**0.330**	**0.330**	**0.630**	**0.630**	**0.630**	**0.530**	**0.530**	**0.530**
Fat phase total	**40.000**	**40.000**	**40.000**	**40.000**	**40.000**	**40.000**	**40.000**	**40.000**	**40.000**
RECIPE total (calc. batchsize)	**100.000**	**100.000**	**100.000**	**100.000**	**100.000**	**100.000**	**100.000**	**100.000**	**100.000**

The emulsifiers tested in 40% W/O TAG spreads samples according to Table 5.4.3 are as follows:

11. DIMODAN® UJ 0.3%
12. Moringa MAG (191) 0.3%
13. Lesquerella 0.3%
14. DIMODAN® UJ 0.6%
15. Moringa 0.6%
16. Lesquerella 0.6%
17. DIMODAN® UJ 0.3% and GRINDSTED® PGPR 90 0.2%
18. Moringa MAG (191) 0.3% and GRINDSTED® PGPR 90 0.2%
19. Lesquerella 0.3% and GRINDSTED® PGPR 90 0.2%

Table 5.4.4 Pilot plant processing conditions for the 40% TAG spread samples

Pilot Plant									
Processing (3-tube lab perfector):	**11**	**12**	**13**	**14**	**15**	**16**	**17**	**18**	**19**
Oil phase temperature	50	50	50	50	50	50	50	50	50
Water phase temperature	50	50	50	50	50	50	50	50	50
Emulsion temperature	50	50	50	50	50	50	50	50	50
Centrifugal pump	Auto	Auto	Auto	Auto	Auto	Auto	Auto	Auto	Auto
Capacity high pressure pump	40	40	40	40	40	40	40	40	40
Cooling (NH3) tube 1:	-10	-10	-10	-10	-10	-10	-10	-10	-10
Cooling (NH3) tube 2:	-10	-10	-10	-10	-10	-10	-10	-10	-10
Cooling (NH3) tube 3:	-10	-10	-10	-10	-10	-10	-10	-10	-10
Rpm tube 1:	1000	1000	1000	1000	1000	1000	1000	1000	1000
Rpm tube 2:	1000	1000	1000	1000	1000	1000	1000	1000	1000
Rpm tube 3:	1000	1000	1000	1000	1000	1000	1000	1000	1000

Texture analysis was carried out with a Stable Micro Systems: TA-XT2i texture analyser and run under standard methodology for measuring hardness (2.0).

5.4.3 Validation Trials

The recipes and plant conditions for the validation trails are given below in Tables 5.4.5 and 5.4.6. Moringa MAG 191 is the same Moringa MAG identified in 5.2 and 5.3. Tests with Lesquerella MAG were not repeated, but abandoned from this point, because of obvious emulsion separation (refer to results).

Table 5.4.5 Recipe for 40% TAG spreads (validation test)

Ingredient Name	1	2	3	4	5	6
Water (Tap)	57.300	57.300	57.300	57.300	57.300	57.300
Salt	1.000	1.000	1.000	1.000	1.000	1.000
Skimmed milk powder (MILEX 240)	0.100	0.100	0.100	0.100	0.100	0.100
GRINDSTED® LFS 560	1.500	1.500	1.500	1.500	1.500	1.500
Potassium Sorbate	0.100	0.100	0.100	0.100	0.100	0.100
Butter Flavouring 050001 T03007	0.010	0.010	0.010	0.010	0.010	0.010
Water phase total	**60.010**	**60.010**	**60.010**	**60.010**	**60.010**	**60.010**
pH	5.5	5.5	5.5	5.5	5.5	5.5
PK4 - INES	25.000	25.000	25.000	25.000	25.000	25.000
Rapeseed oil	75.000	75.000	75.000	75.000	75.000	75.000
Fat blend total	**100.000**	**100.000**	**100.000**	**100.000**	**100.000**	**100.000**
DIMODAN U/J	0.300		0.600		0.300	
PGPR 90 - K					0.200	0.200
Moringa MAG (191)		0.300		0.600		0.300
TOCO 50						
Butter Flavouring 050001 T04184	0.020	0.020	0.020	0.020	0.020	0.020
Other fat ingredients total	**0.320**	**0.320**	**0.620**	**0.620**	**0.520**	**0.520**
Fat phase total	**39.990**	**39.990**	**39.990**	**39.990**	**39.990**	**39.990**
RECIPE total (calc. batchsize)	**100.000**	**100.000**	**100.000**	**100.000**	**100.000**	**100.000**

The samples in the validation trials (Table 5.4.5) are as follows:

1. DIMODAN® UJ 0.3%
2. Moringa 0.3%
3. DIMODAN® UJ 0.6%
4. Moringa 0.6%
5. DIMODAN® UJ 0.3% / GRINDSTED® PGPR 90, 0.2%
6. Moringa 0.3% / GRINDSTED® PGPR 90, 0.2%

Table 5.4.6 Plant process conditions for the 40% TAG spreads (Validation test)

Processing (3-tube lab perfector):	Default	1	2	3	4	5	6
Oil phase temperature	50	50	50	50	50	50	50
Water phase temperature	50	50	50	50	50	50	50
Emulsion temperature	50	50	50	50	50	50	50
Centrifugal pump	Auto	Auto	Auto	Auto	Auto	Auto	Auto
Capacity high pressure pump	40	40	40	40	40	40	40
Cooling (NH3) tube 1:	-10	-10	-10	-10	-10	-10	-10
Cooling (NH3) tube 2:	-10	-10	-10	-10	-10	-10	-10
Cooling (NH3) tube 3:	-10	-10	-10	-10	-10	-10	-10
Rpm tube 1:	1000	1000	1000	1000	1000	1000	1000
Rpm tube 2:	1000	1000	1000	1000	1000	1000	1000
Rpm tube 3:	1000	1000	1000	1000	1000	1000	1000

5.4.4 Results and Discussion

5.4.4.1 60% TAG based W/O Spreads

Table 5.4.7 shows the DSD for the samples from 60% TAG spreads based on those trials shown in Table 5.4.1

Table 5.4.7 DSD for 60% TAG spread samples

Sample	Emulsifier	2.5% <μm	50% <μm	97.5% <μm
1	DIMODAN® RT 0.3%	0.92	3.24	11.43
	St. Dev	0.04	0.09	1.06
2	DIMODAN® RT 0.6%	1.79	2.80	4.39
	St. Dev	0.18	0.06	0.25
3	Moringa 0.3%	1.59	6.36	25.44
	St. Dev	0.04	0.06	1.07
4	Moringa 0.6%	1.46	4.38	13.14
	St. Dev	0.06	0.12	1.22
5	Lesquerella 0.3%	1.63	17.90	212.35
	St. Dev	0.24	3.43	115.68
6	Lesquerella 0.6%	2.27	26.59	312.09
	St. Dev	0.09	0.82	7.18

The DSD reveals that water droplet size volume at 97.5% <μm, are grouped, with the exception of samples containing Lesquerella, which considered highly unstable. At 60% TAG concentration the Moringa and DIMODAN® RT results suggest stable emulsions and thereby smaller water droplet sizes. The DSD data suggests the presence of "large lakes" of water. This assumption is further supported by the data of the distribution as expressed graphically in Figure 5.4.1.

Clearly visible in Figure 5.4.1 is the distribution of the water droplet sizes for the 60% TAG spreads, showing the extremely large size of water droplets corresponding to Lesquerella. Conversely, Moringa sample 4 at the concentration of 0.6% is showing a water droplet size broadly akin to that of sample 1 which corresponds to DIMODAN® RT at 0.3%. This suggests that the stability of the 0.6% Moringa is potentially similar DIMODAN® RT 0.3% sample.

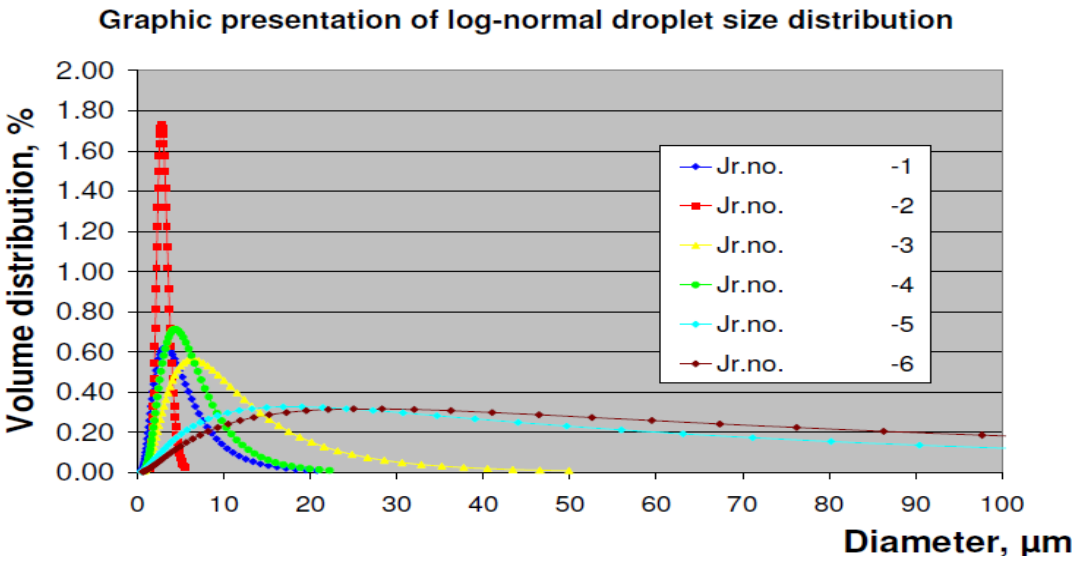

Figure 5.4.1 Water droplet size distribution (DSD) of the 60% TAG blends.

The data presented in Figures 5.4.2 to 5.4.7 are the CLSM images of application trials 1 – 6, as described in Table 5.4.1. Four images at two magnifications (40X and 100X) were taken respectively. The images are then reproduced (scaled) to 375 x 375 µm and 188 x 188µm. All samples are stained with FITC, stains protein green, and Nile Red, stains TAG red.

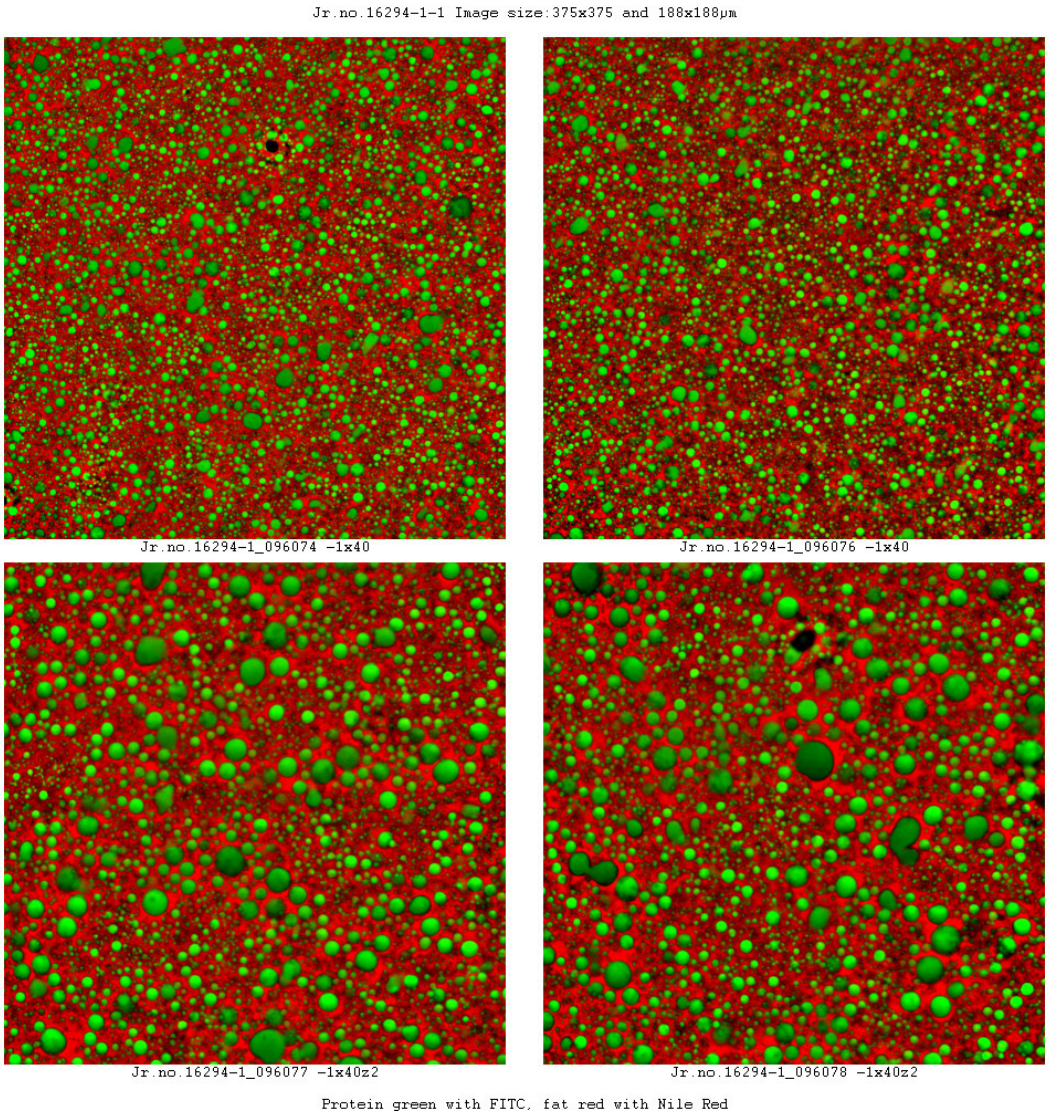

Figure 5.4.2 CLSM image of 60% TAG spread with DIMODAN® RT at 0.3% concentration. (Top images 375 x 375 µm. Bottom images 188 x 188µm)

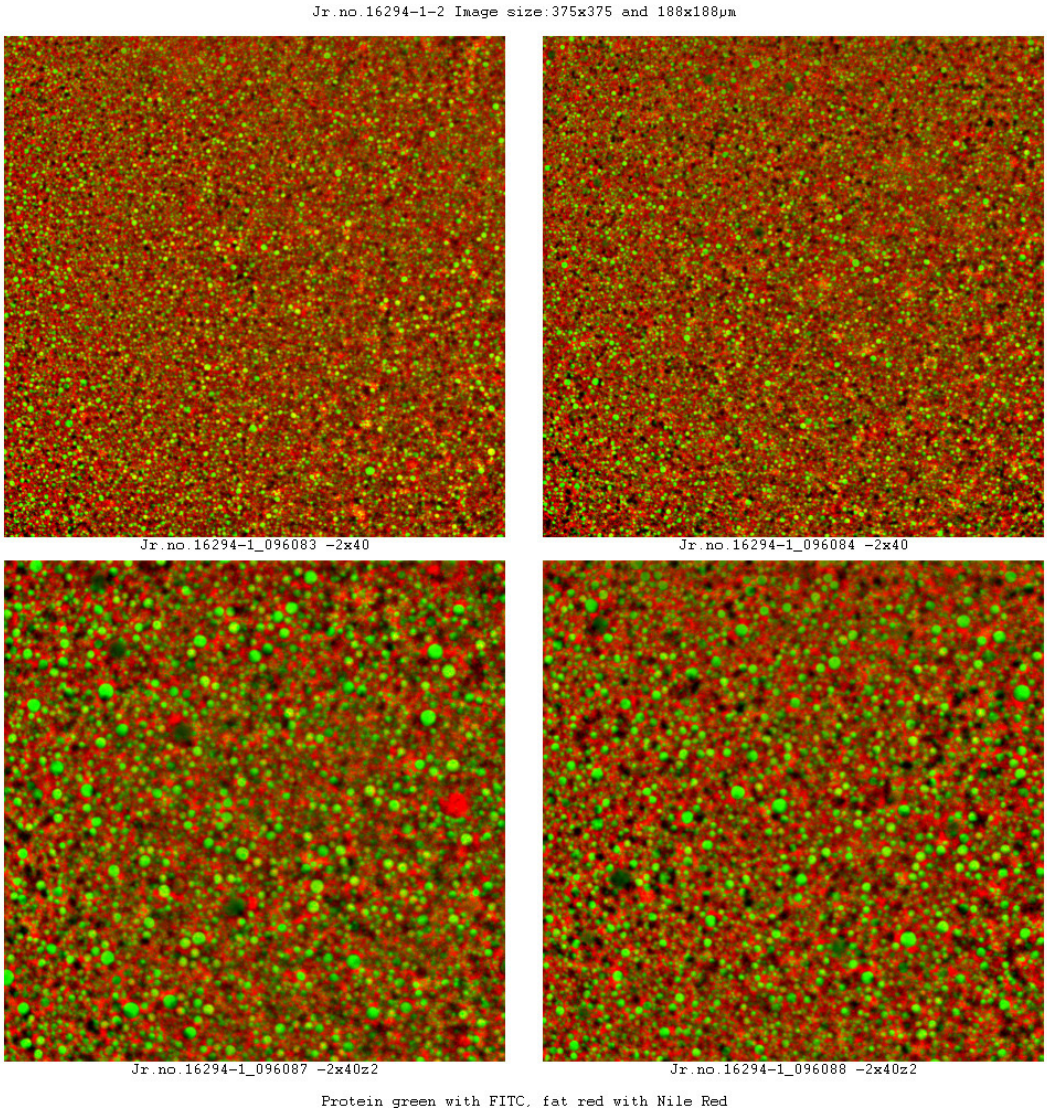

Figure 5.4.3 CLSM image of 60% TAG spread with DIMODAN® RT at 0.6% concentration (Top images 375 x 375 µm. Bottom images 188 x 188µm)

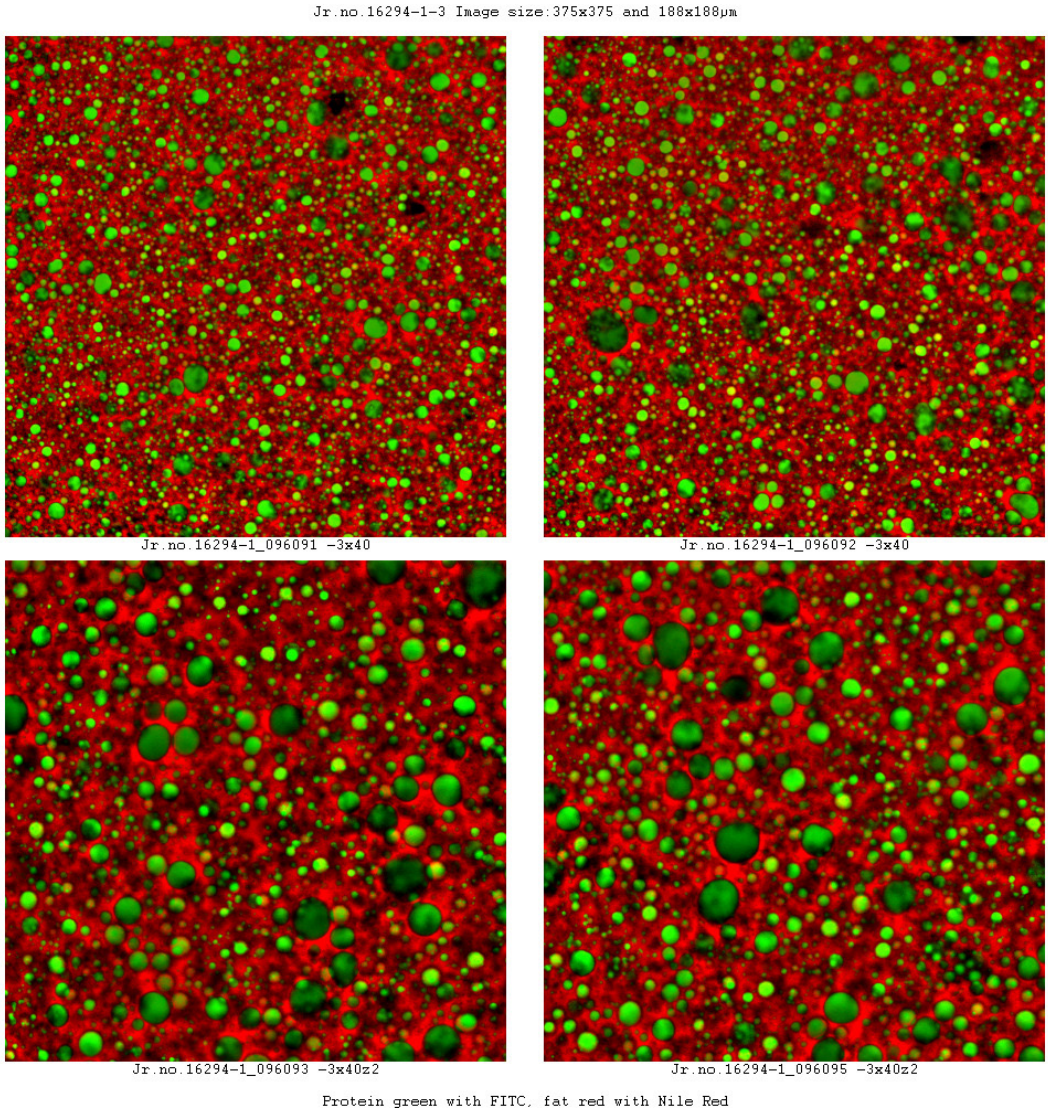

Figure 5.4.4 CLSM image of 60% TAG spread with Moringa at 0.3% concentration. (Top images 375 x 375 µm. Bottom images 188 x 188µm)

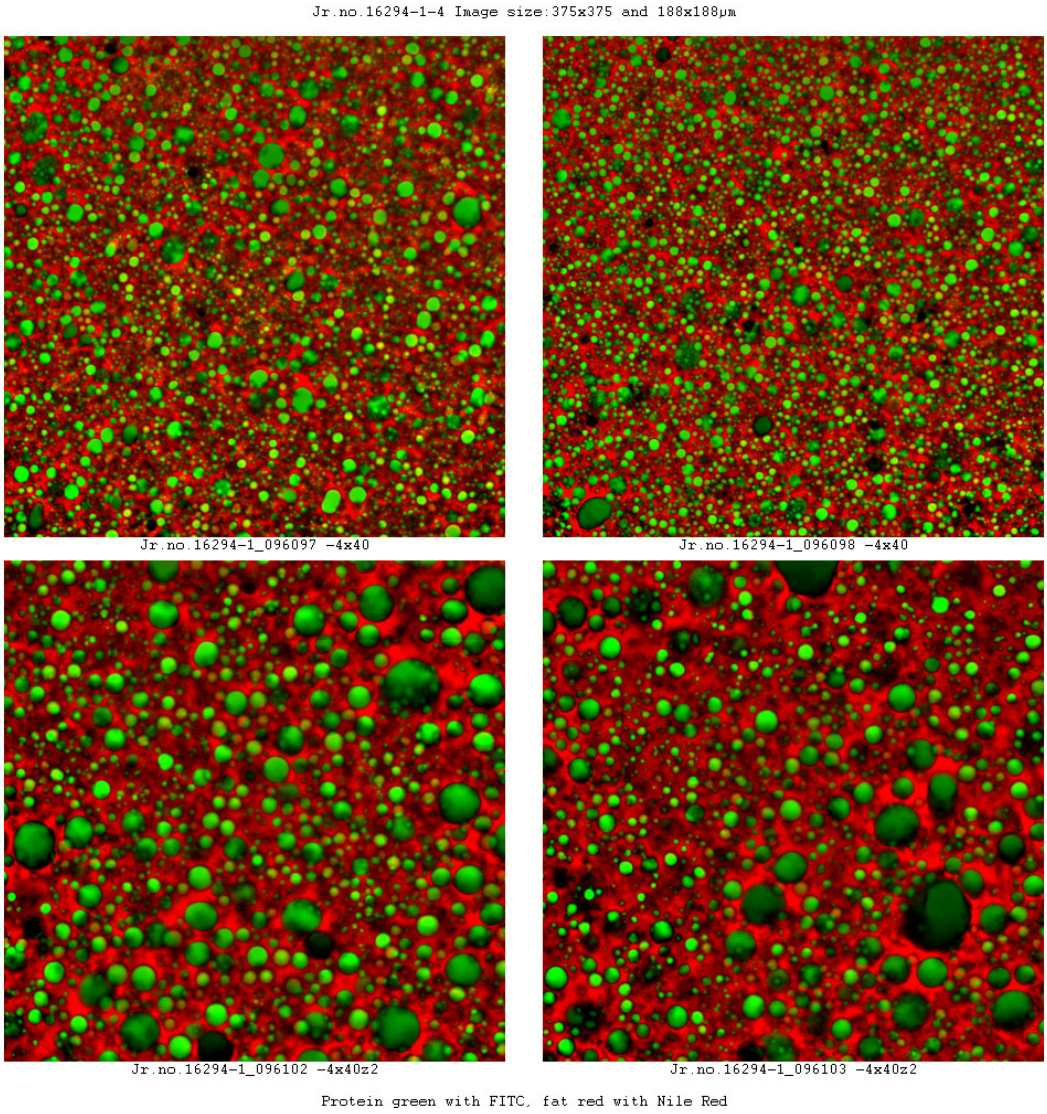

Figure 5.4.5 CLSM image of 60% TAG spread with Moringa at 0.6% concentration. (Top images 375 x 375 µm. Bottom images 188 x 188µm)

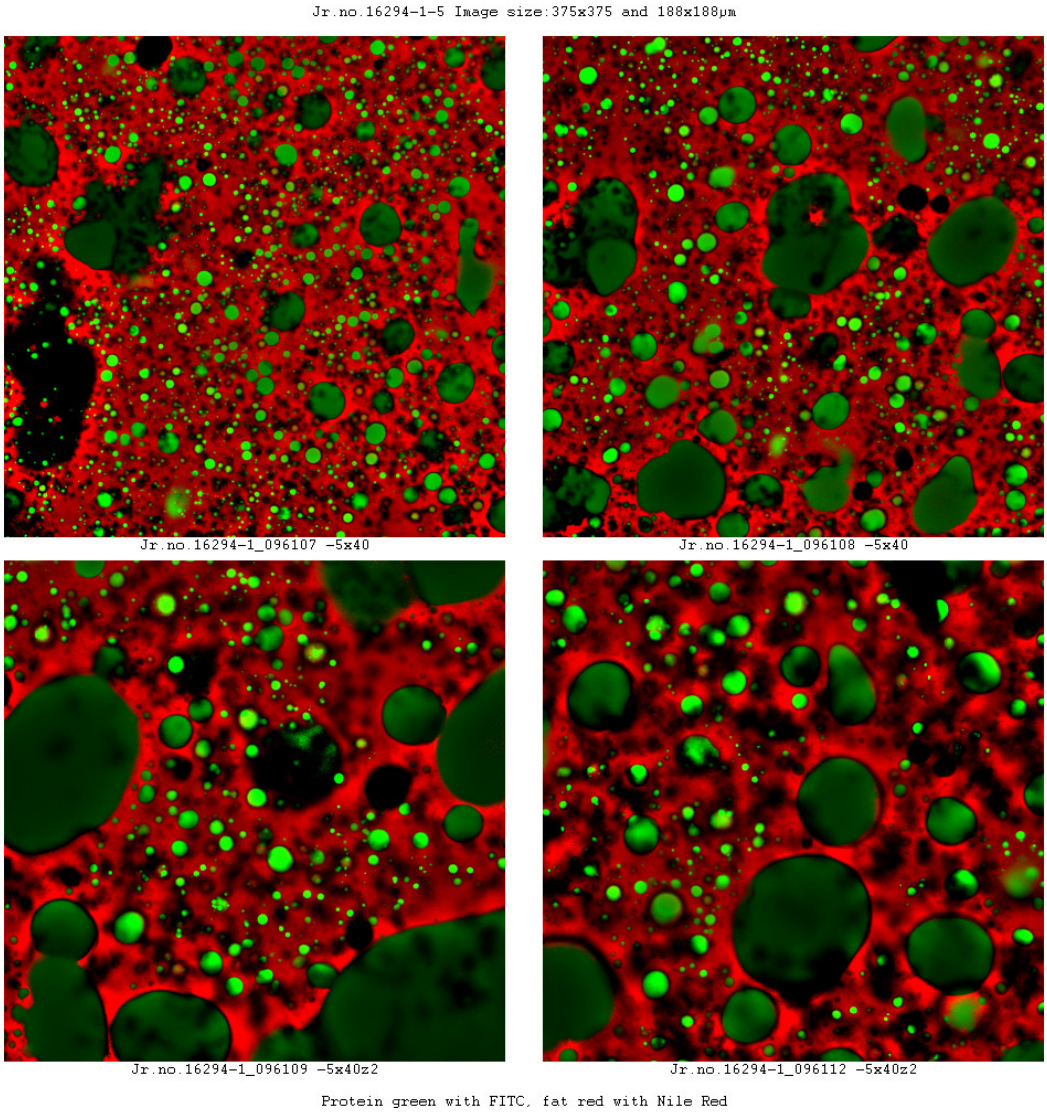

Figure 5.4.6 CLSM image of 60% TAG spread with Lesquerella at 0.3% concentration. (Top images 375 x 375 µm. Bottom images 188 x 188µm)

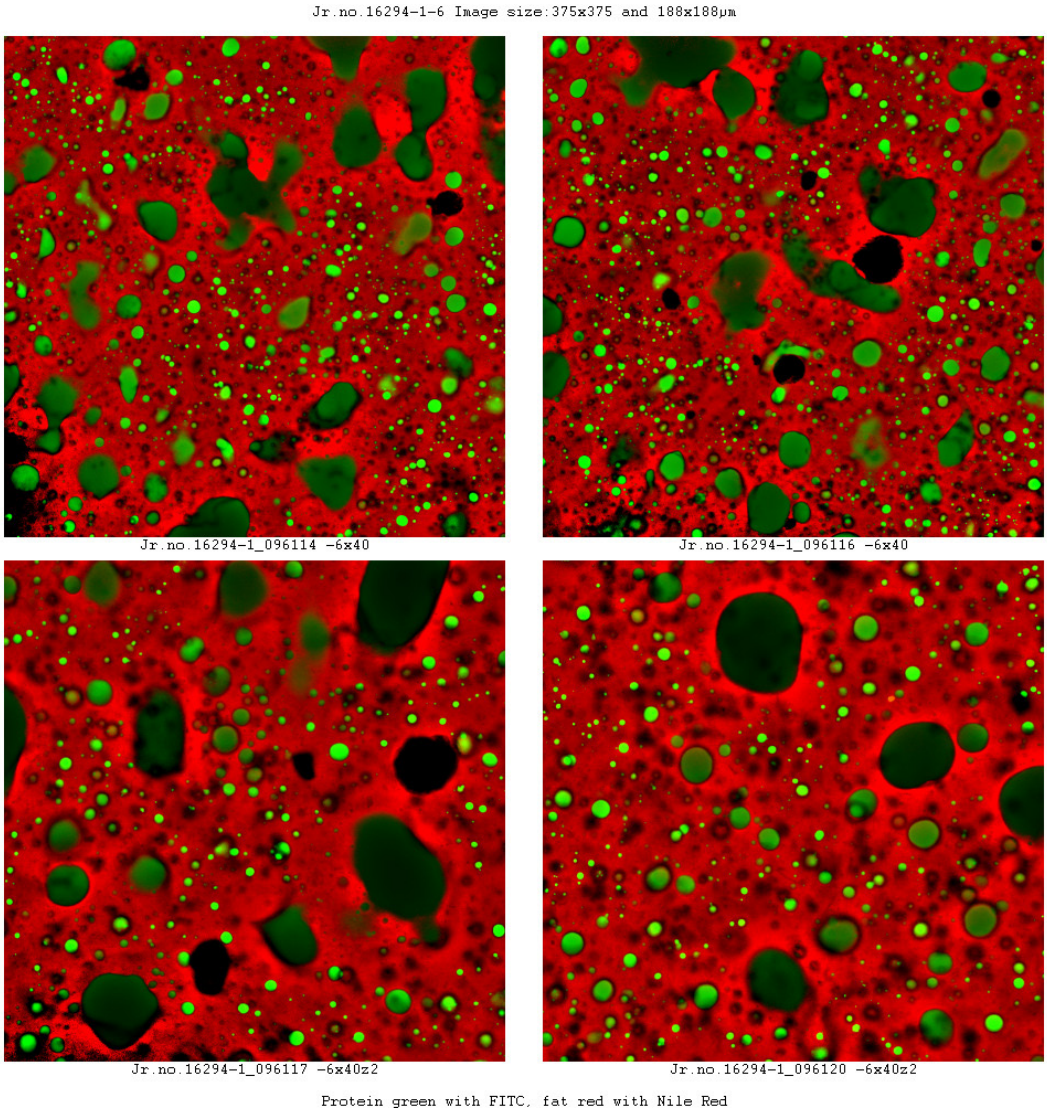

Figure 5.4.7 CLSM image of 60% TAG spread with Lesquerella at 0.6% concentration. (Top images 375 x 375 µm. Bottom images 188 x 188µm)

The slides above in Figures 5.4.2 to 5.4.7 present excellent visual images to support the data in Table 5.4.7 and Figure 5.4.1. DIMODAN® RT 0.3% and 0.6% samples have a small water droplet size and a narrow water droplet distribution. The water droplets are seen via the green or dark colouring, since the protein sits at or in the water phase, these appear together. Apart from Lesquerella (Figures 5.4.6 & 5.4.7) these systems are inherently stable. To help determine stability, sensory properties are discussed later.

Figures 5.4.4 and 5.4.5 refer to the samples with Moringa at 0.3% and 0.6% respectively, and it can be seen that the water droplet size is considerably larger in Figure 5.4.4 at 0.3% as opposed to 0.6% - Figure 5.4.5. These images do not show the very small water droplet structures as in Figure 5.4.3 (DIMODAN® RT 0.6%), however, in Figure 5.4.5, where Moringa is at 0.6% concentration the CLSM images are similar to those for DIMODAN® RT at 0.3%. This is also indicated in the graphical data shown in Figure 5.4.1, and indicates that Moringa here is behaving in a manner that is capable of forming stable spread products and this high TAG concentration is in parity with DIMODAN® RT – albeit at a higher concentration.

Figures 5.4.6 and 5.4.7, corresponding to Lesquerella at 0.3 and 0.6% respectively show the presence of large areas of coalesced water droplets (lakes of water). This was enough to confirm that this product was not stable and basically would fail any storage, sensory or spreading test post production. In 60% W/O TAG spread emulsions Lesquerella MAG is not recommended.

5.4.4.2 40% TAG based W/O Spreads

Use of Moringa MAG (E471) in low TAG (<41%) applications could represent a cleaning up of the food product ingredient label since there would be potential opportunity to omit a co-emulsifier, PGPR (E476). With this objective all MAG based emulsifier components, plus PGPR were then tested in 40% TAG spreads with the aim of assessing the effect of stabilising W/O low TAG content emulsions. The water droplet size results (DSD) are shown in Table 5.4.8.

All samples relating to Lesquerella in 40% TAG spreads show the similar tendency as for the results above for 60% TAG spreads i.e. the water droplet size was so large that the emulsion samples have failed. When combined with a co-emulsifier PGPR, the recovery and stabilisation of the water droplet size was insufficient, leading to emulsion failure.

Moringa showed a trend that is also similar to the 60% TAG spreads, where in 40% TAG spreads, the droplet size where Moringa is present is smaller than all samples with DIMODAN® UJ either alone, or in combination with PGPR. This suggests from DSD analysis that the spreads made with Moringa were stable and exhibit adequate function similar to standard palm or hydrogenated MAG products for reduced or low TAG spreads.

Table 5.4.8 Water droplet size distribution for 40% TAG spread samples.

Sample	Emulsifiers	2.5% <µm	50%<µm	97.5%<µm
11	DIMODAN® UJ 0.3%	1.88	10.18	55.54
	St. Dev	0.11	0.18	2.23
12	Moringa 0.3%	1.31	7.47	42.41
	St. Dev	0.04	0.19	2.87
13	Lesquerella 0.3%	5.21	70.28	991.49
	St. Dev	0.75	26.35	606.24
14	DIMODAN® UJ 0.6%	1.47	12.47	106.38
	St. Dev	0.07	0.26	8.45
15	Moringa 0.6%	0.95	6.04	38.56
	St. Dev	0.06	0.32	6.86
16	Lesquerella 0.6%	9.95	96.07	987.00
	St. Dev	3.61	6.81	236.67
17	DIMODAN® UJ 0.3% / PGPR 90 0.2%	2.47	10.48	44.62
	St. Dev	0.07	0.42	4.39
18	Moringa 0.3% PGPR 90 0.2%	1.27	5.58	24.46
	St. Dev	0.02	0.14	0.94
19	Lesquerella 0.3% / PGPR 90 0.2%	6.82	68.46	722.91
	St. Dev	0.09	10.25	291.67

The graphical distribution of data in Table 5.4.8 is shown in Figure 5.4.8.

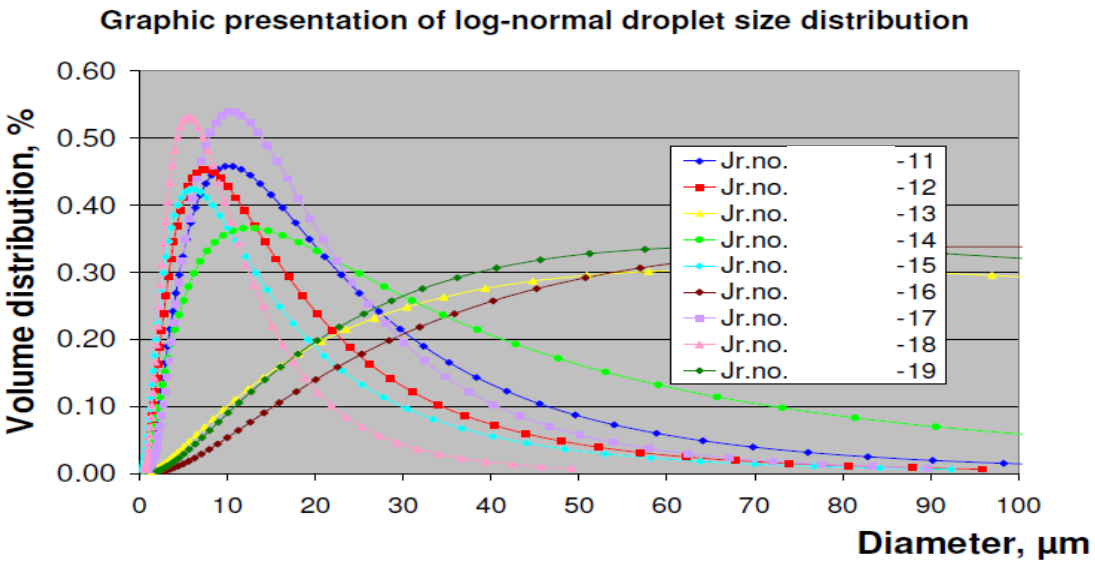

Figure 5.4.8 Water droplet size distribution (DSD) of W/O 40% TAG blends.

Results in Figure 5.4.8 show the samples having the tightest water droplets - samples 12, 15, and 18; those with Moringa at 0.3%, Moringa at 0.6% and Moringa 0.3% / PGPR 0.2% respectively. These results suggest the Moringa containing spreads are likely to be stable.

The CLSM images of the 40% TAG spreads are given in Figures 5.4.9 – 5.4.17. All the CLSM images of samples containing Lesquerella showed the presence of very large lakes of water. Visually these are beyond droplet classification and can be deemed as failed.

Sample 18, i.e. Moringa at 0.3% with co-emulsifier PGPR at 0.2%, had the smallest droplet size from Figure 5.4.8. But of particular significance was the CLSM images of Moringa at 0.6% – sample 15, which as a standalone, gave comparatively, the smallest water droplet. Moringa at 0.3% had slightly larger water droplets shown in Figure 5.4.8 and in fact showed the product itself was stable and held up to both storage and spreadability tests. The same argument was confirmed in the basic sensory results (5.4.4.4).

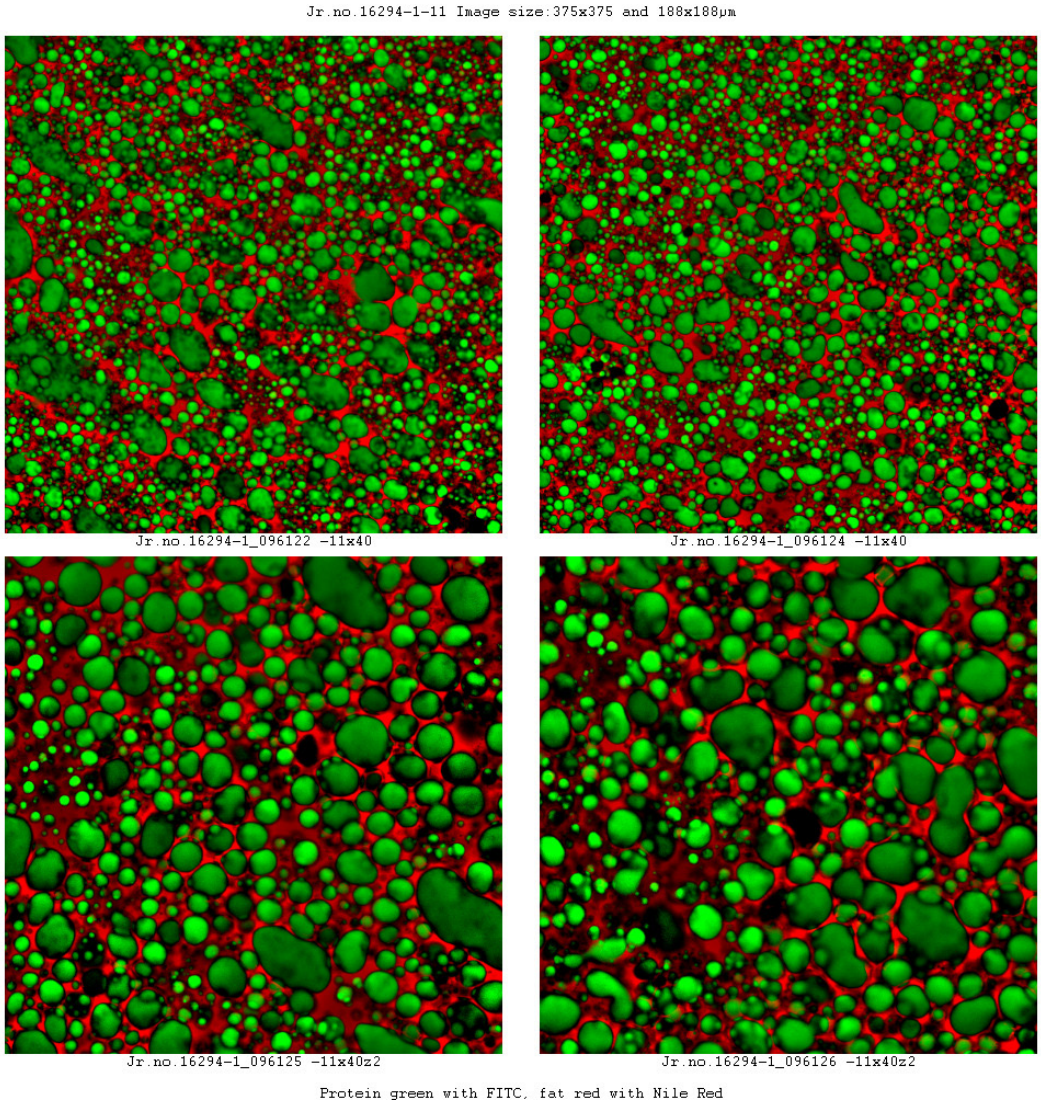

Figure 5.4.9 CLSM image of 40% TAG spread with DIMODAN® UJ at 0.3% concentration. (Top images 375 x 375 µm. Bottom images 188 x 188µm)

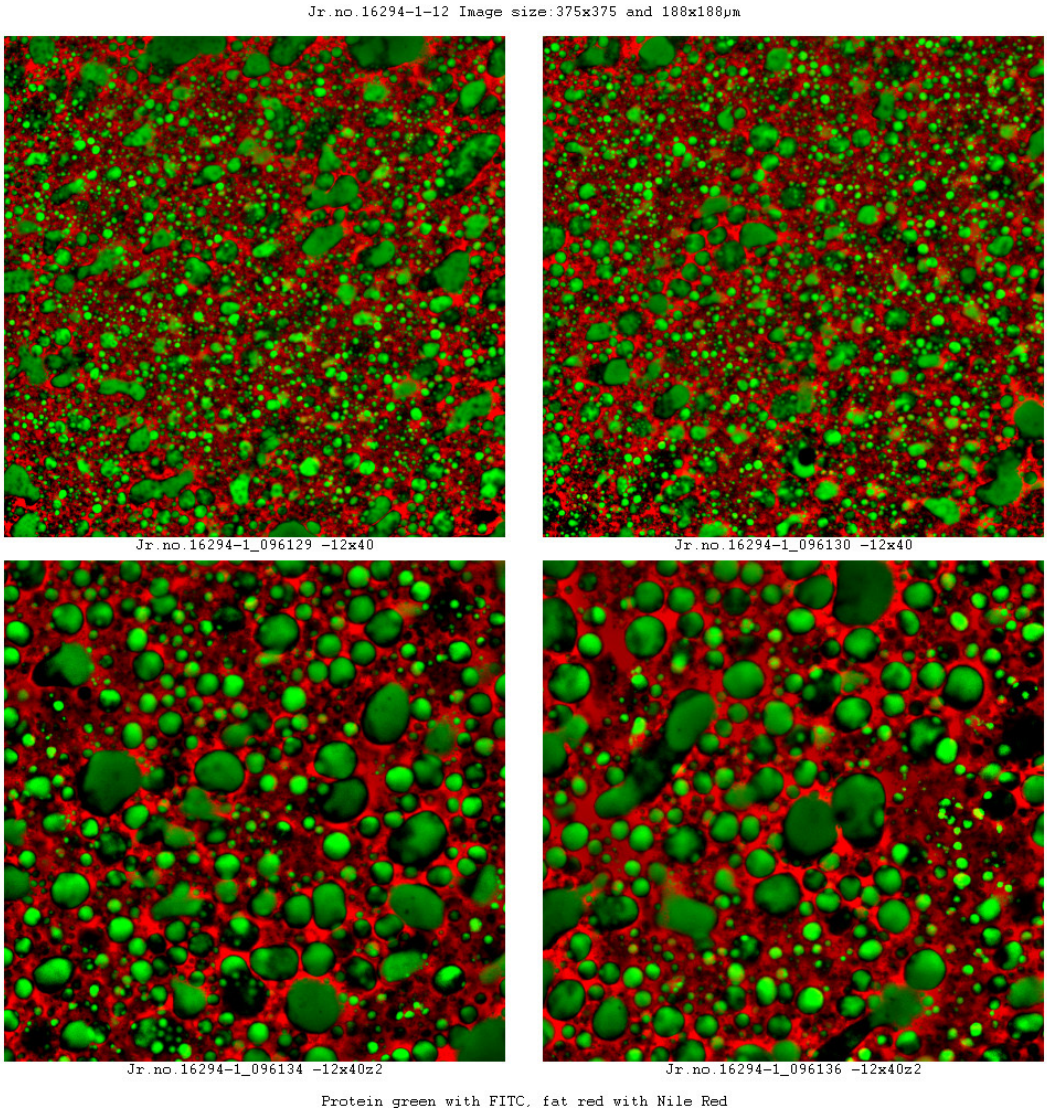

Figure 5.4.10 CLSM image of 40% TAG spread with Moringa at 0.3% concentration. (Top images 375 x 375 µm. Bottom images 188 x 188µm)

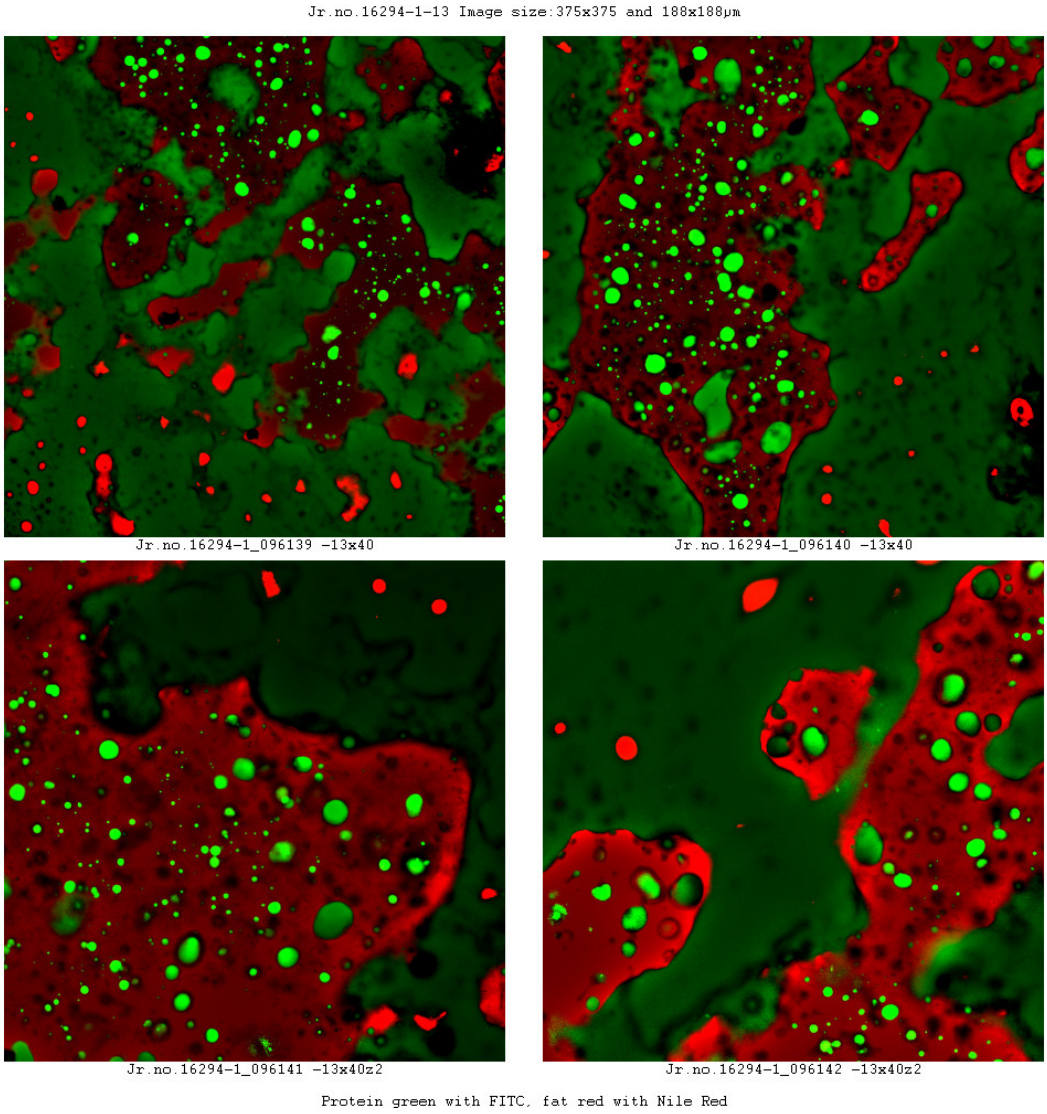

Figure 5.4.11 CLSM image of 40% TAG spread with Lesquerella at 0.3% concentration. (Top images 375 x 375 µm. Bottom images 188 x 188µm)

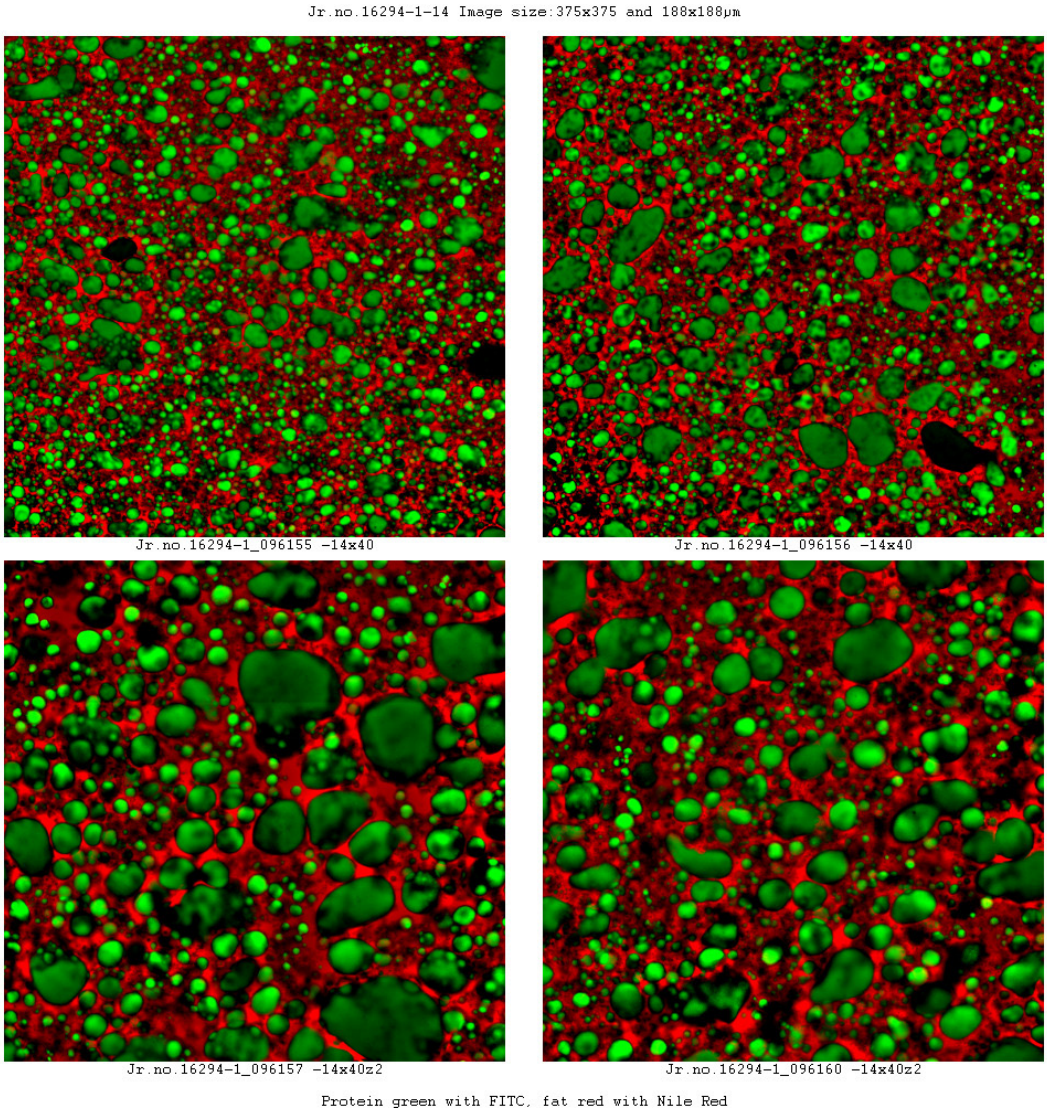

Figure 5.4.12 CLSM image of 40% TAG spread with DIMODAN® UJ at 0.6% concentration. (Top images 375 x 375 µm. Bottom images 188 x 188µm)

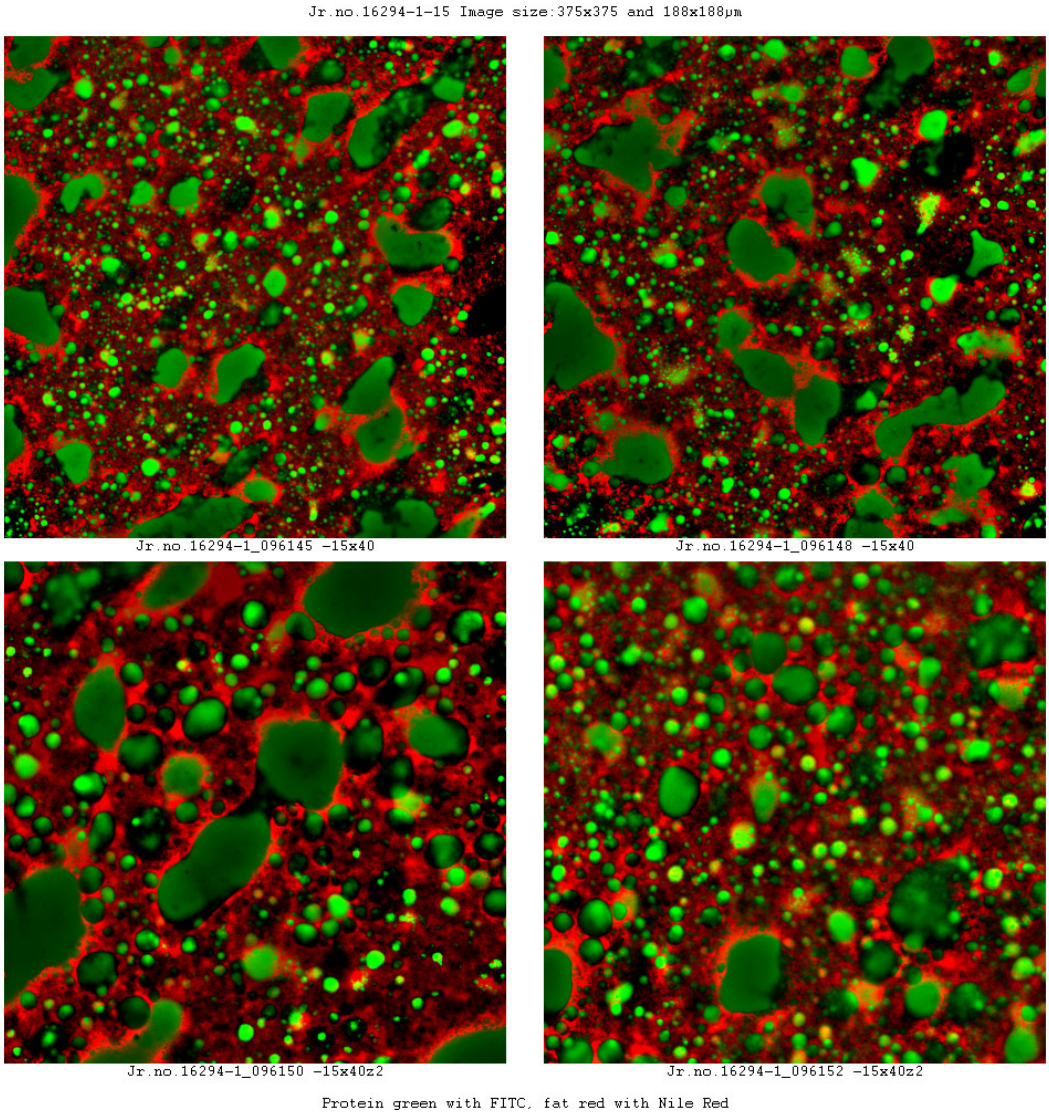

Figure 5.4.13 CLSM image of 40% TAG spread with Moringa at 0.6% concentration. (Top images 375 x 375 µm. Bottom images 188 x 188µm)

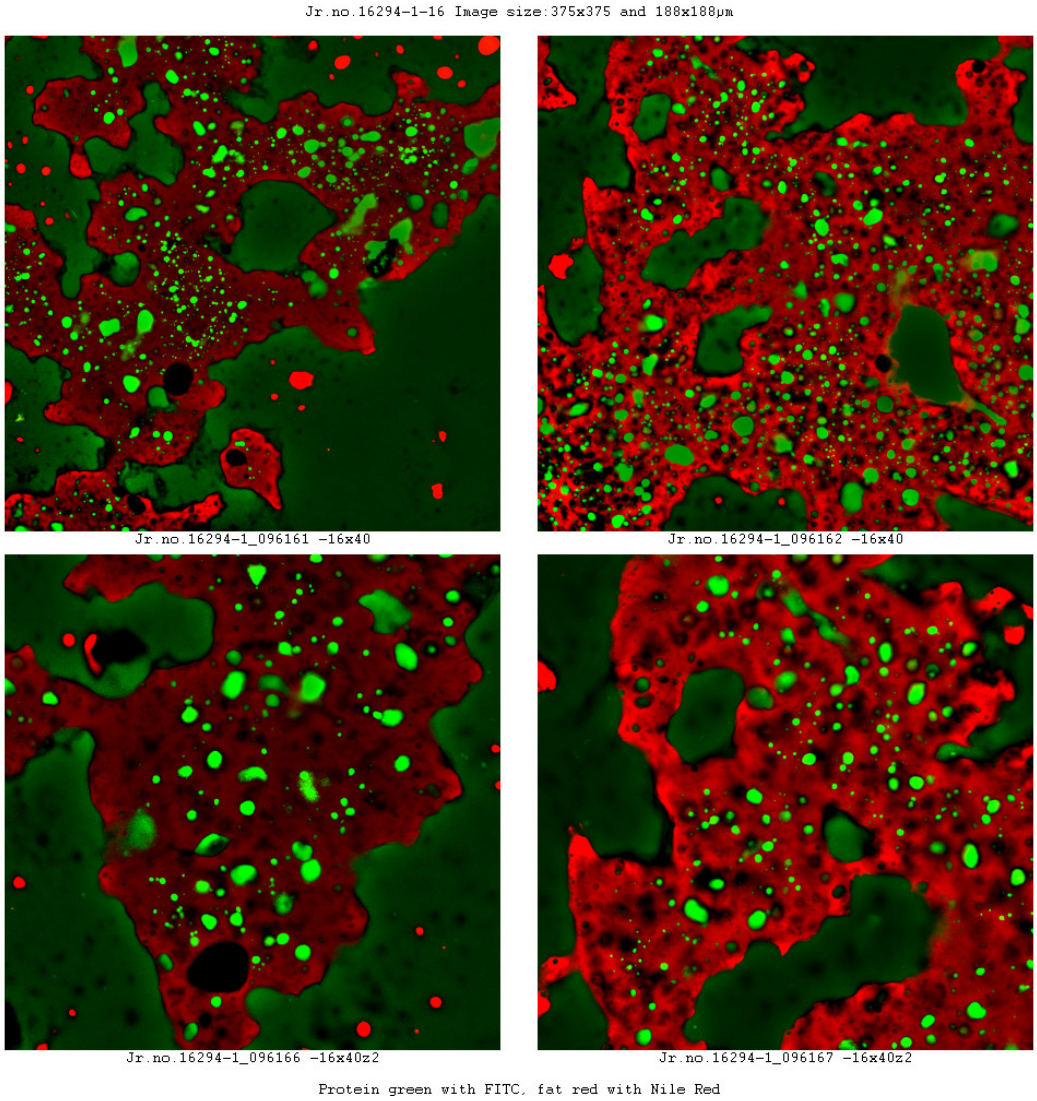

Figure 5.4.14 CLSM image of 40% TAG spread with Lequerella at 0.6% concentration. (Top images 375 x 375 µm. Bottom images 188 x 188µm)

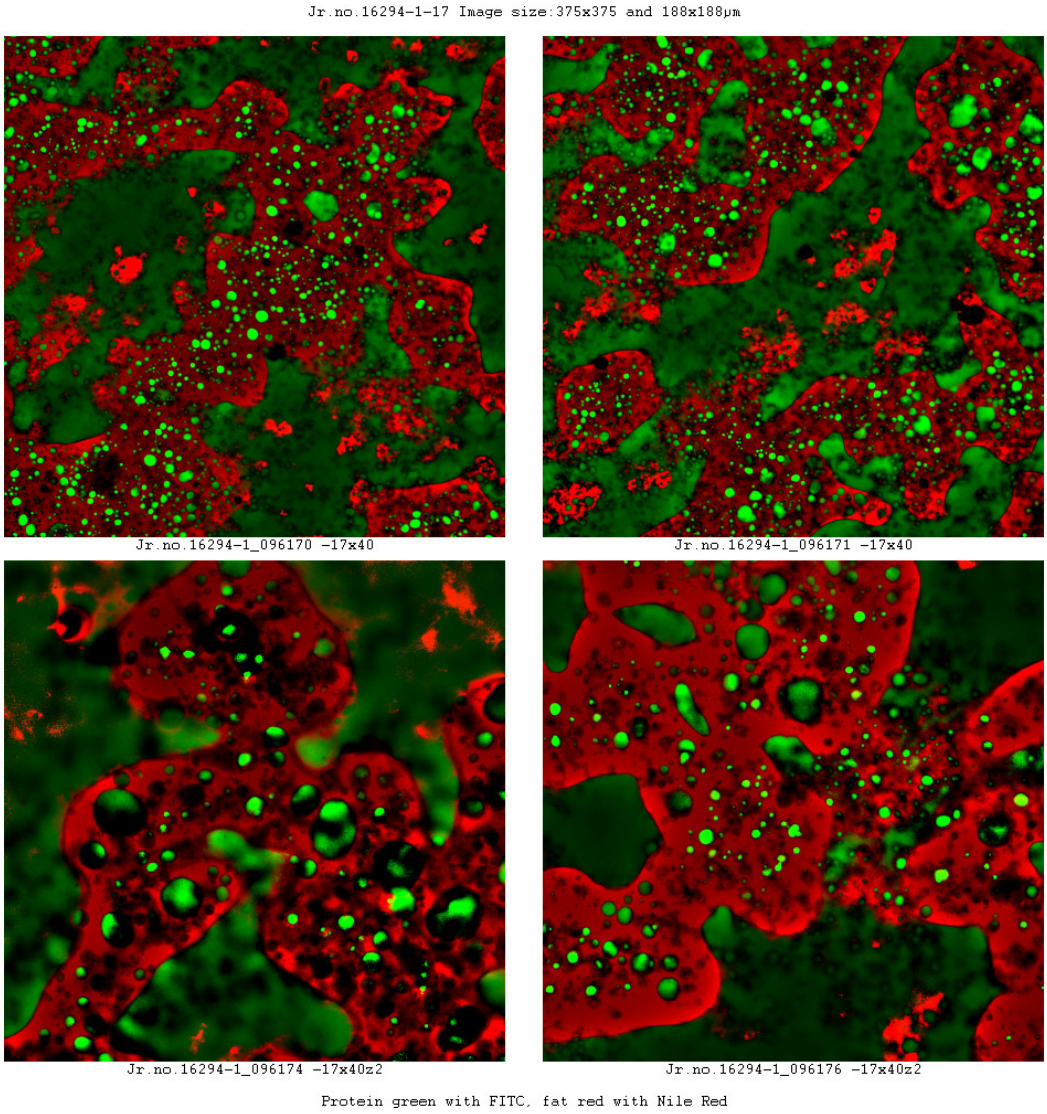

Figure 5.4.15 CLSM image of 40% TAG spread with DIMODAN® UJ 0.3% / GRINDSTED® PGPR 90 at 0.2% concentration. (Top images 375 x 375 µm. Bottom images 188 x 188µm)

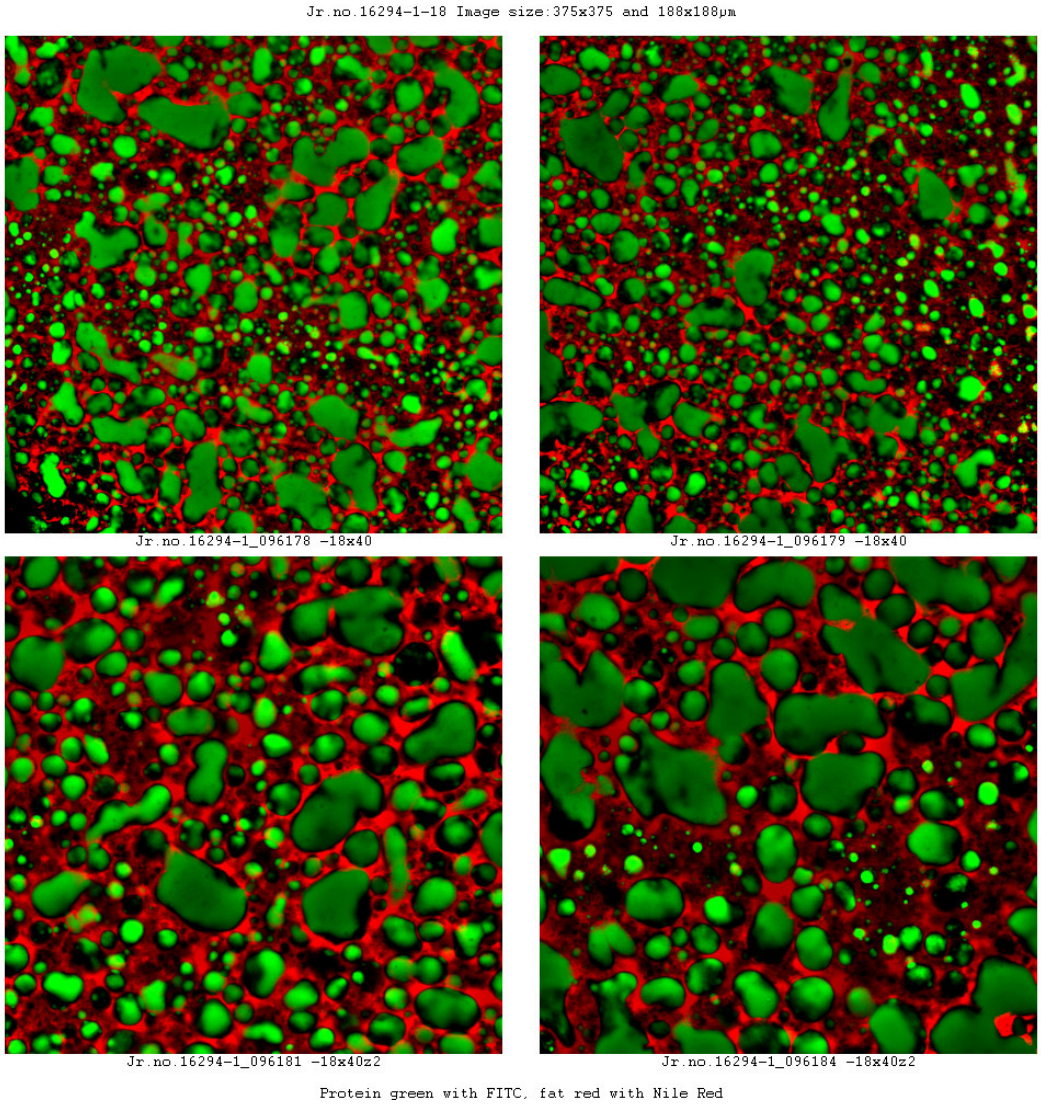

Figure 5.4.16 CLSM image of 40% TAG spread with Moringa 0.3% / GRINDSTED® PGPR 90 at 0.2% concentration. (Top images 375 x 375 µm. Bottom images 188 x 188µm)

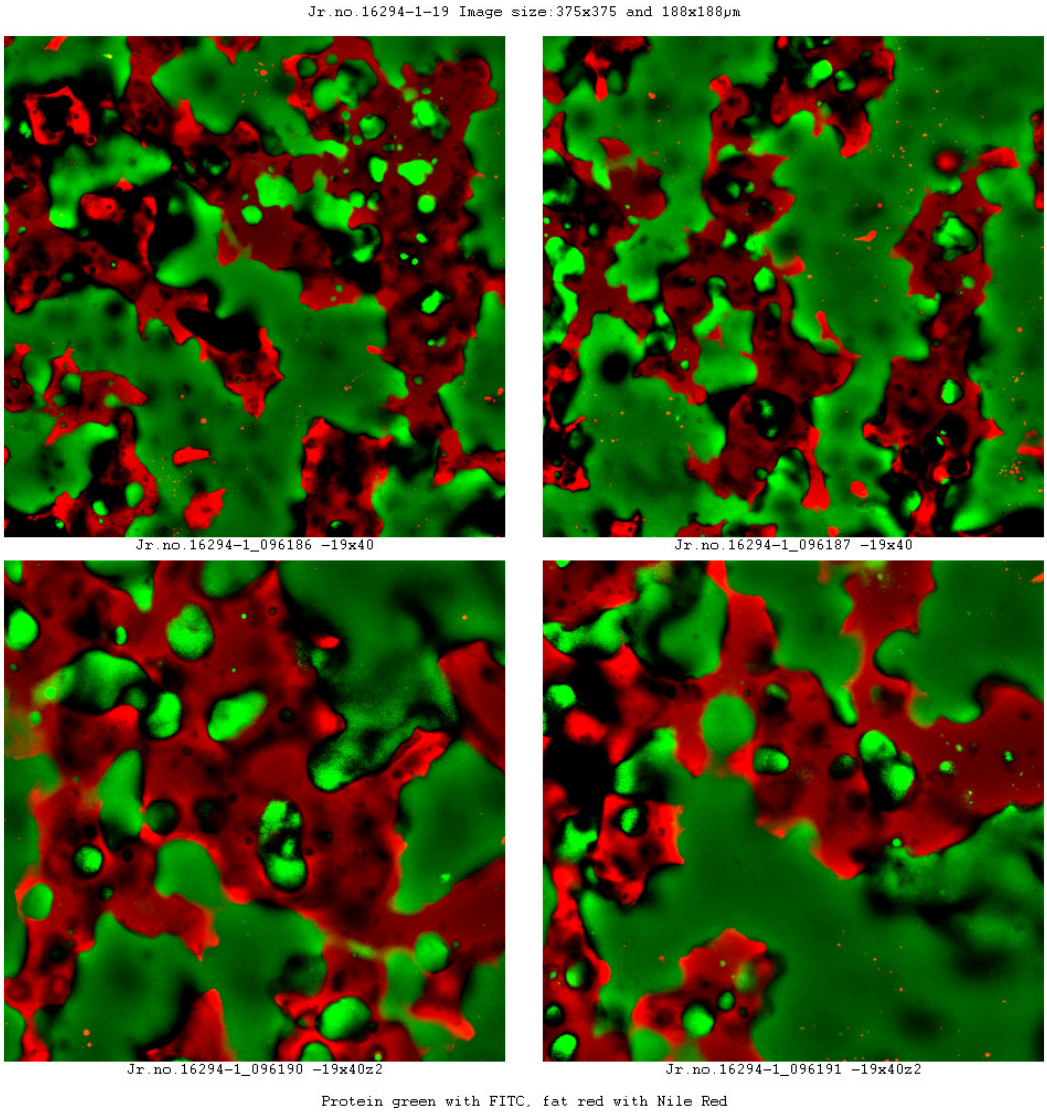

Figure 5.4.17 CLSM image of 40% TAG spread with Lesquerella 0.3% / GRINDSTED® PGPR 90 at 0.2% concentration. (Top images 375 x 375 µm. Bottom images 188 x 188µm)

5.4.4.3 Texture Analysis

Using a Stable Micro-Systems TX2 analyser, the texture of the spread samples was measured and treated together. The grouping on both low TAG and high TAG spreads shown in Figures 5.4.18 (hardness) and Figure 5.4.19 (stickiness).

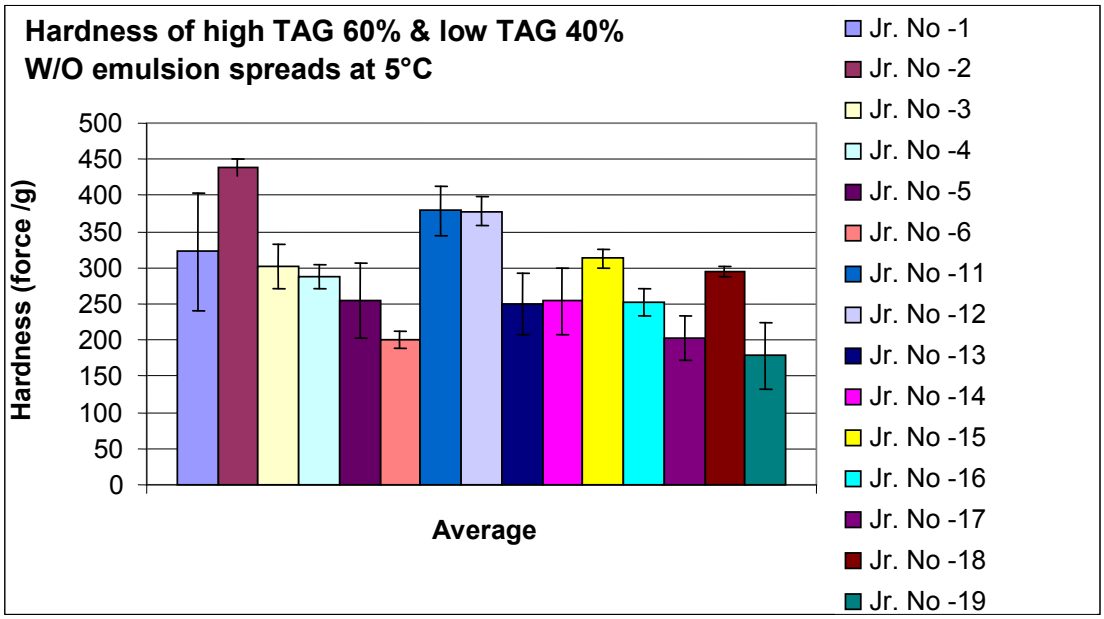

Figure 5.4.18 The hardness of the high TAG (60%) samples – (1-6), and the low TAG (40%) samples – (11-19)

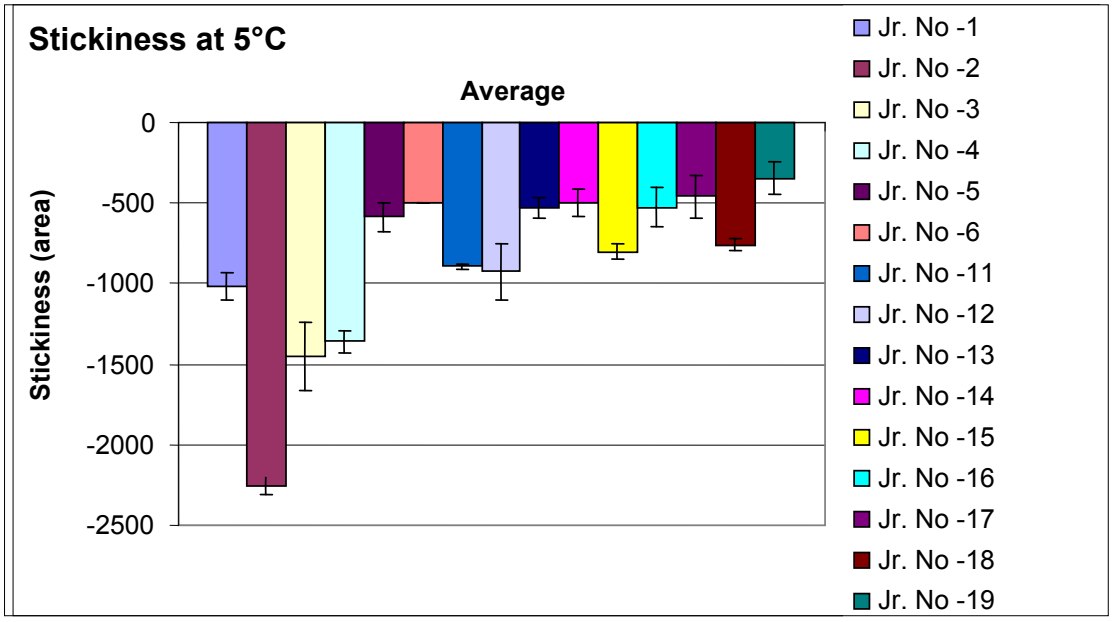

Figure 5.4.19 The stickiness of the high TAG (60%) samples- (1-6), and the low TAG (40%) TAG samples – (11-19)

Considering the 60% TAG samples first, it was clear that the DIMODAN® RT spreads resulted in the greatest degree of hardness, but with the exception of sample 2 where the DIMODAN® RT concentration is 0.6%, the hardness level of the Moringa samples was broadly comparable. The hardness of the Lesquerella samples was significantly less for all concentrations and was difficult to measure because of total product failure.

For the 40% TAG spreads, samples 11-19 in Figures 5.4.18 and 5.4.19, the hardness results showed that DIMODANT® UJ at 0.3% and Moringa at 0.3% gave the highest results, higher than the 60% spreads. The remaining samples showed hardness values similar to the 60% spreads, although the presence of PGPR seemed to result in a decrease in hardness for both DIMODAN® UJ and Lesquerella. Moringa and PGPR resulted in a much firmer product, and could indicate a synergy, a co-emulsifier relationship taking place. In terms of stickiness the same general trends were observed.

5.4.4.4 Objective Sensory Analysis

Sensory tasting of the 60% TAG spreads (1-6) by an expert panel resulted in the following comments for the high TAG samples, 24hrs post production:

Sample 1. (DIMODAN® RT - 0.3%) Soft and smooth with pleasant overall mouth feel.

Sample 2. (DIMODAN® RT - 0.6%) Firmer than sample 1 and generally still soft and smooth. This resulted in a firmer mouth feel, but one that was still acceptable.

Sample 3. (Moringa - 0.3%) Soft and smooth with a pleasant overall mouth feel

Sample 4. (Moringa - 0.6%) Firmer than sample 3, softer than sample 2, and smooth to taste but firmer over all mouth feel than sample 3.

Sample 5. (Lesquerella - 0.3%) Very soft, yellow in appearance, appeared unstable.

Sample 6. (Lesquerella - 0.6%) Very soft, yellow in appearance, appeared unstable.

The conclusions which were drawn for 60% TAG spreads, was that Moringa at 0.3% or 0.6% concentration can form acceptable stable spreads. The degree of firmness achieved was comparable to the control (DIMODAN® RT).

Sensory tasting of the 40% TAG spreads (11- 19) by an expert panel resulted in the following comments for the high TAG samples, 24hrs post production:

Sample 11. (DIMODAN® UJ - 0.3%) Very pleasant and smooth, good overall mouth feel.

Sample 12. (Moringa – 0.3%) Very pleasant and smooth, good overall (thick) mouth feel.

Sample 13. (Lesquerella - 0.3%) Appeared unstable.

Sample 14. (DIMODAN® UJ - 0.6%) Pleasant, smooth and good overall mouth feel.

Sample 15. (Moringa – 0.6%) Very pleasant and smooth, good overall (thick) mouth feel

Smaple 16. (Lesquerella – 0.6%) Unstable.

Sample 17. (DIMODAN® UJ 0.3% / GRINDSTED® PGPR 90 – 0.2%) Very pleasant and smooth, good overall mouth feel.

Sample 18. (Moringa – 0.3% / GRINDSTED® PGPR 90 – 0.2%) Very pleasant and smooth, good overall (thick) mouth feel.

Sample 19. (Lesquerella 0.3% / GRINDSTED® PGPR 90 – 0.2%) Unstable.

These results confirmed the results from earlier, relating to the water droplet size and the CLSM images. Lesquerella failed in the 40% spread emulsions, as it did for 60% spreads. However, Moringa performed well and provided both firmness and good mouth feel characteristics to the emulsion in question. There was also evidence of a potential synergistic interaction with PGPR.

5.4.4.5 Validation Testing

In order to validate results from samples 1 – 6 and 11- 19 (Specifically Moringa samples), additional new application trial samples were assembled.

Only 40% TAG spreads were examined, and the samples of Lesquerella were omitted due to obvious product failure (including 60%). The 40% TAG samples were produced according to repeat formula / conditions as previously described in Tables 5.4.3 and 5.4.4. Validation samples and conditions are described in Tables 5.4.5 and 5.4.6

The results tabulated in Table 5.4.9 show the validated water droplet size distributions for samples 1 – 6 (Table 5.4.5) compared to earlier trial samples 11, 12, 14, 15, 17, 18 in Table 5.4.3.

Table 5.4.9 Validated water droplet size distribution (DSD) results (plain text) of 40% low TAG spreads. Figures in **bold** are the results from the original samples (Table 5.4.8)

Sample	Emulsifier	2.5% <µm	50% <µm	97.5% <µm
1	DIMODAN® UJ 0.3%	2.69 **1.88**	13.81 **10.18**	71.05 **55.54**
	St.Dev	0.06	0.17	0.35
2	Moringa 0.3%	2.07 **1.31**	7.59 **7.46**	28.21 **42.41**
	St. Dev	0.12	0.66	6.73
3	DIMODAN® UJ 0.6%	1.73 **1.47**	8.59 **12.47**	42.79 **106.48**
	St. Dev	0.11	0.35	5.67
4	Moringa 0.6%	1.30 **0.95**	5.77 **6.04**	25.59 **38.56**
	St. Dev	0.03	0.13	1.65
5	DIMODAN® UJ 0.3% / PGPR 90, 0.2%	1.87 **2.47**	6.07 **10.48**	19.74 **44.62**
	St. Dev	0.05	0.05	0.66
6	Moringa 0.3% / PGPR 90, 0.2%	1.39 **1.27**	4.85 **5.58**	16.99 **24.46**
	St. Dev	0.06	0.12	1.51

The DSD validation results for a 40% TAG spread in Table 5.4.9, compared well with the previous results (shown bold within same table), showing that Moringa performs equally as well compared to the initial trials in producing stable spreads with small DSD. In each case the Moringa samples showed smaller DSD than the

initial trials. Moringa MAG used in the validation is the same identical Moringa monoglyceride 191 as used in previous work.

Figure 5.4.20 shows graphically the data presented in Table 5.4.9, but without data from Figure 5.4.8. However, a comparison clearly reveals that generally, all peaks in this validation are in a narrow range. This was possibly attributed to absence of TOCO 50 (antioxidant) a minor component (0.01% w/w) containing 50% tocopherol, a wetting agent.

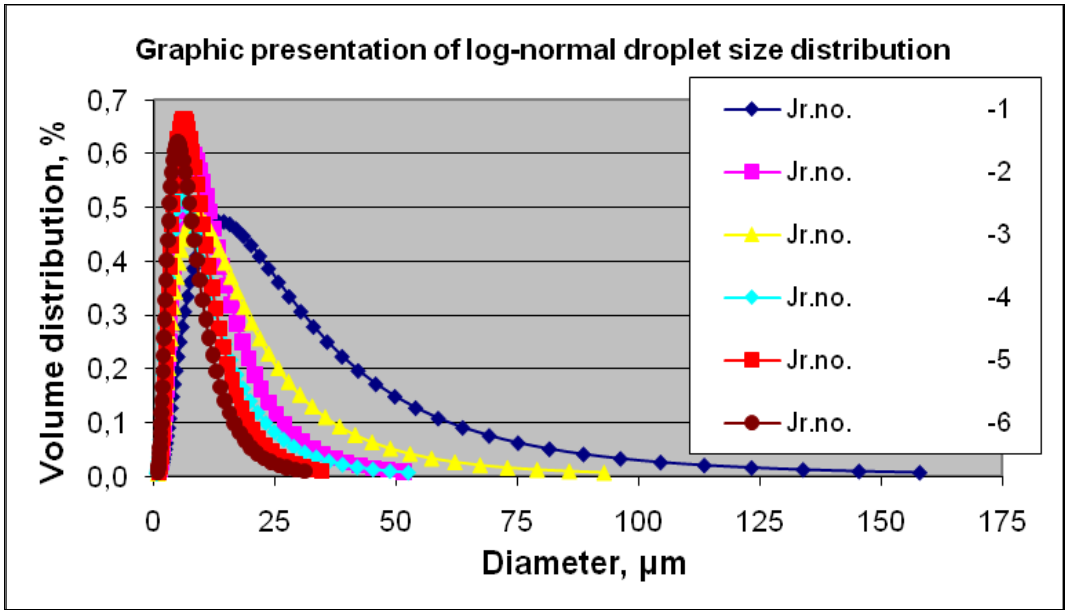

Figure 5.4.20 Water droplet size distributions for the 40% low TAG spreads of the validation tests.

With the exception of sample 5 which had DIMODAN® UJ and GRINDSTED® PGPR 90 combined, the smallest DSD was when Moringa was present. Where DIMODAN® UJ was present in isolation it can be seen this led to the largest DSD. The same was found in the original trials.

CLSM images of the validation studies are presented in Figures 5.4.21 to 5.4.26.

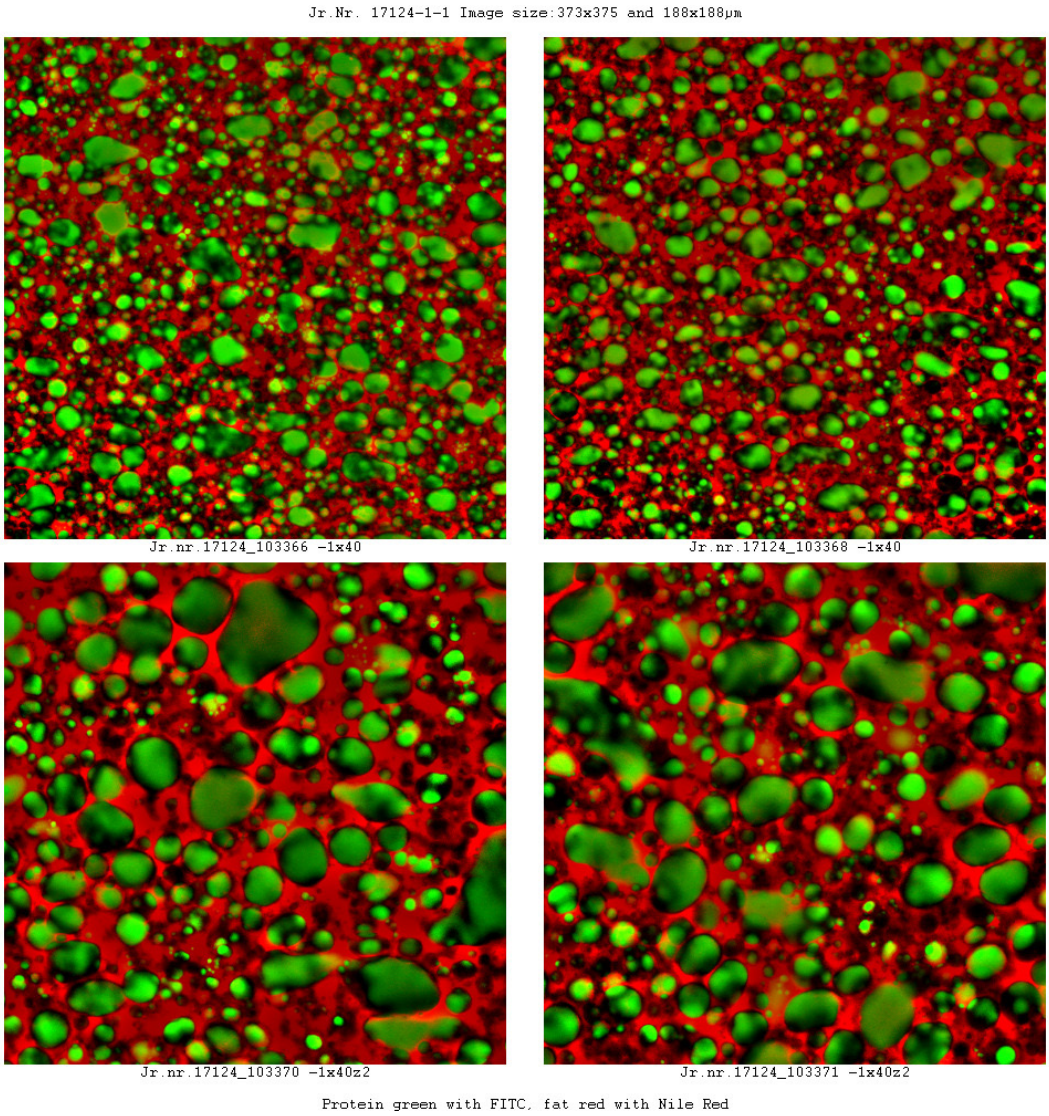

Figure 5.4.21 CLSM image of 40% TAG spread with DIMODAN® UJ - 0.3% concentration. (Top images 375 x 375 µm. Bottom images 188 x 188µm)

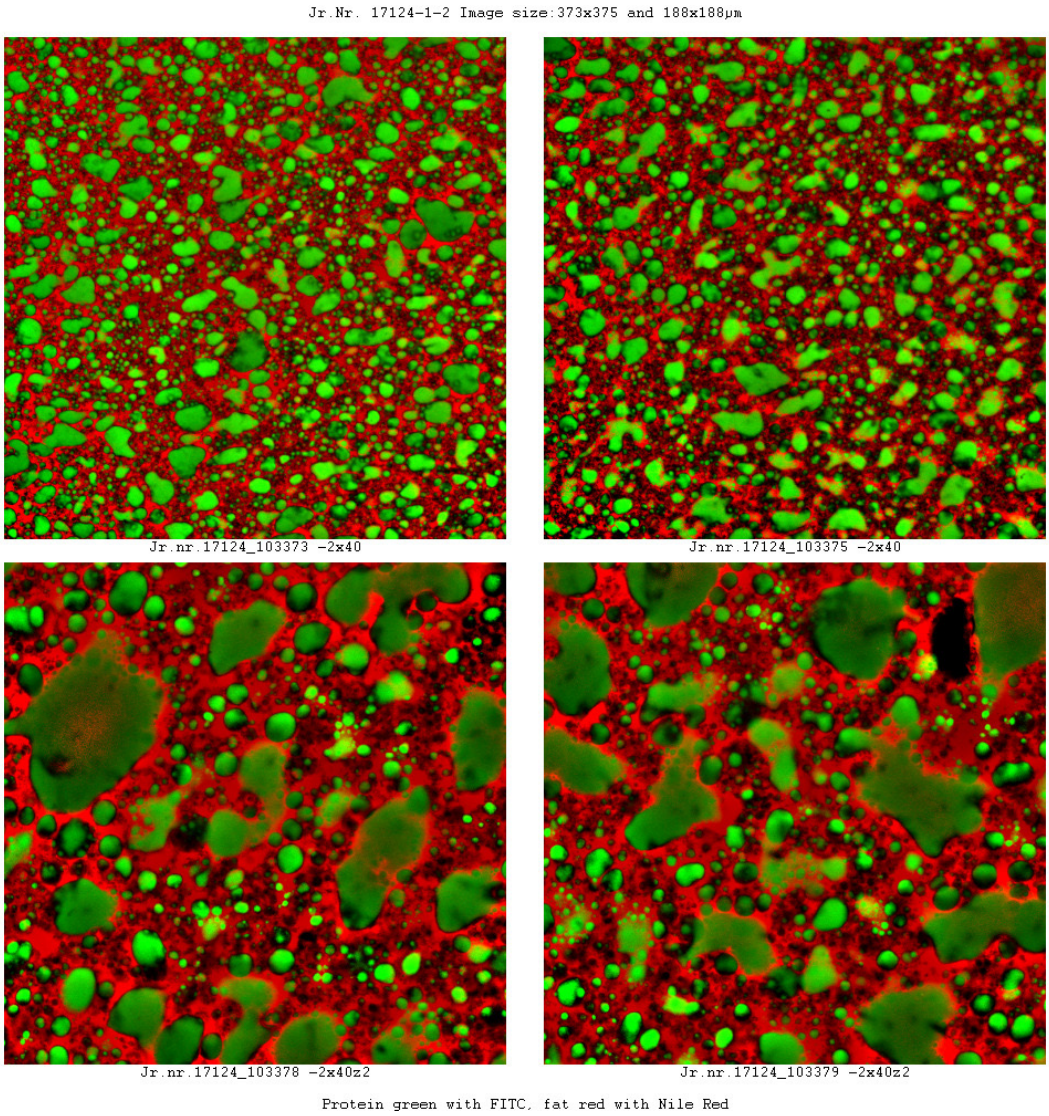

Figure 5.4.22 CLSM image of 40% TAG spread with Moringa - 0.3% concentration. (Top images 375 x 375 µm. Bottom images 188 x 188µm)

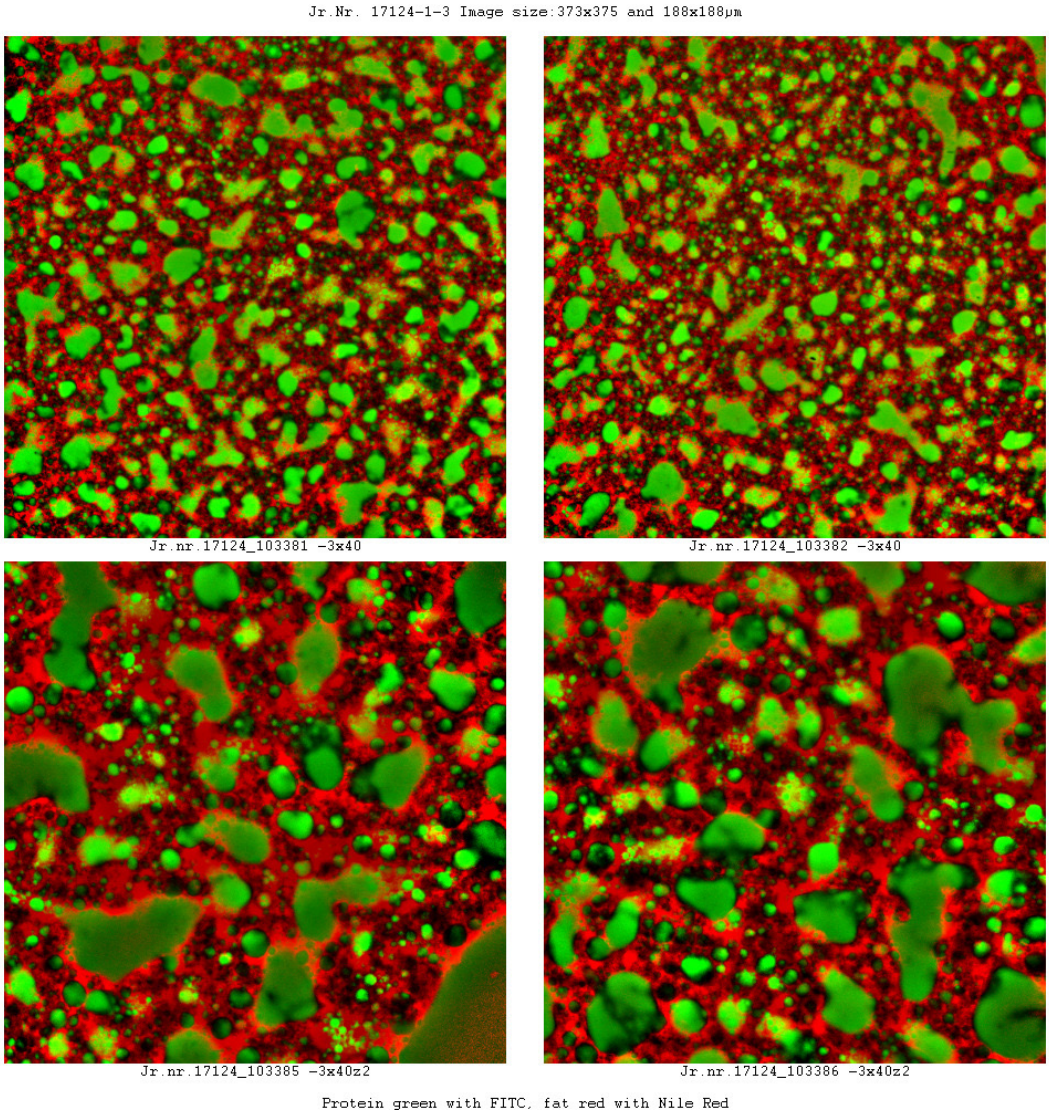

Figure 5.4.23 CLSM image of 40% TAG spread with DIMODAN® UJ - 0.6% concentration. (Top images 375 x 375 µm. Bottom images 188 x 188µm)

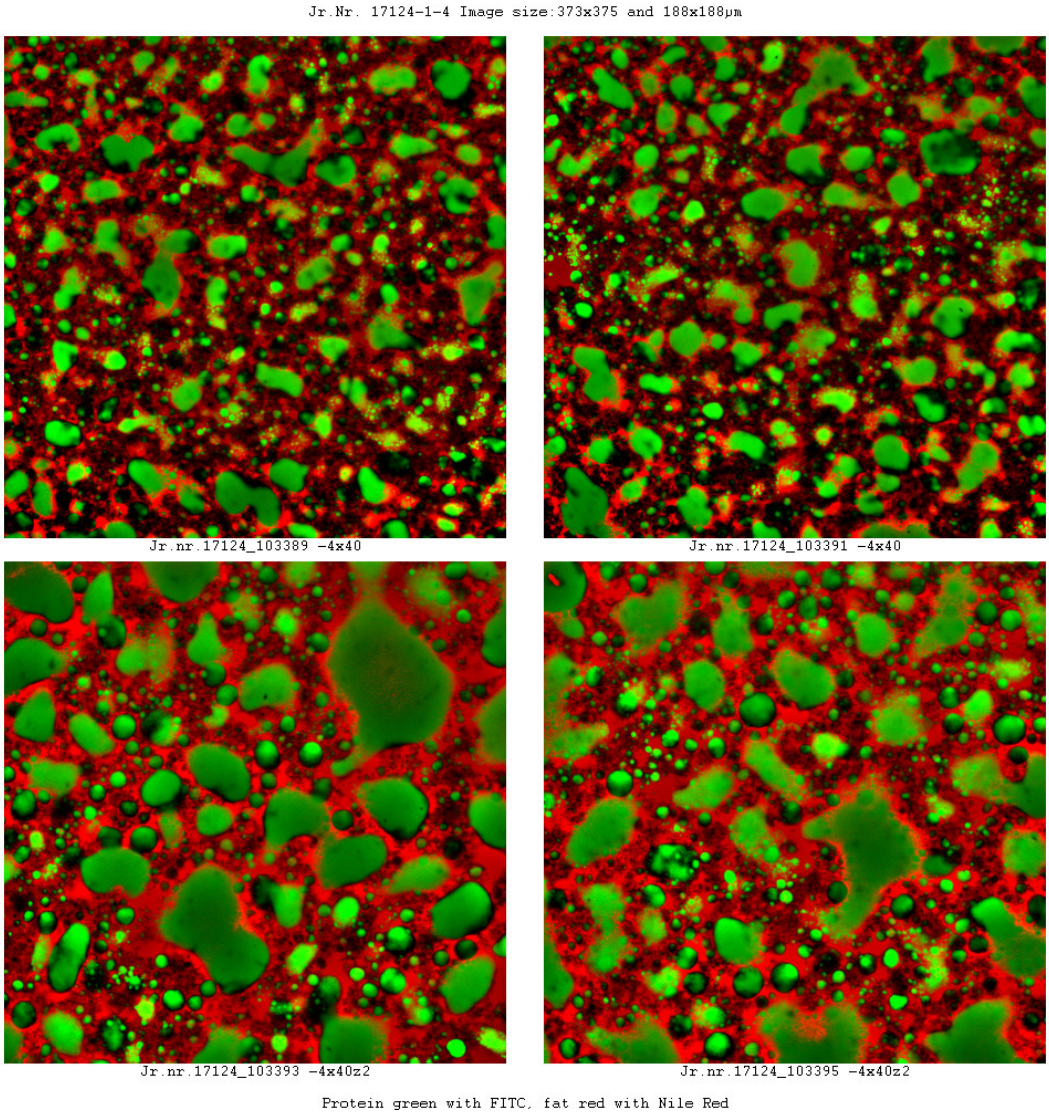

Figure 5.4.24 CLSM image of 40% TAG spread with Moringa - 0.6% concentration. (Top images 375 x 375 µm. Bottom images 188 x 188µm)

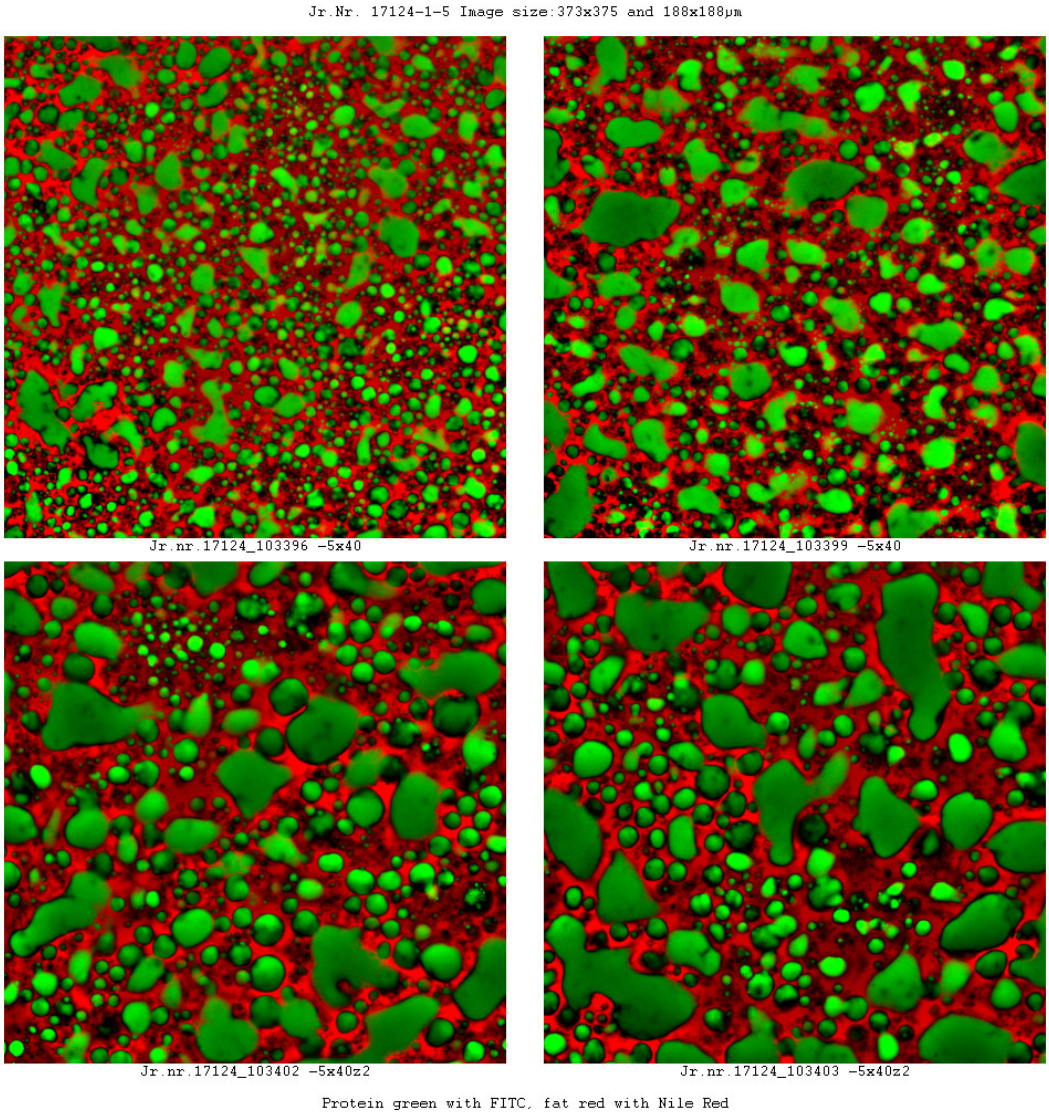

Figure 5.4.25 CLSM image of 40% TAG spread with DIMODAN® UJ - 0.3% / GRINDSTED® PGPR 90 – 0.2% concentration. (Top images 375 x 375 µm. Bottom images 188 x 188µm)

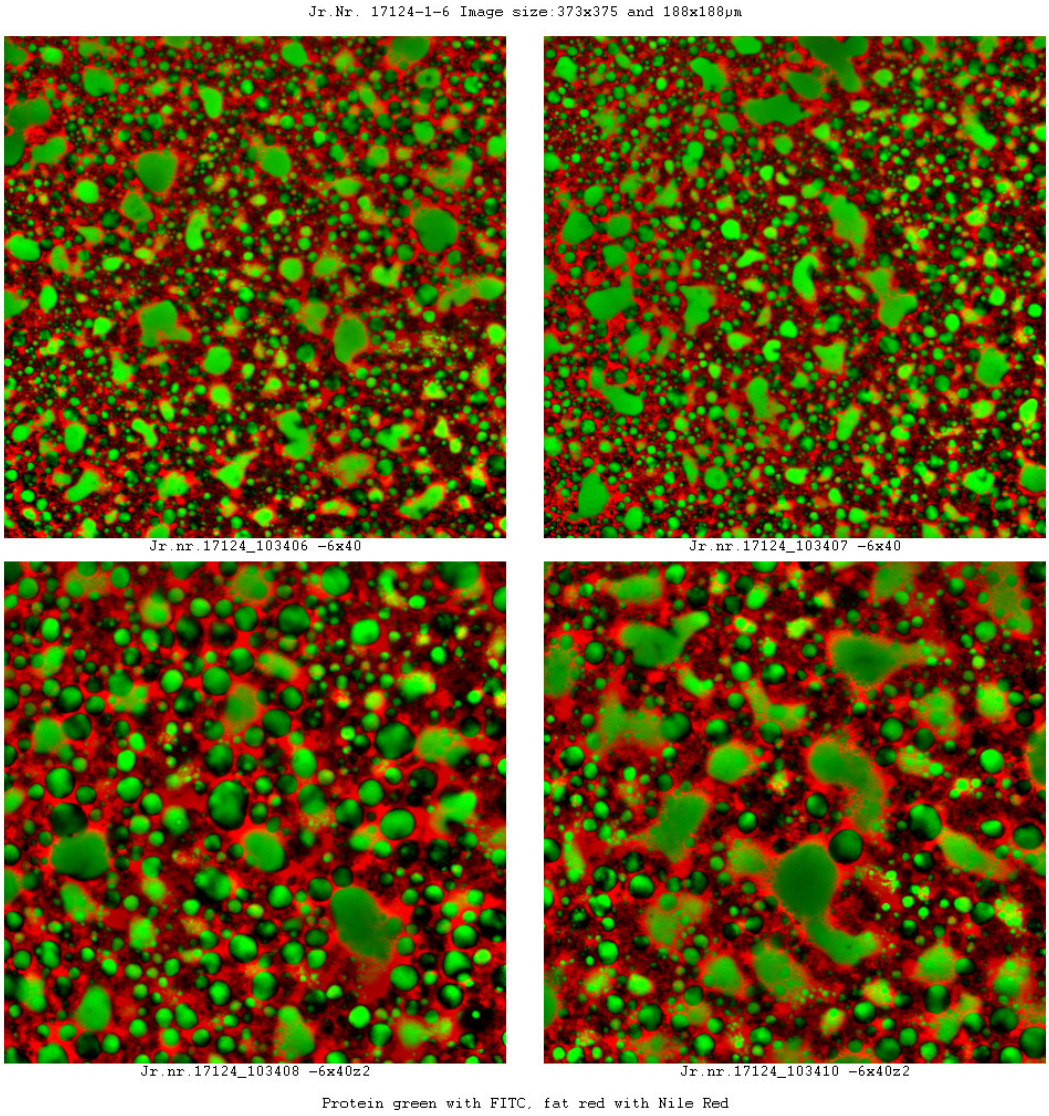

Figure 5.4.26 CLSM image of 40% TAG spread with Moringa - 0.3% / GRINDSTED® PGPR 90 – 0.2% concentration. (Top images 375 x 375 µm. Bottom images 188 x 188µm)

In comparing these CLSM images above (Figures 5.4.21 – 5.4.26) with the original trials for the corresponding samples in Figures 5.4.9 to 5.4.17 there are similarities, especially with the samples that contain Moringa. Taking Figures 5.4.10 and 5.4.22, both of which represent Moringa at 0.3% concentration, when viewed together as a whole, there is similarity. In Figure 5.4.13 and 5.4.24,

Moringa at 0.6% concentration, it appears that Figure 5.4.24 has the smallest water droplets, as indeed indicated by the water droplet size results (DSD). For Figures 5.4.16 and 5.4.26, where Moringa was present together with PGPR, again broad similarities in the image were found. Similar trends were seen for the samples which contain DIMODAN® UJ when compared against the original trials, with the exception of DIMODAN® UJ in the presence of PGPR, where large lakes of water are seen in Figure 5.4.15, which are not present in Figure 5.4.25. The DIMODAN® UJ used in the validation trials came from a new commercial sample than that used in the initial trials (Its material specification being consistent with the first commercial sample). In Figure 5.4.25 the droplets are larger, but remain as discrete droplets. This is possibly explained by the number of variations of selected surfactants used in each trial, and which are run continuously, without any separate product processing interface between each trial. Validation trials were fewer in number, and as previously indicated excluded Lesquerella MAG.

The texture analysis results for the validation testing showing the hardness of the validation samples at 5°C is given in Figure 5.4.27.

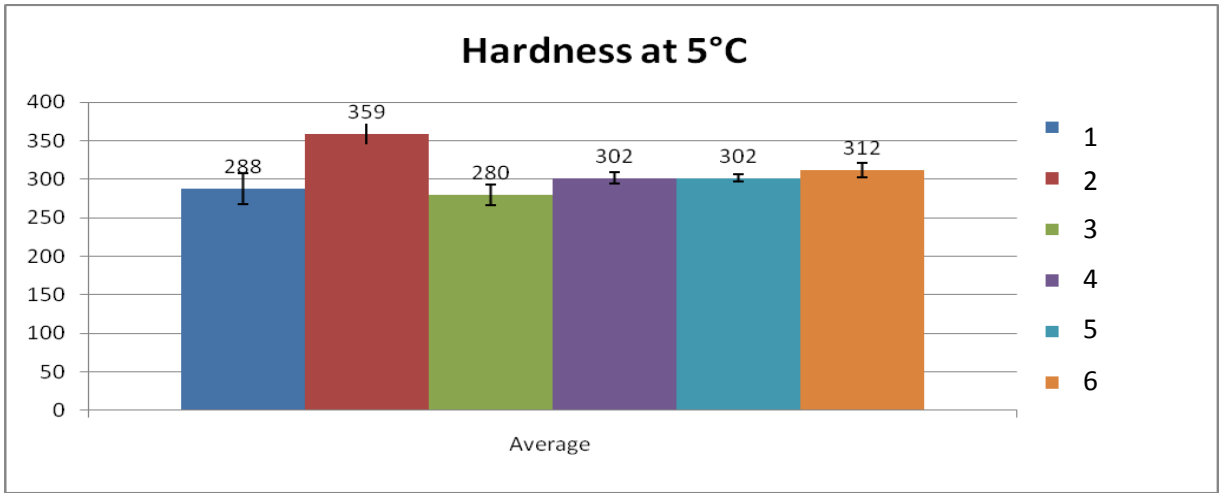

Figure 5.4.27 Textural hardness for the 40% low TAG spread validation tests, where the order from left to right is as follows; DIMODAN® UJ, 0.3%; Moringa 0.3%; DIMODAN® UJ, 0.6%, Moringa, 0.6%; DIMODAN® UJ, 0.3% and GRINDSTED® PGPR 90, 0.2%; Moringa 0.3% and GRINDSTED® PGPR 90, 0.2%.

The validation test confirmed the suggestion that Moringa MAG seems to be outperforming DIMODAN® UJ and also in combination with PGPR, there is small increased firmness. This could coincide with reduced DSD. But, only at the lower concentration of 0.3% is the difference in textural firmness significant where Moringa MAG is present.

5.4.5 Discussion

In summary, the results strongly indicate the functionality of Moringa MAG in high and low TAG spreads is such that it is capable of producing W/O emulsion products that have stable water droplet size capable of inferring additional textural resilience (thicker mouth feel qualities) as well as good flavour release properties. It seems that TAG based systems containing Moringa MAG can tolerate typical processing and storage conditions to make commercially viable products.

Based on evidence of dendrite structures observed earlier (5.3), which compared favourably with the structures of PGPR when examined under microscope, it is possible that dendrite behaviour may be linked to interfacial stabilisation (Ghosh et al., 2011). If these fern-like (dendrite) structures in the model systems transfer across into real food systems as noted for other crystallisation systems (Mullin, 1993), this may account for the development of the final interfacial structure (or its proximity i.e in the bulk) that give the W/O emulsions with Moringa MAG, enhanced (surface-active) functional properties (4.0) i.e. textural resilience and decreased DSD.

The water binding properties of PGPR are one of the reasons that it is essentially the stabilising emulsifier of choice for many water – oil based system food systems (refer to 1.2; 1.5). However, the level of stability that the PGPR can confer is often such that any re-work of the system is made difficult, and this can result in production down time. This has commercial implications because of the negative effects of PGPR on emulsion breakdown characteristics and

consequently, this also has a powerful sensory impact on melting and flavour release.

An emulsifier that is able to maintain a stable and robust emulsion (crucially PGPR is absent), and yet unlike PGPR, behave "abnormally" to allow re-work, enables the potential removal of E476. Wassell et al. (2012a; 2012b; 2012c; 2012d; 2012e) and Bech et al. (2013), show that while the DSD data may be an indicator of product stability, the emulsions should not be 'overly' stable that potential re-work is hindered.

All samples were made with natural Moringa MAG. Proof of concept to ascertain the performance of MAG compositions to mimic Moringa MAG is required. Therefore, this would be systems based on blended fatty acid compositions to match the fatty acid profile of naturally based (*Moringa oleifera*) Moringa MAG to achieve similar functionality. This is plausible because it has already been shown in bulk TAG model systems that such compositions were performing similar to natural versions (refer to 5.3).

5.4.6 Conclusion

The results presented, show that Moringa MAG, when incorporated into a high TAG spread (60%) or a low TAG spread (40%), is highly functional, resulting in a commercially acceptable product which is both stable to processing and storage. The formed emulsions had both acceptable commercial structure and flavour release. Compared to other MAGs in this work, weight for weight, a Moringa MAG conferred additional textural resilience and spreadability.

Further application trials would support the model system results (4.0); because it was shown previously (5.3), that synthetic (blended composition) MAG samples seemed to behave similarly to the naturally based (*Moringa oleifera*) Moringa MAG samples, as used in this study.

5.5 Microscopy Examination of a Forced Cooled Model TAG Based System Containing a Distilled Moringa MAG, Behenic Based MAG and PGPR

5.5.1 Introduction

Processing conditions usually run at faster cooling rates than 1°C per minute, but typical examinations are often run at this much slower cooling rate. This is to avoid excessive temperature gradients and therefore nullify any potential anomaly that may occur. However, this approach may alter the perspective of the original measurement when the cooling rate is changed closer to industrially relevant cooling rates, as used in 5.4.

In a previous study (5.3), cooling rates of 1°C/min from the melt to 20°C resulted with interesting dendrite crystal structure. Therefore the aim of this study is to investigate the effect of forced cooling on the crystal structure of TAG based systems where the cooling rate moves over two orders of magnitude, i.e. from 1°C/min to 100°C/min.

Microscopy examination on the thermal response behaviour of anhydrous TAG continuous samples containing Moringa MAG, PGPR and CRY110, when compared to a blank control, may provide new insight into resultant physical properties.

5.5.2 Materials and Methods

The control TAG blend was 70% Palm Stearin (IV35), and 30% Palm Olein (IV56). Emulsifiers were added to the control sample at 1% of either Moringa MAG, or GRINDSTED® Crystallizer 110 or 0.5% GRINDSTED® PGPR 90 as per the previous study (5.3); the same method is also used. The microscopy was run using an Olympus BX 60 with all images taken using PLM at x200 magnification. The samples were heated to 85°C to remove any previous crystal

history and then treated to the following cooling rates: 1°C/min, 10°C/min, 50°C/min, and 100°C/min to a final ambient temperature of 20°C. Refer to General Materials & Methods (2.0) for additional detail.

5.5.3 Results and Discussion

The results in Figures 5.5.1 – 5.5.4 show the micrographs of the control sample, CRY110, PGPR and Moringa MAG. Each Figure is split further into four individual micrographs that correspond to the four different cooled temperature rates.

In Figure 5.5.1, the control shows a slow cooling rate of 1°C/min the formation of what can be described as clear evidence of TAG crystallisation; with pentagonal and hexagonal snowflake (dendrite) like patterned crystal structures are very apparent.

When the cooling rate is increased to 10°/min, the formation of dendrites become smaller and less distinct; therefore, this is taken as clear indication that the forced cooling at a faster rate as a significant effect on the kinetics of crystal formation. At 50°C/min, the polarised image was poor and it was difficult to draw conclusions, but at 100°C/min no evidence of dendrite structure is visible and the crystals are smaller relative to those at 1°C/min.

Figure 5.5.2, shows the results over the same cooling rates for 1% of CRY110. The polarised image shows homogenous distribution of many small crystals. A similar micrograph image has been observed by Basso et al. (2010) when they used a behenic based monoglyceride. However, the effect is dramatic in their observation probably due to the degree of total saturation of the TAG solvent used (Basso et al., 2010). Moving to faster cooling rates simply reduces the size of the crystal structures progressively, at no point with CRY110 is there any indication of dendrite or any other structural connotation.

Figure 5.5.3 shows results from 0.5% PGPR at 1°C/min cooling rate. The polarised image is dominated by dramatic dendrite structures. There is no evidence of small discrete crystals. In this respect it appears as though PGPR has completely altered the crystallisation kinetics of the bulk system, crystal nuclei have developed into fern-like dendrite structures of notable size in comparison to Figure 5.5.1.

Accelerating the cooling rate to 10°C/min, the large dendrite crystal structures have reduced in number and size. The dark background, non-crystallised region (liquid olein) as seen at 1°C/min is now dominated by homogeneous scattering of mixed crystal shape and size. At 50°C/ min are not obvious and the crystal distribution is now more uniform in size and shape; increasing the cooling rate still further to 100°C/min, results in a structure similar to the polarised image as shown in Figure 5.5.1 and 5.5.2 at the same cooling rate (100°C).

Lastly, Figure 5.5.4 shows the results for Moringa MAG. At 1°C/min there appears to be a composite distribution across the polarised micrograph. Several regions within image appear similar the micrographs at 1°C in Figure 5.5.2, and Figure 5.5.3. This could suggest that Moringa MAG influences crystal behaviour similar to both CRY110 and PGPR. There are areas where fern-like structures are visible as well as areas where discrete crystal clusters are to be found. Increasing the cooling rate to 10°C/min reduces the size of the crystals, but importantly the fern-like structures and clusters are still present; they are more numerous compared to the PGPR in Figure 5.5.3 at the same cooling rate. At a cooling rate of 50°C/min the dendrite structures are arguably still visible, but the overall crystal numeration is possibly more compared to either PGPR or CRY110. Increasing the cooling rate to 100°C/min, results in a vastly reduced crystal structure and no apparent indication of fern-like dendrite structures.

The relevance of these results is in the context of the aim, which is to approach cooling gradients associated with typical production processes. However, this is highly dependent on flow rates and the nature of the product itself, not least the fact that alterations in the TAG solvent will immediately alter the thermal response

and hence solubility potential of forming crystal structures (Metin & Hartel 2005). Conservative estimates suggest that the cooling rates on closed scrapped surface heat-exchanger plants can be anything between 35°C/min., to 45°C/min. Unlike environments associated with real process conditions, these observations were performed under static conditions, as opposed to the dynamic cooling gradients and shear conditions in real processes. Therefore, these results can be taken as indication as to what is potentially happening in the dispersion or bulk TAG phase of a W/O or O/W emulsion system at accelerated cooling rates. Until now, this information was not found within the literature.

There are clear physical differences in the influence of crystal forming kinetics of Moringa MAG, compared with a behenic rich MAG (CRY110), and consequently, these may exert on performance and functionality. As discussed previously (5.2 & 5.3), Moringa MAG has portions of its fatty acid profile composed of C22:0 which is the main component of CRY110 (~89%). Moringa MAG contains approximately 5 - 8% of C22:0 which could be significant.

The polarised micrograph evidence also suggests parallels with the crystal forming nature of PGPR. These parallel crystal formations, coupled with the parallel functionality in high TAG (60%) and low TAG (40%) spreads, is supportive evidence to commercial applications in a number of food products, containing a TAG crystal network structure (Wassell et al., 2012a; 2012b; 2012c; 2012d; 2012e; Bech et al., 2013).

Clearly, and most importantly, Moringa MAG shown in Figure 5.5.4 reveals similar physical properties to PGPR shown in Figure 5.5.3. Theoretically, it is possible that similar behaviour could be manifest at cooling rates experienced in production process conditions, where these crystal structures may influence and be transposed into the final products, so that if present, would influence the physical properties of the bulk oil (refer to 5.4).

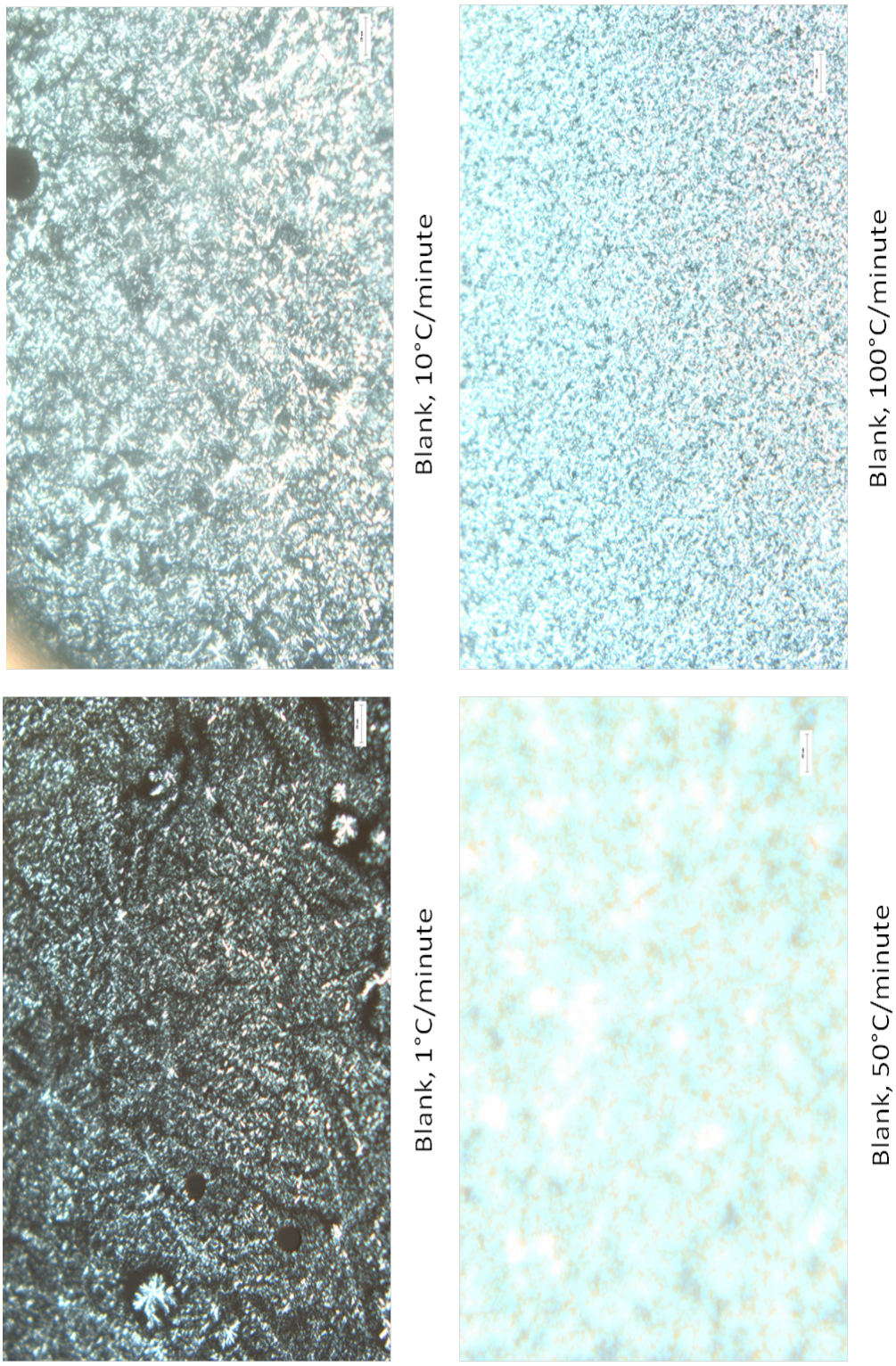

Figure 5.5.1 Micrographs of blank control exposed to forced cooling from 1 – 100°C/min (scale bars = 20µm).

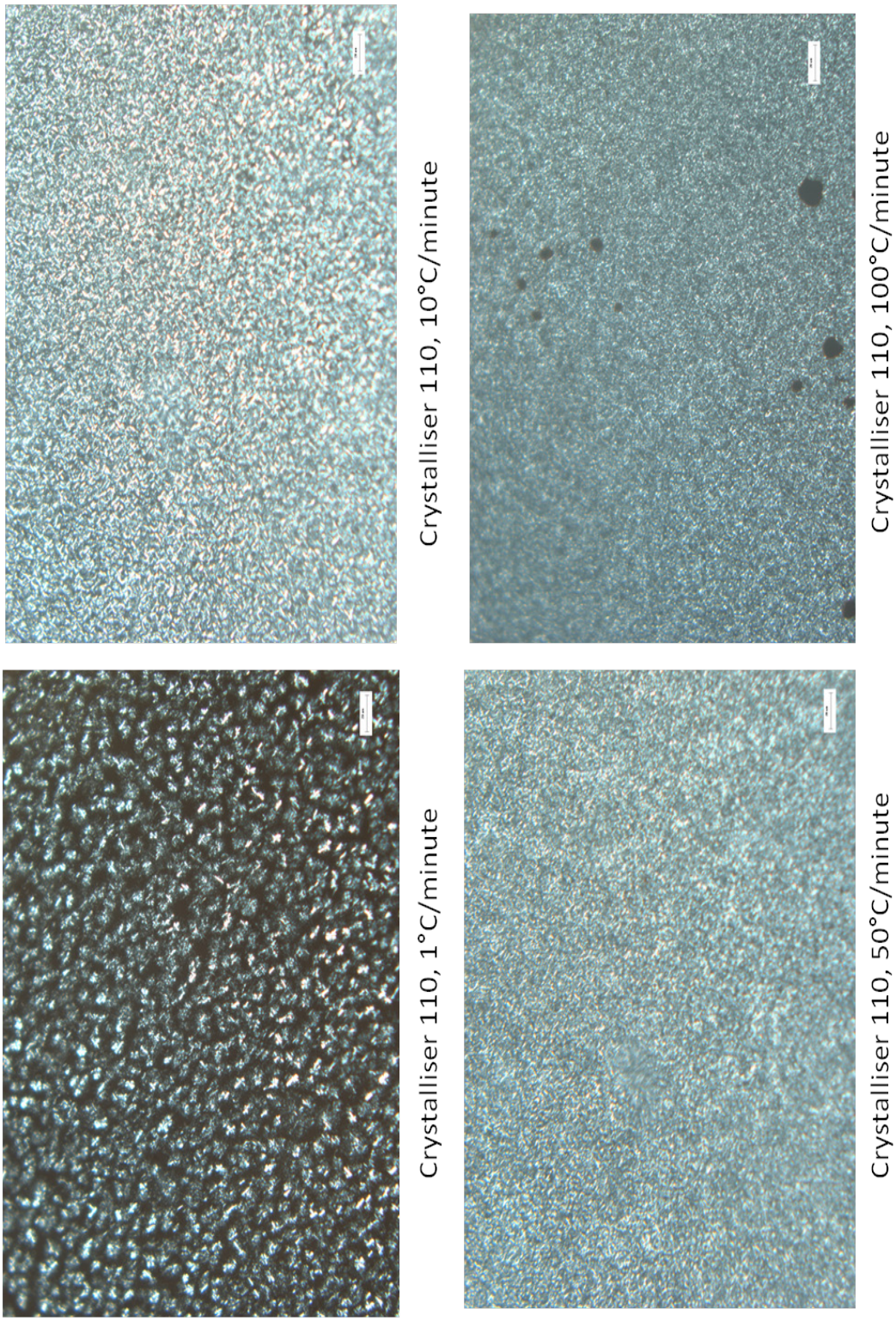

Figure 5.5.2 Micrographs of CRY110 exposed to forced cooling from 1 – 100°C/min (scale bars = 20µm).

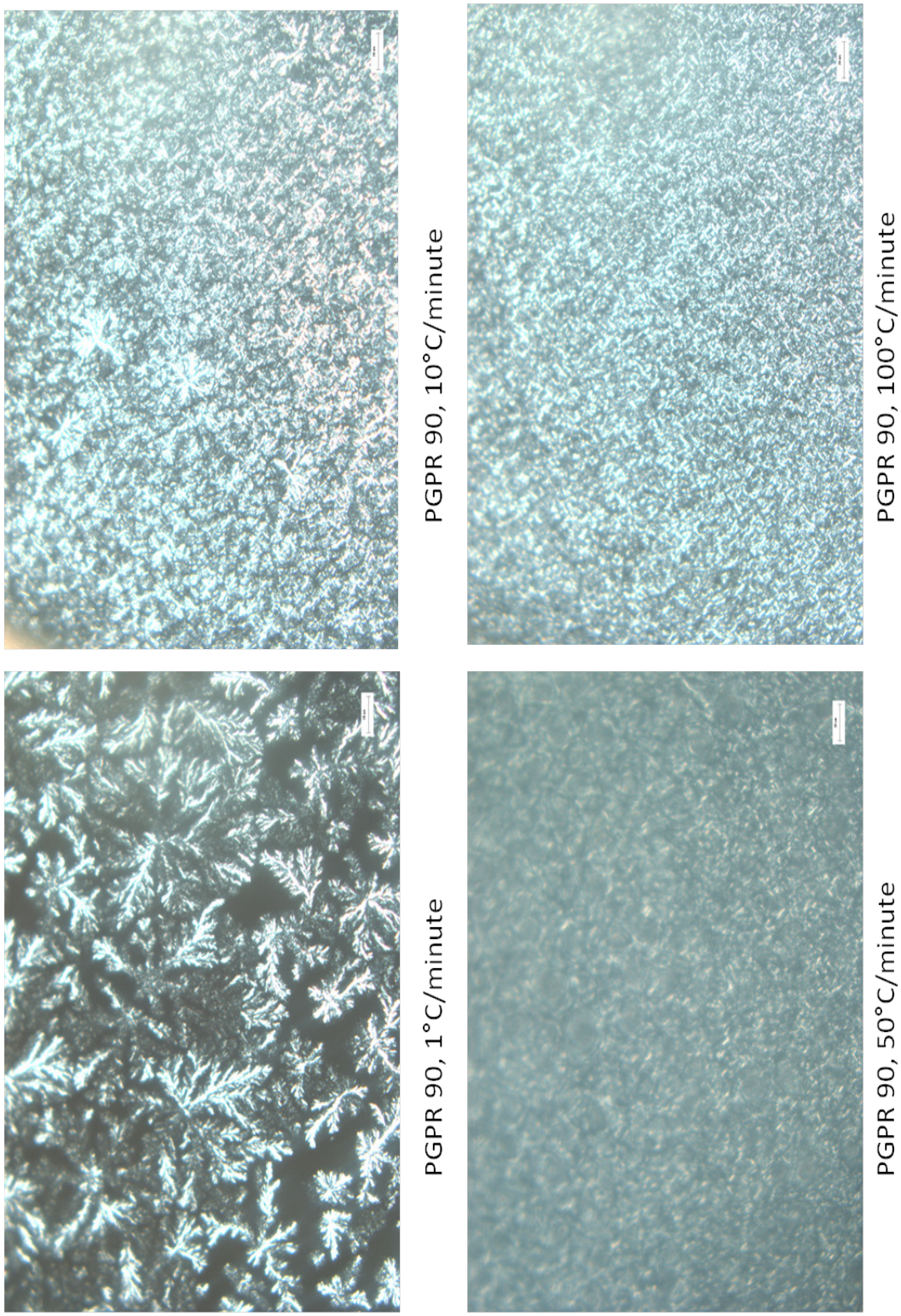

Figure 5.5.3 Micrographs of PGPR 90 exposed to forced cooling from 1 – 100°C/min (scale bars = 20µm).

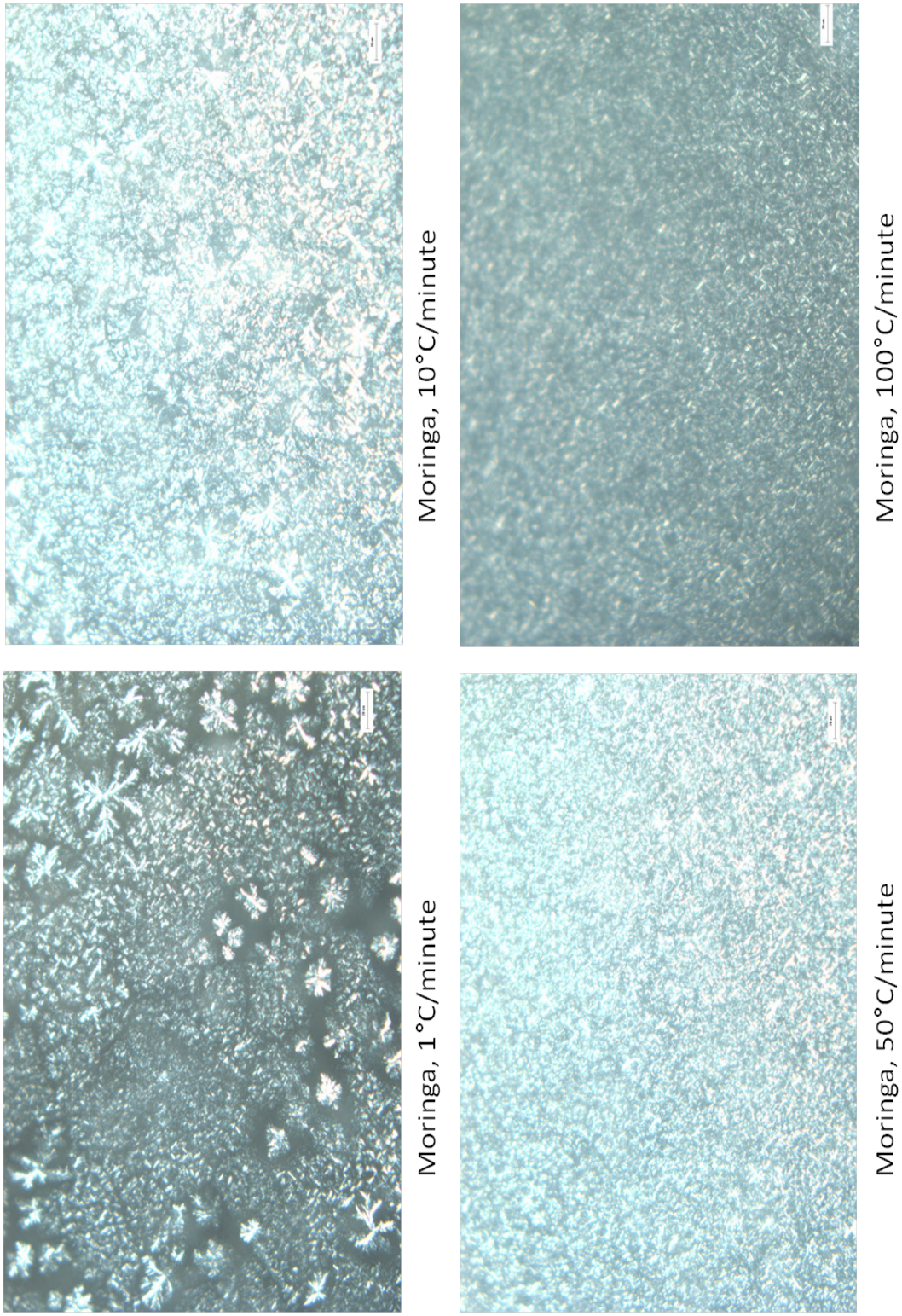

Figure 5.5.4 Micrographs of Moringa MAG exposed to forced cooling from 1 – 100°C/min (scale bars = 20µm).

5.5.4 Conclusion

The results demonstrate that TAG-based systems containing MAG based on natural Moringa TAG (*Moringa oleifera*) are able to influence crystallisation to produce crystal forms which look similar to crystal forms when using PGPR (GRINDSTED® PGPR) and GRINDSTED® Crystallizer 110 (CRY110), a behenic rich MAG. These modes of forming crystals are kept intact at forced cooling rates up to 50°C per minute. These findings may help to explain the influence of Moringa MAG on the physical properties of dispersions (5.2; 5.3) or emulsions (5.4) which potentially transpose bi-functional benefits towards the food systems in which they might be used. The rheological properties of this crystallisation behaviour required further investigation, which was conducted next.

5.6 The Rheological Behaviour of Model TAG Systems Containing a Behenic based MAG, PGPR and Moringa MAG, During Forced Cooling Velocities

5.6.1 Introduction

Investigations into the crystal behaviour of TAG blends containing a behenic based MAG (GRINDSTED® Crystallizer 110), PGPR (GRINDSTED® PGPR 90), and a Moringa MAG based on *Moringa oleifera* TAG have been studied previously (5.3; 5.5). The influence on crystal structure seen through polarised light microscopy showed that PGPR and Moringa MAG had influence on the physical behaviour of the TAG blend, resulting in similar dendrite crystal structures at a range of thermal conditions.

The aim of this study is to investigate a model TAG blend under large scale deformatory rheology and examine if there are similarities in behaviour between PGPR 90 and Moringa MAG.

As in the previous studies (5.3; 5.5), the cooling gradient of the rheological experiments ranged between 1°C/min to 30°C/min. With both cooling and shear, an attempt to reach super-cooled conditions is sought, because of its effects on the level of structure that occurs for a given rate of cooling (Ghosh & Rousseau 2009). Schematically, it can be viewed as in Figure 5.6.1 which shows the energy barrier to crystallisation and the relative amount of structure formed as a function of cooling temperature (Section 1.3).

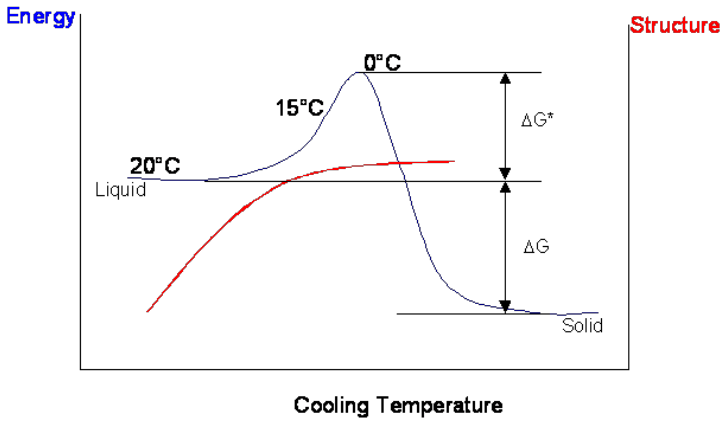

Figure 5.6.1 Schematic diagram of the energy barrier to crystallisation together with the relative amount of structure formed for a given cooling rate.

A schematic in Figure 5.6.1 clearly shows how supercooling leads to structure. Depending on the thermal properties of the solvent, eventually benefits are no longer apparent despite the increased energy input (cooling) temperature, or indeed the cooling rate.

5.6.2 Materials and Methods

Two TAGs blends with differing degrees of saturation were used as the solvent. First a blend consisting of 70% palm stearin (35 IV) and 30% palm olein (56 IV), then secondly a more unsaturated blend consisting of 70% palm olein (56 IV) and 30% palm stearin (35 IV), to which in both cases respectively, the emulsifiers GRINDSTED® Crystallizer 110 (CRY110), GRINDSTED® PGPR 90 (PGPR), and Moringa MAG (191) were added at 1%, 0.5% and 1%.

All samples were run on a Rheometrics SR 5 controlled stress rheometer, which was operated in simulated controlled strain mode set to a constant target shear rate of 10s-1. The geometry was a set of 40mm parallel plates, where the gap was 1mm. The crystal history was removed through melting and holding to 90°C for 15 minutes prior to measurement. The temperature ramp for the experiment was 70°C to 25°C at a fixed cooling rate of either 1°C, 10°C or 30°C. Before

commencement of shear each sample was subject to a 2 minute waiting time with the temperature held at 70°C. The TAG blend and selected emulsifiers were pre-heated to 90°C to remove all crystallisation history prior to rheological measurements. Refer to General Materials & Methods (2.0) for additional detail.

5.6.3 Results and Discussion

5.6.3.1 Cooling Velocity - 1°C/min

The results in Figure 5.6.2(a) and 5.6.3(c) show the entire curve for all the samples cooled at the rate of 1°C/min, where the control sample represents the TAG blend of 70% palm stearin / 30% palm olein and 70% palm olein / 30% palm stearin respectively. The remaining samples are combinations of the TAG blend and the emulsifiers under investigation: CRY110, PGPR 90, and Moringa MAG. Figures 5.6.2(a) and 5.6.2(c) show a large portion of the graph from 70°C to about 45°C where there is only a gradual increase in viscosity. It is viewed that in this portion of the graph essentially nothing is happening to the TAG based system due to the fact that it is still in the melt, and therefore expected to behave in true Newtonian fashion. Below 45°C however, dramatic increase in viscosity is observed occurring at several temperatures depending on the nature of the sample. The dramatic increase in viscosity is possibly the onset of crystallisation, and indeed the values which can be taken from Figure 5.6.1 correspond well with previous results for similar systems containing CRY110 (Young et al., 2008), where onset temperatures for CRY110 in TAG based samples also occurred around 42°C – 45°C.

For clarity, the area of viscosity in Figures 5.6.2(b) and 5.6.3(c) show the expanded section of Figures 5.6.2(a) and 5.6.3(c), where the data is expressed from 50°C and cooler.

Figures 5.6.2(b) and 5.6.3(d) show that CRY110 alone begins the onset of viscosity increase at 40°C and 38°C respectively, whereas the samples with

CRY110 and PGPR 90 or Moringa MAG show an onset at 42.5°C and 41°C respectively. In isolation, Figure 5.6.2(b) shows PGPR 90 and Moringa MAG first show an onset of viscosity rise at around 31-32°C, and the control sample increases from 34°C. Figure 5.6.3(d) shows PGPR 90 and Moringa MAG with onset of viscosity at approximately 30°C-34°C, and the control sample increases from approximately 27°C.

The results from Figure 5.6.2(b) and 5.6.3(d) clearly suggest that when PGPR 90 and Moringa MAG are used in isolation, they both behave similarly, showing the onset of viscosity increase to occur at essentially the same temperature. This similarity in behaviour was suggested earlier (5.3; 5.5), where strong similarities in crystal structure, (i.e. the presence of fern-like dendrite structures) were clearly observed.

When CRY110 is mixed with a co-emulsifier; PGPR 90 and Moringa MAG, there are obvious distinctions. The combination of CRY110 with PGPR 90 shows the earliest onset of viscosity, occurring at 42.5°C. This is likely attributed to several aspects discussed previously (see 4.0), namely, crystal structure and surface activity respectively. The micrographs reported previously (5.3 & 5.5) showed PGPR 90 has an inherent influence on crystal kinetics of TAG toward dendrite structures - (which is likely governed by the "inherent" thermal response behaviour of a given solvent); so that at a cooling rate of 1°C/min, a slow cooling gradient, there is adequate time for PGPR molecules to influence crystal kinetics (Marze 2009), such that PGPR molecules could act as a co-emulsifier (template), to explain the early onset of the CRY110 / PGPR 90 system viscosity increase. Observations by others confirm that PGPR is highly surface active (Rousseau, 2000) as is a behenic based MAG (Krog & Larsson, 1992). This interactive relationship of CRY110 / PGPR 90 was observed earlier (see 4.0) and revealed through thermal treatment that PGPR lowers interfacial tension – early and the second emulsifier (CRY110) dominates the surface tension faster as the emulsifier mixture approaches ($T\gamma$). Then a dramatic fall of interfacial tension occurs once the critical temperature is reached.

In trying to explain the mechanism in the anhydrous bulk, it is known that PGPR adsorbs at polar sites from anhydrous solution. In one example Dedinaite & Campbell (2000) showed that mixture of phospholipids (PE) and PGPR in a anhydrous liquid vegetable oil (triolein), facilitated the adsorption of non-polar PE crystals on a polar surface. In this study two TAG based solvents were used having differing degrees of saturation. Dedinaite & Campbell (2000) explain how PGPR is able to induce crystal kinetics in bulk TAG blends containing a smaller molecular weight surfactant (e.g. behenic MAG). The onset of viscosity occurs at higher temperatures with the CRY110 / PGPR 90 combination than with CRY110 alone, or in combination with Moringa MAG.

Figure 5.6.2(b) shows CRY110 and Moringa MAG have onset of viscosity increases which begins at a slightly cooler temperature of 41°C. Approaching 38°C, viscosity builds almost one order of magnitude more compared with CRY110 alone. The reason for this is possibly explained from the evidence in the work reported previous (5.5), which showed that both Moringa MAG and PGPR strongly influenced TAG crystals towards dendrite structures (5.5 also used the same TAG solvent as in this study). Both Moringa MAG and PGPR appear to have a similar physical response pattern. This similarity may possibly explain why Moringa MAG and PGPR both behave according to a similar mechanism when combined with CRY110 (Wassell et al., 2012a; 2012b; 2012c; 2012d; 2012e; Bech et al., 2013).

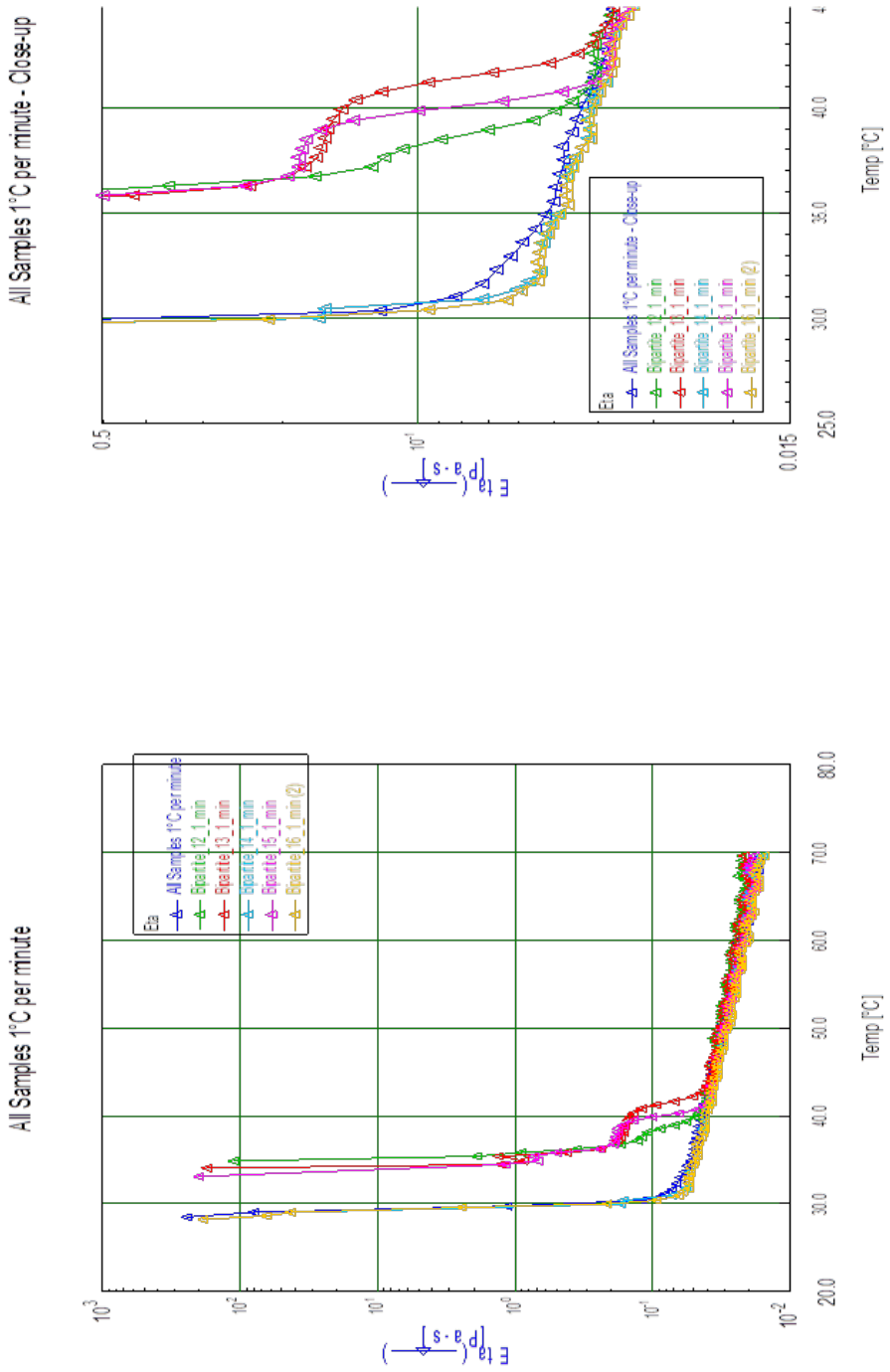

Figure 5.6.2 a / **b** Viscosity cooling curves at 1°C/min of base TAG blend (70% palm stearin/ 30% palm olein) [dark blue]; 1% CRY110 [green]; 1% CRY110 / 0.5% PGPR 90 [red]; 0.5% PGPR 90 [light blue]; 1% CRY110 / 1% Moringa MAG [pink]; and 1% Moringa MAG [yellow]

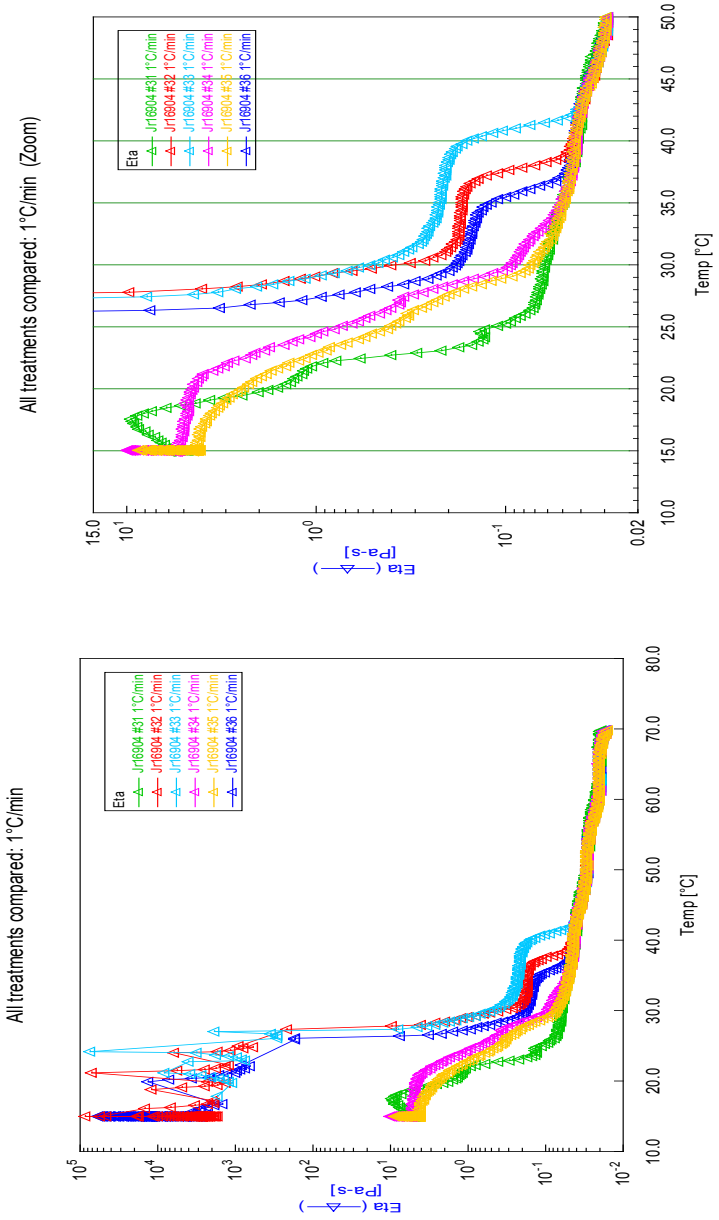

Figure 5.6.3 c / d Viscosity cooling curves at 1°C per minute of base fat blend (70% palm olein / 30% palm stearin) [green]; 1% CRY110 [red]; 1% CRY110 / 0.5% PGPR 90 [light blue]; 0.5% PGPR 90 [pink]; 1% CRY110 / 1% Moringa MAG [dark blue]; and 1% Moringa MAG [yellow]

5.6.3.2 Cooling Velocity - 10°C/min

Figure 5.6.4(a) and 5.6.4(b) show the same rheological cooling profiles for the same samples, measured at a faster cooling rate of 10°C/min. The response behaviour when compared to the slower cooling rate of 1°C/min in Figures 5.6.2(a) and 5.6.2(b), shows on closer examination, a delay in onset temperature to lower values in Figure 5.6.4(a) and 5.6.4(b).

Figure 5.6.4(b) reveals Moringa MAG and PGPR 90 behave similarly, until a temperature of 28°C whereupon differences in their profiles are seen. This manifests itself as a large 'kink' in the profile shape, where there is first a lowering of viscosity followed by another rise in viscosity. Given that the rheometer geometry is rotating throughout the measurement, such a profile may be attributed to an initial build up of viscosity (i.e. structure) which reached a critical point and is then broken by the continual applied shear (Corke, 2007). Quite why this should be observed for the Moringa MAG and PGPR 90 and not the control sample of the base TAG blend alone is not altogether clear. It is possible that the presence of PGPR may influence molecular kinetics in the bulk oil phase, it being highly surface active (Rousseau, 2000; Claesson et al, 1997). If this in turn caused different dielectric parts of the mixed TAG systems to have irregular crystal shapes – dendrites (Ghosh & Rousseau 2010), this together with the presence of a nano-crystalline formation adhered by non-polar polyricinoleate part of the PGPR may cause adhesive properties (Dedinaite & Campbell, 2000).

Shearing through was also not observed in the slower cooling rate of 1°C, and this might be attributed to the slower cooling rate allowing the structure more time to arrange such that breakage or adhesive properties are stronger (Marze 2009).

This would then tend to suggest that the faster cooling rates lead to weaker structures. However, closer examination of Figures 5.6.2(a) and 5.6.4(a) show that the final viscosity value of the sample cooled at 10°C/min in fact gives the highest viscosity. Similar cooling rate structural observations, i.e. greater structure development after gelation onset has been reported in the literature (Ojijo et al,

2004). This suggests that although faster cooling rates may influence differences in either crystallisation onset or shearing through, this does not equate to lower levels of final structure in the final application (Toro-Vazquez et al, 2001).

Clearly, the influence of cooling and its consequential effects to the bulk reaching equilibrium conditions cannot be underestimated. Marze, (2009) demonstrated the effects of PGPR concentrations in sunflower oil, and observed behaviour is controlled by long relaxation times, whereas shorter time relaxation becomes manifest, and takes over when approaching and exceeding the saturation of interfacial concentration. This was reported and understood as a shift from a diffusion-dominated (long process) regime to a rearrangement-dominated (faster process) regime. The significance of this is important and enhances appreciation for, other environmental conditions affecting the bulk, e.g. temperature ramp, solvent type, degree of water activity (Wells, 1998).

Figure 5.6.4(b) with CRY110, shows that the onset of the viscosity rise – essentially gelation – has reduced to between 36°C and 37.5°C at this faster cooling rate of 10°C/min, compared to the onset temperatures of 41°C to 42.5°C in Figure 5.6.2(b). The same trend observed in Figure 5.6.2(b) is seen that the crystalliser sample with PGPR 90 still has the onset at the highest temperature, here being 37.5°C compared to the crystalliser sample with Moringa MAG (36°C). The profile for the CRY110 and Moringa MAG/ CRY110 were essentially the same throughout the cooling regime of 10°C/min, contrary to the results obtained for the slower cooling rate in Figure 5.6.2(b).

The observation that the CRY110 based samples are showing delayed onset of gelation – or viscosity increase – at the higher cooling rate of 10°C/min is understood as super-cooling. Specifically for monoglycerides, any increase in cooling rate, results in crystallisation temperature below normal, due to 'super-cooling' effect (Krog, 2001). There is confirmation of this seen in Figures 5.6.5 and 5.6.6, which show the rheological curves at the accelerated cooling rate of 30°C/min.

5.6.3.3 Cooling Velocity - 30°C/min

In the case of higher saturation and faster cooling rates (Figure 5.6.5), the Moringa MAG and PGPR 90 still show behavioural patterns that are the same, (as seen at lower temperature gradient), and basically follow the control sample, but the viscosity increase has dropped to lower temperatures. When used in combination with CRY110 the onset of viscosity increase – gelation, has also moved to lower temperatures, but still maintaining a distinct gap from the control and single samples.

The new onset temperature for the combined Moringa MAG with CRY110 and PGPR 90 with CRY110 is now the same at 32°C. There appears to be no difference between the sample containing PGPR 90 or Moringa MAG.

Figure 5.6.6 (less saturation faster cooling rate) shows similar response behaviour. However, it is clear that examination of the Moringa MAG and PGPR 90 as single additives cause quicker induction rates compared to the control (without additive). Benefits are also seen again when combining Moringa MAG with CRY110 and PGPR 90 with CRY110.

The increased cooling rate has exerted influence on the onset temperature of the control sample. The data in Figures 5.6.5 and 5.6.6 show, the combined samples and the control and individual samples converge at the lower temperatures and merge. Therefore, this would seem to indicate a physical limit is being reached. At higher cooling rates the non-isothermal crystallisation temperature is reached at shorter periods, but in this case, the time it takes to reach the critical lamellar size for nucleation is prolonged. (Toro-Vazquez et al, 2001).

The results in Figures 5.6.2, 5.6.3, 5.6.4, 5.6.5 and 5.6.6 are very specific for the given model TAG blends and emulsifier concentrations, as well as the selected process conditions. Both Toro-Vazquez et al (2001) and Fredrick et al (2008), suggest conditions ultimately dictate the induction time for crystallisation, and therefore will change for other TAG blends. Ojijo et al (2004) goes on to report that at slow cooling rates sufficient time is available for lamellar structures to

form, these being the precursors to crystal nuclei, and they can form to such an extent as to reach a given critical size for nucleation. This critical size is then reached before the isothermal temperature is reached, whereas at faster rates of cooling much of the lamellar organisation and formation takes place at the isothermal temperature – and therefore more time is required to reach the critical lamellar size. In this case, longer time results in a lower temperature being reached before any onset of viscosity increase is seen, and hence the apparent delay in onset temperatures.

The cooling rate and the solvent have considerable impact and bearing on the mechanical and physical properties, including aspects like stability of the final network structure. In this study two palm oil fractions palm stearin (IV35) and palm olein (IV56), were used at two ratios' to achieve differing unsaturation. Other ratio may have given a different outcome. Studies of palm oil and its numerous fractions show that crystallisation behaviour changes depending on the degree of supercooling (Fredrick et al, 2008).

When comparing the effect of increased cooling rates with their consequences on the structures to the results from the work in 5.5, there is agreement, in that during higher cooling rates the TAG crystals formed were smaller at the same given temperatures than was the case for lower cooling rates.

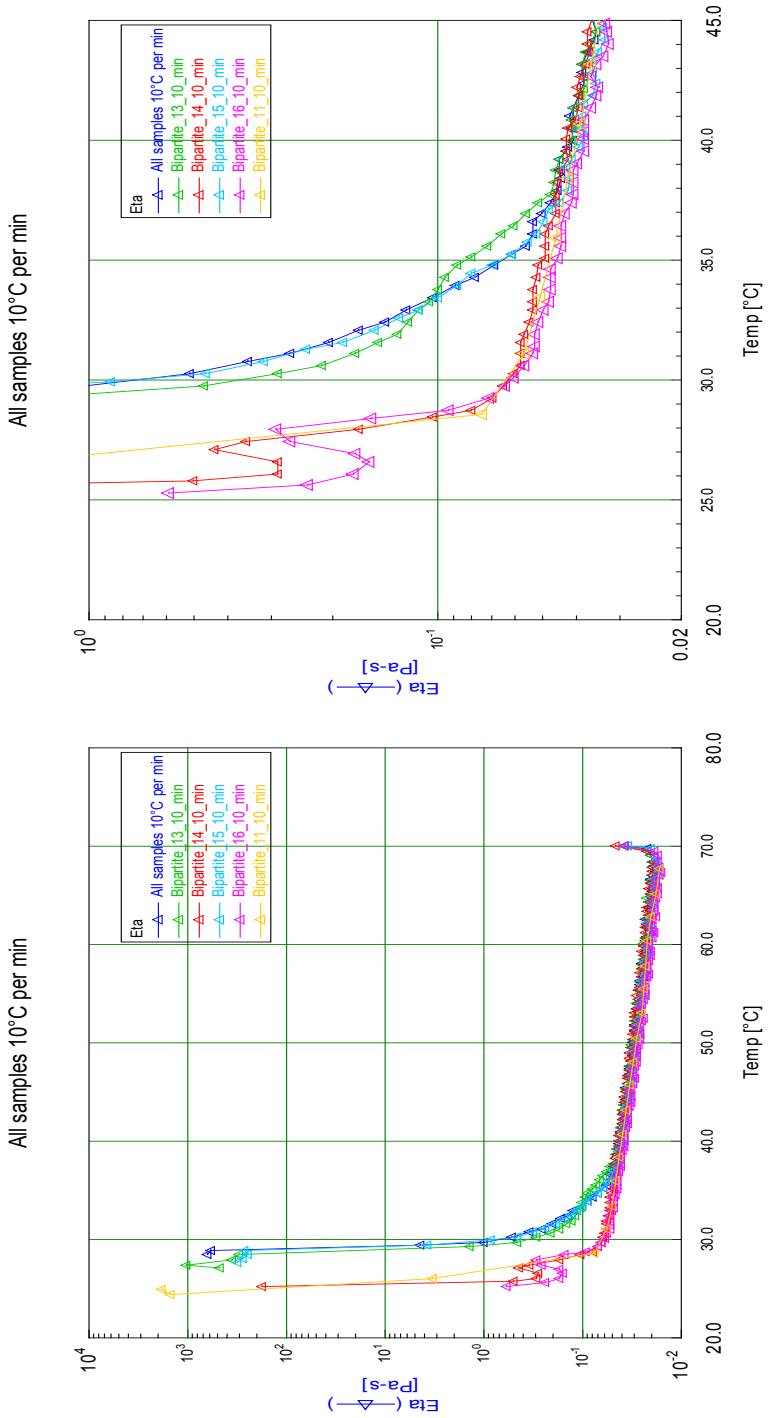

Figure 5.6.4 a / **b** Viscosity cooling curves at 10°C/min of base TAG blend (70% palm stearin/ 30% palm olein) [yellow]; 1% CRY110 [green]; 1% CRY110 / 0.5% PGPR 90 [green]; 0.5% PGPR 90 [red]; 1% CRY110 / 1% Moringa MAG [blue]; and 1% Moringa MAG [pink]

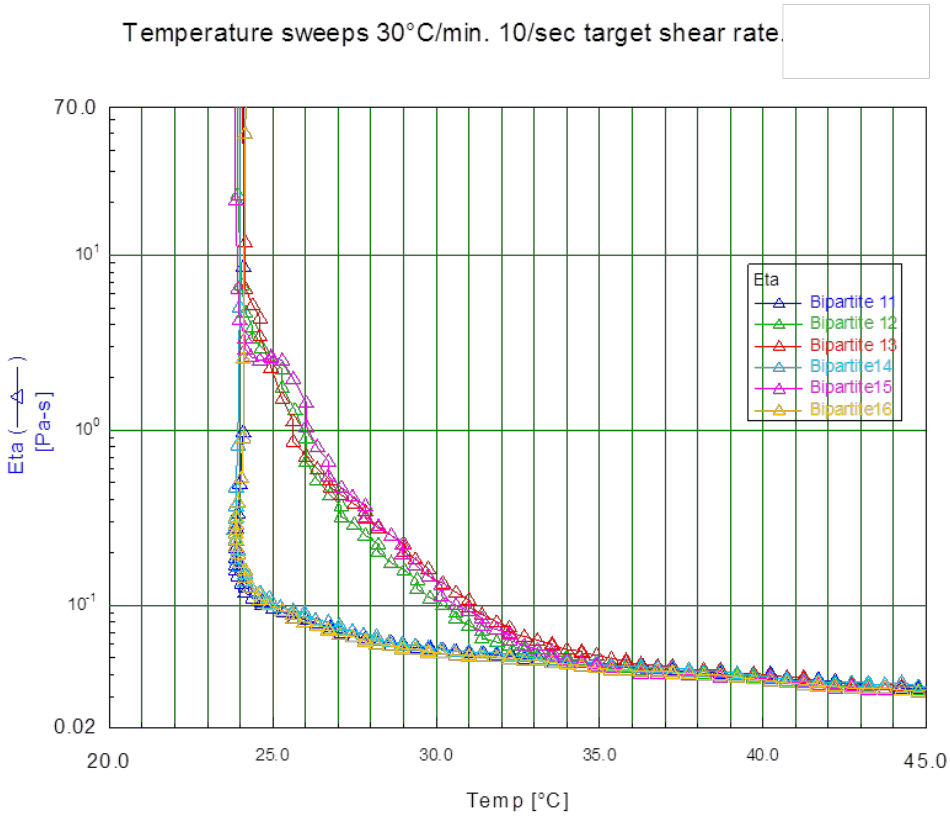

Figure 5.6.5 Viscosity cooling curves at 30°C/min of base TAG blend (70% palm stearin/ 30% palm olein) [Blue]; 1% CRY110 [green]; 1% CRY110 / 0.5% PGPR 90 [red]; 0.5% PGPR 90 [light blue]; 1% CRY110 / 1% Moringa MAG [pink]; and 1% Moringa MAG [yellow]

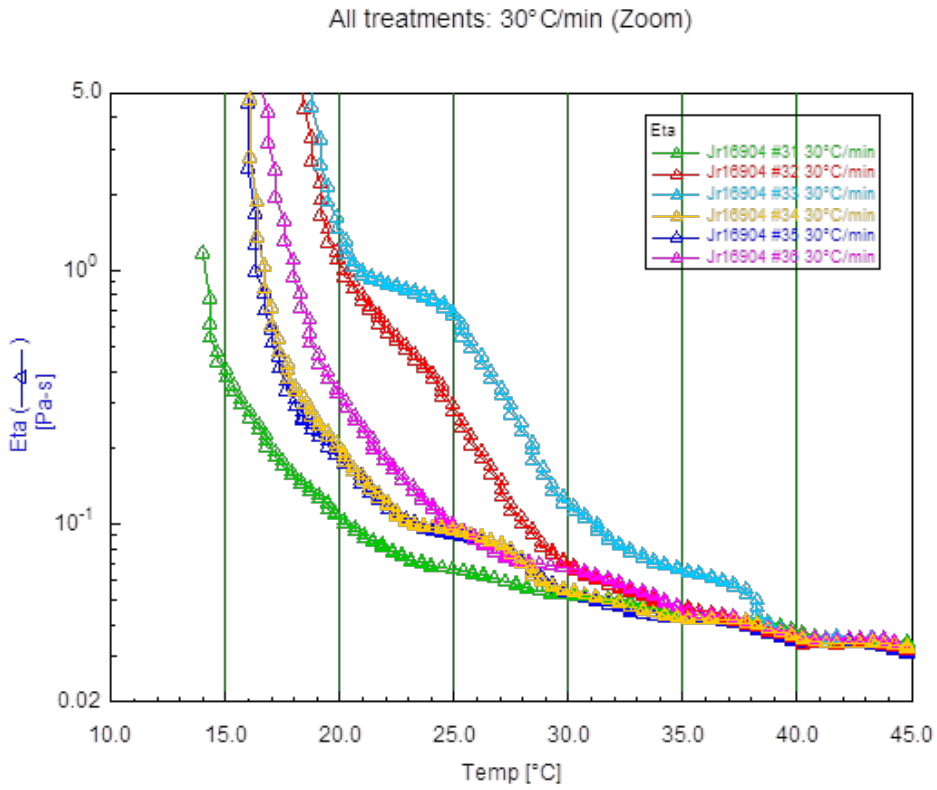

Figure 5.6.6 Viscosity cooling curves at 30°C per minute of base fat blend (70% palm olein / 30% palm stearin) [green]; 1% CRY110 [red]; 1% CRY110 / 0.5% PGPR 90 [light blue]; 0.5% PGPR 90 [yellow]; 1% CRY110 / 1% Moringa MAG [pink]; and 1% Moringa MAG [dark blue]

It is known that addition of hard material, i.e. CRY110 based on C22:0 can, under specific usage and process conditions, induce template nucleation (Wassell et al 2010). The crystalliser material can 'anchor' the surface, but at high dosages, act as a destabilising influence, especially in low saturated TAG systems (Low fat emulsions). However, if a less saturated material were added which still possessed sufficient ratio of saturation : unsaturation to interact with a PGPR dominated surface or have characteristics similar to PGPR, then additional surface strengthening might occur. Based on model systems and application trials in sections 5.3; 5.4 and 5.5, Moringa MAG is such a material.

Coinciding with this study, it has previously been demonstrated (5.7; 5.8) that Moringa MAG is capable of producing stable W/O low fat emulsions where addition of CRY110 or even PGPR (5.8) alone does not. This could suggest that Moringa MAG may fit into the schematic diagram given in Figure 5.6.7 in potentially two distinct manners.

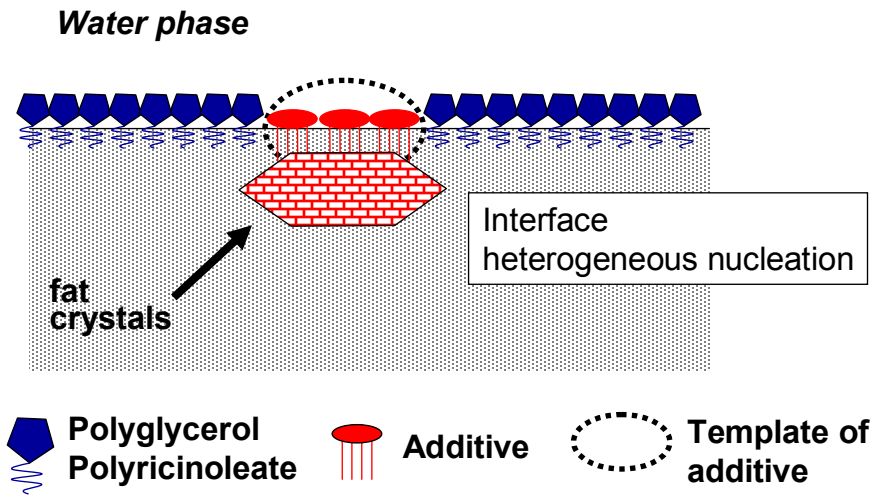

Figure 5.6.7 Additive to induce crystal nucleation, whilst retarding crystal growth. From Wassell, Bonwick, Smith, Almiron-Roig, and Young (2010)

In Figure 5.6.7 the blue PGPR molecules are dominating the surface and only the presence of the co-emulsifier (CRY110) at a Tγ, influences surface kinetics and TAG crystals. Moringa MAG could fulfil combined roles outlined in this schematic model.

5.6.4 Conclusion

Previous studies (3.0; 4.0; 5.2; 5.3; 5.4; 5.5) along with this work should be used as part of a composite conclusion, which suggests that *Moringa oleifera* based MAG is capable of performing a bi-functional role - template nucleation as well as surface stabilising.

These results have established a clear link between cooling rate and onset of gelation (viscosity increase) of both saturated and less saturated TAG systems. At a cooling rate of 1°C/min the onset for PGPR 90 / CRY110 was 42.5°C, whereas at a cooling rate of 10°C/min was 37.5°C. The corresponding onset temperatures for *Moringa oleifera* based MAG / CRY110 were 41°C and 36°C respectively. At a cooling rate of 30°C/min the onset temperature has fallen further to 32°C.

This study showed that a *Moringa oleifera* based MAG and PGPR 90 behave very similarly when used in the given TAG blend alone, but in combination with CRY110 differences do occur within cooling rates of 1°C/min to 30°C/min. Acceleration of gelation was more evident with CRY110 combined with PGPR in the less saturated TAG blend (70% palm olein / 30% palm stearin). These differences are explained via difference in surface activity because of either diffusion and or rearrangement of molecular geometry of the tested surfactants (Bergenståhl 2008). Although a strict relation between surface activity and cooling rate is sought, it is realistic to recognise the complexity of many environmental conditions. At the highest cooling rate studied, 30°C/min, no difference was found between the *Moringa oleifera* based MAG or PGPR 90 when used in combination with CRY110 in the highly saturated TAG blend. The convergence of the curves at the cooler temperature, the final diffusion behaviour and or rearranged interfacial structures resulting from addition of surfactants cannot be quantified within the scope of this measurement.

A study at the same cooling rate (30°C), in a less saturated TAG blend, revealed the same gelation patterns are as distinct to those observed for 1°C/min, although at lower onset temperature.

5.7 Impact of Fatty Acid Profile: Distinctions Between Moringa MAG and Behenic Based MAG in Low TAG W/O Emulsions

5.7.1 Introduction

A previous study (5.4) of W/O low TAG spread emulsions with Moringa MAG concentrated solely on the functionality of the Moringa MAG as being a convincing functional ingredient for commercial applications (Wassell et al., 2012a; 2012b; 2012c; 2012d; 2012e; Bech et al., 2013). The effectiveness of Moringa MAG may in part be due to its natural fatty acid profile consisting of C20:0, C22:0, and >C24:0.

Both CRY110 and PGPR 90 were used as comparisons in previous studies (5.2; 5.3; 5.4; 5.5; 5.6) for several reasons. First, the behenic (C22:0) based MAG (CRY110) is characterised by its high C22:0 content. Moringa MAG is 6 – 8% C22:0 (total >C20:0 = ~10%) which may be unusually high for a natural MAG (Wassell et al., 2012a; 2012b; 2012c; 2012d; 2012e; Bech et al., 2013). Second, the PGPR is normally used in conjunction with a second emulsifier (1.6; 1.7) for low TAG emulsions (<41%). Studies in this thesis have revealed Moringa MAG to have unusual rheological (5.2; 5.6), crystallisation (5.3; 5.5) and interfacial (4.0) similarities to PGPR.

It is known that to stabilise a low TAG W/O emulsion (<50%) using fully saturated MAG is not conducive to stability; especially where a fully saturated and/or longer chain saturated fatty acid e.g. C22:0 (behenic acid) is used. However, evidence in this thesis (1.5) has shown the presence of a C22:0 rich MAG (CRY110) can and does aid structuring performance and in low TAG systems, provided dosage, process conditions and ingredient balance is correct – primarily this mechanism is linked to the presence of the C22:0 fatty acids (Sakamoto et al, 2003; Wassell & Young 2007; Wassell et al., 2010a).

Therefore, assuming that Moringa MAG seems to have a bi-functional effect (5.6), it is necessary to distinguish by application tests, a comparison of only a C22:0 based MAG (CRY110) and Moringa MAG in low TAG emulsion systems.

5.7.2 Materials and Methods

Two TAG concentrations were studied, 35% and 40%/, in W/O emulsions formula's given in Tables 5.7.1 and 5.7.2. In the 35% TAG samples (Table 5.7.1) the water phase is empty, i.e. does not contain hydrocolloid thickeners and represent a spread that is "stressed". In the 40% TAG spreads (Table 5.7.2) the water phase contains GRINDSTED® LFS 560 Stabiliser System (Pectin / Alginate blend). The plant process conditions are subsequently given for the 35% and 40% TAG samples in Table 5.7.3, and were the same in each case. The Moringa MAG 191 is the same specification as described previously (5.3 - Tables 5.3.4 & 5.3.6), see Table 5.7.4. The emulsifier concentrations were 0.15, 0.3, 0.6 and 1.2%. The reliability of Moringa MAG at 0.3% and 0.6% is already confirmed positive (5.4), but the extreme low 0.15% and high 1.2% concentration had not been tested until now. Refer to General Materials & Methods (2.0) for emulsion assembly procedure.

Table 5.7.1 Formula of spread samples at 35% TAG content.

Ingredients in %						
Ingredient Name	**21**	**22**	**23**	**24**	**25**	**26**
Water phase						
Water (Tap)	64.000	64.000	64.000	64.000	64.000	64.000
Salt (Sodium Chloride)	1.000	1.000	1.000	1.000	1.000	1.000
Butter Flavouring 050001 T03007	0.010	0.010	0.010	0.010	0.010	0.010
Water phase total	**65.010**	**65.010**	**65.010**	**65.010**	**65.010**	**65.010**
pH	5.5	5.5	5.5	5.5	5.5	5.5
Fat phase						
Fat blend						
PK4 - INES	25.000	25.000	25.000	25.000	25.000	25.000
COLZAO	75.000	75.000	75.000	75.000	75.000	75.000
Fat blend total	**100.000**	**100.000**	**100.000**	**100.000**	**100.000**	**100.000**
Other fat ingredients						
Moringa. monoglyceride 191		0.150				1.200
GRINDSTED® CRYSTALLIZER 110 Distilled Monoglyceride	0.150		0.300	0.600	1.200	
2% sol. beta-carotene	0.020	0.020	0.020	0.020	0.020	0.020
Butter Flavouring 050001 T04184	0.020	0.020	0.020	0.020	0.020	0.020
Other fat ingredients total	**0.190**	**0.190**	**0.340**	**0.640**	**1.240**	**1.240**
Fat phase total	**34.990**	**34.990**	**34.990**	**34.990**	**34.990**	**34.990**
RECIPE total (calc. batchsize)	**100.000**	**100.000**	**100.000**	**100.000**	**100.000**	**100.000**

Table 5.7.2 Formula of spread samples at 40% TAG content.

Ingredients in %						
Ingredient Name	**11**	**12**	**13**	**14**	**15**	**16**
Water phase						
Water (Tap)	57,300	57,300	57,300	57,300	57,300	57,300
Salt (Sodium Chloride)	1,000	1,000	1,000	1,000	1,000	1,000
Skimmed milk powder (MILEX 240)	0,100	0,100	0,100	0,100	0,100	0,100
GRINDSTED® LFS 560 Stabiliser System	1,500	1,500	1,500	1,500	1,500	1,500
Potassium Sorbate	0,100	0,100	0,100	0,100	0,100	0,100
Butter Flavouring 050001 T03007	0,010	0,010	0,010	0,010	0,010	0,010
Water phase total	**60,010**	**60,010**	**60,010**	**60,010**	**60,010**	**60,010**
Ph	5,5	5,5	5,5	5,5	5,5	5,5
Fat phase						
Fat blend						
PK4 – INES	25,000	25,000	25,000	25,000	25,000	25,000
COLZAO	75,000	75,000	75,000	75,000	75,000	75,000
Fat blend total	**100,000**	**100,000**	**100,000**	**100,000**	**100,000**	**100,000**
Other fat ingredients						
Moringa, monoglyceride 191	0,150					1,200
GRINDSTED® CRYSTALLIZER 110 Distilled Monoglyceride		0,150	0,300	0,600	1,200	
2% sol. beta-carotene	0,020	0,020	0,020	0,020	0,020	0,020
Butter Flavouring 050001 T04184	0,020	0,020	0,020	0,020	0,020	0,020
Other fat ingredients total	**0,190**	**0,190**	**0,340**	**0,640**	**1,240**	**1,240**
Fat phase total	**39,990**	**39,990**	**39,990**	**39,990**	**39,990**	**39,990**
RECIPE total (calc. batchsize)	**100,000**	**100,000**	**100,000**	**100,000**	**100,000**	**100,000**

Table 5.7.3 Pilot plant processing conditions for the formula's in Tables 5.7.1 and 5.7.2

Processing (3-tube lab perfector):	
Oil phase temperature	50
Water phase temperature	50
Emulsion temperature	50
Centrifugal pump	Auto
Capacity high pressure pump	40
Cooling (NH3) tube 1:	-10
Cooling (NH3) tube 2:	-10
Cooling (NH3) tube 3:	-10
Rpm tube 1:	1000
Rpm tube 2:	1000
Rpm tube 3:	1000

Refer to General Materials & Methods (2.0) for emulsion assembly procedure.

Table 5.7.4 Fatty acid profiles for Moringa MAG 191 and CRY110 (5.3 - Tables 5.3.4 & 5.3.6)

Fatty acid chain length	% in Moringa 191	% in CRY110 (courtesy: Danisco A/S
C12:0	<0.1	
C14:0	0.1	
C15:0	<0.1	
C16:0	6.5	
C16:1	1.8	
C17:0	0.2	
C18:0	5.8	2.0
C18:1	71.2	
C18:2	1.5	
C18:3	0.3	
C20:0	3.4	5.0
C20:1	1.9	
C20 unsaturated	0.3	
C22:0	6.0	89.0
C22 unsaturated	0.2	0.3
C24:0	0.8	3.0

The methods of analysis for water droplet size distribution (DSD) and confocal laser scanning microscopy (CLSM), scaled to 375 x 375µm are outlined in 2.0. All samples are stained with FITC, stains protein green, and Nile Red, stains fat red. Texture analysis was outlined previously (5.3). Photographic images were recorded using a Canon G12.

5.7.3 Results and Discussion

Table 5.7.5 Water droplet size distribution (DSD) for 40% TAG spreads (samples 21-26), and 35% TAG spreads (sample 11-16).

Sample ID	Average/ St.dev	2.5% <μm	50% <μm	97.5% <μm
11	Average	1.08	5.38	26.80
	St.dev	0.02	0.07	0.54
12	Average	1.10	5.62	28.80
	St.dev	0.05	0.03	1.14
13	Average	0.84	6.50	50.41
	St.dev	0.04	0.13	2.75
14	Average	0.60	10.14	171.08
	St.dev	0.04	0.20	17.17
16	Average	2.01	3.64	6.58
	St.dev	0.09	0.02	0.36
21	Average	0.23	3.46	51.73
	St.dev	0.01	0.07	5.26
22	Average	0.58	3.81	24.82
	St.dev	0.03	0.06	1.16
23	Average	0.91	10.20	115.23
	St.dev	0.05	0.75	21.16
24	Average	1.01	21.66	481.56
	St.dev	0.05	3.66	196.53
25	Average	0.85	23.01	665.20
	St.dev	0.13	4.21	346.97
26	Average	3.48	3.48	3.49
	St.dev	0.01	0.01	0.01

The results presented in Table 5.7.5 show the water droplet size distribution for the 35% TAG spreads (samples 21-26) and the 40% TAG spreads (samples 11-16).

Sample 15 could not be measured due weak to signal. Samples 21, 22, 23 and 24 covering the 35% TAG spreads were phase separated (except sample 26); abundance of liquid oil was in the bottom of the 150g sample container. This observation indicates instability. An indicator of instability is revealed by large water droplet size distribution (DSD).

The clear conclusion that is drawn from the results given in Table 5.7.5 is that the size of the water droplets for all samples containing CRY110 are large and

therefore the spread samples are prone to instability, and hence separation. This was found irrespective of TAG content, either 35% or 40%, although the samples at 40% were distinctly more stabilised, likely because of 5% more TAG content and aided by stabiliser in the water phase.

A different situation was apparent for the samples containing Moringa MAG. These samples generally showed a stable performance, with the exception of sample 22, which contained Moringa MAG at 0.15% dosage in the 35% TAG spreads. This was the most stressed of the Moringa MAG containing samples since the water phase of this spread was empty, i.e. no hydrocolloid thickener. Sample 22 showed clear phase separation and therefore instability. In a 35% W/O emulsion, and empty water phase, it is possible that 0.15% Moringa MAG is the lower inclusion limit.

At the higher Moringa MAG inclusion level sample 26, dosed at 1.2% for the same 35% TAG spread with empty water phase, resulted in a dramatic reduction of the water droplet size, and no phase separation, adding positively to previous results (5.4).

In the 40% TAG spreads, with the water phase stabilised with GRINDSTED® LFS 560 Stabiliser System, Moringa MAG dosed at 0.15% (sample 11) showed water droplet sizes of 26.8, which was enough to provide a stable emulsion, whereas when the dose is increased to 1.2% (sample 16) the water droplet size dropped to 6.58, and the level of stability increased.

Basic photographic (Canon G12) evidence of the samples is shown when spreading onto cardboard (post production, after 24 hours), and while still in the plastic sample pots highlights the structure in Figure 5.7.1a to e. Here the relative stability or breakdown can be readily seen. It is already established (5.4) that Moringa MAG dosage at 0.3 and 0.6% are stable.

In Figures 5.7.1a to c the cardboard test is seen for the samples at 40% TAG content with a stabilised water phase. Sample 11, containing Moringa MAG at 0.15% produced a thick and creamy emulsion that was stable, and acceptable to

spread testing. There was no adverse sign of emulsion breakdown or leakage of water.

Samples 12 – 15 all contained CRY110 (high C22:0) alone at increasing concentrations from 0.15, 0.3, 0.6 and 1.2% respectively and showed increasing instability with increasing concentration. All samples resulted with increasing water release and lumpy inhomogeneous structure. Sample 15 was inverted and essentially an O/W emulsion (CLSM in Figure 5.7.2e).

Sample 16 (Moringa MAG at 1.2%) demonstrated a very thick and stable emulsion, but with very slow flavour release. The emulsion here was essentially too stable, and melting breakdown by mouth was insufficient. These results suggest that Moringa MAG can stabilise in low TAG spread applications beyond the capability of CRY110.

The results suggest that the optimum Moringa MAG dose for low TAG W/O emulsions lies between 0.15% and 1.2%. As demonstrated previously (5.4) where a co-emulsifier (PGPR) might be added, it is now shown that PGPR is not required.

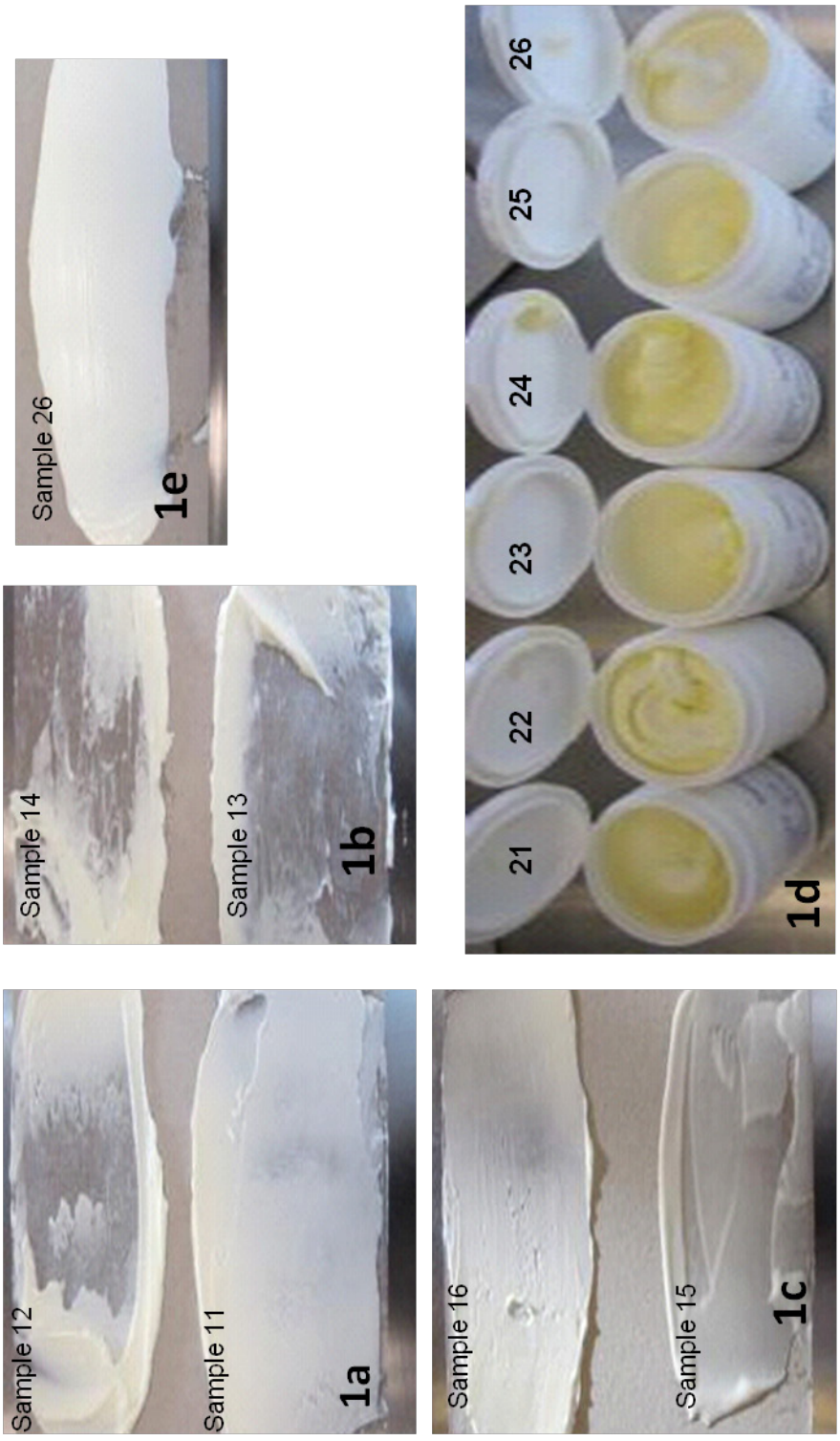

Figure 5.7.1, (**1a)** Spread test for samples 11 and 12; (**1b)** spread test for samples 13 and 14; (**1c)** spread test for samples 15 and 16; (**1d)** samples in storage tub for samples 21, 22, 23, 24, 25 and 26; (**1e)** spread test for sample 26

5.7.3.1 CLSM

The data presented in Figures 5.7.2 a to f (samples 11 to 16), and Figures 5.7.3 a to f (samples 21 to 26) show the confocal laser scanning microscopy (CLSM) images for the samples of full water phase and a TAG content of 40%, and empty water phase and a TAG content of 35% respectively. Images are reproduced from x40 magnification and scaled to 375 x 375 μm.

For Figure 5.7.2 a and f, which contain Moringa MAG at 0.15% and 1.2% respectively, the CLSM images show a compact-like water droplet size distribution. This is indicative of a stable emulsion.

Samples pertaining to Figures 5.7.2 b to e show the sample containing CRY110 at increasing concentration from 0.15%, 0.3%, 0.6% and 1.2% respectively, and basically show the increasing instability of the emulsions until the image corresponding to sample 15 (Figure 5.7.2 e) shows complete breakdown.

In terms of a maximum Moringa MAG limit (1.2%), the CLSM image in Figure 5.7.3 f (sample 26), appears unstable. It is suggested this is possibly an artefact of an O/W/O emulsion, where Moringa MAG has gone beyond critical micelle concentration, and formed a separate laminar phase. Figure 5.7.1 e (Sample 26) shows a highly stable white emulsion, demonstrated by the tight emulsion (97.5% DSD = 3.49).

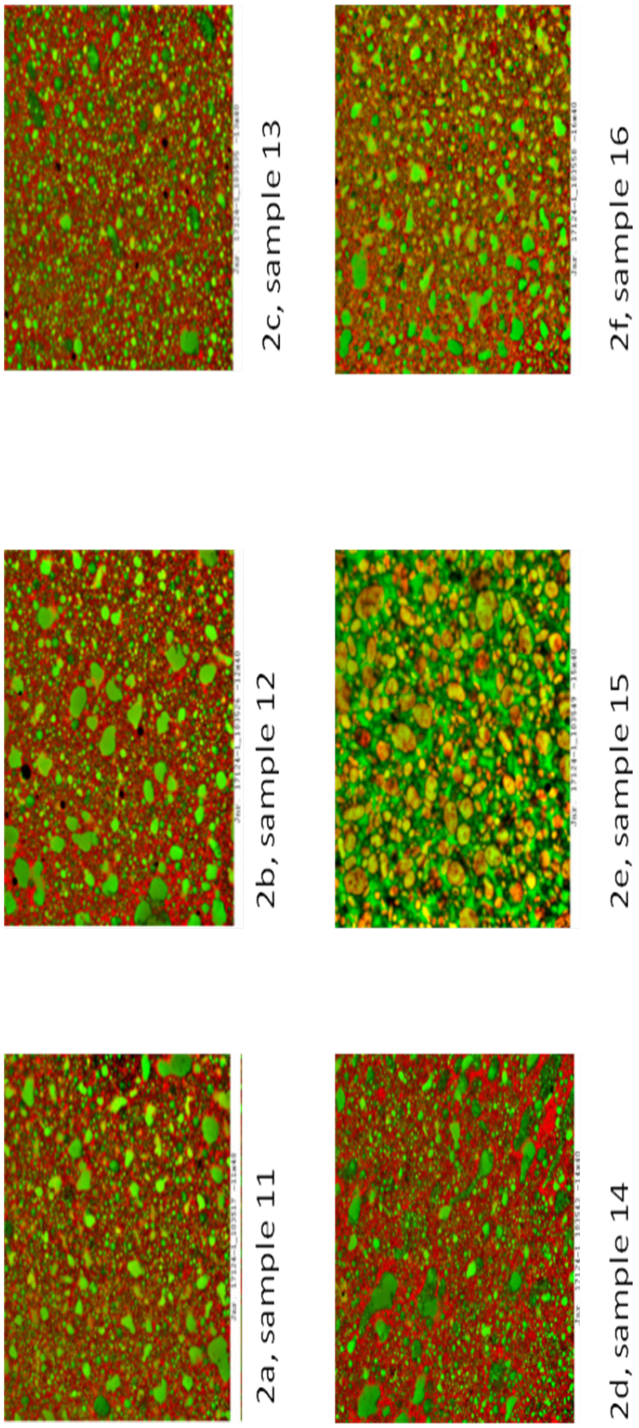

Figure 5.7.2 (2a – 2f) CLSM images of low TAG (40%) spread samples 11 to 16, with stabilised water phase

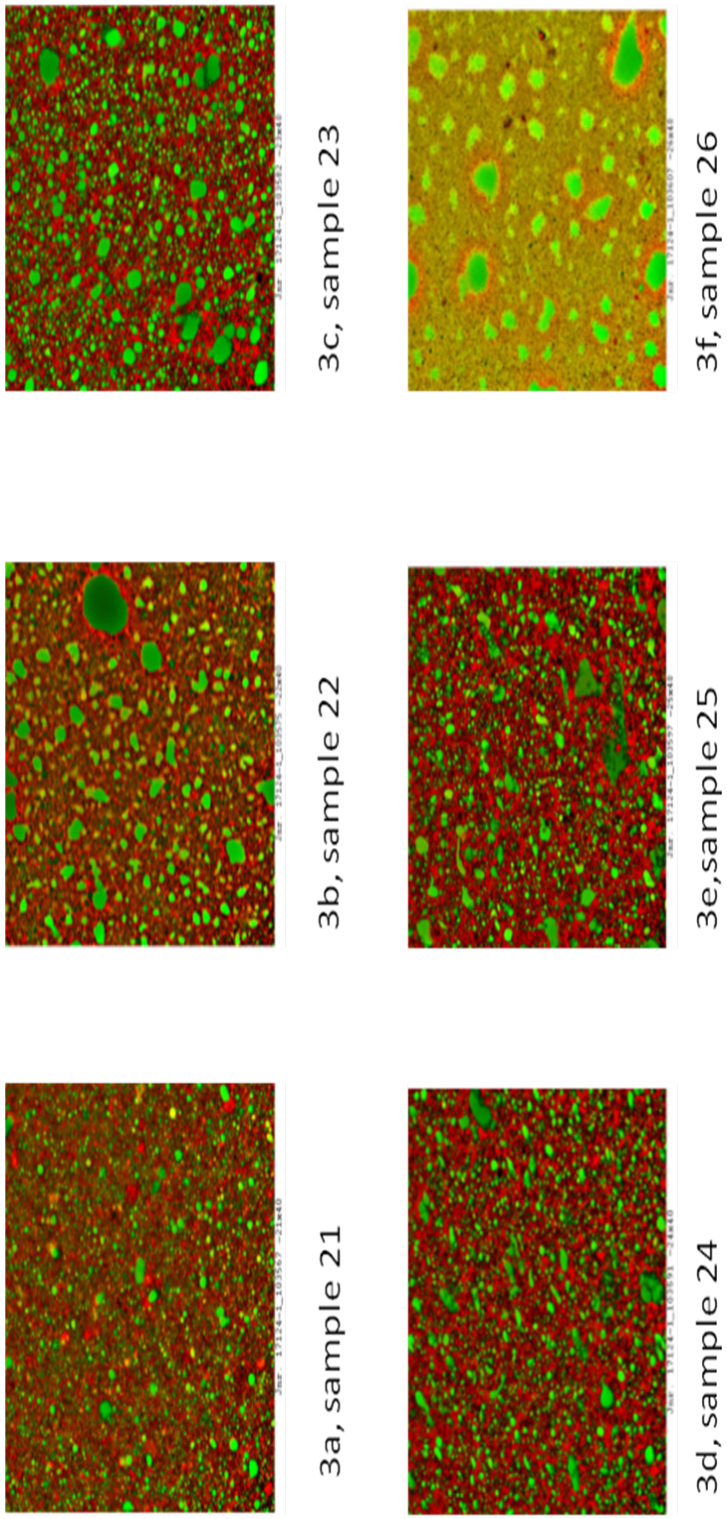

Figure 5.7.3 (3a – 3f) CLSM images of low TAG (35%) spread samples 21 – 26 with empty water phase

5.7.3.2 Texture Analysis

Textural firmness of measured samples (those measurable) are given in Figures 5.7.4 and 5.7.5. Figure 5.7.4 shows the hardness results for samples 11 to 16, i.e. full water phase, 40% TAG content. Figure 5.7.5 shows the hardness results only for sample 26, i.e. Moringa MAG at 1.2% with the empty water phase and 35% TAG content.

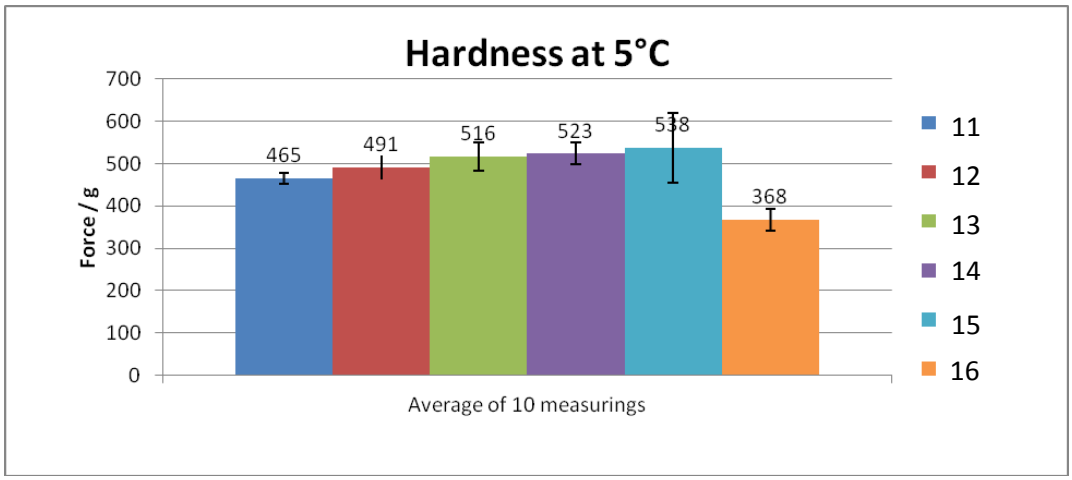

Figure 5.7.4 Hardness results: texture analysis for samples 11 to 16, 40% TAG, full water phase

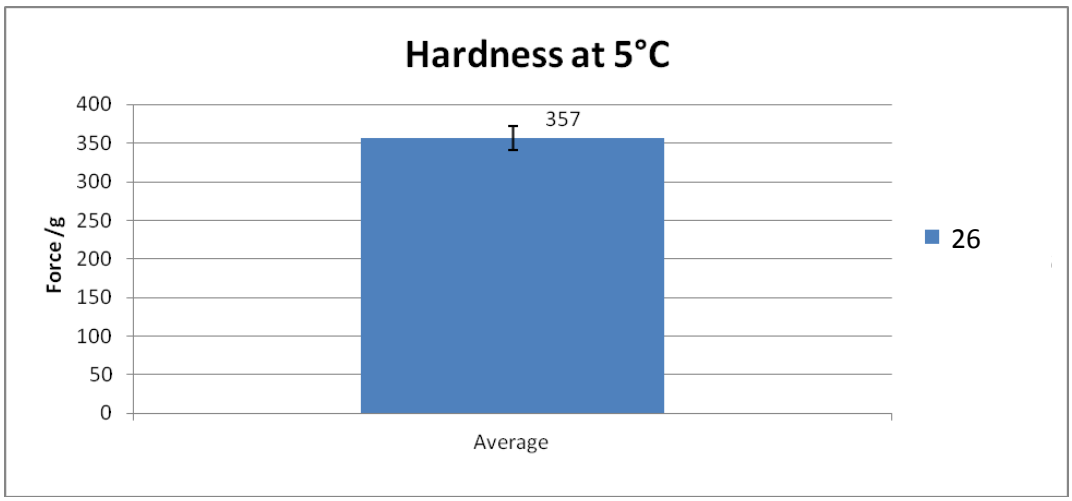

Figure 5.7.5 Hardness result: texture analysis for sample 26, 35% TAG, empty water phase.

Figure 5.7.4 shows (samples 11 – 16) a gradual increase in hardness, i.e. moving from Moringa MAG at 0.15% and CRY110 from 0.15%, 0.3%, 0.6% and 1.2% respectively. The emulsion firmness at the higher crystalliser concentrations is harder and this could be attributed to the continued water leakage from the emulsion making the solid part of the sample appear harder than would otherwise have been. At 1.2% sample 16 (Moringa MAG) is much softer. It is worth noting that despite this leakage of water being attributed for the increase in hardness, the level of water leakage has not led to the catastrophic failure of the systems represented in samples 21 to 25. It can be seen that Figure 5.7.5 only has data for one sample, the Moringa MAG containing Sample 26 at 1.2% dosage. All other samples in this range failed and were not possible to measure. Interestingly, the effect of Moringa MAG at 1.2% in either the 35% empty water phase or 40% hydrocolloid-protein enriched water phase W/O emulsion gives basically the same textural force response.

Given the water leakage apparent for the samples in Figure 5.7.4, it is difficult to assign these textural results to a particular trend, as they are perhaps best described as average apparent values.

5.7.4 Conclusion

The results in this study have differentiated the distinction between a natural non-hydrogenated monoglyceride based on *Moringa oleifera* TAG and a fully saturated long chain monoglyceride based mainly on C22:0, (GRINDSTED® Crystallizer 110), in W/O low TAG emulsions. The results show that low TAG spreads cannot be adequately stabilised by behenic based (89% C22:0) MAG (CRY110) alone in either normal full, or empty water phase environments at 40% or 35% TAG content. All results show there is water leakage resulting in breakdown of the emulsion or indeed complete emulsion failure.

In contrast to this, Moringa MAG were shown to be able to stabilise the emulsions in the full water phase 40% TAG content systems at dosages between 0.15% and

1.2%, with the optimal being in between this range (5.4). These systems did not exhibit water leakage, were stable and spreadable. At a high concentration of 1.2%, a tendency towards over stabilisation resulted, leading to the inability of the emulsion to give good flavour release. When stressing the systems further by reducing the TAG content and keeping the water phase empty, the Moringa MAG at 0.15% dosage could not stabilise the spread. This is possibly an artefact of dosage, where a dose of 0.15% is below the lowest limit of securing stability, while a 1.2% dosage leads to over stabilisation.

There is clear distinction between two distilled MAG, one both natural, non-hydrogenated (Moringa MAG), and one fully hydrogenated (CRY110). Moringa MAG is able to stabilise low TAG spread emulsions, which might be attributed in part to the presence of its approximately 30% range of saturated fatty acids including C16:0, C18:0, C20:0, C22:0, C24:0 and C26:0, but clearly not exclusively because of this, but also because of a significant proportion being >C20:0. Possibly there are also other aspects of a *Moringa oleifera* based MAG structure and combination of fatty acids (~70% C18:1) that allow it to stabilise low TAG spread emulsions, where as a single emulsifier, CRY110 (essentially ~85% - 90% C22:0) does not. In the product applications and at the concentrations tested in this investigation, the addition CRY110 as a single emulsifier in low TAG W/O emulsions led to instability.

5.8 Effect of PGPR Concentration in Low TAG W/O Emulsions

5.8.1 Introduction

The strong water binding properties of Polyglycerol Polyricinoleate (PGPR) are well known (Claesson, Dedinaite, Bergenståhl, Campbell, & Christenson, 1997; Marze, 2009; Dedinaite & Campbell, 2000; Rousseau, 2000) and is normally, used in conjunction with a second emulsifier (1.5; 1.6) for low TAG (<41%) emulsions (Garti & Remon 1984).

For comparison, studies in this thesis have revealed that a MAG based on *Moringa oleifera* TAG has unusual rheological (5.2; 5.6), crystallisation (5.3; 5.5; 5.6) and interfacial properties (4.0) similar to PGPR. The evidence suggests that the optimum Moringa MAG dose for low TAG W/O emulsions is positioned between 0.15% and 1.2%. As demonstrated previously (5.4 & 5.7) where a co-emulsifier (PGPR) might be added, it was shown that PGPR is not required. However to support the argument that Moringa MAG seems to have a bi-functional effect (5.6), it was necessary to distinguish by application tests, a comparison solely of a behenic based MAG (CRY110) and Moringa MAG as single emulsifiers in low TAG emulsion systems (5.7). Goubran and Garti (1988) reported the benefit of using high molecular weight polyglycerols (PGPR) and recognised that while much had been reported on their behaviour in O/W emulsions, there appeared to be little reported regarding their behaviour in W/O emulsions.

The effect of PGPR as a single emulsifier is now tested in the context of the maximum permitted dose of PGPR in food emulsions is 0.4 wt%, and specifically it is limited in use to emulsions of less than 41% fat/oil (permitted use of E476 - EC Directive 95/2/EC). The aim in this study is to distinguish the effect PGPR 90 as a single emulsifier system at varying concentration in W/O 40% low TAG emulsions in comparison with a Moringa MAG tested previously (5.6; 5.7). (Wassell et al., 2012a; 2012b; 2012c; 2012d; 2012e; Bech et al., 2013).

5.8.2 Materials and Methods

GRINDSTED® PGPR 90 (PGPR) was used as a single emulsifier in a series of W/O 40% low TAG emulsions (in full water phase as per section 5.7), prepared according to Table 5.8.1, and then processed using the conditions in Table 5.8.2. Droplet size distribution (DSD), Confocal Laser Scanning Microscopy (CLSM), texture analysis and simple cardboard (abuse) test are carried out to achieve a balanced conclusion of the samples. More comprehensive detail is provided in General Materials & Methods (2.0).

Table 5.8.1 Formulations for low TAG W/O (40%) emulsions

Ingredients in %				
Ingredient Name	**61**	**62**	**63**	**64**
Water phase				
Water (Tap)	57.300	57.300	57.300	57.300
Salt	1.000	1.000	1.000	1.000
Skimmed milk powder (MILEX 240)	0.100	0.100	0.100	0.100
GRINDSTED® LFS 560	1.500	1.500	1.500	1.500
Potassium Sorbate	0.100	0.100	0.100	0.100
Butter Flavouring 507104 A	0.010	0.010	0.010	0.010
Water phase total	**60.010**	**60.010**	**60.010**	**60.010**
pH	5.5	5.5	5.5	5.5
Fat phase				
Fat blend				
PK4 - INES	25.000	25.000	25.000	25.000
Rapeseed oil	75.000	75.000	75.000	75.000
Fat blend total	**100.000**	**100.000**	**100.000**	**100.000**
Other fat ingredients				
PGPR 90	0.150	0.300	0.600	1.200
2% sol. beta-carotene	0.020	0.020	0.020	0.020
Butter Flavouring 050001 T04184	0.020	0.020	0.020	0.020
Other fat ingredients total	**0.190**	**0.340**	**0.640**	**1.240**
Fat phase total	**39.990**	**39.990**	**39.990**	**39.990**
RECIPE total (calc. batchsize)	**100.000**	**100.000**	**100.000**	**100.000**

Table 5.8.2 Processing parameters used for formula in Table 5.8.1

Pilot Plant				
Processing (3-tube lab perfector):	**61**	**62**	**63**	**64**
Oil phase temperature	50	50	50	50
Water phase temperature	50	50	50	50
Emulsion temperature	50	50	50	50
Centrifugal pump	Auto	Auto	Auto	Auto
Capacity high pressure pump	40	40	40	40
Cooling (NH3) tube 1:	-10	-10	-10	-10
Cooling (NH3) tube 2:	-10	-10	-10	-10
Cooling (NH3) tube 3:	-10	-10	-10	-10
Rpm tube 1:	1000	1000	1000	1000
Rpm tube 2:	1000	1000	1000	1000
Rpm tube 3:	1000	1000	1000	1000

5.8.3 Results and Discussion

5.8.3.1 Droplet Size Distribution (DSD)

Table 5.8.3 shows the W/O 40% emulsions samples 61 – 64 to test the PGPR DSD, at following inclusions: 0.15, 0.3, 0.6, 1.2%, and illustratively in Figure 5.8.1. These results must be viewed in comparison to the relatively increased DSD, when compared to the natural Moringa MAG (~91% mono) as shown in Table 5.8.4 (Samples originally prepared for synchrotron radiation Macrobeam and microbeam X-ray diffraction measurements (6.0). Presented University of Chester PGR Conference: Structuring and Texturing Low Saturated Fat Systems. 19th May 2011)). The comparison is important in the context of permitted use in food stuffs (EC Directive 95/2/EC) because at 0.6% PGPR (maximum use is 0.4%), droplet size is significantly larger than Moringa MAG (191) at the same dose (0.6%). However, when comparing PGPR at 0.4% (Table 5.8.4) with Moringa MAG 191, the Moringa MAG is almost half the DSD at 97.5% of the mean volume. For comparison, Table 5.8.4 also shows the DSD for PGPR at 0.3%, combined with CRY110 at 0.15% (6.0).

The results reveal an apparent inconsistency. PGPR at 0.6% has larger DSD (average 47.56μm) than PGPR at 0.4% (average 6.10μm). One would imagine the 35% TAG emulsion to be relatively less stable and have larger DSD, but the

results in Table 5.8.4 show that PGPR at 0.4% results in a smaller DSD. The reason for the discrepancy is possibly explained, because 0.6% PGPR is within a 40% TAG emulsion and contains skimmed milk powder (SMP), which can destabilise the emulsion, which seems contradictory, but protein within the SMP is often used to "open" the emulsion and enhance flavour release and melting behaviour. Therefore, despite 5% less TAG content and hence increased water phase for the 35% TAG, it is possibly easier to process than the 40% TAG.

Table 5.8.3 Low TAG W/O (40%) emulsions samples 61 – 64 to test PGPR water droplet size distribution at concentrations: 0.15, 0.3, 0.6 & 1.2%

Sample ID	Average/ St.dev	2.5% <µm	50% <µm	97.5% <µm	Dose wt%
61	Average	1.46	12.54	107.93	0.15
	St.dev	0.05	0.46	10.39	
62	Average	1.02	12.89	164.41	0.30
	St.dev	0.04	0.67	22.91	
63	Average	0.93	6.59	47.56	0.60
	St.dev	0.09	0.37	9.61	
64	Average	1.82	4.23	9.84	1.20
	St.dev	0.03	0.05	0.27	

Table 5.8.4 Results of average DSD volumes for low TAG W/O (35%) emulsions (no protein / stabiliser) 0.6% Moringa 191; 0.4% PGPR 90 and 0.3% PGPR + 0.15% CRY110))

Sample ID	Average/ St.dev	2.5% <µm	50% <µm	97.5% <µm	Dose wt%
7	Average	3.52	3.54	3.56	0.6% Moringa 191
	St.dev	0.05	0.03	0.02	
8	Average	1.92	3.42	6.10	0.4% PGPR
	St.dev	0.10	0.02	0.28	
18	Average	3.58	3.59	3.60	0.3% PGPR + 0.15% CRY110
	St.dev	0.01	0.01	0.02	

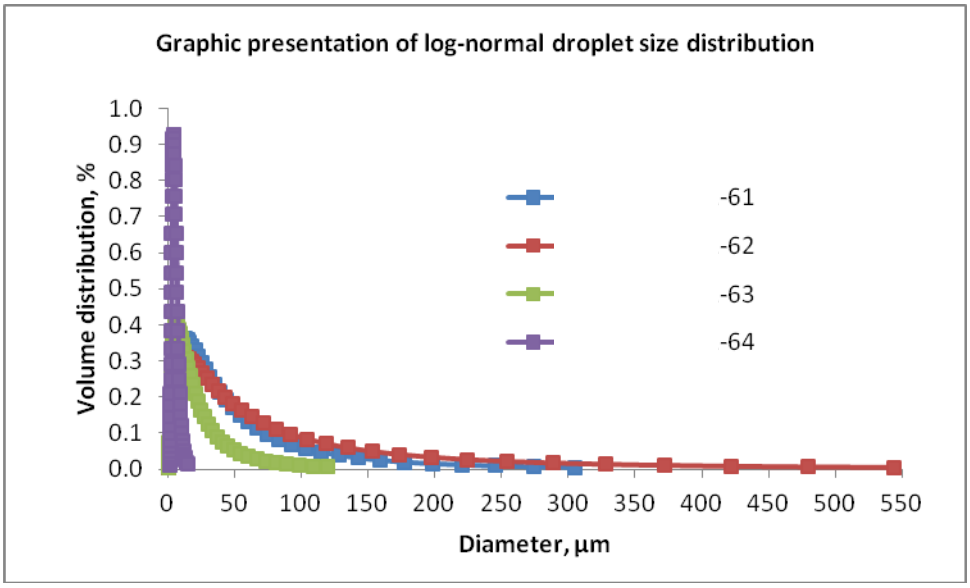

Figure 5.8.1 DSD normal distribution shows data from Table 5.8.3

5.8.3.2 Texture Analysis

Figure 5.8.2 shows the textural firmness of PGPR at increasing dose, leading to decreased firmness. These results are discussed further under the heading CLSM.

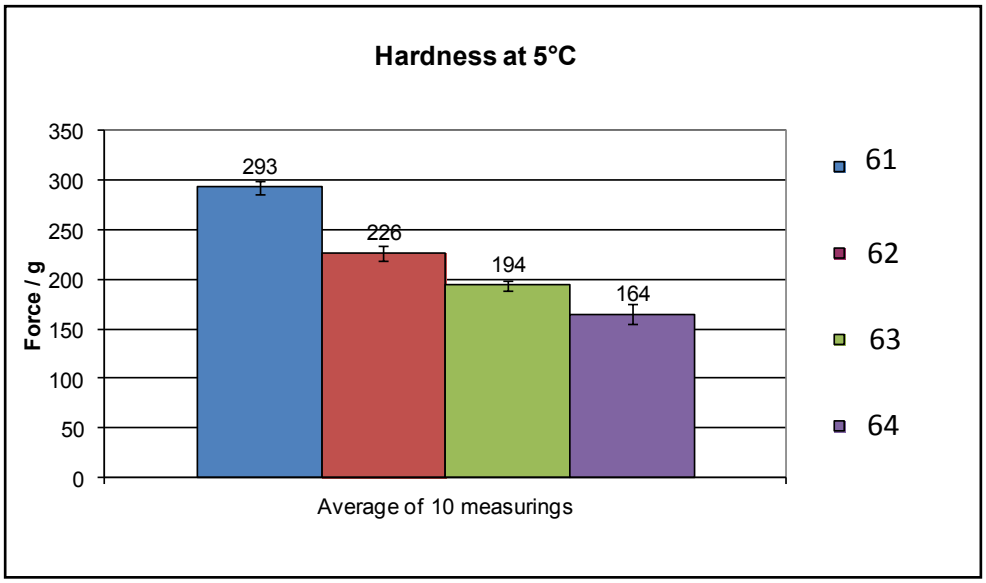

Figure 5.8.2 Texture analysis on 61 – 64; average of 10 measurements shows decreasing hardness with increasing PGPR concentration: 0.15, 0.3, 0.6 & 1.2%

5.8.3.3 CLSM

Confocal laser scanning microscopy (CLSM) images show trials 61 – 64, in Figures 5.8.3 - 5.8.6. Each figure shows four images at two magnifications (40X top and 100X bottom) and then scaled to 375 x 375µm and 188 x 188µm. All samples were stained with FITC, stains protein green, and Nile Red, stains fat red.

Comparing Figure 5.8.3 (sample 61, 0.15% PGPR) and Figure 5.8.4 (sample 62, 0.3% PGPR) there is apparent similarity in size and shape of water droplets despite significant difference in PGPR dose. The DSD data in Table 5.8.3 shows that as concentration is increased from 0.15% to 0.3% an increase in droplet size occurs, this is an unexplained anomaly.

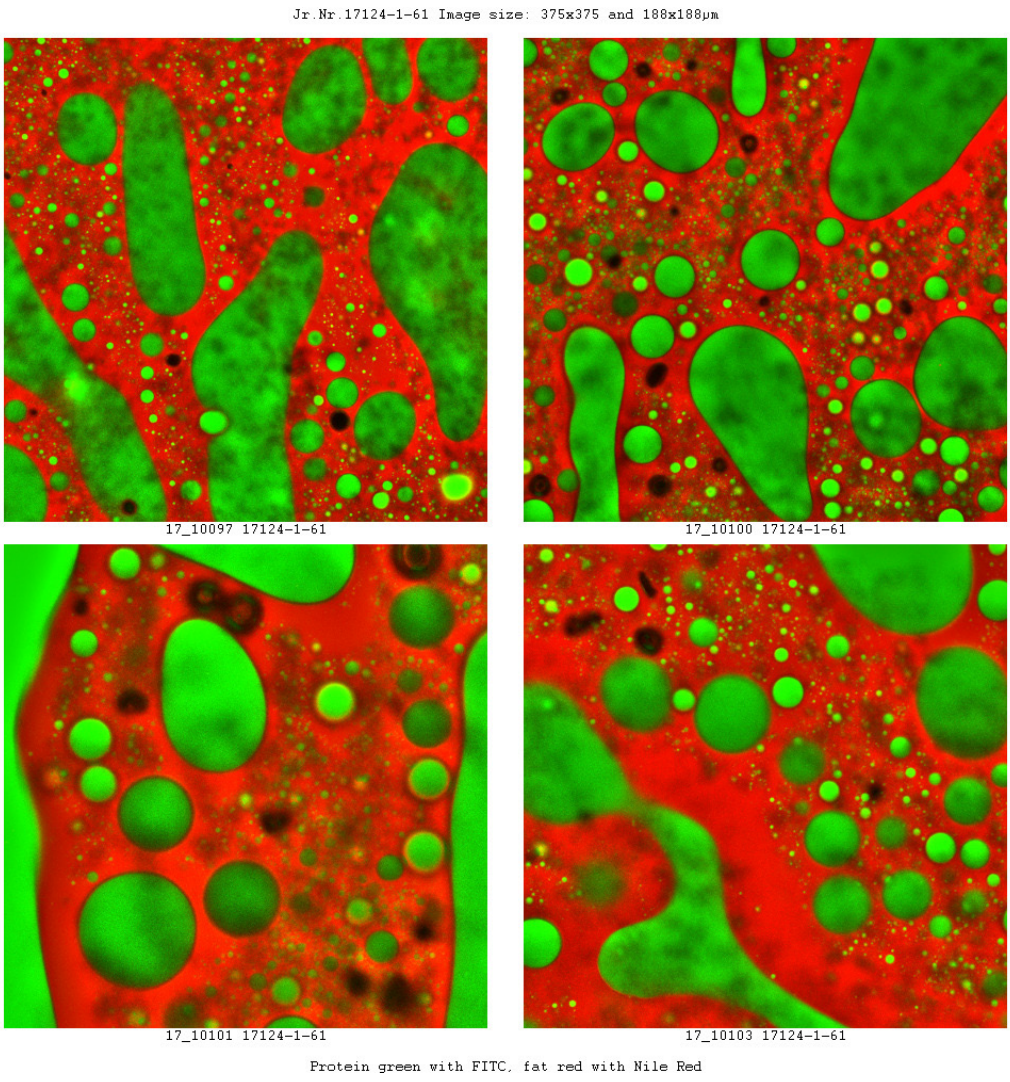

Figure 5.8.3 CLSM image of 40% TAG emulsion (Sample 61, dose 0.15% PGPR)

As emulsifier load is increased to 0.6% PGPR (sample 63, Figure 5.8.5) and 1.2% PGPR (sample 64, Figure 5.8.6) the results show decreased droplet size. This is consistent with the DSD and textural analysis.

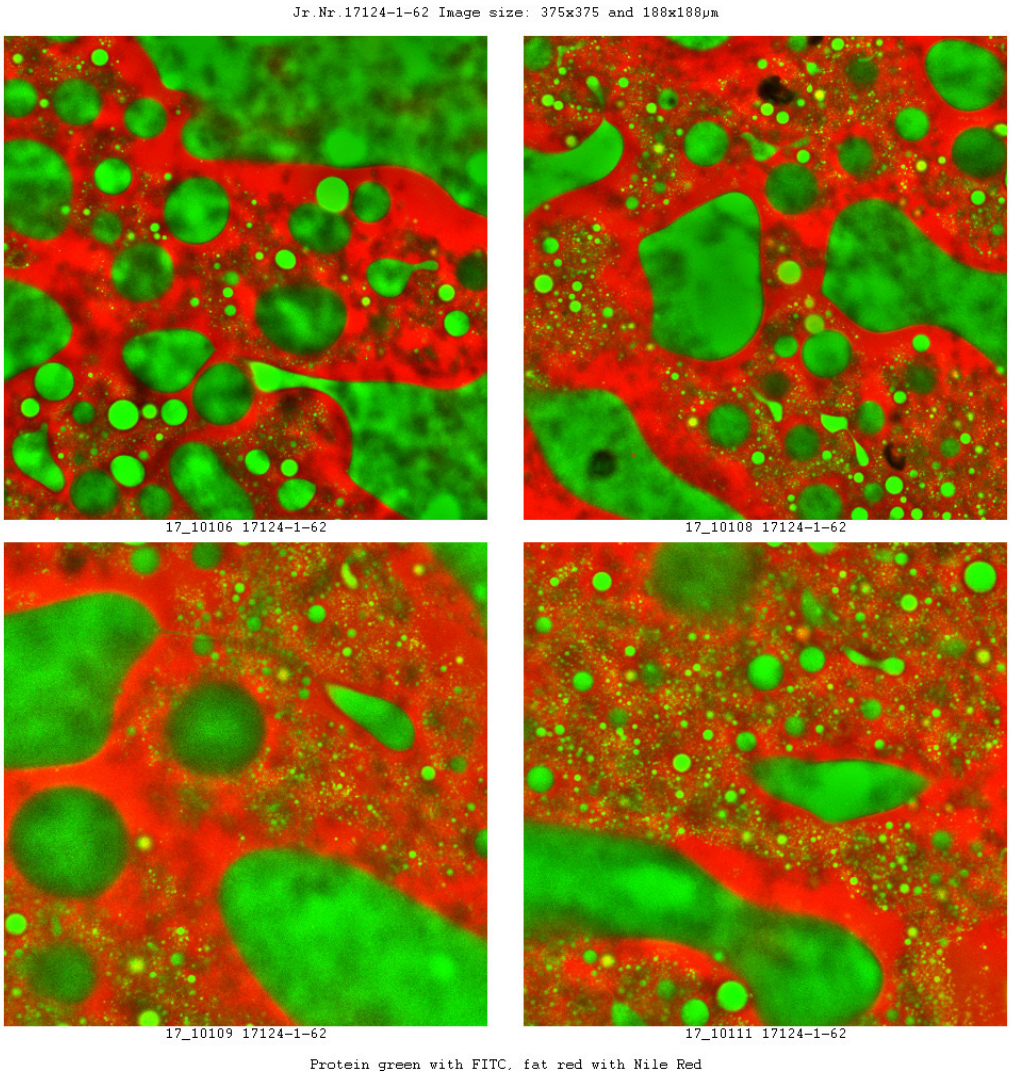

Figure 5.8.4 CLSM image of 40% TAG emulsion (Sample 62, dose 0.3% PGPR)

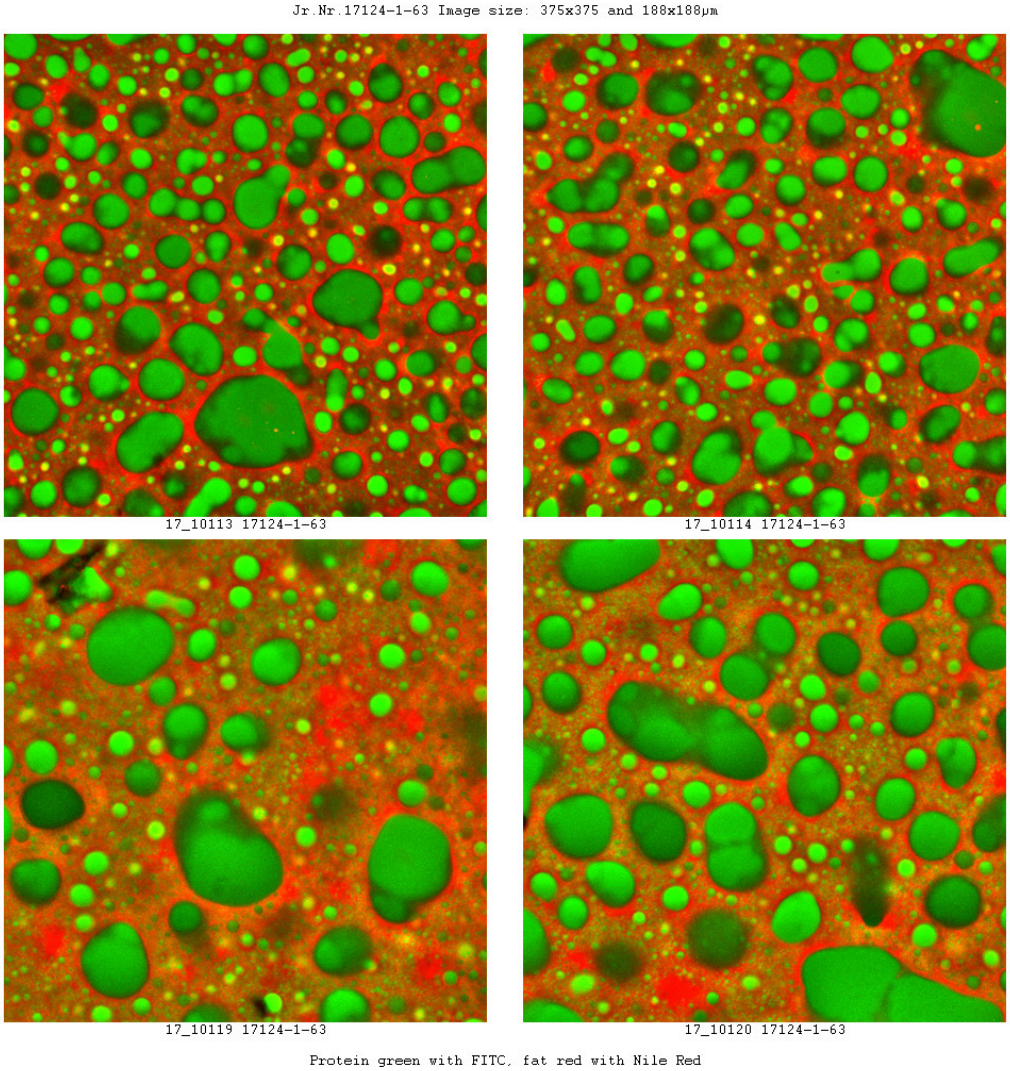

Figure 5.8.5 CLSM image of 40% TAG emulsion (Sample 63, dose 0.6% PGPR)

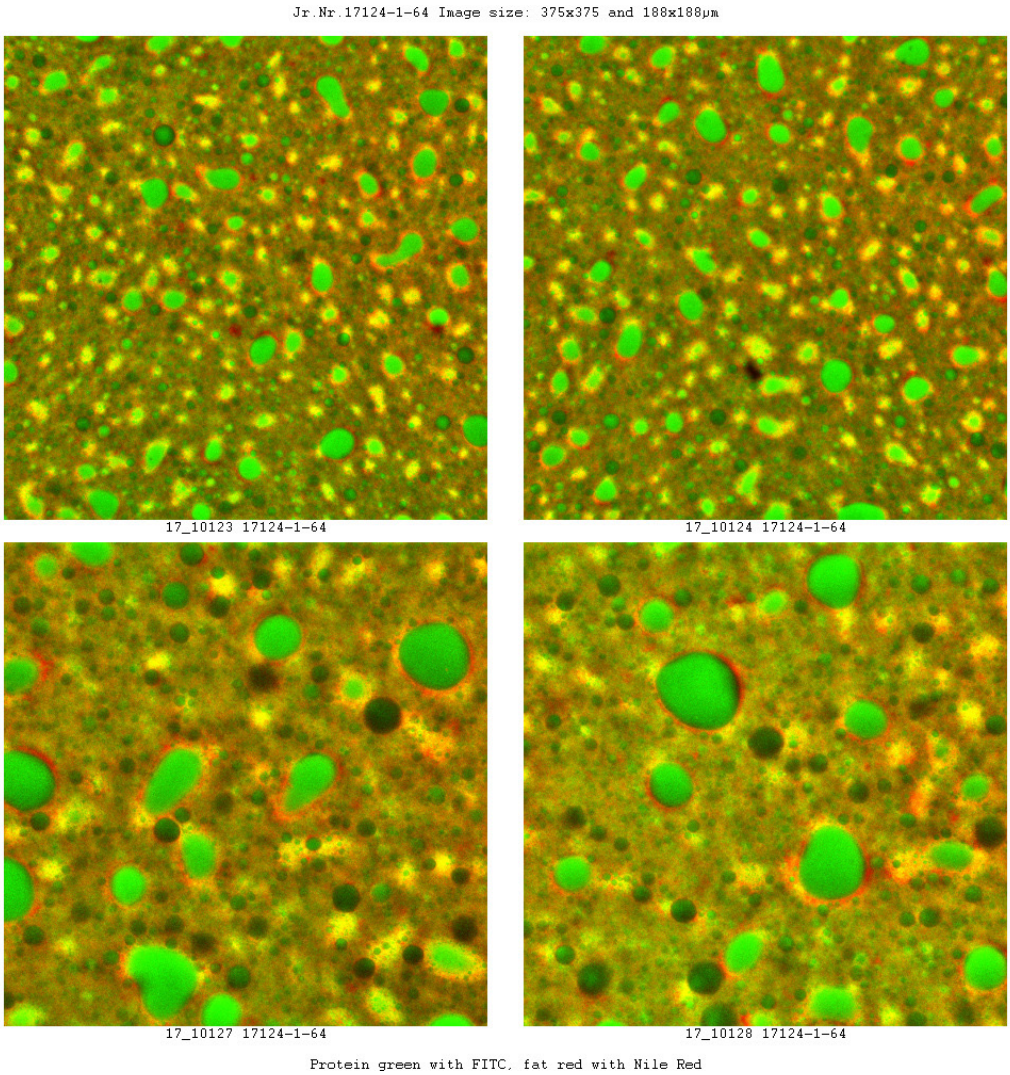

Figure 5.8.6 CLSM image of 40% TAG emulsion (Sample 64, dose 1.2% PGPR)

5.8.3.4 Cardboard Test

In Figure 5.8.7 simple cardboard test (abuse test) results are shown for PGPR samples at 0.15, 0.3, 0.6 and 1.2% dosages. The sensory comments were: At 0.15%, the emulsion was falling apart, was generally weak, a watery mouth feel. At 0.3%, signs of water separation, non-creamy and watery mouth feel. At 0.6% acceptable, mouth feel thicker than at 0.3% (sample 62), chewy in character. At 1.2%, good stability, but mouth feel was very chewy.

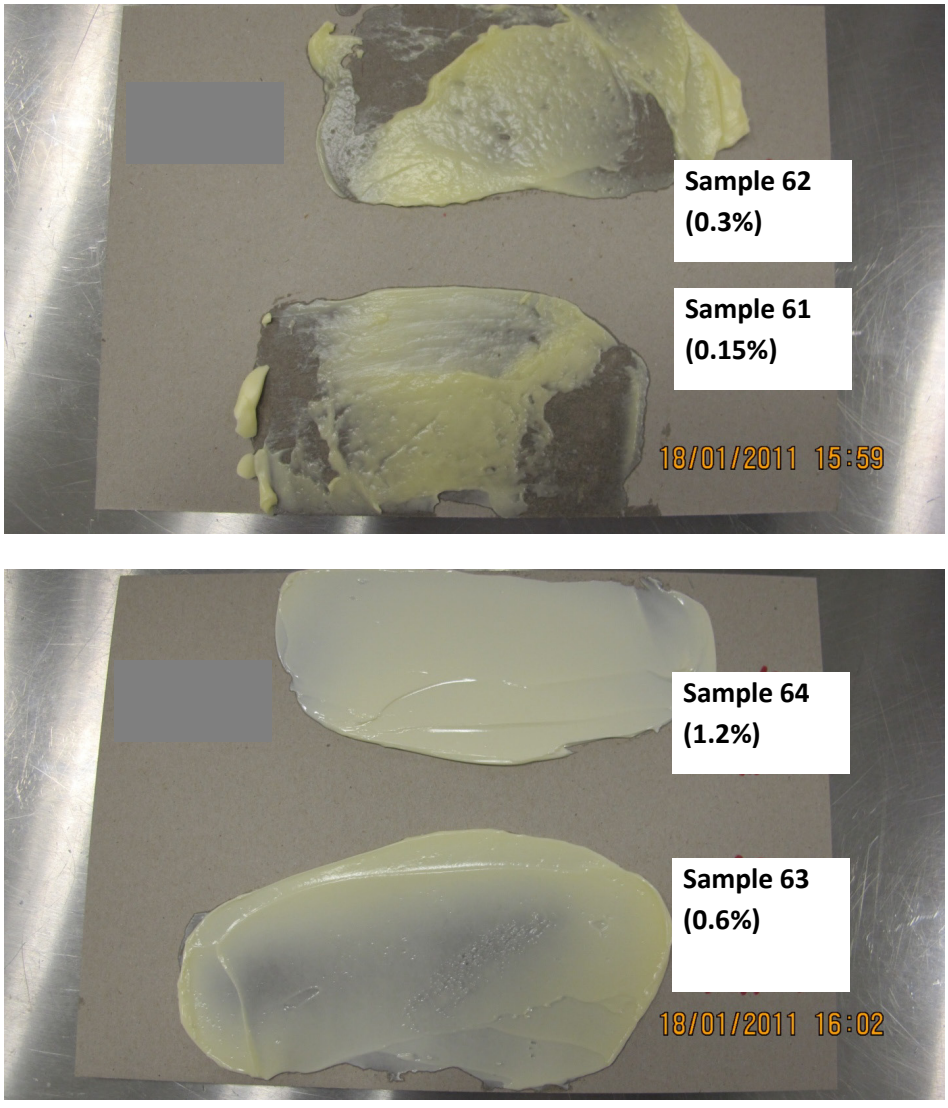

Figure 5.8.7 Photographic evidence of spread tests: PGPR at 0.15% & 0.3% (top) and 0.6% & 1.2% (bottom)

The sensory and simple cardboard test shows the use of PGPR as a single emulsifier in low TAG W/O emulsions is to be severely inadequate at stabilising the emulsion at 0.15 to 0.3%. At low emulsifier concentrations, which are possibly below the surface excess concentration, larger droplets are formed because of insufficient surface coverage, in turn leading to coalescence. Smaller droplets with increasing concentrations are formed because of sufficient surface coverage and less coalescence (Taylor, 2011). However, other considerations must also be weighed, such as sensory, and spreadability. Likely between 0.3 and 0.6% there is sufficient PGPR concentration to stabilise the emulsion; according to sensory and abuse test, the emulsion at 0.6% is stabilised (Figure 5.8.7).

The water binding properties of PGPR 90 are one of the reasons that it is essentially the stabilising emulsifier of choice for many water – oil based food systems (1.2.8; 1.6; 1.7). Hence, PGPR is normally used in conjunction with a second emulsifier for low TAG emulsions <41% (Garti & Remon 1984). However, the maximum permitted dose of 0.4% (EC Directive 95/2/EC) is potentially insufficient to achieve stability. This examination has shown that PGPR is not adequately able to stabilise low TAG W/O emulsions to 0.3%. In contrast, Moringa MAG (191) was shown to be able to stabilise the emulsions in a full water phase 40% TAG emulsion at between 0.15% and 1.2%, with the optimal being in between this range (5.4). These systems did not exhibit water leakage, were stable and spreadable.

In typical TAG blends e.g. low fat W/O emulsions, there is usually a proportion which is higher melting. On cooling, the higher melt will eventually crystallise out of solution and in doing so establish additional surfaces for the emulsifier to adsorb to. A higher melting emulsifier e.g. behenic rich MAG, when crystallising out of solution, may establish a template structure of micro or nano crystalline material (Taylor, 2011) for new born crystal growth within the bulk TAG solvent.

The use of a highly surface-active emulsifier such as PGPR may result in a strengthened interface; so that there is mutual dependence with a co-emulsifier. It is suggested that Moringa MAG has a bi-functional role, first as co-emulsifier acting as a template for nucleation (5.2; 5.3; 5.5; 5.6) and secondly high surface activity (4.0).

5.8.4 Conclusions

As part of a multidisciplinary approach a series of measurements (5.2; 5.3; 5.4; 5.5; 5.6; 5.7) have attempted to quantify the potential bi-functional effects of a novel monoglyceride based on *Moringa oleifera* TAG (Table 5.8.4) compared with PGPR. Results have already distinguished by application tests, a comparison of a behenic based (CRY110) MAG (5.7), *Moringa oleifera* based MAG and now PGPR in low TAG W/O emulsion systems.

PGPR as a single emulsifier results in relatively increased volume of water droplet size, when compared to *Moringa oleifera* based MAG (~91% mono). Crucially, the DSD, sensory and abuse test showed the use of PGPR as a single emulsifier in a low TAG W/O (40%) emulsion to be severely inadequate towards stability between concentrations of 0.15% and 0.3%.

5.9 The Performance of Varying Distillations of Moringa MAG in Low TAG W/O (40%) Emulsions

5.9.1 Introduction

Previously, the use of fully distilled Moringa MAG 191, from *Moringa oleifera* TAG has been studied for high (60%) and low (40%) TAG W/O emulsion systems (5.4). The purpose of this study was to examine the behaviour of previously untested partially distilled Moringa MAG 102 / 105 samples in 40% low TAG W/O emulsions (5.3) and compare the results obtained from 5.4.

5.9.2 Materials and Methods

The Moringa MAG used in this study were the same as outlined in previous work (5.3). Briefly, the fatty acid profiles of the samples of the monoglyceride from *Moringa oleifera* TAG are given in Table 5.9.1, and Table 5.9.2 shows their mono-, di-, and tri-glycerides. It should be noted here that Moringa MAG 191 (~91% mono) was not used in this particular study, because it has previously been tested, validated and documented earlier (5.4).

Table 5.9.1 Fatty acid composition of MAG based on *Moringa oleifera* TAG

Fatty acid chain length	% present
C12:0	<0.1
C14:0	0.1
C15:0	<0.1
C16:0	6.5
C16:1	1.8
C17:0	0.2
C18:0	5.8
C18:1	71.2
C18:2	1.5
C18:3	0.3
C20:0	3.4
C20:1	1.9
C20 unsaturated	0.3
C22:0	6.0
C22 unsaturated	0.2
C24:0	0.8

Table 5.9.2 Moringa (*Moringa oleifera*) based MAG: mono, di- & tri-glycerides ($^{\#}$2559/104 = 105 with antioxidant)

Analysis (%)	**2559/102**	**2559/104#**	**2472/191**
GL	0.11	1.27	0.76
Digl	0.05	0.08	0.07
FFA	0.2	0.4	0.3
Mono	53.16	82.55	91.14
Di	42.05	15.67	7.75
Tri	4.39	0.02	0
Approx mono content %	53	82	91

The sample formulation used in this work can be seen in Table 5.9.3, together with the processing parameters for the same in, Table 5.9.4.

The sample number, concentration and identification are given as follows:

Sample no.	Conc. (%)	Moringa ID.
41	0.15	Moringa 102
42	0.30	Moringa 102
43	0.60	Moringa 102
44	1.20	Moringa 102
45	0.15	Moringa 105
46	0.30	Moringa 105
47	0.60	Moringa 105
48	1.20	Moringa 105

Table 5.9.3 Formulations: low TAG W/O (40%) emulsions with *Moringa oleifera* based MAG

Ingredients in %								
Ingredient Name	**41**	**42**	**43**	**44**	**45**	**46**	**47**	**48**
Water phase								
Water (Tap)	57.300	57.300	57.300	57.300	57.300	57.300	57.300	57.300
Salt	1.000	1.000	1.000	1.000	1.000	1.000	1.000	1.000
Skimmed milk powder (MILEX 240)	0.100	0.100	0.100	0.100	0.100	0.100	0.100	0.100
GRINDSTED® LFS 560	1.500	1.500	1.500	1.500	1.500	1.500	1.500	1.500
Potassium Sorbate	0.100	0.100	0.100	0.100	0.100	0.100	0.100	0.100
Butter Flavouring 050001 T03007	0.010	0.010	0.010	0.010	0.010	0.010	0.010	0.010
Water phase total	**60.010**	**60.010**	**60.010**	**60.010**	**60.010**	**60.010**	**60.010**	**60.010**
pH	5.5	5.5	5.5	5.5	5.5	5.5	5.5	5.5
Fat phase								
Fat blend								
PK4 - INES	25.000	25.000	25.000	25.000	25.000	25.000	25.000	25.000
Rapeseed oil	75.000	75.000	75.000	75.000	75.000	75.000	75.000	75.000
Fat blend total	**100.000**	**100.000**	**100.000**	**100.000**	**100.000**	**100.000**	**100.000**	**100.000**
Other fat ingredients								
Moringa MAG102	0.150	0.300	0.600	1.200				
Moringa MAG105					0.150	0.300	0.600	1.200
2% sol. beta-carotene	0.020	0.020	0.020	0.020	0.020	0.020	0.020	0.020
Butter Flavouring 050001 T04184	0.020	0.020	0.020	0.020	0.020	0.020	0.020	0.020
Other fat ingredients total	**0.190**	**0.340**	**0.640**	**1.240**	**0.190**	**0.340**	**0.640**	**1.240**
Fat phase total	**39.990**	**39.990**	**39.990**	**39.990**	**39.990**	**39.990**	**39.990**	**39.990**
RECIPE total (calc. batchsize)	**100.000**	**100.000**	**100.000**	**100.000**	**100.000**	**100.000**	**100.000**	**100.000**

Table 5.9.4 Processing conditions for low TAG W/O emulsions

Pilot Plant								
Processing (3-tube lab perfector):	**41**	**42**	**43**	**44**	**45**	**46**	**47**	**48**
Oil phase temperature	50	50	50	50	50	50	50	50
Water phase temperature	50	50	50	50	50	50	50	50
Emulsion temperature	50	50	50	50	50	50	50	50
Centrifugal pump	Auto	Auto	Auto	Auto	Auto	Auto	Auto	Auto
Capacity high pressure pump	40	40	40	40	40	40	40	40
Cooling (NH3) tube 1:	-10	-10	-10	-10	-10	-10	-10	-10
Cooling (NH3) tube 2:	-10	-10	-10	-10	-10	-10	-10	-10
Cooling (NH3) tube 3:	-10	-10	-10	-10	-10	-10	-10	-10
Rpm tube 1:	1000	1000	1000	1000	1000	1000	1000	1000
Rpm tube 2:	1000	1000	1000	1000	1000	1000	1000	1000
Rpm tube 3:	1000	1000	1000	1000	1000	1000	1000	1000

The procedure for water droplet size distribution (DSD) analysis, confocal laser scanning microscopy (CLSM), and texture analysis were reported earlier (5.4; 5.7). Four images at two magnifications (40X and 100X) were taken respectively. The images are then reproduced (scaled) to 375 x 375 μm and 188 x 188μm. All samples are stained with FITC, stains protein green, and Nile Red, stains fat red.

5.9.3 Results and Discussion

The DSD data is given in Table 5.9.5 for samples 102 and 105, and Table 5.9.6 for comparison shows sample 191 (5.4).

Table 5.9.5 DSD data: samples 41-44 (concentration 0.15, 0.3, 0.6 and 1.2%) correspond to Moringa MAG 102, monoglyceride content ~53%; samples 45-48 (concentration 0.15, 0.3, 0.6 and 1.2%) correspond to Moringa MAG 105, monoglyceride content ~83%

Sample ID	Average/ St.dev	2.5% <µm	50% <µm	97.5% <µm	Dose wt%
41	Average	2.12	9.17	39.71	0.15
	St.dev	0.03	0.20	2.08	
42	Average	2.02	7.80	30.12	0.30
	St.dev	0.03	0.21	1.32	
43	Average	1.65	6.33	24.30	0.60
	St.dev	0.02	0.02	0.48	
44	Average	1.29	4.84	18.20	1.20
	St.dev	0.07	0.08	1.54	
45	Average	2.06	11.61	66.25	0.15
	St.dev	0.01	0.80	11.62	
46	Average	1.88	8.95	43.37	0.30
	St.dev	0.05	0.27	3.55	
47	Average	1.45	6.51	29.32	0.60
	St.dev	0.01	0.21	1.92	
48	Average	1.46	4.13	11.71	1.20
	St.dev	0.04	0.09	0.80	

Table 5.9.6 DSD: low TAG W/O (40%) spreads containing Moringa MAG 191 (monoglyceride content of ~91%)

Moringa MAG 191	2.5% <µm	50%<µm	97.5%<µm
Moringa, 0.3%	1.31	7.47	42.41
St. Dev	0.04	0.19	2.87
Moringa, 0.6%	0.95	6.04	38.56
St. Dev	0.06	0.32	6.86

5.9.3.1 Droplet Size Distribution (DSD)

Table 5.9.5 shows the DSD for Moringa 102 at 0.15, 0.30, 0.60 and 1.2% concentrations, corresponding to 97.5 % of droplet volume of 39.71, 30.12, 24.30, and 18.20μm. This shows a clear decreased DSD with increasing concentration. Similarly for Moringa 105 over the same concentrations, 97.5 % of droplet volume was 66.25, 43.37, 29.32 and 11.71μm, showing an increasing trend towards decreased DSD. These results are in good agreement with the trends shown earlier (5.3). For comparison Table 5.9.6, shows the DSD for Moringa 191 which had good stability and mouth feel properties. Noteworthy, is that the DSD for Moringa 191 (91% mono) at 0.3% and 0.6% concentrations are closer to those from Table 5.9.5 for Moringa 105 (~83% mono) than Moringa 102 (~53% mono). The DSD for Moringa 102 is smallest overall. This leads to the assumption that stability is not inherently linked only to monoglyceride content or DSD exclusively.

Figure 5.9.1 shows photographic images of the samples after preparing an abuse test of spreading arbitrary portion of the sample onto cardboard, then manually spreading backward / forward. As the concentration of the Moringa MAG increased the samples became more resilient (thicker).

Sensory comments were made for the samples which started for Moringa 102 at sample 44, working to more dilute systems. The emulsion was stable, thick and creamy, and then with subsequent dilutions proceeded to become less thick, and less creamy in mouth feel. The regression in texture continued until the lowest concentration was reached whereby the emulsion was described as uneven.

For Moringa 105, again starting at the highest concentration (sample 48), a regression was found, from a stable and thick emulsion to one that is showing clear signs of water separation, and not as thick or creamy in terms of mouth feel (sample 45). Samples 46 / 47 sat placed on a sliding scale between these (sample 45 / 48) two extremes.

5.9.3.2 CLSM

The data presented in Figures 5.9.2 and 5.9.3 show the confocal laser scanning microscopy (CLSM) images relating to Moringa MAG samples 102, and 105 respectively. Four images at magnification 40X were taken respectively. The images are then reproduced (scaled) to 375 x 375μm

In both Figures 5.9.2 and 5.9.3 it can be seen that the images corresponding to the lower dosage of the given Moringa MAG (top left) showed a much looser structure compared to the remaining images where concentration increases. This is manifested in larger DSD.

As concentrations increased, the DSD decreased, similar to results seen previously (5.4; 5.7), indicating a general increase towards stability.

Fig. 1b

Fig. 1d

Fig. 1a

Fig. 1c

Figure 5.9.1 (**1a)** Spread tests: samples 41 & 42 (Moringa MAG 102); (**1b)** 43 & 44 (Moringa MAG 102); (**1c)** 45 & 46 (Moringa MAG 105) and (**1d)** 47 & 48 (Moringa MAG 105)

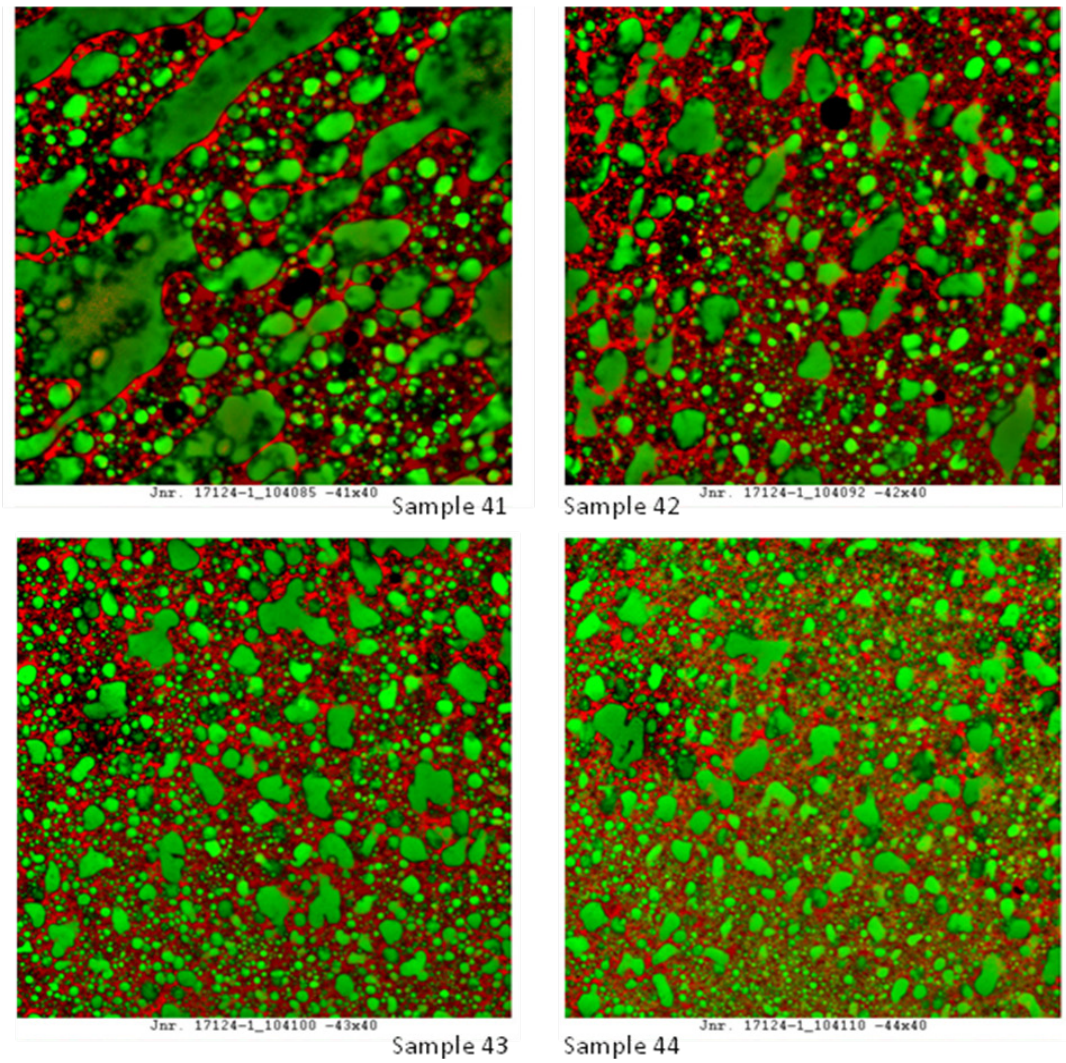

Figure 5.9.2 CLSM images, Moringa MAG 102: sample 41 (0.15%); sample 42 (0.3%); sample 43 (0.6%), and sample 44 (1.2%) (scaled to 375 x 375µm)

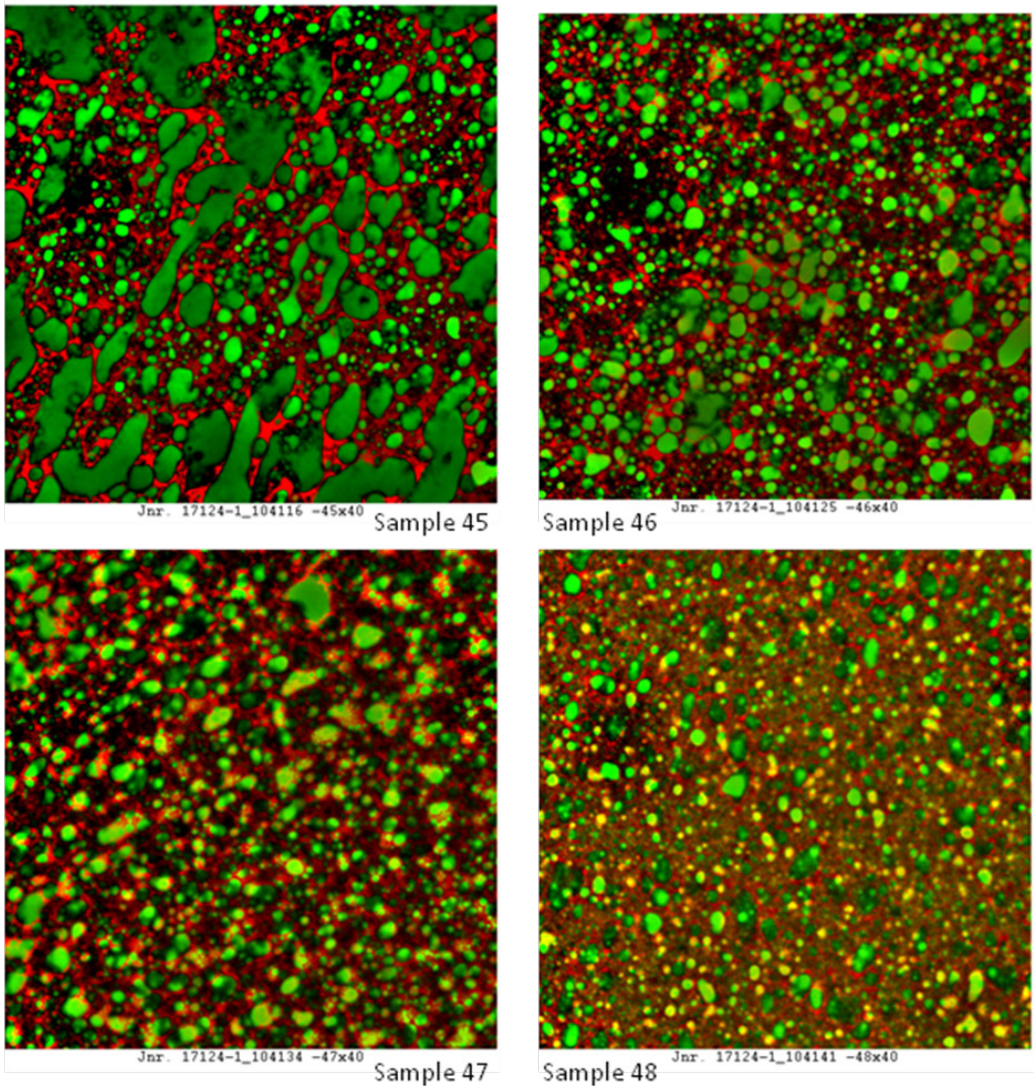

Figure 5.9.3 CLSM images, Moringa MAG 105: sample 45 (0.15%); sample 46 (0.3%); sample 47 (0.6%), and sample 48 (1.2%) (scaled to 375 x 375µm)

5.9.3.3 Texture Analysis

Texture analysis results on hardness are presented in Figure 5.9.4, and show a general reduction in hardness as the concentration of either Moringa MAG 102 or 105 increases.

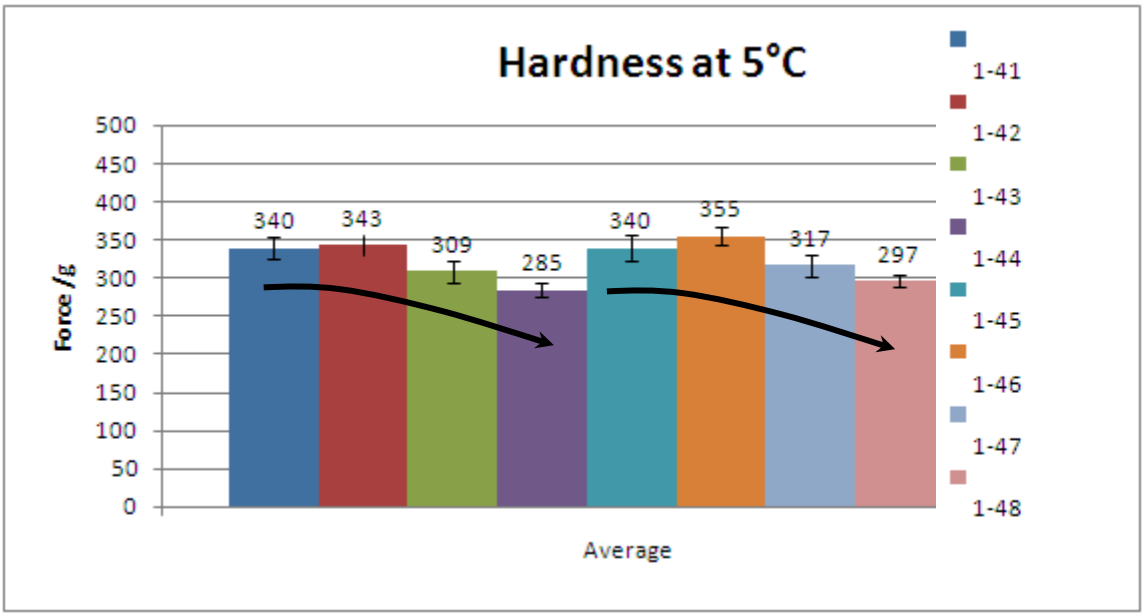

Figure 5.9.4 Texture analysis: hardness profile for Moringa MAG 102 emulsions (41-44) and Moringa MAG 105 emulsions (45-48), at 5°C

There appeared to be a slight increase in firmness occurring from 0.15% until reaching 0.3%, then decline. Whereas, with an increased Moringa MAG concentration of 1.2% (samples 44 and 48), there was a general decrease in firmness. This occurred from a concentration of 0.3% (samples 42 and 46). These results are in agreement with textural data reported previously (5.4), where textural hardness results were very similar.

The outcome of this study was to test the integrity of W/O low TAG emulsion spreads; which was shown to be positive when using natural Moringa MAG with lower mono % contents. Generally, the results have confirmed acceptable stability.

Next would be to ascertain if an earlier study (5.3) where synthetic Moringa MAG were tested, would have any correspondence to the degree of final mono % shown in resulting samples produced with Moringa (*Moringa oleifera* TAG) based MAG distillations in this work.

5.9.4 Conclusion

When compared to natural Moringa MAG with lower mono contents, it is generally concluded from combined DSD analysis that smaller water droplets resulted as the *Moringa oleifera* based MAG concentration increased. CLSM, texture analysis, photographic images, combined with the effects of abuse tests, showed positive emulsion stability.

In comparison to a fully distilled *Moringa oleifera* based MAG (191) tested earlier (5.4), this work concludes that low TAG W/O emulsion spreads made with a *Moringa oleifera* based MAG with mono contents of 53.16% and 82.55%, are equally capable of producing commercially viable low TAG W/O emulsions.

5.10 Blended MAG compositions to Equal Moringa Based MAG in Low TAG W/O Emulsions

5.10.1 Introduction

Previous studies have shown the use of Moringa MAG (based on *Moringa oleifera* TAG) in low TAG W/O emulsion systems with natural distillations (5.4; 5.9) and comparisons have been made to a specific MAG identified as being characterised rich in C22:0 (5.7). Natural Moringa MAG contains in total ~10% of the three saturated fatty acids: C20:0 + C22:0 + C24:0. The aim of this study was to assess the effect blended commercial MAG compositions to reproduce a synthetic version of natural Moringa MAG. The natural Moringa MAG samples were made from base *Moringa oleifera* TAG as a raw material to give MAG as outlined previously (5.3).

5.10.2 Materials and Methods

MAG were blended to contain specific amounts of a behenic based monoglyceride (GRINDSTED® Crystallizer 110), which has been established as a critical component of the total fatty acids of Moringa MAG (4.0; 5.3; 5.4; 5.5; 5.6; 5.7; 5.9). The blending ratios and other compositional details for mimicking natural Moringa MAG are given in Tables 5.10.1 – 5.10.3. In this examination the same MAG blends (synthetic samples) were assembled as shown previously (5.3).

Table 5.10.1 Blending ratios for synthetic MAG

	SM 90*	SM 60**	SM 80***
GRINDSTED® CRYSTALLISER 110	10	10	10
DIMODAN RT	90		50
GRINDSTED® Mono-di PR40		90	40
Total %	100	100	100
Mono (approximate %)	* 96	** 64	*** 82

Table 5.10.2 Fatty acid composition of synthetic MAG

Fatty acid (%)	(SM 90)	(SM 60)	(SM 80)
C10:0	<0.1	0.0	0.0
C12:0	0.1	0.1	0.1
C14:0	0.1	0.5	0.3
C15:0	<0.1	<0.1	<0.1
C16:0	5.3	21.5	12.7
C16:1	0.1	0.1	0.2
C17:0	0.1	0.1	0.1
C18:0	10.9	4.1	7.8
C18:1	64.6	23.9	47.6
C18:2	5.2	10.8	7.7
C18:3	0.0	3.8	2.0
C20:0	1.3	1.0	1.0
C20:1	1.4	2.6	1.8
C20:unsaturated	0.1	0.9	0.7
C22:0	10.7	8.8	7.2
C22:1	0.0	20.7	10.0
C22:unsaturated	0.0	0.8	0.4
C24:0	0.3	0.3	0.3
C24:1	0.0	0.4	0.2

Table 5.10.3 Total distribution of natural Moringa MAG saturated, unsaturated fatty acids in relation to synthetic MAG and actual total saturated chain length from C20:0

Distribution of SAT / un-SAT chain length (%)	Moringa MAG 191	SM90	SM60	SM80
Saturated	22.7	28.6	36.3	29.4
unsaturated	77.2	71.4	63.6	70.6
Total	100 ± 0.1	100 ± 0.1	100 ± 0.1	100 ± 0.1
SATs from C20:0 >	10.2	12.3	10.1	8.5

Table 5.10.4 Formulations for 40% low TAG emulsions with synthetic MAG (SM90 SM60)

Ingredients in %								
Ingredient Name	**31**	**32**	**33**	**34**	**35**	**36**	**37**	**38**
Water phase								
Water (Tap)	57.300	57.300	57.300	57.300	57.300	57.300	57.300	57.300
Salt (Sodium Chloride)	1.000	1.000	1.000	1.000	1.000	1.000	1.000	1.000
Skimmed milk powder (MILEX 240)	0.100	0.100	0.100	0.100	0.100	0.100	0.100	0.100
GRINDSTED® LFS 560 Stabiliser System	1.500	1.500	1.500	1.500	1.500	1.500	1.500	1.500
Potassium Sorbate	0.100	0.100	0.100	0.100	0.100	0.100	0.100	0.100
Butter Flavouring 507104 A	0.010	0.010	0.010	0.010	0.010	0.010	0.010	0.010
Water phase total	**60.010**	**60.010**	**60.010**	**60.010**	**60.010**	**60.010**	**60.010**	**60.010**
pH	5.5	5.5	5.5	5.5	5.5	5.5	5.5	5.5
Fat phase								
Fat blend								
PK4 - INES	25.000	25.000	25.000	25.000	25.000	25.000	25.000	25.000
COLZAO (Rapeseed Oil)	75.000	75.000	75.000	75.000	75.000	75.000	75.000	75.000
Fat blend total	**100.000**	**100.000**	**100.000**	**100.000**	**100.000**	**100.000**	**100.000**	**100.000**
Other fat ingredients								
Synthetic Moringa – 1 **(SM90)**	0.150	0.300	0.600	1.200				
Synthetic Moringa – 2 **(SM60)**					0.150	0.300	0.600	1.200
2% sol. beta-carotene	0.020	0.020	0.020	0.020	0.020	0.020	0.020	0.020
Butter Flavouring 050001 T04184	0.020	0.020	0.020	0.020	0.020	0.020	0.020	0.020
Other fat ingredients total	**0.190**	**0.340**	**0.640**	**1.240**	**0.190**	**0.340**	**0.640**	**1.240**
Fat phase total	**39.990**	**39.990**	**39.990**	**39.990**	**39.990**	**39.990**	**39.990**	**39.990**
RECIPE total (calc. batchsize)	**100.000**	**100.000**	**100.000**	**100.000**	**100.000**	**100.000**	**100.000**	**100.000**

Table 5.10.5 40% low TAG emulsions with synthetic MAG (SM80)

Ingredients in %				
Ingredient Name	**49**	**51**	**52**	**53**
Water phase				
Water (Tap)	57.300	57.300	57.300	57.300
Salt (Sodium Chloride)	1.000	1.000	1.000	1.000
Skimmed milk powder (MILEX 240)	0.100	0.100	0.100	0.100
GRINDSTED® LFS 560 Stabiliser System	1.500	1.500	1.500	1.500
Potassium Sorbate	0.100	0.100	0.100	0.100
Butter Flavouring 050001 T03007	0.010	0.010	0.010	0.010
Water phase total	**60.010**	**60.010**	**60.010**	**60.010**
pH	5.5	5.5	5.5	5.5
Fat phase				
Fat blend				
PK4 - INES	25.000	25.000	25.000	25.000
COLZAO (Rapeseed Oil)	75.000	75.000	75.000	75.000
Fat blend total	**100.000**	**100.000**	**100.000**	**100.000**
Other fat ingredients				
Synthetic Moringa – 3 **(SM80)**	0.150	0.300	0.600	1.200
2% sol. beta-carotene	0.020	0.020	0.020	0.020
Butter Flavouring 050001 T04184	0.020	0.020	0.020	0.020
Other fat ingredients total	**0.190**	**0.340**	**0.640**	**1.240**
Fat phase total	**39.990**	**39.990**	**39.990**	**39.990**
RECIPE total (calc. batchsize)	**100.000**	**100.000**	**100.000**	**100.000**

Refer to General Materials & Methods (2.0) for emulsion assembly procedure. The processing conditions on the plant for all samples are given in Table 5.10.6.

Table 5.10.6 Pilot plant scraped surface processing conditions for all samples

Processing (3-tube lab perfector):	
Oil phase temperature	50
Water phase temperature	50
Emulsion temperature	50
Centrifugal pump	Auto
Capacity high pressure pump	40
Cooling (NH3) tube 1:	-10
Cooling (NH3) tube 2:	-10
Cooling (NH3) tube 3:	-10
Rpm tube 1:	1000
Rpm tube 2:	1000
Rpm tube 3:	1000

Analytical measurements, DSD, CLSM and texture analysis were carried out as described earlier (2.0; 5.4).

5.10.3 Results and Discussion

The results for DSD are shown in Table 5.10.7.

Table 5.10.7 DSD data for SM 90 (samples 31-34), SM60 (samples 35-38), and SM80 (samples 49-53)

Sample ID	Average/ St.dev	2.5% <μm	50% <μm	97.5% <μm	Dose wt%
31	Average	1.33	5.19	20.22	0.15
	St.dev	0.03	0.07	0.94	
32	Average	1.31	4.39	14.70	0.30
	St.dev	0.05	0.02	0.60	
33	Average	1.38	3.95	11.34	0.60
	St.dev	0.08	0.04	0.81	
34	Average	1.33	3.73	10.56	1.20
	St.dev	0.15	0.03	1.22	
35	Average	1.61	6.32	24.75	0.15
	St.dev	0.02	0.04	0.45	
36	Average	1.48	5.52	20.51	0.30
	St.dev	0.04	0.05	0.72	
37	Average	1.36	4.34	13.90	0.60
	St.dev	0.01	0.03	0.20	
38	Average	1.90	3.52	6.53	1.20
	St.dev	0.11	0.04	0.47	
49	Average	1.72	6.50	24.58	0.15
	St.dev	0.05	0.04	1.06	
51	Average	1.47	5.33	19.37	0.30
	St.dev	0.06	0.14	1.00	
52	Average	1.39	4.27	13.12	0.60
	St.dev	0.04	0.01	0.42	
53	Average	1.72	3.42	6.81	1.20
	St.dev	0.07	0.03	0.17	

The data from Table 5.10.7 shows a trend as seen previously, where at lower synthetic MAG concentrations DSD is larger, and decreases as synthetic MAG concentration increases. The smaller the DSD led a tendency towards more stable emulsion. The mean DSD during the emulsification process was heavily dependent on emulsifier concentration. At low emulsifier concentrations, which

are possibly below the surface excess concentration, larger droplets were formed because of insufficient surface coverage, in turn leading to coalescence. Smaller droplets with increasing concentrations were formed because of sufficient surface coverage (Taylor 2011). However, other considerations must also be weighed, such as sensory, and spreadability (5.8).

While there has been attempt to control all variables, there was always "natural" process variation (with a normal distribution) from batch to batch processing conditions. From a pilot scale perspective, the natural process variation made it extremely difficult to statistically validate because the pilot plant setup for the studies in this work and others (5.4; 5.7; 5.9) was exclusively setup for this product specification. However, where there were anomalies, these have been mentioned.

The DSD data showed all synthetic (SM 90 / 60 / 80) MAG concentrations were considerably lower than the corresponding natural Moringa MAG reported earlier at the 0.3% and 0.6% emulsifier load. This immediately suggests that the synthetic MAG at 0.3 / 0.6% gave tighter structures (5.4; 5.7). For ease of comparison the DSD from previous tests of Moringa MAG at 0.15 0.3, 0.6, 1.2%, are shown in Tables 5.10.8 and 5.10.9. As previously mentioned, the anomaly, may possibly have been attributed to batch to batch variation.

Table 5.10.8 DSD data for 40% TAG spread samples containing natural Moringa MAG 191 monoglyceride ~91% (from Table 5.4.8 in: 5.4; and Table 5.7.5 in: 5.7)

Moringa MAG 191	2.5% <µm	50%<µm	97.5%<µm	Dose wt%
Average	1.08	5.38	26.80	0.15
St. Dev	0.02	0.07	0.54	
Average	1.31	7.47	42.41	0.3
St. Dev	0.04	0.19	2.87	
Average	0.95	6.04	38.56	0.6
St. Dev	0.06	0.32	6.86	
Average	2.01	3.64	6.58	1.2
St. Dev	0.09	0.02	0.36	

Table 5.10.9 DSD data from 5.9 shows: samples 41-44 (conc. 0.15, 0.3, 0.6, 1.2%) correspond to Moringa MAG 102 (mono 53%); and samples 45-48 (conc. 0.15, 0.3, 0.6, 1.2%) correspond to Moringa MAG 105 (mono 83%)

Sample ID	Average/ St.dev	2.5% <µm	50% <µm	97.5% <µm	Dose wt%
41	Average	2.12	9.17	39.71	0.15
	St.dev	0.03	0.20	2.08	
42	Average	2.02	7.80	30.12	0.30
	St.dev	0.03	0.21	1.32	
43	Average	1.65	6.33	24.30	0.60
	St.dev	0.02	0.02	0.48	
44	Average	1.29	4.84	18.20	1.20
	St.dev	0.07	0.08	1.54	
45	Average	2.06	11.61	66.25	0.15
	St.dev	0.01	0.80	11.62	
46	Average	1.88	8.95	43.37	0.30
	St.dev	0.05	0.27	3.55	
47	Average	1.45	6.51	29.32	0.60
	St.dev	0.01	0.21	1.92	
48	Average	1.46	4.13	11.71	1.20
	St.dev	0.04	0.09	0.80	

It was observed that SM90 (31-34) where the monoglyceride content was highest (96.50%) was not the sample resulting with the smallest water droplet size at 1.2% concentration, as may have been expected. The high concentrations of SM60 and SM80 with monoglyceride contents of ~64%, and ~82% respectively were lower and similar to each other. This seems to suggest that the monoglyceride / diglyceride content of the synthetic blended MAG may play a more specific role in adjusting water droplet size than was previously thought.

Also to consider is that DSD is not the only determining factor to confirm a stabilised emulsion; the interfacial film thickness and strength are likely also important considerations. This aspect has shown the importance of interfacial tension and visco-elastic behaviour especially, in conjunction with combined emulsifiers (4.0) e.g GRINDSTED® Crystallizer 110 (CRY110) and GRINDSTED® PGPR90 (PGPR). It was shown previously (5.6) that Moringa MAG (191), has similar viscous profiles to PGPR and yet these two emulsifiers could not be more molecularly dissimilar, given that monoglycerides are low molecular weight, compared to the high molecular weight PGPR.

Application tests have characterised and made distinction between a behenic based MAG (CRY110) and Moringa MAG and have shown a behenic rich C22:0 ~89%) MAG is not conducive to stabilised W/O low TAG emulsions (5.7).

The strong water binding properties of PGPR are also well known (Claesson et al, 1997; Garti & Remon 1984; Marze, 2009; Dedinaite & Campbell, 2000; Rousseau, 2000). Application tests have shown that PGPR used alone in low TAG W/O emulsions, resulted in relatively increased volume of water droplet size, when compared to the natural Moringa MAG (5.8)

How does Moringa MAG work at the interface? Fatty acid compositions showed (Tables 5.10.2 and 5.10.3) that the synthetic MAG have roughly 8.5 – 12.3% of their saturation starting from C20:0. Importantly, for the natural Moringa MAG, diversity exists from the same fatty acid chain length (C20:0) and there is a significant proportion of C22:0 and C24:0 as seen in Table 5.10.2 (also detected

C26:0, but not shown). Whereas, within the same spectrum, CRY110 (5.7) and synthetic MAG are mainly centred at the C22:0 chain length. Another distinction is that natural Moringa MAG also contain lower chain (C16:0 and C18:0) and a high degree of unsaturated fatty acids (~72%). Given the complexity of the natural Moringa MAG fatty acid profile it was not possible within the scope of this examination to precisely mimic this fatty acid range exactly for the synthetic MAG.

Factors such as resilience / abuse (cardboard test) and compression (texture test) must also be considered.

5.10.3.1 Spread Test

The next test looked at integrity of the samples by way of a physical spreading (abuse) test. The results of which are shown in Figure 5.10.1. The samples were spread out manually onto a piece of cardboard using a regular kitchen knife. The use of cardboard is designed to mimic a surface offering resistance e.g bread / toast and the tongue to a certain degree, i.e. the cardboard although smooth is a roughened surface (specification not known). The spreading action gives a better representation than would be the case for spreading on plastic, glass or steel. Together with the spread tests, sensory evaluation of the sample was also completed. These results can be summarised as follows:

SM90 with monoglyceride ~96% (samples 31-33) had acceptable structure, a thick and creamy mouth feel and acceptable in the mouth melt profile, indicating good flavour release. SM 90 sample 34 gave an acceptable emulsion, but the mouth feel was not as smooth or creamy, and the melt profile was slower. This is at high concentration – 1.2%.

SM60 with monoglyceride 64.56% (sample 35) gave an acceptable emulsion, but was duller in appearance, though creamy as the preceding samples (SM90 31-33), but the in mouth melt profile was poorer. SM60 sample 36 gave a better emulsion

and was creamy and thicker than SM60 sample 35. SM60 sample 37 gave a good thick emulsion and was creamy and thick in the mouth feel. SM60 sample 38 gave a thick emulsion was creamy and thick to taste, but showed a slow melting profile. Likely this was again attributed to high concentration 1.2%.

SM80 with monoglyceride ~82% (sample 49) gave a good emulsion and was thick and creamy to taste. SM80 sample 51 gave a good shiny emulsion, was thick, but not as creamy as SM80 sample 49. SM80 sample 52 gave an acceptable thick emulsion with a creamy taste. SM80 sample 53 gave a very thick emulsion, with an equally thick mouth feel, and poor flavour release, once again attributed to high concentration 1.2%.

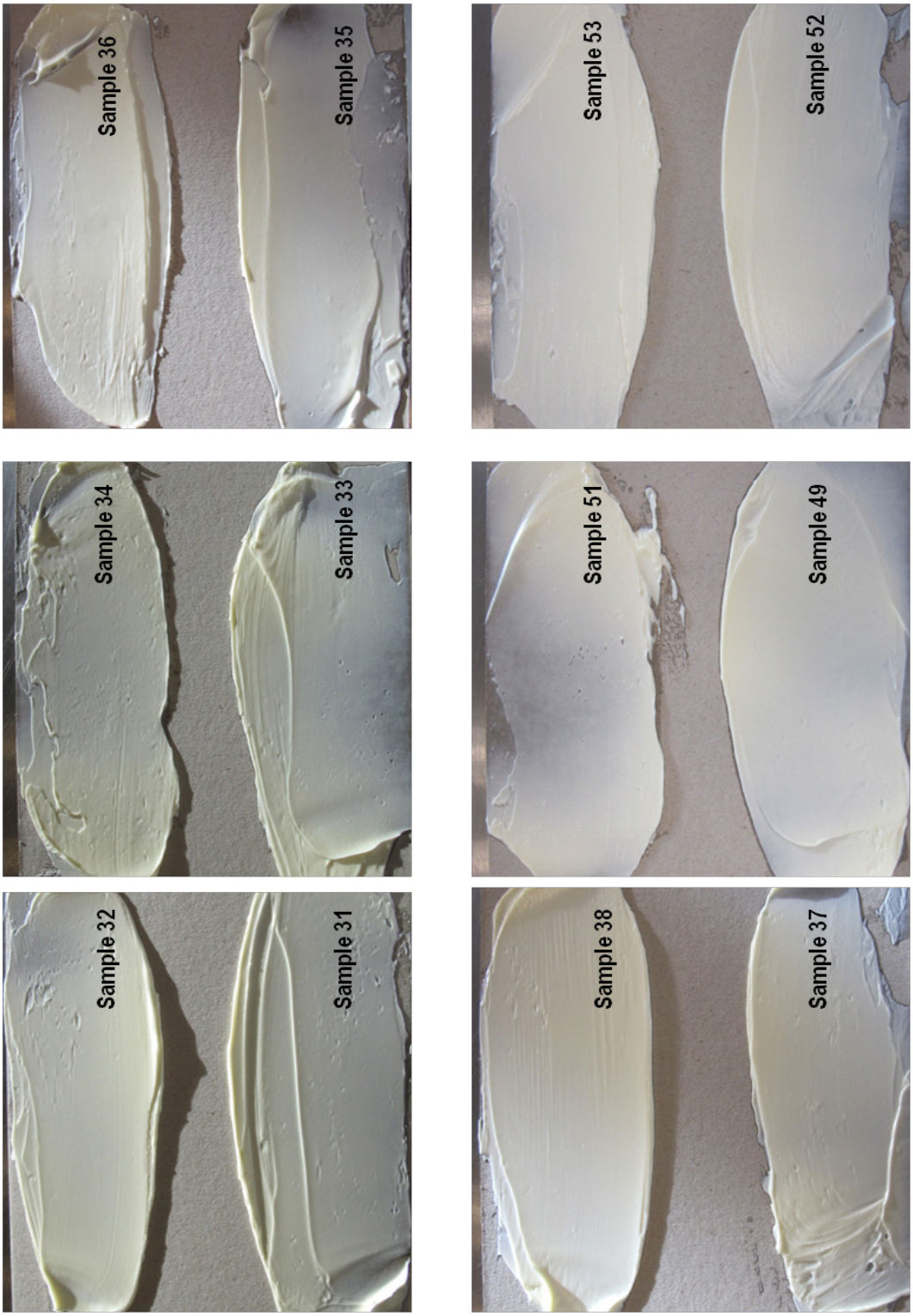

Figure 5.10.1 Photographic evidence of spread testing of the synthetic MAG 31-34 (SM90); 35-38 (SM60); and 49, 51-53 (SM80)

As is seen from the sensory results and images in Figure 5.10.1, an increase in concentration of the synthetic Moringa MAG generally leads to greater emulsion stability, but eventually at a concentration between 0.6% and 1.2%, mouth feel and the flavour release became poor. It was also interesting to compare back to the natural Moringa MAG spreads described earlier (5.9) to note that as the concentration of the natural Moringa MAG samples increased, there was not the same consistent comment regarding poor flavour release despite the concomitant increase in emulsion stability. This suggests the synthetic MAG have different interfacial film behaviour and are interfacially active according to a different mechanism when compared directly to the natural Moringa MAG. This aspect has been shown through tensiometry measurements (method as before: 2.0; 4.0), whereby natural Moringa MAG (191) was similar to, or more surface active (lower tension), than synthetic equivalents as shown in Figure 5.10.2.

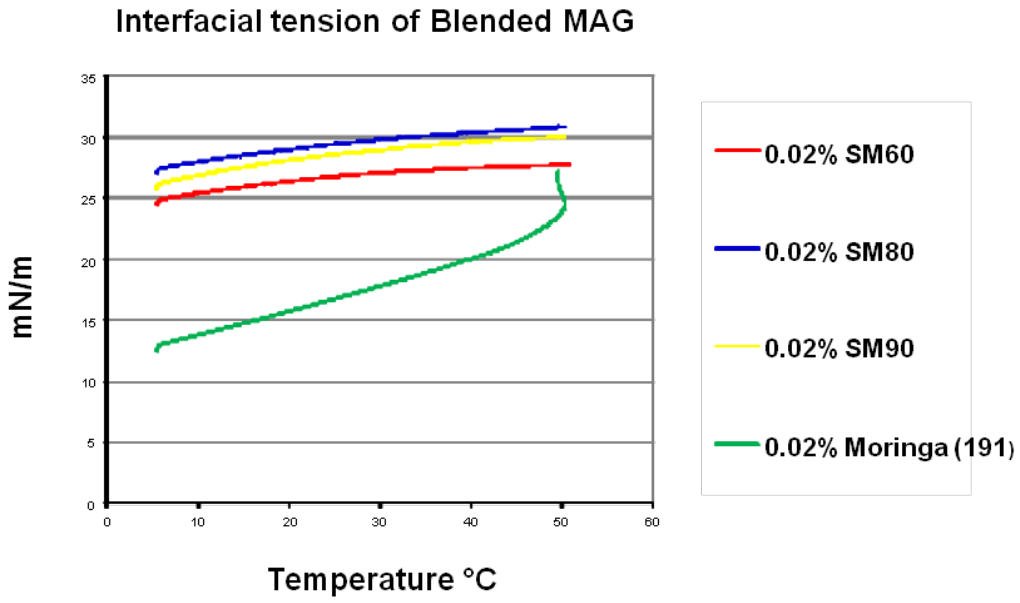

Figure 5.10.2 Interfacial tension behaviour of blended synthetic MAG to mimic natural Moringa MAG

It is important to note that where measured and studied, the viscosity (G'') and elastic (G') modulus of several fatty acid variations of commercial MAG, showed that only behenic rich (CRY110) and mixtures of the same blended together with

other MAG, resulted in development of both G'' / G' in samples (4.0). All three synthetic MAG (SM90, SM80, SM60) contained a minimum of ~7.2% behenic contribution from CRY110 (see Table 5.10.2). Interfacial tension measurements shown throughout this work have also shown CRY110 is highly surface active at ~<20°C, within the final exit temperature (packing T°C) of the W/O emulsions (Bech et al., 2013).

5.10.3.2 CLSM

Figures 5.10.3 to 5.10.5 show confocal laser scanning microscopy (CLSM) images, which are consistent with the DSD results shown in Table 5.10.9. Images are scaled to 375 x 375 µm (unless otherwise indicated). All samples were stained with FITC, stains protein green, and Nile Red stains fat red.

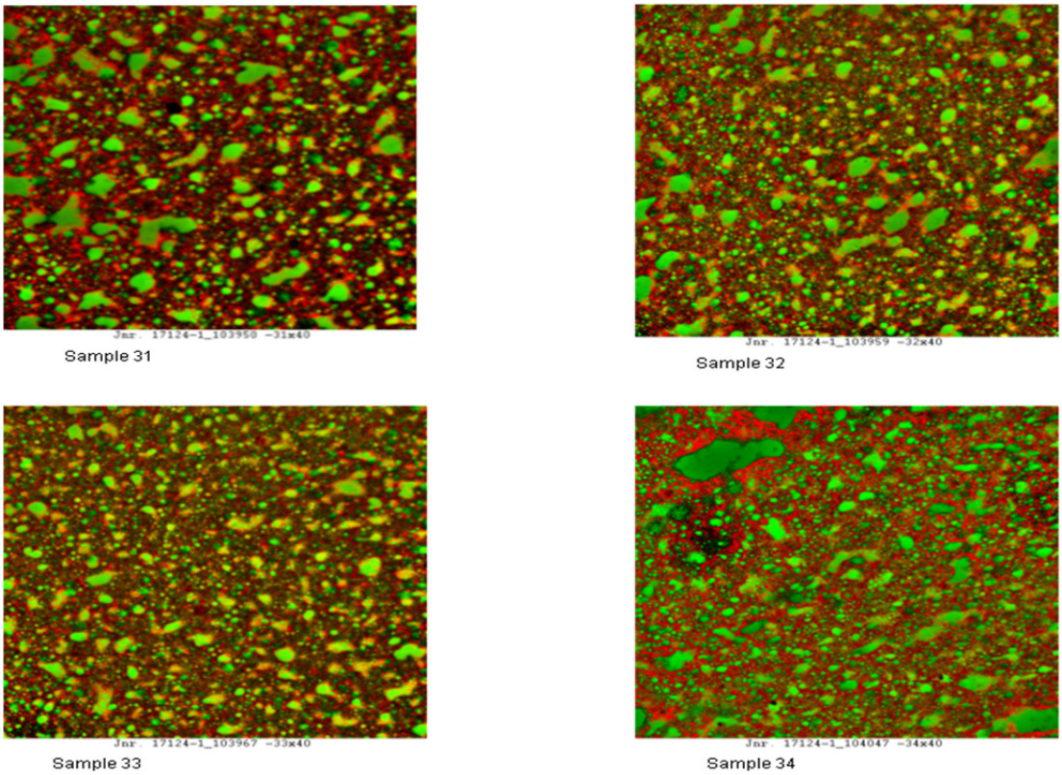

Figure 5.10.3 CLSM images of synthetic MAG (SM90) mono content ~96%, samples 31, 32, 33, & 34, of concentration 0.15, 0.3, 0.6 & 1.2% respectively

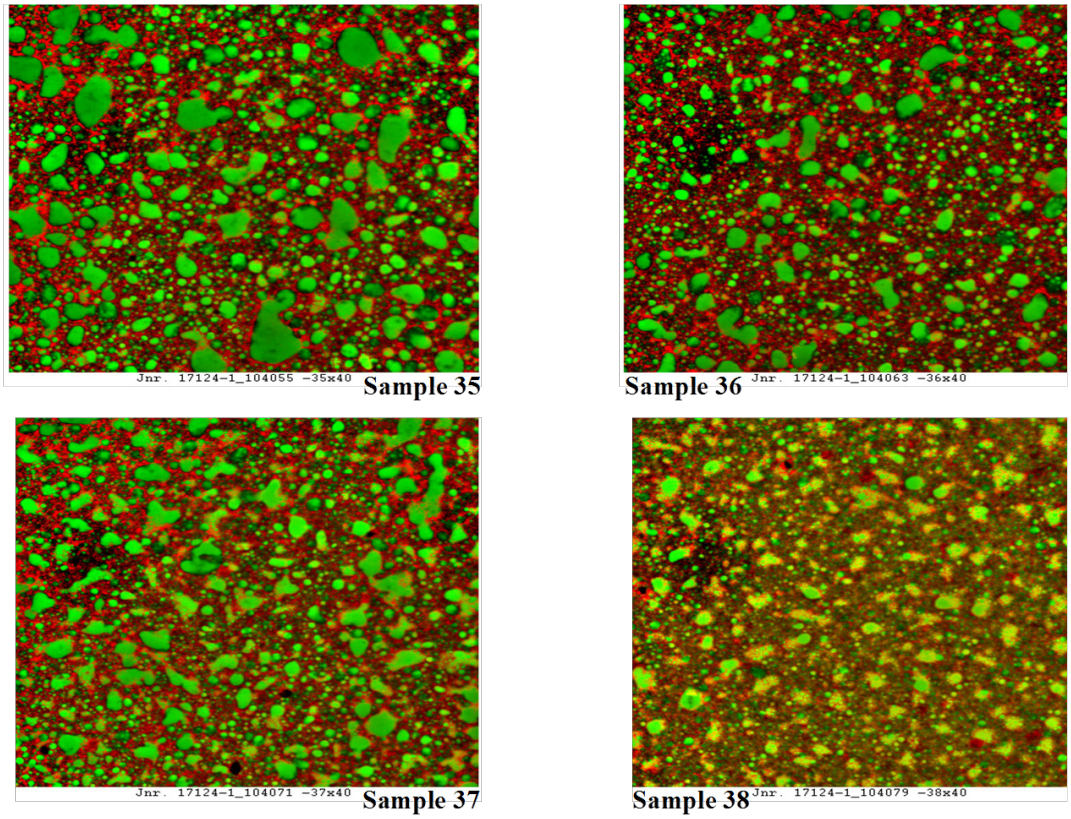

Figure 5.10.4 CLSM images of synthetic MAG (SM60), mono content ~64%, samples 35, 36, 37, & 38, of concentration 0.15, 0.3, 0.6 & 1.2% respectively

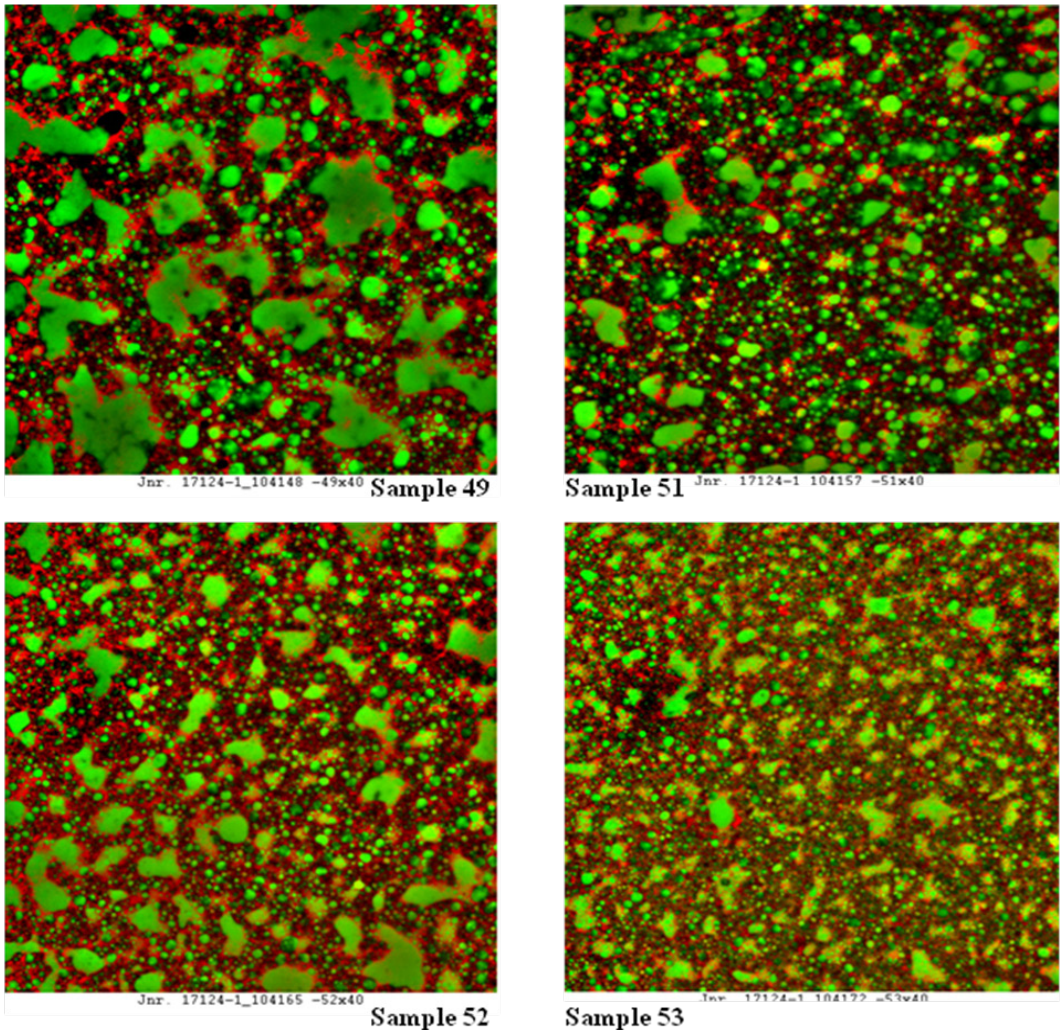

Figure 5.10.5 CLSM images of synthetic MAG (SM80) mono content ~82%, samples 49, 51, 52, & 53, of concentration 0.15, 0.3, 0.6 & 1.2% respectively

5.10.3.3 Texture Analysis

Texture analysis data is presented in Figure 5.10.6 and 5.10.7.

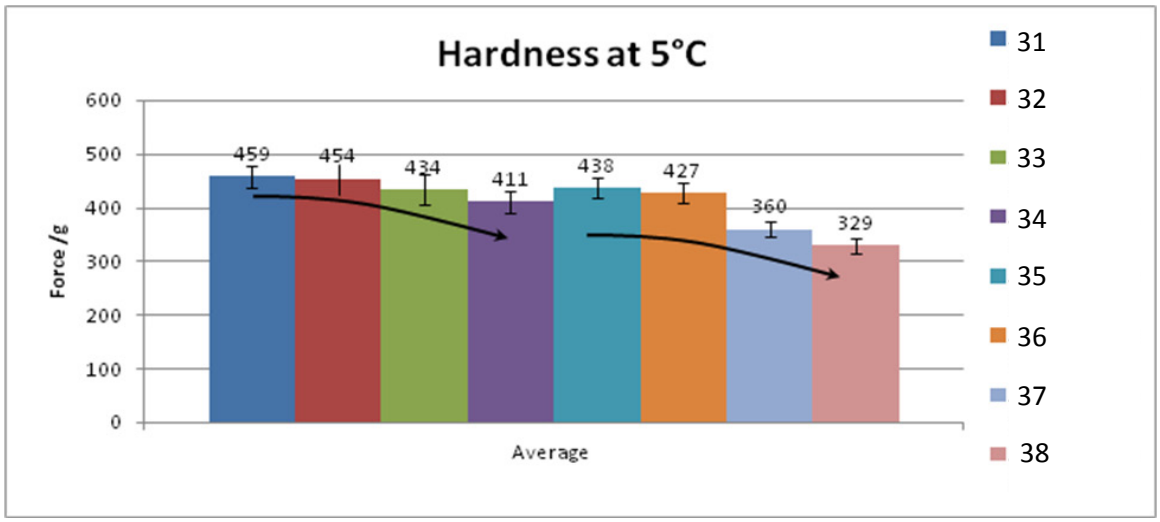

Figure 5.10.6 Hardness results from texture analyser for synthetic SM90 (31 to 34) and synthetic SM60 (35 to 38)

Figure 5.10.6 shows textural hardness data for synthetic MAG (SM90 / SM60) with mono contents of ~96% and ~64 respectively, which broadly agree with findings in previous work (5.9). The hardness values decreased as the concentration of the Moringa MAG increased, and the same was observed with synthetic MAG. The hardness values themselves were greater for the synthetic MAG than was the case for the natural Moringa MAG described earlier by between 50 to 100g (5.9).

Figure 5.10.7 shows synthetic MAG (SM80) with a mono content of ~82%, which did not correlate with decreasing hardness with increasing emulsifier concentration. The hardness values were still more than the values for the corresponding natural Moringa MAG. This is likely explained by the ratio of saturated fatty acids to unsaturated. The natural Moringa MAG have a higher degree of unsaturation, hence softer, which is known to have proven advantages for manufacture of low TAG W/O emulsion spreads (1.2.6; 1.5; 1.6).

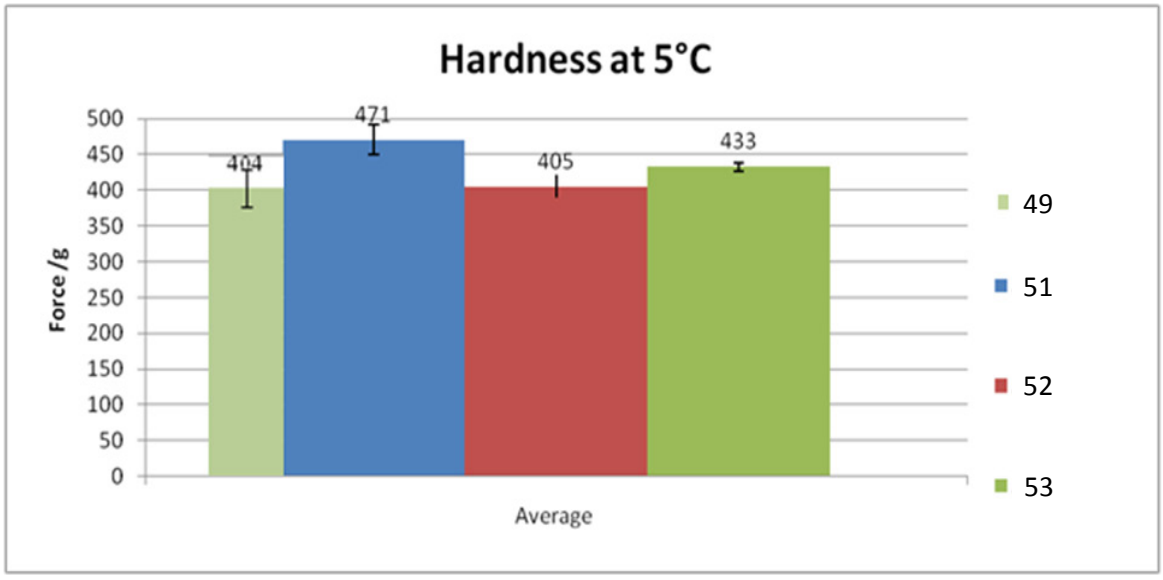

Figure 5.10.7 Hardness results from texture analyser for synthetic SM80 (49, 51, 52 & 53)

Where the synthetic MAG have been blended to mimic the natural, non-hydrogenated Moringa MAG samples, the same diversity of long chain fatty acids (>C22:0) is not viable because of availability and hence price prohibitive. Therefore, synthetic samples are essentially based on the fully hydrogenated CRY110. From a commercial perspective there is implication; synthetic MAG are able to produce firmer spreads, which have a smaller average water droplet size than natural Moringa MAG. Whereas the natural non-hydrogenated MAG samples may result in a softer, creamier mouth feel, whilst maintaining interfacial film strength and which can fulfil re-work / re-melt requirements.

5.10.4 Conclusion

These results show that a synthetic MAG composition is capable of producing commercially viable spreads, which are firmer than their naturally based (*Moringa oleifera* TAG) Moringa MAG counterparts. By mimicking the fatty acid profile of *Moringa oleifera* based MAG, it was possible to produce W/O low TAG emulsions which have similar physical properties (Bech et al., 2013) to those made using a MAG based on *Moringa oleifera* TAG.

5.11 Effect of High and Low Temperature Distillation on the Functionality of MAG based on *Moringa oleifera* TAG in Low TAG W/O Emulsions

5.11.1 Introduction

In earlier studies covering the use of a Moringa Monoglyceride (Moringa MAG), questions were raised as to why a Moringa MAG might function, given its interfacial behaviour (4.0). The first approach in answering this question is thought to be linked to its fatty acid composition. A comprehensive comparison of natural Moringa MAG (5.4; 5.9) with a series of blended synthetic MAG (5.3; 5.10), results in approximately 8.5 – 12.3% of saturated fatty acids centring from C20:0. Natural Moringa MAG starts from the same fatty acid (C20:0) but with more significant amounts of C22:0 and C24:0 (C26:0 detected but not shown). Whereas, with the blended (synthetic) MAG (5.7; 5.10), its fatty acid spectrum is primarily based on a C22:0 rich MAG (CRY110), this being the primary component.

Another distinction is that natural Moringa MAG also contain other fully saturated fatty acids of shorter chain lengths (C16:0 and C18:0) and a high degree of unsaturated fatty acids (~72%). Given the complexity of the natural Moringa MAG fatty acid profile it is was not possible within the scope of previous examination (5.10), to precisely mimic its fatty acid range exactly (5.6 – 5.10).

The distillation process used to synthesise Moringa MAG from the raw TAG material was carried out at an unusually higher temperature than normal, because distillation at high temperature preserves a wider spectrum of fatty acids of different chain lengths, as high as plus C24:0, thereby resembling the natural fatty acid profile of the original TAG composition. However, could the same functional properties be achieved from a Moringa MAG when distilled at a lower, normal distillation temperature?

The aim of this study was to investigate two samples of Moringa MAG, distilled at two temperatures, 210°C and 185°C respectively, and to test if functional

differences are apparent. The resultant Moringa MAG were tested in W/O low TAG emulsions (40% and 35% TAG), at similar process conditions described earlier (5.4, 5.7 – 5.10).

5.11.2 Materials and Methods

The emulsions were made in general accordance to the principles outlined in previous work (5.4), and the exact recipe conditions and plant processing conditions are given in Tables 5.11.1 and 5.11.2. Details of the distillation process conditions are outlined in Wassell et al. (2012a; 2012b; 2012c; 2012d; 2012e) and Bech et al. (2013). Also refer to General Materials & Methods (2.0).

Water DSD was carried out using a Bruker Minispec NMS (20MHz) according to the standard method (outlined in Materials & Methods 2.0). Texture analysis was carried out using a TA-XT2i texture analyser from Stable Micro Systems. Visual evaluation of the emulsions was carried out after 16 weeks storage at 5°C, by spreading with a typical kitchen table knife onto cardboard (abuse test), and the results photographed. The W/O emulsions were evaluated by an expert sensory panel, for texture / mouth feel and flavour release parameters. Table 5.11.3 gives the fatty acid profile of the high (210°C) and low (185°C) temperature distillations for two Moringa MAG distillations from *Moringa oleifera* TAG (see 2.0):

Sample 2559/132 (87% Monoglyceride – high temperature distillation 210°C).
Sample 2559/134 (97% Monoglyceride – low temperature distillation 185°C).

Table 5.11.1 Formulations for 35% and 40% TAG emulsions using two Moringa MAG distillations: sample 2559/132 (87% Monoglyceride - high temperature distillation 210°C) and sample 2559/134 (97% Monoglyceride – low temperature distillation 185°C)

Ingredients in %								
Ingredient Name	**71**	**72**	**73**	**74**	**75**	**76**	**77**	**78**
Water phase								
Water (Tap)	57.300	57.300	57.300	57.300	64.000	64.000	64.000	64.000
Salt	1.000	1.000	1.000	1.000	1.000	1.000	1.000	1.000
Skimmed milk powder (MILEX 240)	0.100	0.100	0.100	0.100				
GRINDSTED® LFS 560	1.500	1.500	1.500	1.500				
Potassium Sorbate	0.100	0.100	0.100	0.100				
Butter Flavouring 507104 A	0.010	0.010	0.010	0.010	0.010	0.010	0.010	0.010
Water phase total	**60.010**	**60.010**	**60.010**	**60.010**	**65.010**	**65.010**	**65.010**	**65.010**
pH	5.5	5.5	5.5	5.5	5.5	5.5	5.5	5.5
Fat phase								
Fat blend								
PK4 - INES	25.000	25.000	25.000	25.000	25.000	25.000	25.000	25.000
Rapeseed oil	75.000	75.000	75.000	75.000	75.000	75.000	75.000	75.000
Fat blend total	**100.000**	**100.000**	**100.000**	**100.000**	**100.000**	**100.000**	**100.000**	**100.000**
Other fat ingredients								
87% Monoglyceride (Moringa oil), 2559/132	0.300		0.600		0.300		0.600	
97% Monoglyceride (Moringa oil), 2559/134		0.300		0.600		0.300		0.600
Butter Flavouring 050001 T04184	0.020	0.020	0.020	0.020	0.020	0.020	0.020	0.020
Other fat ingredients total	**0.320**	**0.320**	**0.620**	**0.620**	**0.320**	**0.320**	**0.620**	**0.620**
Fat phase total	**39.990**	**39.990**	**39.990**	**39.990**	**34.990**	**34.990**	**34.990**	**34.990**
RECIPE total (calc. batchsize)	**100.000**	**100.000**	**100.000**	**100.000**	**100.000**	**100.000**	**100.000**	**100.000**

Table 5.11.2 Processing conditions for 35% and 40% TAG W/O emulsions

Journal No.	17124-1-71							
Date	12-04-2011							
Sample No.	71	72	73	74	75	76	77	78
Time	10:25	10:32	10:39	10:45	10:53	11:03	11:13	11:21
Log	---	---	---	---	---	---	---	---
Pump capacity (kg)	42,00	42,00	42,00	42,00	42,00	42,00	42,00	42,00
Centrifugal Pump (bar)	0,50	0,50	0,50	0,50	0,50	0,50	0,50	0,50
Pump pressure (bar)	19,10	19,10	20,00	22,70	23,30	25,20	26,50	28,40
Emulsion temp. C	42,80	46,20	48,00	49,10	48,90	48,50	50,00	53,00
NH3 (1st tube) °C	-10,10	-10,10	-10,10	-10,10	-10,10	-10,10	-10,10	-10,10
NH3 (2nd tube) °C	-10,10	-10,10	-10,10	-10,10	-10,10	-10,10	-10,10	-10,10
NH3 (3nd tube) °C	-10,10	-10,10	-10,10	-10,10	-10,10	-10,10	-9,30	-10,10
Temp (1st tube) °C	8,40	8,00	8,40	9,00	8,90	8,30	6,80	10,90
Temp (2nd tube) °C	11,30	11,20	11,60	12,60	13,30	14,40	14,60	14,60
Temp (3rd tube) °C	11,50	11,60	11,90	12,20	12,60	13,50	13,80	14,10
Amp (1st tube)	292,00	294,00	298,00	300,00	314,00	295,00	294,00	312,00
Amp (2nd tube)	319,00	319,00	319,00	332,00	321,00	334,00	333,00	333,00
Amp (3rd tube)	312,00	312,00	315,00	326,00	328,00	332,00	333,00	343,00
Speed Tankunit 1	38,00	52,00	48,00	45,00	37,00	47,00	25,00	11,00
Speed Tankunit 2	53,00	53,00	55,00	52,00	57,00	58,00	55,00	55,00
Speed Perf 1 [rpm]	1000	1000	1000	1000	1000	1000	1000	1000
Speed Perf 2 [rpm]	1000	1000	1000	1000	1000	1000	1000	1000
Speed Perf 3 [rpm]	1000	1000	1000	1000	1000	1000	1000	1000

Table 5.11.3 Fatty acid compositions of high and low temperature MAG distillations from Moringa *oleifera* TAG

	MAG	**MAG**	**Original TAG**
ID no.	**2559/132**	**2559/134**	***Moringa oleifera***
	210°C	**185°C**	
	%	%	%
GL	0.88	0.52	No data
DIGL	0.15	0.22	No data
FFA	0.2	0.2	1.5
MONO	**86.92**	**97.95**	No data
DI	**11.80**	**1.06**	**3.3**
TRI	0.03	0.02	No data
C12:0	<0.1	<0.1	0.2
C14:0	0.1	0.1	0.1
C16:0	**6.3**	**6.4**	**5.9**
C16:1	1.9	1.9	1.8
C17:0	0.1	0.1	0.1
C18:0	**5.5**	**5.7**	**5.5**
C18:1	72.6	75.3	71.8
C18:2	1.5	1.5	1.6
C18:3	0.2	0.2	0.0
C20:0	**3.2**	**2.9**	**3.3**
C20:1	1.8	1.7	1.9
C20:u	0.2	0.2	0.1
C21:0	<0.1	0.0	0.0
C22.0	**5.8**	**3.6**	**6.3**
C22:1	0.1	0.0	0.1
C23:0	<0.1	<0.1	1.0
C24:0	**0.8**	**0.3**	**1.0**
C26:0	**detected**	**detected**	**detected**

5.11.3 Results and Discussion

5.11.3.1 Droplet Size Distribution (DSD)

The results from the water droplet size distribution (DSD) are given in Table 5.11.4 where emphasis is placed towards 97.5% <µm.

Table 5.11.4 DSD analysis results for W/O emulsions (samples 71 – 78)

Sample	2.5% <µm	50% <µm	97.5% <µm
71. 40% **high** T°C (0.3% dosage)	1.79	5.7	18.19
St. Dev	0.03	0.08	0.70
72. 40% **low** T°C (0.3% dosage)	1.90	6.48	22.05
St. Dev	0.04	0.19	0.82
73. 40% **high** T°C (0.6% dosage)	1.46	4.76	15.44
St. Dev	0.03	0.10	0.86
74. 40% **low** T°C (0.6% dosage)	1.47	5.09	17.61
St. Dev	0.02	0.12	0.83
75. 35% **high** T°C (0.3% dosage)	2.25	3.66	6.02
St. Dev	0.27	0.03	0.77
76. 35% **low** T°C (0.3% dosage)	3.65	3.66	3.66
St. Dev	0	0.01	0.01
77. 35% **high** T°C (0.6% dosage)	3.47	3.52	3.56
St. Dev	0.07	0.03	0.07
78. 35% **low** T°C (0.6% dosage)	3.55	3.56	3.59
St. Dev	0.02	0.02	0.03

The 40% TAG (water phase with hydrocolloid / protein) emulsion (samples 71 – 74), DSD (97.5% <µm), indicates all emulsions are likely to be stable with minimal phase separation, but need to be concluded in relationship to sensory tests. These results are different from those previously found (Table 5.4.8 in 5.4; & Table 5.7.5 in 5.7), where Moringa MAG from high temperature distillation (Lot 2559/ 191) only were tested.

Previous DSD results (5.4 & 5.7) for Moringa MAG at 0.3% concentration and Moringa MAG at 0.6% were; 42.41, and 38.56 respectively, which compares to 18.19, and 15.44 here. This suggests that the stability of these new samples is greater than the stability of the original samples tested previously (5.4 & 5.7). A

possible reason is the difference in diglyceride content which, although not discussed here, is known to aid emulsification (Shimada and Ohashi 2003). Factors such as insufficient emulsification or inconsistencies in the shear scraped surface heat exchanger process may also have a bearing.

The low temperature distillation samples (72 & 74) gave larger respective DSD sizes compared to the high temperature distillations; where the low temperature distillation samples showed here are within the DSD range shown earlier (5.4) and correspond to samples that were fundamentally stable in appearance and abuse testing (spreading).

The 35% TAG (empty water phase) emulsions, samples 75 – 78, gave DSDs to values consistently under 10 microns. This tends to indicate an extremely stable emulsion, indeed if not over-stable, which would negatively impact the flavour release properties (see 5.11.4.2). No material difference could be seen from high temperature distillation to the low temperature distillation samples.

5.11.3.2 Sensory

It was often difficult to make final conclusions from the DSD alone, and therefore a visual (photographic) evaluation combined with sensory evaluation, where each sample was spread onto cardboard and then tasted and characterised organoleptically was carried out. Comments from sensory after spreading and tasting are given as follows:

71. Very stable, seemed as if break down would occur but did not. Improved with more working. Mouth feel; initially thick/creamy, breaks down easily, good flavour release.

72. As stable as 71, no separation. Mouth feel; not as thick as 71, but persists in the mouth for longer not breaking down as easily.

73. Very thick, bit of separation to begin with, then stabilised. Mouth feel; thicker than 71/72, but still acceptable flavour release. Retains structure longer, does not breakdown so easily, not as sticky/waxy as 71/72.

74. Very thick, some oiling out, but emulsion ok, slightly more unstable than 73. Mouth feel; not as thick as 73, detection of lumps possible, like scrambled eggs.

75. Very very stable emulsion, thick, very spreadable. Mouth feel; thick, not too tight, firm, breaks down, melting ok, bit lumpy.

76. Very very stable, thick spreadable. Mouth feel; thick, but more salt release than 75.

77. Extremely stable emulsion, thick, spreadable. Mouth feel; smooth, thick, slow flavour release.

78. Extremely stable, spreadable, thick, slightly more sticky than 74. Mouth feel; smooth, thick, no breakdown, possibly stabilised?

40% W/O emulsions: On assessment of samples 71-74, the 40% TAG emulsions, the samples with the high temperature distillation, (71 and 73) seemed to form stable emulsions, but are breaking down in the mouth easier than the low temperature counterparts, giving good flavour release. It would seem that the Moringa MAG produced via the high temperature distillation, i.e. with the broadest range of fatty acids (see Table 5.11.3), seem to infer a beneficial function in terms of in-mouth sensorial properties and flavour release.

35% W/O emulsions: At 35% TAG level, a similar trend is observed; the high temperature distillation samples resulted with products which had improved mouth feel perception and flavour release. However, all the 35% TAG emulsions as a whole were extremely stable and as such could not be classified (in the opinion of expert sensory panel) as being representative of a typical table emulsion. These could be summarised as all being too stable and too thick for acceptable product use. Probably for a more realistic consistency, the dosage of the Moringa MAG should be reduced to perhaps 0.15%. Again, although the stability and taste levels

of the high temperature distillation samples were improved, the low temperature samples were not unacceptable.

Photographic images of samples 71 – 74 (40% TAG emulsions) and samples 75-78 (35% TAG emulsions) are shown in Figures 5.11.1 and 5.11.2. Whilst the samples in Figure 5.11.1 are eminently stable, it is clearly evident that those depicted in Figure 5.11.2 are more stable; having additional intensity of whiteness and less translucence, due to smaller DSD and or, though not measured here, more crystal numeration. Importantly, none of the samples showed signs of oiling out or other phase separation. It was difficult to observe from the photographs the differences tasted during evaluation between the high temperature and low temperature distillations, therefore making it important to take a holistic view to the sample evaluation.

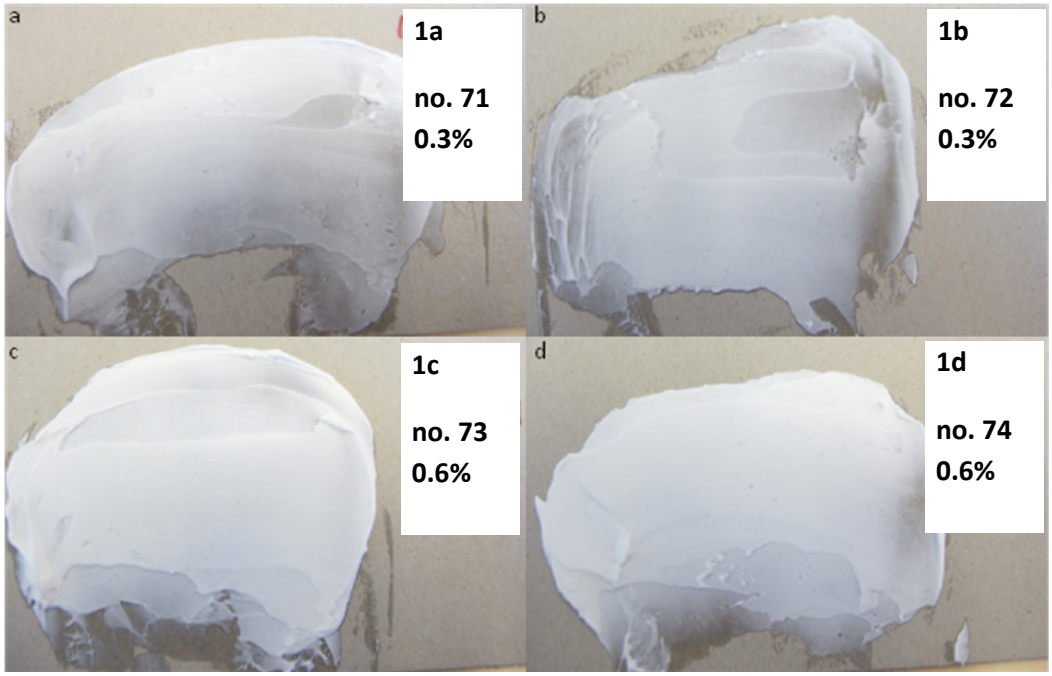

Figure 5.11.1 40% emulsion samples: (1a) no.71, 0.3% dose, HIGH T°C distillation; (1b) no.72, 0.3% dose, low T°C distillation; (1c) no.73, 0.6% dose, HIGH T°C distillation; (1d) no.74, 0.6% dose, low T°C distillation

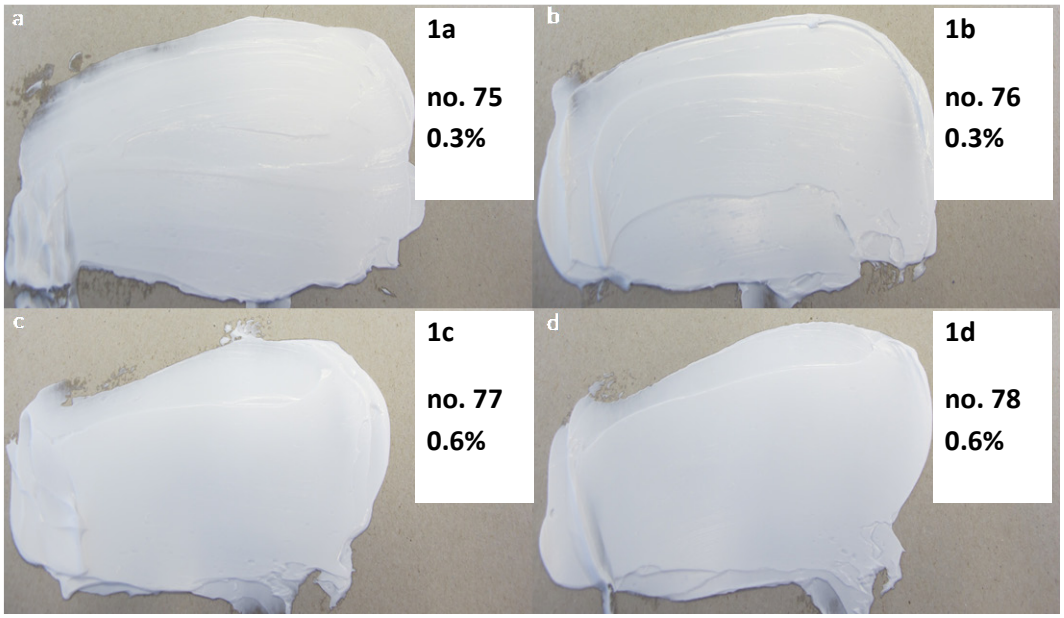

Figure 5.11.2 35% emulsion samples: (1a) no.75, 0.3% dose, HIGH T°C distillation; (1b) no.76, 0.3% dose, low T°C distillation; (1c) no.77, 0.6% dose, HIGH T°C distillation; (1d) no.78, 0.6% dose low T°C distillation

Texture analysis

The results from texture analysis in terms of hardness are given in Figure 5.11.3 after measurement at 5°C.

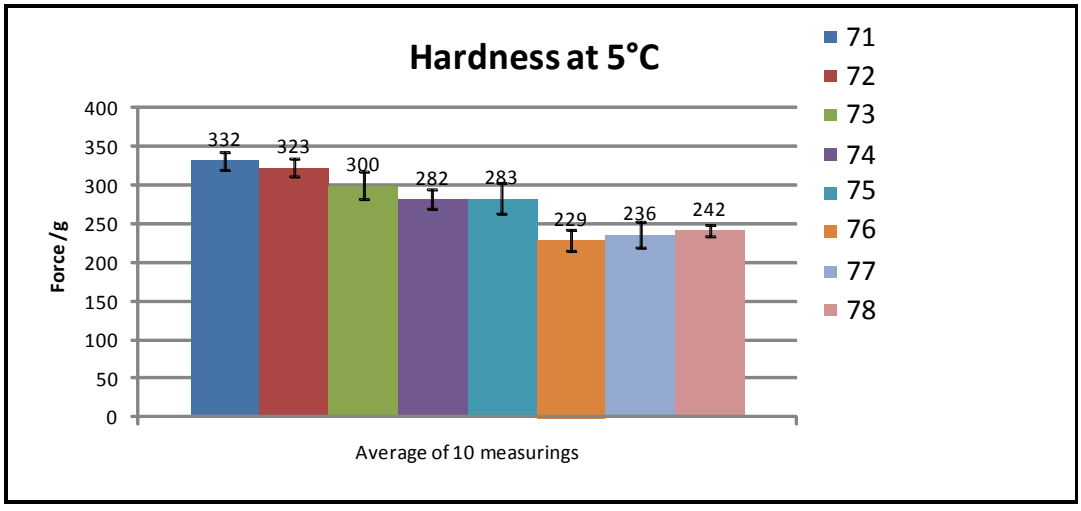

Figure 5.11.3 Texture analysis: hardness for 40% TAG emulsions (samples 71-74), and 35% TAG emulsions (samples 75-78)

5.11.3.3 Effect of Distillation at 0.3% Moringa MAG Concentration

When comparing sample 71 / 72, there appeared to be agreement with sensory results; sample 71 was firmer compared with 72. This also fits with water-droplet distribution. The effect was more pronounced when comparing samples 75 / 76.

5.11.3.4 Effect of distillation at 0.6% Moringa MAG Concentration

When comparing samples 73 / 74, though small, there appeared similar agreement when compared to water-droplet sizes. The same pattern did not follow for samples 77 / 78. This was probably attributed because at the emulsifier concentrations and shear on the emulsion, a mean DSD of approximately 3 - 4μm, had already approached the maximum decreased droplet size.

The result of high shear during emulsification and cooling will always produce droplets, however the Laplace pressure within the droplets increases as droplet size decreases, consequentially resulting in a resistance to further deformation. The addition of an emulsifier decreases the Laplace pressure allowing the production of smaller droplets. However, 0.6% Moringa MAG in this examination probably exceeds the concentration necessary to produce stable emulsions.

The results of Figure 5.11.3 showed a somewhat contradictory trend to those expressed from the spreading tests and mouth feel evaluation which all led to the conclusion that increasing the concentration leads to an increase in mouth resilience. The results from DSD indicated that while there tended to be decreased DSD according to an increase in Moringa MAG, this did not necessarily translate to increased firmness. It has been shown that increasing Moringa MAG concentration tended to "soften" the bulk TAG (5.4; 5.7 – 5.10).

In the case of 40% emulsions, the initial trend in textural resilience is thought to be reliable. The "elastic" resilience experienced in sensory observations is likely the

effect of strengthened interfacial film properties (4.0) at the water-oil surface (observed in the pilot studies in 1.5). This may have some connection with the miscibility of the Moringa MAG, where the proportion of saturated fatty acids >C20:0 are likely to be more surface-active (Krog 1992), forming an insoluble microcrystalline arrangement, where an interstitial stabilised interface may exist (Johansson, Bergenståhl & Lundgren, 1995).

Data for 35% emulsions did not show any significant trend in the case of DSD – evident from droplets at <5µm. The expert sensory findings follow a similar pattern to the 40% emulsions. It is assumed therefore, that such resilience was the effect of maintaining the whole preserved fatty acid profile in the high temperature distillation, 87% mono (2559/132), and this is despite the higher mono content (97%) in the low temperature distillation (2559/134).

Finally for both 40% and 35% TAG emulsion – in all cases - both high and low temperature distillations were an improvement on PGPR as shown previously (Tables 5.11.3; 5.11.4 in 5.11 & 5.8).

5.11.4 Conclusion

The results show a direct effect of securing a diversified fatty acid spectrum. It is concluded that Moringa MAG synthesised at a higher distillation temperature has generally led to direct increase on the influence of initial firmness and is manifest through sensory resilience, compared to normal distillations. These physical properties have a direct functional effect, leading to “elastic” resilience because of strengthened interfacial film properties (4.0) at the water-oil surface (observed in the pilot studies in 1.5). This may have some connection with the miscibility (Ueno et al., 1994) of the *Moringa oleifera* based MAG, where the proportion of saturated fatty acids >C20:0 are likely to be more surface-active (Krog 1992), forming Pickering and insoluble microcrystalline arrangement; in turn, a steric, interstitial stabilised interface may exist (Johansson, Bergenståhl & Lundgren, 1995).

5.12 Inventions: a Moringa MAG and Modified Crystalliser Composition

5.12.1 Summary

Inventive steps have successfully provided solutions to several unresolved problems, primarily within crystallisation and emulsification of low TAG W/O emulsions (Wassell et al., 2012a; 2012b; 2012c; 2012d; 2012e; Bech et al., 2013). These key findings have been found through a multidisciplinary investigation (Wassell & Young 2007; Wassell et al., 2010a; 2010b; 2012; Young et al 2008) involving a range of analyses and product application (proof of concept) tests (3.0; 4.0; 5.1 – 5.11; 6.0). Theories and conclusions concerning Pickering stabilisation, a metastable region and dendrite behaviour are discussed.

5.12.2 *Moringa oleifera* based Monoglycerides

Recently, there has been a need to find ways to promote crystallisation in oil / fat blends (triacylglycerols) which require an increase in their crystal kinetics (Wassell & Young 2007; Wassell et al., 2010b; Young et al., 2008). One issue is the removal of *trans* isomers which are derived from partial hydrogention of liquid triacylglycerol (TAG) and semisolid triacylglycerols (TAGs). It is known that partial *trans* isomers which have a degree of saturation (low iodine value) are able to induce crystallisation (Flöter & van Duijn 2006).

There is still a problem to find materials which can overcome crystallisation and emulsification issues when formulating TAG based oil blends which meet the following criteria:- First, componants are *trans* free. Second, they should not come from fully hydrogenated hardstock, and third, they should provide adequate function within a low saturated TAG environment (Wassell et al., 2010a). These may be especially interesting for applications where water-in-oil or oil-in-water emulsions are used.

Currently, commercial reasons dictate a need to find a solution for substituting fully hydrogenated fats (Wassell et al., 2010a). While these do not inherently contain *trans* isomers of any significance, the perception in the media and more importantly from medical sources, is that these should also be removed because hydrogenation is linked to formation of *trans* and human coronory risks. Therefore there is now requirement even with minor ingredients to make these fit under the category of non-hydrogenated material (Wassell et al., 2010a), therefore attaining a more natural and/or ethical status (Bech et al., 2008; Carmichael 2011; Wang et al., 2012).

A monoglyceride providing a relatively rich source of C22:0, having a longer fatty acid moiety than commonly used fatty acids may have some important advantages, both from a crystallisation and emulsification perspective in low and high TAG spreads (1.6, 3.0, 4.0 5.0). However, the problem to date is finding and developing emulsifiers which contain a significant source of long chain moieties, but yet, have not undergone hydrogenation or other modification steps.

Emulsifiers designed from *Moringa oleifera* TAG (4.0, 5.0), are thought to be able to provide unique functions because of the following reasons:-

A monoglyceride (MAG) based on *Moringa oleifera* TAG provides a natural source of behenic fatty acid, approximately 6 – 8% (In fact total >C20:0 > 10%). The *Moringa oleifera* TAG is a natural source of behenic, which has been used as an oil structuring and solidifying agent in margarine, shortening, and foods containing liquid, semi-solid and solid TAG, eliminating the need to hydrogenate (5.11).

A rich source of saturated fatty acids (>C20:0) is interesting for use in W/O emulsions, particularly, low TAG (<41%) W/O emulsions, where it is common industrial practice to include the use of Polyglycerol Polyricinoleate (PGPR) (1.6, 1.7.2). There is strong evidence to suggest that low TAG emulsions (W/O) could be successfully assembled without PGPR (5.8). This particular aspect could provide a powerful solution in emulsion "break-down" of highly stabilised emulsions, where PGPR is present within emulsion systems.

A bi-functional Moringa MAG could be a "one-stop" solution for both low and high TAG systems (5.4), where emulsification and crystallisation are deemed critical.

Moringa oleifera TAG based monoglycerides may also provide unique new esters of monoglycerides. Therefore, this could lead to construction of a monoglyceride designed with a diverse fatty acid range, which may or may not contain a significant degree of diglyceride content (possibly similar to Moringa MAG) (5.9, 5,10, 5.11).

Finally, application trials (5.0), to test performance of Moringa MAG have successfully investigated the suitability of a *Moringa oleifera* based MAG in 60% and 40% TAG W/O emulsion spreads. In the case of 40% spreads, these were all tested with and without PGPR (5.4; 5.7; 5.8; 5.9; 5.11).

5.12.3 Interim Conclusion

In all cases, the use of a Moringa MAG enhanced emulsion stability and improved water size droplet distribution. In the case of low TAG (<40%) W/O emulsions, there was strong stability without the use of PGPR (5.0).

Interfacial tensiometry has shown unusual decreased tension measurement, close to that of PGPR (4.0). All other tested MAG, irrespective of their fatty acid compositions had higher tension measurements across the measured temperature spectrum (50°C - 5°C). This was considered significant, especially where rheological measurements also showed evidence of visco-elastic structural changes (4.0, 5.6). Aside from the inventive bi-functional use of a Moringa MAG, there was also potential benefits to couple a second emulsifier (5.3; 5.6) within a wide range of food emulsion / dispersion systems, but primarily for use in the design, structuring and texturing of low saturated TAG systems (Abdulkarim et al., 2005; Lalas & Tsaknis 2002; Wassell et al., 2012a; 2012b; 2012c; 2012d; 2012e).

5.12.4 Modified Crystalliser Composition

It has been previously shown in discussion (5.12.2 & 5.12.3), that a minor ingredient can be strongly effective at influencing crystallisation and interfacial behaviour (3.0; 4.0; 5.0). An essential feature of CRY110 is that it provides a relatively rich source of behenic (C22:0), longer chain fatty acid moiety than commonly used fatty acids (Krog & Larsson 1992). This feature is considered to offer some important advantages, both from a crystallisation and emulsification perspective in low and high TAG spreads (1.5). However, it has been demonstrated that a MAG characterised as behenic based is not suitable as a standalone solution in low TAG (<41%) based water-in-oil emulsion spreads, and either causes destabilisation or fails quickly (days) during shelf life (5.7).

A second emulsifier may enhance the first emulsifier in such systems. This is particularly the case in demanding applications such as low (<41%) TAG based spreads (Bech et al., 2013). A MAG having a bi-functional effect would be desirable to provide a composition which can function as both an emulsifier and a crystallisation improver. An emulsifier able to satisfy the following would provide unique functions:-

A rich source of saturated fatty acids is interesting for use in W/O emulsions, particularly low TAG W/O (<41% oil) where it is common industrial practice to include the use of Polyglycerol Polyricinoleate (PGPR) (1.5). There was strong evidence to suggest that low TAG emulsions (W/O) could be successfully assembled without the use of PGPR (5.4; 5.8; 5.9; 5.11). Depending on its inclusion level, PGPR has tendency to “over stabilise” the emulsion, leading to adverse sensory (5.8) resilience. Therefore, where there is a preference to include PGPR, the dosage can be reduced (5.8) thereby offering potential cost-in-use savings.

It was found that MAG with fatty acid composition (FAC) containing in the region of 8.5 – 12.3% saturation starting from C20:0 seemed to enhance emulsification and crystallisation properties (5.0) In natural Moringa MAG, diversity in the FAC

starts from the same chain length (C20:0) and there is a significant proportion of C22:0 and C24:0 (Table 5.10.2). Natural Moringa MAG also contain lower chain (C16:0 and C18:0) and a high degree of unsaturated fatty acids (~72%). A similar designed fatty acid composition, using alternatively sourced MAG to mimic a natural Moringa MAG is considered novel. Wassell et al (2012a; 2012b; 2012c; 2012d; 2012e), describe the use of a MAG based on natural Moringa TAG), where it could provide a "one-stop" solution for both low and high TAG systems (5.3; 5.10). Optionally, when combined with e.g. PGPR (a co-emulsifier) this may also provide additional structuring advantages (Bech et al., 2013).

5.12.5 Interim Conclusion

The use of modified crystalliser, based on MAG, enables improved emulsion stability, and improved water size droplet distribution. In the case of low TAG (<40%) W/O emulsions, there is good stability without the use of PGPR (5.10).

A modified crystalliser composition may find applications in a wide range of food emulsion / dispersion systems, but primarily for use in the design, structuring and texturing of low saturated TAG systems.

A series of application trials have revealed the possibility to make a synthetic like Moringa monoglyceride by mimicking the fatty acid composition (5.3; 5.10) of *Moringa oleifera* based monoglycerides, thereby overcoming potential restrictions of supply and dependence on sources of *Moringa oleifera* TAG (Wassell et al., 2012a; 2012b; 2012c; 2012d; 2012e; Bech et al., 2013).

5.12.6 Significance for Pickering Stabilisation

Most studies have looked at the effect of high TAG Pickering stabilisation compared to low TAG Pickering stabilisation. Garti et al., (1998) found sub-microcrystalline surface-active fully hydrogenated palm stearin, could in the

presence of PGPR, stabilise water droplets (25% aqueous phase in 75% TAG consisting of liquid soybean oil). Ghosh and Rousseau (2011) investigated surface active fully hydrogenated canola TAG in the presence of GMO (a Glycerol monooleate based MAG), testing in emulsions consisting 80% liquid canola oil / 20% aqueous phase. Both these studies and others (Johansson et al., 1995) have shown effects of Pickering stabilisation to reduce coalescence and smaller droplet size for a given TAG crystal concentration and speed of thermal treatment (Hodge & Rousseau 2005). However, these were found to be very system specific, and subsequently this has technical consequences for low TAG W/O emulsions.

The effects of shear and non-isothermal crystallisation have a dramatic effect on the bulk TAG network structure (Rousseau et al., 2005). With consideration of this aspect, crystalline material aiding emulsion stability would need to be smaller than the dispersed aqueous droplets (Ghosh & Rousseau 2010). Rousseau and Hodge (2005), say the visco-elastic behaviour of the interfacial film is attributed to wetted TAG crystal, how they are wetted and dependent on the composition and initial surface properties of the TAG particles.

Since conducting this thesis, Ghosh and Rousseau (2011) have shown Pickering stabilisation to be more efficient with TAG (HCO) and GMS (a Glycerol monostearate based MAG), than with TAG (HCO) in the presence of GMO (a Glycerol monooleate based MAG). Stabilisation appeared superior with the more saturated MAG. This could be due to hydrogen bonding with the TAG solvent (Chen, van Damme, & Terentjev, 2009). It is therefore suggested that when TAG particles are covered by an adsorbed layer of an emulsifier, the interaction may strongly influence the macroscopic properties of the TAG continuous phase (Bergenståhl 2008). Further, if the adsorbed emulsifier is of a liquidus nature e.g. PGPR, this would cause the Pickering TAG crystals to be more surface-active (Ghosh & Rousseau 2011).

Rousseau et al. (2003), say in the presence of fewer TAG crystals, stabilisation must be dependent on the interfacial properties, so that any visco-elastic behaviour could take place. It would therefore seem to be the case that an interstitial region

and its interaction with Pickering surface-active TAG and MAG crystals are therefore critical. Rousseau et al. (2003), also alluded to this when examining low (38%) TAG margarine, indicating this aspect had not been examined.

The low TAG W/O emulsions measured in this research had considerably decreased bulk TAG network. Consequently, network stabilisation would have had even less influence on interfacial stabilisation. In this situation, Pickering surface-active TAG / MAG crystals are more important, so that in the presence of a co-emulsifier such as PGPR or additional MAG (4.0; 5.4; 5.11), this effect would be enhanced. Additionally, should crystal structures exist as smaller, liquidus and or nano-arrays, then this might also account for interfacial visco-elastic behaviour, stabilising the W/O emulsion (4.0; Johansson et al., 1995; Rousseau, 2000).

5.12.7 Metastable Region

It is not certain if the bi-functional behaviour of e.g. Moringa MAG might be attributed to the miscibility (Ueno et al., 1994) of its fatty acids: ~30% range of saturated fatty acids (SAFA) including C16:0, C18:0, C20:0, C22:0, C24:0 of which ~10% is >C20:0 coupled with ~70% C18:1 (5.0). The textural resilience measured in the low TAG (<41%) W/O emulsions is considered to be the effect of strengthened interfacial film properties (4.0) at the water-oil surface (1.5; 5.0). For a Moringa MAG, where the proportion of SAFA >C20:0 are likely to be more surface active (Krog 1992), these may form insoluble / metastable microcrystalline arrangements through polar interaction with the remaining liquidus fatty acids causing a steric, interstitial stabilised interface to be formed (Johansson, Bergenståhl & Lundgren, 1995). Further, Sato (1998), suggests oleic acid (C18:1) may be responsible for cohesive interactions (Claesson et al., 1997) when these chains are forced to interact with SAFA chains in the same lamellar.

The interface may be induced to a different structure, especially with a decreasing bulk TAG network (Goubran & Garti 1988). This is possibly due to dielectric influence compared to the bulk, where dipolar interactions between a polar

aqueous surface and ester groups of TAG occur (Claesson et al., 1997; Petrov et al., 1995). The nature of the solvent plays a vital role on surface interactions (Dedinaite & Campbell 2000). Though not adequately explained here or understood (5.6), PGPR may induce additional adhesive properties when mixed with another emulsifier in the presence of water. Additionally, the polar region of the PGPR may influence the water droplet properties (Ghosh & Rousseau 2009).

It is hoped that subsequent SR-XRD synchrotron studies or more powerful analysis could provide more insight to characterise a metastable phase / interstitial region. It could also lead to new insight, that could help to explain further details, behind the behaviour of Pickering MAG crystals (based on a quantity of >C20:0) becoming viscous and sticky at their surfaces by adsorbing Liquidus PGPR (Mullin, 1993). The structure of this system in the presence of an aqueous phase is still not known (Dedinaite & Campbell 2000).

5.12.8 Dendrite Structure

Dendrite structures were observed (2-D) microscopically (5.3; 5.5) in the bulk phase. Logically, this situation 3-D, combined with their proliferation would likely influence the total G* due to their relative surface area. The phenomenon of dendrite structures (Ben-Jacob & Garik 1990) observed in this thesis (5.0) is possibly linked to both saturation, the rate of thermal treatment of the TAG blends (5.3) and irregularity of the structure magnifying existing wetting properties (Rousseau 2002). This is possibly linked to the effect of the adsorbed emulsifier enhancing crystallisation (Marikkara & Ghazali 2011), causing dendrite forms. In the presence of water and oil, this could be additional explanation for comparative thickening observed in the W/O emulsions (5.4; 5.7, 5.11), where adhesion is caused by increased polarity (Rousseau 2002). The additional sites of contact on wetted TAG crystal due to the presence of adsorbed emulsifier (forming surface active crystals) e.g. Moringa MAG or PGPR combined with CRY110 (5.6), could also explain observed rheological and interfacial behaviour (4.0).

6.0 Synchrotron Radiation Macrobeam and Microbeam X-ray Diffraction Studies of Interfacial Crystallisation of Fats in Water-in-Oil Emulsions

6.1 Introduction

A synchrotron radiation macrobeam and microbeam X-ray diffraction study of interfacial crystallisation to clarify the effects of emulsifier additives on low fat water-in-oil (W/O) emulsions was conducted (Wassell et al., 2012). Emulsifiers having long-chain saturated fatty acid moieties have been found to be effective due to their melting and surface active characteristics at the water-oil interface (4.0; 5.0; Wassell et al., 2012a; 2012b; 2012c; 2012d; 2012e; Bech et al., 2013).

6.2 Background

It is known that given a certain concentration of emulsifier, triacylglycerol (TAG) crystals become more polar in behaviour because the emulsifier is adsorbed at the crystal surface. Indeed Boyd, Krog and Sherman (1976), suggested that there may be a connection between the stability of a lipid bilayer, dependant on molecular packing conditions in the bulk [containing emulsifiers] and viscoelasticity of adsorbed films of the same emulsifiers at the TAG – water interface.

A mixed emulsifier system is suggested in theory to produce a more rigid interfacial structure (Boyd et al., 1976), which may be conducive to minimising coalescence (Rousseau 2000). The selection of the emulsifier is therefore critical, because even when complexes of emulsifiers are located at the W/O interface it is possible that the emulsions will still be unstable (Boyd et al., 1976).

Rosen (1989) states, selection of a co-emulsifier, a polar compound of intermediate chain length is preferred over long-chain polar compounds because these are generally not desirable as co-emulsifiers since they tend to form liquid-crystalline structures that may increase the viscosity of the system and the rigidity

of the interface. There would seem to be contradiction, because studies have shown (Arima et al., 2009; Tanaka et al., 2009) long-chain saturated fatty acid moieties (behenic rich) to be effective emulsifier additives at the interface of TAG and water emulsion droplets (O/W).

Investigations into rheological properties using a modified technique to assess both elastic and viscous moduli in the bulk in model emulsions have been made (4.0). Interfacial tension measurements have revealed strong interactions between PGPR and behenic rich MAG (4.0). The purpose of using the SR-μ-SAXD in this study is to explain more fully why this interaction may occur.

A technique to more precisely observe microstructures of lamellar plane directions, to thereby aid understanding to the mechanism of structure at interfaces e.g. W/O emulsions, and how these might be modified through emulsifier-initiated processes, was carried out as part of the multidisciplinary investigation. Following bulk and interfacial examinations (3.0; 4.0; 5.0), the purpose of this investigation was to study the influence of PGPR, and then PGPR combined with a behenic based monoglyceride (MAG (CRY110)) in W/O emulsions needed to be studied in low TAG (<41%) emulsions to determine the cause and effect on crystal behaviour at the interface. It was considered important to tie this new learning with previous multiple observations in 3.0, 4.0 & 5.0 (Wassell & Young 2007; Wassell et al., 2010a; 2010b; Young et al., 2008).

It has been shown (Wassell et al., 2010a) that some emulsifiers can template with other emulsifiers resulting in increased strength of the interfacial membrane between the water and TAG phases so that the surfaces of the water droplets are either partially or wholly covered, forming monolayers for heterogeneous crystallisation. This feature has been analysed in TAG oil-in-water emulsions (Arima et al., 2009), but has not been investigated in water-in-TAG oil emulsions (Figure 6.1).

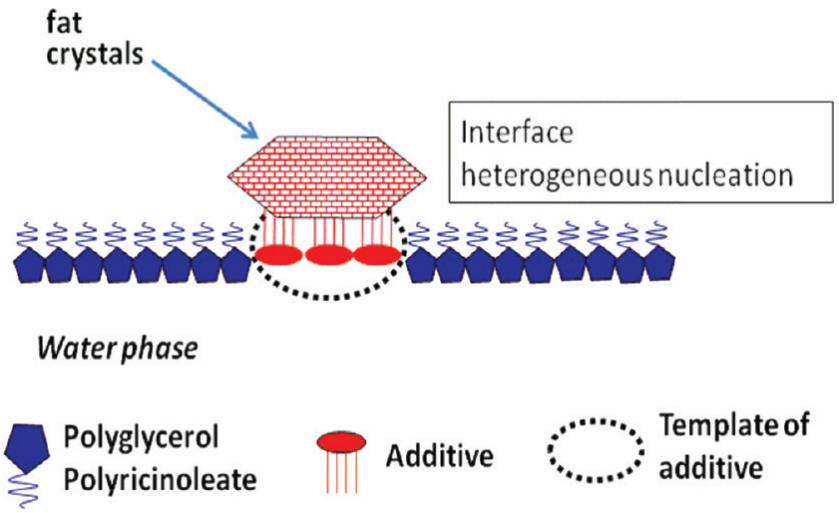

Figure 6.1 Proposed schematic showing interfacial crystallisation at the water-in-oil interface.

As described earlier (1.5; 4.0; 5.0), it is common practice to use two emulsifiers (e.g., polyglycerol polyricinoleic acid (PGPR) and monoacylglycerol (MAG)) in the production of W/O emulsions, in which MAG may act as a templating agent, whereas PGPR assures emulsion stability.

The effect of PGPR and MAG has been studied in high TAG (>75%) W/O emulsions (Garti et al., 1998; Ghosh & Rousseau, 2009), but until now it is not specifically known about the interactive behaviour of a long-chain MAG and PGPR in low TAG (<41%) W/O emulsions (Wassell et al., 2012).

PGPR is highly surface active and has a large complex structure (molecular weight (MW) range >4000 g/mol)), compared to MAG which has a smaller molecular structure (MW 580 g/mol) than PGPR. Interactions of the two emulsifiers have an interesting effect on interfacial and bulk crystallisation behaviour. According to available information, the influence of PGPR and MAG containing behenic acid moiety (monobehenate (MB) previously abbreviated as CRY110 or MB90 (2.0 General Materials & Methods)) has not previously been analysed to determine the effects of interfacial heterogeneous crystallisation of low TAG (35% oil phase) W/O emulsions (See Table 2.22 in Materials and Methods (2.0)).

Synchrotron radiation X-ray diffraction (SR-XRD) macrobeam and microbeam small angle X-Ray diffraction (SR-μ-SAXD) analysis, DSC, polarised optical Microscopy (POM) were used to enable observation of TAG crystals near the W/O interface because this method can provide microscopic information about crystallised materials on the order of micrometer to submicrometer dimensions and provide learning about the interactions between TAGs and emulsifiers in the continuous TAG phase and at the W/O interface.

6.3 Results and Discussion

6.3.1 DSC Thermograms and Macrobeam SR-XRD Measurements

Figure 6.2 depicts the DSC cooling thermopeaks of two emulsions using PGPR alone and PGPR + MB. Although not shown here, the DSC heating thermograms did not indicate any differences between the two emulsion samples, whereas the cooling thermopeaks were quite different.

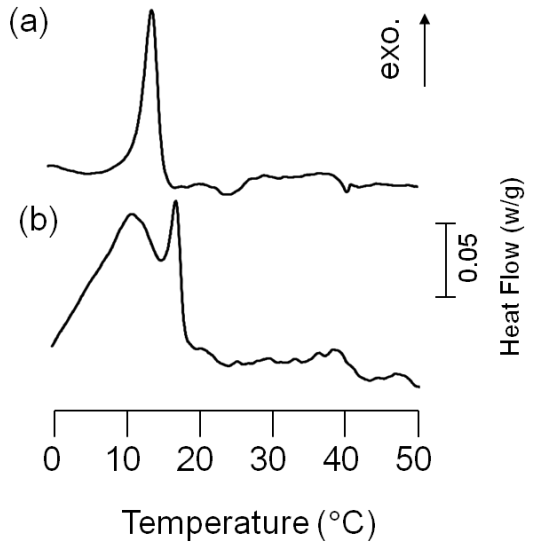

Figure 6.2 DSC cooling thermopeaks taken for (a) PGPR emulsion and (b) PGPR + MB emulsion

The emulsifiers influenced kinetic crystallisation processes at 16.1°C in the PGPR emulsion, whereas the crystallisation temperature increased to 17.9 °C in the PGPR + MB emulsion. Exothermic behaviour resulted in a single peak (PGPR emulsion) to double peak (18°C and 10 °C in the PGPR + MB emulsion). This may have been caused by the promotion of the crystallisation of a high-melting fraction of solid TAG by the addition of MB.

The melting and crystallisation of the PGPR emulsion were examined by macrobeam SR-XRD (Figure 6.3). At 5 °C, the SAXD and WAXD patterns exhibited a long spacing peak of 4.07 nm (Figure 6.3a), a strong peak of 0.462 nm, and a weak peak of 0.386 nm (Figure 6.3b). The WAXD peaks correspond to β polymorph, which represents $T_{\parallel}$ subcell structure. The reason for the presence of β form in the emulsion sample is that the sample was stored over a long period and the most stable form of the fat crystals in the emulsion was formed.

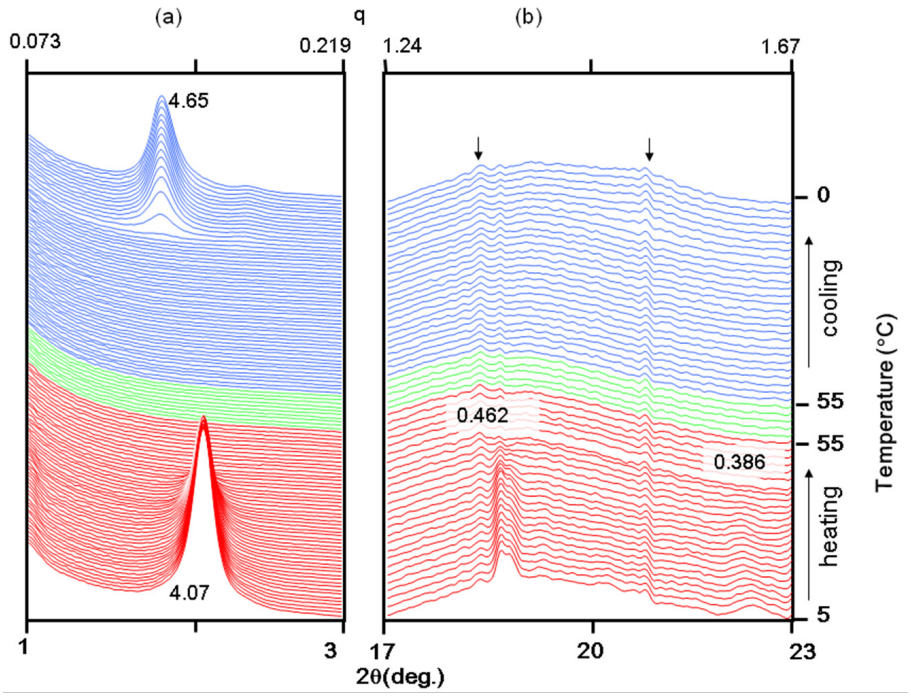

Figure 6.3 Macrobeam SR-XRD patterns of PGPR emulsion taken during heating and cooling. Unit: nm. Experiment noise is denoted by arrows

When the emulsion was heated, both SAXD and WAXD patterns disappeared at 40 °C, due to the melting of the β form. During cooling, crystallisation was detected with the occurrence of the SAXD peak of 4.65 nm at 14 °C, corresponding to the exothermic peak of crystallisation observed in the DSC cooling pattern (Figure 6.2a). The long spacing of 4.65 nm means that the polymorphic form of these crystals is α form, as the chain axis in the TAG crystals is normal to the lamellar interface (Sato & Ueno 2011). In addition, the α form tends to crystallise faster than the other more stable forms during the ambient rate of cooling. Despite the strong SAXD peak, no strong peaks were detectable in the WAXD area during cooling (Figure 6.3b). This may be due to the weak diffraction of the hexagonal subcell packing of α form in the W/O emulsion. Figure 6.4 depicts the melting and crystallisation of the PGPR + MB emulsion examined by macrobeam SR-XRD. Similar to the PGPR emulsion, the SAXD patterns confirmed the presence of the β form at 5 °C, as evidenced by a long spacing peak of 4.07 nm (Figure 6.4a), and the WAXD patterns of strong peaks of 0.462 nm and weak peaks of 0.386 nm (Figure 6.4b).

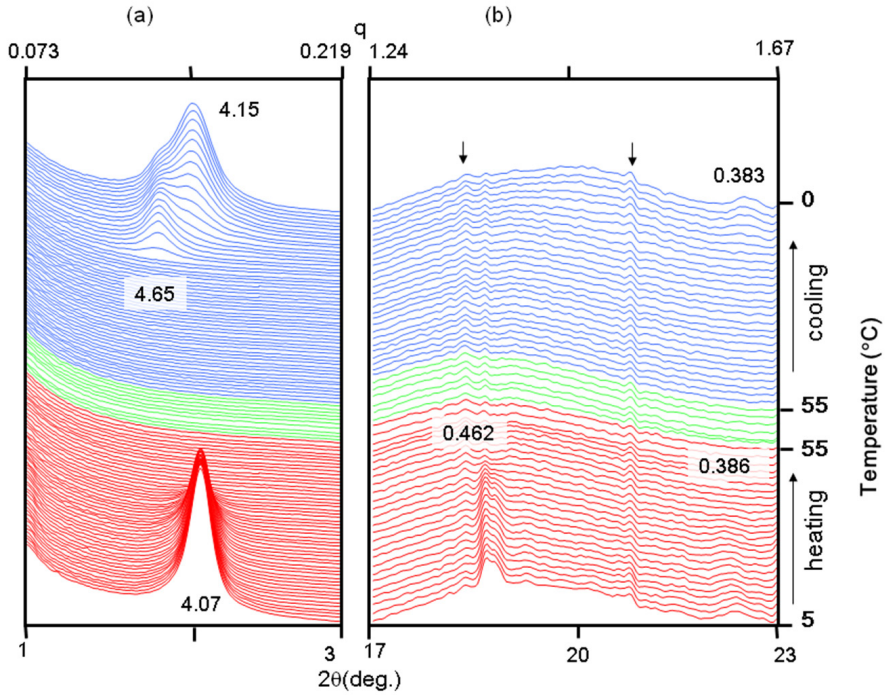

Figure 6.4 Macrobeam SR-XRD patterns of PGPR + MB emulsion taken during heating and cooling. Unit: nm. Experiment noise is denoted by arrows

No strong peak was detectable in the WAXD area when the strong SAXD peak of 4.65 nm appeared. However, a weak WAXD peak of 0.383 nm appeared when the SAXD peak of 4.15 nm appeared below 10 °C. It is assumed that this form is a low temperature sub-α form (Yano et al., 1999).

The macrobeam XD patterns taken during cooling from 55 °C exhibited two-stage crystallisation profiles. The first peak (4.65 nm) appeared at 16 °C and the second peak (4.15 nm) appeared at 10 °C. This two-stage crystallisation observed in the SR-XRD experiment also corresponds to split DSC exothermic peaks taken during cooling (Figure 6.2b).

6.3.2 μ-SAXD Measurements: Azimuthal Angle (χ) Extension Patterns.

PGPR: The lamellar directions of the fat crystals near the W/O interface are found parallel to the W/O interfacial plane using PGPR alone as the emulsifier agent. The azimuthal angle (χ) extension patterns did not reveal this tendency for all positions in the bulk TAG phase, but it may be assumed that the PGPR membrane at the W/O interface may induce the interfacial heterogeneous crystallisation illustrated in Figure 6.1.

PGPR + MB Emulsion: When compared to PGPR only, the two emulsions had basically common results in terms of lamellar directions of the TAG crystals at the positions near the W/O interface. These were confirmed by analysis of the χ extension patterns at various positions surrounding the water droplets. However, the intensity of the diffracted X-ray beams was less in the PGPR + MB emulsion than in the PGPR emulsion, possibly due to the formation of tiny TAG crystals (see Polarised Optical Microscope (POM) micrographs Figure 6.5)) caused through addition of MB. This effect made analysis of the results of μ-SAXD data from the PGPR + MB emulsions difficult for calculating the degree of orientation of the lamellar planes of TAG crystals; these are evaluated by calculating the half width of χ value (Δχ). A smaller Δχ yields a higher degree of orientation of the lamellar planes. The lamellar planes of the TAG crystals in the PGPR + MB

emulsion were more highly ordered than those in the PGPR emulsion. However, such a comparison of $\Delta\chi$ values could not be made for all positions of the PGPR + MB emulsion, hence making it difficult to obtain a clear conclusion about the preferred orientation of the lamellar planes of the TAG crystals, near the W/O interface in the PGPR + MB emulsion and in comparison with those in the PGPR emulsion.

6.3.3 Polarised Optical Microscopic (POM) Observation

The crystal morphology and dimensions of the fat crystals were observed in the PGPR emulsion and PGPR + MB emulsion polarised optical microscope (Figure 6.5). Clear differences were detectable between the crystal morphologies of the two emulsions, in that no large crystal aggregate is observed in the TAG phase in the PGPR + MB emulsion. Instead, thin layers of bright images were attached to the water phases (arrows in Figure 6.3). This morphological change can be explained by the addition of MB increasing the crystallisation temperature, as confirmed by the cooling experiments of SR-XRD and by the reduction in crystal size due to increased rates of crystal nucleation.

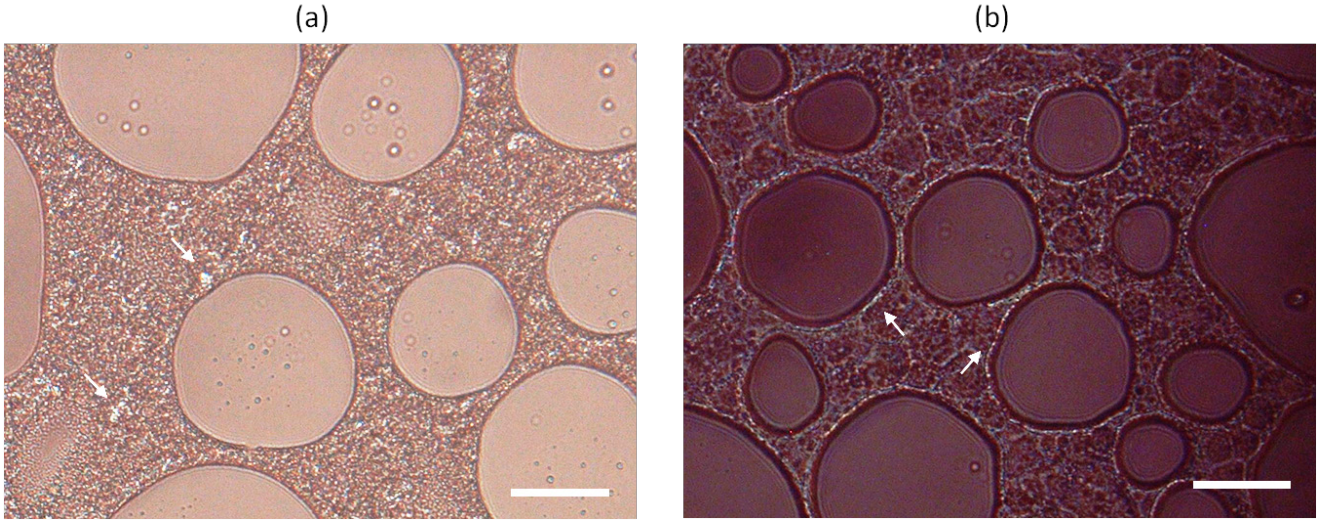

Figure 6.5 Polarised optical micrographs of W/O emulsions. (a) PGPR emulsion and (b) PGPR + MB emulsion. Scale bar: 25μm

It should be noted that 35% W/O emulsions assembled for these measurements, originally had a smaller water droplet size (see Table 5.8.4) to that inferred in Figure 6.5. Due to confidentiality (Wassell et al., 2012a; 2012b; 2012c; 2012d; 2012e) several samples (containing *Moringa oleifera* based MAG) were not measured. The POM images of Figure 6.5 (originally Figure 13 in Wassell et al., 2012) were the result of heating the sample to 50°C, then cooling to 5°C at a rate of 2°C/min and keeping at this temperature for 10 minutes. By comparison, this may explain the difference in droplet sizes observed in this multiple study (5.0) which shows other examples of low fat (<41%), W/O emulsions (Wassell et al., 2012c).

6.4 Conclusions and Recommendations

This study (Wassell et al., 2012) revealed the following results. First, the addition of MB promoted TAG crystallisation as observed by DSC and macrobeam SR-XRD analysis. Second, the microbeam SR-XRD indicated that the lamellar planes of TAG crystals near the water and oil interfaces were arranged almost parallel to the interface planes in both the PGPR emulsion and the PGPR + MB emulsion. No appreciable differences between them were confirmed. Third, the POM observations indicated that adding MB eliminated the formation of large crystal aggregates, resulting in the formation of tiny TAG crystals.

Although PGPR contains large amounts of liquidus fatty acid moieties at the temperatures examined in the present μ-SAXD experiments, it can be assumed that certain molecular interactions between PGPR and TAG molecules may be operating at the W/O interface to cause interfacial crystallisation to some extent, and the addition of MB may strengthen this interfacial crystallisation. Such interactions may include not only hydrophobic chain-chain interactions between the fatty acid moieties of the emulsifiers and TAG molecules, but also hydrophilic interactions between the polar groups of the emulsifiers and glycerol groups of TAG molecules (Ghosh & Rousseau, 2011; Ghosh et al., 2011).

Regarding the effects of adding MB on intensifying the interfacial crystallisation illustrated in Figure 6.1, which was considered plausible to observe at the beginning of this study, no significant evidence was observed, except for the promotion of TAG crystallisation in the continuous TAG phase and close to the water phase perimeter. A possible reason may be low adsorption of MB at the W/O interface in cooperation with PGPR membranes, whose adsorbability exceeds that of MB.

Not to be overlooked, is that should a liquidus interstitial region exist between either the Pickering stabilised TAG (Rousseau & Hodge, 2005) and or (not discounting) Pickering surface-active MAG (MB) crystals (4.2.3; 4.2.8), this may partially explain previously observed visco-elastic behaviour (4.0); caused by the liquidus PGPR. A *Moringa oleifera* based MAG (currently not measured (6.3.3)) having unusual miscibility (Ueno et al., 1994; Sato 1998), could influence liquidus TAG / MAG structure (4.0) at the interstitial region at nanoscopic dimensions (Rousseau et al., 2005).

The polymorph behaviour of Pickering TAG and MAG (Malkin, 1954) crystalline material has been examined but requires more research. Possibly a relationship exists between their form, quantity and quality. Hodge and Rousseau (2005) found in their study of W/O emulsions that TAG based on hydrogenated canola was more resistant to destabilisation in the β-form (Basso et al., 2010). When comparing the relative β intensity (R β) within W/O emulsions, Shiota et al. (2011), using TAG blends prepared with MAG based on palmitic, stearic, and behenic acid, found that the influence of the behenic based MAG resulted in the lowest (R β) within W/O emulsions.

It is known that distilled MAG crystallise into metastable α-crystal, then transform into higher melting β-form. Metastable β'-form does not occur in commercial MAG. On cooling, a solid state transition occurs to sub-α (Krog, N., Danisco / DuPont TP18-1e). The behaviour of MAG / TAG in hydrophobic solutions is shown not to be the same or similar as in water, because hydrogen bonding of glycerol groups would be different (Chen et al., 2009). The lamellar phase

structure appears more ordered at a low temperature, where a sub-α form result in rigidity of lamellar bilayers (Chen et al., 2009). It is not known if assumed low temperature sub-α form seen in macrobeam SR-XRD patterns of PGPR + MB (CRY110) emulsion (Wassell et al., 2012) could also explain interfacial (4.0) and macroscopic (5.0) visco-elastic properties (Rousseau & Hodge 2005; Bergenståhl 2008). These areas require more research.

A limitation of the synchrotron radiation macrobeam and microbeam X-ray diffraction studies of the interfacial crystallisation of TAG based W/O emulsions could be the actual TAG volume. Initially, W/O emulsions with TAG contents of 18% and 25% were prepared, but were difficult to measure and inconclusive. The TAG content was raised to 35%. A solution to achieving meaningful measurements at lower TAG contents could likely provide clearer data. A potential weakness is perhaps that the microbeam needs sufficiently strong intensity to achieve refraction of a lyotropic liquid crystal, because the radiation time must be limited to approximately 5 seconds to avoid thermal damage. A more intense method (e.g Diamond Synchrotron) to examine the interface may reveal vital information about the liquidus region between any Pickering TAG / MAG crystal.

It should be noted that a *Moringa oleifera* based MAG in a 35% TAG W/O emulsion (5.4) was assembled for μ-SAXD measurement, but not analysed (6.3.3) due to confidentiality (WIPO applications: Wassell et al., 2010a; 2012; 2012a; 2012b; 2012c; 2012d; 2012e). Analysis of this sample would still be ideal in order to compare with those measured previously (Wassell et al., 2012).

7.0 General Discussion, Final Conclusions and Recommendations

7.1 Multidisciplinary Approach to Structuring in Reduced Triacylglycerol (TAG) Based Systems

Since the commencement of this thesis, both a literature and critical review (Wassell & Young 2007; Wassell et al., 2010a) have clearly shown the need for a multiple focus approach to solving some structuring problems of TAG based water – oil systems, specifically those already characterised as reduced and low fat.

A simultaneous study by Vereeken et al. (2010), looked at complex mixtures of both saturated and unsaturated MAG in the presence of both liquid and solid TAG and investigated their application (designed to contain maximum 30% total SAFA). In anhydrous systems, they found that mixtures of C16:0 / C22:0 MAG did not differ from a C16:0 / C18:0 MAG, and explained this might be attributed to non-ideal phase behaviour (Vereeken et al., 2009). However, water tended to have a decreasing effect on the SFC, which they attributed to hydrophobicity of the fatty acid complex. Their investigation varied the water concentration between 0% and 20% (Vereeken et al., 2010), which are characterised between anhydrous bulk fats to full fat margarines.

In contrast, this study investigated the effects of a MAG that contains a significant content of C22:0 in anhydrous bulk fats (3.0; 4.0; 5.0). It then investigated the same effect in emulsions with aqueous phase contents initially at 82% (1.5), then between 35% and 65% (5.0; 6.0). These emulsions systems have inherently reduced total TAG (containing SAFA) and are more complex to stabilise. Further TAG reduction whilst avoiding impact on structure and functional properties (Wassell & Young 2007; Wassell et al., 2010a) is more problematic where a food is already regarded as low saturated (1.4; 1.6; 1.7).

This study has investigated the effects of emulsifier on the physical behaviour, both to the TAG, and at the TAG/water interface and shows new information

about interfacial properties to be of considerable importance (Wassell et al., 2010a; 2012; 2012a; 2012b; 2012c; 2012d; 2012e; Bech et al., 2013).

In contrast to other studies (1.6; 1.7), this study (Wassell & Young 2007; Wassell et al., 2010a) has shown that C22:0 rich MAG, or its significant inclusion, has a pronounced effect on crystallisation (Wassell et al., 2010b; 2012; Young et al., 2008) and interfacial kinetics (4.0). New interfacial measurements clearly demonstrated an unusual surface-interactive relationship of longer chain MAG compositions, both with and without PGPR in W/O emulsions and anhydrous TAG systems. This is thought to partially explain textural behaviour observed in multiple application trials (1.5; 5.0; 6.0; Wassell et al., 2010b; 2012; Young et al., 2008).

Results show that the influence on interfacial tension by a single MAG emulsifier is more pronounced with long-chain MAG than with medium-chain MAG (4.0). The relative decrease in interfacial tension upon decreased temperature, was greater the longer the chain length. While this confirms studies by others (Krog & Larsson 1992), this thesis moreover, now provides new additional insight, because bulk and interfacial rheology showed that the presence of C22:0 fatty acids have a pronounced effect on both G' and G''. This effect was more manifest in the presence of an aqueous phase.

This study has considered rheology and surface-interactive behaviour of mixed surfactant systems, specifically the affect of typical co-emulsifiers commonly used in low TAG spread (<41%) applications. Results show that mixtures of PGPR and MAG rich in C18:1 / 18:2 and C16:0 / C18:0 did not decrease the interfacial tension compared with PGPR alone. Only a composition containing MAG with significant proportion of C22:0 impacted interfacial tension.

An emulsifier composition of PGPR and a C22:0 based MAG (CRY110) resulted with decreasing tension, commencing from ~20°C and is initially dominated by PGPR. Then, through interfacial reorganisation, the surface is rapidly dominated

by C22:0 fatty acids. This resulting interactive behaviour may partially explain increased textural resilience (thickening) due to viscoelasticity (4.0; 5.0).

Results from interfacial tensiometry measurements on a *Moringa oleifera* based MAG showed unusual decreased interfacial tension behaviour not dissimilar to PGPR. All other tested MAG (excluding a C22:0 based MAG), irrespective of their fatty acid compositions resulted in higher interfacial values across the measured temperature spectrum (50°C to 5°C). The explanation for this is likely linked to maintaining a wide and diverse fatty acid profile (5.11) of the original TAG source (*Moringa oleifera*). Practically, it was found that a high temperature distillation of *Moringa oleifera* TAG to preserve its longer chain fatty acids (decreased mono- %), when tested in 35% and 40% TAG W/O emulsions, resulted with decreased DSD when compared to a low temperature distillation (higher mono- %), which had a more narrow fatty acid profile (5.11).

Critically, an essential element of the multidisciplinary approach was to cross-examine and verify results in real multi component systems and under process conditions relevant to the actual food product (Johansson, 1994; Mazzanti et al., 2005; Rousseau 2000). Only by applying these results in real products, could "proof of concept" be achieved (McClements 2007).

Application studies of *Moringa oleifera* based MAG in low TAG (35% - 41%) W/O emulsions, resulted with high emulsion stability without a co-surfactant (PGPR) 4.0; 5.0)). These results provided positive verification of the interfacial and rheological analyses (4.0, 5.6). This may offer technological advantage, where under certain circumstances, a co-emulsifier (PGPR) can be avoided (1.7).

When tested separately, both a *Moringa oleifera* based MAG and PGPR seemed to have similar influence on the crystallisation kinetics of the particular anhydrous TAG systems (5.3; 5.5; 5.6). A combination of either of these two emulsifiers with a behenic rich (CRY110) MAG, resulted in enhanced gelation onset behaviour, which was dependent on the rate of thermal treatment and selected solvent (5.5; 5.6).

Additional application studies confirmed the potential to mimic the fatty acid composition of *Moringa oleifera* TAG (5.3; 5.10), meaning restriction of supply and dependence on a particular TAG source is now reduced (Bech et al., 2013).

The combination of several analytical techniques was considered invaluable. Pilot studies (1.5; Appendix B; C; D) did not reveal a complete representation of the influence on crystallisation of a C22:0 based MAG. By utilisation of the UVP-PD technique, it has been possible to examine the effect of a C22:0 based MAG in an anhydrous TAG system whilst in a dynamic non-isothermal condition (3.0). This non-invasive technique can conclusively validate structural events.

Combined interfacial tension and rheological measurements, to assess both elastic and viscous moduli in the bulk model systems have conclusively revealed strong interactions between PGPR and a C22:0 rich (CRY110) MAG (4.0; 5.6). To explain more fully why this interaction occurs, the Macrobeam and SR-μ-SAXD X-Ray (6.0) was utilized. This method revealed that addition of a C22:0 based MAG promoted TAG crystallisation as observed by DSC analysis. This was confirmed with POM observations, which indicated that C22:0 rich MAG eliminated the formation of large crystal aggregates, resulting in the likely formation of tiny Pickering TAG / MAG crystals (6.0).

It is thought that PGPR, which has liquidus fatty acid moieties at the temperatures examined in the μ-SAXD measurements, may have certain molecular interactions with TAG molecules at the W/O interface to cause a degree of interfacial crystallisation. The addition of a MAG containing long-chain C22:0 may strengthen the interfacial crystallisation (4.3.8) of liquidus interstitial crystals near the aqueous droplets (Shiota et al, 2011).

The following sections now examine the implications of several of these findings, summarise the key results and then discuss implementation of innovative outcomes from this study and future use.

7.1.1 Implications for Pickering Stabilisation

Studies and outcomes in this thesis (1.4; 1.5; 4.0; 5.0; 6.0; Wassell et al., 2012b), collectively now provide new insight concerning the effects of Pickering surface-active MAG (with significant content of >C20:0) in reduced and low TAG W/O emulsions. The low TAG W/O emulsions measured in this research had considerably decreased bulk TAG network. Network stabilisation would have had less influence on interfacial stabilisation. In this situation, it is likely that Pickering surface-active TAG / MAG crystals become strongly mobilised to the interface due to dielectric interaction.

It is concluded that the presence of surface-active MAG crystals are strongly linked to increased fatty acid chain length, which influence viscoelasticity (4.0; 5.0; 6.0). With the presence of a co-emulsifier e.g. PGPR or additional MAG (4.0; 5.0; 6.0), this effect is enhanced. Should crystal structures exist as smaller, liquidus and or nano-arrays, these may induce and also account for interfacial visco-elastic behaviour, stabilising the W/O emulsion (Johansson et al., 1995; Rousseau, 2000).

7.1.2 Interfacial Stabilisation in a Metastable Region

The bi-functional behaviour of e.g. a *Moringa oleifera* based MAG might be attributed to the miscibility (Ueno et al., 1994) of its fatty acids: ~30% range of saturated fatty acids (SAFA) including C16:0, C18:0, C20:0, C22:0, C24:0 of which ~10% is >C20:0 coupled with ~70% of C18:1 (5.0). The textural resilience measured in the low TAG (<41%) W/O emulsions is considered to be the effect of strengthened interfacial film properties (4.0) at the water-oil surface (1.5; 5.0). It is thought that SAFA is likely to be more surface-active in a *Moringa oleifera* based MAG, whose proportion of >C20:0 is ~10% (Krog 1992). In this situation, the presence of long-chain SAFA may cause insoluble / metastable microcrystalline arrangements through polar interaction with any proximate liquidus fatty acids,

causing a steric, interstitial stabilised interface to be formed (Johansson, Bergenståhl & Lundgren, 1995).

Subsequent SR-XRD synchrotron (6.0) studies or more powerful analysis could provide deeper insight to characterise a metastable phase / interstitial region. It could also help to explain further details, behind the behaviour of Pickering MAG (7.1.1) crystals (linked to increased chain length), becoming viscous and sticky at their surfaces by adsorbing liquidus PGPR (Mullin, 1993). The structure of this combined system in the presence of an aqueous phase is still not known (Dedinaite & Campbell 2000). As a single system, the results suggested that a *Moringa oleifera* based MAG, could perform a similar function.

7.1.3 Dendrite Behaviour

Through a multidisciplinary approach, dendrite crystal structures were observed (2-D) microscopically (5.3; 5.5) in the bulk phase, leading to increased surface area of the TAG crystal structure. This is possibly attributed to the effect of the adsorbed emulsifier enhancing dendrite behaviour. If this situation occurs in the presence of water and oil, this could also be another explanation for the comparative thickening (textural resilience) observed in the W/O emulsions (5.4; 5.7, 5.11), where increased adhesion is probably caused by increased polarity (Rousseau 2002). The additional sites of contact on the wetted TAG crystal due to the presence of adsorbed emulsifier (forming surface active crystals) and or co-emulsifier e.g. *Moringa oleifera* based MAG or PGPR combined with CRY110 (5.6), may also explain observed rheological and interfacial behaviour (4.0).

7.2 Key Findings:

Moringa oleifera based MAG compared to PGPR resulted in similar interfacial tension values (4.0).

Strong interactions occur between a behenic rich (CRY110) MAG combined with PGPR and results in direct influence of interfacial and viscoelasticity (4.0; 5.6).

Separately, the physical effect of a *Moringa oleifera* based MAG to form dendrite structures, is very similar to the effect of PGPR (5.3; 5.5). When compared, the rheological behaviour observed under forced cooling conditions in two different TAG solvents, showed that a *Moringa oleifera* based MAG resulted in almost identical gelation patterns to PGPR, (5.6).

The influence of a behenic rich (CRY110) MAG combined with PGPR resulted in the formation of dendrite structures. The same result occurred with a behenic rich (CRY110) MAG combined with *Moringa oleifera* based MAG (5.3; 5.5). Forced cooling showed PGPR enhanced the rate of gelation when combined with a behenic rich (CRY110) MAG (5.6).

A *Moringa oleifera* based MAG can successfully stabilise low TAG (35% - 41%) WO emulsions without PGPR (5.4; 5.7; 5.8; 5.11). Moreover, a *Moringa oleifera* based MAG is distinctly more functional and contrasted in performance to a behenic rich (CRY110) MAG used as a single emulsifier (5.7; 5.8). Maintaining the whole fatty acid composition, close to the original (*Moringa oleifera*) TAG profile is shown to be more functional (5.10., 5.11; 5.12).

7.3 Novelty and Future Context

The literature (1.4; 1.6) shows health and sustainability have become important reasons for finding alternative lipid materials for the function of structuring / stabilising food products (Beaglehole et al., 2011; Bradley 2012; Carmichael 2011; Gortmaker et al., 2011; Menaa et al., 2013; Wang et al., 2012; Wassell & Young 2007; Wassell et al., 2010a;). The reformulation of reduced fat systems is not simple (Pothiraj et al., 2012; Wassell et al., 2010a; Windwood, 2011).

While low fat emulsion technology is not new, the use of one or several novel applications of long-chain e.g. behenic (C22:0) based emulsifiers to low or reduced TAG W/O emulsions was not found in the literature (1.4; 1.6). This novel research aimed to observe rheological and interfacial crystallisation behaviour in W/O emulsions and anhydrous bulk TAG (Wassell et al., 2010b; Young et al., 2008; 4.0; 5.0; 6.0). It has discovered potential advantages for the inclusion of certain concentrations of saturated long chain fatty acids for stabilising and emulsifying low TAG (<41%), W/O emulsions and dispersions. A study of *Moringa oleifera* as a new TAG material has resulted in the development of a MAG, which is a novel approach to stabilising TAG based W/O emulsions or dispersions (Wassell et al., 2012a; 2012b; 2012c; 2012d; 2012e).

In consideration of regulatory requirements (FAO/WHO 2011) of novel materials, this research has also resulted in novel use of MAG compositions from traditional sources, that may incidentally mimic a *Moringa oleifera* based MAG (Bech et al., 2013). Significantly, with or without a co-emulsifier, these novel solutions provide new possibilities and function with the option of avoiding the use of lipid materials which are either palm TAG based and/ or hydrogenated (Wassell & Young 2007; Wassell et al., 2010a).

From this multidisciplinary study, there are resulting inventions (Patents) that contribute towards consumer requirements for foods that satisfy the current and future demand for natural, sustainable sources of raw materials. These are briefly described:-

WO2012168722: **A novel, bi-functional, non-hydrogenated, monodiglyceride** (*Moringa oleifera* MAG).

WO2012168727: A bi-functional non-hydrogenated emulsifier **to aid crystallisation** onset with or without a co-emulsifier.

WO2012168726: A bi-functional non-hydrogenated emulsifier replacement for use in **water-in-oil emulsions and described as low fat**, so as to replace or reduce the addition a co-emulsifier e.g. PGPR.

WO2012168723: A **food or non-human feed dispersion** stabilised with a novel, bi-functional, non-hydrogenated, monodiglyceride

WO2012168724: A bi-functional non-hydrogenated emulsifier replacement for use in **high or reduced fat water-in-oil emulsions**.

WO2013050944: A novel fatty acid **composition** comprising monodiglycerides with minimum C22:0 content of 4.5wt%.

Practical application of these inventions may also potentially extend to areas such as: pharmaceutical products, cosmetics and bio-fuel.

7.4 Recommended Research

7.4.1 Additional Measurements

Further research should include a series of rheological and interfacial analyses (4.0), initially to measure MAG rich in C20:0 and C24:0. These should be tested with the addition of a co-emulsifier e.g. PGPR, or *Moringa oleifera* based MAG (or similar composition). Also to consider, is the synthesis of novel MAG from natural non-hydrogenated TAG sources (1.6) such as milk TAG fractions, combined with natural sources of saturated long chain fatty acids from e.g. Rambutan (*Nephelium lappaceum L.*), Sirisompong, Jirapakkul & Klinkesorn, 2011)).

Despite MAG structures having radically different fatty acid configurations (7.1.2), binary MAG mixtures are apparently still miscible (Ueno et al., 1994; Sato 1998). A rheological examination (4.0) of binary ratio's of MAG, analysed using software able to accommodate changing densities (refer to 4.3.3), may reveal undiscovered transition temperatures (Ueno et al., 1994). Software development is necessary for method. Such investigations will give more insight into the interfacial behaviour of saturated longer chain fatty acids and their potential use as surface interactive co-emulsifiers.

7.4.2 High Internal Aqueous Phase Emulsions

Low TAG (<41%) W/O emulsions contain a large dispersed aqueous phase, whose composition cannot be overlooked (Keogh 2006; Rousseau et al., 2003), because ionic strength may influence hydrophilic stabilisation (Larsson et al., 1969). This aspect was not within the scope of this thesis. Scherze et al (2006), suggest electrolytes may have a bearing on the rigidity of the interfacial film, because in TAG (70%) based W/O emulsions they found PGPR in the presence of NaCl

seemed to stiffen the interface. Further research may demonstrate this is caused by influence to the polar region of the PGPR molecule.

Research from studies within other disciplines may bring insight into high internal phase emulsions (Peng et al., 2009) where the influence of the droplet curvature must be considered (Shinohara et al., 2008). In turn dielectric behaviour may possibly influence mobility of surface-active crystals to the interface stronger than van der Waals forces where there is decreasing bulk TAG network, as in low (<41%) TAG emulsions (Goubran & Garti 1988). These factors could also have implications in more complex emulsions e.g. O/W/O or W/O/W.

Furthermore, and in the context of earlier discussion / conclusions (7.1; 7.1.1; 7.1.2), it must also be recognised that studies have shown the interfacial aqueous region continues to be a rich area for research (Berkowitz & Vácha 2012; Qiao, Sega & Holm, 2012).

7.4.3 Interactions at the Interfacial Region

Interactions have been observed by application of several MAG characterised (3.0; 4.0; 5.0) by their intrinsic fatty acid profiles (Wassell et al., 2010a). It would be beneficial to understand the impact of hydrophobicity on the glycerol region (Chen et al., 2009) of a MAG due to any modifications of its hydroxyl groups coupled with longer chain length fatty acids (Valentin & Mouloungui 2013).

7.5 Concluding Remarks

A multidisciplinary approach, encompassing wide ranging methods of analysis and novel solutions (2.0; 3.0; 4.0; 5.0; 6.0), has provided new information on structuring in reduced TAG based systems and has specifically enhanced current understanding of structuring in low TAG W/O emulsions.

With reference to Figures 6.1 and 6.5 (6.0), subsequent studies regarding emulsion stabilisation should give attention to the interstitial region. Figure 7.1 shows some important elements to consider at the W/O interface. In addition, there are questions regarding the interrelationship of aspects such as super-cooling / shear, time / adsorption development, crystal structure / morphology and aqueous phase behaviour at the interfacial region, which are areas for further research.

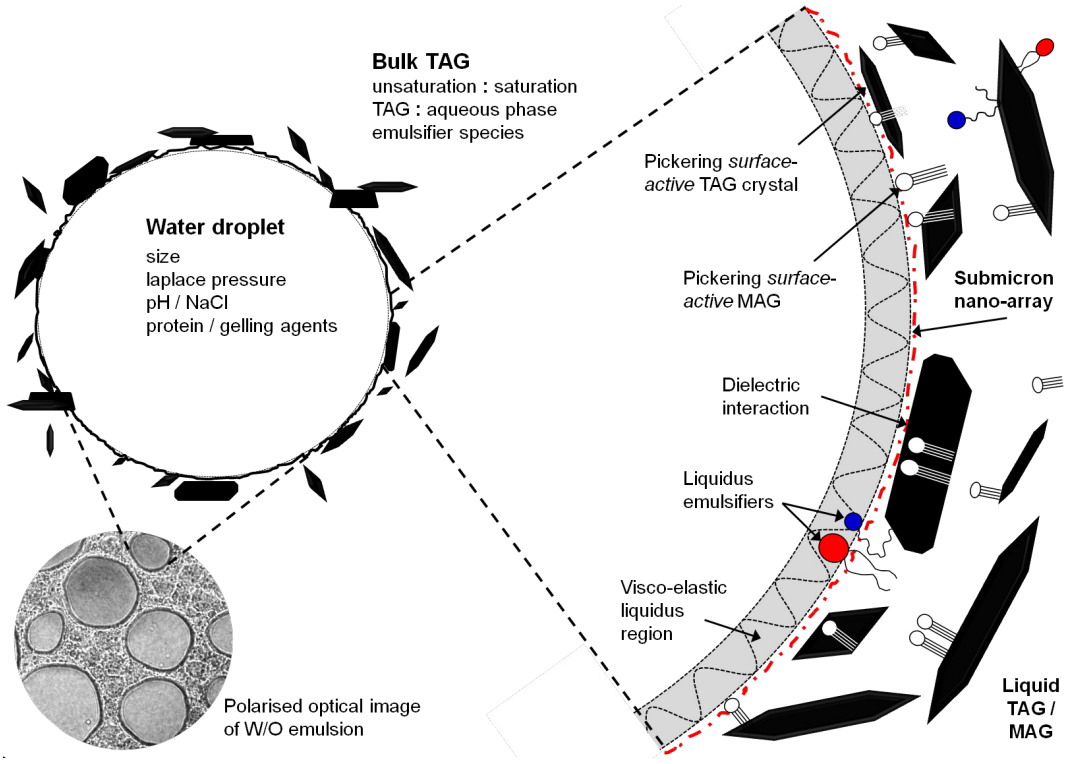

Figure 7.1 A schematic diagram of important elements at the interfacial region

References

Abdulkarim, S.M., Long, K., Lai, O.M., Muhammad, S.K.S., Ghazali, H.M., (2005). Some physico-chemical properties of Moringa oleifera seed oil extracted using solvent and aqueous enzymatic methods. Food Chemistry. 93, 253–263.

Annon. (2005). GRAS Exemption Notification. PGPR - Polyglycerol polyricinoleic acid for Use in Margarines, Low Fat Margarines, Spreads, Creamers and Dairy Analogs. Office of Premarket Approval, Center for Food Safety and Applied Nutrition. Food and Drug Administration.

Anwar, F., and Rashid, U. (2007). Physico-Chemical Characteristics of *Moringa Oleifera* and seeds and Seed oil from a wild provenance of Pakistan, Pak. J. Bot., 39 (5): 1443-1453.

Arima, S., Ueji, T., Ueno, S., Ogawa, A. and Sato, K. (2007). Retardation of crystallisation-induced destabilization of PMF-in-water emulsion with emulsifier additives. Colloids and Surfaces B: *Biointerfaces*, 55, 98–106.

Arima, S., Ueno, S., Ogawa, A. and Sato, K. (2009). Scanning microbeam small-angle X-ray diffraction study of interfacial heterogeneous crystallisation of fat crystals in oil-in-water emulsion droplets. Langmuir, 25, 9777–9784.

Asano, Y. and Sotoyama, K., (1999). Viscosity change in oil/water food emulsions prepared using a membrane emulsification system. Food Chemistry. 66: 327-331.

Awad, T. and Sato, K. (2001). Effects of Hydrophobic emulsifier on crystallisation behaviour of palm mid-fraction in oil-in-water emulsion. JAOCS, 78, 837–842.

Awad, T. and Sato, K. (2002). Acceleration of crystallisation of palm kernel oil in oil-in-water emulsion by hydrophobic emulsifier additives. Colloids and Surfaces B: Biointerfaces, 25, 45–53.

Awad, T.S., Moharram, H.A., Shaltout, O.E., Asker, D. and Youssef, M.M. (2012). Applications of Ultrasound in Analysis, Processing and Quality Control of Food: A Review, Food Research International. 48 (2), 410-427.

Basheva, E.S., Gurkov, T.D., Ivanov, I.B., Bantchev, G.B., Campbell, B., and Borwankar, R.P., (1999). Size Dependence of the Stability of Emulsion Drops Pressed against a Large Interface. Langmuir. 15: 6764-6769.

Basso, R.C., Ribeiro, A.P.B., Masuchi, M.H., Gioielli, L.A., Gonçalves, LA. G., Santos, A.O., Cardoso, L.P. and Grimaldi, R. (2010). Tripalmitin and monoacylglycerols as modifiers in the crystallisation of palm oil, Food Chemistry, 122, 1185–1192.

Basiron, Y. (2005). Palm oil in: Bailey's, Industrial Oil and Fat Products, 6th ed. (edited by F. Shahidi). New York: John Wiley & Sons.

Bastida-Rodríguez, J., (2013). The Food Additive Polyglycerol Polyricinoleate (E-476): Structure, Applications, and Production Methods, ISRN Chemical Engineering, vol. 2013, Article ID 124767, 21.

Beaglehole, R., et al., (2011). Priority actions for the non-communicable disease crisis. The Lancet, 377, (9775) 1438 – 1447.

Bech, A.T., Farmer, M., Forrest, B.A., Wassell, P., Young, N.W.G., DuPont Nutrition Biosciences APS, (2013). *Composition*. World Intellectual Property Organisation No. WO2013050944.

Bech, A.T., Wassell, P. and Hornholt, M. (2008). Method of preparing non-hydrogenated emulsifiers. Patent: WO/2008/059220.

Bell, A., Gordon, M.H., Jirasubkunakorn, W. and Smith, K.W. (2007). Effects of composition on fat rheology and crystallistation. Food Chemistry, 101, 799–805.

Ben-Jacob, E. and Garik, P., (1990). The formation of patterns in non-equilibrium growth. Nature. 343. 523-530.

Bergenståhl, B. (2008). Physicochemical Aspects of an Emulsifier Functionality. In: G.L. Hasenhuettl and R.W. Hartel (eds.), Food Emulsifiers and Their Applications. 2nd ed. Springer, New York.

Berger, K.G. and Idris, N.A. (2005). Formulation of zero-*trans* acid shortenings and margarine and other food fats with products of the oil palm. Journal of the American Oil Chemists Society, 82, 775–782.

Berkowitz, M.L. and Vácha, R., (2012). Aqueous Solutions at the Interface with Phospholipid Bilayers. Accounts of Chemical Research, 45, 74-82.

Birkhofer, B., Jeelani, S.A.K., Windhab, J., et al. (2008). Monitoring of fat crystallisation process using UVP-PD technique. Flow Measurement and Instrumentation, 19, 163–169.

Bockisch, M. (1998). Fats and Oils Handbook. Champaign, AOCS Press, 838.

Boodhoo, M.V., Humphrey, K.L. and Narine, S.S. (2009). Relative hardness of fat crystal networks using force displacement curves. International Journal of Food Properties, 12, 1129–1144.

Bot, A., den Adel, Regkos, C., Sawalha, H., Venema, P., and Flöter, E. (2011). Structuring in β-sitosterol + γ-oryzanol-based emulsion gels during various stages of a temperature cycle. Food Hydrocolloids 25, 639-646.

Bot, A., Veldhuizen, Y.S.J., del Adel, R. and Roijers, E.C. (2009). Non-TAG structuring of edible oils and emulsions. Food Hydrocolloids, 23, 1184–1189.

Boyd, J.V., Krog, N., Sherman, P., (1976). Comparison of Rheological Studies on Adsorbed Emulsifier Films with X-Ray Studies of the Bulk Solutions, in: A.L. Smith, edit., Proceedings of a Symposium by Society of Chemical Industry, Brunel University, September 16-18, 1974., Theory and Practice of Emulsion Technology., Academic Press. 123-133.

Boyd, J.V., Parkinson, C. and Sherman, P. (1972). Factors Affecting Emulsion Stability, and the HLB Concept. J. Coli. Interface Sci. 41, 2, 359-370.

Bradley, P. (2012). Diet composition and obesity. The Lancet, 379, (9821), 1100.

van Camp, D., Hooker, N.H., and Lin, C.J., (2012). Changes in fat contents of US snack foods in response to mandatory *trans* fat labelling. Public Health Nutrition. 15, (6), 1130-1137.

Carmichael, H. (2011). Palmed off? Chemistry & Industry. Society of Chemical Industry, (7) 22-24.

Cerdeira, M., Martini, S., Hartel, R.W. and Herrera, M.L. (2003). Effect of sucrose ester addition on nucleation and growth behaviour of milk fat-sunflower oil blends. Journal of Agricultural Food and Chemistry, 51, 6550–6557.

Cerdeira, M., Pastore, V., Vera, L.V., Martini, S., Candal, R.J. and Herrera, M.L. (2005). Nucleation behaviour of blended high-melting fractions of milk fat as affected by emulsifiers. European Journal of Lipid Science and Technology, 107, 877–885.

Cerdeira, M., Martini, S., Candal, R.J. and Herrera, M.L. (2006). Polymorphism and growth behaviour of low-*trans* fat blends formulated with and without emulsifiers. JOACS, 83, 489–496.

Chakraborty, M., C. Bhattacharya, and S. Datta, (2003). Effect of drop size distribution on mass transfer analysis of the extraction of nickel(II) by emulsion liquid membrane Colloids and Surfaces A: Physiochem. Eng. Aspects. 224: 65-74.

Charteris, W.P. (2007). Physicochemical aspects of the microbiology of edible table spreads. International Journal of Dairy Technology, 48, 87–96.

Chen, C.H., Van Damme, I., Terentjev, E.M., (2009). Phase Behavior of C18 monoglyceride in hydrophobic solutions, Soft Matter, 5, 432-439.

Chrysan, M.M. (2005). Margarines and Spreads in: Bailey's, Industrial Oil and Fat Products, 6th edn (edited by F. Shahidi). New York: John Wiley & Sons.

Claesson, P. M., Dedinaite, A., Bergenståhl, B., Campbell, B. and Christenson, H. (1997). Langmuir, 13, 1682.

Corke, H. (2007). “Speciality Cereal and Noncereal Starches.” In: The RVA Handbook , Eds. Crosbie, G.B., and Ross, A.S. AACC International, USA: 49-62.

Dassanayake, L.S.K., Kodali, D.R. and Ueno, S. (2011). Formation of oleogels based on edible lipid materials, Current Opinion in Colloid & Interface Science, 16, (5) 432-439.

Dedinaite, A. and Campbell, B. (2000). Interactions between Mica Surfaces across Triglyceride Solution Containing Phospholipid and Polyglycerol Polyricinoleate, Langmuir (16), 2248-2253.

Delamarre, S. and Batt C.A. (1999). Review – The microbiology and historical safety of margarine. Food Microbiology, 16, 327─333.

Dierig, D.A. and Thompson, A.E., (1993). Vernonia and Lesquerella potential for commercialization. In: J. Janick and J.E. Simon, Editors, New Crops. Proceedings of the Second National Symposium. New Crops: Exploration, Research, Commercialization Indianapolis, Ind., October 6–9, 1991, John Wiley & Sons, Inc., New York, 362–367.

Dierig, D.A., Thompson, A.E., and Nakayama, F.S., (1993). Lesquerella commercialization efforts in the United States. Ind. Crops Prod. 1, 289–293.

Drewnowski, A. and Almiron-Roig, E. (2009). Human perceptions and preferences for fat-rich foods. In: Fat detection: taste, texture, and post-ingestive effects (edited by J.-P. Montmayeur & J. le Coutre). Boca Raton, Florida: CRC Taylor & Francis Group.

Drewnowski, A., Shrager, E.E., Lipsky, C., Stellar, E. and Greenwood, M.R.C. (1989). Sugar and fat: sensory and hedonic evaluations of liquid and solid foods. Physiology and Behavior, 45, 177–183.

Duffy, N., Blonk, H.C.G., Beindorff, C.M., Cazade, M., Bot, A. and Duchateau, G.S. (2009). Organogel-based emulsion systems, microstructural features and impact on in vitro digestion. JAOCS, 86, 733–741.

van Duijn, G., Dumelin, E.E. and Trautwein, E.A. (2006). Virtually *trans* free oils and modified fats. In: Improving the Fat Content of Foods (edited by C. Williams & J. Buttriss). p 490–507. Cambridge: Woodhead Publishing.

Euston, S.R. (2008). Emulsifiers in Dairy Products and Dairy Substitutes. In: G.L. Hasenhuettl and R.W. Hartel (eds.), Chp 7., Food Emulsifiers and Their Applications (2ed). Springer, New York.

Fahey, J.W., (2005). *Moringa oleifera*: A Review of the Medical Evidence for Its Nutritional, Therapeutic, and Prophylactic Properties. Part 1. Trees for Life Journal (1:5)., http://www.TFLJournal.org/article.php/20051201124931586

FAO/WHO. (2011). Codex Alimentarius Commission, STANDARD FOR NAMED VEGETABLE OILS. 210-1999.

Firestone D (2004). Official methods and recommended practices of the American Oil Chemists' Society, 5th ed. AOCS, Champaign. USA.

Flöter, E. and van Duijn, G. (2006). Trans-free fats for use in food. In: Modifying Lipids for Use in Food (ed. F.D. Gunstone). 429–443. Cambridge: Woodhead Publishing.

Ford, R. (2012). Weight-Watchers gets back into dairy spreads with Half Fat, The Grocer, William Reed Business Media Ltd., UK.

Foster, T., Russell, A., Farrer, D. et al. (2007). Instant emulsions. In: Food Colloids – Self Assembly and Material Science (edited by E. Dickinson & M. Leser). 413–422. London: RSC Publishing.

Fredrick, E., Foubert, I., De Sype, J. and Dewettinck, K. (2008). "Influence of Monoglycerides on the Crystallisation Behaviour of Palm Oil" Crystal Growth and Design. 8, (6) 1833-1839.

Food Standards Agency (FSA) (2008). Saturated fat and energy intake programme. http://www.food.gov.uk/multimedia/pdfs/satfatprog.pdf (last accessed 15th April 2013).

Fujiwara, K., Nagahisa, S., Yano, J., Ueno, S. and Sato, K. (2000). Kinetics of heterogeneous nucleation, of n-alcohol crystals from solution assisted by template thin films of monoacylglycerols and fatty acids. Journal of Physical Chemistry, 104, 8116–8123.

Garbolino, C., Bartoccini, M. and Floter, E. (2005). The influence of emulsifiers on the crystallization behavior of a palm oil-based blend. Eur J Lipid Sci Technol. 107, 616-626.

Garti, N., Binyamin, H. and Aserin, A. (1998). Stabilization of water-in-oil emulsions by submicrocrystalline α-form fat particles. J. Am. Oil Chem. Soc. 75, (12) 1825-1831.

Garti, N. and Remon, G. (1984). Relationship between nature of vegetable oil, emulsifier and the stability of w/o emulsion. J. Food Technology 19, 711-717.

Garti, N. and Sato, K. (2001). Crystallization Processes in Fats and Lipid Systems, Marcel Dekker, New York.

Ghosh, S. and Rousseau, D. (2009). Freeze–thaw stability of water-in-oil emulsions. Journal of Colloid and Interface Science 339, 91–102.

Ghosh, S and Rousseau, D. (2010). Effect of emulsifier type on interfacial crystallization in water-in-oil emulsions. Book of abstracts: Hiroshima International Forum on Functionality of Lipids. March 24-27, Hiroshima University, Higashi-Hiroshima, Japan.

Ghosh, S and Rousseau, D. (2011). Fat crystals and water-in-oil emulsion stability. Current Opinion in Colloid & Interface, 16 (5), 421-431.

Ghosh, S., Tran, T. and Rousseau, D. (2011). Comparison of Pickering and Network Stabilization in Water-in-Oil Emulsions. Langmuir, 27 (11), 6589–6597.

Gortmaker, S.L., Swinburn, B.A., Levy, D., Carter, R., Mabry, P.L., Finegood, D.T., Huang, T., Marsh, T. and Moodie, M.L. (2011). Changing the future of obesity: science, policy, and action. The Lancet. 378, (9793), 838-847.

Goubran, R.. and Garti, N. (1988). Stability of W/O Emulsions Using High Molecular Weight Emulsifiers, J. Dispersion Sci. Technol. 9 (2), 131–148.

De Graef, V., Dewettinck, K., Verbeken, D. & Foubert, I. (2006). Rheological behaviour of crystallizing palm oil. European Journal of Lipid Science and Technology, 108, 864–870.

Gülseren, I., and Corredig, M., (2012). Interactions at the interface between hydrophobic and hydrophilic emulsifiers: polyglycerol polyricinoleate (PGPR) and milk proteins, studied by drop shape tensiometry, Food Hydrocolloids. 29, (1) 193–198.

Halliday, J. (2011). The long, expensive, worthwhile road to reducing saturated fat, http://www.foodnavigator.com (Last accessed 15th April 2013).

Hartel, R.W. (2001). Crystallization in Foods. Gaithersburg: Aspen Publishers.

Hernqvist, L. (1988). Crystal structures of fats and fatty acids. In: Crystallisation and polymorphism of fats and fatty acids, Ed. by Garti N. and Sato K., Marcel Dekker Inc., New York. p. 97-137.

Himawan, C., Starov, V.M. and Stapley, A.G.F. (2006). Thermodynamic & kinetic aspects of fat crystallisation. Advances in Colloid and Interface Science, 122, 3–33.

Hoerr, C. W. (1960). Morphology of fats, oils and shortening. J. Am. Oil Chem. Soc., (37) 539-546.

Hodge, S.M. and Rousseau, D., (2005). Continuous-phase fat crystals strongly influence water-in-oil emulsion stability, J. Am. Oil Chem. Soc., 82, (3), 159–164.

Holmberg, K. (2002). Handbook of Applied Surface and Colloid Chemistry. New York, Wiley and Sons: 219.

Hughes, N., Marangoni, A.G., Wright, A.J., Rogers, M.A. and Rush, J.W.E. (2009). Potential food applications of edible oil organogels. Trends in Food Science & Technology, 20, 470–480.

ICI Americas Inc. (1980). The HLB System: A Time-saving Guide to Emulsifier Selection. Wilmington, DE 19897, USA.

Ishizuka, C., Ahmed, T., Arima, S. and Aramaki, K. (2009). Viscosity boosting effect of added ionic surfactant in nonionic wormlike micellar aqueous solutions. Journal of Colloid and Interface Science, 339, 511–516.

Janssen, P.W.M. and MacGibbon, A.K.H. (2007). Non-isothermal crystallisation of bovine milk fat. JAOCS, 84, 871–875.

Johansson, D. (1994). Colloids in Fat: The fat crystal as a functional particle. Ph.D. Institute for Surface Chemistry. Stockholm, Sweden and Department of Food Technology, Lund University, Lund, Sweden.

Johansson, D. and Bergenstahl, B. (1995). Sintering of fat crystal networks in oil during post-crystallization processes, J. Am. Oil Chem. Soc. 72, (8): 911-920.

Johansson, D., Bergenståhl, B. And Lundgren, E. (1995). Water-in-triglyceride oil emulsions. Effect of fat crystals on stability. J. Am. Oil Chem. Soc. 72 (8): 939-950.

Juriaanse, A.C. and Heertje, I., (1988). Microstructure of Shortenings, Margarine and Butter – A Review. Food Microstructure, Scanning Microscopy International. USA. Vol. 7, 181-188.

Katsuragi, T. (1999). Interactions between surfactants and fats. In: Physical Properties of Fats, Oils and Emulsifiers (edited by N. Widlak). 211–219. USA: AOCS Press.

Keogh, M.K., (2006). Chemistry and Technology of Butter and Milk Fat Spreads in: Advanced Dairy Chemistry. Vol 2: Lipids, 3rd edition. Ed. P.F. Fox and P.L.H. McSweeney, Springer, New York. 333-363.

Kodali, D.R. (2005). Trans fats – chemistry, occurrence, functional need in foods and potential solutions. In: Trans Fats Alternatives (edited by Dharma R. Kodali & G. List). USA: AOCS Press.

Kristensen, C.J. and Wassell, P. (2006). Diglycerides in palm oil – influence on crystallisation behaviour in production of puff pastry margarine. Poster and abstract from 4th Euro Fed Lipid Congress, 1–4 October 2006, University of Madrid (UCM), Madrid, Spain. 491.

Kristensen, C.J., Wassell, P., Mikkelsen, J.D. and Søe, J.B. (2005). Enzymatic treatment of oils. Danisco A/S, Denmark, International patent: WO/2005/066351.

Kristott, J.U. (1999). Physical Properties of Edible Vegetable Oils. In: LFRA Oils and Fats Handbook Series, Vol. 1. Vegetable Oils and Fats. (B. Rossell, ed.). Leatherhead Food RA, Leatherhead UK.

Krog, N. (1975). Interactions between water and surface active lipids in food systems. In: DUCKWORTH, R. B. (ed.). Water relations of foods. Academic Press: New York.

Krog N. (1977). Function of Emulsifiers in Food Systems, JAOCS. (54), 124-131.

Krog N. (1990). Thermodynamics of Interfacial Films in Food Emulsions. In: EI-Nokaly, M and Cornell, D (ed) Microemulsions and emulsions in food. 138-145.

Krog, N.J. (1997). 'Food emulsifiers and their Chemical and physical properties', in Friberg, S.E. and Larsson, K., (eds). Food Emulsions, Third Edition, Revised and Expanded. New York, Marcel Dekker. 141-188.

Krog N. (2001). Danisco A/S Technical Paper- TP-17., New Insights in Food Emulsions. Paper: South African Association for Food Science and Technology 16th Int. Congress. Durban Elangeni, 10-12 September, 2001 by: N. Krog, Danisco A/S, DK-8220 Brabrand, Denmark.

Krog, N. and Larsson, K. (1992). Crystallization at interfaces in food emulsions - a general phenomenon, Fat Sci Technol, 94, 55 – 57.

Krog, Niels and Vang Sparsø, Flemming (2003). Food Emulsifiers Their Chemical And Physical Properties. In Food Emulsion: - Edited by: Stig E. Friberg, Kåre Larsson and Johan Sjöblom.

Kyriakidis, N.B. and Katsiloulis, T. (2000). Calculation of iodine value from measurements of fatty acid methylesters of some oils: Comparison with relevant American Oil Chemists Society method, JOACS 77(12), 1235-1238.

Lalas, S. and Tsaknis, J. (2002). Characterization of Moringa oleifera Seed Oil Variety Periyakulam 1, J. Food Composition & Analysis, 15, 65-77.

Larsson, K., Lundquist, M., Stållberg-Stenhagen, S. and Stenhagen, E., (1969). Some Recent Studies on the Structural Arrangements of Lipids in Surface Layers and Interphases, Journal of Colloid and Interface Science, 29, 2, 268-278.

Lee, H.O., Jiang, T.L., Jiang, TS. and Avramdis, K.S. (1991). Measurements of Interfacial Shear Viscoelasticity with an Oscillatory Torsional Viscometer. J. Colloid Interface Sci. 146 (1) 90-122.

Lida, H.M.D.N. and Ali, R.M. (1998). Physicochemical characteristics of palm-based oil blends for production of reduced fat spreads. Journal of the American Oil Chemists Society, 75, 1625–1631.

Lin, C., He, G.H., Dong, C.X., Liu, H.J., Xiao, G.K. and Liu, Y.F. (2008). Effect of Oil Phase Transition on Freeze/Thaw-Induced Demulsification of Water-in-Oil Emulsions, Langmuir 24 (10) 5291–5298.

Lucas, L. and Rappeport, A. (2012). Fatty food clampdown is hard to swallow. Financial Times, June 8th, London.

Lupi, F.R., Gabriele, D., de Cindio, B., (2011a). Effect of Shear Rate on Crystallisation Phenomena in Olive Oil-Based Organogels. Food and Bioprocess Technology. Food Biopr Tech., 4: 111-17.

Lupi, F.R., Gabriele, D., de Cindio, B., Sánchez, M.C., Gallegos, C., (2011b). A rheological analysis of structured water-in-olive oil emulsions, Journal of Food Engineering, 107, (3–4), 296-303.

Madsen, J. (1987). Emulsifiers used in margarine, low calorie spread, shortening bakery compound and filling. Fett-Wiss. Technol., 89, 165-172.

Madsen, J. (1990). In D. Erickson, ed., World Conference Proceedings, Edible Fats and Oils Processing: Basic Principles and Modern Practices, American Oil Chemists' Society, Champaign, Illinois, 1990, 221–227.

Madsen, J. (2003). Fat Crystallography – A Review. Technical Paper: TP 1504-2e, Dansico A/S (DuPont).

Maleky, F., Campos, R. and Marangoni, A.G. (2007). Structural and mechanical properties of fats quantified by ultrasonics. JAOCS, 84, 331–338.

Malkin T. (1954). The polymorphism of glycerides. Prog Chem Fats Other Lipids; 2: 1-50.

Marangoni, A.G. (2005). Fat Crystal Networks. Marcel Dekker, New York.

Marangoni, A.G. (2007). A *trans*-free and low-saturate future? – A commentary Inform, 18(4), 281–283.

Marangoni, A.G., Acevedo, N., Maleky, F., Co, E., Peyronel, F., Mazzanti, G., Quinn, B., and Pink, D. (2012). Structure and functionality of edible fats. Soft Matter, 8, 1275-1300.

Marikkara, J.M.N. and Ghazali, H.M. (2011). Effect of Moringa Oleifera Oil Blending on Fractional Crystallization Behavior of Palm Oil. International Journal of Food Properties. 14 (5), 1049-1059.

Martini, S., Awad, T. and Marangoni, G., (2006). Structure and properties of fat crystal networks. In: *Modifying lipids for use in food*, Ed by Gunstone, F.D., Woodhead publishing, England. 142 – 169.

Marze, S. (2009). Relaxation processes of PGPR at the Water/Oil interface inferred by oscillatory or transient viscoelasticity measurements. Langmuir. 25 (20) 12066-12072.

Mazzanti, G., Guthrie, S.E., Sirota, E.B., Marangoni, A.G. and Idziak, S.H.J. (2003). Orientation and phase transition of fat crystals under shear. Crystal Growth & Design. 3, 721-725.

Mazzanti, G., Marangoni, A.G., Guthrie, S.E., Idziak, S.H.J., Sirota, E.B., (2005). Crystallisation of Bulk Fats Under Shear in: Soft Materials Structure and Dynamics. Dutcher, J.R. and Marangoni, A.G. (Eds). Marcel Dekker, N.Y.

McClements, D.J., (1999). Food emulsions. CRS Press. 89.

McClements, D.J. (2007). Critical review of techniques and methodologies for characterization of emulsion stability: in Food Science and Nutrition 47 (7), 611-649.

McClements, D.J. and Povey, M.J.W. (1987). Solid fat content determination using ultrasonic velocity measurements. International Journal of Food Science and Technology, 22, 491–499.

McClements, D.J. and Povey, M.J.W. (1988). Comparison of pulsed NMR and ultrasonic velocity techniques for determining solid fat content. International Journal of Food Science and Technology, 23, 159–170.

McClements, D.J. and Rao, J., (2011). Food-Grade Nanoemulsions: Formulation, Fabrication, Properties, Performance, Biological Fate, and Potential Toxicity. Critical Reviews in Food Science and Nutrition. 51, (4), 285-330.

McNeill, G.P. (2009). Saturated fats and the risk of heart disease. *inform*, AOCS, 20, 340–341.

Merchant, A.T., Kelemen, L.E., de Koning, L. et al. (2008). Interrelation of saturated fat, *trans* fat, alcohol intake, and subclinical atherosclerosis. American Journal of Clinical Nutrition, 87, 68–74.

Menaa, F., Menaa, A., Tréton, J. and Menaa, B. (2013). Technological Approaches to Minimize Industrial Trans Fatty Acids in Foods. Journal of Food Science. 78 (3), 377–386.

Metin, S. and Hartel, R.W. (2005). Crystallization of Fats and Oils, in: Bailey's, Industrial Oil and Fat Products, 6th ed (edited by F. Shahidi). New York: John Wiley & Sons.

Micha, R. and Mozaffarian, D. (2010). Saturated Fat and Cardiometabolic Risk Factors, Coronary Heart, J Lipids.

Mohammed, A.S., Lai, O.M., Muhammad, S.K.S., Long, K., and Ghazali, H.M. (2003). *Moringa oleifera*, Potentially a New Source of oleic acid-type oil for Malaysia. In: Investing in Innovation 2003, Vol 3: Bioscience and Biotechnology, ed. Mohd. Ali Hassan et al., pp 137-140. Universiti Putra Malaysia Press, Serdang Press, Selangor, Malaysia

Mojet, J. and Koster, E.P. (2005). Sensory memory and food texture. Food Quality and Preference, 16, 251–266.

Morris, V.J. (2011). Emerging roles of engineered nanomaterials in the food industry - Review Article. Trends in Biotechnology. 10, 509-516.

Mozaffarian, D., Jacobson, M.F., Greenstein, J.S. (2010). Food Reformulations to Reduce Trans Fatty Acids. The New England Journal of Medicine, 362, 2037-2039.

Moziar, C., De Man, J.M. and De Man, L. (1989). Effect of Tempering on the Physical Properties of Shortening, Can. Inst. Food Sci. Technol. J. 22: 238–242.

Mullin, J.W. (1993). Crystallisation, (3rd ed), Butterworth-Heinemann, Oxford., 293.

Nagarajan, R., Chung, S.I. and Wasan, D.T. (1998). Biconical Bob Oscillatory Interfacial Rheometer. J. Colloid Interface Sci. 204, 53-60.

Narine, S.S. and Marangoni, A.G. (1999). Relating structure of fat crystal networks to mechanical properties: a review, Food Research International, 32 (4), 227–248.

Narine, S.S and Humphrey K.L., (2004). A comparison of lipid functionality as a function of molecular ensemble and shear: Microstructure, polymorphism, solid fat content and texture. *Food Res Int,* 37, 28-38.

NICE, (2010). Public Health Guidance 25: Prevention of cardiovascular disease at population level. National Institute for Health and Clinical Excellence.

Oh, S.G. and Slattery, J.C. (1978). Disk and Biconical Interfacial Viscometers. Journal of Colloid and Interface Science. 67 (3) 516-525.

Ojijo, N.K.O., Neeman, I., Eger, S. and Shimoni, E. (2004). Effects of monoglyceride content, cooling rate and shear on the rheological properties of olive oil/ monoglyceride gel networks. Journal of Food Science and Agriculture, 84, 1585–1593.

Okamura, A., Wassell, P., Young, N.W.G., Bonwick, G., Smith, C., Almiron-Ruig, E., Sato, K., Ueno, S., (2011). Influence of Emulsifiers in W/O Low Fat Spreads for Fat Crystallization. (PC-007) Physical chemistry poster session. 9th Euro Fed Lipid Congress, Rotterdam, 18-21 September 2011.

Pandey, A., Pradheep, K., Gupta, R., Roshini Nayar, E., Bhandari, D.C., (2011). 'Drumstick tree' (*Moringa oleifera* Lam.), a multipurpose potential species in India, Genetic Resources and Crop Evolution. 58 (3), 453-460.

Pernetti, M., van Malssen, K.F., Flöter, E. and Bot, A. (2007). Structuring of edible oils by alternatives to crystalline fat. Current Opinion in Colloid & Interface Science, 12, 221–231.

Peng, J., Xia, H., Liu, K. et al. (2009). Water-in-oil gel emulsions from a cholesterol derivative Structure and unusual properties. Journal of Colloid and Interface Science, 336, 780–785.

Pérez-Martínez, J.D., Reyes-Hernández, J., Dibildox-Alvarado E., and Toro-Vazquez. J.F. (2012). Physical Properties of Cocoa Butter/Vegetable Oil Blends Crystallized in a Scraped Surface Heat Exchanger. *JAOCS*. 89, (2), 199-209.

Petrov, P., Miklavcic, S., Olsson, U., Wennerstroem, H. (1995). A Confined Complex Liquid. Oscillatory Forces and Lamellae Formation from an L3 Phase. Langmuir, 11 (10), 3928–3936.

Pickering, S.U. (1907). Emulsions. J. Chem. Soc., Trans. 91, 2001-2021.

Piller, D., (2011). Innovations in the "post-*trans*" era of fats and oils. *inform*. AOCS., 22(10), 647-648.

Podmore, J. (2008). Food applications of *trans* fatty acids. In: Trans Fatty Acids (edited by A. Dijkstra, R.J. Hamilton & W. Hamm). 203–217. London, UK: Blackwell Publishing.

Pothiraj, C., Zuñiga, R., Simonin, H., Chevallier S. and Le-Bail, A. (2012). Methodology assessment on melting and texture properties of spread during ageing and impact of sample size on the representativeness of the results. Journal of Stored Products and Postharvest Research. 3 (10), 137 – 144.

Povey, M.J.W. (2001). Crystallization of Oil-in-Water Emulsions, in: Crystallization Processes in Fats and Lipid Systems, (Eds). Garti N and Sato, K, Marcel Dekker, NY., 255-288.

Povey, M.J.W., Awad, T.S. Huo, R. and Ding, Y. (2007). Crystallization in Monodisperse Emulsions with Particles in Size Range 20-200nm. In: Food Colloids, Self Assembly and Material Science Eds E. Dickinson and M.E. Leser, RSC Publishing, London, 399-411.

Povey, M.J.W. and Challis, R.E. (2006). Applications of Ultrasound to Analysis/Quantitation of Dairy Lipids, Advanced Dairy Chemistry Volume 2 – Lipids, Third Edition Eds P.F. Fox and P.L.H. McSweeney, Springer, New York, 709-721.

Prakash, M.N.K. and Ramana, K.V.R. (2003). Ultrasound and its application in the food industry. Journal of Food Science and Technology, 40, 563–570.

van Putte, K. and van den Enden, J.C. (1974). Fully automated determination of solid fat content by pulsed NMR. *JAOCS*, 51, 316–320.

Qiao, B.F., Sega, M., Holm, C., (2012). Properties of water in the interfacial region of a polyelectrolyte bilayer adsorbed onto a substrate studied by computer simulations. Phys. Chem. Chem. Phys 14, 11425–11432.

Ray, Y.C., Lee, H.O., Jiang, T.L. and Jiang, TS. (1987). Oscillatory Torsional Interfacial Viscometer. J. Colloid Interface Sci. 119 (1) 81-99.

Riekel, C., Burghammer, M., Muller, M. (2000). Microbeam small-angle scattering experiments and their combination with micro diffraction. J Appl Cryst., 33: 421-423.

Rogers, M.A. (2009). Novel structuring strategies for unsaturated fats – meeting the zero-*trans*, zero-saturated fat challenge: A review. Food Research International, 42, 747–753.

Rosen, M., (1989). Emulsification by Surfactants in: Surfactants and Interfacial Phenomena (2nd edition) John Wiley & Sons, USA.

Rousseau, D. (2000). Fat crystals and emulsion stability - a review, Food Research International, (33), 3-14.

Rousseau, D. (2002). Fat Crystal Behavior in Food Emulsions, in: Physical Properties of Lipids. Edited by: Alejandro G. Marangoni, Suresh S. Narine. Marcel Dekker, New York. 219 – 264.

Rousseau, D., Hodge, S.M., Nickerson, M.T. and Paulson, A.T. (2005). Regulating the Beta prime to Beta polymorphic transition in food fats, JAOCS, 82 (1), 7-12.

Rousseau, D., Ghosh, S. and Park, H. (2009). Comparison of the dispersed phase coalescence mechanisms in different tablespreads. Journal of Food Science 74 (1), E1-E7.

Rousseau, D. and Hodge, S.M. (2005). Stabilization of water-in-oil emulsions with continuous phase crystals. Coll. Surf. A 260, 229–237.

Rousseau, D., Zilnik, L., Khan, R. and Hodge, S. (2003). Dispersed phase destabilization in table spread. J Am Oil Chem Soc. 80, 957-961.

Sahasranamam, U.M. (2005). EU Patent EP1552751 A1 Trans free hard structural fat for margarine blend and spread.

Sakamoto, M., Mauro, K., Kuiryama, J., Kouno, M., Ueno, S. and Sato, K. (2003). Effects of adding polyglycerol behenic acid esters on the crystallisation of palm oil. Journal of Oleo Science, 52, 639–645.

Sakamoto, M., Ohba, A., Kuiryama, J., Mauro, K., Ueno, S. and Sato, K. (2004). Influences of fatty acid moiety and esterification of polyglycerol fatty acid esters on the crystallisation of palm mid fraction in oil-in-water emulsion. Colloids and Surfaces, B, Biointerfaces, 37, 27–33.

Sato, K. (1989). Crystallization of fats and fatty acids. In: Crystallisation and polymorphism of fats and fatty acids, Ed. by Garti N. and Sato K., 227-260.

Sato, K. (1998). Newest understandings of molecular structures and interactions of unsaturated fats and fatty acids. Progress in Colloid & Polymer Science. 108: 58-66.

Sato, K. (2001). Crystallization behaviour of fats and lipids – a review. Chemical Engineering Science, 56, 2255–2265.

Sato, K., Ueno, S. (2011). Crystallization, transformation and microstructures of polymorphic fats in colloidal dispersion states. Curr. Opin. Colloid Interface Sci. 2011, 16, (5) 384-390.

Schaink, H.M., van Malssen, K.F., Morgado-Alves, S., Kalnin, D. and van der Linden, E. (2007). Crystal network for edible oil organogels: possibilities and limitations of the fatty acid and fatty alcohol systems. Food Research International, 40, 1185–1193.

Scherzea, I., Knotha, A., Muschiolika, G. (2006). Effect of Emulsification Method on the Properties of Lecithin- and PGPR-Stabilized Water-in-Oil-Emulsions. Journal of Dispersion Science and Technology, 27, (4), 427 – 434.

Shigemi, U. (2006). Patent: Plastic Oil and Fat Composition and Method for Producing the Same. Japan: Fuji Oil Co. Ltd. JP2006129819.

Shimada, A. and Ohashi, K. (2003). Interfacial and Emulsifying Properties of Diacylglycerol. Food Sci. Technol. Res., 9 (2).142- 147.

Shinohara, Y., Takamizawa, T., Ueno, S., Sato, K., Kobayashi, I., Nakajima, M. and Amemiya., Y. (2008). Microbeam X-ray diffraction analysis of interfacial heterogeneous nucleation of n-hexadecane inside oil-in-water emulsion droplets. Cryst. Growth Des. 8, 3123–3126.

Shiota, M., Iwasawa, A., Kotera, M., Konno, M., Isogai, T., Tanaka, L., (2011). Effect of Fatty Acid Composition of Monoglycerides and Shear on the Polymorph Behavior in Water-in-Palm Oil-Based Blend. J Am Oil Chem Soc. 88 (8) 1103-1111.

Siew, W.L. (2002). Understanding the Interactions of Diacylglycerols with Oils for Better Product Performance, Palm Oil Developments. No. 36. Malaysian Palm Oil Board. 6–12,

Siew, W.L. and Ng, W.L. (1990). Influence of diglycerides on the crystallization of palm oil. Journal of the Science of Food and Agriculture, 79, 722–726.

Silva, H.D., Cerqueira M.A., and Vicente, A.A., (2011). Nanoemulsions for Food Applications: Development and Characterization. Food and Bioprocess Technology. 5, (3), 854-867.

Sirisompong, W., Jirapakkul, W., Klinkesorn, U., (2011). Response surface optimization and characteristics of rambutan (*Nephelium lappaceum L.*) kernel fat by hexane extraction. LWT - Food Science and Technology, 44 (9), 1946–1951.

Siri-Tarino, P. W., Sun, Q., Hu, F. B., Krauss, R. M. (2010). Meta-analysis of prospective cohort studies evaluating the association of saturated fat with cardiovascular disease. Am J Clin Nutr., 1 – 12.

Smith, K.W., Bhaggan, K., Talbot, G. and van Malssen, K.F. (2011). Crystallization of Fats: Influence of Minor Components and Additives. JAOCS, 88, (8), 1085-1101.

Stender, S., Astrup, A. and Dyerberg, J. (2009). What went in When *trans* went out? New England Journal of .Medicine, 361, 314–316.

Stewart, M.F. and Hughes, E.J., (1972). Polyglycerol Esters as Food Additives, Process Biochemistry, 7 (12), 27-28.

Swinburn, B.A., Sacks, G., Hall, K.D., McPherson, K., Finegood, D.T., Moodie, M.L. and Gortmaker, S.L. (2011). The global obesity pandemic: shaped by global drivers and local environments. Lancet, 378, (9793), 804-814.

Talbot, G., Favre, L. and ThÖrig, L. (2007). Palm oil: The healthy alternative to *trans* fats. Inform, 18, 198–200.

Tanaka, L., Tanaka, K., Yamato, S., Ueno, S. and Sato, K. (2009). Microbeam X-ray diffraction study of granular crystals formed in water-in-oil emulsion. Food Biophysics, 4, 331–339.

Tang, D. and Marangoni, A.G. (2006b). Microstructure and fractal analysis of fat crystal networks. JAOCS, 83, 377–388.

Taylor, M.S. (2011). Stabilisation of water-in-oil emulsions to improve the emollient properties of Lipstick. MRes dissertation, University of Birmingham, UK.

Timms, R. E. (1984). Phase behaviour of fats and their mixtures. Progress in Lipid Research; 23 (1) 1-38.

Timms, R.E. (1985). Physical properties of oils and mixtures of oils. Journal of American Oil Chemists Society, 62, 241–249.

Timms, R.E. (1991). Crystallisation of Fats, Chemistry & Industry (SCI), May 20th, 342-344.

Timms, R.E. (2007). Fat Crystallisation: mechanism and methods for studying OFI Middle East: SCI Technical Conference Edible Oils and Fats Lecture-Trends in Raw Materials, Processing and Applications 20–21 March 2007, Cairo

Toro-Vazquez, J.F., Dibildox-Alvarado, E., Herrera-Coronado, V. and Charo-Alonso M.A. (2001). Triglyceride crystallization in vegetable oils: application of models, measurements, and limitations, in Crystallization and Solidification Properties of Lipids. Ed by Widlak N, Hartel R and Narine S. AOAC Press, Champaign, IL, 53–78.

Ueno, S., Suetake, T., Yano, J., Suzuki, M., Sato, K., (1994). Structure and polymorphic transformations in elaidic acid, (*trans*-ω9-octadecenoic acid). Chemistry and Physics of Lipids. 72, 27-34.

Ueno, S., Nishida, T., Sato, K., (2008). Synchrotron Radiation Microbeam X-ray Analysis of Microstructures and the Polymorphic Transformation of Spherulite Crystals of Trilaurin. Cryst. Growth Des. 8 (3), 751–754.

Urick, R.J. (1947). A sound velocity method for determining the compressibility of finely divided substances. Journal of Applied Physics, 18, 983–987.

Valentin, R. & Mouloungui, Z., (2013). Superhydrophilic surfaces from short and medium chain solvo-surfactants. Oléagineux, Corps Gras, Lipides. 20 (1) 33-44.

Vereecken, J., Foubert, I., Smith, K.W., and Dewettinck, K., (2009a). Effect of SatSatSat and SatOSat on crystallisation of model fat blends, Eur J, Lipid Sci, Technology, 111, 243-258.

Vereecken, J., Foubert, I., Meeussen, W., Lesaffer, A., and Dewettinck, K., (2009b). Fat Structuring with partial acylglycerols, Effect on solid fat profiles, Eur J, Lipid Sci, Technology, 111, 259-272.

Vereecken, J., Meeussen, W., Foubert, I., Lesaffer, A., Wouters, J., and Dewettinck, K., (2009c). Comparing the crystallization and polymorphic behaviour of saturated and unsaturated monoglycerides, Food Research International, 42, 1415-1425.

Vereecken, J., Meeussen, W., Lesaffer, A., Dewettinck, K., (2010). Effect of water and monoglyceride concentration on the behaviour of monoglyceride containing fat systems. Food Research International, 43, 872–881.

Verstraete, E. (2011). MSc thesis: Methods for monitoring fat crystallization under shear for margarine applications. Faculty of Bioscience Engineering. University Gent.

Vesper, H.W., Kuiper, H.C., Mirel, L.B., Johnson, C.L. and Pirkle, J.L. (2012). Levels of plasma *trans*-fatty acids in non-Hispanic white adults in the United States in 2000 and 2009. JAMA. 8, 307 (6), 562-3.

Wang, F., Liu, Y., Jin, Q., Huang, J., Meng, Z., Wang, X., (2011). Kinetic analysis of isothermal crystallization in hydrogenated palm kernel stearin with emulsifier mixtures, Food Research International, 44, (9), 3021-3025.

Wang, Y.C., McPherson, K., Marsh, T., Gortmaker, S.L. and Brown M. (2011). Health and economic burden of the projected obesity trends in the USA and the UK. The Lancet., Vol 378, (9793), 815-825.

Wang, R.., Xu, X. and Jiang, Y. (2012). Vegetable oils and fats in China: current and future trends. *inform*. AOCS. 23 (5), 329-334.

Wassell, P. and Young, N.W.G (2007). Food applications of *trans* fatty acid substitutes. International Journal of Food Science and Technology, 42, 503–517.

Wassell, P., Bonwick, G., Smith, C. J., Almiron-Roig, E. and Young, N.W.G. (2010a). Towards a Multidisciplinary Approach to Structuring in Reduced Saturated Fat- Based Systems – A Review. International Journal of Food Science & Technology, **45**, 642–655.

Wassell, P., Wiklund, J., Stading, M., Bonwick, G., Smith, C. J., Almiron-Roig, E. and Young, N. W. G. (2010b). Ultrasound Doppler based in-line viscosity and solid fat profile measurement of fat blends, International Journal of Food Science and Technology, **45**, 877 - 883.

Wassell, P., Farmer, M., Warner, S.A., Bech, A.T., Young, N.W.G., Bonwick, G., Smith, C., DuPont Nutrition Biosciences APS, (2012a). *Food or Feed Including Moringa Oil*. World Intellectual Property Organisation No. WO2012168722.

Wassell, P., Farmer, M., Warner, S.A., Bech, A.T., Young, N.W.G., Bonwick, G., Smith, C., DuPont Nutrition Biosciences APS, (2012b). *Triglyceride Fat Crystallisation*. World Intellectual Property Organisation No. WO2012168727.

Wassell, P., Farmer, M., Warner, S.A., Bech, A.T., Young, N.W.G., Bonwick, G., Smith, C., DuPont Nutrition Biosciences APS, (2012c). Low Fat Spread. World Intellectual Property Organisation No. WO2012168726.

Wassell, P., Farmer, M., Warner, S.A., Bech, A.T., Young, N.W.G., Bonwick, G., Smith, C., Forrest, B.A., DuPont Nutrition Biosciences APS, (2012d). *Dispersion of Triglycerides*. World Intellectual Property Organisation No. WO2012168723.

Wassell, P., Farmer, M., Warner, S.A., Bech, A.T., Young, N.W.G., Bonwick, G., Smith, C., DuPont Nutrition Biosciences APS, (2012e). *Spread*. World Intellectual Property Organisation No. WO2012168724.

Wassell, P., Okamura, A., Young, N.W.G., Bonwick, G., Smith, C., Sato, K. and Ueno, S., (2012). Synchrotron Radiation Macrobeam and Microbeam X-ray Diffraction Studies of Interfacial Crystallization of Fats in Water-in-Oil Emulsions. Langmuir 28 (13), 5539-5547.

Wells, M.A. (1998). Emulsifiers in Chocolate. Wells, M. A., Ed. SCI: London,73.

WHO (2011). Global status report on non-communicable diseases 2010.

Wiklund, J. (2007).Ultrasound Doppler Based In-Line Rheometry – Development, Validation and Application. PhD thesis, Lund, Sweden: Lund University, ISBN 978-91-628-7025-6.

Wiklund, J., Shahram, I. and Stading, M. (2007). Methodology for inline rheology by ultrasound Doppler velocity profiling-and pressure difference techniques. Chemical Engineering Science, 62, 4277–4293.

Wiklund, J. and Stading, M. (2008). Application of in-line ultrasound Doppler based UVP-PD rheometry method to concentrated model and industrial suspensions. Flow Measurement and Instrumentation, 19, 171–179.

Willett, W. and Mozaffarian, D. (2008). Ruminant or industrial sources of *trans* fatty acids: Public Health Issue or Food Label Skirmish? American Journal of Clinical Nutrition, 87, 515–516.

Winwood. R. (2011). So you think you know the effects of dietary lipids on human health? – Fat Chance! J. Food Science and Technology, (25), 2, 26-28.

Wood, A.B. (1964). A textbook of Sound, 3rd edn. London: Bell and Sons.

Yamagishi, K., Iso, H., Yatsuya, H., Tanabe, N., Date, C., Kikuchi, S., Yamamoto, A., Inaba, Y. and Tamakoshi, A., (2010). "Dietary intake of saturated fatty acids and mortality from cardiovascular disease in Japanese: the Japan Collaborative Cohort Study for Evaluation of Cancer Risk Study" American Journal of Clinical Nutrition.

Yano, J., Sato, K., Kaneko, F., Small, D.M., and Kodali, D.R., (1999). Structural analyses of polymorphic transitions of sn-1,3-distearoyl-2-oleoylglycerol (SOS) and sn-1,3-dioleoyl-2-stearoylglycerol (OSO): assessment on steric hindrance of unsaturated and saturated acyl chain interactions. J. Lipid Res. 40: 140–151.

Yap, P. H., deMan, J. M. and deMan, L. (1989). Polymorphic stability of hydrogenated canola oil as affected by addition of palm oil. Journal of American Oil Chemists' Society, 66 (12), 1784-1791.

Young, N.W.G. (2011). Food's next 40 years – challenges, implications, perspectives and consequences. J. Food Science & Technology, (25), 3, 14-15.

Young, N.W.G. and Wassell, P. (2008). Margarines and Spreads. In: G.L. Hasenhuettl and R.W. Hartel (eds.), Food Emulsifiers and Their Applications, 2nd ed. Springer, New York.

Young, N.W.G., Wassell, P, Wiklund, J. and Stading, M. (2008). Monitoring structurants of fat blends with ultrasound based in-line rheometry (UVP-PD). International Journal of Food Science and Technology, 43, 2083–2089.

Yusoff, M.S.A., Kifli, H., Lida, H.M.D.N. & Rozie, M.P. (1998). The formulation of *trans* fatty acid-free margarines. In: Proceedings of the World Conference on Oilseed and Edible Oils Processing (ed. S.S. Koseoglu). 156–158. Champaign, IL: AOCS Press.

Appendices

APPENDIX A

UniCamp Brazil, Independant Data

Dr. Renato Grimald, Fats & Oils group, tested the crystallisation of palm oil and palm kernel oil behaviour with additive. Independently, his team tested a sample of DIMODAN® MB-90 (CRY110) and found an increase in palm oil crystallisation speed. Their study found it was possible to increase fat kinetics in biscuit cream filling fats and firmness. From DSC evaluation of Dimodan MB-90 (CRY110) using the following:

1. Palm Oil (PO); 2. Palm Oil + MB-90 (0.5% DIMODAN® MB-90); 3. Palm kernel Oil (PKO)

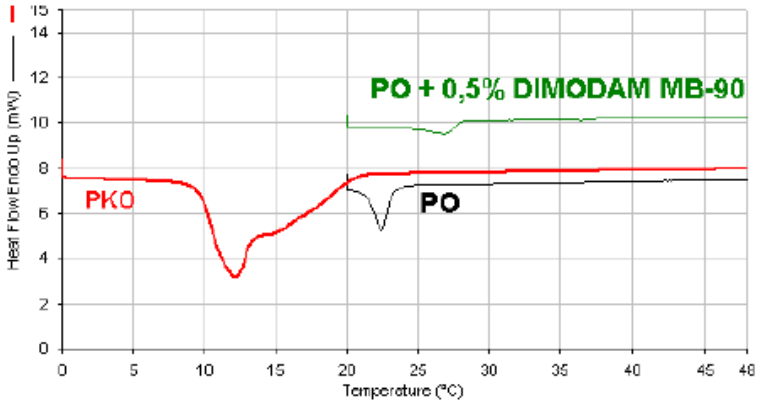

Figure A1.1

PO and PKO have different crystallisation behaviour, when decreasing temperature from:

- 50°C to 20°C at 2°C/min (PO)
- 50°C to 0°C at 2°C/min (PKO)

The peak shows energy liberation. This situation was static (no shear) at 20°C for crystallisation. PO without MB-90 showed peak with max intensity at 22°C was still liquid at 20°C. PKO was very exothermic, seen by large peak intensity. MB-90 promotes two effects: earlier crystallisation. Exothermic effect decreased significantly (peak almost disappears). **Conclusion:** This independent data from UNICAMP showed crystallisation was modified.

APPENDIX B

Additional Pilot Studies

Twelve different emulsifier combinations were tested and applied into commercially available fat blends. As shown in pilot study 1.5, a behenic rich MAG (DIMODAN® MB-90) does seem to enhance the crystallisation onset when applied in blends regarded as industrial "hard" fat blends. Softer fat blends (retail types) might possibly benefit from alternative pro-crystallisation additives based on TAG / MAG mixtures. The possibilities may be highly dependent on the application. Therefore, a dilution / blend of DIMODAN® MB-90 and HLEAR might be used for retail (softer, more unsaturated) products

Materials and Methods

In order to accommodate a range of fats with varying solid fat content (SFC), the emulsifier blends were applied into three fat blends, otherwise known as hard, medium and soft. The emulsifier blends shown in Table B1.1, were designed to enable to compare performance of monoglyceride and triglyceride with similar fatty acid profile, such as palm based products like: DIMODAN® HP (Monoglyceride) and GRINDSTED® PS 101 (Triglyceride). All emulsifier blends were applied at 1% dosage, and then rate of crystallisation and DSC were determined.

Table B1.1 – Description of emulsifier blends composition

Emulsifier Ingredient	1	2	3	4	5	6	7	8	9	10	11	12
DIMODAN® MB-90	100	50	50	50	50	50	50	50	70	30	34	34
DIMODAN® HP		50							30	70	33	33
DIMODAN® HR			50								33	
GRINDSTED® PS101				50								
HLEAR (low erucic)					50							
PS105 ALT1						50						
PS105 ALT2							50					
HHEAR (high erucic)								50				33

Remarks:

a) GRINDSTED® PS 101 – represent the same triglyceride as used in the synthesis of DIMODAN® HP (similar fatty acid profile).
b) HLEAR (low erucic) = fully hardened low erucic acid rapeseed oil = GRINDSTED® PS 104 – represent the same triglyceride as used in the synthesis of DIMODAN® HR.
c) HHEAR (high erucic) = fully hardened high erucic acid rapeseed oil. GRINDSTED® PS 209 contains 89 parts of it.
d) PS 105 ALT1 = 52% HHEAR (high erucic) + 48% HLEAR (low erucic).
e) PS 105 ALT2 = 52% HHEAR (high erucic) + 48% GRINDSTED® PS101.
f) Based on product description DIMODAN® MB-90 contains 80% behenic acid as part total of its fatty acid composition.
g) Emulsifier blends were applied into fat at 1% dosage (100g samples were prepared).
h) Fat blend and emulsifier were melted together at 90°C for 2 hours, in order to guarantee homogeneous samples fast cooling was simulated using ice bath and manual agitation.

Table B1.2 – Glyceride fatty acid composition

	A	B	C	D				89% **A** 11% m/90% HPPaSt	100% **C** or **D**
Item No.	**126269**	**042301**	**035800**	**004556**		**European PS 105**		**126324**	**061191**
Fatty acid	HHEAR	HLEAR	HPAST	HP	PS 105	ALT 1 (52%**A** 48%**B**)	ALT2 (52%**A** 48%**D**)	PS 209	PS 101
C 12	-	-	0,2	0,5		-	0,2	0,0	
C 14	0,2	-	1,2	2,5		0,1	1,3	0,3	
C 15	4,1	-	0,1	-		2,1	2,1	3,8	
C 16	-	6,0	58,0	43,0	9,5	2,9	20,6	4,9	
C 17	0,1	-	0,1	-		0,1	0,1	0,1	
C 18	39,0	91,0	40,0	51,0	58,0	64,0	44,8	39,1	
C 18-1	-	-	0,3	0,3		-	0,1	0,0	
C 20	8,9	2,0	0,7	1,5		5,6	5,3	8,2	
C 22	46,0	0,6	-	-	24,0	24,2	23,9	42,1	
C 24	1,1	-	-	-		0,6	0,6	1,0	
Sum	99,4	99,6	100,6	98,8	91,5	99,5	99,1	99,5	

Fat blends:

A. Palm Oil

B. A Brazilian commercial low *trans* table margarine fat blend.

C. Puff pastry margarine fat blend, composed of:

- 60% palm stearin
- 25% palm oil
- 15% rapeseed oil

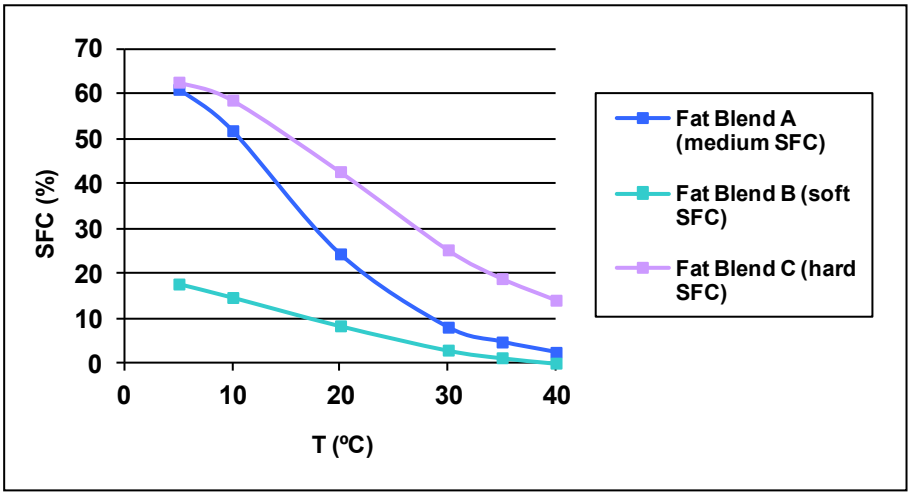

Figure B1.1 – Fat blends solid fat content – SFC% (Bruker-pNMR)

Table B1.3 – Fatty acid composition of selected triglyceride blends

Fatty Acid	Fat Blend A	Fat Blend B	Fat Blend C
C8:0		0.3	0.1
C10:0		0.3	0.1
C12:0		4	0.6
C14:0	1	1.5	1.2
C15:0		0.1	0.1
C16:0	43	12	46.3
C16:1		0.1	0.2
C17:0		0.3	0.1
C18:0	5	9.3	4.4
C18:1	40	23.2	35.2
C18:2	10	42.7	9
C18:3		5	1.6
C20:0	0.5	0.5	0.5
C20:1		0.3	0.4
C22:0		0.5	0.1
C22:1		-	0.2

Analytical methods

Table B1.4 DSC determination

Sample	Rate of Crystallisation	DSC
Fat Blend A (pure and emulsifier added)	Melt at 90°C Measure SFC/min at 20°C	Heat 1 5°C/min Cool -10°C/min Heat 2 5°C/min
Fat Blend B (pure and emulsifier added)	Melting 90°C Measure SFC/min at 15°C	
Fat Blend C (pure and emulsifier added)	Melting 90°C Measure SFC/min at 20°C	

Remarks:

a) Rate of crystallisation was run in triplicates. Rate of crystallisation by triplicate determination and averages were plotted together to see standard deviation – Figure B1.2 (example)
   i. Weigh ….g of sample.
   ii. Keep sample for 1h at 90°C.
   iii. Cool down to 20°C (or 15°C) and start SFC measurement.

b) DSC was duplicated. Figure B1.3 duplicate determination of DSC
   i. Heat the sample from 5°C to 80°C by heating rate of 5°C/min.
   ii. Cool down from 80°C to 5°C by cooling rate of -10°C/min.
   iii. Heat the sample again from 5°C to 80°C by heating rate of 5°C/min.

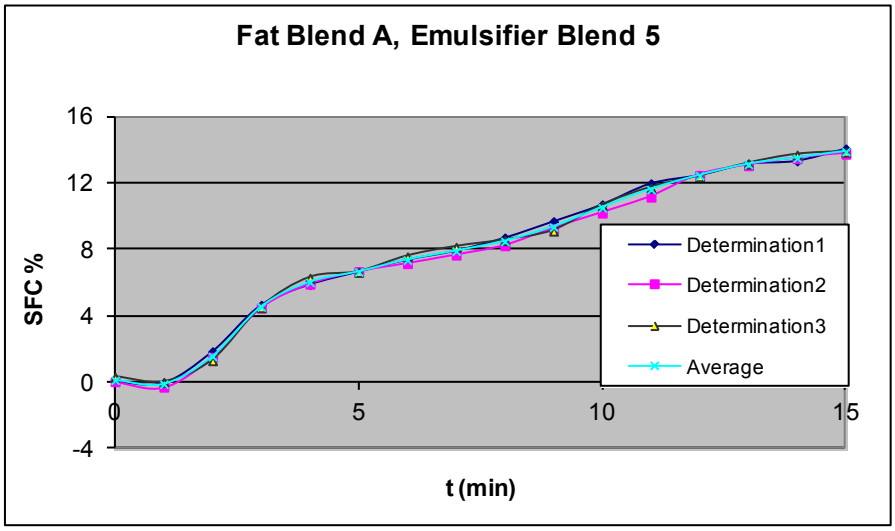

Figure B1.2 Triplicate determination of rate of crystallisation, example

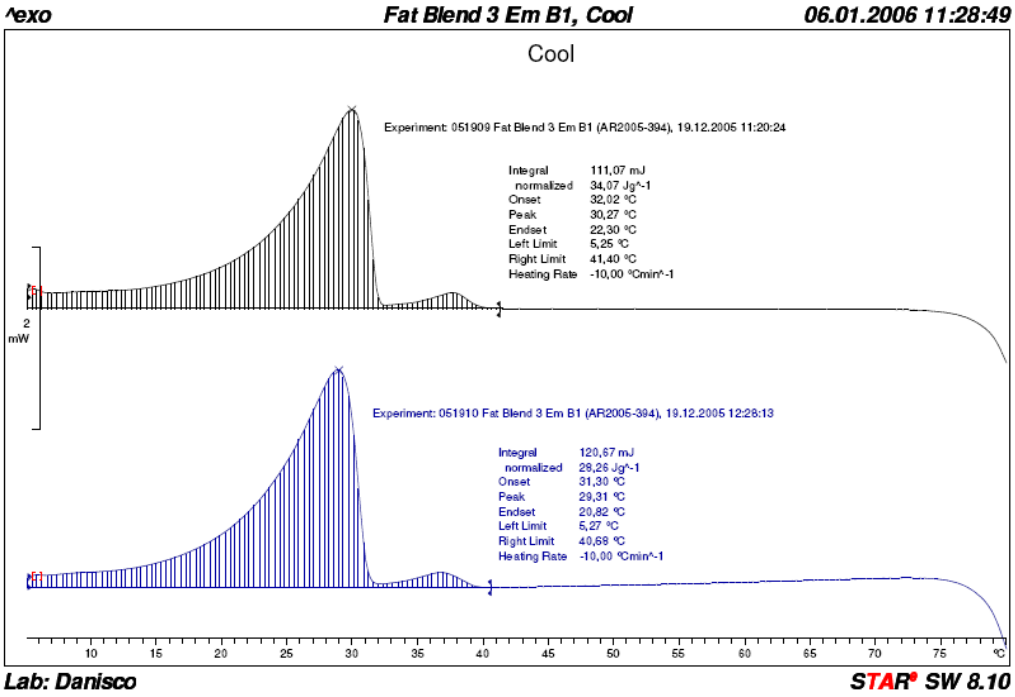

Figure B1.3 Duplicate determination of DSC, example

Results

Results are shown using average values from Rate of Crystallisation triplicate determinations (**Appendix C**).

MEDIUM Fat Blend A - (Palm Oil)

Figure B1.4 shows all variants tested in the medium (palm oil) fat blend. The following

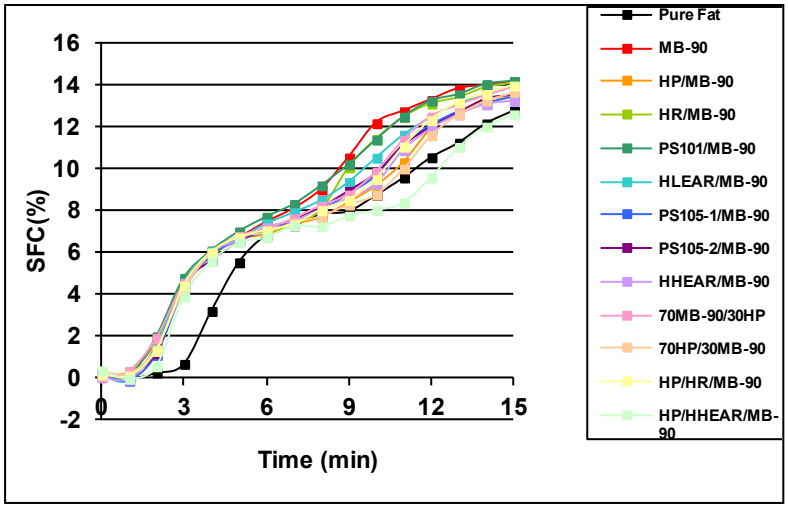

Figure B1.4 Rate of crystallisation (at 20°C, 15min plotted), 1% emulsifier blend dosage.
Comments are made:

a) Time 0 to 6 min - it is difficult to determine difference between emulsifiers, but all have early onset rate of crystallisation on the pure fat blend.

b) Comparing all applied monoglycerides, MB-90 presented best performance followed by HR/MB-90.

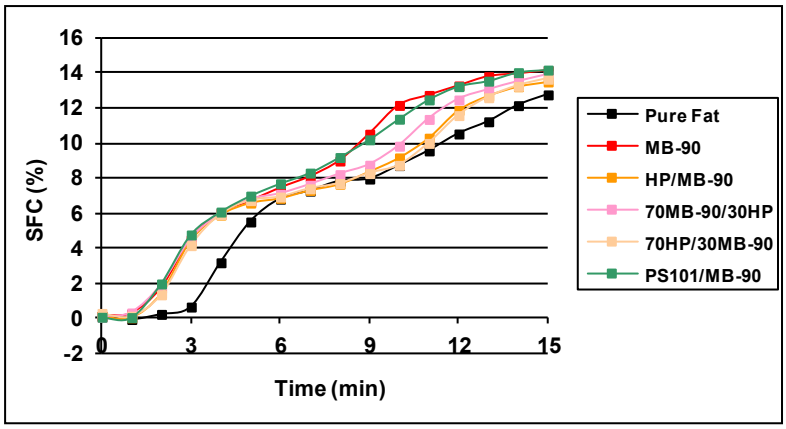

Figure B1.5 Rate of crystallisation (at 20°C, 15min plotted), 1% emulsifier blend dosage.

c) Different combinations of HP and MB-90 showed less performance when compared to pure MB-90 after ~ 6 mins.

d) Comparing monoglyceride (HP) versus triglyceride (PS101) with similar fatty acid profile, triglyceride presented better performance than monoglyceride in this specific application.

e) Monoglyceride (HR) performed better than triglyceride (HLEAR and HHEAR).

In general pure MB-90 performed best.

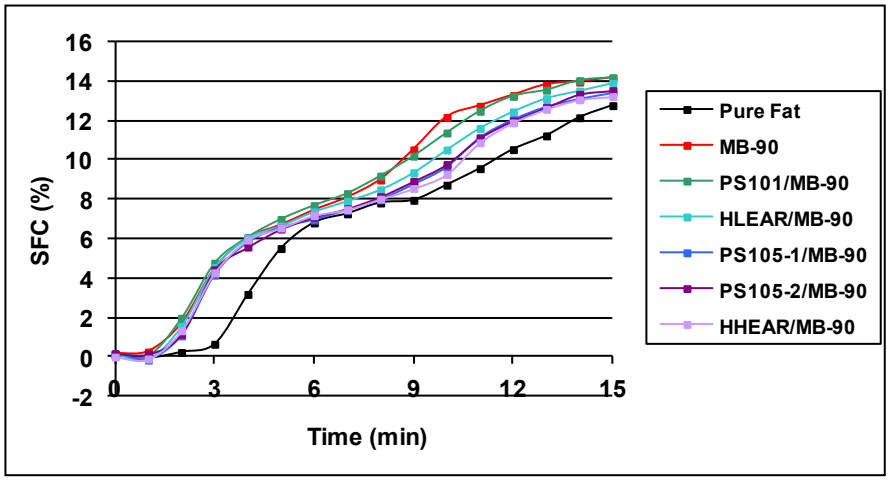

Figure B1.6 Rate of crystallisation (at 20°C, 15min plotted), 1% emulsifier blend dosage.

Comments (after 6 min): Looking at all triglyceride blends, PS 101 and HLEAR presented better performance than other combinations, but still poorer than MB-90.

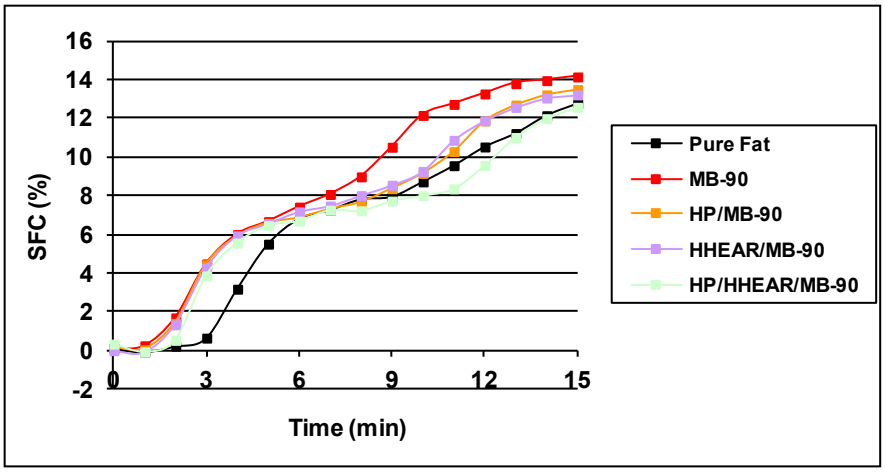

Figure B1.7 Rate of crystallisation (at 20°C, 15min plotted), 1% emulsifier blend dosage.

Comments (after 6 min): A three component blend of triglyceride (HHLEAR), monoglycerides HP and MB-90 did not improve the performance comparing with blends of two components (HP/MB-90 and HHEAR/MB-90).

DSC

Data is provided in **Appendix D**

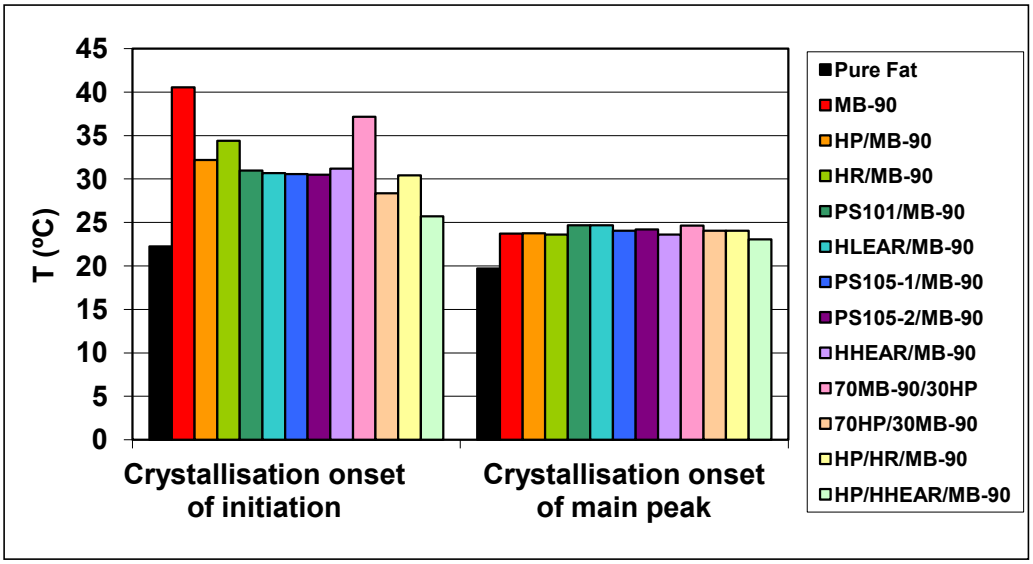

Figure B1.8 DSC – Cooling curve data (cooling -10°C/min), 1% emulsifier dosage

Comments:

Crystallisation onset of initiation, correspond to the temperature where crystallisation begins and is taken from the DCS cooling curve described as "Right Limit".

Crystallisation onset of main peak corresponds to the temperature where most of the fat crystallisation takes place and is described in the DSC cooling curve as "Onset".

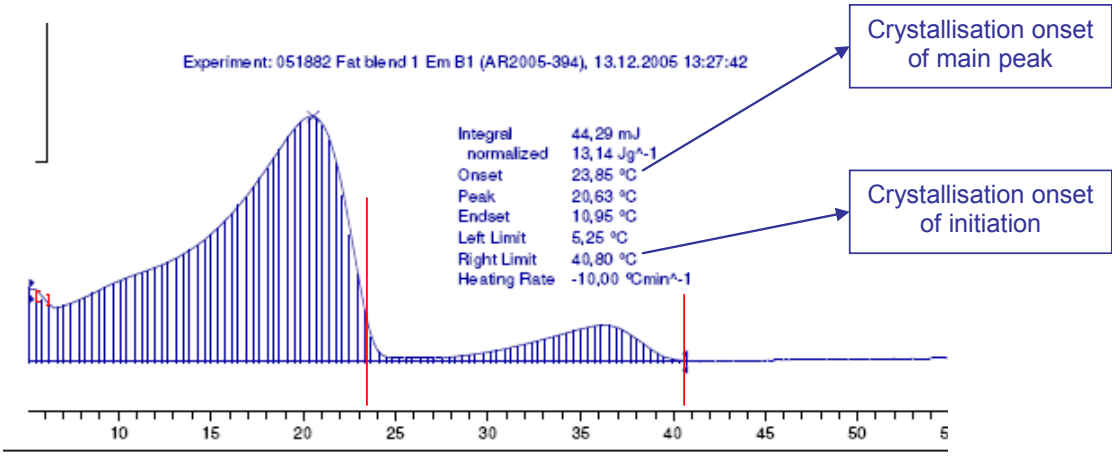

Figure B1.9 Example of DSC data

SOFT Fat Blend B **(low trans Brazilian blend)**

Rate of crystallisation (at 15°C, 15min plotted), 1% emulsifier blend dosage.

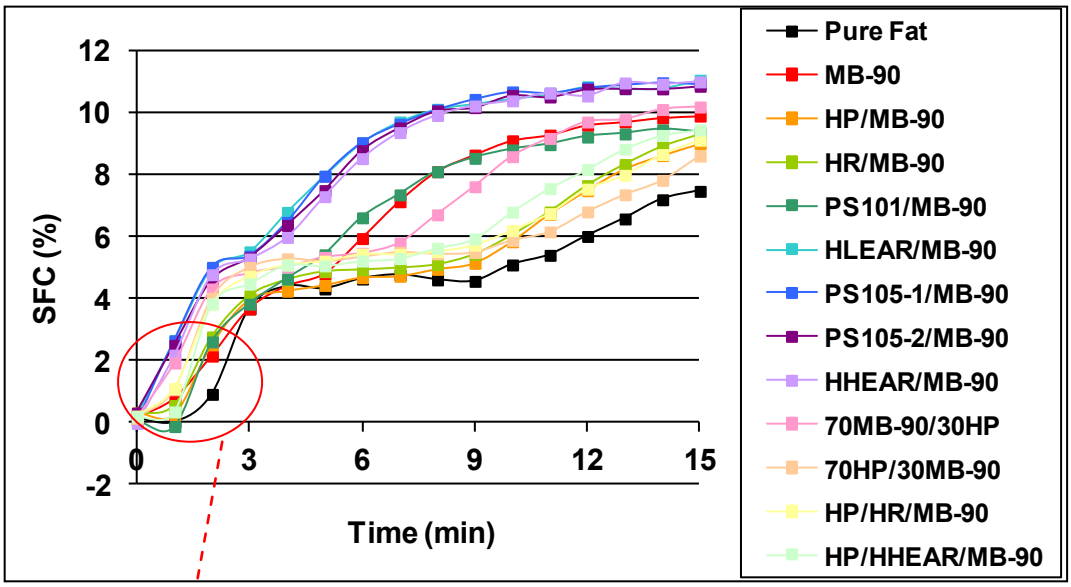

Figure B1.10

Comments: In general, blends containing triglyceride based crystal promotors presented much better performance than blends containing monoglycerides. Both triglyceride and monoglycerides enhanced the rate of crystallisation when compared to pure fat.

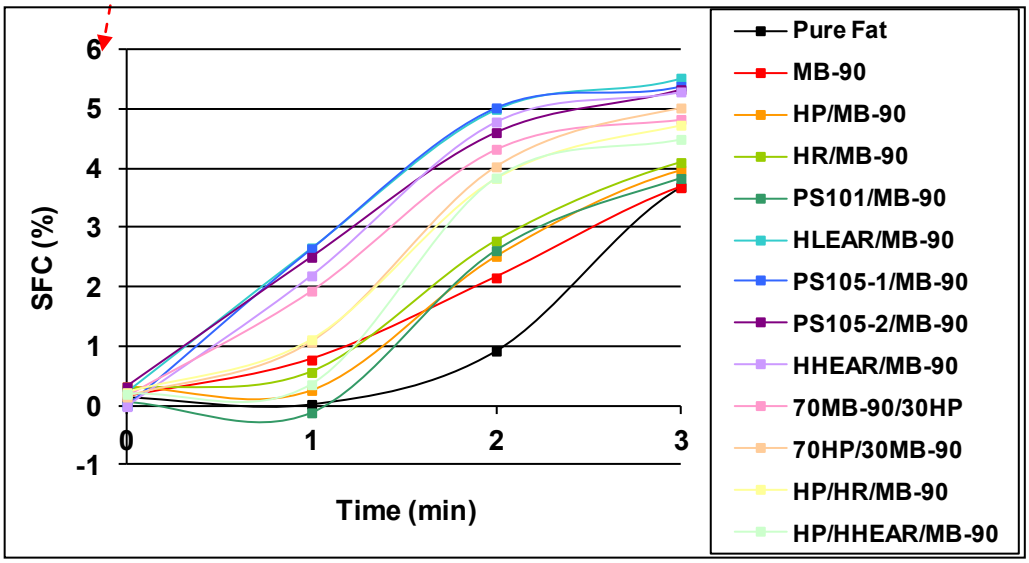

Figure B1.11

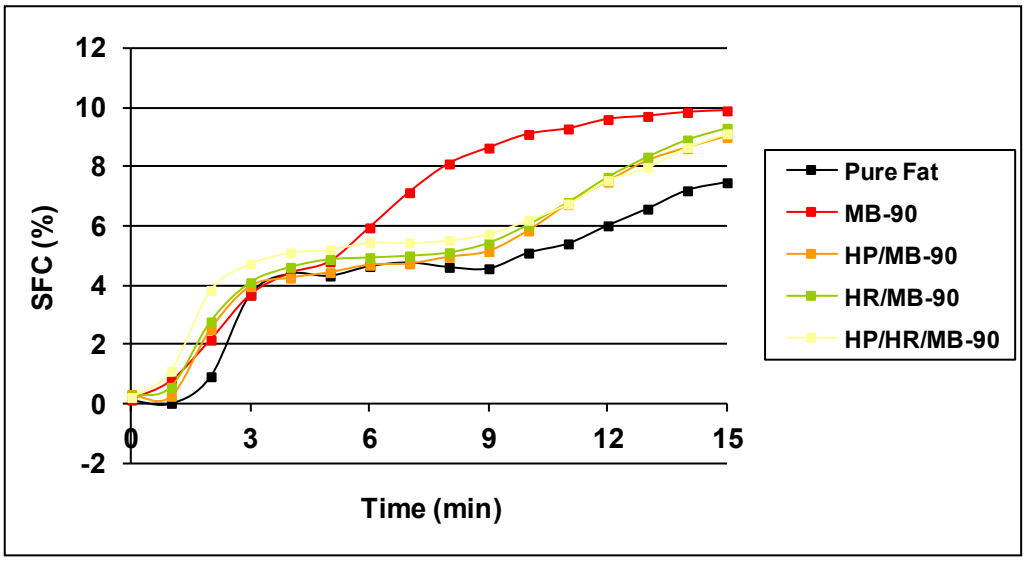

Figure B1.12

Comments: From the beginning (first 3 mins), both blends with HP and HR improved the onset temperature comparing with pure fat blend. But, after 6 min MB-90 was more efficient.

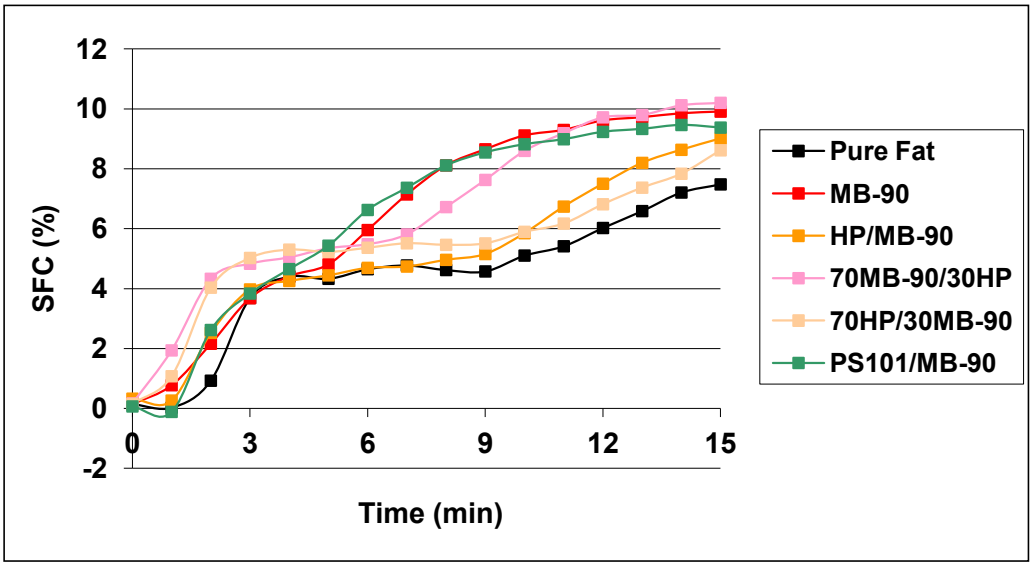

Figure B1.13

Comments (after 6 min): PS 101 / MB-90 continued to show similar performance to pure MB-90 from ~ 6 mins to ~ 10mins.

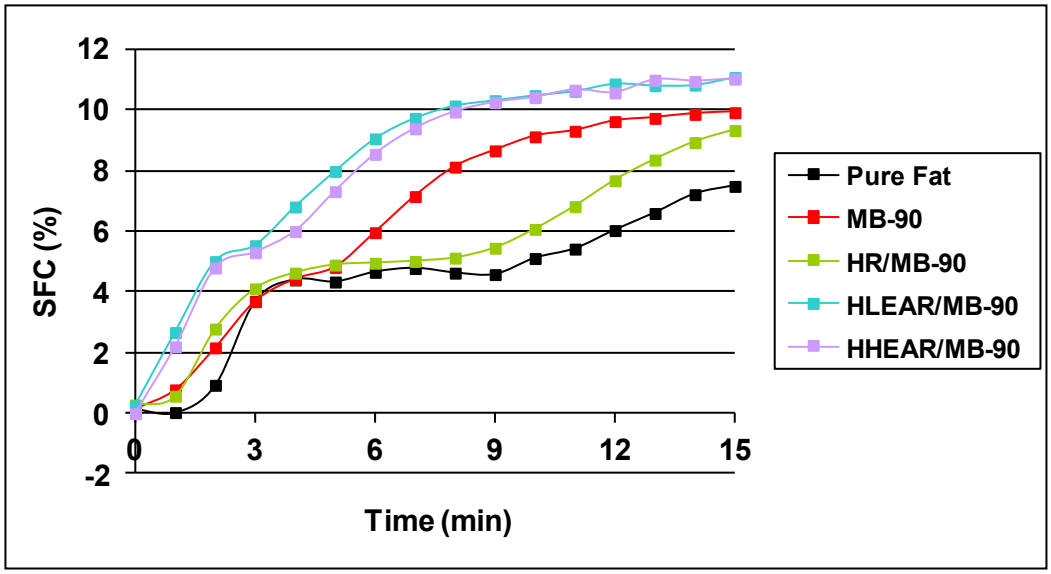

Figure B1.14

Comments:

Blends containing triglycerides (HLEAR and HHEAR) performance much better than the blend HR/MB-90 (monoglycerides), the onset temperature was clearly enhanced.

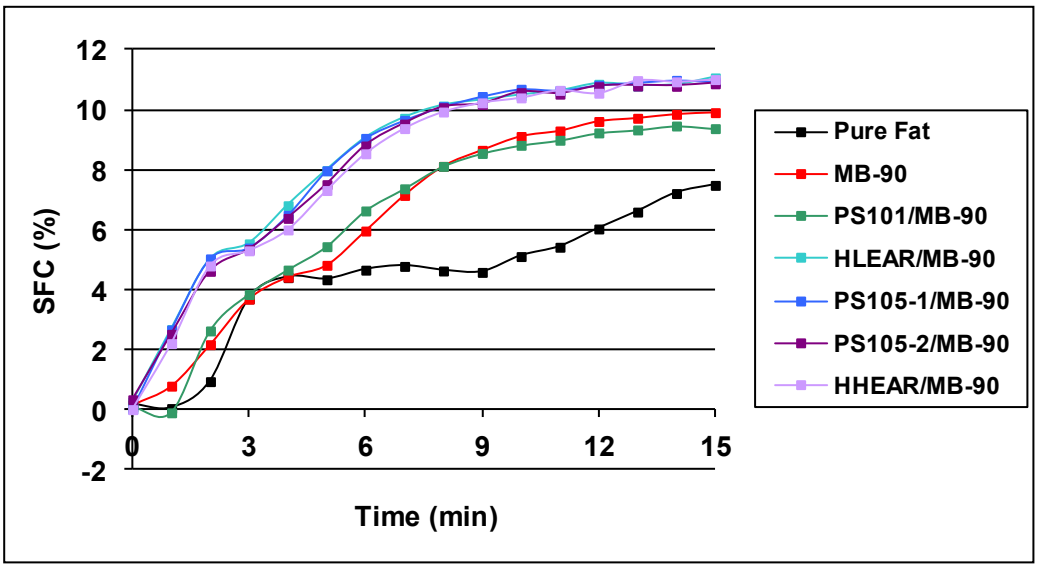

Figure B1.15

Comments:

All blends containing triglycerides perform more or less the same and better than MB-90. Except for PS101/MB-90 blend.

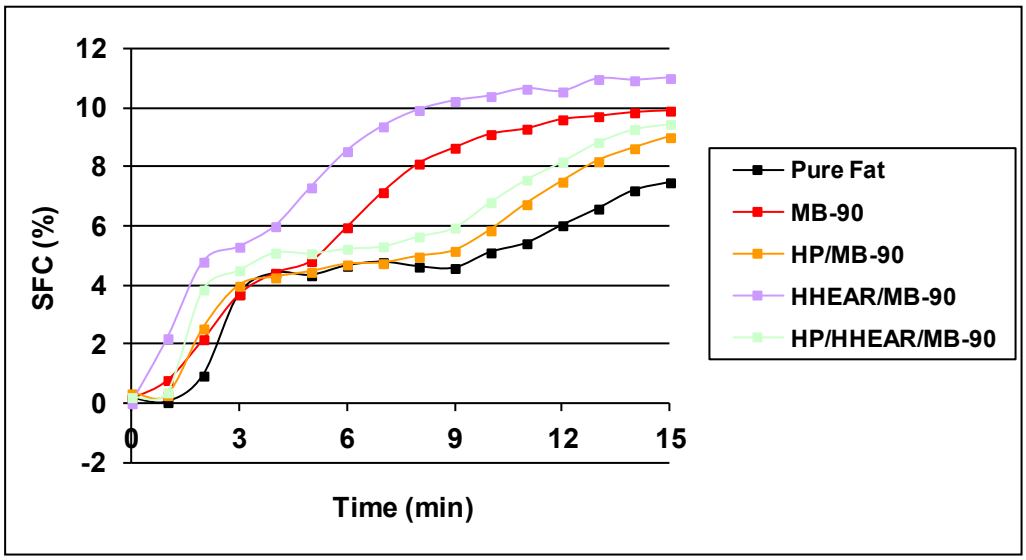

Figure B1.16

Comments: In general best onset was obtained for HHEAR/MB-90 followed by MB-90.

DSC – Cooling curve data (cooling -10°C/min), 1% emulsifier blend dosage.

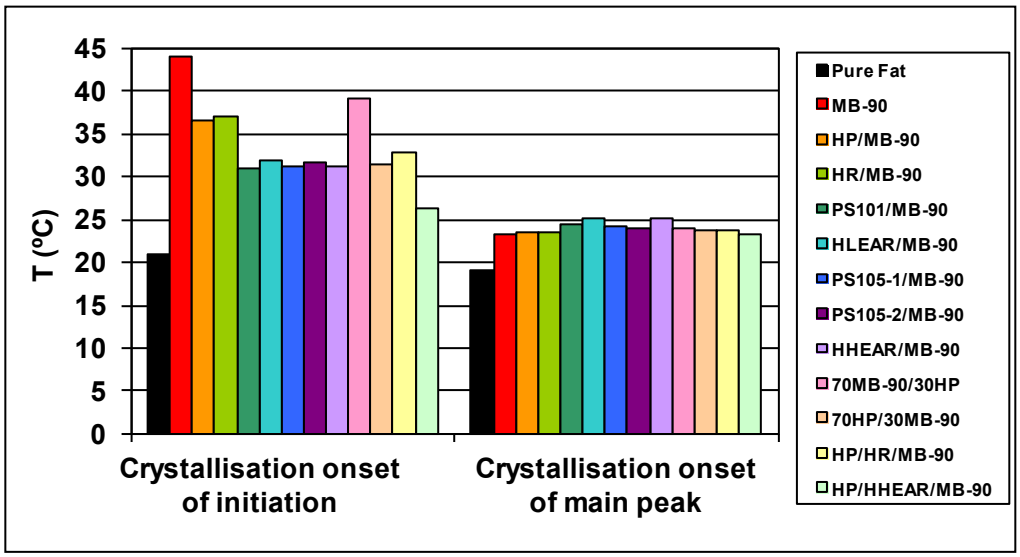

Figure B1.17

HARD Fat Blend C (60% palm stearin / 25% palm oil / 15% rapeseed oil)

Rate of crystallisation (at 20°C, 15min plotted), 1% emulsifier blend dosage.

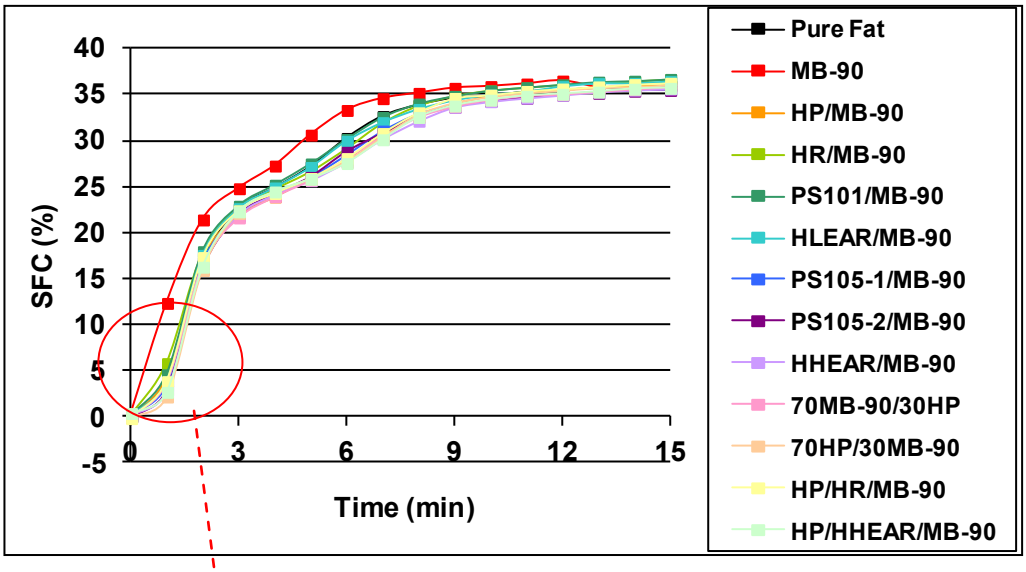

Figure B1.18

Comments: Pure MB-90 is the only emulsifier that clearly made positive difference on the onset temperature. It means that only MB-90 improved the rate of crystallisation in this fat blend.

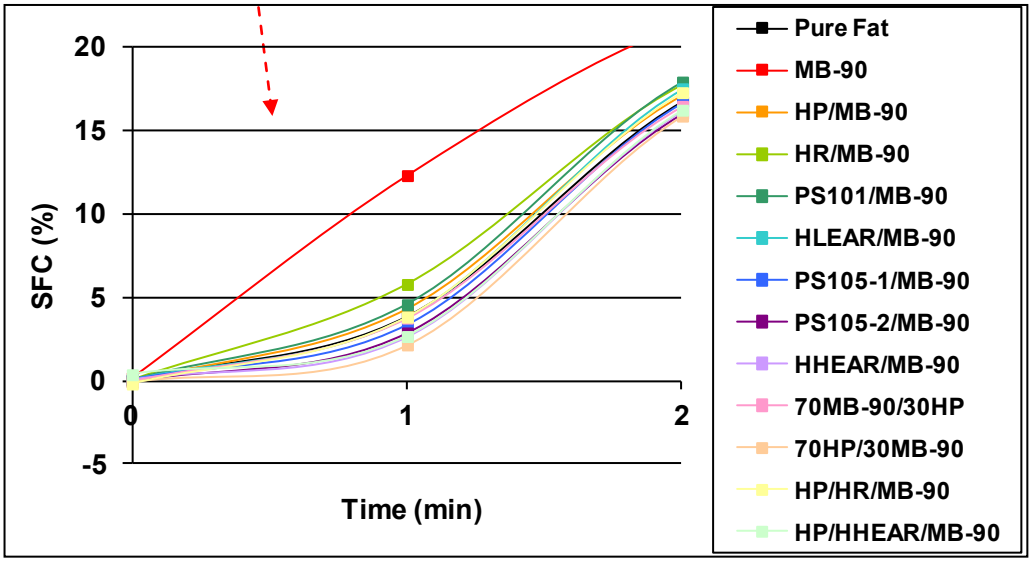

Figure B1.19

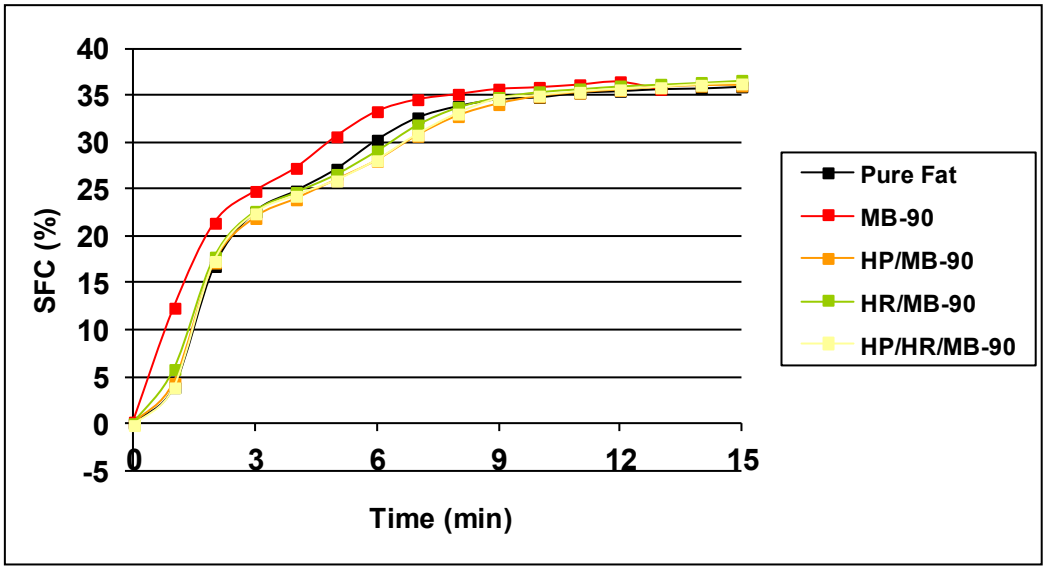

Figure B1.20

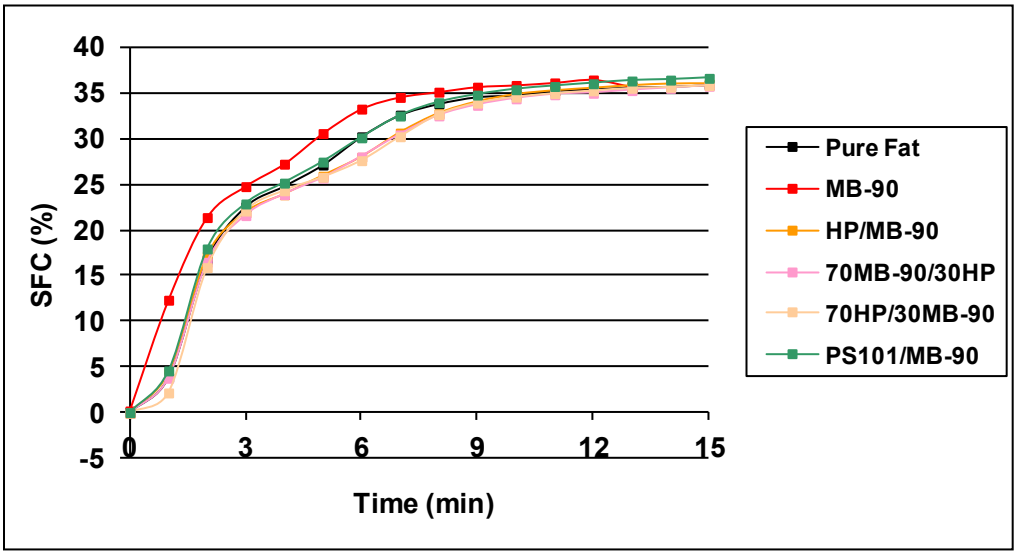

Figure B1.21

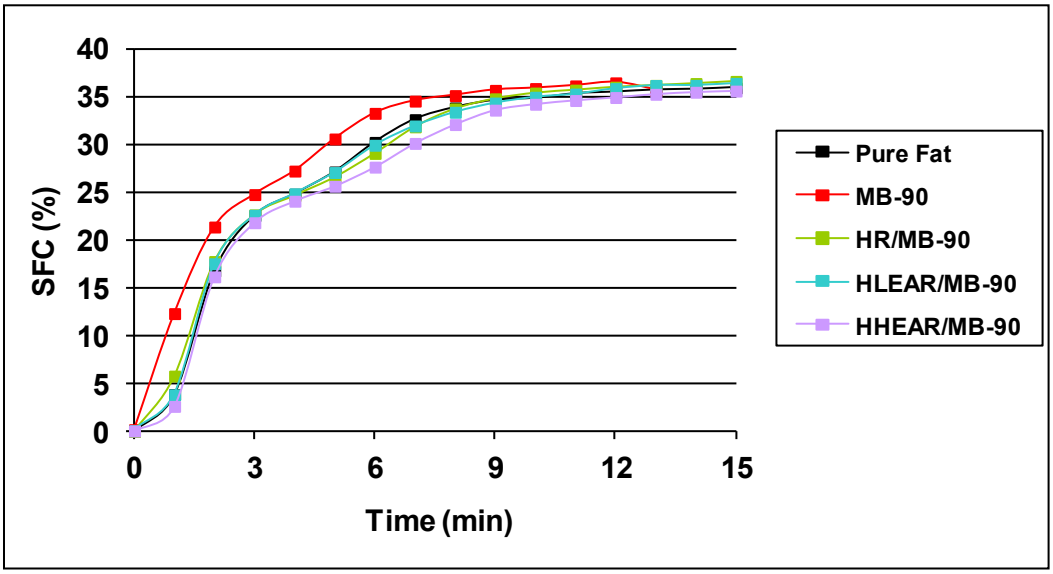

Figure B1.22

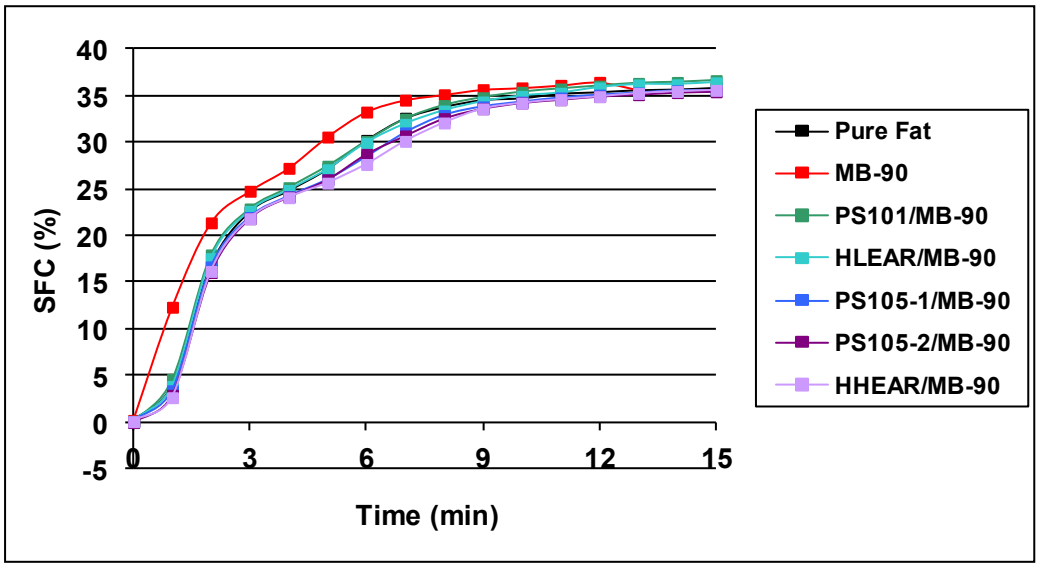

Figure B1.23

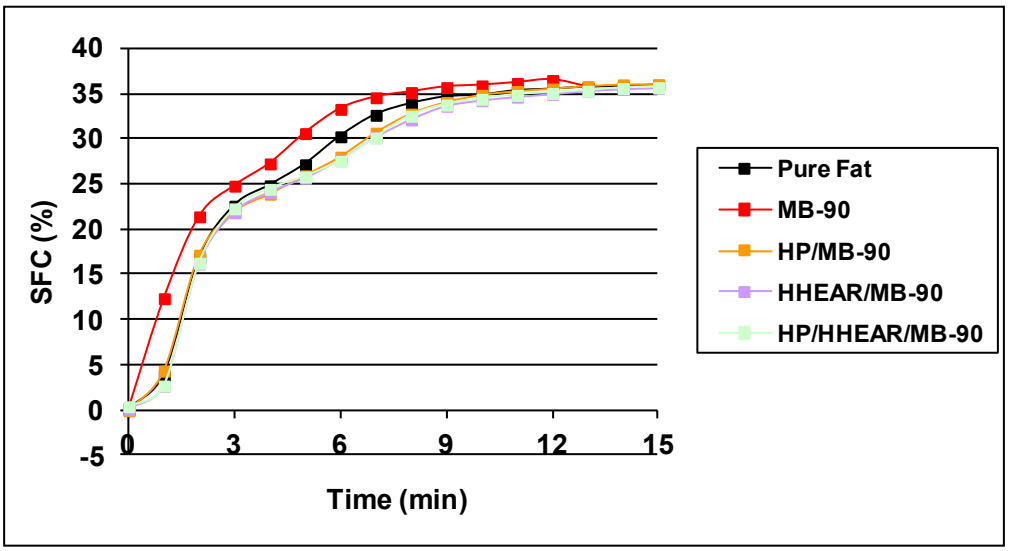

Figure B1.24

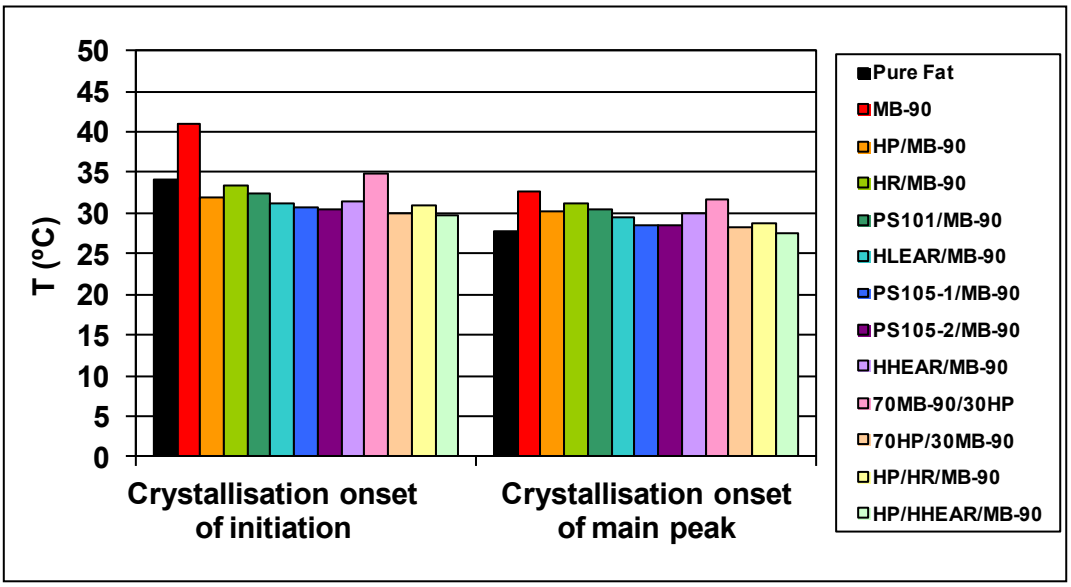

Figure B1.25 DSC – Cooling curve data (cooling -10°C/min), 1% emulsifier blend dosage

RESULTS – (Additional test materials)

Determinations using a new monoglyceride sample, then applied into the same fat blends.

Table B1.5 Description of the emulsifier blends composition

	1a	2a	3a	4a
DIMODAN® MB-90		50	30	100 (applied at 0.5% into fat)
TS-XYZ	100	50	70	

Remarks:

a) TS-XYZ is a composition of DIMODAN® HB-90. It also contains a second monoglyceride based on HLEAR (DIMODAN®HR), resulting in approximately half of the C22 found in DIMODAN® MB-90)

b) Emulsifier blends from 1 to 3 were applied at 1% dosage into the three fat blends described throughout previous examples within this study. Blend 4, represents DIMODAN® MB-90 at 0.5%.

MEDIUM Fat Blend A (Palm)

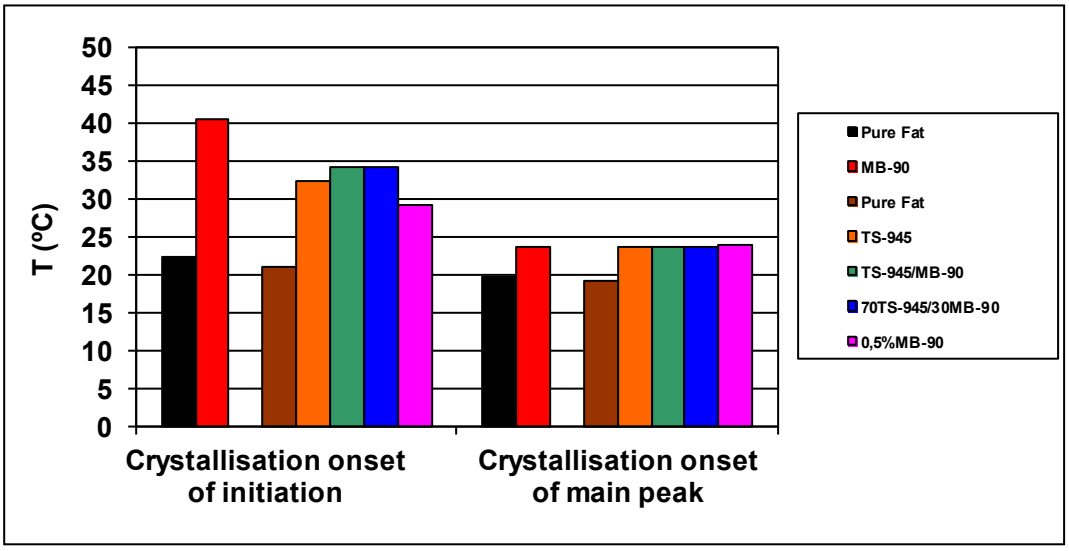

Figure B1.26 DSC – Cooling curve data (cooling -10°C/min)

SOFT Fat Blend B (low trans)

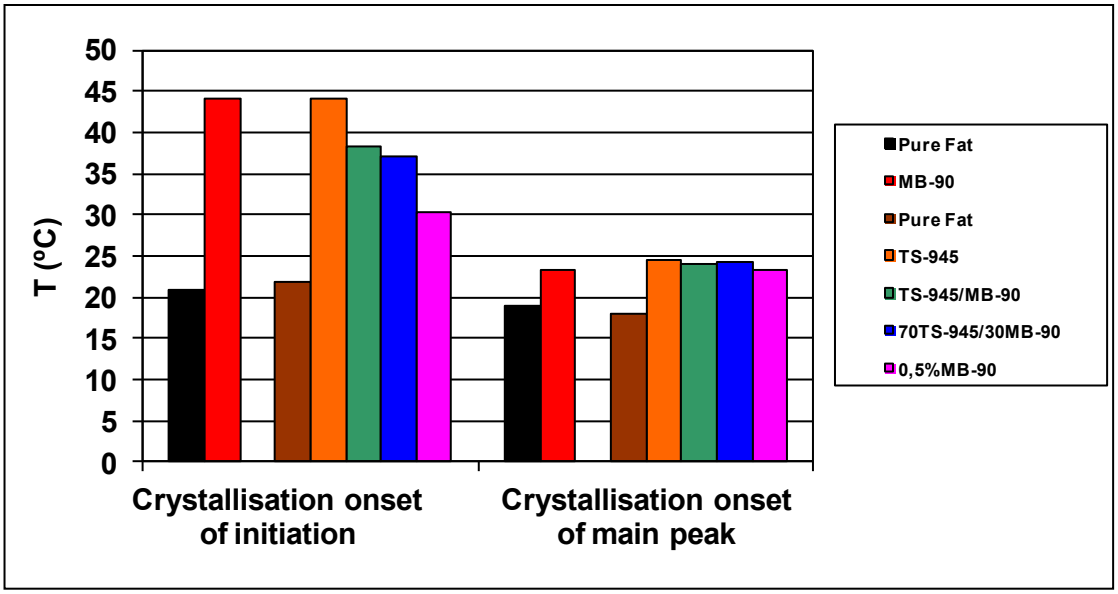

Figure B1.27 DSC – Cooling curve data (cooling -10°C/min)

HARD Fat Blend C

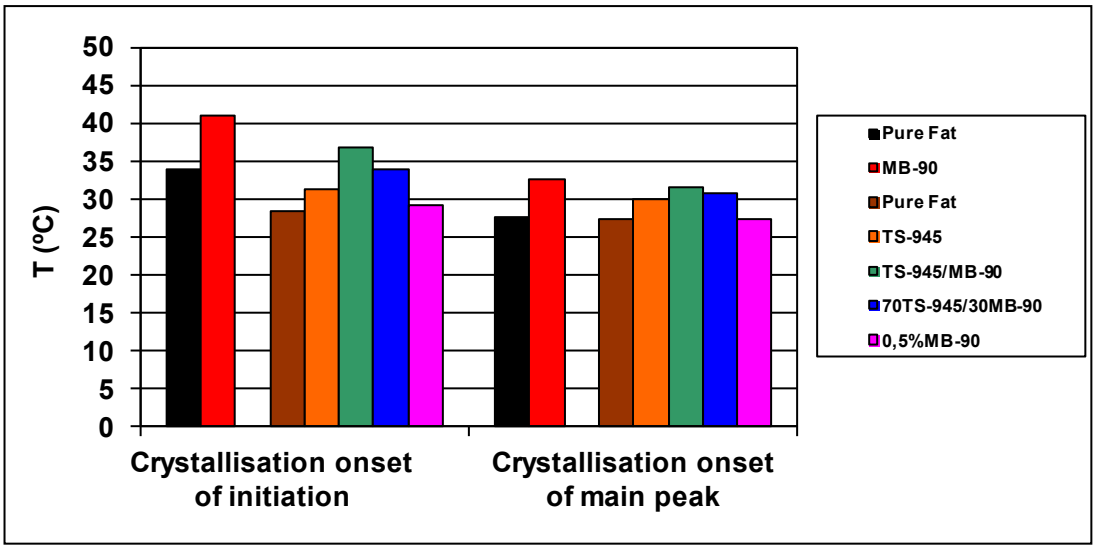

Figure B1.28 DSC – Cooling curve data (cooling -10°C/min)

Conclusion

DIMODAN MB-90 (Now known as Grindsted Crystalliser 110), has a positive effect on all fat blends studied in this work. For hard blend (fat blend C, puff pastry), it is clear that only monoglyceride based on C22:0 promoted higher rate of crystallisation and earlier onset than others within this study.

Generally it can be concluded from this study that the harder the fat blend, the better the monoglyceride performance when compared to triglyceride. The following is found:

Alternatives for **Hard blends** – (blend C)

- MB-90 offers excellent performance.
- TS-XYZ could be used either singular or combined with MB-90
- It is better to have C22 +C18 blended than only C22 in a low dosage, and therefore it probably better to use at least 1% DIMODAN® MB or MB-90+HR than 0.5% MB-90 alone.

Alternatives for **Soft blends** – (blend B)

- In general, blends containing triglyceride based crystal promoters presented much better performance than blends containing monoglycerides. Anyway, both triglyceride and monoglycerides enhanced the rate of crystallisation when compared to pure fat. TS-XYZ could be used either singular or combined with MB-90
- Blends containing triglycerides (HLEAR and HHEAR) performed better than blends of HR/MB-90.

Alternatives for **Medium blends** – (blend A)

- It is hard to see difference between emulsifiers, but all of them have provided improved rate of crystallisation on the pure fat blend.MB-90 presented best performance followed by HR/MB-90.Monoglyceride (HR) performed better than triglyceride (HLEAR and HHEAR).
- In general pure MB-90 performed best.

Due to the difficulty of unlimited combinations of possible oil formulations, the study is limited to several typical commercial fat blends, and has shown some potential combinations of monoglyceride and triglyceride alternatives to Dimodan® MB-90, which might have more commercial cost incentives.

Pure MB-90 increased the rate of crystallisation and the onset temperature. The degree of saturation of the harder fat blend has an intrinsic influence; so that the DIMODAN® MB-90 performance compared better with other alternatives.

When a softer fat blend is used, more options (alternatives) can be found which could change positively the fat crystallisation behaviour. An example, such as 50:50 combination of DIMODAN® MB-90 + HLEAR (fully hardened low erucic acid rapeseed oil) showed a good alternative in performance.

Note:

Supporting crystallisation and DSC data are provided in **APPENDICES C & D**

APPENDIX C

Rate of Crystallisation: Triplicate Determination of Results from Appendix B

Fat blend A – Palm Oil

Pure Fat Blend A

t (min)	Determ.1	Determ.2	Determ.3	Average
0	0,002	0,022	0,322	0,115
1	-0,076	-0,175	0,036	-0,072
2	0,316	0,139	0,208	0,221
3	0,567	0,447	0,904	0,639
4	3,293	2,866	3,358	3,172
5	5,414	5,218	5,879	5,504
6	6,746	6,604	7,077	6,809
7	7,173	7,109	7,523	7,268
8	7,763	7,859	7,845	7,822
9	7,861	7,793	8,219	7,958
10	8,762	8,630	8,791	8,728
11	9,506	9,348	9,848	9,567
12	10,451	10,433	10,720	10,535
13	11,176	11,085	11,437	11,233
14	12,073	12,302	12,092	12,156
15	12,630	12,603	13,079	12,771
16	13,287	13,150	13,445	13,294
17	13,632	13,638	13,918	13,729
18	14,045	13,965	13,982	13,997
19	14,339	14,281	14,474	14,365
20	14,638	14,425	14,577	14,547
25	15,476	15,356	15,535	15,456

Emulsifier 1 (1%)

t (min)	Determ.1	Determ.2	Determ.3	Average
0	0,215	0,034	0,103	0,117
1	0,133	0,266	0,334	0,244
2	1,518	1,838	1,707	1,688
3	4,170	4,510	4,760	4,480
4	5,874	6,039	6,090	6,001
5	6,593	6,730	6,694	6,672
6	7,514	7,466	7,290	7,423
7	8,084	7,992	8,153	8,076

8	9,328	8,861	8,777	8,989
9	11,089	10,364	10,116	10,523
10	12,558	12,070	11,882	12,170
11	12,917	12,772	12,533	12,741
12	13,362	13,284	13,199	13,282
13	13,893	13,841	13,701	13,812
14	14,122	13,838	13,952	13,971
15	13,957	14,371	14,157	14,162
20	14,944	14,910	14,679	14,844

Emulsifier 2 (1%)

t (min)	Determ.1	Determ.2	Determ.3	Average
0	0,232	-0,070	0,184	0,115
1	0,132	-0,147	0,096	0,027
2	1,562	1,484	1,163	1,403
3	4,418	4,584	4,295	4,432
4	5,765	6,099	5,830	5,898
5	6,695	6,772	6,286	6,584
6	6,928	6,929	6,706	6,854
7	7,264	7,443	7,211	7,306
8	7,516	7,839	7,634	7,663
9	8,377	8,422	8,329	8,376
10	9,409	9,080	9,013	9,167
11	10,363	10,507	10,020	10,297
12	11,962	12,057	11,627	11,882
13	12,773	12,803	12,542	12,706
14	13,241	13,289	13,177	13,236
15	13,553	13,546	13,428	13,509
20	14,608	15,016	14,803	14,809

Emulsifier 3 (1%)

t (min)	Determ.1	Determ.2	Determ.3	Average
0	0,313	0,212	0,215	0,247
1	0,132	0,424	0,205	0,254
2	1,542	2,145	1,595	1,761
3	4,298	5,022	4,594	4,638
4	5,916	5,747	5,640	5,768
5	6,781	6,650	6,501	6,644
6	7,017	6,787	6,907	6,904
7	6,982	7,623	7,367	7,324
8	7,747	8,151	8,160	8,019
9	9,875	10,153	10,138	10,055

10	11,313	11,612	11,308	11,411
11	12,358	12,491	12,552	12,467
12	12,937	13,324	13,052	13,104
13	13,148	13,432	13,610	13,397
14	13,644	14,078	13,929	13,884
15	13,881	14,071	14,305	14,086

Emulsifier 4 (1%)

t (min)	Determ.1	Determ.2	Determ.3	Average
0	0,192	0,293	-0,320	0,055
1	0,017	0,110	-0,013	0,038
2	1,710	2,481	1,689	1,960
3	4,353	5,013	4,919	4,762
4	5,916	5,992	6,309	6,072
5	6,730	7,166	7,057	6,984
6	7,440	7,872	7,755	7,689
7	8,269	8,485	8,114	8,300
8	8,937	9,313	9,321	9,190
9	10,079	10,372	10,156	10,202
10	11,347	11,552	11,242	11,380
11	12,484	12,550	12,417	12,484
12	13,237	13,225	13,266	13,243
13	13,346	13,761	13,562	13,556
14	13,803	14,141	14,184	14,043
15	13,965	14,248	14,358	14,190

Emulsifier 5 (1%)

t (min)	Determ.1	Determ.2	Determ.3	Average
0	0,039	0,041	0,297	0,126
1	-0,035	-0,291	0,001	-0,108
2	1,850	1,517	1,302	1,556
3	4,647	4,476	4,498	4,540
4	5,889	5,916	6,281	6,029
5	6,662	6,677	6,630	6,656
6	7,385	7,155	7,570	7,370
7	7,930	7,669	8,145	7,907
8	8,704	8,232	8,541	8,492
9	9,689	9,272	9,113	9,358
10	10,704	10,201	10,644	10,516
11	11,975	11,164	11,702	11,614
12	12,488	12,477	12,393	12,453
13	13,166	13,057	13,163	13,129

14	13,349	13,479	13,701	13,510
15	14,072	13,749	13,877	13,899
16	14,192	14,034	14,102	14,109

Emulsifier 6 (1%)

t (min)	Determ.1	Determ.2	Determ.3	Average
0	0,148	0,128	0,108	0,128
1	-0,245	-0,123	-0,132	-0,167
2	1,123	1,057	1,018	1,066
3	4,103	4,122	4,246	4,157
4	5,691	5,825	5,890	5,802
5	6,502	6,671	6,467	6,547
6	6,931	6,847	7,096	6,958
7	7,619	7,541	7,361	7,451
8	8,001	7,882	8,065	7,983
9	8,761	8,636	8,878	8,758
10	9,933	9,413	9,581	9,642
11	11,008	11,235	11,178	11,140
12	11,950	12,233	11,984	12,056
13	12,788	12,465	12,880	12,711
14	13,018	13,201	13,116	13,112
15	13,340	13,569	13,332	13,414

Emulsifier 7 (1%)

t (min)	Determ.1	Determ.2	Determ.3	Average
0	0,435	0,235	-0,181	0,163
1	0,267	0,062	0,096	0,142
2	1,156	1,300	1,009	1,155
3	4,557	4,426	4,299	4,427
4	5,979	5,537	5,218	5,578
5	6,485	6,573	6,424	6,494
6	7,131	7,210	6,971	7,104
7	7,652	7,509	7,553	7,531
8	8,123	8,097	8,197	8,139
9	8,814	8,858	9,096	8,923
10	9,820	9,567	9,946	9,778
11	10,918	11,094	11,334	11,115
12	12,001	12,049	11,924	11,991
13	12,720	12,737	12,540	12,666
14	13,265	13,363	13,399	13,342
15	13,413	13,440	13,745	13,533

Emulsifier 8 (1%)

t (min)	Determ.1	Determ.2	Determ.3	Average
0	-0,124	0,027	0,057	-0,013
1	-0,191	-0,271	0,141	-0,107
2	1,289	1,281	1,406	1,325
3	3,898	4,246	4,670	4,271
4	5,761	5,842	6,205	5,936
5	6,287	6,591	6,776	6,551
6	7,007	7,136	7,391	7,178
7	7,606	7,561	7,403	7,482
8	7,994	7,994	8,067	8,018
9	8,501	8,568	8,602	8,557
10	9,352	9,105	9,356	9,271
11	10,785	10,706	11,150	10,880
12	12,025	11,656	12,002	11,894
13	12,420	12,507	12,826	12,584
14	13,048	12,940	13,215	13,068
15	13,158	13,167	13,368	13,231

Emulsifier 9 (1%)

t (min)	Determ.1	Determ.2	Determ.3	Average
0	-0,056	0,106	0,096	0,049
1	0,18	0,371	0,351	0,301
2	2,030	1,892	1,705	1,876
3	4,635	4,379	4,476	4,497
4	5,965	6,218	5,626	5,936
5	6,724	6,836	6,708	6,756
6	6,950	7,085	7,224	7,086
7	7,284	7,581	7,634	7,608
8	8,158	8,272	8,209	8,213
9	8,737	8,795	8,718	8,750
10	9,849	9,979	9,684	9,837
11	11,409	11,296	11,399	11,368
12	12,364	12,444	12,628	12,479
13	12,992	13,301	12,767	13,020
14	13,552	13,452	13,446	13,483
15	13,714	13,969	13,973	13,885

Emulsifier 10 (1%)

t (min)	Determ.1	Determ.2	Determ.3	Average
0	0,336	0,139	0,352	0,276

1	0,182	0,283	-0,112	0,118
2	1,813	0,871	1,326	1,337
3	4,556	3,984	3,912	4,151
4	6,014	5,768	6,032	5,938
5	6,851	6,577	6,747	6,725
6	6,842	6,924	7,023	6,930
7	7,210	7,358	7,441	7,400
8	7,560	7,763	7,789	7,704
9	8,448	8,208	8,159	8,272
10	8,974	8,498	8,758	8,743
11	10,349	9,753	9,891	9,998
12	11,794	11,524	11,442	11,587
13	12,626	12,492	12,706	12,608
14	13,299	13,166	13,313	13,259
15	13,747	13,614	13,636	13,666

Emulsifier 11 (1%)

t (min)	Determ.1	Determ.2	Determ.3	Average
0	0,091	0,230	0,051	0,124
1	0,077	0,181	-0,075	0,061
2	1,408	1,266	1,091	1,255
3	4,549	4,187	4,429	4,388
4	5,992	6,018	5,930	5,980
5	6,652	6,705	6,672	6,676
6	6,990	7,129	6,971	7,030
7	7,095	7,389	7,227	7,308
8	8,060	7,938	8,015	8,004
9	8,647	8,352	8,458	8,486
10	9,820	9,181	9,473	9,491
11	11,659	10,700	10,772	11,044
12	12,623	12,256	12,057	12,312
13	13,351	12,994	13,125	13,157
14	13,624	13,432	13,654	13,570
15	14,203	13,848	13,865	13,972

Emulsifier 12 (1%)

t (min)	Determ.1	Determ.2	Determ.3	Average
0	0,485	0,374	0,127	0,329
1	-0,318	-0,036	0,147	-0,069
2	0,420	0,377	0,772	0,523
3	3,407	4,082	4,089	3,859
4	5,125	5,656	5,898	5,560

5	6,032	6,618	6,728	6,459
6	6,224	6,894	6,973	6,697
7	6,591	7,291	7,232	7,262
8	6,615	7,458	7,627	7,233
9	7,361	7,769	8,072	7,734
10	7,435	8,294	8,299	8,009
11	7,984	8,578	8,538	8,367
12	8,986	10,070	9,673	9,576
13	10,508	11,381	11,197	11,029
14	11,492	12,152	12,365	12,003
15	12,091	12,801	12,885	12,592
16	12,474	13,463	13,134	13,024

Fat blend B – Table Margarine

Pure Fat Blend B				
t (min)	Determ.1	Determ.2	Determ.3	Average
0	0,290	0,317	-0,162	0,148
1	-0,042	-0,054	0,179	0,028
2	1,407	0,693	0,681	0,927
3	3,775	3,672	3,623	3,690
4	4,415	4,347	4,435	4,399
5	4,281	4,250	4,457	4,329
6	4,691	4,613	4,646	4,650
7	4,881	4,682	4,763	4,775
8	4,622	4,551	4,694	4,622
9	4,698	4,288	4,740	4,575
10	5,036	5,198	5,079	5,104
11	5,575	5,478	5,192	5,415
12	5,949	6,137	5,990	6,025
13	6,704	6,620	6,442	6,589
14	7,122	7,310	7,196	7,209
15	7,303	7,697	7,443	7,481
16	8,082	7,995	7,818	7,965
17	8,268	8,258	8,414	8,313
18	8,483	8,390	8,432	8,435
19	8,646	8,557	8,627	8,610
20	8,817	8,701	8,677	8,732

Emulsifier 1 (1%)

t (min)	Determ.1	Determ.2	Determ.3	Average
0	0,202	0,292	-0,066	0,143
1	1,038	0,678	0,613	0,776
2	2,375	2,266	1,843	2,161
3	3,671	3,716	3,656	3,681
4	4,144	4,596	4,498	4,413
5	4,776	4,917	4,740	4,811
6	6,057	5,986	5,826	5,956
7	7,021	7,056	7,359	7,145
8	8,080	8,221	8,043	8,115
9	8,628	8,785	8,542	8,652
10	9,108	9,223	9,010	9,114
11	9,286	9,416	9,192	9,298
12	9,615	9,677	9,552	9,615
13	9,674	9,857	9,635	9,722
14	9,839	9,789	9,931	9,853
15	9,730	10,019	9,980	9,910
20	10,086	10,042	9,898	10,009

Emulsifier 2 (1%)

t (min)	Determ.1	Determ.2	Determ.3	Average
0	0,418	0,289	0,275	0,327
1	-0,150	0,585	0,358	0,264
2	2,089	2,762	2,720	2,524
3	3,472	4,253	4,196	3,974
4	3,756	4,614	4,400	4,257
5	4,058	4,507	4,767	4,444
6	4,172	5,069	4,841	4,694
7	4,302	4,927	4,986	4,738
8	4,342	5,433	5,110	4,962
9	4,927	5,374	5,166	5,156
10	5,280	6,178	6,097	5,852
11	5,955	7,138	7,124	6,739
12	7,014	7,829	7,663	7,502
13	7,697	8,401	8,495	8,198
14	8,100	8,841	8,963	8,635
15	8,606	9,374	9,052	9,011
16	8,646	8,538	9,376	8,853
17	9,197	9,727	9,638	9,521

Emulsifier 3 (1%)

t (min)	Determ.1	Determ.2	Determ.3	Average
0	0,301	0,227	0,303	0,277
1	0,716	0,718	0,266	0,567
2	2,859	2,911	2,569	2,780
3	3,883	4,147	4,285	4,105
4	4,534	4,655	4,679	4,623
5	4,863	5,036	4,761	4,887
6	4,748	5,177	4,926	4,950
7	4,849	4,985	5,194	5,009
8	5,008	5,063	5,283	5,118
9	5,363	5,471	5,499	5,444
10	6,062	5,948	6,182	6,064
11	6,632	6,819	6,996	6,816
12	7,590	7,679	7,731	7,667
13	8,243	8,272	8,530	8,348
14	8,962	8,854	8,959	8,925
15	9,337	9,251	9,373	9,320
16	9,422	9,471	9,564	9,486

Emulsifier 4 (1%)

t (min)	Determ.1	Determ.2	Determ.3	Average
0	-0,097	0,218	0,083	0,068
1	-1,221	0,060	0,818	-0,114
2	0,890	2,767	4,202	2,620
3	3,285	4,388		3,837
4	3,633	5,122	5,203	4,653
5	4,489	5,823	5,991	5,434
6	6,030	6,964	6,886	6,627
7	6,244	7,850	8,007	7,367
8	7,413	8,365	8,563	8,114
9	7,861	8,939	8,840	8,547
10	8,139	9,070	9,247	8,819
11	8,154	9,370	9,440	8,988
12	8,712	9,529	9,459	9,233
13	8,644	9,592	9,762	9,333
14	8,703	9,905	9,783	9,464
15	8,634	9,784	9,709	9,376

Emulsifier 5 (1%)

t (min)	Determ.1	Determ.2	Determ.3	Average
0	0,344	0,135	0,244	0,241
1	2,724	2,517	2,756	2,666
2	4,997	4,841	5,168	5,002
3	5,678	5,470	5,436	5,528
4	6,854	6,696	6,856	6,802
5	8,153	8,039	7,729	7,974
6	9,151	8,964	9,025	9,047
7	9,799	9,472	9,894	9,722
8	10,023	10,149	10,222	10,131
9	10,161	10,381	10,381	10,308
10	10,624	10,335	10,464	10,474
11	10,710	10,538	10,592	10,613
12	10,810	10,963	10,802	10,858
13	10,628	10,974	10,788	10,797
14	10,812	10,887	10,750	10,816
15	11,151	11,040	11,019	11,070

Emulsifier 6 (1%)

t (min)	Determ.1	Determ.2	Determ.3	Average
0	0,025	-0,123	0,109	0,004
1	2,989	2,656	2,308	2,651
2	4,929	5,116	5,037	5,027
3	5,500	5,226	5,441	5,389
4	6,327	6,476	6,635	6,479
5	8,074	8,082	7,744	7,967
6	9,043	9,251	8,859	9,051
7	9,722	9,561	9,668	9,650
8	9,919	10,324	10,085	10,109
9	10,311	10,681	10,357	10,450
10	10,568	10,855	10,654	10,692
11	10,583	10,790	10,583	10,652
12	10,606	10,983	10,879	10,823
13	10,954	11,089	10,703	10,915
14	10,939	10,827	11,200	10,989
15	10,900	10,988	10,926	10,938

Emulsifier 7 (1%)

t (min)	Determ.1	Determ.2	Determ.3	Average
0	0,220	0,411	0,336	0,322
1	2,726	2,715	2,082	2,508
2	4,482	4,530	4,819	4,610
3	5,514	5,355	5,133	5,334
4	6,551	6,254	6,332	6,379
5	7,656	7,411	7,452	7,506
6	8,756	8,845	8,787	8,796
7	9,584	9,348	9,651	9,528
8	10,335	9,937	9,954	10,075
9	10,316	10,065	10,171	10,184
10	10,859	10,405	10,471	10,578
11	10,739	10,354	10,488	10,527
12	10,909	10,508	10,910	10,776
13	10,866	10,647	10,876	10,796
14	10,970	10,607	10,789	10,789
15	11,079	10,736	10,803	10,873

Emulsifier 8 (1%)

t (min)	Determ.1	Determ.2	Determ.3	Average
0	-0,176	-0,288	0,437	-0,009
1	2,872	1,957	1,755	2,195
2	5,104	4,548	4,714	4,789
3	5,394	5,339	5,154	5,296
4	5,975	6,088	5,916	5,993
5	7,422	7,262	7,242	7,309
6	8,775	8,688	8,144	8,536
7	9,429	9,292	9,410	9,377
8	10,252	9,702	9,839	9,931
9	10,391	10,121	10,199	10,237
10	10,590	10,304	10,314	10,403
11	10,725	10,672	10,560	10,652
12	10,962	10,386	10,330	10,559
13	11,149	10,944	10,850	10,981
14	11,039	10,943	10,835	10,939
15	11,241	10,891	10,911	11,014

Emulsifier 9 (1%)

t (min)	Determ.1	Determ.2	Determ.3	Average

0	-0,160	0,360	0,301	0,167
1	2,670	1,789	1,358	1,939
2	4,523	4,387	4,078	4,329
3	4,966	4,787	4,743	4,832
4	5,044	4,952	5,132	5,043
5	5,463	5,321	5,259	5,348
6	5,362	5,611	5,473	5,482
7	5,837	5,737	5,861	5,812
8	6,929	6,690	6,551	6,723
9	7,757	7,635	7,498	7,630
10	8,563	8,613	8,623	8,600
11	9,204	9,337	9,029	9,190
12	9,733	9,790	9,633	9,719
13	9,687	9,825	9,878	9,797
14	10,056	9,932	10,380	10,123
15	10,279	10,093	10,237	10,203
16	10,130	10,183	10,164	10,159

Emulsifier 10 (1%)

t (min)	Determ.1	Determ.2	Determ.3	Average
0	0,597	-0,023	-0,119	0,152
1	1,659	1,105	0,463	1,076
2	4,193	4,103	3,803	4,033
3	4,971	4,971	5,133	5,025
4	5,223	5,288	5,395	5,302
5	5,356	5,276	5,042	5,225
6	5,145	5,402	5,549	5,365
7	5,422	5,562	5,557	5,514
8	5,446	5,534	5,408	5,463
9	5,667	5,508	5,359	5,511
10	5,943	5,934	5,815	5,897
11	6,547	6,086	5,882	6,172
12	7,021	6,731	6,698	6,817
13	7,786	7,350	6,977	7,371
14	8,015	7,763	7,731	7,836
15	9,002	8,572	8,279	8,618
16	9,026	9,091	8,674	8,930
17	9,606	9,352	9,054	9,337
18	9,758	9,704	9,470	9,644
19	9,884	9,883	9,507	9,758
20	9,889	10,143	9,819	9,950
25	10,574	10,661	10,446	10,560

Emulsifier 11 (1%)

t (min)	Determ.1	Determ.2	Determ.3	Average
0	0,380	0,120	0,178	0,226
1	1,883	1,153	0,319	1,118
2	4,250	3,865	3,398	3,838
3	4,953	4,731	4,522	4,735
4	5,312	5,228	4,792	5,111
5	5,386	5,106	5,179	5,224
6	5,362	5,572	5,431	5,455
7	5,548	5,458	5,330	5,445
8	5,524	5,618	5,469	5,537
9	6,083	5,537	5,617	5,746
10	6,480	6,051	6,115	6,215
11	6,824	6,780	6,682	6,762
12	7,919	7,410	7,331	7,553
13	8,329	7,999	7,670	7,999
14	8,858	8,621	8,534	8,671
15	9,264	9,156	8,980	9,133
16	9,661	9,602	9,420	9,561
17	10,211	9,618	9,604	9,811
18	9,873	9,880	9,706	9,820
19	10,227	10,065	9,903	10,065
20	10,324	10,34	10,116	10,26

Emulsifier 12 (1%)

t (min)	Determ.1	Determ.2	Determ.3	Average
0	0,191	0,225	0,180	0,199
1	1,043	0,141	-0,103	0,360
2	4,229	3,643	3,660	3,844
3	4,836	4,318	4,335	4,496
4	5,258	4,917	5,119	5,098
5	5,437	4,802	4,987	5,075
6	5,426	4,902	5,361	5,230
7	5,334	5,121	5,479	5,311
8	5,905	5,420	5,606	5,644
9	6,373	5,712	5,749	5,945
10	7,188	6,571	6,658	6,806
11	8,120	7,337	7,250	7,569
12	8,434	8,167	7,950	8,184
13	9,262	8,510	8,749	8,840

14	9,490	9,073	9,295	9,286
15	9,771	9,220	9,401	9,464
16	10,018	9,287	9,740	9,682
17	9,982	9,58	9,703	9,755

Fat blend C – Puff pastry margarine

Pure Fat Blend C

t (min)	Determ.1	Determ.2	Determ.3	Average
0	0,272	-0,080	-0,055	0,046
1	4,146	5,598	1,828	3,857
2	18,046	17,165	15,123	16,778
3	22,973	22,898	21,842	22,571
4	25,175	24,928	24,368	24,824
5	27,557	26,744	-	27,151
6	30,535	30,216	29,987	30,246
7	32,830	32,749	32,295	32,625
8	34,131	34,027	33,398	33,852
9	34,860	34,871	34,072	34,601
10	34,695	35,207	34,508	34,803
11	35,412	35,517	34,917	35,282
12	35,744	35,735	34,888	35,456
13	35,905	35,991	35,126	35,674
14	36,075	35,931	35,233	35,746
15	36,126	36,345	35,319	35,930

Emulsifier 1 (1%)

t (min)	Determ.1	Determ.2	Determ.3	Average
0	0,212	0,436	-0,087	0,187
1	12,462	12,388	12,142	12,331
2	21,329	21,489	21,352	21,390
3	24,778	24,758	24,816	24,784
4	27,312	27,368	27,053	27,244
5	30,778	30,581	30,448	30,602
6	33,399	33,187	33,265	33,284
7	34,519	34,626	34,549	34,565

8	35,061	35,092	35,272	35,142
9	35,706	35,752	35,613	35,690
10	35,850	35,802	35,988	35,880
11	36,217	36,134	36,118	36,156
12	36,459	36,672	36,301	36,477
13	35,563	35,870	35,552	35,662
14	-	-	-	-
15	-	-	-	-

Emulsifier 2 (1%)

t (min)	Determ.1	Determ.2	Determ.3	Average
0	-0,122	0,001	-0,104	-0,075
1	4,549	4,369	4,031	4,316
2	16,825	17,245	17,371	17,147
3	21,673	21,779	22,235	21,896
4	23,676	23,858	24,132	23,889
5	25,649	26,065	26,061	25,925
6	27,800	28,078	28,114	27,997
7	30,277	30,752	30,938	30,656
8	32,539	32,754	32,991	32,761
9	33,815	34,067	34,240	34,041
10	34,627	34,953	34,949	34,843
11	35,162	35,140	35,475	35,259
12	35,290	35,562	35,763	35,538
13	35,708	35,658	36,085	35,817
14	35,826	35,908	36,263	35,999
15	35,756	36,156	36,167	36,026

Emulsifier 3 (1%)

t (min)	Determ.1	Determ.2	Determ.3	Average
0	-0,054	0,251	-0,140	0,019
1	4,151	5,331	7,900	5,794
2	16,872	17,546	18,922	17,780
3	21,964	22,598	23,426	22,663
4	24,158	24,704	25,164	24,675
5	26,149	26,449	27,193	26,597
6	28,810	28,871	29,595	29,092
7	31,555	31,539	32,518	31,871
8	33,331	33,725	34,204	33,753
9	34,294	34,800	35,328	34,807

10	34,907	35,467	35,851	35,408
11	35,157	35,937	36,056	35,717
12	35,542	36,262	36,272	36,025
13	35,645	36,320	36,673	36,213
14	35,765	36,594	36,855	36,405
15	35,951	36,751	37,187	36,630

Emulsifier 4 (1%)

t (min)	Determ.1	Determ.2	Determ.3	Average
0	0,543	-0,222	-0,303	0,006
1	4,650	5,299	3,788	4,579
2	17,777	18,549	17,525	17,950
3	22,594	23,274	22,785	22,884
4	25,303	25,360	24,845	25,169
5	27,540	27,691	27,190	27,474
6	30,271	30,436	29,697	30,135
7	32,484	32,681	32,406	32,524
8	33,763	34,245	33,947	33,985
9	34,631	35,314	34,528	34,824
10	35,350	35,538	35,340	35,409
11	35,673	36,021	35,588	35,761
12	35,847	36,429	35,928	36,068
13	36,176	36,630	36,282	36,363
14	36,206	36,751	36,439	36,465
15	36,648	36,883	36,444	36,658

Emulsifier 5 (1%)

t (min)	Determ.1	Determ.2	Determ.3	Average
0	0,124	0,311	-0,176	0,086
1	3,952	4,541	3,014	3,836
2	17,329	17,761	17,552	17,547
3	22,619	22,649	22,603	22,624
4	24,766	25,023	24,817	24,869
5	26,855	27,459	26,969	27,094
6	29,836	30,264	29,734	29,945
7	31,892	32,231	31,768	31,964
8	33,216	33,627	33,352	33,398
9	34,340	34,487	34,262	34,363
10	35,025	34,976	34,911	34,971
11	35,208	35,451	35,256	35,305

12	35,807	35,995	35,831	35,878
13	36,242	36,156	36,204	36,201
14	36,143	36,418	36,089	36,217
15	36,332	36,597	36,338	36,422

Emulsifier 6 (1%)

t (min)	Determ.1	Determ.2	Determ.3	Average
0	0,224	-0,085	0,064	0,068
1	3,683	3,480	2,949	3,371
2	16,798	16,537	16,660	16,665
3	21,956	21,806	22,160	21,974
4	24,056	24,379	24,195	24,210
5	26,144	25,803	26,087	26,011
6	28,352	28,431	28,562	28,448
7	30,912	30,766	31,464	31,047
8	32,697	32,913	33,146	32,919
9	33,797	33,711	34,016	33,841
10	34,177	34,387	34,497	34,354
11	34,799	34,725	34,867	34,797
12	35,116	34,808	35,389	35,104
13	35,287	35,246	35,465	35,333
14	35,550	35,425	35,727	35,567
15	35,788	35,552	35,393	35,578

Emulsifier 7 (1%)

t (min)	Determ.1	Determ.2	Determ.3	Average
0	-0,071	0,024	-0,091	-0,046
1	1,802	4,174	2,669	2,882
2	15,387	17,165	15,620	16,057
3	21,274	22,398	21,820	21,831
4	23,761	24,451	24,245	24,152
5	25,706	26,261	26,074	26,014
6	27,921	29,265	29,046	28,744
7	30,309	31,058	30,796	30,721
8	32,230	32,911	32,605	32,582
9	33,489	33,729	33,694	33,637
10	33,852	34,503	34,410	34,255
11	34,434	34,596	34,777	34,602
12	34,825	34,885	35,125	34,945
13	34,973	35,063	35,408	35,148

14	35,130	35,321	35,666	35,372
15	35,275	35,386	35,712	35,458

Emulsifier 8 (1%)

t (min)	Determ.1	Determ.2	Determ.3	Average
0	-0,070	0,238	-0,008	0,053
1	2,498	2,716	2,654	2,623
2	15,717	16,701	16,114	16,177
3	21,539	22,011	21,970	21,840
4	23,741	24,389	24,139	24,090
5	25,565	25,710	25,685	25,653
6	27,328	27,892	27,750	27,657
7	29,881	30,330	30,207	30,139
8	31,579	32,506	32,244	32,110
9	33,432	33,705	33,720	33,619
10	33,771	34,356	34,575	34,234
11	34,304	34,808	34,763	34,625
12	34,687	35,029	35,105	34,940
13	35,060	35,364	35,406	35,277
14	35,178	35,604	35,695	35,492
15	35,271	35,652	35,915	35,613

Emulsifier 9 (1%)

t (min)	Determ.1	Determ.2	Determ.3	Average
0	0,135	0,065	-0,311	-0,037
1	4,525	4,439	2,350	3,771
2	16,781	17,210	15,487	16,493
3	21,516	22,084	21,221	21,607
4	23,895	24,221	23,602	23,906
5	25,761	25,981	25,393	25,712
6	28,066	28,268	27,773	28,036
7	30,581	30,434	30,354	30,456
8	32,472	32,740	32,401	32,538
9	33,637	33,800	33,654	33,697
10	34,263	34,492	34,473	34,409
11	34,686	34,960	34,919	34,855
12	34,884	35,087	35,078	35,016
13	35,160	35,499	35,281	35,313
14	35,326	35,692	35,646	35,555
15	35,373	36,096	35,893	35,787

Emulsifier 10 (1%)

t (min)	Determ.1	Determ.2	Determ.3	Average
0	-0,139	-0,128	0,119	-0,049
1	2,439	1,698	2,348	2,162
2	16,024	15,736	15,952	15,904
3	21,911	22,212	22,199	22,107
4	24,392	24,332	24,255	24,326
5	25,709	25,833	25,883	25,808
6	27,509	27,615	27,766	27,630
7	30,238	30,301	30,221	30,253
8	32,791	32,662	32,582	32,678
9	33,954	33,963	33,894	33,937
10	34,612	34,467	34,709	34,596
11	34,971	34,990	34,998	34,986
12	35,309	35,271	35,278	35,286
13	35,607	35,462	35,626	35,565
14	35,729	35,706	35,596	35,677
15	35,763	35,901	35,928	35,864

Emulsifier 11 (1%)

t (min)	Determ.1	Determ.2	Determ.3	Average
0	-0,094	-0,093	-0,371	-0,186
1	4,660	3,815	3,017	3,831
2	17,413	17,780	16,745	17,313
3	22,086	22,731	22,358	22,392
4	24,268	24,366	24,168	24,267
5	25,692	26,191	25,811	25,898
6	27,845	28,191	28,127	28,054
7	30,625	30,932	30,786	30,781
8	33,010	33,071	33,019	33,033
9	34,104	34,435	35,235	34,591
10	34,649	35,205	34,997	34,950
11	34,976	35,603	35,476	35,352
12	35,282	35,781	35,779	35,614
13	35,427	36,072	36,033	35,844
14	35,922	36,254	36,123	36,100
15	36,027	36,379	36,324	36,243

Emulsifier 12 (1%)

t (min)	Determ.1	Determ.2	Determ.3	Average
0	0,301	0,351	0,468	0,373
1	2,127	2,407	3,470	2,668
2	16,177	16,039	16,560	16,259
3	22,339	21,818	22,660	22,272
4	24,375	24,204	24,716	24,432
5	25,702	25,602	26,101	25,802
6	27,421	27,334	27,802	27,519
7	29,905	30,130	30,264	30,100
8	32,349	32,447	32,771	32,522
9	33,841	33,571	33,876	33,763
10	34,188	34,379	34,631	34,399
11	34,816	34,597	35,073	34,829
12	35,035	34,919	35,178	35,044
13	35,223	35,083	35,531	35,279
14	35,726	35,389	35,655	35,590
15	35,652	35,447	35,952	35,684

APPENDIX D

DSC: Cooling - Duplicate Determination of Results from Appendix B

Fat blend A – Palm Oil (fat blend A = fat blend 1)

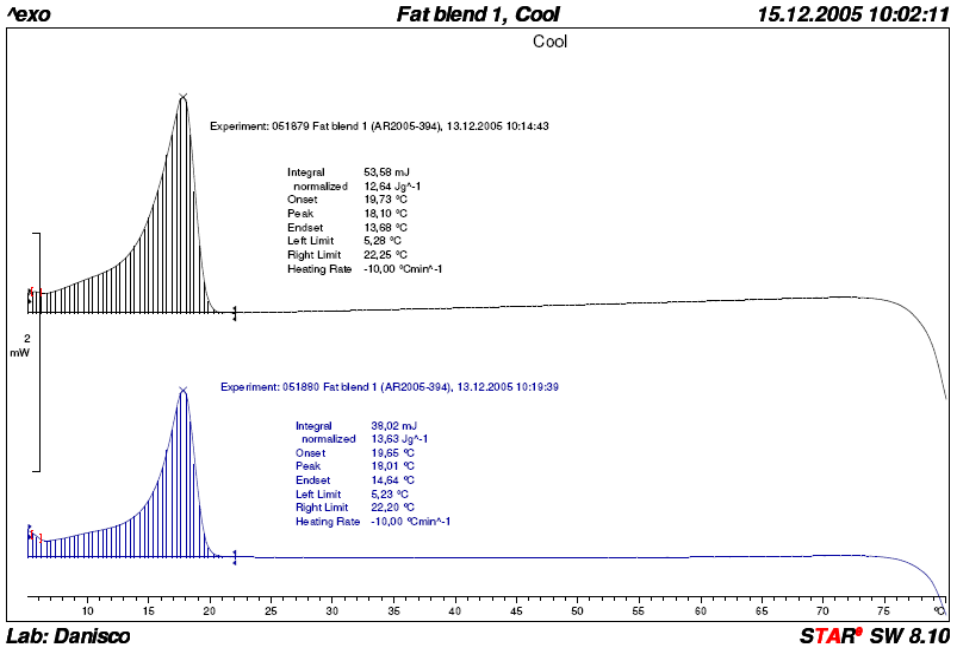

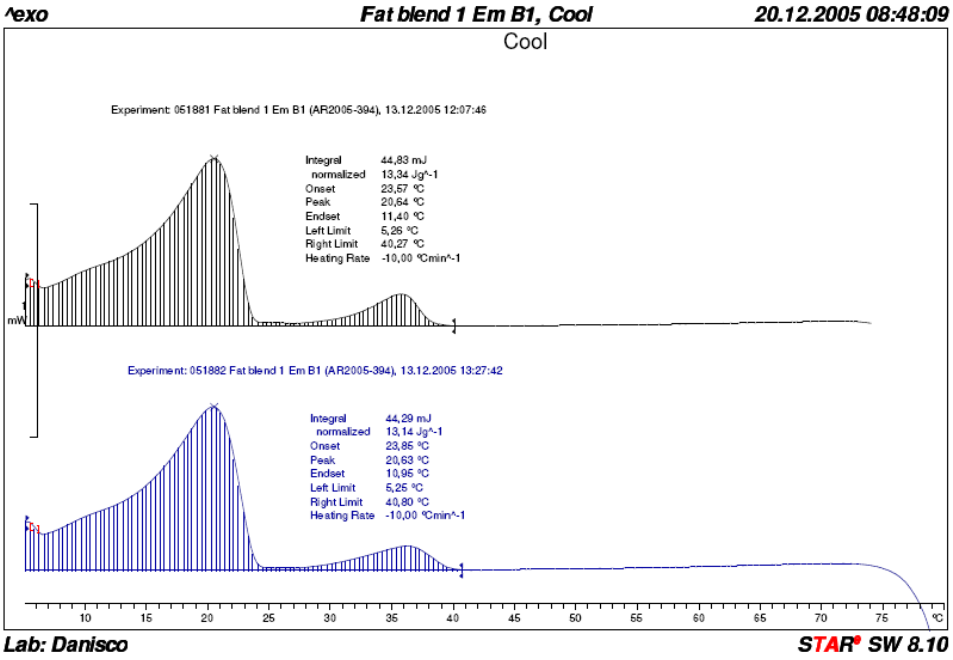

^exo **Fat blend 1 Em B2, cool** **20.12.2005 09:08:19**

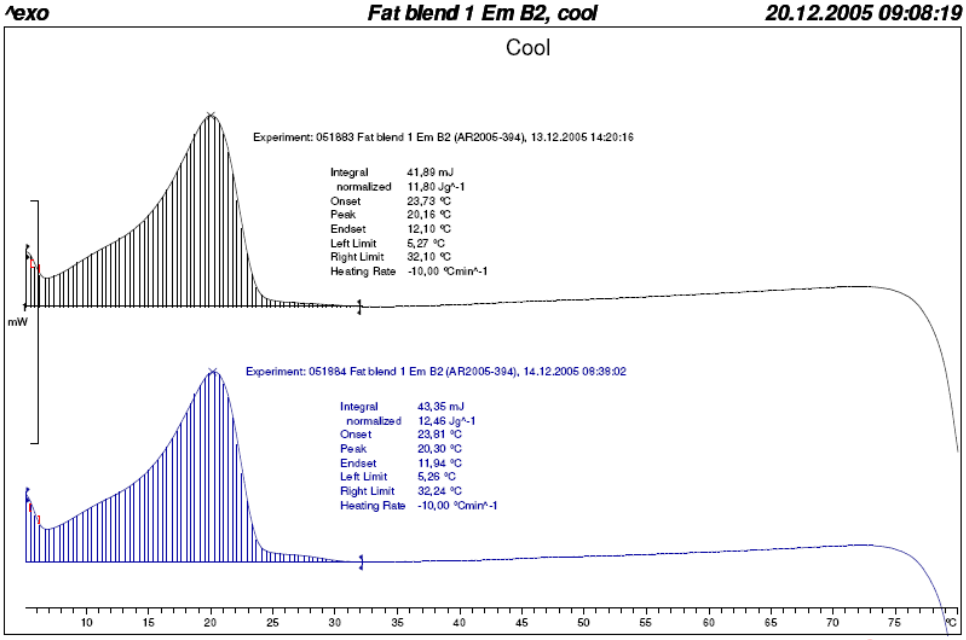

Lab: Danisco **STAR° SW 8.10**

^exo **Fat blend 1 Em B3, Cool** **20.12.2005 09:49:52**

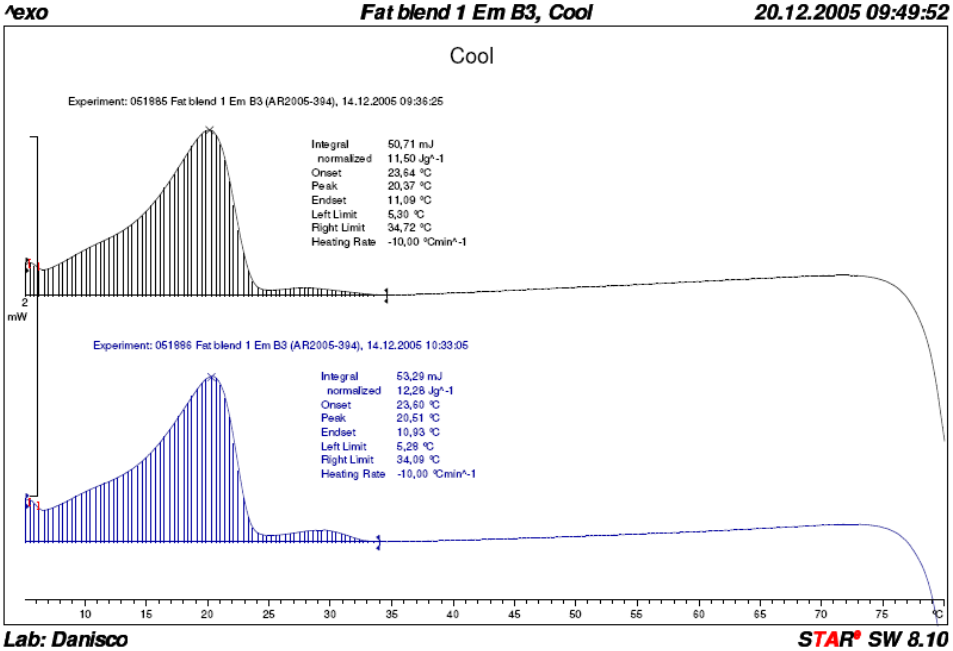

Lab: Danisco **STAR° SW 8.10**

^exo **Fat blend 1 Em B4, Cool** **20.12.2005 09:58:16**

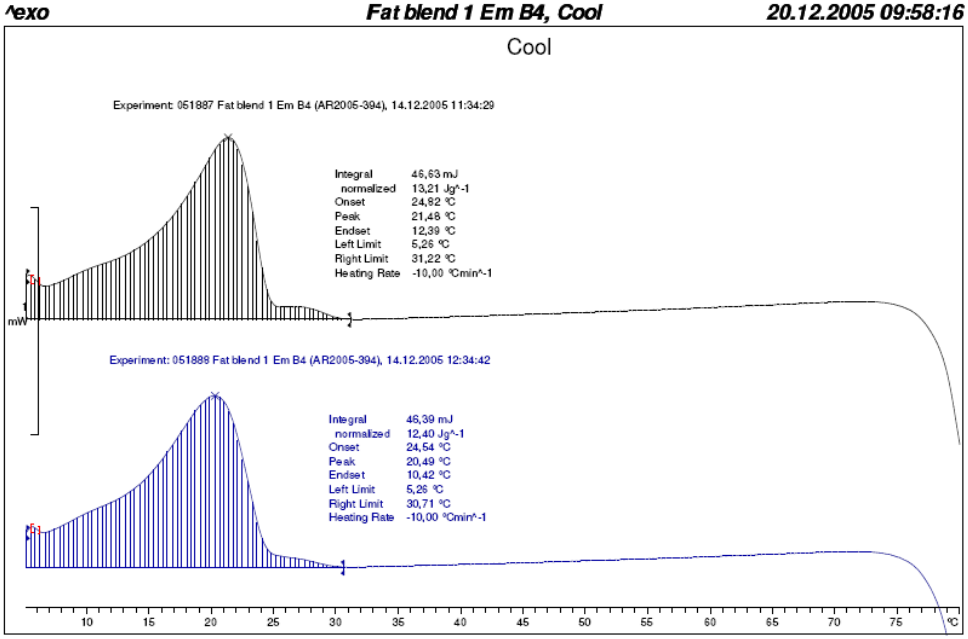

Lab: Danisco **STAR° SW 8.10**

^exo **Fat blend 1 Em B5, Cool** **20.12.2005 10:25:15**

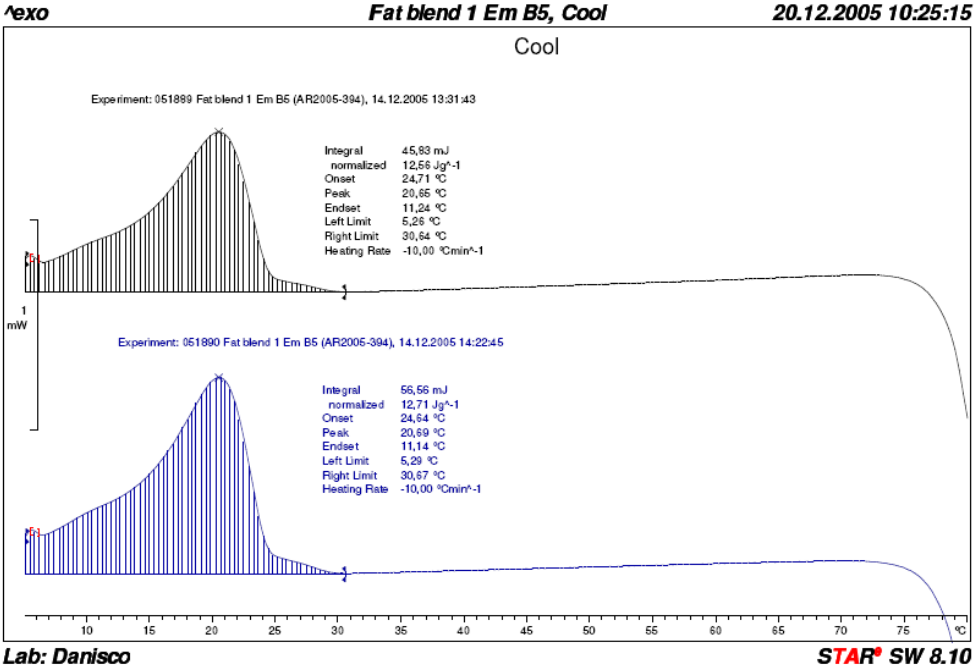

Lab: Danisco **STAR° SW 8.10**

^exo **Fat blend 1 Em B6, Cool** **20.12.2005 10:31:35**

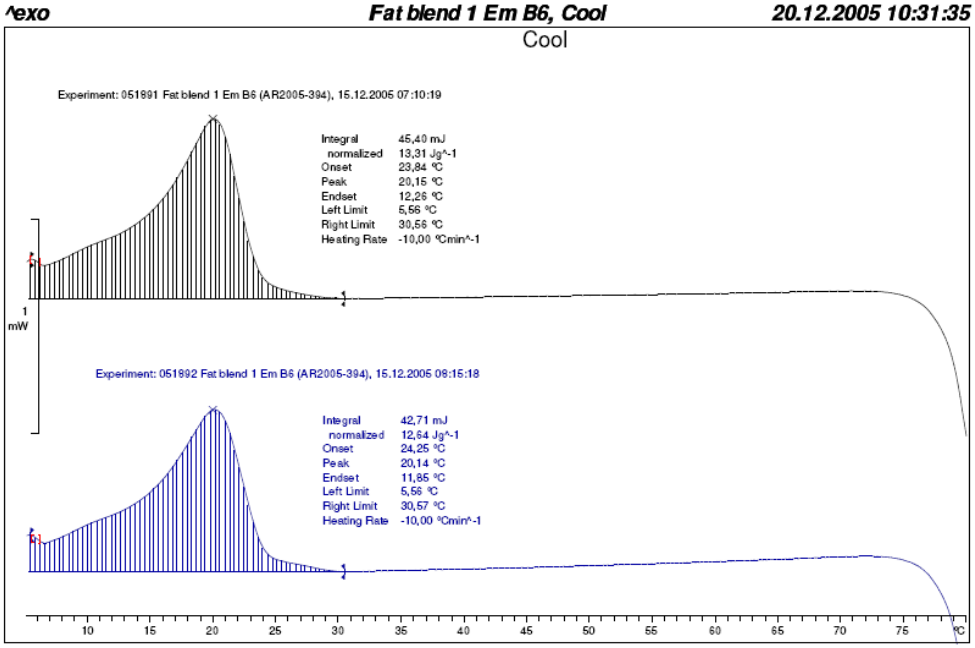

Lab: Danisco **STAR° SW 8.10**

^exo **Fat blend 1 Em B7, Cool** **20.12.2005 11:40:17**

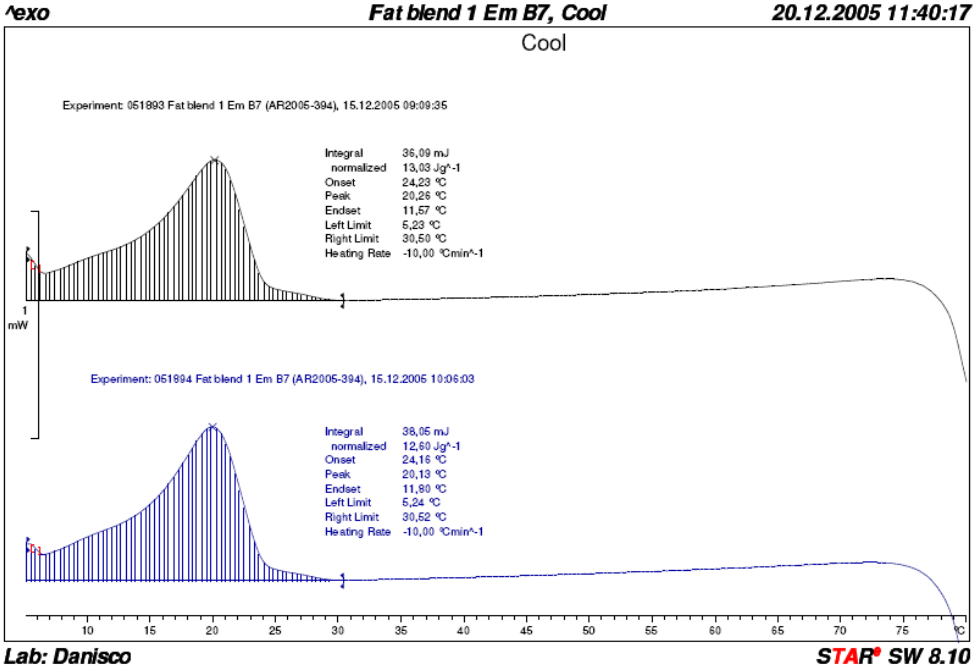

Lab: Danisco **STAR° SW 8.10**

^exo **Fat blend 1 Em B8, Cool** **20.12.2005 11:50:19**

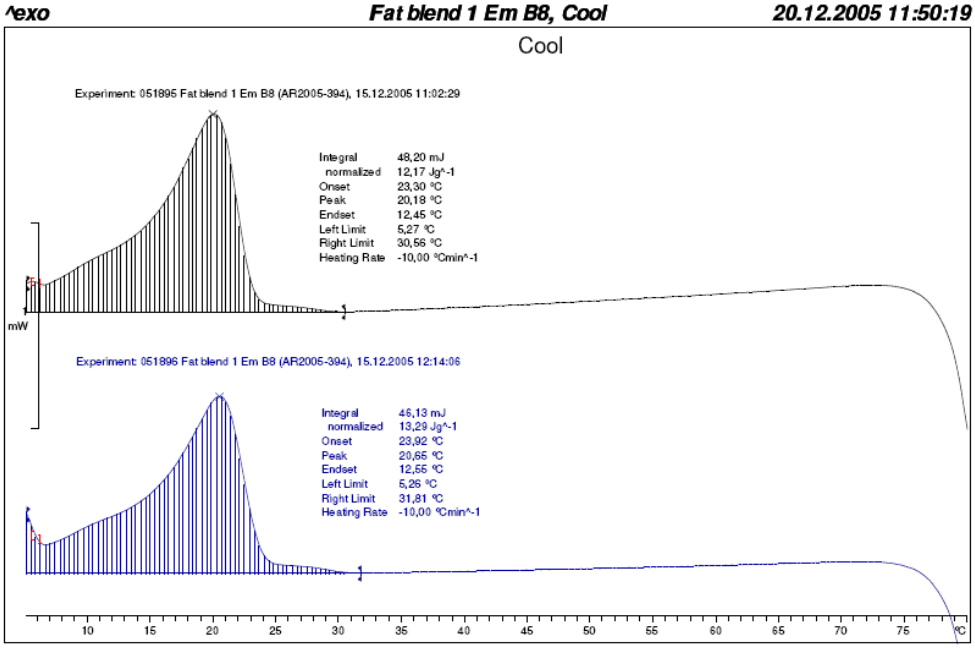

Lab: Danisco **STAR° SW 8.10**

^exo **Fat blend 1 Em B9, Cool** **20.12.2005 11:56:56**

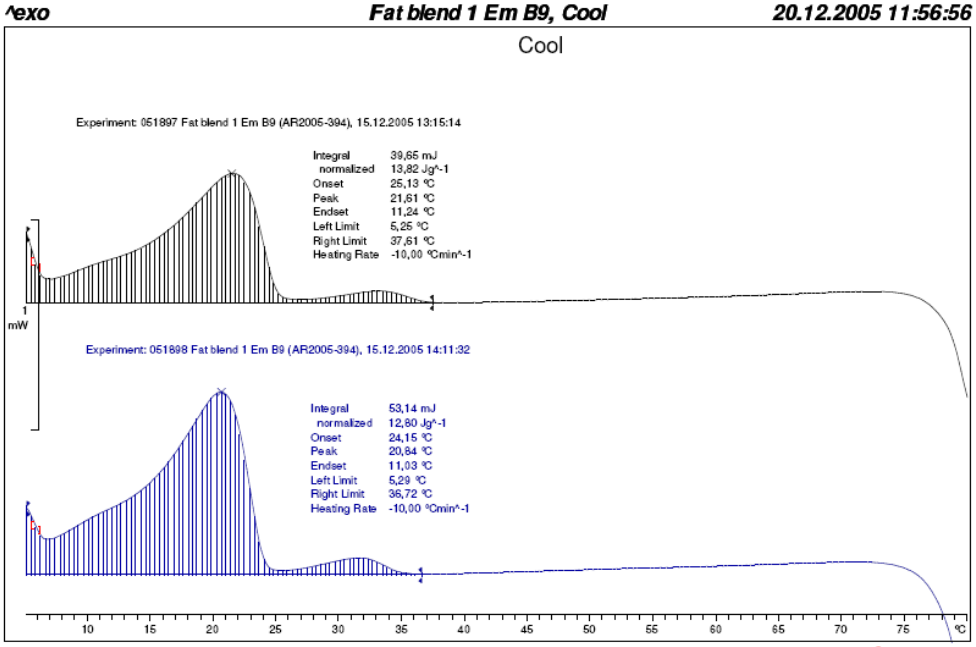

Lab: Danisco **STAR° SW 8.10**

^exo **Fat Blend 1 Em B10, Cool** **21.12.2005 09:38:20**

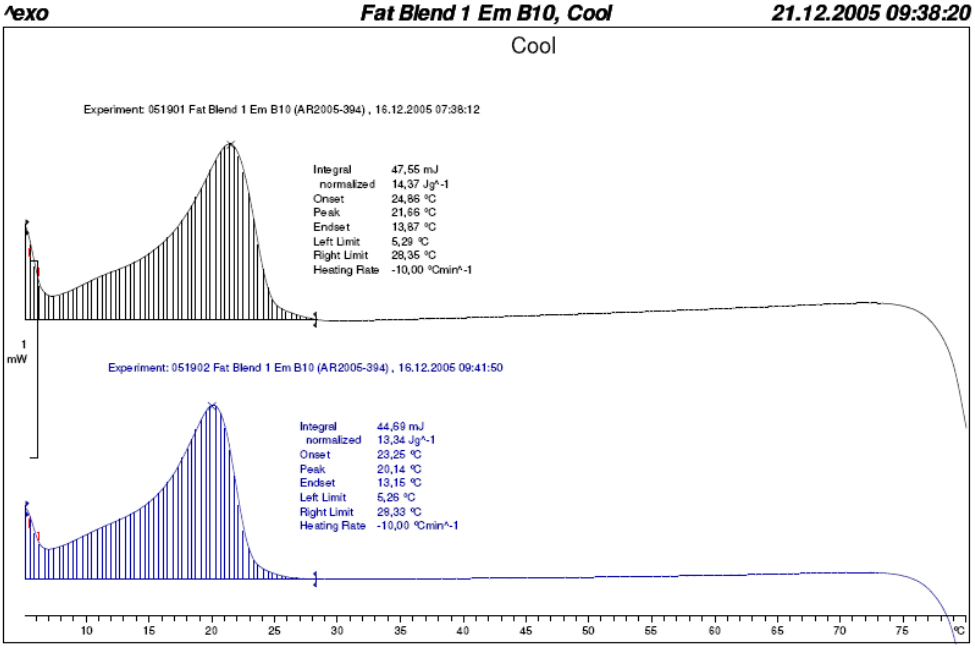

Lab: Danisco **STAR^e SW 8.10**

^exo **Fat Blend 1 Em B11, Cool** **21.12.2005 09:44:42**

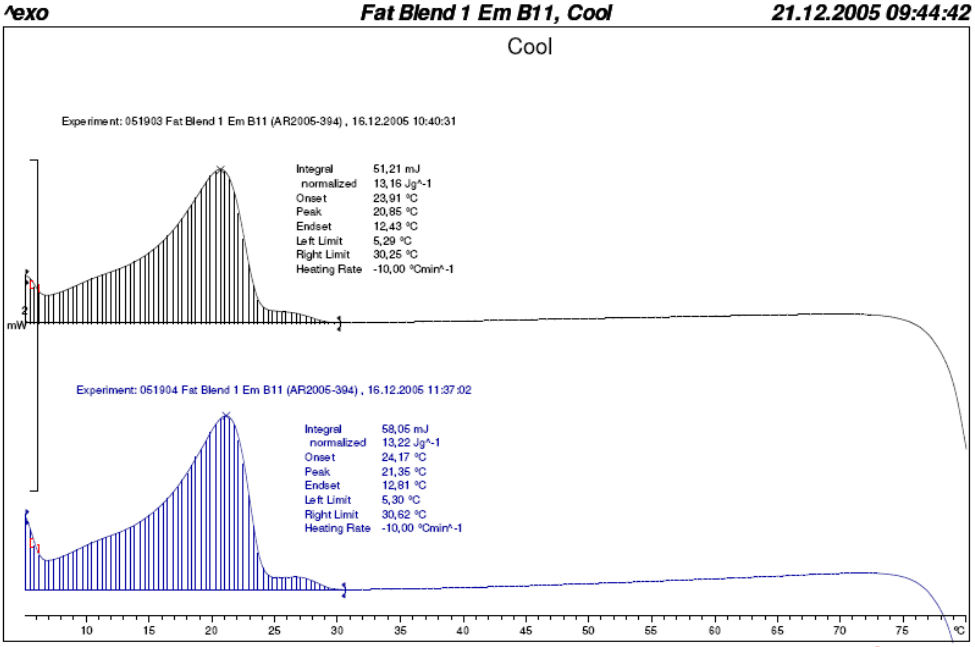

Lab: Danisco **STAR^e SW 8.10**

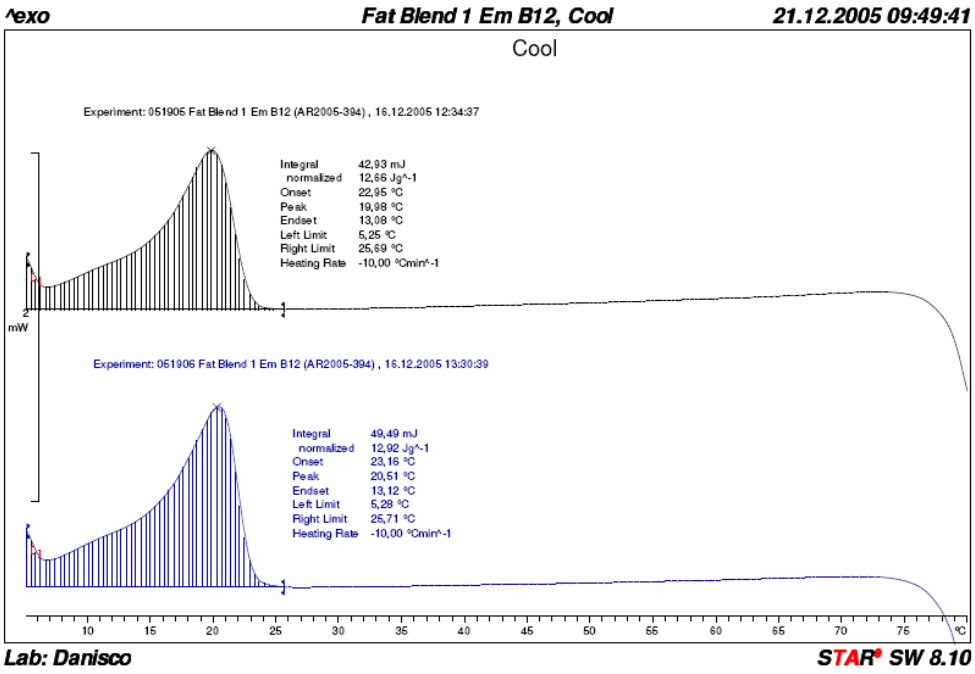

Fat blend B – Table margarine (fat blend B = fat blend 2)

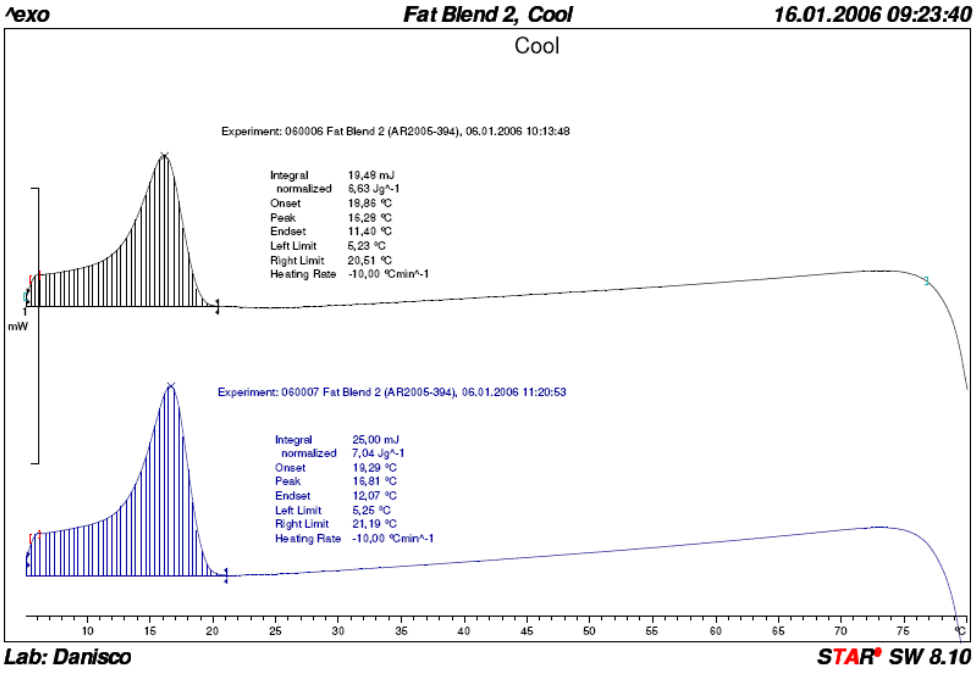

^exo **Fat Blend 2 Em B1, Cool** **16.01.2006 09:35:16**

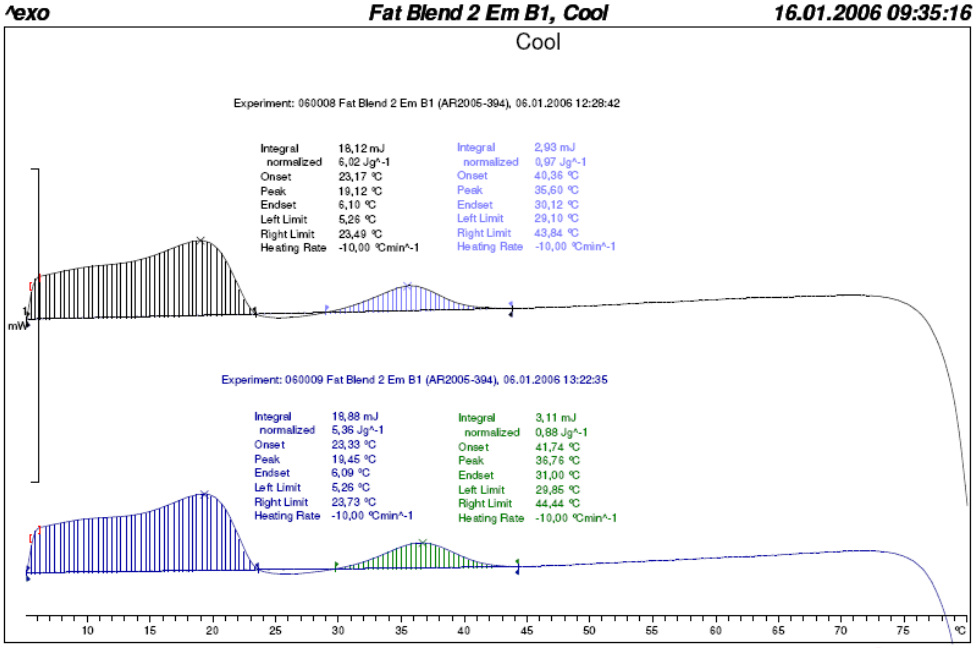

Lab: Danisco **STAR® SW 8.10**

^exo **Fat Blend 2 Em B3, Cool** **16.01.2006 09:58:16**

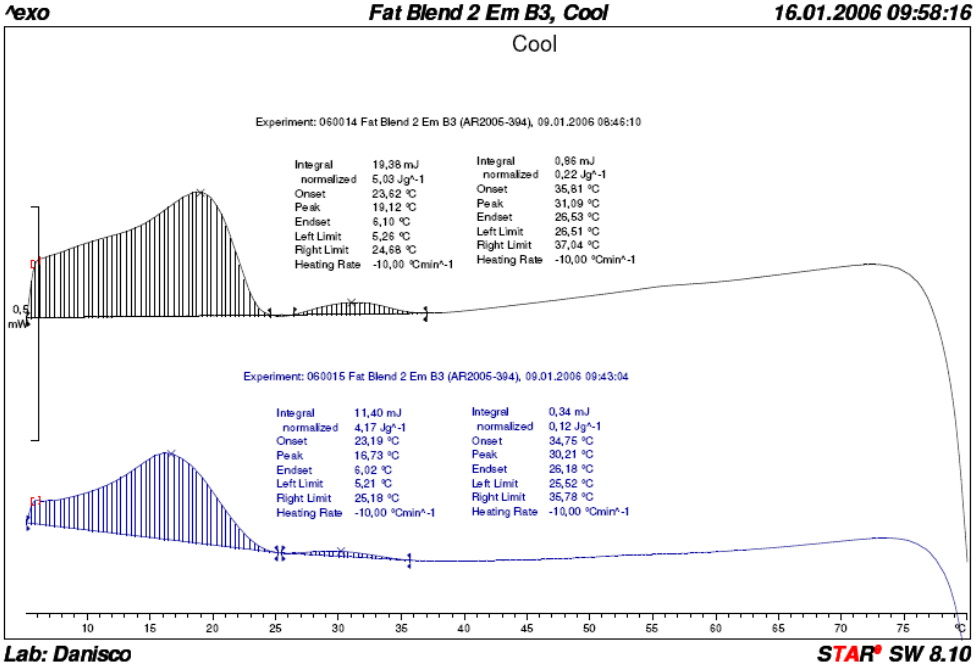

Lab: Danisco **STAR® SW 8.10**

^exo **Fat Blend 2 Em B4, Cool** **16.01.2006 10:05:12**

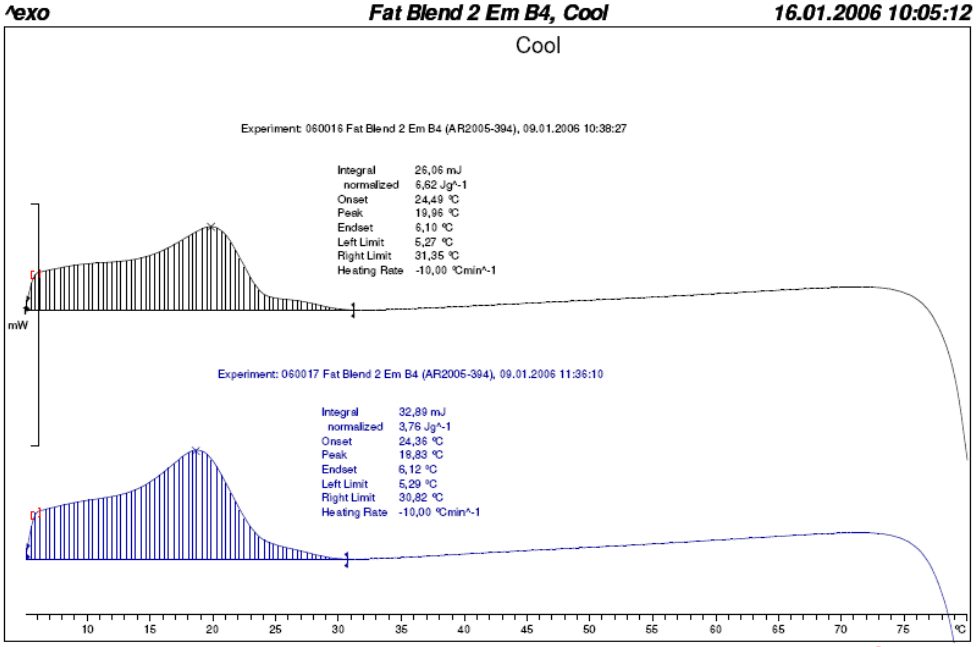

Lab: Danisco **STAR^e SW 8.10**

^exo **Fat Blend 2 Em B5, Cool** **19.01.2006 11:00:38**

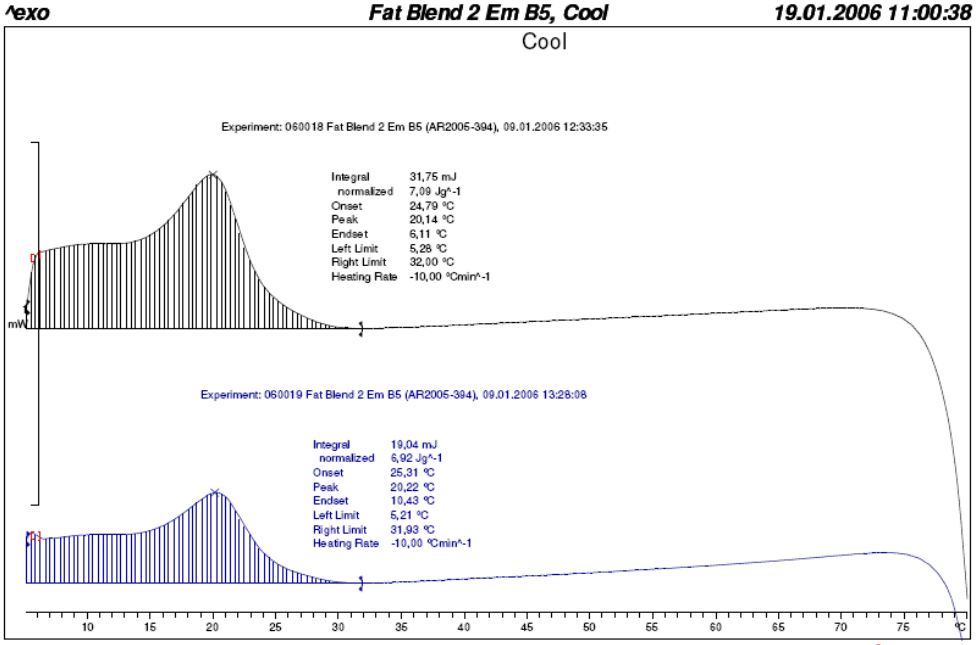

Lab: Danisco **STAR^e SW 8.10**

^exo **Fat Blend 2 Em B6, Cool** **19.01.2006 11:06:42**

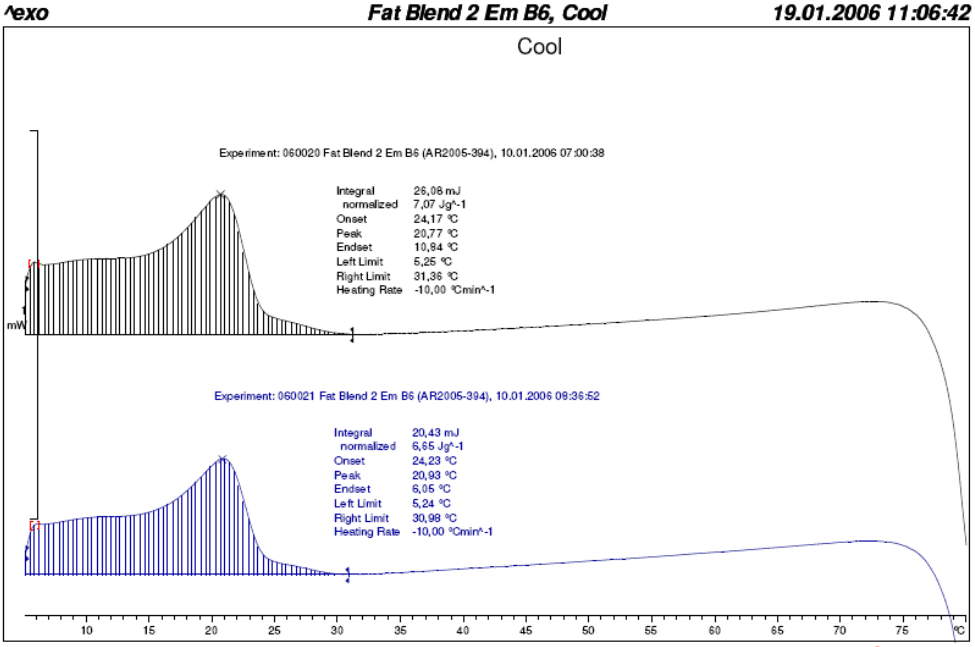

Lab: Danisco **STAR° SW 8.10**

^exo **Fat Blend 2 Em B7, Cool** **19.01.2006 11:13:07**

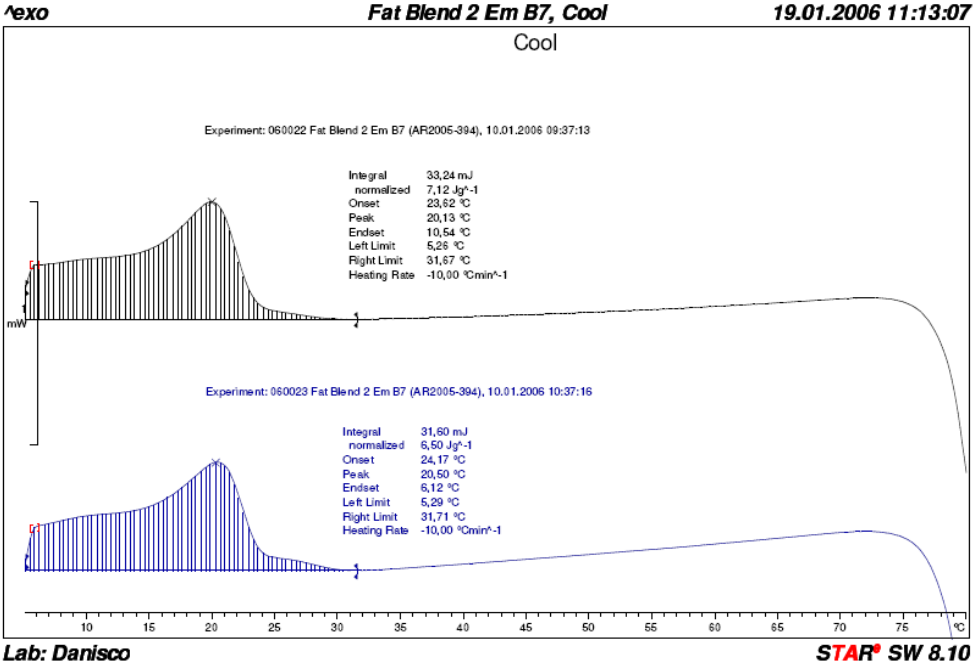

Lab: Danisco **STAR° SW 8.10**

^exo **Fat Blend 2 Em B8, Cool** **19.01.2006 12:22:28**

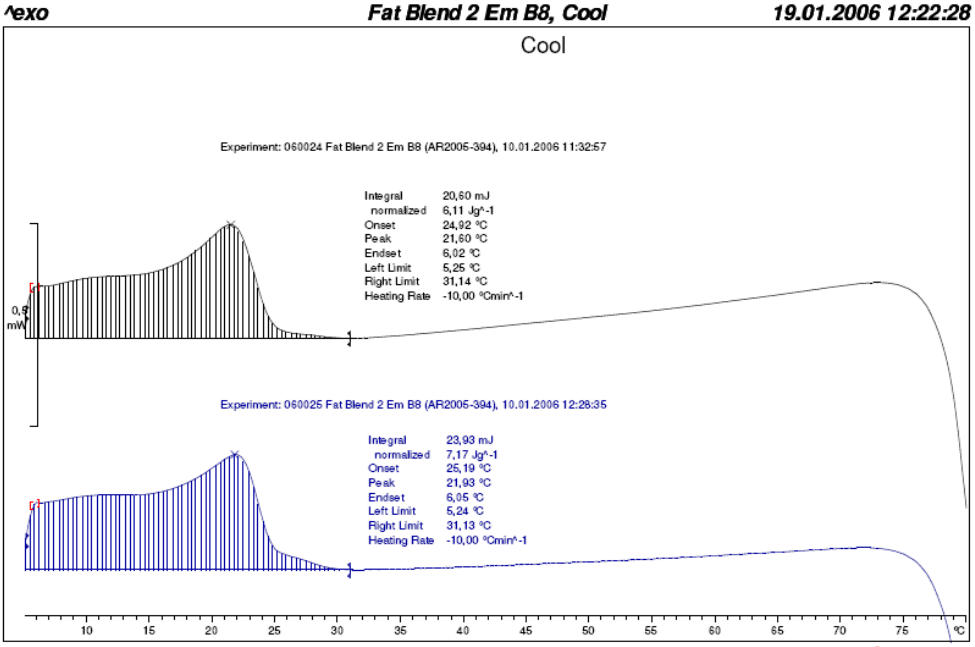

Lab: Danisco **STAR^e SW 8.10**

^exo **Fat Blend 2 Em B9, Cool** **19.01.2006 12:28:28**

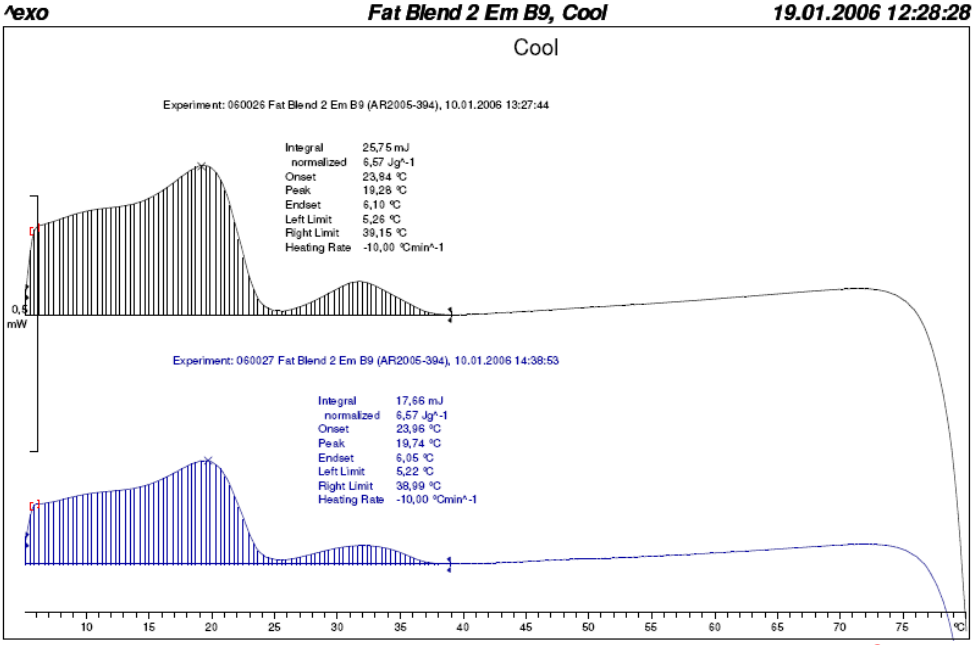

Lab: Danisco **STAR^e SW 8.10**

^exo **Fat Blend 2 Em B10, Cool** **19.01.2006 13:03:30**

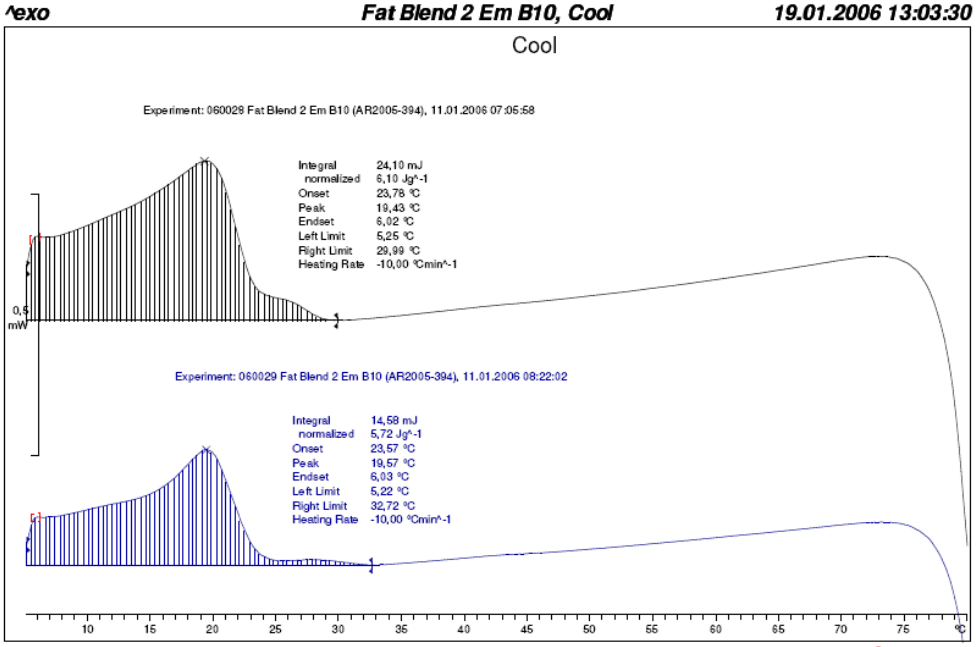

Lab: Danisco **STAR^e SW 8.10**

^exo **Fat Blend 2 Em B11, Cool** **19.01.2006 13:09:41**

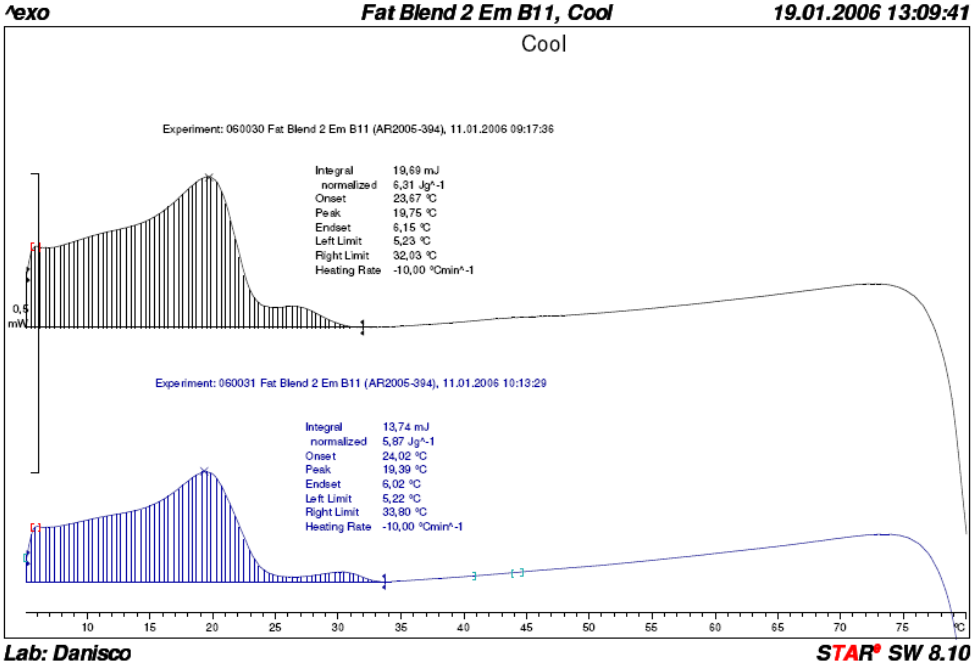

Lab: Danisco **STAR^e SW 8.10**

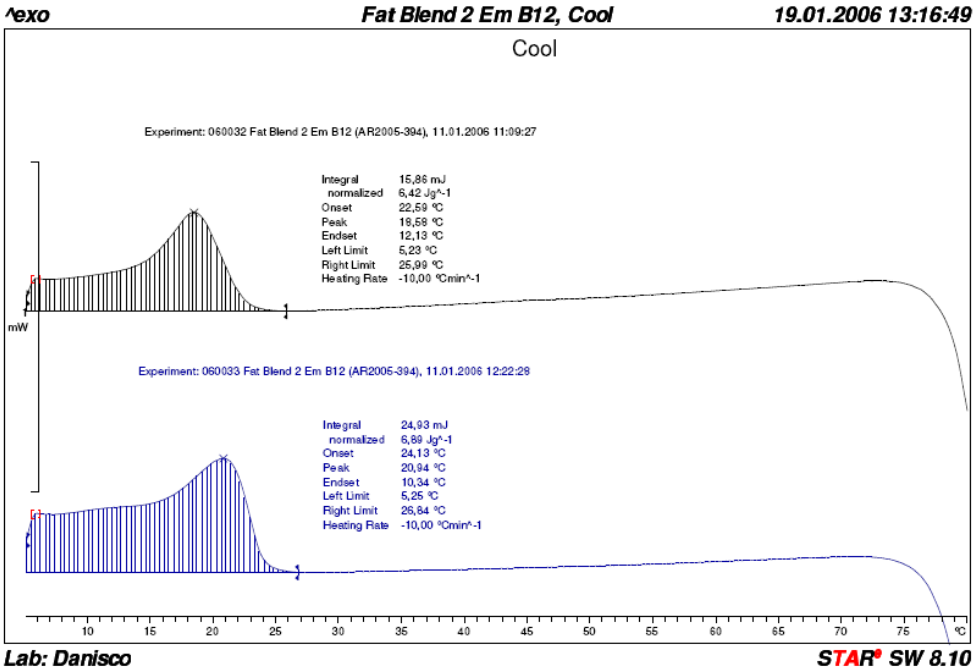

Fat blend C – Puff pastry margarine (fat blend C = fat blend 3)

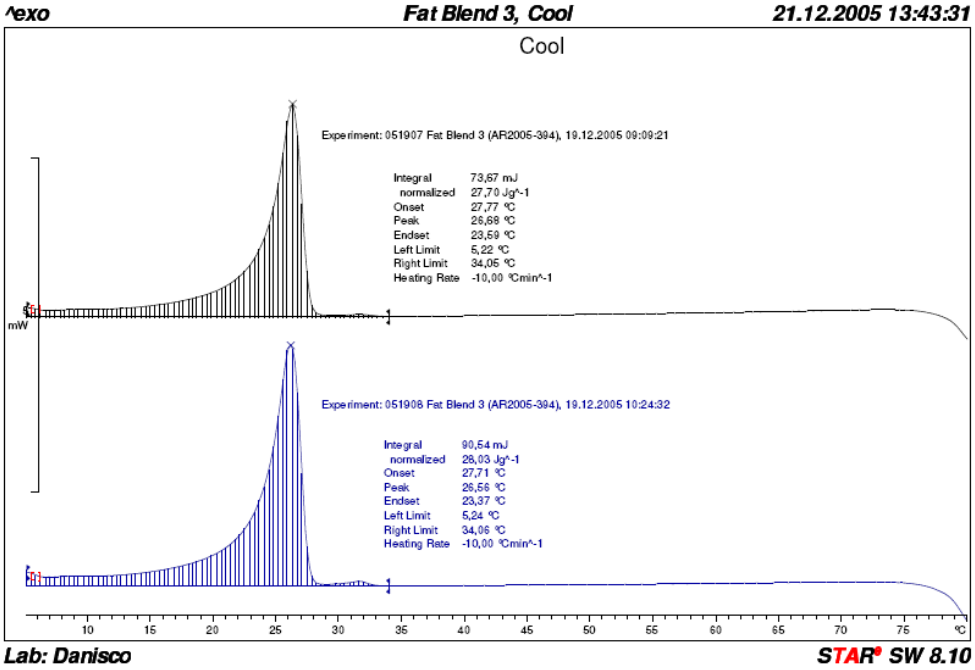

^exo **Fat Blend 3 Em B1, Cool** **06.01.2006 11:28:49**

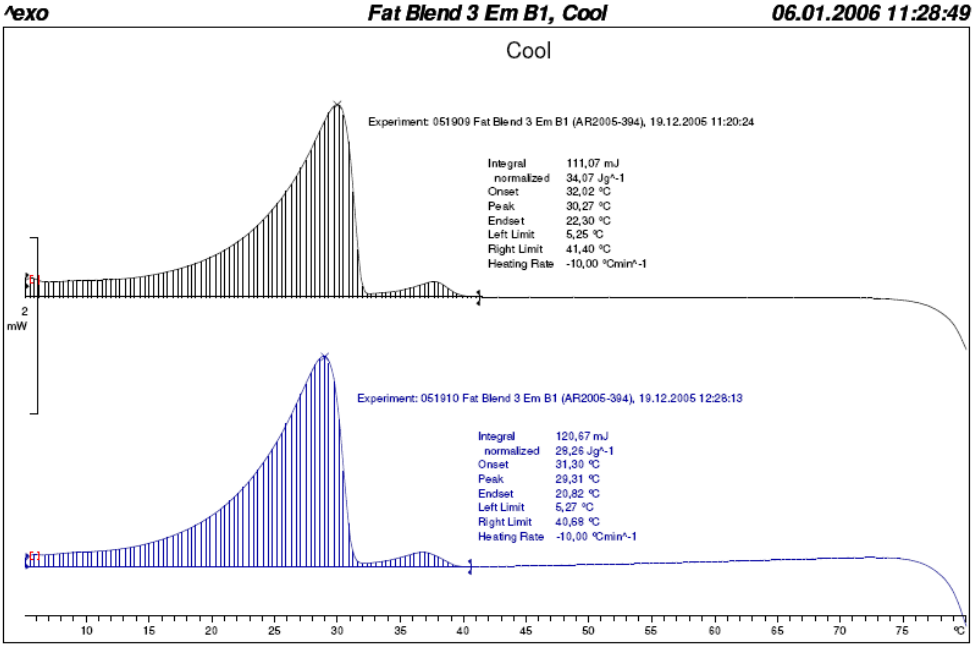

Lab: Danisco **STAR^e SW 8.10**

^exo **Fat Blend 3 Em B2, Cool** **09.01.2006 08:51:13**

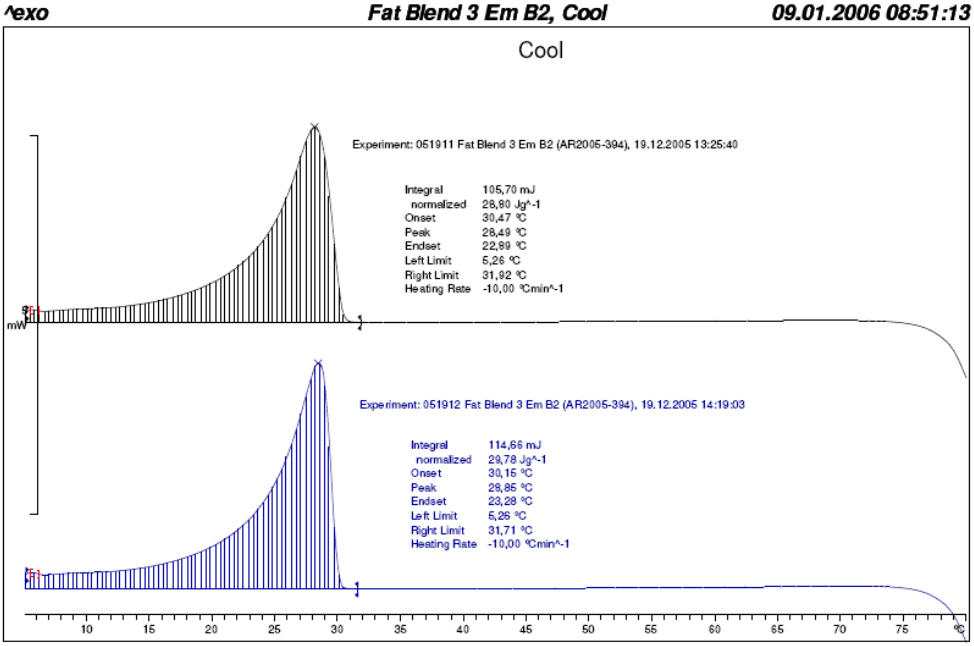

Lab: Danisco **STAR^e SW 8.10**

^exo **Fat Blend 3 Em B3, Cool** **09.01.2006 06:49:35**

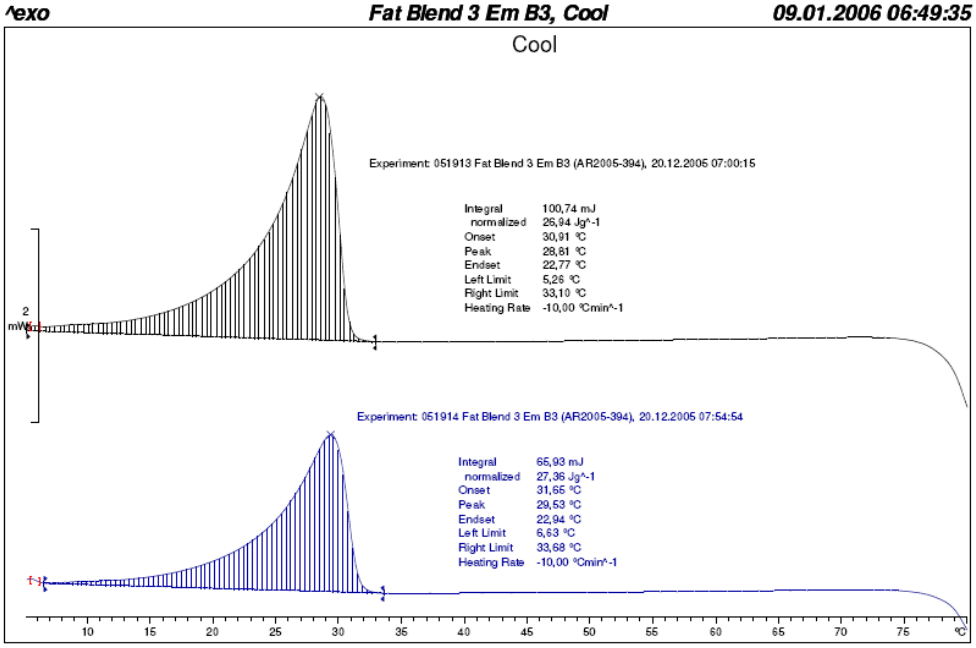

Lab: Danisco **STAR° SW 8.10**

^exo **Fat Blend 3 Em B4, Cool** **09.01.2006 09:11:13**

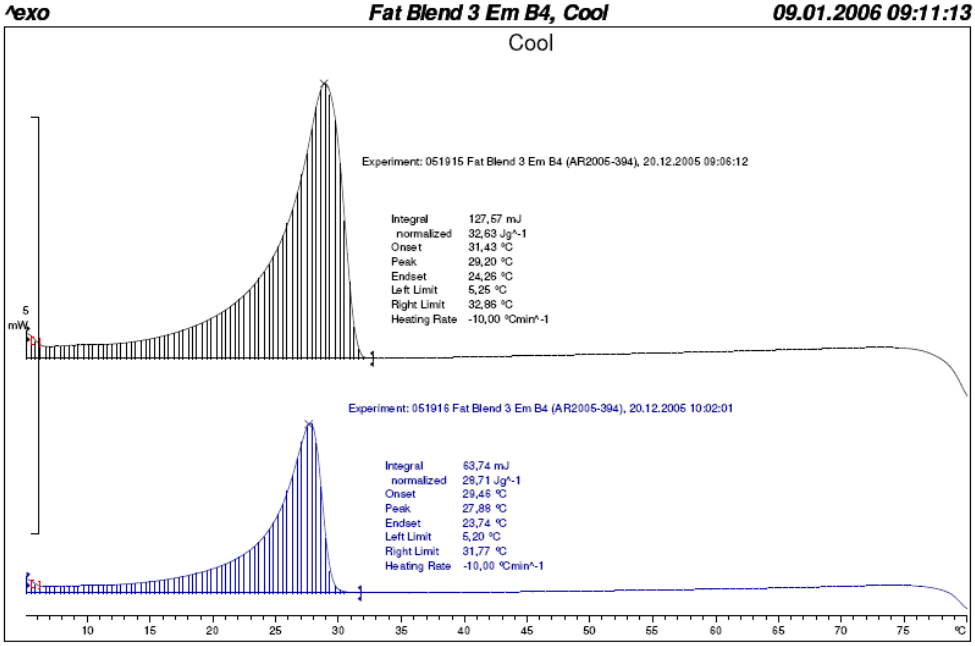

Lab: Danisco **STAR° SW 8.10**

^exo **Fat Blend 3 Em B5, Cool** **09.01.2006 09:20:24**

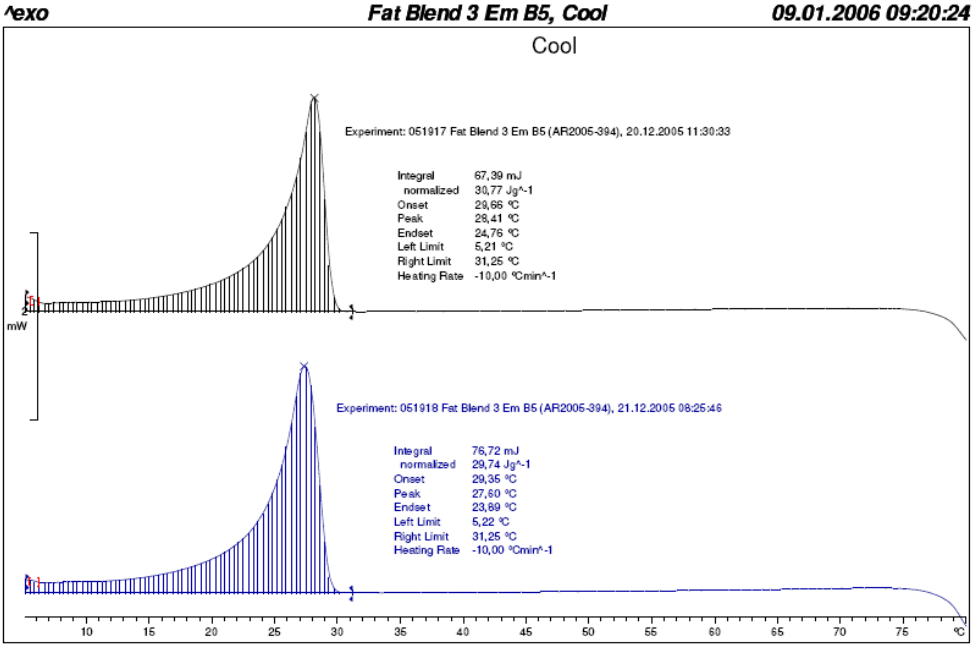

Lab: Danisco **STAR° SW 8.10**

^exo **Fat Blend 3 Em B6, Cool** **09.01.2006 12:17:54**

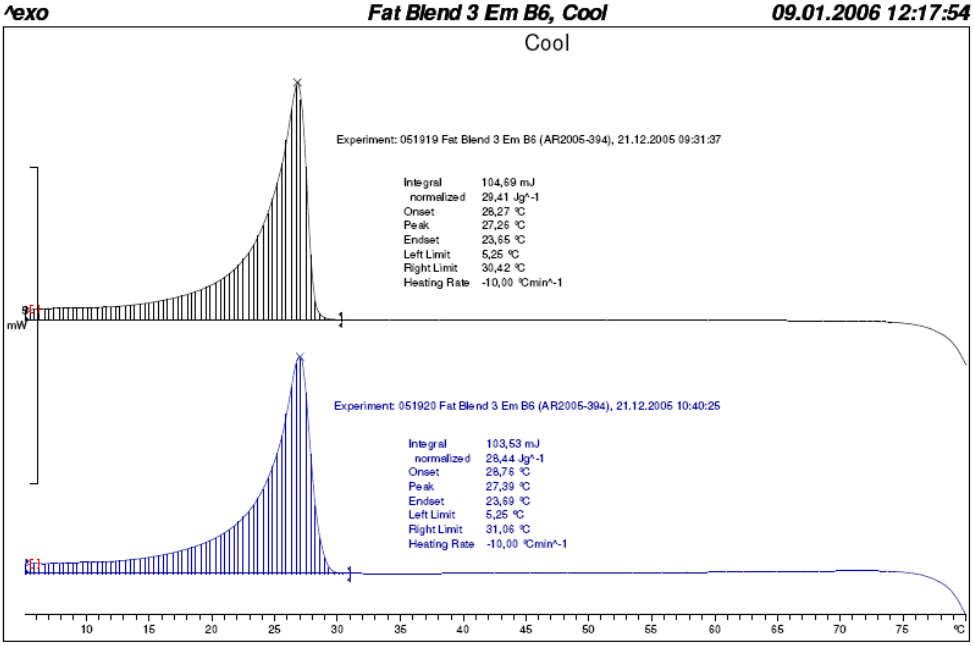

Lab: Danisco **STAR° SW 8.10**

^exo **Fat Blend 3 Em B7, Cool** **09.01.2006 12:28:56**

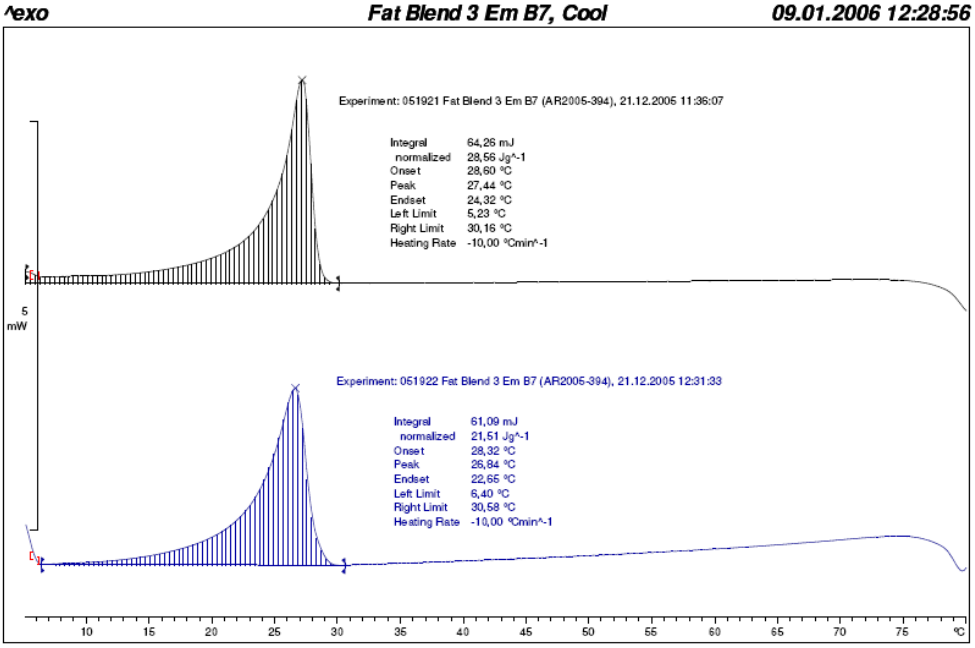

Lab: Danisco **STAR° SW 8.10**

^exo **Fat Blend 3 Em B8, Cool** **10.01.2006 13:05:19**

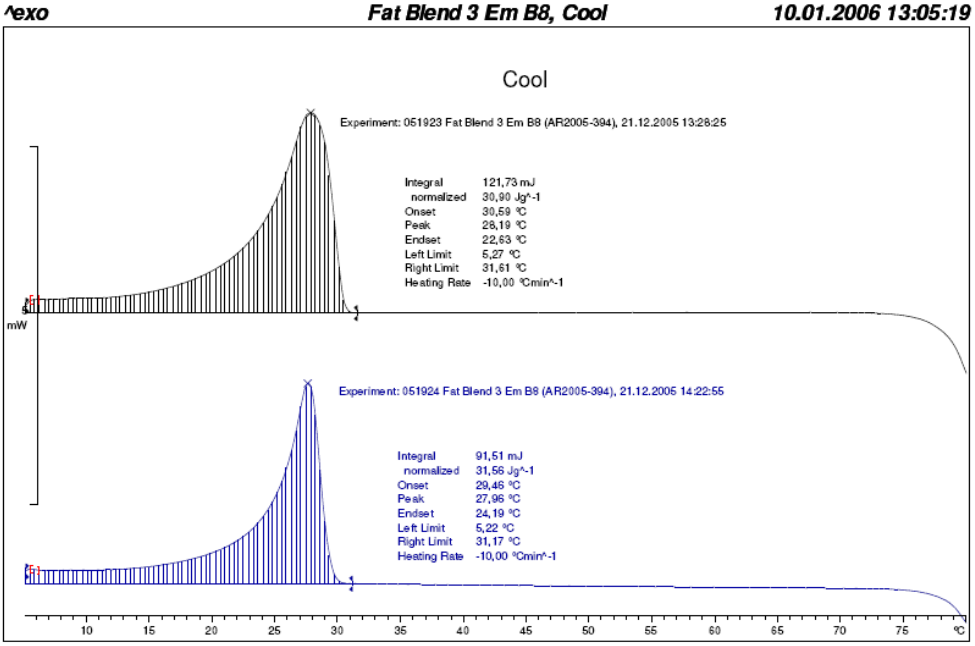

Lab: Danisco **STAR° SW 8.10**

^exo **Fat Blend 3 Em B9, Cool** **10.01.2006 13:28:57**

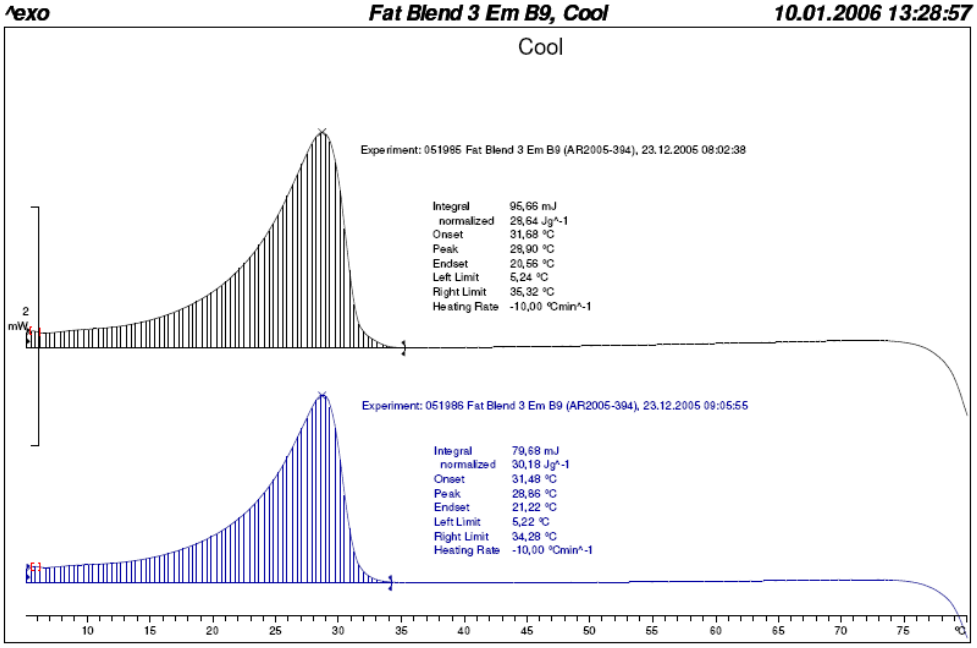

Lab: Danisco **STAR° SW 8.10**

^exo **Fat Blend 3 Em B10, Cool** **10.01.2006 13:34:55**

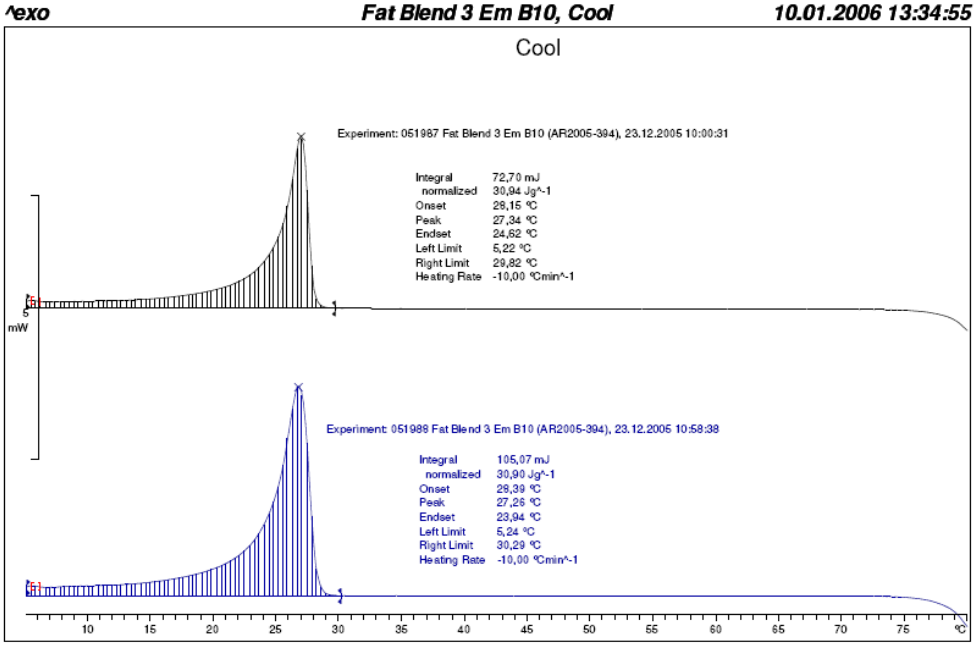

Lab: Danisco **STAR° SW 8.10**

^exo **Fat Blend 3 Em B11, Cool** **11.01.2006 10:03:28**

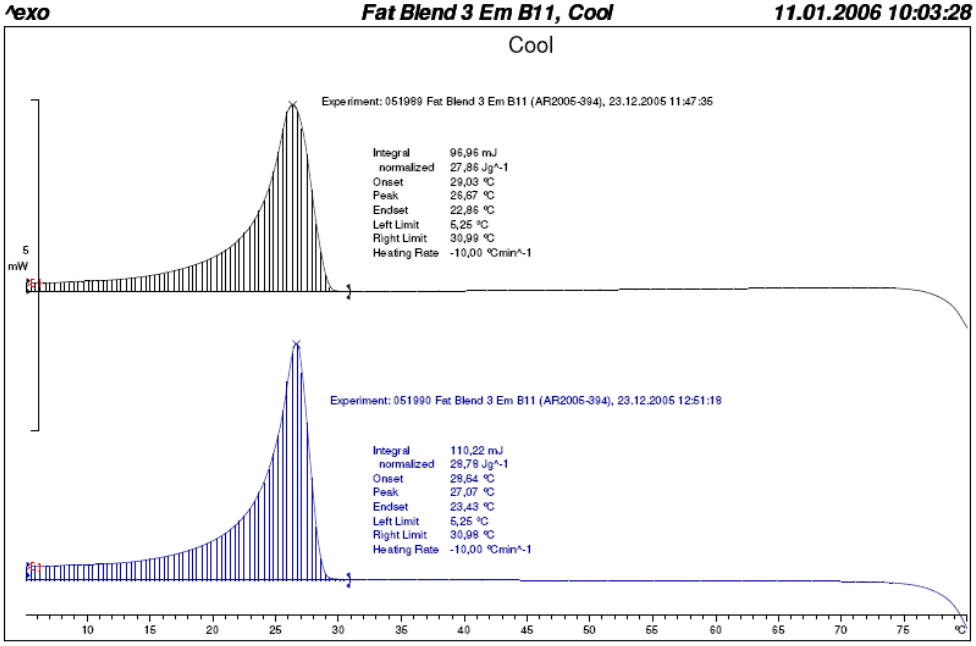

Lab: Danisco **STAR® SW 8.10**

^exo **Fat Blend 3 Em B12, Cool** **11.01.2006 10:12:44**

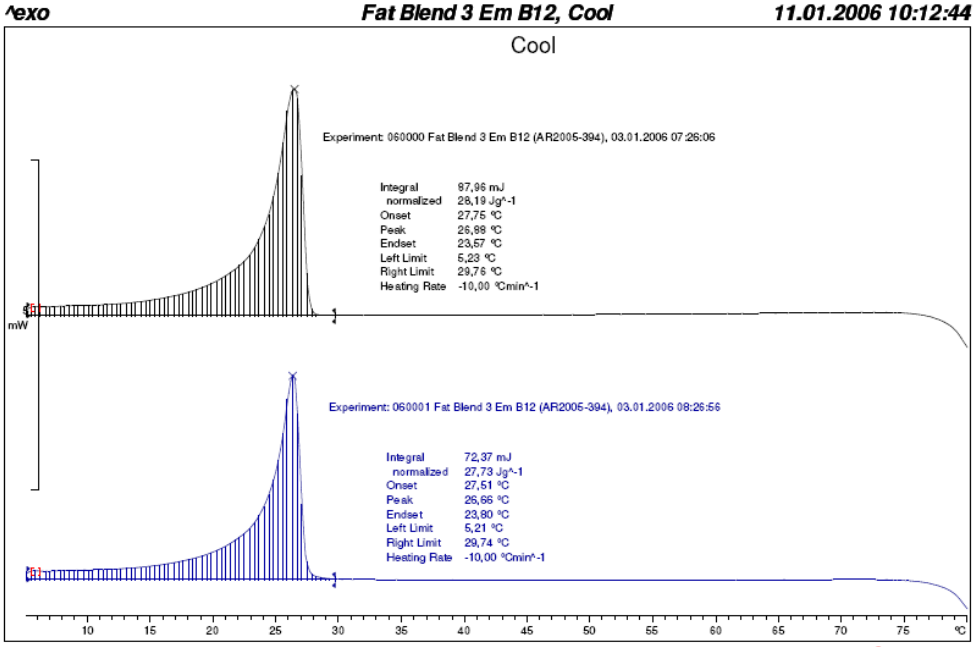

Lab: Danisco **STAR® SW 8.10**

APPENDIX E

Pilot Scale UVP Apparatus

The details of the UVP-PD equipment are the same as before, and have been adequately outlined previously (Wassell et al., 2010b = Paper 4; Young, Wassell, Wiklund, & Stading, 2008 = Paper 3), with the exception of the transducer sensors.

The experimental Oils and Fats pilot plant flow loop at Danisco A/S consists of a closed stainless steel piping circulation system with the possibility to switch between different heat exchanger combinations etc. The sample fluids can be re-circulated through the 12 mm piping from a stainless steel tank with an agitator using a centrifugal pump. The project started with the adaptation of the UVP-PD in-line measuring section to the Oils and Fats pilot plant at Danisco A/S, Braband, Denmark. The measuring section, featuring a custom made flow adapter cell, was fitted with a pair of ultrasound transducers and a pair of pressure sensors.

Figures E1-2 show photos of the experimental Oils and Fats pilot plant flow loop at Danisco A/S together with the UVP-PD in-line measuring section.

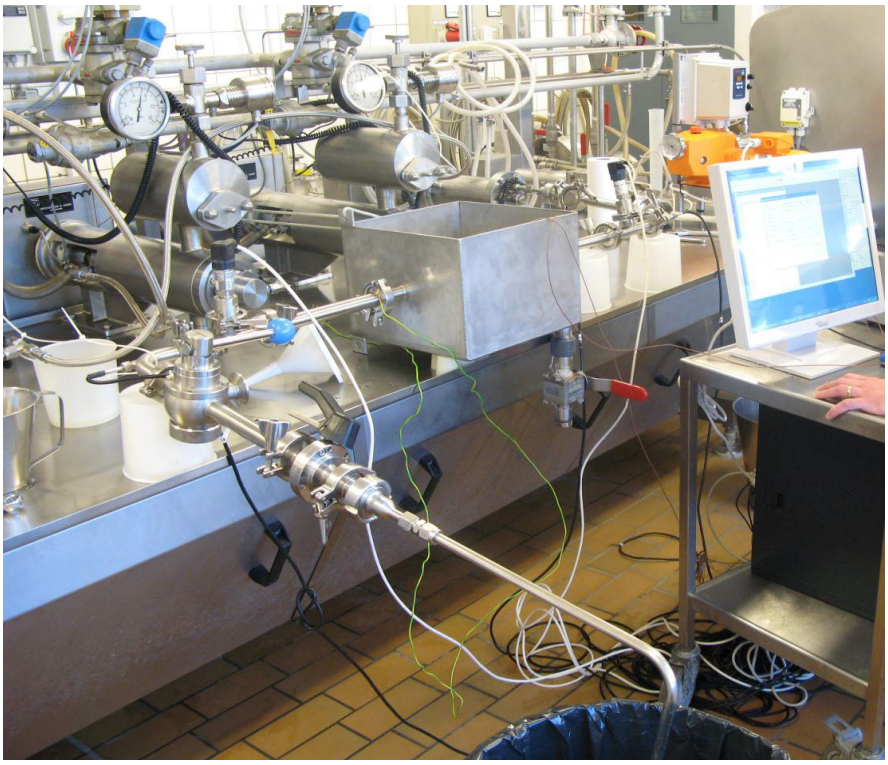

Figure E1: Pilot plant at Danisco A/S installation of UVP-PD in-line measuring section

The UVP-PD in-line measuring section was connected to the pilot plant piping through an expansion and had an inner diameter of 22.5 mm. The measuring section was attached to the exit of the pin roller and the pilot plant loop could easily be modified to closely mimic real industrial conditions

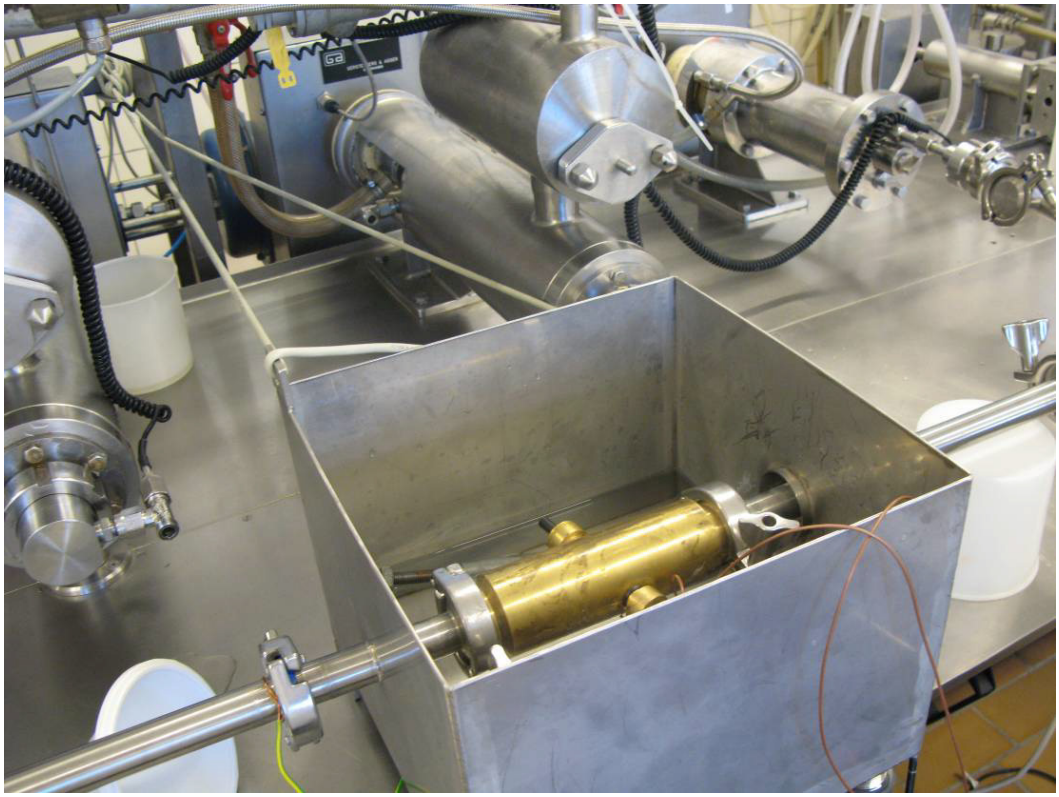

Figure E2 shows close up of UVP-PD in-line measuring section and flow adapter cell fitted with two ultrasound transducers

Images of previous test section are shown in Figure E3 (not previously shown) from the schematic Figure 3.2 in 3.0. The current apparatus is shown in Figure E4

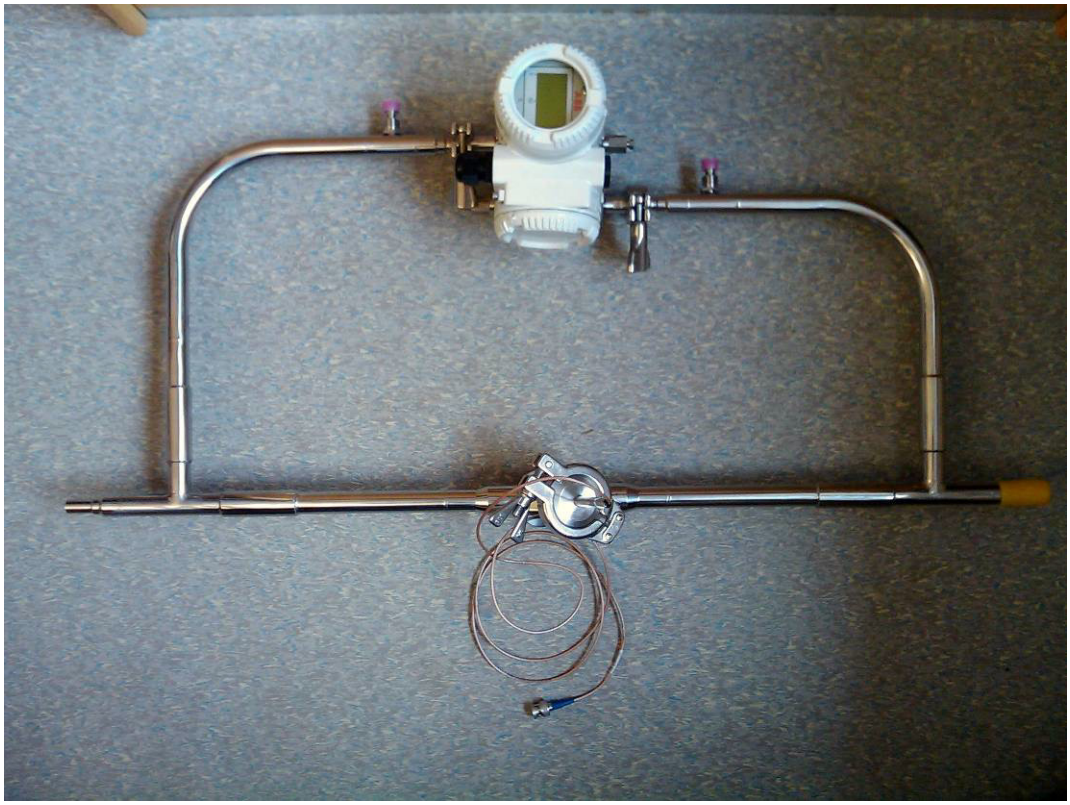

Figure E3 UVP section as described in Figure 3.2

Briefly, the UVP-PD test section was collaboratively developed by Danisco, Denmark, SIK, Sweden, and AB WI-KA Mekaniska Verksted, Sweden. This same test section contained housings also for a differential pressure sensor (ABB 265DS; STP80, ABB Automation Technology Products AB, Sollentuna, Sweden).

The current flow cell and pressure sensor apparatus shown in Figure E4, was used to investigate DAG concentration in palm products (Wassell, Wiklund, Farmer, Hogan Bonwick, Smith, Young, *Dynamic In-Line and Static Off-Line Rheological Profiling on Palm Oil and the Effect of Diglyceride Content on Structure Formation* (for publication)

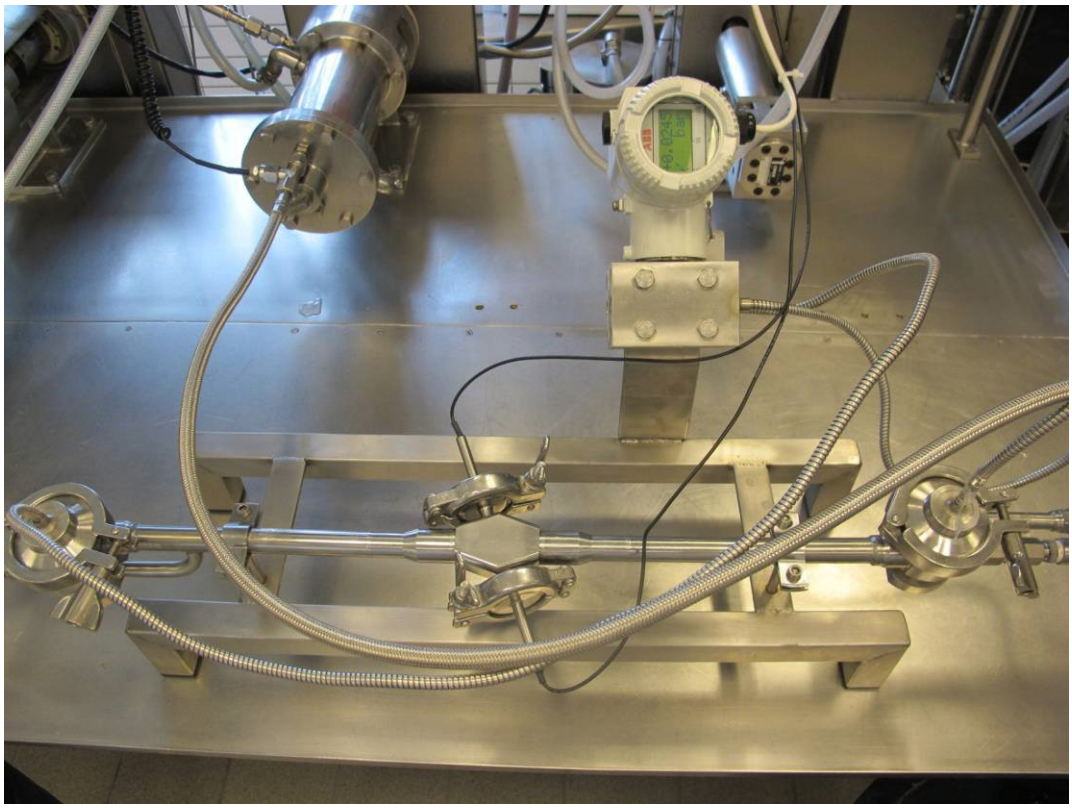

Figure E4 Photographic image of current UVP-PD flow cell apparatus. The flow cell is in the centre with two fixed delay line transducers in place. Far right and left are the pressure sensors which in turn are connected to the pressure gauge (top right).

APPENDIX F

Moringa Oil *(Moringa oleifera)*

From seeds of Moringa tree, also known as Horseradish tree, drumstick tree, Ben tree (Figure F1)

Unusually long shelf life (strong antioxidant, mild taste)

Seed contain 22-40% oil; used in cosmetics and as fuel; rich in Behenic Acid ("Ben oil")

Used already at 400 BC in ancient Greece, now mainly from Philippines, India, Africa

Regarded as "World´s most useful tree" (almost all parts used for food)

Figure F1 Moringa Oil *(Moringa oleifera),* image courtesy of Danisco / DuPont 2009

Available and traded in commercial scale, Moringa is cultivated in semi-arid, tropical, and subtropical areas in Africa, Central and South America, Sri Lanka, India, Mexico, Malaysia, Indonesia and the Philippines. It is also native to the southern foothills of the Himalayas in northwestern India. It grows to about 10-12m in height, in cultivation it is cut back annually to ~1-2m.

The tree is considered one of the world's most useful trees, as almost every part of the Moringa tree can be used for food, or has some other beneficial

property. The tree's bark, roots, fruit, flowers, leaves, seeds, and gum are also used medicinally.

The Moringa seeds yield 38–40% edible oil, called ben oil from the high concentration of behenic acid contained in the oil.

While it grows best in dry sandy soil, it tolerates poor soil, including coastal areas. It is a fast-growing (3m in 10 months from seed) drought-resistant tree.

References:

Lalas, S. Tsaknis, J. (2002) Characterization of *Moringa oleifera* Seed Oil Variety "Periyakulam 1" Journal of Food Composition and Analysis, 15 (1), 65-78.

Tsaknis, J. Lalas, S. Gergis, V. Dourtoglou, V. Spiliotis, V. (1999) Characterization of *Moringa oleifera* variety Mbololo seed oil of Kenya. Journal of agricultural and food chemistry. 47 (11) 4495-4499.

Tsaknis, J. Lalas, S. Gergis, V. Spiliotis, V. (1998) A total characterisation of *Moringa oleifera* Malawi seed oil. Rivista Italiana delle Sostanze Grasse. 5, (1) 21 – 27.

Somali, M.A. Bajneid, M.A. Al-Fhaimani, S.S. (1984) Chemical composition and characteristics of *Moringa peregrina* seeds and seeds oil. Journal of the American Oil Chemists' Society, 61 (1) 85-86.

Vernacular Names of *Moringa oleifera*

(Source: http://www.moringanews.org/biblio_en.html)

EUROPE

ENGLISH: Horseradish tree, Radish tree, Drumstick tree, Mother's Best Friend, West Indian ben.

FRENCH: Bèn ailé, Benzolive, Ben oléifère, Arbre radis du cheval.

GERMAN: Behenbaum, Behenussbaum, Flügelsaniger bennussbaum, Pferderettichbaum

ITALIAN: Sàndalo ceruleo

PORTUGUESE: Acácia branca, Marungo, Muringa, Moringuiero; Cedro (Brazil)

SPANISH: Árbol del ben, Ben, Morango, Moringa

AFRICA

BENIN:

(Adia): Kpashima

(Bariba): Yuru ara, Yorwata, Yoroguma

(Dendi): Windibundu

(Fon): Patima, Kpatima, Yovokpatin, Kpano, Yovotin

(Gun): Ékwè kpatin, Kpajima

(Mina): Yovo vigbe, Yovo kpati

(Natemba): Tekpinda

(Peul): Guildandeni, Latj iri, Legi-Lakili

(Saxwe): Kotba

(Waama): Yori kununfa

(Yoruba): Ewé ilé

(Yoruba-Nago): Ewé igablé, Ewé ilé, Ewé oyibo (White man's tree), Agun, Manyieninu, Ayere, Oyibo.

BURKINA FASO :

(Bwaba): La-Banyu.

(Dioula): Ardjeneyiri, Ardjian jirri.

(Gourmanche/Gourmantchema): Alj an-tiiga, Ki gambaga (region of Tapua), Diegu kanlobuga (region of Gnagna) (meaning "one will never lack a child in the courtyard"), Makkakomboanga.

(Fulfuldé): Aljannahi, Guilgandani, Gigandjah.

(Morée/Mossi): Argentiga, Arzan tiiga ("The tree of paradise").

CAMEROUN:

(Daggai): Paizlava

(Foulfouldé): Guiligandja, Giligandjahi

(Hausa): Zogalagandi

(Mafa): Gagawandalahai

(Mandara): Djhiré

(Moundang): Naa-toukoré

(Podoko): Chabané

(Toupouri): Naa-nko

CHAD:

(Sara): Kag n'dongue

(Shuwa Arabic): Alim, Halim

COMOROS ARCHIPELAGO:
Anambo, Mvungué.

GHANA:

(Ewe): Atiuwuse (the tree with tender/slim leaves), Babati, Babatsi, Kpotowuzie (feeble tree; easily broken). Kpokpoti (the "illness tree"), Nukunaya (wonderful news), Yevu-ti (white man's tree), Yevutsi
(Dagari): Obnukuo, Ornyyukuo, Zangala.

KENYA:

(Swahili): Mlonge, Mronge, Mrongo, Mlongo, Mzunze, Mzungu., Mjungu moto, Mboga chungu, Shingo.

(Sokoki - Indian spoken in Mombasa): Mborongi.

MADAGASCAR:

(Malagasy): Anamambo, Anamorongo, Feliimorongo, Felikambo, Felikamoranga, Landihazo, Moringa, Moringy.

MALAWI:

(Chichewa): Cham'mwanba, Kangaluni.

(Lomwe): Sangoa, Shangoa

(Senna): Nsangoa.

(Yao): Kalokola.

ALSO: Maula tengo, Mpundi, Muula, Mbula, Mpempu, Chakate, Mpenba

MALI:

(Bambara): Gnougou Jirini, Kandjirini, Manjirini, Massa Jirini.

(Segou): Verdaye

MAURITIUS:

(Creole): Drède mouroungue.

(Indian Creole): Mouroungue

NIGER:

(Hausa): Zôgala gandi.

(Shuwa Arabic): Alim, Halim.

(Zarma): Windi-bundu.

NIGERIA:

(Fulani): Gawara, Gaware, Konamarade, Rini maka, Habiwal hausa.

(Hausa): Bagaruwar maka, Bagaruwar masar, Barambo, Koraukin zaila, Rimin nacara, Rimin turawa, Samarin danga, Shipka hali, Shuka halinka, Zogall, Zogalla-gandi,

(Ibo): Odudu oyibo,Okwe oyibo,Okwe olu,Uhe,Oku-ghara-ite, Okochi egbu ("cannot be killed by the dry season").

(Nupe): Chigban Wawa

(Yoruba): Adagba malero, Ewele, Ewé ilé, Ewe igbálé, Idagbo monoyé ("The tree which grows crazily").

SENEGAL:

(Wolof): Neverday, Nébéday, Sap-Sap.

(Serer): Nébéday.

SEYCHELLES :

(Creole): Drède mouroungue.

SIERRA LEONE:

Boganja

SOMALIA:

(Indian): Mrongo

SUDAN:

(Arabic): Ruwag, Alim, Halim, Shagara al ruwag.

(Dinka): Anid.

(Kordofan Arabic): Shagara zaki al moya.

TANZANIA:

(Swahili): Mlonge, Mronge, Mrongo, Mlongo, Mzunze, Mzungu., Mjungu moto, Mboga chungu, Shingo.

TOGO:

(Dagomba): Baganlua, Bagaelean.

(Ewe): Kpotima, Kpoti, Yevu-ti, Yovoviti.

(Hausa): Mágurua maser.

(Mina): Yovoviti.

(Moba): Gambaduk.

(Mouroungue): Jevoti, Jovoviti.

ALSO: Amedoti, Ekpoti, Molo-Kpoti.

ZAMBIA:

(Tonga): Zagalanda, Zakalanda

ZIMBABWE:

(Tonga): Mupulanga, Zakalanda.

ASIA

BURMA:

(Burmese): Dandalun, Daintha, Dandalun-bin, Dandalonbin.

CAMBODIA:

Ben ailé, Daem mrum.

INDIA :

(Bengalese): Munga ara, Sajna, Sojna, Sujana

(Gujarati): Midho-saragavo, Saragavo, Saragvo, Suragavo.

(Hindi): Munga ara, Shajmah, Shajna, Segra.

(Hindi/Orissa): Sanjna, Saijna, Shajna, Soandal

(Kanarese): Nugga egipa, Nugge, Noogay, Nuggi Mara.

(Kol): Mulgia, Munga ara, Mungna

(Kumao – Himalayan region): Sunara

(Konkani/Goa): Moosing, Mosing

(Malayalam): Sigru, Moringa, Muringa, Murinna, Morunna.

(Marathi): Sujna, Shevga, Shivga.

(Modesia/W. Bengal): Mangnai

(Monghye/Punjab): Sejana

(Oriya): Munigha, Sajina.

(Punjabese): Sanjina, Soanjana.

(Rajasthan): Lal Sahinjano

(Sanskrit): Danshamula, Shobhanjana, Sigru Shobhanjan, Sobhan jana.

(Sindhi): Swanjera

(Tamil): Morunga, Murungai, Murunkak-kai.

(Telegu): Sajana, Tella-Munaga.

(Teling): Morunga, Morungai

(Urdu): Sahajna

(Central provinces): Mulaka, Saihan

(Western region): Sundan

ALSO: Sweta Maricha

INDONESIA:

(Alor): Maroenga, Motong.

(Bali): Kelor, Tjelor.

(Flores): Moltong

(Java): Kelor

(Madura): Marongghi

(Moluccan islands): Oho Gaairi

(Roti): Kafok, Kai fok

(Sumatra): Kalor, Kerore

(Sumba): Kawona, Wona

(Ternate): Kelo, Oege Kelo

(Tidore): Kelo

(Timor): Baoe fo, Maroenga

ALSO: Remoenggai, Sajor Kelor

LAOS:

(Lao): B'Loum

MALAYSIA:

Kachang Kelur, Lemunggai, Meringgai, Semunggai, Smunggai, Semunggai, Remunggai

NEPAL:

Sitachini

PAKISTAN:

Saijan, Sohanjna

PHILIPPINES:

(Tagálog): Kalungai, Kamalungua, Malongai, Malungai, Mulanggay, Malunkai.

(Bikol): Kalungai

(Bisáya): Alúngai, Dool, Malungit.

(Kisaya): Kalungai

(Ibanág): Marongai, Marungai

(Ilóko): Marongai, Marungai, Komkompilan

(Pampángan): Dool, Kamalungua, Malúngit.

(Panay Bisáya): Kalamúngai, Kamalongan

(Pangasinán): Rúnggai

(Sambáli): Marongai, Marungai

(Simeulue): Aroenggai

THAILAND:

(Thai): Kaanaeng-doeng, Phak eehuem, Phak eehum, Phak-nuea-kai, Se-cho-ya

(Central highlands): Ma rum

(North): Ma khonkom

VIETNAM:

Chum Ngay

YEMEN:

(Arabic?): Saisam

SOUTH & CENTRAL AMERICA, CARRIBEAN

BELIZE:

(Spanish): Maranga calalu

CAYMAN ISLANDS:

(Spanish): Mawonga.

COLOMBIA:

(Spanish): Aceite, Aceitoso, Angela, Colirio, Goma, Jeringa, Marango, Maranjo, Marangon, Sen de la tierra.

COSTA RICA:

(Spanish): Marango, Marangon.

CUBA:

(Spanish): Acacia, Ben, Calicita, Leno nefrítico, Palo blanco, Palo de jeringa, Palo de Tambor, Paraíso francés.

DOMINICAN REPUBLIC:

(Spanish): Ben, La libertad, Libertad, Palo de abejas, Palo de aceiti.

DUTCH ANTILLES:

(Dutch): Ben boom

(Spanish): Brenolli, Morenga, Orselli.

EL SALVADOR:

(Spanish): Ceiba, Marengua, Narango, Paraíso extranjero, Teberinto.

GUADALOUPE:

(Spanish): Maloko, Moloko, Ben-ailé.

GUATAMALA:

(Spanish): Perla, Perlas, Paraíso blanco.

GUYANA:

Saijhan.

HAITI:

(French): Benzolive, Benzolivier, Ben oleifere, Bambou-bananier, Graines benne, Olivier.

(English): Benzolive tree.

HONDURAS:

Maranga calalu.

MEXICO:

(Spanish): Arbol de las perlas, Chinto borrgo, Flor de Jacinto, Jacinto, Paraíso blanco, Paraíso de Espana, Perla, Perlas, Perla de la India, Perlas del oriente, San Jacinto.

NICARAGUA:

(Spanish): Marango, Maranjo, Marangon.

PANAMA:

(Spanish): Jacinto.

PANAMA CANAL ZONE:

(English): Horseradish tree.

PUERTO RICO:

(Spanish): Angela, Ben, Colirio, Jasmin francés, Resada, Sen de la tierra.

SAN SALVADOR:

(Spanish): Marango, Marangon, Maranjo.

SURINAM:

(Dutch): Peperwortel boom.

(Indonesian): Kelor.

TRINIDAD:

(Hindi?): Saijan.

VENEZUELA:

(Spanish): Aceite de Ben, Azucarillo, Ben, Sen.

ALSO: Arbol do los aspáragos, Bamboubamamoer, Cedro, Cenauro, Chinto borrego, Chuva de prata, Desengaño, Gailito, Guaireña, Hoja de sen, Macasar, Marenque, Moongay, Moriengo, Noz de bem, Orenga, Palo de geringa, Palo jeringa, Paraíso, Pois quinique, Quiabo de tres quinas, Sainto John, Salaster, Salibau, Sen, Seringa.

VERNACULAR NAMES: OTHER MORINGA VARIETIES

MORINGA CONCANENSIS

India

(Tamil: Murungai (The same name is used for *Moringa oleifera*).

MORINGA DROUHARDII

MADAGASCAR

(Malagasy): Hazomalana, Maroserano, Moringy.

MORINGA LONGITUBA

ETHIOPIA

(Somali): Hane, Mane.

KENYA

(Somali): Borrant, Haduma.

(Boran): Saffara.

SOMALIA

(Majindi?): Fintir.

(Somali): Hawe, Mawe, Mawow, Wame, Wuame.

MORINGA OVALIFOLIA

ANGOLA Hungua, Mungua.

NAMIBIA

(Afrikansk): Meelsakboom.

(Herero): Omutindi.

MORINGA PEREGRINA

EGYPT, SYRIA, ARABIAN PENINSULA

(Arabic): Bãn, El bãn, Vassar, Ithi, Yassar

IRAN

Gazrokh, Gazroghan.

ORAN

(Arabic): Shuh

SOMALIA

(Somali): Dankap, Dongop, Dumok, Mereh, Moroh.

SUDAN

(Arabic): Shagara al rauwãq.

(Bisharin, Hadendowa): Mai

(Tigri): Khal erbal.

ETHIOPIA

(Tigri): Khal erbal.

MORINGA STENOPETALA

ETHIOPIA

(Konso): Shifara, Shalchada.

KENYA

(Turkana): Etebusoit.

(Njemps): Loresienjo.

(Samburu): Larsanjo, Lorsenjo, Lossantscho.

(Somali): Mau, Mawa.

(Boran): Saffara. (Konso): Shifara, Shalchada, Shalqueida.

APPENDIX G

Lesquerella Oil *(Lesquerella fendleri)* Potential for Commercialisation

Source from: (Dierig et al., 1993; Dierig and Thompson, 1993)

As stated:-

”Lesquerella produces a triglyceride oil that is two-thirds or more lesquerolic acid, a hydroxy fatty acid (HFA). Hydroxy fatty acids are now used in nylon-11 and nylon-6,10, lithium greases, coatings, sulfated and sulfonated oil, sebacic acid, ethoxylated oil, food grade lubricants, polyurethanes, and cosmetics. The current source of HFAs is ricinoleic acid from castor (Ricinus communis L.), which was formerly cultivated in the United States. Approximately 41,000 million tons are now imported, primarily from Brazil and India, at a value exceeding $100 million per year. Lesquerella is native to the United States. and could be established as a domestic HFA source and reduce reliance on castor oil importation.

Lesquerella has several novel properties that set it apart from castor and other oilseeds. One property, is its oil functionality, including difunctional hydroxy moities (in contrast to other seed oils such as castor that are trifunctional). Lesquerella has been reported to contain natural estolides (secondary esters derived from the addition of a fatty acid moiety to the hydroxyl functionality of the hydroxy triglyceride) that improve performance of the oil. Estolides have been encountered in only a few other seed oils, and are not naturally found in castor oil (although they can be synthetically fabricated). Estolides have been shown to improve vegetable oil performance in motor oils by improving pour points (temperature at which the oil no longer pours), and estolides have also been used as viscosity modifiers in lubricating oils. The second of lesquerella's novel properties is its antioxidants, converted from the seed meal fraction that contain unique glucosinolates and have superior oxidative stability properties. The seed meal also has a binder application, unique for seed meals. The third novel property is the seed coat of lesquerella, which contains a unique gum that has rheological properties equivalent to guar or xanthan that can be useful in

coatings and food thickeners" (Dierig et al., 1993; Dierig and Thompson, 1993).

*Lesquerella produces a triglyceride oil that is two-thirds or more lesquerolic acid, a hydroxy fatty acid (HFA). This rich source of hydroxy moieties was thought to be interesting for use in low fat w/o emulsions.

- *Lesquerella fendleri* is a plant from the familiy of Brassicaceae (like Rapeseed)
- Richest source of "Bladderpod Oil"
- 24% oil content in the seeds (Rapeseed 40%, Sunflower 50%)
- Oil: Reddish-brown colour
- Seed coat: Natural Gum, maybe a food additive like Xantham
- Native in South-West US, northern Mexico
- Production not yet industrialized
- Development in trials stadium
- No progress in breeding so far

Information source: Maricopa Agricultural Center, University of Arizona; Texas A&M University 2009

APPENDIX H

IRS Recalculation of Complex Interfacial Behaviour Based on Absolute Constants

Example is shown here of recalculations based on more absolute constants. Ideally, the calculation of complex interfacial viscosity eta-i, is done for each of the 151 data points. However, the example here uses constants at 5°C interval from 50°C to 5°C. As discussed in 4.2.3, calculations based on absolute values, present problems in the regression analysis, where a small negative G´ is introduced, causing "overcompensation".

Calculation of interfacial rheological values during a temperature sweep								
	Result		Technical informations					
			Upper fluid (oil)			Lower fluid (water)		
			Density	Re(visc)	Im(visc)	Density	Re(visc)	Im(visc)
Temp	G'_i	G''_i		eta2'	eta2"		eat1'	eta1"
°C	Pa·m	Pa·m	g/ml	Pa·s	Pa·s	g/ml	Pa·s	Pa·s
5	-0.713	0.290	0.9229	0.97800	0.90100	1.0000	0.00152	0.00000
10	-0.528	0.343	0.9195	0.69200	0.58700	0.9997	0.00131	0.00000
15	-0.171	0.446	0.9160	0.37000	0.17900	0.9992	0.00114	0.00000
20	0.135	0.268	0.9125	0.09180	0.01180	0.9983	0.00100	0.00000
25	0.047	0.113	0.9091	0.06220	0.00988	0.9971	0.00089	0.00000
30	0.047	-0.016	0.9056	0.05130	0.01140	0.9957	0.00080	0.00000
35	0.015	-0.003	0.9023	0.04630	0.01000	0.9941	0.00072	0.00000
40	0.002	0.000	0.8989	0.03280	0.00655	0.9923	0.00065	0.00000
45	0.000	-0.003	0.8954	0.03470	0.00960	0.9902	0.00060	0.00000
50	0.002	-0.002	0.8920	0.02750	0.00875	0.9880	0.00055	0.00000

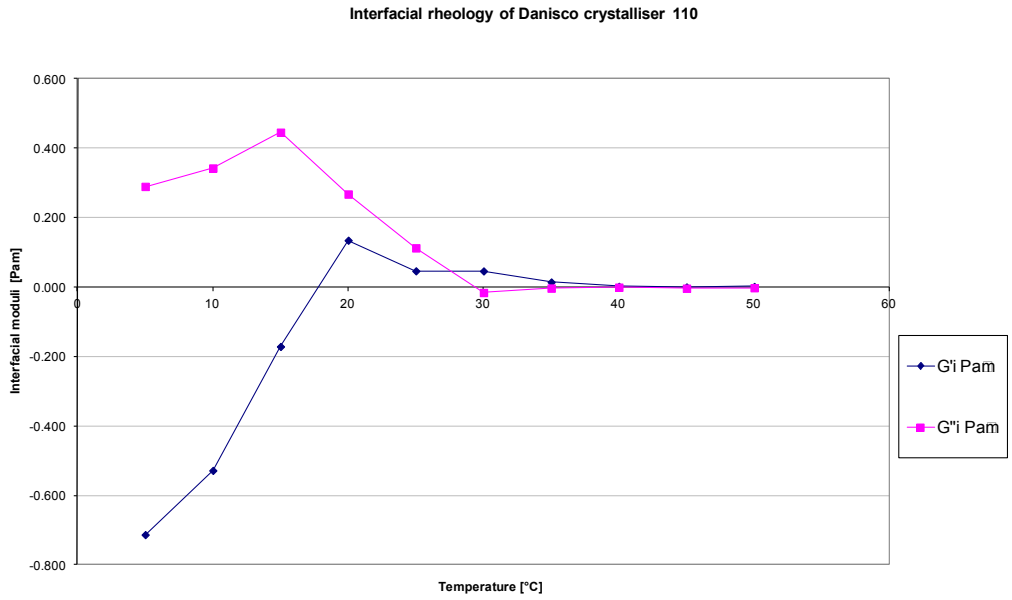

APPENDIX I

Example Data: Anton Paar RHEOPLUS software

Complex viscosity is based on constants of upper fluid density (0.8912 g/cm^3), viscosity (0.0252 Pas) parameter for Sunflower oil at 50°C; lower fluid density (0.98802 g/cm^3), viscosity (0.000547 Pas) parameter for water at 50°C. These constants were used as a function of all 151 data points.

Example data from RHEOPLUS/32 V3.21 shows upper fluid parameter: bulk sunflower oil at 50°C and lower fluid parameter: water at 50°C

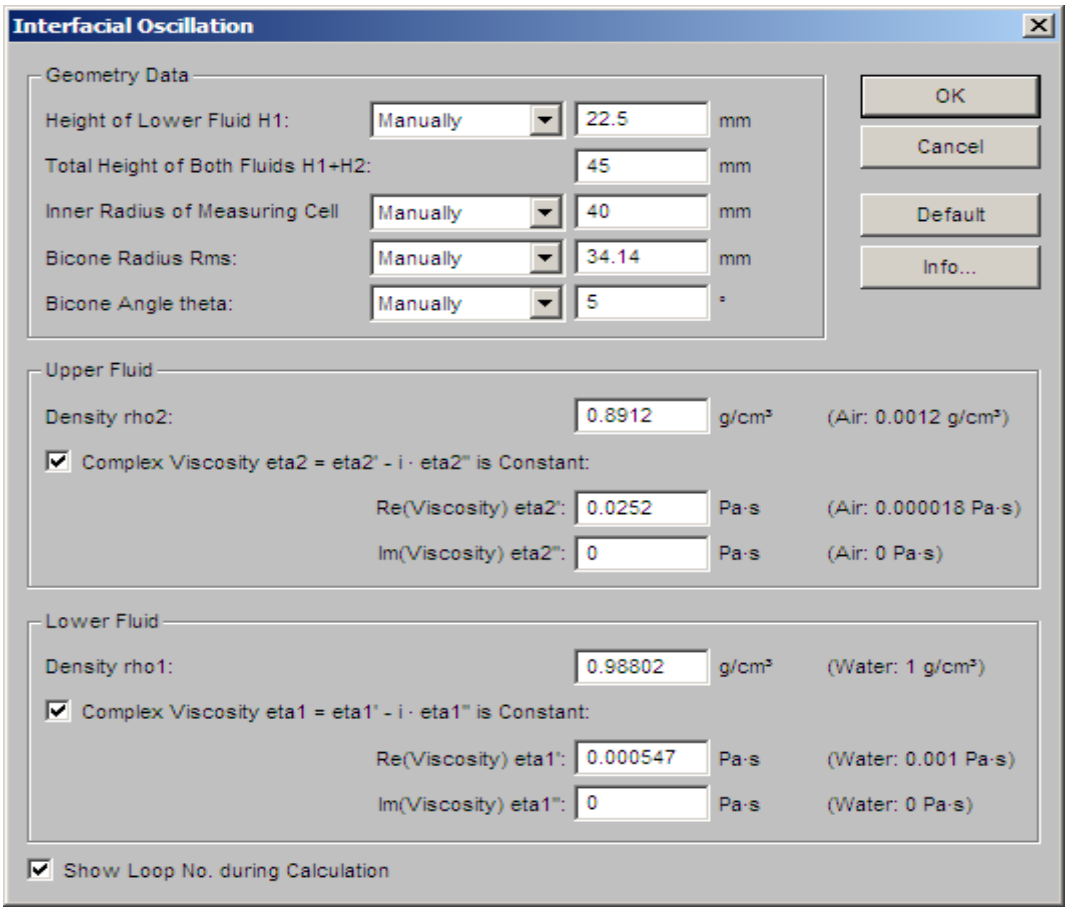

APPENDIX J

Test Settings: Stable Micro Systems Texture Analyser (TA-XT2i) Software (version 2.64)

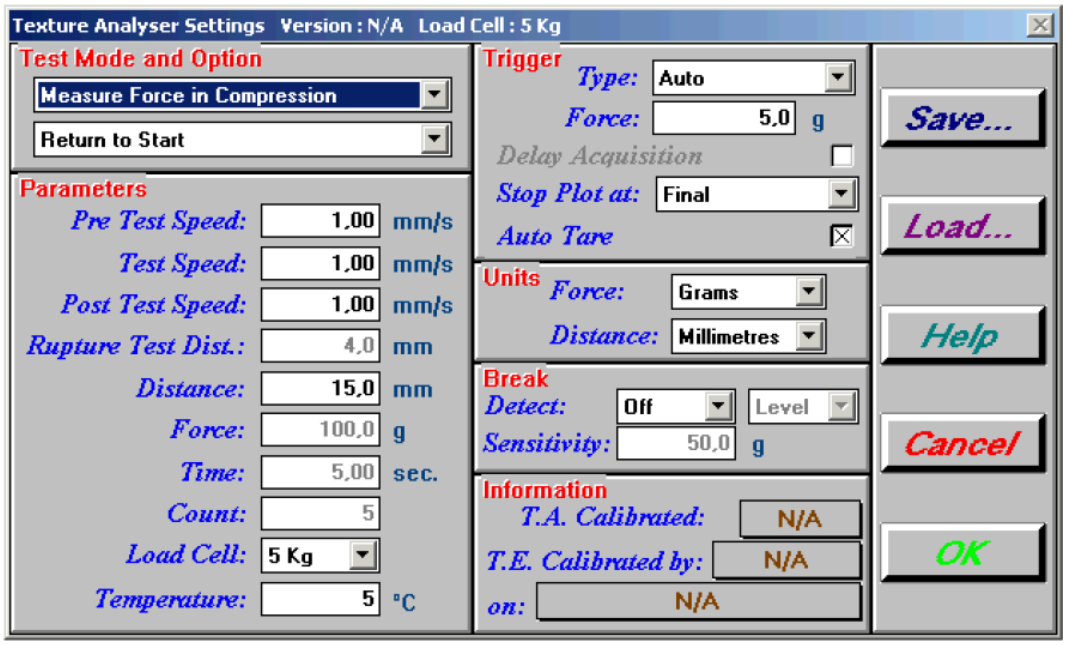

Example of Stable Micro Systems Texture Analyser software: Texture expert version 2.64